LI
LABORATORY INVESTIGATION
THE BASIC AND TRANSLATIONAL PATHOLOGY RESEARCH JOURNAL
VOLUME 100 | SUPPLEMENT 1 | MARCH 2020

ABSTRACTS

GASTROINTESTINAL PATHOLOGY (612-832)

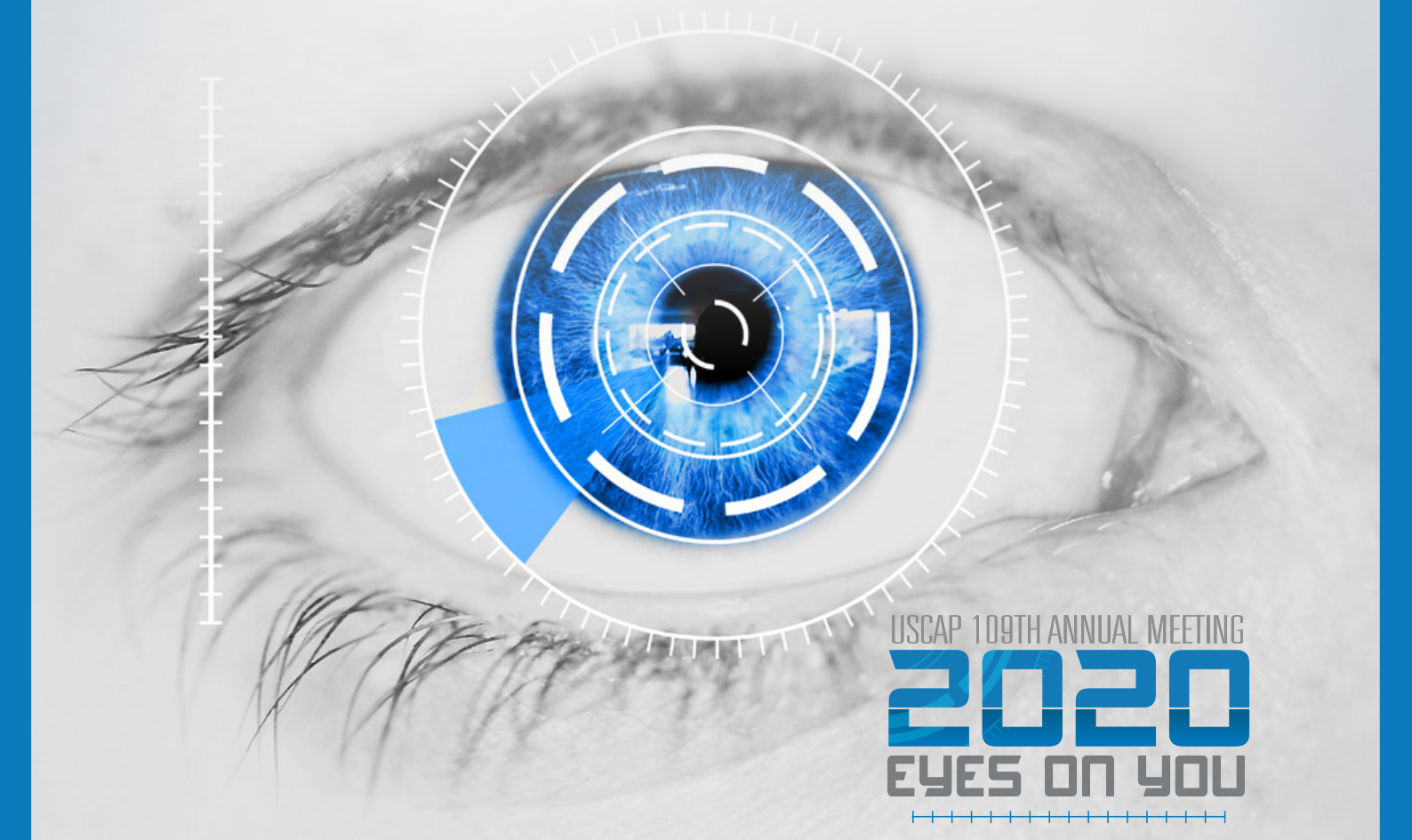

FEBRUARY 29-MARCH 5, 2020

LOS ANGELES CONVENTION CENTER
LOS ANGELES, CALIFORNIA

Published by
SPRINGER NATURE
www.ModernPathology.org

USCAP Creating a Better Pathologist
AN OFFICIAL JOURNAL OF THE UNITED STATES AND CANADIAN ACADEMY OF PATHOLOGY

EDUCATION COMMITTEE

Jason L. Hornick, Chair

Rhonda K. Yantiss, Chair, Abstract Review Board and Assignment Committee

Laura W. Lamps, Chair, CME Subcommittee

Steven D. Billings, Interactive Microscopy Subcommittee

Raja R. Seethala, Short Course Coordinator

Ilan Weinreb, Subcommittee for Unique Live Course Offerings

David B. Kaminsky (Ex-Officio)

Zubair Baloch
Daniel Brat
Ashley M. Cimino-Mathews
James R. Cook
Sarah Dry
William C. Faquin
Yuri Fedoriw
Karen Fritchie
Lakshmi Priya Kunju
Anna Marie Mulligan
Rish K. Pai
David Papke, Pathologist-in-Training
Vinita Parkash
Carlos Parra-Herran
Anil V. Parwani
Rajiv M. Patel
Deepa T. Patil
Lynette M. Sholl
Nicholas A. Zoumberos, Pathologist-in-Training

ABSTRACT REVIEW BOARD

Benjamin Adam
Narasimhan Agaram
Rouba Ali-Fehmi
Ghassan Allo
Isabel Alvarado-Cabrero
Catalina Amador
Roberto Barrios
Rohit Bhargava
Jennifer Boland
Alain Borczuk
Elena Brachtel
Marilyn Bui
Eric Burks
Shelley Caltharp
Barbara Centeno
Joanna Chan
Jennifer Chapman
Hui Chen
Beth Clark
James Conner
Alejandro Contreras
Claudiu Cotta
Jennifer Cotter
Sonika Dahiya
Farbod Darvishian
Jessica Davis
Heather Dawson
Elizabeth Demicco
Katie Dennis
Anand Dighe
Suzanne Dintzis
Michelle Downes
Andrew Evans
Michael Feely
Dennis Firchau
Gregory Fishbein
Andrew Folpe
Larissa Furtado
Billie Fyfe-Kirschner
Giovanna Giannico
Anthony Gill
Paula Ginter
Tamara Giorgadze
Purva Gopal
Anuradha Gopalan
Abha Goyal
Rondell Graham
Alejandro Gru
Nilesh Gupta
Mamta Gupta
Gillian Hale
Suntrea Hammer
Malini Harigopal
Douglas Hartman
John Higgins
Mai Hoang
Mojgan Hosseini
Aaron Huber
Peter Illei
Doina Ivan
Wei Jiang
Vickie Jo
Kirk Jones
Neerja Kambham
Chiah Sui Kao
Dipti Karamchandani
Darcy Kerr
Ashraf Khan
Francesca Khani
Rebecca King
Veronica Klepeis
Gregor Krings
Asangi Kumarapeli
Alvaro Laga
Steven Lagana
Keith Lai
Michael Lee
Cheng-Han Lee
Madelyn Lew
Zaibo Li
Faqian Li
Ying Li
Haiyan Liu
Xiuli Liu
Yen-Chun Liu
Lesley Lomo
Tamara Lotan
Anthony Magliocco
Kruti Maniar
Emily Mason
David McClintock
Bruce McManus
David Meredith
Anne Mills
Neda Moatamed
Sara Monaco
Atis Muehlenbachs
Bita Naini
Dianna Ng
Tony Ng
Michiya Nishino
Scott Owens
Jacqueline Parai
Yan Peng
Manju Prasad
Peter Pytel
Stephen Raab
Joseph Rabban
Stanley Radio
Emad Rakha
Preetha Ramalingam
Priya Rao
Robyn Reed
Michelle Reid
Natasha Rekhtman
Jordan Reynolds
Michael Rivera
Andres Roma
Avi Rosenberg
Esther Rossi
Peter Sadow
Steven Salvatore
Souzan Sanati
Anjali Saqi
Jeanne Shen
Jiaqi Shi
Gabriel Sica
Alexa Siddon
Deepika Sirohi
Kalliopi Siziopikou
Sara Szabo
Julie Teruya-Feldstein
Khin Thway
Rashmi Tondon
Jose Torrealba
Andrew Turk
Evi Vakiani
Christopher VandenBussche
Paul VanderLaan
Olga Weinberg
Sara Wobker
Shaofeng Yan
Anjana Yeldandi
Akihiko Yoshida
Gloria Young
Minghao Zhong
Yaolin Zhou
Hongfa Zhu
Debra Zynger

To cite abstracts in this publication, please use the following format: **Author A, Author B, Author C, et al. Abstract title (abs#). In "File Title."** ***Laboratory Investigation*** **2020; 100 (suppl 1): page#**

612 Tumor Stroma Ratio and Tumour Budding as Independent Predictors for Survival in Colorectal Cancer Patients

Lamia AboElnasr[1], Hala El-Rebey[1], Asmaa El Dein Mohamed[1], Asmaa Abdou[1]
[1]Pathology Department, Faculty of Medicine, Menoufia University, Shebin Elkom, Menoufia, Egypt

Disclosures: Lamia AboElnasr: None; Asmaa El Dein Mohamed: None; Asmaa Abdou: None

Background: Although TNM staging system remains the cornerstone of risk assessment in patients with colorectal cancer (CRC), clinical behaviour is diverse within the same stage. More additional prognostic markers are needed for better stratification.

Tumor stroma ratio (TSR) is an estimate of the proportion of epithelial and stromal cells which play a central role in the invasion-metastasis cascade. Tumour budding (TB) is defined as the presence of single tumor cells or small clusters of up to 5 cells in the tumor stroma. TB is considered to be associated with epithelial mesenchymal transition at the invasive front and thus might represent the cell-biological correlate of the tumour-stroma interphase.

The potential relationship between TB and TSR, however, is sparsely mentioned in the literature. The aim of this study was to assess TB and TSR in CRC surgical specimens and test their correlation with each other and with survival data.

Design: A cohort of 93 randomly selected CRC surgical specimens was retrospectively reviewed and evaluated using hematoxylin and eosin sections. One tumour block representing the deepest invasive front was selected from each case. The extent of TB per high power field (HPF) was assessed at the invasive tumor margin, classified as high-grade budding (≥ 10 buds) and low-grade budding (< 10 buds). TSR was assessed in one field with tumour cells present at all borders (north-east-south-west), scored as low TSR (> 50% stroma/ HPF) and high TSR (≤ 50% stroma/ HPF).

Results: Low TSR score was associated with worse recurrence-free survival (RFS) ($p < .0001$) and worse overall survival (OS) ($p < .0001$). Data analysis revealed also a significant statistical difference between both patterns of TB scoring regarding survival data. High TB score was associated with worse RFS ($p < .0001$) and worse OS ($p < .0001$).Furthermore, the mean number of buds per HPF was inversely correlated to TSR (increasing number of buds was associated with a lower TSR) ($P<0.01$).

Figure 1 - 612

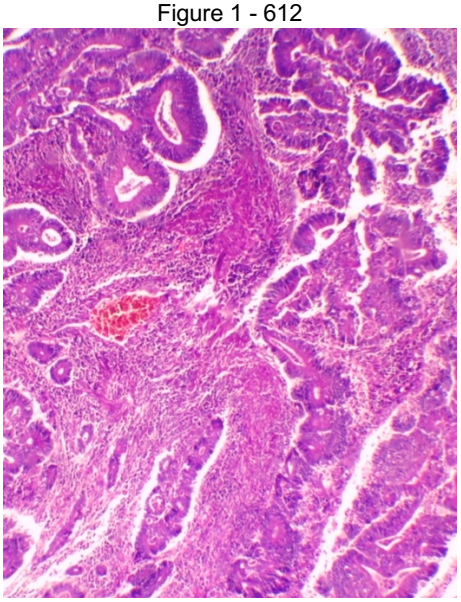

Figure 2 - 612

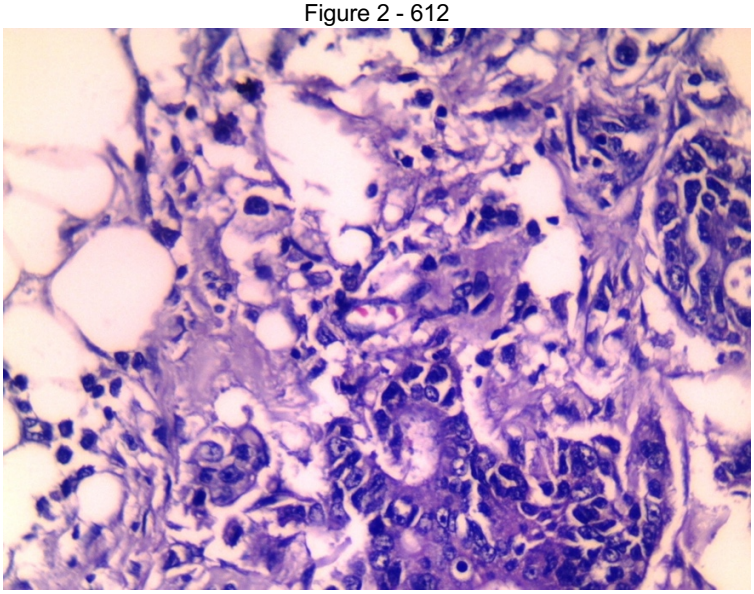

Conclusions: Both TB and TSR scoring are independent prognostic pathological factors in CRC that could be used to stratify patients into risk groups. Those parameters can be easily assessed in routine hematoxylin and eosin stained sections.

613 Polypoid Undifferentiated Rhabdoid Carcinoma in the Intestine: A Distinctive Presentation of Metastatic -Mostly Occult -Undifferentiated Non-small Cell Lung Carcinoma Illustrated in a Series of 12 Cases

Abbas Agaimy[1], Ondrej Daum[2], Michal Michal[2], Arndt Hartmann[3], Gregory Lauwers[4]
[1]Universitätsklinikum Erlangen, Germany, Erlangen, Germany, [2]Biopticka laborator s.r.o., Plzen, Czech Republic, [3]Institut fur Pathologie, Erlangen, Germany, [4]H. Lee Moffitt Cancer Center & Research Institute, University of South Florida, Tampa, FL

Disclosures: Abbas Agaimy: None; Ondrej Daum: None; Michal Michal: None; Arndt Hartmann: None; Gregory Lauwers: None

Background: Primary small bowel carcinomas are uncommon. Among these, undifferentiated and rhabdoid variants are exceedingly rare with frequent SWI/SNF complex inactivation. Since these tumors usually lack epithelial component, are occasionally multifocal and have a nonspecific immunophenotype, distinction of “primary vs. metastatic disease” is challenging.

Design: We herein present 12 cases of distinctive and under-recognized pattern of metastatic mostly occult (synchronous) non-small cell lung cancer (NSCLC) presenting as undifferentiated rhabdoid carcinomas in the bowel. Immunohistochemical analyses were performed. The metastases were tested for common mutations using the TST15 gene panel.

Results: The cohort was composed of 6 females and 6 males aged 52 to 80 yrs (median, 60) who presented with unifocal (n=7) or multifocal (n=5) tumors. Bowel metastases and primary NSCLCs were synchronous in 8 cases and metachronous in four. Synchronous metastasis was diagnosed 1 and 4 (x2) months after NSCLC (missing details in 1). Most patients presented with acute abdomen, obstruction, or bleeding, necessitating emergency surgery. The primary tumor was biopsy-proven in 8 cases and was diagnosed by imaging in four. Primary tumor histology was obtained via endobronchial or core biopsy in 8 cases. It was concordant with metastasis (both undifferentiated) in 3 and discordant (4 adenocarcinomas, 1 combined with undifferentiated carcinoma and 1 squamous cell carcinoma) in 5 cases. Metastases showed diffuse sheets of large poorly cohesive cells with variable rhabdoid morphology and prominent mainly neutrophilic mixed background inflammation. No adenoma component or dysplasia was noted. Immunohistochemistry (IHC) showed at least focal pankeratin and/or EMA expression, but not TTF1. SWI/SNF IHC showed loss of SMARCA2 (n=6), SMARCA4 (n=1), or both (n=1). Molecular testing of the metastasis revealed BRAF (4/8; 50%) or KRAS (2/8; 25%) mutations; 2 were wildtype. None had EGFR mutations.

Figure 1 - 613

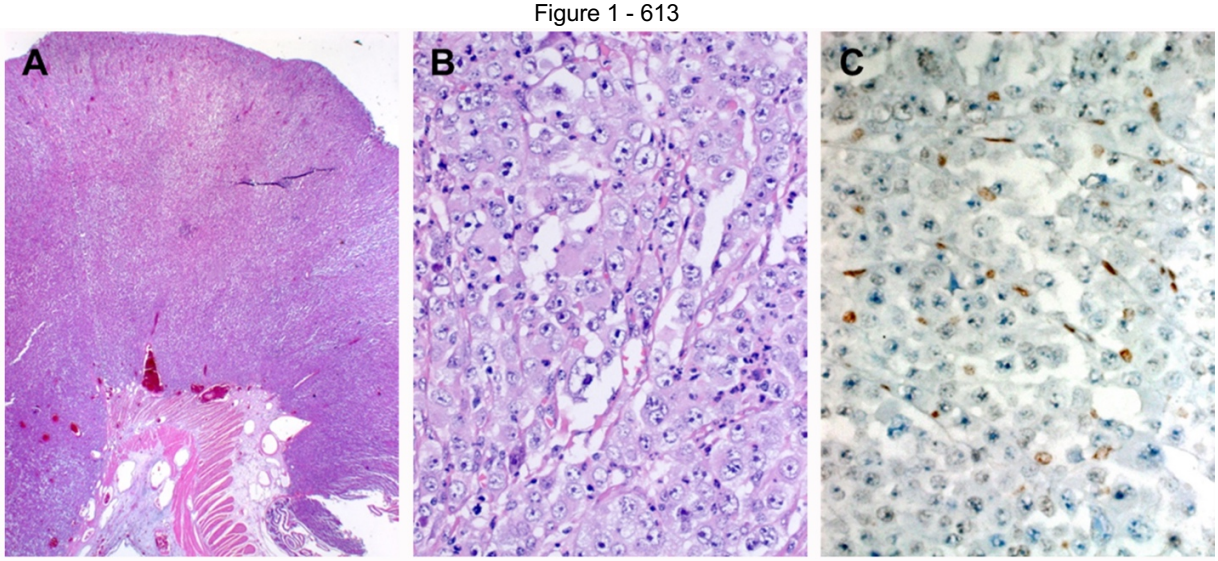

A: Overview of polyploid jejunal metastasis from undifferentiated NSCLC.
B: At high power, large anaplastic cells with vesicular nuclei and central macronucleoli, note neutrophilic infiltration in the background.
C: Loss of SWI/SNF components (mainly SMARCA2 and SMARCA4) are frequent.

Conclusions: This series highlights a distinctive pattern of metastatic, mainly occult, undifferentiated NSCLC closely mimicking primary intestinal rhabdoid carcinoma with predilection for small intestine (mainly jejunum). Recognition of this presentation is critical for appropriate therapy and prognostication. Discordant histology between primary and metastatic tumor points to the rare phenomenon of dedifferentiation limited to metastasis; alternatively, the undifferentiated component might have been missed in the lung biopsy.

614 Histologic Subclassification of Esophageal Adenocarcinoma has Prognostic Significance

Ashna Aggarwal[1], Iván González[2], Hsiang-Chih (Sean) Lu[3], Horacio Maluf[2], Deyali Chatterjee[4]
[1]Barnes Jewish Hospital/Washington University, St. Louis, MO, [2]Washington University School of Medicine, St. Louis, MO, [3]Washington University School of Medicine in St. Louis, St. Louis, MO, [4]Washington University in St. Louis, St. Louis, MO

Disclosures: Ashna Aggarwal: None; Iván González: None; Hsiang-Chih (Sean) Lu: None; Horacio Maluf: None; Deyali Chatterjee: None

Background: The WHO classification of esophageal adenocarcinoma (EA) has no recognized subtypes. However, morphologic variants can be identified in large resection specimens, that often appear distinctive even after neoadjuvant treatment. We undertook this study to systematically analyze the clinicopathologic significance of these histologic patterns.

Design: With IRB approval, detailed histologic review of all archival slides of esophagectomy specimens for EA was performed. Cases with at least 10% viable tumor in the tumor bed, were included. Based on morphology, EA was classified into three specific patterns. Tumors with glandular formation was recognized as tubular, with a subset of them displaying a diffuse infiltrative pattern of invasion, labeled “tubular-infiltrative” (T-I; fig. 1A). The other distinct pattern of gland-forming tumor was arranged predominantly into closely spaced, rounded configuration, labeled “tubular-lobulated” (T-L; fig. 1B). Cribriforming, micropapillary, and papillary formations within the tubular structures were allowed in this group. The third distinct pattern was tumor cells predominantly composed of non-cohesive signet ring-like cells, disposed in extracellular pools of mucin, labeled mucinous-signet-ring cell (M-S; fig 1C).

Results: A total of 69 resected tumors (proximal esophagus: 1, distal esophagus: 11, gastroesophageal junction: 57 cases) from 56 males and 13 females were included, with mean age of 63.3 years (range 35.2 -89.2 years). 65 cases (94%) received neoadjuvant therapy, with a mean percentage of residual tumor in the examined tissue of 56% (range 10-100%). 38 cases were classified into the T-I group, 25 cases into the T-L group, and 6 cases belonged to M-S group. Demographic information and clinicopathologic correlation is outlined in Table 1. Mean follow-up period was 821 days. Log-rank (Mantel-Cox) test shows significant differences in terms of both recurrence-free survival (RFS; p=0.001) and overall survival (OS; p=0.018) between the tumor groups (Fig 2).

Histologic parameter	**Tubular-infiltrative (T-I)**	**Tubular-lobulated (T-L)**	**Mucinous signet-ring (M-S)**	**p-value**
Tumor Budding				**0.0037**
Intermediate/high (39, 57%)	28	10	1	
No/low (30, 43%)	10	15	5	
Tumor Infiltrative Lymphocytes (>5/HPF)				**<0.001**
Yes (33, 48%)	9	24	0	
No (36, 52%)	29	1	6	
Desmoplasia with myxoid stroma (intra/peritumoral)				**0.0279**
Yes (17, 25%)	14	3	0	
No (52, 75%)	24	22	6	
(y)pT stage				**0.02**
T1	9	6	1	
T2	5	8	2	
T3	24	11	2	
T4	0	0	1	
(y)pN stage				0.72
N0	18	14	3	
N1	9	4	0	
N2	7	3	2	
N3	4	4	1	
Peritumoral lymphocytic response				0.08
Brisk (21, 30%)	10	11	0	
Not significant (48, 70%)	28	14	6	

Figure 1 - 614

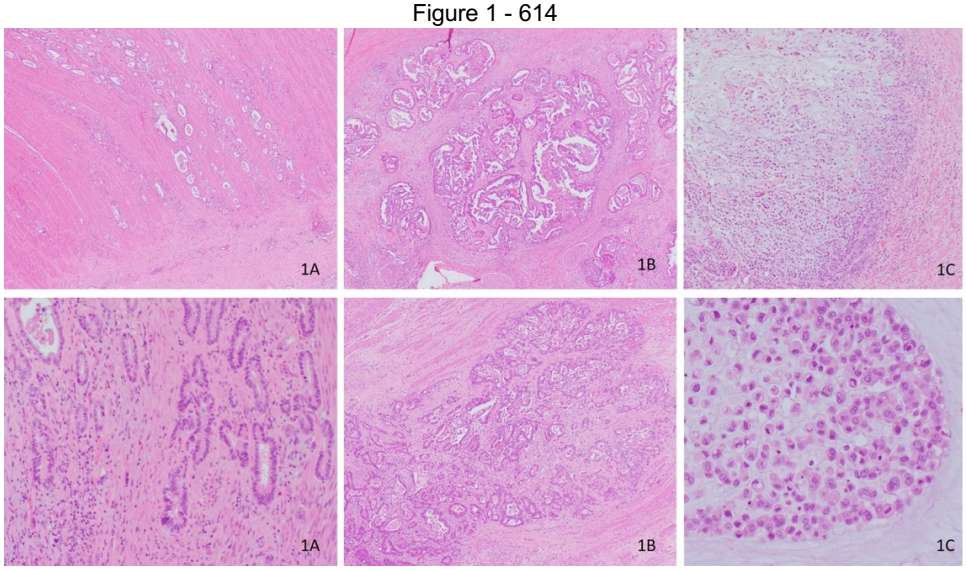

Figure 2 - 614

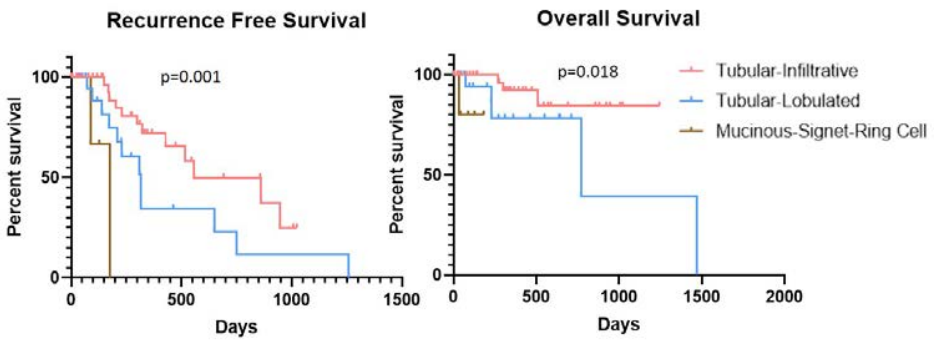

Conclusions: The significant differences among these histologic groups in terms of RFS and OS, as well as with prognostic histologic features such as tumor budding, tumor infiltrating lymphocytes, desmoplastic stroma, and tumor stage, suggest that it is clinically relevant to subclassify EA.

615 Increased Tumor Necrosis is an Independent Predictor of Poor Prognosis in Patients with Colorectal Carcinoma and Correlates with Stage and KRAS Gene Mutation

Mouyed Alawad[1], Donghai Wang[1], Rachelle Mendoza[1], Absia Jabbar[1], Ghulam Ilyas[1], M. Haseeb[1], Raavi Gupta[1]
[1]SUNY Downstate Medical Center, Brooklyn, NY

Disclosures: Mouyed Alawad: None; Donghai Wang: None; Rachelle Mendoza: None; Absia Jabbar: None; Ghulam Ilyas: None; M. Haseeb: None; Raavi Gupta: None

Background: Tumor necrosis is a well-known indicator of poor prognosis in various neoplasms. However, its role in colorectal carcinomas (CRC) has not been well understood. Our study aims to quantify and correlate the amount of tumor necrosis in CRC with clinicopathologic data.

Design: We identified 288 CRC resection specimens and recorded their clinicopathologic data. At least 3 representative tumor sections were reviewed for each case. Clinical stage was coded as early (I and II) or late (III and IV). Tumor necrosis was quantified by two pathologists and scored absent (score 0), focal (score 1, ≤10%), moderate (score 2, 10%-30%), and high (score 3; >30%). Correlations between different parameters were determined by Pearson's Chi-Squared test; $p<0.05$ was considered significant. Disease-free survival (DFS) and overall survival (OS) were calculated by Kaplan-Meier method and analyzed by log-rank test and Cox regression analysis (SPSS, v.22.0).

Results: Majority of the patients were African-American (78.8%) and the mean age was 63.4 years. Tumor necrosis showed significant correlation with the pathologic stage (pT,N,M) (p<0.0001), clinical stage (p<0.0001), KRAS mutation (p<0.0001), and lymphovascular invasion (LVI) (p=0.013) (*Table*). No correlation was observed between tumor necrosis and age, race, sex and mismatch repair gene expression. Higher tumor necrosis (score 3) was associated with shorter DFS (p=<0.0001 for early and p=0.007 for late stage) and OS (p=0.002 adjusted for stage). Score 3 tumor necrosis remained a predictor for shorter DFS (p=0.001) and OS (p=0.045) after controlling for age, tumor invasion (pT), lymph node status (pN), metastasis (pM) and clinical stage (*Figure*). We observed a trend for DFS and OS with increasing tumor necrosis scores in both early and late clinical stages.

Characteristics^		Tumor Necrosis Score				
		0 (Absent)	1 (Focal, ≤10%)	2 (Moderate, 10-30%)	3 (High, > 30%)	P value
		N (%)	N (%)	N (%)	N (%)	
Tumor Invasion (pT)	Tis	0 (0.0)	3 (100)	0 (0.0)	0 (0.0)	0.0001
	1	8 (29.6)	16 (59.3)	3 (11.1)	0 (0.0)	
	2	7 (12.5)	34 (60.7)	13 (23.2)	2 (3.6)	
	3, 3a	6 (3.7)	36 (22.0)	77 (47.0)	45 (27.4)	
	4, 4a, 4b	1 (2.7)	6 (16.2)	19 (51.4)	11 (29.7)	
DFS		569*	870*	899*	473*	log rank ‡
OS		643*	984*	991*	669*	log rank ‡
Lymph Node Status (pN)	0	18 (11.3)	80 (50.3)	42 (26.4)	19 (11.9)	0.0001
	1, 1a	0 (0.0)	5 (10.0)	34 (68.0)	11 (22.0)	
	1b	1 (3.8)	4 (15.4)	10 (38.5)	11 (42.3)	
	1c	1 (7.1)	2 (14.3)	9 (64.3)	2 (14.3)	
	2, 2a	0 (0.0)	1 (4.3)	12 (52.2)	10 (43.5)	
	2b	1 (8.3)	2 (16.7)	5 (41.7)	4 (33.3)	
Metastasis (pM)	x	22 (9.1)	90 (37.3)	94 (39.0)	35 (14.5)	0.0001
	1	0 (0.0)	4 (8.9)	18 (40.0)	23 (51.1)	
Clinical Stage	0	0 (0.0)	1 (100)	0 (0.0)	0 (0.0)	0.0001
	I	13 (18.8)	49 (71.0)	6 (8.7)	1 (1.4)	
	II	5 (6.0)	30 (36.1)	34 (41.0)	14 (16.9)	
	III	3 (3.6)	9 (10.7)	54 (64.3)	18 (21.4)	
	IV	0 (0.0)	5 (10.4)	18 (37.5)	25 (52.1)	
KRAS	Wild-type	1 (3.0)	6 (18.2)	18 (54.5)	8 (24.2)	0.0001
	Mutant	1 (2.9)	3 (8.6)	2 (5.7)	29 (82.9)	
LVI	Absent	18 (9.0)	75 (37.7)	72 (36.2)	34 (17.1)	0.013
	Present	2 (3.2)	13 (21.0)	29 (46.8)	18 (29.0)	
*Mean						
Tis: Carcinoma in situ; DFS: Disease-free survival ; OS: Overall survival; LVI: Lymphovascular Invasion						
^ Only values of statistically significant factors are listed.						
‡ log rank p value						

Figure 1 - 615

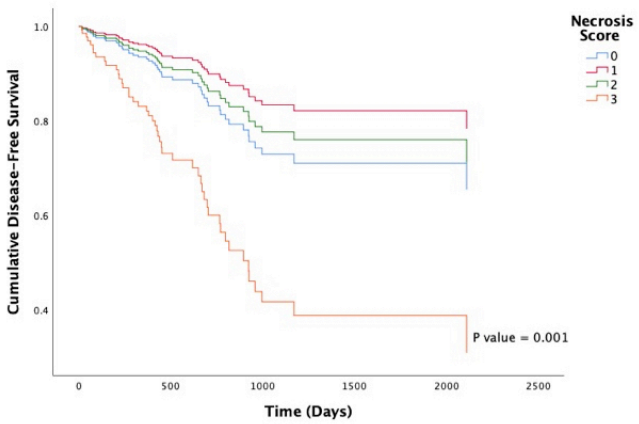

Conclusions: Higher tumor necrosis is an independent predictor of poor survival in CRC. It correlates with pathologic and clinical stages, as well as KRAS mutation and LVI. It could be a useful prognostic feature to be included in pathology reports.

616 Concurrent Gene Mutational Profile and Clinicopathologic Characteristic of SMAD4 Mutated Colorectal Adenocarcinomas

Andrew Alexander[1], Ryan Jones[2], Juehua Gao[3], Guang-Yu Yang[2]
[1]Northwestern University Feinberg School of Medicine, Chicago, IL, [2]Northwestern University, Chicago, IL, [3]Northwestern Memorial Hospital, Chicago, IL

Disclosures: Andrew Alexander: None; Ryan Jones: None; Juehua Gao: None; Guang-Yu Yang: None

Background: Sporadic *SMAD4* mutations are present in 2.1-20% of colorectal cancers and often occur in association with mutations involving *KRAS*, *NRAS* and *BRAF*. To date there is limited data regarding the potential impact concurrent mutation have in defining the clinicopathologic characteristics of *SMAD4* mutated colorectal adenocarcinomas. In this study, we evaluated a set of *SMAD4* mutated colorectal adenocarcinomas to determine the presence of concurrent mutations including *KRAS*, *NRAS*, *BRAF*, and *TP53* mutations. We then assessed the pathologic and clinical characteristics of these tumors.

Design: We searched the molecular-surgical pathology database of colorectal cancers (CRC) in our institution from 2015-2019. Out of 635 colon cancer specimens with comprehensive next generation sequencing (NGS) analysis, we identified 67 cases of *SMAD4* mutated colorectal adenocarcinomas. NGS analysis for the targeted 22 cancer-related gene panels (including *KRAS, EGFR, BRAF, PIK3CA, AKT1, ERBB2, PTEN, NRAS, STK11, MAP2K1, ALK, DDR2, CTNNB1, MET, TP53, SMAD4, FBX7, FGFR3, NOTCH1, ERBB4, FGFR1* and *FGFR2 genes)* was performed for all 635 cases of CRC. Clinical and pathologic features associated with this set of tumors was also analyzed.

Results: Based on NGS analysis, all of the 67 SMAD4 mutations were missense mutations with a wide spectrum of mutations, but clustered at codon 1081 (29.8%, 20/67), at codon 1067 (10.4%, 7/67), and at codon 1051 (6.0%, 4/67). The most common concurrent gene mutations were observed in *KRAS* (52.2%, 35/67), *TP53* (50.7%, 34/67), *PIKC3A* (16.4%, 11/67), *BRAF* (13.4%, 9/67) and *FBX7* (13.4%, 9/67). In 56.7% (38/67) of cases two or more additional mutations were observed and only rare cases (6%, 4/67) showed an isolated *SMAD4* mutation. The most common pair of additional genes mutated were *KRAS* and *TP53* (14/67) followed by *KRAS* and *PIKC3A* (8/67). 86.6% (58/67) of cases were MSI stable tumors and only 13.4% (9/67) of cases showed microsatellite instability. In all five cases with loss of MLH1 and PMS2 expression, a *BRAF* V600E mutation was identified. The majority of cases were located in right colon (21/67), left colon (25/67) and rectum (16/67) with rare cases arising in the transverse colon (3/67), appendix (1/67) and urachus (1/67).

Conclusions: A wide spectrum of missense mutation appears to be the dominant genetic alteration in *SMAD4* mutant colorectal cancers. Such missense mutations, together with either KRAS or p53 mutation, is a critical pathogenic event leading to development of colorectal cancer.

617 Impact of Mentorship on Interobserver Agreement in Assessment of Inflammatory Bowel Disease-Associated Dysplasia

Lindsay Alpert[1], Namrata Setia[1], Huaibin Mabel Ko[2], Stephen Lagana[3], Meredith Pittman[4], Melanie Johncilla[5], Michael Drage[6], Lei Zhao[7], Marcela Salomao[8], Xiaoyan Liao[6], Won-Tak Choi[9], Sarah Jenkins[10], John Hart[1], Noam Harpaz[11], Lysandra Voltaggio[12], Gregory Lauwers[13], Robert Odze[14], Helen Remotti[15], Thomas Smyrk[10], Rondell Graham[10]
[1]The University of Chicago, Chicago, IL, [2]Icahn School of Medicine at Mount Sinai, New York, NY, [3]New York-Presbyterian/Columbia University Medical Center, New York, NY, [4]New York-Presbyterian/Weill Cornell Medical Center, New York, NY, [5]New York-Presbyterian Hospital/Weill Cornell Medical Center, Petit Valley, Trinidad and Tobago, [6]University of Rochester Medical Center, Rochester, NY, [7]Brigham and Women's Hospital, Harvard Medical School, Boston, MA, [8]Mayo Clinic, Scottsdale, AZ, [9]University of California San Francisco, San Francisco, CA, [10]Mayo Clinic, Rochester, MN, [11]Mount Sinai Medical Center, New York, NY, [12]Baltimore, MD, [13]H. Lee Moffitt Cancer Center & Research Institute, University of South Florida, Tampa, FL, [14]Boston, MA, [15]Columbia University Medical Center, New York, NY

Disclosures: Lindsay Alpert: None; Namrata Setia: None; Huaibin Mabel Ko: None; Huaibin Mabel Ko: None; Stephen Lagana: None; Meredith Pittman: None; Melanie Johncilla: None; Michael Drage: None; Lei Zhao: None; Marcela Salomao: None; Xiaoyan Liao: None; Won-Tak Choi: None; Sarah Jenkins: None; John Hart: None; Noam Harpaz: None; Lysandra Voltaggio: None; Gregory Lauwers: None; Robert Odze: None; Helen Remotti: None; Thomas Smyrk: None; Rondell Graham: None

Background: The diagnosis and grading of inflammatory bowel disease (IBD)-associated dysplasia can be challenging, and past studies have demonstrated considerable interobserver variability in such diagnoses. During GI pathology fellowship, experienced GI pathologists teach trainees how to navigate this difficult area, but the impact of such mentorship on interobserver agreement is unknown.

Design: Twelve early-career GI pathologists from 8 institutions contributed 163 H&E slides of colon biopsies from IBD patients. Slides were de-identified, scanned using a Philips digital scanner, and uploaded to an online slide-viewing site (VMicro). Early-career GI pathologists and their 7 fellowship mentors rendered a diagnosis of negative for dysplasia, indefinite for dysplasia, low grade dysplasia, or high grade dysplasia and provided a confidence level (not confident, somewhat confident, or confident) for each case. Cohen's and Fleiss' kappa statistics were used to assess interobserver agreement.

Results: Interobserver agreement between mentor/mentee pairs ranged from κ=0.31-0.49, with an average agreement of 59.8% (SD 5.6, 54.6-65.2%) (Figure). Five mentors had 2 mentees each, and interobserver agreement between mentees of the same mentor ranged from κ=0.34-0.55, with an average agreement of 62.2% (SD 6.2, 56.4-69.9%). Agreement between mentors from different institutions compared pairwise ranged from κ=0.27-0.50, with an average agreement of 56.3% (SD 5.6, 45.4-66.3%) and a combined kappa coefficient of 0.39 (95% CI: 0.34-0.43). The combined kappa coefficient for all mentees was 0.44 (95% CI: 0.39-0.48). Overall, mentors used the diagnosis of indefinite for dysplasia slightly less often than mentees (13.6% vs. 15.8%) and were confident in a greater percentage of cases (75.4% vs. 63.7%), but these differences did not reach statistical significance (Table).

Overall comparison of ratings among mentors and mentees

N = total ratings

	Mentee ratings (N=1956)	Mentor ratings (N=1141)	P-value
Diagnosis			
Negative for dysplasia	830 (42.4%)	435 (38.2%)	0.20
Low grade dysplasia	577 (29.5%)	353 (31.0%)	0.69
High grade dysplasia	239 (12.2%)	196 (17.2%)	0.13
Indefinite for dysplasia	310 (15.8%)	155 (13.6%)	0.50
Confidence			
Not confident	143 (7.6%)	61 (5.4%)	0.64
Somewhat confident	539 (28.7%)	218 (19.2%)	0.19
Confident	1197 (63.7%)	856 (75.4%)	0.20

Figure 1 - 617

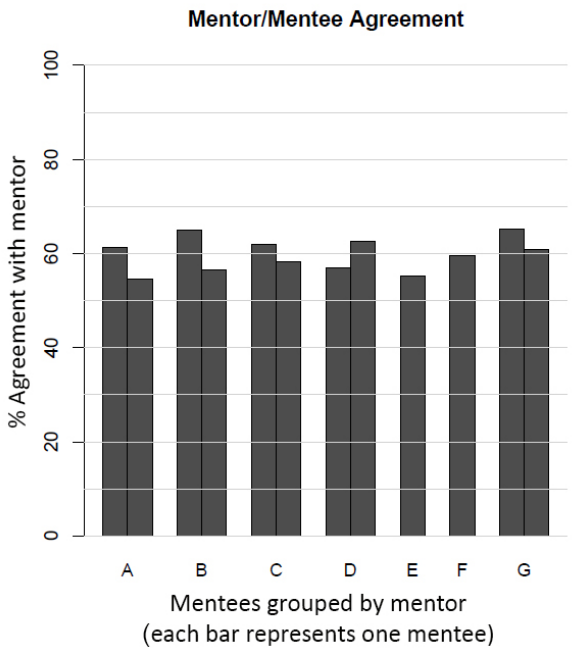

Conclusions: Mentorship during GI pathology fellowship does not appear to be the main factor contributing to interobserver variability in IBD dysplasia diagnoses, as agreement between mentor/mentee pairs was not significantly better than agreement between mentees overall. However, increased experience also does not appear to improve interobserver agreement, as GI pathology mentors did not have higher agreement levels than mentor/mentee pairs or mentees overall.

618 Interobserver Agreement and Confidence in the Diagnosis of Inflammatory Bowel Disease-Associated Dysplasia Among Subspecialist GI Pathologists

Lindsay Alpert[1], Namrata Setia[1], Huaibin Mabel Ko[2], Stephen Lagana[3], Meredith Pittman[4], Melanie Johncilla[5], Michael Drage[6], Lei Zhao[7], Marcela Salomao[8], Xiaoyan Liao[6], Won-Tak Choi[9], Sarah Jenkins[10], John Hart[1], Noam Harpaz[11], Lysandra Voltaggio[12], Gregory Lauwers[13], Robert Odze[14], Helen Remotti[15], Thomas Smyrk[10], Rondell Graham[10]

[1]The University of Chicago, Chicago, IL, [2]Icahn School of Medicine at Mount Sinai, New York, NY, [3]New York-Presbyterian/Columbia University Medical Center, New York, NY, [4]New York-Presbyterian/Weill Cornell Medical Center, New York, NY, [5]New York-Presbyterian Hospital/Weill Cornell Medical Center, Petit Valley, Trinidad and Tobago, [6]University of Rochester Medical Center, Rochester, NY, [7]Brigham and Women's Hospital, Harvard Medical School, Boston, MA, [8]Mayo Clinic, Scottsdale, AZ, [9]University of California San Francisco, San Francisco, CA, [10]Mayo Clinic, Rochester, MN, [11]Mount Sinai Medical Center, New York, NY, [12]Baltimore, MD, [13]H. Lee Moffitt Cancer Center & Research Institute, University of South Florida, Tampa, FL, [14]Boston, MA, [15]Columbia University Medical Center, New York, NY

Disclosures: Lindsay Alpert: None; Namrata Setia: None; Huaibin Mabel Ko: None; Stephen Lagana: None; Meredith Pittman: None; Melanie Johncilla: None; Michael Drage: None; Lei Zhao: None; Marcela Salomao: None; Xiaoyan Liao: None; Won-Tak Choi: None; Sarah Jenkins: None; John Hart: None; Noam Harpaz: None; Lysandra Voltaggio: None; Gregory Lauwers: None; Robert Odze: None; Helen Remotti: None; Thomas Smyrk: None; Rondell Graham: None

Background: The diagnosis and grading of inflammatory bowel disease (IBD)-associated dysplasia can be challenging, even for experienced gastrointestinal pathologists. Past studies have demonstrated considerable interobserver variability in such diagnoses, but factors influencing this variability have not been closely examined.

Design: Subspecialist GI pathologists contributed 163 examples of colon biopsies from IBD patients with diagnoses of negative for dysplasia (NEG), indefinite for dysplasia (IND), low grade dysplasia (LGD), and high grade dysplasia (HGD). H&E slides were de-identified, scanned using a Philips digital scanner, and uploaded to an online slide-viewing site (VMicro). Nineteen subspecialist GI pathologists reviewed the scanned slides, rendered a diagnosis of NEG, IND, LGD, or HGD, and provided a confidence level (not confident, somewhat confident, or confident) for each case. Cohen's and Fleiss' kappa statistics were used to assess interobserver agreement.

Results: The overall kappa coefficient was 0.42 (95% CI: 0.38, 0.46). The consensus diagnosis (diagnosis most commonly chosen by reviewers for each case) was NEG in 75 cases, LGD in 49 cases, HGD in 26 cases, and IND in 10 cases. In 3 cases, there was no consensus diagnosis due to equal numbers of the two most common diagnoses. In 28 cases, <50% of reviewers agreed with the consensus diagnosis. Common features seen in these low agreement cases included detachment of surface epithelium, poor orientation, a serrated appearance, mucosal atrophy, and decreased goblet cells. Reviewers were significantly less confident in cases for which they rendered a diagnosis of IND (Table). Higher confidence levels were seen in cases with greater agreement among reviewers, though cases diagnosed as HGD had lower agreement levels even when confidence was high (Figure). However, in most cases (14/18, 78%) with a consensus diagnosis of HGD and <66% agreement, LGD was the second most common diagnosis.

Confidence vs. Dysplasia
N = total ratings

	Negative (N=1265)	Low (N=930)	High (N=435)	Indefinite (N=465)
Confidence				
Not confident	44 (3.5%)	30 (3.2%)	18 (4.1%)	112 (27.9%)
Somewhat confident	230 (18.4%)	204 (22.0%)	99 (22.8%)	224 (55.7%)
Confident	975 (78.1%)	694 (74.8%)	318 (73.1%)	66 (16.4%)
Confidence				
N	1249	928	435	402
Mean (SD)	1.75 (0.51)	1.72 (0.52)	1.69 (0.55)	0.89 (0.66)
Median	2.00	2.00	2.00	1.00
Q1, Q3	2.00, 2.00	1.00, 2.00	1.00, 2.00	0.00, 1.00
Range	(0.00-2.00)	(0.00-2.00)	(0.00-2.00)	(0.00-2.00)

Figure 1 - 618

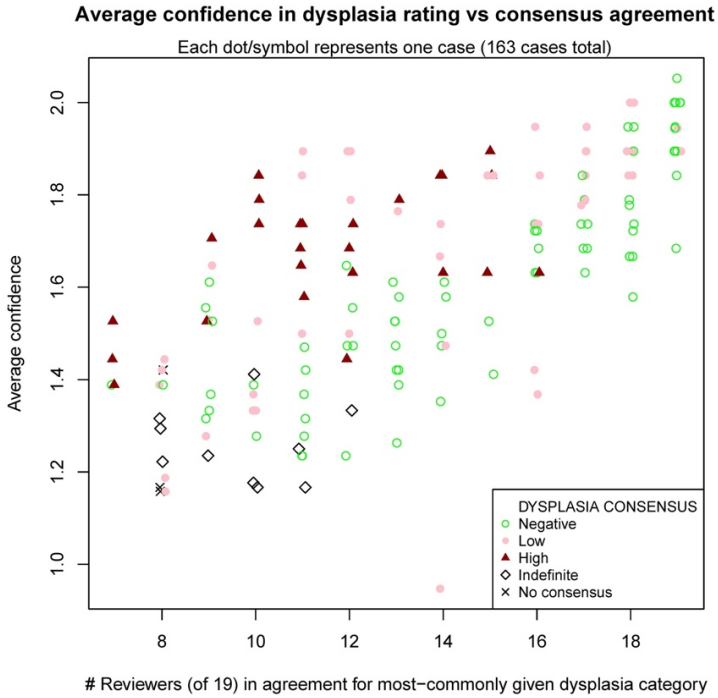

Conclusions: In this curated cohort of IBD dysplasia cases, interobserver agreement among subspecialist GI pathologists was fair to moderate. Both processing artifacts and the presence of certain histologic features (serration, atrophy, decreased goblet cells) appear to contribute to diagnostic variability. Increased confidence in a diagnosis generally correlates with higher interobserver agreement.

619 Traditional Serrated Adenomas in Familial Adenomatous Polyposis Syndrome

Zainab Alruwaii[1], Elizabeth Montgomery[2], Laura Wood[3], Tatianna Larman[4]
[1]The Regional Laboratory and Blood Bank, Dammam, Eastern Province, Saudi Arabia, [2]Johns Hopkins Medical Institutions, Baltimore, MD, [3]Johns Hopkins Hospital, Baltimore, MD, [4]Johns Hopkins University School of Medicine, Baltimore, MD

Disclosures: Zainab Alruwaii: None; Elizabeth Montgomery: None; Laura Wood: None; Tatianna Larman: None

Background: Small intestinal serrated polyps encompassing hyperplastic polyps, sessile serrated adenomas/polyps and traditional serrated adenomas (TSA) have been highlighted in a few studies. Of these serrated lesions, polyps with TSA-like morphology have shown aggressive behavior. However, these polyps have not been studied in patients with familial adenomatous polyposis (FAP). Herein, we describe the pathologic features of FAP-associated TSAs.

Design: A retrospective electronic search of pathology records for small bowel adenomas from patients with FAP syndrome (2000-2018) was done. 64 specimens (endoscopic=62; resection=3) from 45 patients were identified. H&E slides were reviewed to identify adenomas that showed areas with slit-like serration, cells with eosinophilic cytoplasm, and vesicular nuclei. Small bowel adenomas with the same features were also selected from 53 consecutive specimens (endoscopic=34; resection=19) from 51 non-syndromic patients. Lynch syndrome and inflammatory bowel disease patients were excluded. B-catenin immunostain was done on the available blocks. Clinical data were obtained from the patients' charts.

Results: Of the 177 polyps from 45 FAP patients and 60 polyps from 51 non-syndromic patients,18 adenomas from 9 FAP patients (20%) and 10 adenomas from the non-syndromic group (19.6 %) showed TSA features. TSAs from FAP group presented at a younger age than those in the non-syndromic group (median:43 vs. 66; P=.0048). All were discovered during screening/resection for FAP-associated adenomas in asymptomatic patient. In contrast, all non-syndromic patients were symptomatic (abdominal pain=4, biliary obstruction-related symptoms=4, anemia=1, and weight loss=1. Associated extra-intestinal malignancies were identified in 5 non-syndromic cases. FAP patients had smaller lesions compared to the those in the other group (median:0.6 cm vs. 2.5 cm; p=.00006). Histologically, adenomas exhibited similar morphologic features in both groups; however, advanced adenomas with high-grade dysplasia and adenocarcinoma were identified only in the non-syndromic lesions (n=6,60%). Abnormal B-catenin staining was seen in 1 adenoma from the FAP patients and in 3 advanced adenomas from the other group.

Conclusions: Adenomas with TSA-like morphology in the setting of FAP syndrome are characterized by smaller size, and lower rate of associated high-grade dysplasia or carcinoma than sporadic adenomas with the same morphology. This presumably reflects the intensified screening offered to FAP patients.

620 Implementation of the International Tumor Budding Consensus Conference (ITBCC) Directives on Colorectal Adenocarcinoma: Limited Value in Treated Rectal Cancer?

Mitchell Arbogast[1], Richard Davis[2], Shannon Mccall[1], Diana Cardona[1], Cynthia Guy[3], Lani Clinton[4]
[1]Duke University Medical Center, Durham, NC, [2]Duke University, Durham, NC, [3]Duke University, Chapel Hill, NC, [4]Duke University Medical Center, Mebane, NC

Disclosures: Mitchell Arbogast: None; Richard Davis: None; Shannon Mccall: None; Diana Cardona: None; Cynthia Guy: None; Lani Clinton: None

Background: Tumor budding (TB) is widely accepted as a prognosticator in colorectal cancer, but standardized scoring is essential for clinical care. The 2016 International Tumor Budding Consensus Conference (ITBCC) set forth a three-tiered system of TB: low, intermediate, or high (0-4, 5-9, or >/=10 buds, respectively). The College of American Pathologists recommends documenting TB in colorectal cancer synoptic reports per the ITBCC. However, many patients with rectal cancers undergo chemoradiation before resection. Thus, the question of true TB versus tumor regression/treatment effects as well as the prognostic importance of TB in treated rectal cancer arises. The aim of this study is to assess the recent ITBCC guidelines in colon and rectal cancers, individually.

Design: After obtaining IRB approval, 109 colorectal adenocarcinomas (CRC) were identified during a 32-month period (Feb 2016-Oct 2018). The H&E slides were reviewed to assess TB per the ITBCC. Histologic features such as tumor grade, stage, lymph node (LN) status, and lymphovascular invasion (LVI) were collected. Binomial logistic regression analysis with TB as the independent variable assessed impact on the aforementioned features.

Results: Among 109 total cases of CRC, 65 (60%) colonic and 44 (40%) rectal cancers were identified (Table 1). 9% of colonic cancers received neoadjuvant therapy compared with 81% of rectal cancers. 57% of colonic and 86% of rectal cancers had low TB. Intermediate TB was seen in 23% of colonic and 7% of rectal cancers; high TB was found in 20% of colonic and 7% of rectal cancers. In colonic cancer, 77% of high TB cases and 53% of intermediate TB cases had LVI compared with only 22% of low TB cases (OR=2.20, p<0.005; OR=1.42, p<0.05, respectively). Surprisingly, this finding was not replicated in rectal cancers. Furthermore, among colon cancers, 69% of cases with high TB had positive LNs compared with 49% of cases with low TB (OR=1.46, p<0.05). In rectal cancers, approximately 1/3 had positive LNs across all three TB categories, thus no statistical significance was identified.

Table 1. Lymphovascular invasion and lymph node status per tumor budding category.

	LVI		Positive LN	
	Colon (n=65)	Rectum (n=44)	Colon (n=65)	Rectum (n=44)
Low TB (0-4 buds)	8/37=22%	10/38=26%	18/37=49%	14/38=37%
Intermediate TB (5-9 buds)	8/15=53%*	0/3=0%	6/15=40%	1/3=33%
High TB (>/= 10 buds)	10/13=77%**	0/3=0%	9/13=69%*	1/3=33%

* p<0.05, **p<0.005

Conclusions: Using the 2016 ITBCC guidelines, we show that, only for colon cancers, high TB was a significant predictor of LVI and positive LN status when compared to low TB. In contrast, in rectal cancers, most of which had neoadjuvant therapy, TB was not a significant predictor. Prior studies show conflicting data regarding TB in treated rectal cancer; our findings suggest that TB in treated rectal cancers is of limited value.

621 Recurrence in Early-Stage Colon Cancer is Determined by Subclonal Copy Number Alterations

Ivan Archilla[1], Sara Lahoz[2], Elena Asensio[2], Eva Hernandez-Illan[2], Queralt Ferrer[2], Antoni Castells[3], Jordi Camps[4], Miriam Cuatrecasas Freixas[5]
[1]Hospital Clinic, University of Barcelona, Barcelona, Spain, [2]Hospital Clinic-IDIBAPS, University of Barcelona, Barcelona, Spain, [3]Hospital Clinic of Barcelona, Barcelona, Spain, [4]Hospital Clinic-IDIBAPS, Universitat de Barcelona, Barcelona, Spain, [5]Hospital Clinic, Universitat de Barcelona, Barcelona, Spain

Disclosures: Ivan Archilla: None; Sara Lahoz: None; Elena Asensio: None; Eva Hernandez-Illan: None; Queralt Ferrer: None; Antoni Castells: None; Jordi Camps: None; Miriam Cuatrecasas Freixas: None

Background: Stage II colon cancer (CC) holds a major therapeutic challenge since 10-15% of patients develop recurrence after surgical curative intent. Therefore, predicting tumor relapse in early-stage CC is of utmost importance to identify patients at high risk of metastasis who might benefit from adjuvant chemotherapy. Besides, chromosome instability leads to the co-existence of distinct subclonal cell populations, resulting in intratumor heterogeneity (ITH), which has already been associated with poor clinical outcome in some cancer types.

Design: SNP-arrays were performed in 84 stage II colon carcinomas, including 38 from patients who developed recurrence after 5-years follow-up. None of the patients received adjuvant treatment. Fluorescence *in situ* hybridization (FISH) was also utilized to examine the dynamics of copy number alterations (CNAs). Levels of ITH were assessed by measuring the proportion of subclonal CNAs, defined as those being present in <85% of the tumor population. Histopathological analyses were applied in order to evaluate high risk factors such as tumor budding, lymphovascular and perineural invasion (LVPNI), immune infiltration and PDL-1 expression.

Results: Data show that tumors from recurrent patients have larger fractions of altered genomes compared to non-recurrent (P=0.014). Candidate genomic regions displaying higher prevalence in recurrent cancers are the gain of chromosome 13q, loss of 17q21.31-q24.3 and copy-neutral LOH at 17p13.3-p11.1. Given the positive correlation between fractions of altered genome and numbers of subclonal CNAs (Pearson's R=0.66, P<0.0001), we further investigated the contribution of subclonal CNAs as surrogate of ITH levels in disease recurrence. Results from both SNP-arrays and FISH indicate that recurrent tumors have greater proportions of subclonal CNAs (P=0.021). Histopathological factors that also exhibit a statistical association with recurrence are tumor budding, LVPNI and immune infiltration (P<0.05). Survival analyses show that patients with gain of chromosome 13 and high subclonal copy-number heterogeneity have higher risk of developing recurrence (Log-rank P<0.05, HR=2.28-2.96).

Conclusions: These data suggest that genomic ITH along with high-risk histopathological factors are associated with an increased risk of disease relapse in early-stage colon cancer, and therefore could improve prognosis in the context of clinical decision making.

622 Lymph Node Total Tumor Load, Tumor Budding and Poorly Differentiated Clusters as a Tool to Unmask High-Risk Colorectal Carcinomas

Ivan Archilla[1], Iñigo Gorostiaga[2], Jose Javier Aguirre[3], Jose Guerrero[1], Jordi Tarragona[4], María Teresa Rodrigo[5], Natalia Castrejón[6], Jordi Camps[7], Iban Aldecoa[8], Miriam Cuatrecasas Freixas[9]
[1]Hospital Clinic, University of Barcelona, Barcelona, Spain, [2]Araba University Hospital, Vitoria-Gasteiz, Álava/Araba, Spain, [3]Araba University Hospital, Vitoria, Álava/Araba, Spain, [4]Arnau of Vilanova University Hospital, Lleida, Spain, [5]Department of Pathology, Hospital Clinic, Barcelona, Spain, [6]Hospital Clinic Barcelona, University of Barcelona, Barcelona, Spain, [7]Hospital Clinic-IDIBAPS, Universitat de Barcelona, Barcelona, Spain, [8]Hospital Clinic of Barcelona, San Cugat del Valles, Barcelona, Catalonia, Spain, [9]Hospital Clinic, Universitat de Barcelona, Barcelona, Spain

Disclosures: Ivan Archilla: None; Iñigo Gorostiaga: None; Jose Javier Aguirre: None; Jose Guerrero: None; Jordi Tarragona: None; María Teresa Rodrigo: None; Natalia Castrejón: None; Jordi Camps: None; Iban Aldecoa: None; Miriam Cuatrecasas Freixas: None

Background: Tumor budding (TB) and poorly differentiated clusters (PDC) are related to the tumor microenvironment involved in the epithelial-to-mesenchymal transition (EMT) and are related to an aggressive behavior in colorectal carcinoma (CRC). Patients that harbor lymph node (LN) micrometastases not detected by H&E are known to have worse prognosis and could benefit from adjuvant therapy. Molecular detection of CK19 mRNA in LN by the One Step Nucleic Acid Amplification (OSNA) assay is an alternative LN staging method to the standard H&E for early-stage CRC. This molecular method allows to detect the presence of LN tumor burden in 11,5 to 50% of patients diagnosed as pN0 by histological examination. This assay has been validated for breast and CRC LN analysis. We aimed to evaluate the correlation between TB and PDCs with LN total tumor load (TTL), defined as the sum of CK19 mRNA/µL copies present in the LNs of CRC specimens to better select those patients at risk of recurrence.

Design: TB and PDC from 342 CRC from 3 Spanish hospitals were evaluated with H&E and CK19 immunohistochemistry (IHC). The OSNA assay is an automated molecular diagnostic tool that uses nucleic acid amplification technology (RT-LAMP) for the detection of CK19 mRNA. This method was performed in 5.931 freshly isolated LNs from these cases. A TTL> 250 copies/µL was considered positive.

Results: Molecular LN analysis resulted positive in 38% cases with presence of LN TTL>250 copies/µL of CK19 mRNA. Tumor budding was low (Bd1) in 45%, intermediate (Bd2) in 25% and high (Bd3) in 30% of the cases. PDC was low grade-G1 in 53%, intermediate-G2 in 32%, and high-G3 in 15% of cases. A positive correlation was observed between TB and PDC with TTL (r = 0.249, p <0.001 for TB, r = 0.266, p <0.001 for PDC), which was higher with immunohistochemistry evaluation. TB and PDC also correlated with high histological grade, lymphovascular and perineural invasion, pT and pN stages (p <0.001).

Conclusions: Molecular LN analysis is a highly sensitive and a promising approach for LN staging in early CRC. It could evolve into a fast, ready-to-use and reliable alternative to H&E pN staining. The correlation between TTL, TB and PDC could be useful for the detection of high-risk CRC.

623 Clinicopathologic Study of Blue nevi of the Gastrointestinal (GI) Tract: First Case Series

Naziheh Assarzadegan[1], Kevan Salimian[2], Danielle Hutchings[3], Annika Windon[4], Kiyoko Oshima[4], Lysandra Voltaggio[5], Elizabeth Montgomery[6], Abdulsalam Aodah[7]
[1]Department of Pathology, The Johns Hopkins Medical Institutions, Baltimore, MD, [2]Johns Hopkins, Baltimore, MD, [3]Johns Hopkins Medicine, Baltimore, MD, [4]Johns Hopkins Hospital, Baltimore, MD, [5]Baltimore, MD, [6]Johns Hopkins Medical Institutions, Baltimore, MD, [7]Riyad Regional Lab, Riyadh, Saudi Arabia

Disclosures: Naziheh Assarzadegan: None; Kevan Salimian: None; Danielle Hutchings: None; Annika Windon: None; Kiyoko Oshima: None; Lysandra Voltaggio: None; Elizabeth Montgomery: None; Abdulsalam Aodah: None

Background: Blue nevus (BN) is a benign melanocytic proliferation that is typically cutaneous. Extracutaneous BN is infrequent. The most common extracutaneous locations are the mucosa of the head and neck region, female genital tract, spermatic cord, prostate and lymph node. Gastrointestinal (GI) tract BN is rare with only a few case reports in the literature. Here*, we describe the clinicopathologic findings of the largest series (6 cases) of blue nevi of the GI tract.*

Design: A search of our Pathology Data System from 1984 to 2019 identified 6 blue nevi of the GI tract. Clinical information and H&E stained slides were reviewed. All cases were initially reviewed in consultation by one of the authors (E.A.M.) and demographic information was available for all cases. The location, the layer of the GI tract involved, characteristics of the spindle cells, presence of nuclear atypia, mitoses or necrosis were recorded. Follow-up data were obtained through the medical chart or the referring pathologists or clinicians.

Results: Lesions predominantly arose in middle-aged adults with a mean age of 54 (range 27 to 80) and a slight female predominance (N = 4, 66%). The most common sites were rectum and colon (N=5, 83%), followed by stomach (N=1, 17%). Four cases were identified incidentally during endoscopic examination that was performed either for screening or for unrelated symptoms (N=4, 66%). Two patients presented with rectal bleeding (N=2, 33%) unassociated with the BN (hemorrhoids). Endoscopically, most lesions appeared as superficial hyperpigmented areas (N=5, 83%). One case was described as abnormal mucosa (N=1, 17%). Microscopically, the mucosa was involved in all cases (N=6, 100%). One case showed a submucosal proliferation in addition to the mucosal component (N=1, 17%). Lesions were composed of a proliferation of bland spindle cells with abundant granular pigment. No nuclear atypia, mitoses or necrosis were identified. When performed, immunostains showed strong immunoreactivity for melanocytic markers (S100 protein, HMB45, and MART1). Follow-up information was available in 5 patients with no recurrences reported to date.

Conclusions: This is the largest series of GI tract blue nevi to date. BN is a benign melanocytic proliferation and neither our study nor our review of the literature identified malignant examples. It is important to be aware of the occurrence of such lesions outside of the skin and consider the possibility of BN when pigmented lesions are encountered in the GI tract.

624 Comparison of Three Different Histologic Grading Systems in Assessing Pouchitis on Pouch Resections

Ahmed Bakhshwin[1], Isaac Briskin[2], Suha Abushamma[3], Florian Rieder[4], Ilyssa Gordon[5]
[1]Robert J. Tomsich Pathology & Laboratory Medicine Institute, Cleveland Clinic, Pepper Pike, OH, [2]Cleveland Clinic Quantitative Health Sciences, Cleveland, OH, [3]Washington University in St. Louis, St. Louis, MO, [4]Cleveland Clinic Digestive Disease and Surgery Institute, Cleveland, OH, [5]Robert J. Tomsich Pathology & Laboratory Medicine Institute, Cleveland Clinic, Cleveland, OH

Disclosures: Ahmed Bakhshwin: None; Isaac Briskin: None; Suha Abushamma: None; Florian Rieder: None; Ilyssa Gordon: None

Background: Total colectomy with ileal pouch anal anastomosis is the standard of care for refractory ulcerative colitis. Pouchitis is one of the most common complications leading to pouch failure. Two commonly used clinical scores have similar histologic components. Application of a more detailed histologic score may refine pouchitis categorization.

Design: A representative section of resected ileal pouch (n=55) was evaluated for the histologic component of the Pouchitis Activity Score, the Pouch Disease Activity Index, and the Modified Global Histology Activity Score. Score of >4 is moderate/severe pouchitis by Pouchitis Activity Score and Pouch Disease Activity Index; and score of >6 is moderate/severe by Modified Global Histology Activity Score. Additionally, acute and chronic components were compared separately. Agreement on severity was calculated with Fleiss's and Cohen's Kappa statistics. McNemar's exact binomial test was used to compare discordant rates.

Results: There is moderate agreement between all methods in identifying moderate/severe histology overall (75%, $\kappa = 0.54$) and for the chronic items alone (78%, $\kappa = 0.51$). Evaluation of the acute elements alone reveals a statistically significant difference between each of the scoring systems in identifying moderate/severe histology ($p<0.001$ to $p= 0.02$) (Table1).

Table 1. Comparison of Three Histologic Scoring Systems in Pouch Resections

	Overall Moderate/severe (n, %)	Chronic Moderate/severe (n)	Acute Moderate/severe (n)
Modified Global Histology Activity Score	44 (80)	48	46
Pouchitis Activity Score	41 (75)	43	33
Pouch Disease Activity Index	40 (73)	44	25
p-value	>0.1	>0.1	<0.001 to 0.02
Overall Agreement (%, kappa)	75 (0.54)	78 (0.51)	56 (0.38)

Conclusions: Although originally created to assess Crohn's disease, Modified Global Histology Activity Score can effectively be used to evaluate pouch resections. The acute elements of Pouchitis Activity Score, Pouch Disease Activity Index, and Modified Global Histology Activity Score identify histologic features that result in significantly different case categorization. Association with clinical and endoscopic parameters are needed for further study.

625 Sporadic Colorectal Adenomas in Young Adults

Ahmed Bakhshwin[1], Xuefeng Zhang[2]
[1]Robert J. Tomsich Pathology & Laboratory Medicine Institute, Cleveland Clinic, Pepper Pike, OH, [2]Cleveland Clinic, Beachwood, OH

Disclosures: Ahmed Bakhshwin: None; Xuefeng Zhang: None

Background: While the incidence of Colorectal cancer (CRC) in the United States has been declining over the past several decades, paradoxical increase of incidence has been seen in the population younger than 45. Currently, average-risk persons are recommended to start CRC screening at age from 45 to 50. However, incidental colonic adenomas are not uncommon in patients younger than 40. We aim to characterize the demographic and clinicopathological features of this patient population, which could potentially help risk stratifying patients who need colonoscopy before 40.

Design: We retrospectively searched pathology database from 2002 to 2018 for adult patients 40-year-old and younger, who were found to have conventional adenomas when undergoing colonoscopy for GI symptoms. Patients with inflammatory bowel disease, defined genetic syndromes or personal history of colorectal cancer are excluded. Clinical, endoscopic and pathologic data were collected.

Results: A total of 227 patients (52% female) were identified. The age ranged from 18 to 40 years (median 34) (31% <30; 32% 30-35; 38% 36-40). The racial distribution resembled the general population (74% Caucasian, 15% African American, 4% Asian, 3% Hispanic, 4% others/unknown). The majority of the patients (83%) had no family history (FH) of CRC; 7% of the patients had FH of CRC in 1st-degree relatives, and 10% in 2nd-degree relatives. The most common indications for colonoscopy were abdominal pain (30%), bleeding per rectum (29%), and change in bowel habits (27%). Only 3% of patients underwent colonoscopy due to FH in addition to other concurrent symptom(s) that prompted the procedure. Sixty-seven percent of the patients were either overweight (BMI 25-29.9) (27%) or obese (BMI>30) (40%). Average number of adenoma identified was 1.4 (range 1 to 8). Eighteen patients had concurrent serrated polyps. The characteristics and locations of the polyps were depicted in (Table 1). Thirty-six patients (16%) underwent follow-up colonoscopy (1 to 4 colonoscopies), and 16 patients were found to have additional adenomatous polyp(s). Of these 16 patients, 27% were overweight and 60% were obese.

Type of adenoma	n (%)	size (mean) mm	HGD %	Cecum	Ascending	Transverse	Descending	Sigmoid	Rectosigmoid	Rectum
Tubular adenoma	288 (85)	4.97	0	6.7	18.6	27.9	11.4	22.2	4	9.1
Tubulovillous adenoma	16 (5)	16.1	31	11.8	11.8	11.8	23.5	23.5	5.9	11.8
Villous adenoma	1 (0)	5.5	100	0	0	0	0	100	0	50
Sessile serrated adenoma	10 (3)	9.2	0	23.1	23.1	38.5	0	15.4	0	0
Hyperplastic polyp	24 (7)	3.5	0	4	8	8	4	36	16	24

Conclusions: In patients 40-year-old or younger who had sporadic conventional colonic adenomas, the majority did not have a family history of CRC, and therefore may not be considered to have screening colonoscopy before 45. Obesity is very common in this patient population, particularly in those who had additional adenomas on follow-up.

626 Esophageal Adenocarcinoma Showing Extensive Neuroendocrine Differentiation after Induction Chemoradiation: The Molecular View of a Poorly Understood Phenomenon

Cameron Beech[1], Daniela Molena[2], Laura Tang[2], David Klimstra[2], Jinru Shia[2]
[1]New York, NY, [2]Memorial Sloan Kettering Cancer Center, New York, NY

Disclosures: Cameron Beech: None; Daniela Molena: None; Laura Tang: None; David Klimstra: None; Jinru Shia: None

Background: Chemoradiation induced neuroendocrine differentiation (NED) is a well-known phenomenon that can occur in gastrointestinal adenocarcinomas. It remains to be defined whether this phenomenon is driven by specific genomic aberrations. Here we report our genomic findings of paired pre- and post-treatment tumor samples in a patient with an esophageal adenocarcinoma that had undergone profound neuroendocrine differentiation post-therapy.

Design: The study patient was a 70-year-old female who was found on endoscopy to have a 3.5cm ulcerated mass in the distal esophagus. Biopsy revealed a moderately differentiated adenocarcinoma. The disease was appropriately staged, deemed to be locally advanced, and the patient received neoadjuvant treatment according to the MSK PET directed approach followed by esophago-gastrectomy. The resection revealed residual carcinoma, pT3N1, with 30% treatment response. Differing from the initial biopsy, both the primary tumor and metastatic lymph node in the resection exhibited profound NED as demonstrated by both morphology and immunohistochemistry (Fig.1). Targeted NGS via MSK-IMPACT with a 468 gene panel was performed on three tumor samples: pre-treatment biopsy, post-treatment primary tumor with NED, and post-treatment nodal metastasis with NED.

Results: Sequencing data showed conserved somatic mutations within TP53, CCNE1, KMT2A, SMARCA4 across all three samples (Table 1). There was also no difference in microsatellite instability status or tumor mutation burden across samples. CCNE1 amplification was increased approximately fourfold in the resection specimen compared to the biopsy.

		Biopsy	Resection	Lymph node metastasis
MSI Status		MSS	MSS	MSS
MSI sensor score		0.23	0.86	0.07
Tumor mutation burden (mt/Mb)		2.6	2.6	2.6
Somatic variants identified	TP53 exon 8 p.E294* (c.880G>T)	Present	Present	Present
	CCNE1 amplification	Amplified (Fold Change: 6.5)	Amplified (Fold Change: 10.1)	Amplified (Fold Change: 2.4)
	KMT2A exon 27 p.R3232Q (c.9695G>A)	Present	Present	Present
	SMARCA4 exon 14 p.D697A (c.2090A>C)	Present	Present	Present
	BCL2rearrangement: c.585+35197:BCL2_chr18	Present	Present	Present
	SMARCA4 rearrangement c3215+5:SMARCA4_chr19	Present	Present	Present
	TP53 rearrangement:t(17;20)(p13.1;q13.13)(chr17:g.7579520::chr20:g.48328389	Present	Present	Present

Figure 1 - 626

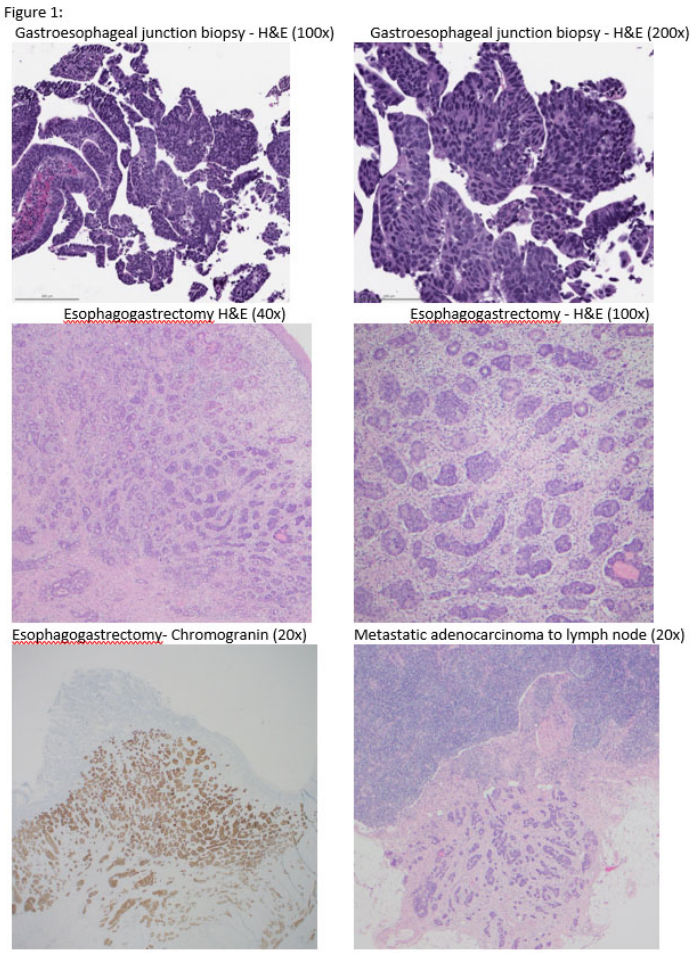

Conclusions: In this analysis of an esophageal adenocarcinoma case, comparative mutational profiling of pre-treatment tumor that did not have NED and post-treatment tumor that acquired profound NED revealed identical mutational signatures. These findings suggest that chemoradiation induced NED is likely driven by mechanisms other than mutational events.

627 Can Histologic Findings in Esophageal Biopsy Specimens Predict Positive Margins in Subsequent Endoscopic Mucosal Resection Specimens?

Phoenix Bell[1], Justin Cates[2], Raul Gonzalez[3]
[1]University of Rochester Medical Center, Rochester, NY, [2]Vanderbilt University Medical Center, Nashville, TN, [3]Beth Israel Deaconess Medical Center, Boston, MA

Disclosures: Phoenix Bell: None; Justin Cates: None; Raul Gonzalez: None

Background: Endoscopic mucosal resection (EMR) is increasingly employed for local control of dysplastic and early malignant processes of the gastrointestinal tract. We previously performed a large-cohort analysis evaluating numerous histologic factors in esophageal EMR specimens, finding that positive margin status was the only microscopic predictor of disease recurrence. We hypothesized that histologic findings in pre-EMR biopsy specimens might predict increased risk of positive margins in the subsequent resection specimen.

Design: We searched our EMR database for patients with available prior biopsy samples, identifying 68 cases. For each, we recorded size of endoscopic lesion, worst biopsy diagnosis (low-grade dysplasia [LGD], high-grade dysplasia [HGD] or esophageal adenocarcinoma [EAC]), percent of biopsy showing disease, presence of intestinal metaplasia (IM), presence of additional foci of disease within 2 cm of the EMR site, and whether disease undermined squamous epithelium. Further, for biopsies with EAC, we assessed tumor budding, tumor differentiation, and tumor depth. These factors were compared to positive margin status in the subsequent EMR specimen using Fisher's exact test, with significance set at $P<0.05$.

Results: Of the 68 pre-EMR biopsies, 57%, 37%, and 6% showed HGD, EAC, and LGD, respectively. Average age at biopsy was 66 years. The majority of patients were male (87%). Median endoscopic lesion size was 1 mm, though this was only available for 16 cases (24%). Additional foci of disease were present in 35% of patients. Percent of biopsy showing disease was 1-33% in 41%, 34-66% in 34%, and 67-100% in 25%. IM was seen in 79% of biopsies, and disease undermined squamous epithelium in 50%. Among biopsies with EAC, 60% were well differentiated, 32% moderately differentiated, and 8% poorly differentiated. Median cancer depth on biopsy was 0 mm (intramucosal EAC). Subsequent positive EMR margins existed for 31% of cases. Only degree of cancer differentiation in the biopsy influenced positive EMR margin status (*P*=0.047), with all poorly differentiated cases having positive margins.

Conclusions: The presence of poorly differentiated EAC in biopsy samples increases the risk of positive margin status in subsequent EMR specimens and thus increases the likelihood of disease recurrence. Such information on biopsy may indicate a need for more aggressive action during the EMR procedure. We lacked sufficient data to determine whether endoscopic lesion size also impacted positive margin risk.

628 A Large Multicenter Series of Post-Transplant Lymphoproliferative Disorders Involving the Gastrointestinal Tract and Liver

Adam Booth[1], Sanam Loghavi[2], Raul Gonzalez[3], Kamran Mirza[4], Brian Cox[5], Grace Malvar[3], L. Jeffrey Medeiros[2], Genevieve Crane[6]

[1]University of Texas Medical Branch, Galveston, TX, [2]The University of Texas MD Anderson Cancer Center, Houston, TX, [3]Beth Israel Deaconess Medical Center, Boston, MA, [4]Loyola University Medical Center, Maywood, IL, [5]Cedars-Sinai Medical Center, Los Angeles, CA, [6]New York-Presbyterian/Weill Cornell Medical Center, New York, NY

Disclosures: Adam Booth: None; Sanam Loghavi: None; Raul Gonzalez: None; Kamran Mirza: None; Brian Cox: None; Grace Malvar: None; L. Jeffrey Medeiros: None; Genevieve Crane: None

Background: Post-transplant lymphoproliferative disorders (PTLDs) are a heterogeneous group of diseases ranging from indolent polymorphic/polyclonal lymphoid proliferations to aggressive monomorphic lymphomas including diffuse large B cell lymphoma and plasmablastic lymphoma. PTLDs occur in the setting of immunosuppression for solid organ (SOT) or allogeneic hematopoietic stem cell transplantation (AHSCT). Risk factors for PTLD include viral infections, graft type, immunosuppressive drug regimen and host immune status. The gastrointestinal (GI) tract and liver are among the most commonly involved sites. Here we report a large, multi-institutional series of patients with PTLDs involving the GI tract and liver.

Design: An electronic medical record search of four large institutions for cases of gastrointestinal tract and liver PTLD was performed. Cases with insufficient history were excluded. Independent Samples T-test and Chi-squared Fischer's Exact test were utilized to evaluate differences in demographics and sample characteristics. In a representative subset, overall survival was assessed via Kaplan Meier survival curve. Multiple binary logistic regressions were used to assess associations with EBV status.

Results: We identified 74 PTLDs (Table), the majority of which were monomorphic. The cohort displayed demographic uniformity in age and gender (p = 0.227) and time to transplant, despite a wide mean 17.2 months (EBV negative = 20) and 48.6 months (EBV positive = 46), p=0.425. AHSCT related PTLD were more often EBV+ (83% vs. 67%), polymorphic (30% vs. 6%), involving multiple sites (26% vs. 2%) and associated with mortality (100% vs. 40% were evaluable). Taken alone, EBV was significantly associated with BM (p=0.022, Figure) and when adjusted for age and gender by regression analysis (p=0.034) with an OR of 5.6 (1.13, 27.58). However, in SOT, liver involvement was associated with cardiac transplant and EBV (11/12, 92%).

Sex	Age	Graft Type	Time from Transplant	Site	Type	EBV Status	Overall Survival
F	50	AHSCT	4.6	Duodenum, stomach, colon	DLBCL	Positive	na
F	50	AHSCT	1242	Liver	DLBCL	Positive	0.72
M	21	AHSCT	9.9	Sigmoid	Polymorphic	Positive	0.07
F	31	AHSCT	4.7	Cecum	DLBCL	Positive	155.34
F	32	AHSCT	4.9	Stomach, duodenum, rectum	DLBCL	Positive	85.55
F	34	AHSCT	11.2	Stomach	Polymorphic	Positive	7.50
M	32	AHSCT	12.4	Duodenum, rectosigmoid	Polymorphic	Positive	92.09
M	60	AHSCT	65.3	Liver	DLBCL	Negative	29.92
M	49	AHSCT	11.9	Liver	DLBCL	Negative	72.10
F	51	AHSCT	1.6	Colon	Polymorphic	Positive	1.28
F	68	AHSCT	11.2	Rectum	DLBCL	Positive	1.51
M	36	AHSCT	3.6	Stomach, duodenum, colon, rectum	DLBCL	Positive	2.50
M	18	AHSCT	2.8	Duodenum	Polymorphic	Positive	58.13
F	54	AHSCT	3.7	Rectum	Polymorphic	Positive	13.28
M	46	AHSCT	10.1	Liver	DLBCL	Positive	6.25
M	72	AHSCT	5.3	Stomach, rectum	DLBCL	Positive	6.18
F	65	AHSCT	3.6	Stomach	DLBCL	Positive	0.53
F	36	AHSCT	2.7	Liver	Polymorphic	Positive	2.40
M	26	AHSCT	25.8	Anus	Plasmablastic lymphoma	Positive	20.28

M	44	AHSCT	3.4	Stomach, duodenum, colon	DLBCL	Positive	3.65
M	61	Liver	62.1	Stomach	DLBCL	Negative	10.95
M	74	Liver	10	Stomach	HGBL	Negative	na
F	72	Kidney	11	Stomach	HGBL	Positive	na
M	61	AHSCT	0.58	Rectum	DLBCL	Positive	na
M	70	AHSCT	1.25	Cecum	DLBCL	Negative	na
M	55	Liver	4.08	Colon	LBCL	Negative	na
F	51.1	Solid organ (unknown type)		Anus	LBCL	Positive	
F	34.2	Heart	0.76	Colon	LBCL	Negative	
F	61.5	Kidney	5.86	Descending colon	DLBCL	Negative	
F	9.2	Liver	8.56	Duodenum	Polymorphic	Negative	
M	49.1	Liver	0.38	Duodenum, pancreas	LBCL	Negative	3.42
M	70.8	Kidney	4.33	Duodenum, mesentery	DLBCL	Negative	
F	25	Kidney	8.69	Ascending colon	DLBCL	Negative	
M	26.6	Liver	2.25	Sigmoid	DLBCL	Negative	
M	70.3	Kidney	5.85	Small intestine	DLBCL	Negative	
F	3.4	Liver	2.61	Small intestine	Plasmacytoma	Negative	1.02
M	52.2	Liver		Small intestine	DLBCL	Negative	
M	19.8	Liver		Colon	Polymorphic	Positive	
F	67.3	Lung		Duodenum	DLBCL	Positive	1.15
F	6.9	Small intestine	4.27	Small intestine	Unspecified type	Positive	
F	44.2	Kidney	8.97	Jejunum	Polymorphic	Positive	
M	27.6	Lung	0.6	Sigmoid	LBCL	Positive	96.30
M	49.9	Solid organ (unknown type)		Small intestine	DLBCL	Positive	
M	32.7	Kidney	12.7	Small intestine	DLBCL	Positive	
M	54.1	Liver	6.22	Small intestine	LBCL	Positive	84.39
F	42.3	Kidney	17.59	Colon	Burkitt lymphoma	Positive	
F	56.6	Kidney	7.55	Sigmoid	DLBCL	Positive	12.16
M	47.2	Kidney	2.02	Liver	DLBCL	Positive	
M	21.8	Heart	2.52	Liver	LBCL	Positive	62.93
F	10.3	Heart	0.58	Liver	Polymorphic	Positive	
M	48	Heart	9.45	Liver	LBCL	Positive	4.96
M	2.4	Liver	2.31	Liver	LBCL	Positive	1.58
M	53.8	Liver		Liver	LBCL	Positive	0.07
M	5.3	Liver	2.37	Liver	Burkitt lymphoma	Positive	
M	69.3	Heart/kidney	7.22	Stomach	Gray zone lymphoma	Negative	
M	52.3	Liver	1.7	Stomach	DLBCL	Negative	56.75
M	81.4	Kidney	10.53	Stomach	DLBCL	Negative	2.33
M	72.8	Solid organ (unknown type)		Stomach	LBCL	Positive	
F	39.9	Kidney		Stomach	LBCL	Positive	
M	30	Lung	5.88	Colon	DLBCL	Positive	na
F	49	Lung	108.33	Small intestine, ascending colon	DLBCL	Negative	na
F	65	Kidney	113.62	Stomach	DLBCL	Positive	na
F	48	Kidney	0	Peritoneal fluid	HGBL	Positive	na
M	54	Liver	55.79	Liver	DLBCL	Positive	na
M	66	Lung	98.17	Mesentery	DLBCL	Positive	na
F	46	Kidney	5.69	Ascending colon, sigmoid	DLBCL	Positive	na
F	44	AHSCT	30.21	Liver	DLBCL	Positive	na
M	62	Lung	88.21	Terminal ileum	DLBCL	Positive	na
M	63	Lung	94.88	Jejunum	DLBCL	Positive	na
M	52	Kidney	132.62	Terminal ileum, appendix	DLBCL	Positive	na
M	52	Kidney	132.2	Ileum	DLBCL	Positive	na
F	38	Kidney	15.81	Liver	Plasmablastic lymphoma	Positive	na
M	49	Liver	11.64	Liver	Plasmablastic lymphoma	Positive	na
M	65	Liver	23.6	Liver	Burkitt lymphoma	Negative	16.73

Figure 1 - 628

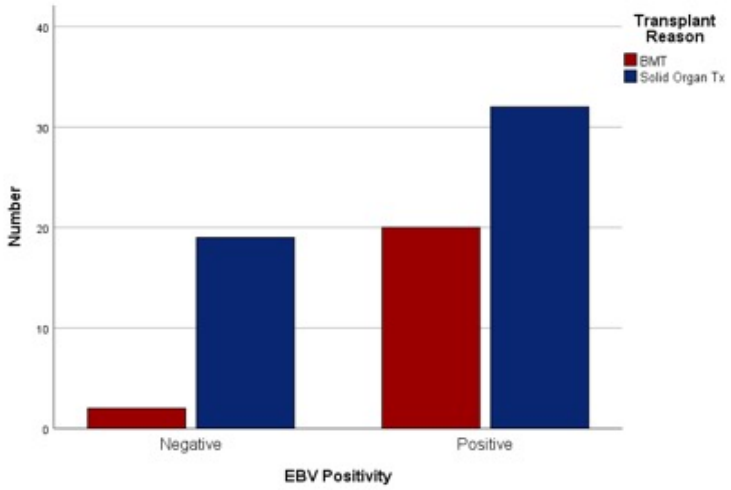

Conclusions: We analyzed a large, multi-institutional cohort of PTLDs arising in the GI tract and liver to assess clinical, morphologic and phenotypic features that may inform prognosis and yield insights into their development. The majority of GI-associated PTLD were of monomorphic type. However, different sites within the GI tract were associated with distinct features. Mortality was high and did not appear to differ between sites of involvement. This study provides the first large scale assessment of both AHSCT and SOTs resulting in PTLDs within the GI tract and liver.

629 Objective Visual Analog Scale for Biopsy Diagnosis of Helicobacter pylori Infection in Clinical Practice

Katherine Boylan[1], Shruti Patrey[1], Phillip Mcmullen[2], Vera Tesic[3], Christopher Weber[1], John Hart[1], Namrata Setia[1]
[1]The University of Chicago, Chicago, IL, [2]University of Chicago Medical Center, Chicago, IL, [3]The University of Chicago, River Forest, IL

Disclosures: Katherine Boylan: None; Shruti Patrey: None; Phillip Mcmullen: None; Vera Tesic: None; Christopher Weber: None; John Hart: None; Namrata Setia: None

Background: The Sydney Classification included visual depictions of increasing inflammatory cell infiltrates in *H. pylori* gastritis, but the scale was subjectively designed. The GIPS guidelines also recommend using visual gestalt to identify *substantial* inflammation for prompting further ancillary stains for *H. pylori* organisms. This study aims to objectively investigate the degree of inflammation that justifies additional workup for *H. pylori* infection.

Design: We retrospectively identified two cohorts of patients who had undergone upper GI endoscopy with gastric biopsies; one with clinical evidence of *H. pylori* infection (n=66), defined as the presence of clinical symptoms with a positive 1) *H.* pylori immunostain, 2) stool antigen test, and/or 3) CLO test, and one without infection (n=81). Biopsies with the highest degree of chronic inflammation were stained for MUM-1, a specific marker for plasma cells. Digital analysis was performed on scanned slides using Aperio GENIE nuclear quantification algorithm to calculate the number of plasma cells/mm^2 in the mucosa, which we termed the “inflammatory score”. The data generated was used for ROC analysis.

Results: Patients with *H. pylori* infection had a median inflammatory score of 1125 plasma cells/mm^2 (± 441 SD), while patients without infection had a median of 246 plasma cells/mm^2 (± 258 SD). The inflammatory score cut-off value of a positive infection was ≥ 645 plasma cells/mm^2 (sensitivity 94%, specificity 94%, Figure 1). The false negative rate of pathologic diagnoses was 0.061 and the false positive rate was 0.062. A visual analogue scale was created based on the review of H&E and MUM-1 stained slides (Figure 2). Site-based variation in inflammation, proportion of plasma cells and neutrophils, and requirement of *H. pylori* immunostain to establish the diagnosis were taken into account. False negative biopsies included partially treated infections (3 cases, 5%) and sampling error (2 cases, 3%). False positive biopsies (5 cases, 6%) included gastric Crohn’s disease, sarcoidosis, and fungal infections. False positive stool antigen tests were identified in 15 cases (18.5%), which included negative biopsies with significant upper GI bleeding, which is a documented cause of a false positive stool antigen test.

Figure 1 - 629

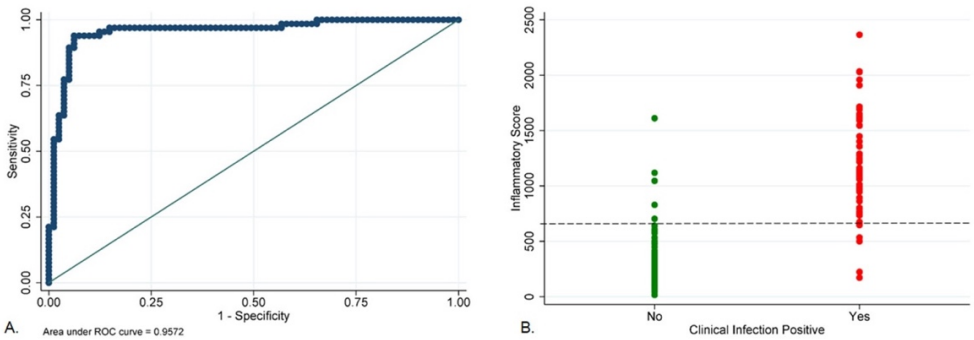

Figure 1. A) ROC curve analysis of clinical *H. pylori* infection versus inflammatory score. B) Perfect test analysis, showing an inflammatory score cut-off of ≥ 645 plasma cells per milimeter squared for positive clinical infection.

Figure 2 - 629

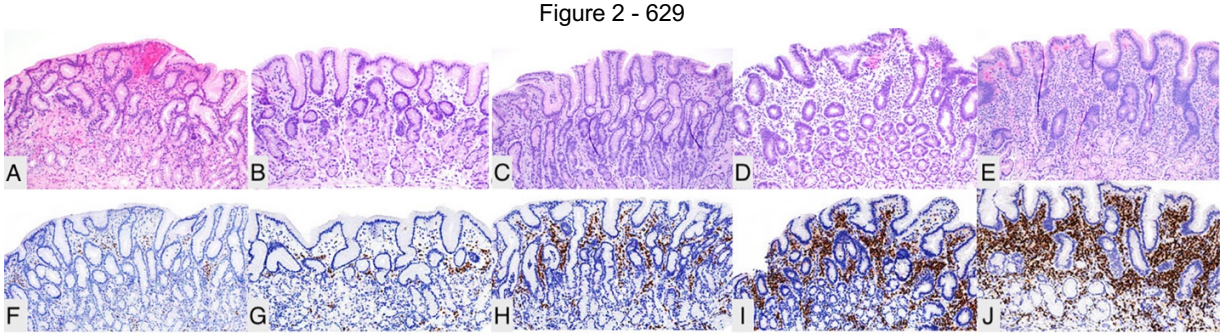

Figure 2. Visual analog scale with top row showing representative H&E sections of antral mucosa & bottom row with corresponding MUM1 stains. A & F) Normal mucosa. B & G) Non-H. pylori inactive gastritis. C & H) H. pylori inactive gastritis, with negative biopsy and immunostain. D & I) H. pylori gastritis at low end of positive inflammatory score. E & J) H. pylori gastritis at high end of positive inflammatory score.

Conclusions: We propose an objective visual analog scale that is associated with a high sensitivity and specificity for diagnosing *H. pylori* infection, which justifies moving away from upfront universal *H. pylori* testing in routine clinical practice.

630 Esophageal GISTs: Molecular Findings, Disease Spectrum, and Diagnostic Pitfalls in a Rare Entity

Amanda Breitbarth[1], Brian Brinkerhoff[2]
[1]Oregon Health & Science University, Portland, OR, [2]OHSU, Portland, OR

Disclosures: Amanda Breitbarth: None; Brian Brinkerhoff: None

Background: Esophageal gastrointestinal stromal tumors (GISTs) comprise less than 1% of all GISTs and may be confused with other mesenchymal tumors of the esophagus. Ancillary testing is critical to the diagnosis, treatment, and disease stratification of these tumors. There is currently limited published data on esophageal GISTs. The goal of this study is to elucidate the molecular and pathologic features as well as diagnostic pitfalls of this rare entity based on our institutional experience.

Design: The OHSU Database was searched from 2000 to present, identifying 6 patients with primary esophageal GISTs. Slides were reviewed by two independent pathologists, stained with an extended IHC panel, and analyzed via the Knight Diagnostic Laboratory next-generation GeneTrails® Solid Tumor Panel.

Results: A spectrum of pathology was observed: 2 incidental GISTs (0.1 cm and 0.4 cm) in the setting of treated gastroesophageal adenocarcinoma, 1 esophageal low-grade GIST with synchronous gastric primary (different molecular profiles), 2 low-grade GISTs, and 1 malignant GIST with mediastinal and liver metastases despite imatinib therapy. 2 cases were initially misdiagnosed as leiomyomas (1 on frozen section, 1 based on limited IHC). By IHC, 100% of cases stained with CD117 and DOG1, 80% with caldesmon, and none with

desmin. *KIT* mutations were identified in all cases: 3 point mutations and 1 deletion in exon 11 (post-imatinib), 3 point mutations in exon 13 (1 post-imatinib), and 1 deletion in exon 17 (post-imatinib). Partial loss of *CDKN2A* was observed in the malignant GIST following therapy. *POLE*, *DICER1*, and *RICTOR* variants were identified. No other mutations or copy number alterations were identified.

Table 1: Patient demographics, pathologic features, and molecular data

Case	Age (years)	Gender	History	Level of esophagus	Treatment	Size (cm)	Mitotic rate (per 50 HPF)	KIT	PDGFRA	CDKN2A	Variants of unknown significance
1	62	Female	Synchronous esophageal and gastric	Mid-upper	Resection	4	5	Exon 13: K642E	None	None	RICTOR p.I1601V
2	44	Female	Primary esophageal with recurrence and metastases to mediastinal lymph node and liver	Distal	Resection and tyrosine kinase inhibition	2.2	11	Exon 11: WK557-558 deletion Exon 13: V654A Exon 17: 819 and 820 deletion	None	Partial loss	None
3	66	Male	Incidental (resection of treated gastroesophageal adenocarcinoma)	Distal	Carboplatin/taxol, radiation, and resection	0.1	1/3	Not done	Not done	Not done	Not done
4	51	Male	Incidental (resection of treated gastroesophageal adenocarcinoma)	Mid	Carboplatin/taxol, radiation, and resection	0.4	<1/10	Exon 11: KIT p.V560D	None	None	None
5	62	Male	Primary	Distal	Enucleation	3.5	2	Exon 11: KIT p.W557G	None	None	POLE and DICER1
6	70	Male	Primary	Distal	Enucleation	3.7	2	Exon 13: KIT p.K642E	None	None	None

Figure 1 - 630

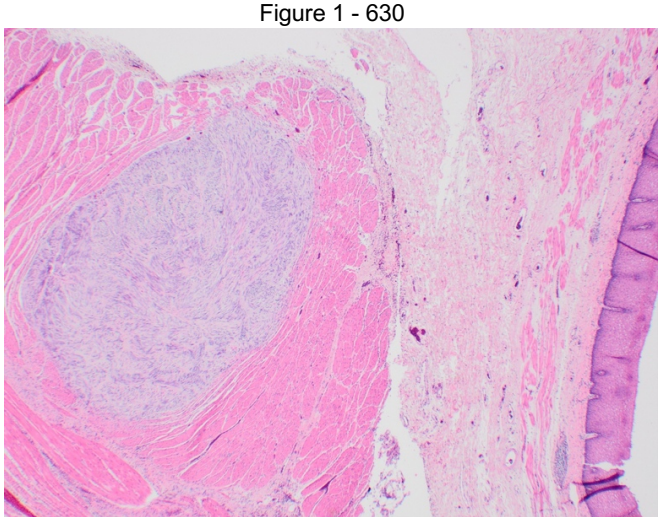

Figure 2 - 630

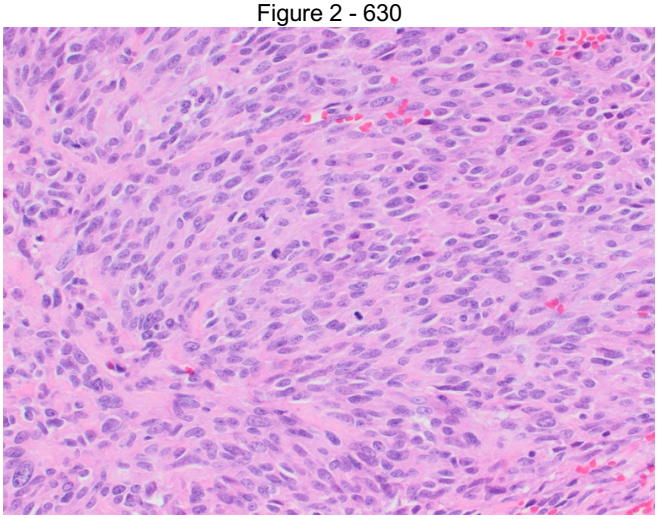

Conclusions: Extended molecular testing revealed novel findings in esophageal GISTs, including acquired partial loss of *CDKN2A*, *POLE*, *DICER1*, and *RICTOR* variants, in addition to more the commonly described *KIT* exon 11, 13, and 17 mutations. Use of next-generation sequencing may yield additional unique molecular profiles in future studies. This series also reports the first 2 cases of incidental esophageal GISTs in the setting of partially treated gastroesophageal adenocarcinoma, suggesting either an association with adenocarcinoma or possibly therapy-induced tumorigenesis. Finally, our institutional experience confirms the challenge of diagnosing this rare tumor, a known mimic of esophageal leiomyoma. A broad IHC panel in the setting of esophageal mesenchymal tumors may help to avoid this diagnostic pitfall.

631 Can Deep Learning Predict PD-L1 Status? A Fine-Tuned InceptionV3 Convolution Neural Network Architecture Accurately Determines PD-L1 Status in Colonic Adenocarcinoma

Devin Broadwater[1], Lynn Messersmith[2], Grant Williams[3], Nathaniel Smith[4]
[1]USAF, San Antonio, TX, [2]SAMMC, Fort Sam Houston, TX, [3]San Antonio Uniformed Services Health Education Consortium, Schertz, TX, [4]Brooke Army Medical Center, San Antonio, TX

Disclosures: Devin Broadwater: None; Lynn Messersmith: None; Grant Williams: None; Nathaniel Smith: None

Background: PD-L1 immunohistochemical staining is becoming increasingly important in the oncological treatment of various neoplasms. Interestingly, colonic adenocarcinomas show PD-L1-dependent morphological changes (medullary phenotype and increased tumor-infiltrating lymphocytes) rendering them potentially amenable to analysis by a Convolutional Neural Network (CNN). Previously, we have shown that CNNs have the potential to reduce costs and turnaround time associated with immunohistochemical (IHC) staining. Herein, we demonstrate that a fine-tuned InceptionV3 CNN architecture is able to accurately and confidently determine PD-L1 status from H&E images.

Design: A total of 1915 H&E images were acquired from 107 (68 PD-L1 negative, 39 PD-L1 positive) archived colonic adenocarcinoma cases. Cases were randomly partitioned into 1532 training (80%) and 383 test images (20%) without individual case overlap between the training and test sets. The training set was used to fine-tune a customized fully-connected layer on top of the InceptionV3 CNN architecture utilizing pre-trained ImageNet convolutional layer weights. The customized FC layer contained a single 256-unit hidden layer and 2 final output units with softmax activation to output a probability distribution over two classes (PD-L1 positive and PD-L1 negative). A ROC curve was used to determine the probability with the highest specificity.

Results: The CNN showed 81.2% overall accuracy. Mean predicted probability of the true class over the entire test set was 0.772 with a standard deviation of 0.299. Of 383 test images, 196 (51.2%) had a predicted class probability of > 0.95 (“Confident Prediction”) while 187 (48.8%) had a probability of 0.5 to 0.95 (“Equivocal Prediction”). The specificities with “confident” and “equivocal” predictions were 88.1% and 63.0%, respectively. IHC utilization with only “equivocal” predictions would result in 51.2% less IHC usage overall. Additionally, 51 cumulative days of turnaround time and up to $2550 worth of reagents are reduced per 100 cases. Figure 1 illustrates predicted PD-L1 status for various colonic adenocarcinoma cases at 200x magnification.

Figure 1 - 631

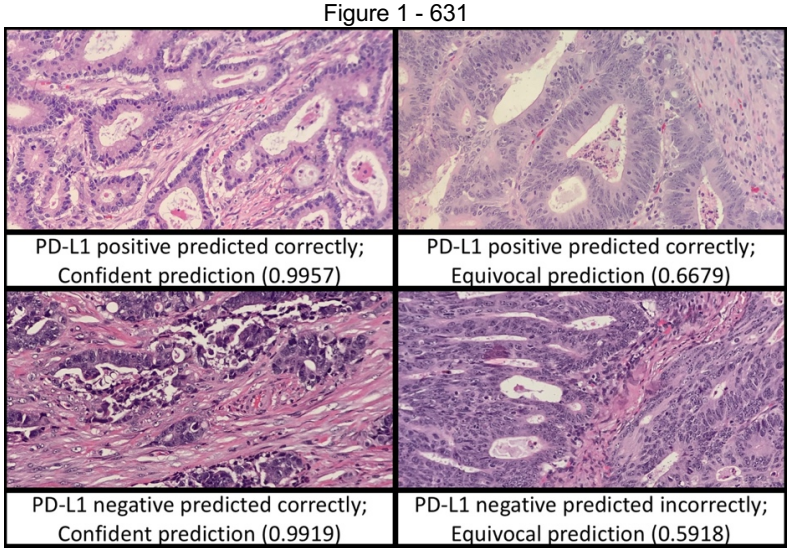

Conclusions: A fine-tuned InceptionV3 architecture provides an accurate and confident CNN model to predict PD-L1 status. We predict even further increases in accuracy as additional training images are collected from future intra- and interdepartmental cases.

632 Mutational Analysis of Colorectal Adenomatous Polyps in Childhood Cancer Survivors Treated with Radiation Therapy Using Targeted Next Generation Sequencing (NGS)

Hussam Bukhari[1], Sammy Au[2], Michael Nimmo[3], Baljinder Salh[2], Nazira Chatur[2]
[1]Vancouver, BC, [2]University of British Columbia, Vancouver, BC, [3]UBC, Vancouver, BC

Disclosures: Hussam Bukhari: None; Sammy Au: None; Michael Nimmo: None; Baljinder Salh: *Speaker*, Pfizer; Nazira Chatur: None

Background: Childhood cancer survivors treated with radiation therapy (RT) are at an increased risk of premalignant and malignant lesions, including early invasive colorectal carcinoma (CRC). It is well-established that RT-associated CRC undergo a preinvasive adenomatous stage where they can be detected and managed by early colonoscopy. Molecular profiling of these polyps using targeted NGS is highly sensitive and specific and may aid in unraveling their molecular composition. We aim to molecularly characterize colorectal adenomatous polyps in young cancer survivors treated with RT using a targeted NGS panel, as well as correlate the genetic findings with their histomorpholy.

Design: We extracted DNA from 18 adenomatous polyps which we acquired from 17 patients who received RT for childhood cancers. The median age is 35 at colonoscopy. The panel comprises 146 hotspots in 30 genes including: BRAF, KRAS, TP53, PIK3CA, PTEN and CTNNB1 etc. Four of the polyps had histopathologic diagnoses of sessile serrated adenoma/polyp (SSA/P) (22.2%), while the remaining 14 polyps were either tubular adenomas (TA), tubulovillous adenomas or TA with submucosal invasion (77.7%). High-risk features were defined as: size of 10 mm or greater, three or more adenoma, tubulovillous or villous histology or adenoma with high-grade dysplasia.

Results: Five polyps elucidated hotspot mutations at cancer-associated genes (27.7%), while the remaining 13 polyps were negative for the mutations tested (72.3%). Of the 5 mutated polyps, 2 polyps harbored substitution mutations in the KRAS gene at exon 2. The two polyps were non-serrated and showed high-risk histological features. Additionally, 2 other polyps showed substitution mutations in the BRAF V600E, with both polyps showing histological features of SSA/P. The last mutated polyp had a histological diagnosis of TA with submucosal invasion and elucidated a substitution mutation at the TP53 gene.

Conclusions: Our analysis demonstrates that RT-associated polyps harbor similar genetic changes to adenomas in the average-risk population. We postulate that RT-associated polyps follow the conventional 'adenoma-carcinoma sequence' or the alternative serrated pathway, making them amenable to detection and management by early colonoscopy. Furthermore, our panel failed to detect novel driving mutations in cancer-associated genes. More comprehensive molecular analysis of these polyps is required to understand their molecular composition and to aid in identifying actionable genetic alterations.

633 A Study on the Relationships between Genetic Characteristics and Prognosis in EBV and MSI Molecular Subtypes of Gastric Cancer

Lei Cai[1], Ruifen Wang[1], Yeqi Sun[1], Juanqing Yue[1], Junlei Li[1], Lifeng Wang[2]
[1]Xinhua Hospital, School of Medicine, Shanghai Jiao Tong University, Shanghai, China, [2]Shanghai, China

Disclosures: Junlei Li: None; Lifeng Wang: None

Background: As the role of MSI and EBV subtype was ever-increasing important in GC immunotherapy, the connections between clinicopathological characteristics and prognostic significance in Asia population remain unresolved. In addition, in-depth molecular mechanism why these two groups could benefit from the immunotherapy was also meaningful to be revealed.

Design: EBV(+) and MSI-H GC were examined in 279 GC cases by utilization of whole tumor paraffin sections. The EBV infection was proved by in situ hybridization. MSI-H was detected by combining PCR and immunohistochemical staining. GSE13911, GSE51575 GSE62254 and TCGA-STAD was downloaded from the GEO datasets or TCGA. WGCNA was used to identify the key modules. According to the expression of CD274(PD-L1 gene), KEGG enrichment and GO enrichment was performed to observe the different patterns. CD274 high expression samples in MSI and EBV was selected to be compared by the GSEA and GSVA.

Results: The MSI-H phenotype gained a good overall survival (P=0.0338, P=0.0028) and could predict the prognosis while it had no significant difference in EBV samples(P=0.5255, P=0.8670) in TCGA-STAD and GSE62254 datasets. MSI-H cases were associated with elderly age(P=0.017), stage(P=0.000)and good prognosis(P=0.013) in 275 definite cases. MSI-H is also nearly an independent prognostic factor(P=0.05, HR=2.33).The key modules were both tightly associated with the immune response in the MSI and EBV subtype and CD274 was one of the intersected gene. In MSI subtype, CD274 high expression was associated with the response to virus and IFN-γ that reflected the higher TMEscore that determined its prognostic values. EBV subtype was more prone to related to the T cell activation and the type 4 allergic reaction. MSI has more active adipogenesis and fatty acid metabolism in CD274 high expression groups.

Conclusions: MSI-H GC has good prognosis independent of different races. But for EBV(+) GC, no prognostic significance could be yielded in this study. The positive regulation of CD274 could be seen in all MSI and EBV related datasets. CD274 expression related to the response to virus and IFN-γ that reflected the high TMEscore in MSI GC subtype. T cell activation and type 4 allergic reactions were more evident in EBV subtype. MSI GC had significant difference in adipogenesis and fatty acid metabolism.

634 Abnormalities of the Appendiceal Orifice in Biopsy Samples: When is a Skip Lesion Not a Lesion?

Carlos Castrodad-Rodriguez[1], Tony El Jabbour[2], Jui Choudhuri[1], Nicole Panarelli[3]
[1]Montefiore Medical Center, Bronx, NY, [2]Tony El Jabbour, Bronx, NY, [3]Montefiore Medical Center, Scarsdale, NY

Disclosures: Carlos Castrodad-Rodriguez: None; Tony El Jabbour: None; Jui Choudhuri: None; Nicole Panarelli: None

Background: The appendix is a well-established "skip lesion" in ulcerative colitis, and inflammatory changes are frequently evident in biopsies from the appendiceal orifice. We have observed that the appendiceal orifice often has an irregular endoscopic appearance, even when the remainder of the colon appears normal. We performed this study to investigate the value of biopsy samples from the appendiceal orifice in the absence of other endoscopic abnormalities.

Design: All biopsy samples of the appendiceal orifice taken over a one-year period were reviewed. Patients undergoing screening colonoscopy or who reported recent onset of gastrointestinal signs and symptoms were included in the study. Those with an established clinical history of inflammatory bowel disease were excluded. The histologic features were correlated with endoscopic findings, clinical presentation, and findings in biopsies taken during the same procedure.

Results: Biopsies from 134 patients were included. Patients presented for screening colonoscopy (n=112), change in bowel habits (n=9), or signs and symptoms of gastrointestinal bleeding (n=13). Sampling was performed for the endoscopic impression of a polyp or nodule (n=93), or congested (n=32) or normal (n=9) mucosa. Most (88%) nodular orifices were detected during screening colonoscopies and some of them proved to harbor polyps (adenoma =22, sessile serrated polyp =7, hyperplastic polyp =12, Schwann cell hamartoma =1). However those detected during colonoscopies for other indications were normal (n=10) or showed focal cryptitis (n=1). Congested mucosa yielded normal biopsies in 27 (84%) cases, but 5 (16%) showed active colitis with (n=2) or without (n=3) features suggesting chronic injury. No patient with inflamed appendiceal orifice mucosa in either group had colitis in biopsies taken from other sites, and they either remained asymptotic or symptoms resolved by their follow-up appointment. Biopsies from normal mucosa were invariably without histologic abnormality.

Conclusions: We conclude that isolated abnormalities of non-polypoid appendiceal orifice mucosa rarely yield histologic findings with clinical implications, and they may lend themselves to over-interpretation, particularly when features of chronic injury are present. Those with features of colitis should be interpreted with caution, since they are usually not associated with abnormalities in the rest of the colon.

635 Expression of SWI/SNF Nucleosome Remodeling Complex Proteins in Colorectal Adenocarcinoma

Ivan Chebib[1], Azfar Neyaz[2], Steffen Rickelt[3], Yasmeen Qwaider[1], David Berger[4], Vikram Deshpande[4]
[1]Massachusetts General Hospital, Harvard Medical School, Boston, MA, [2]Massachusetts General Hospital, Malden, MA, [3]David H. Koch Institute for Integrative Cancer Research, Cambridge, MA, [4]Massachusetts General Hospital, Boston, MA

Disclosures: Ivan Chebib: None; Azfar Neyaz: None; Steffen Rickelt: None; Yasmeen Qwaider: None; David Berger: None; Vikram Deshpande: *Grant or Research Support*, Advanced Cell Diagnostics; *Advisory Board Member*, Viela; *Grant or Research Support*, Agios Pharmaceuticals

Background: Mutations in *SMARCB1/INI1*, member of the SWI/SNF nucleosome remodeling complex, are associated with sarcomas often with rhabdoid morphology. Mutations in other members of the SWI/SNF complex have been increasingly identified in other tumors, some even defined by loss of expression. Although mutations in some SWI/SNF members (ie *ARID1A*) are common, colorectal carcinoma (CRC) only rarely lose expression of SWI/SNF proteins, a subset with rhabdoid morphology. We assessed expression of SWI/SNF complex proteins in a cohort of CRC to determine whether loss of expression is associated with an undifferentiated epithelioid/rhabdoid morphology.

Design: Tissue microarrays (2-mm cores) were created containing CRC in 490 patients. Clinical, pathologic and microsatellite instability status (MSI) data was collected. Presence of an undifferentiated epithelioid or rhabdoid histology was identified. Immunohistochemical staining was performed for SWI/SNF complex proteins: ARID1A, SMARCB1, SMARCA4, SMARCA2, SMARCC1, SMARCC2, and SMARCE1. Nuclear expression was semi-quantitatively scored: 0-no expression; 1-weak expression; 2-strong expression. Loss of expression (score 0) was compared to presence of epithelioid/rhabdoid morphology (Mantel-Haenszel test). Decreased/loss of expression (score 0/1) was compared to MSI status (Fisher exact test). SWI/SNF complex expression was assessed in relation to survival (log-rank test).

Results: There were 490 patient-specimens. Of these, 4.7% showed undifferentiated epithelioid or rhabdoid morphology. There was absent expression of ARID1A in 7.2%, SMARCA4 in 0.7%, SMARCC1 in 0.2%, and SMARCE1 in 0.2%. ARID1A loss was the only marker associated with epithelioid/rhabdoid morphology in CRC (5/21, p=.002); however, ARID1A (16 cases), SMARCA4 (3), SMARCC1 (1) and SMARCE1 (1) showed loss of staining in CRC with conventional morphology and 16 cases showed epithelioid/rhabdoid morphology without loss of marker expression. Of cases with known MSI status, 44% with low/absent SMARCA4 expression were MSI-high, whereas only 20% of CRC with intact SMARCA4 were MSI-high (p=.095). Loss of expression was not associated with survival difference in any of the SWI/SNF evaluated.

Conclusions: Loss of SWI/SNF nucleosome remodeling complex proteins is rare in CRC. ARID1A is most commonly lost and is associated with undifferentiated epithelioid/rhabdoid morphology in a subset of cases. However, most cases with SWI/SNF expression loss maintain conventional CRC morphology.

636 The Changes of Histological Inflammatory Injury and Gene Expression Signatures in Ulcerative Colitis Associated with Colon Cancer Progression

Fengming Chen[1], Yongjun Liu[2], Francesca Ruggiero[3], Bryan Tsao[4], MaryElizabeth Stein[4], Suzanne Hile[4], Kristin Eckert[4]
[1]Penn State Health Hershey Medical Center, Hershey, PA, [2]The University of Wisconsin School of Medicine and Public Health, Madison, WI, [3]Penn State Health Milton S. Hershey Medical Center, Hershey, PA, [4]Penn State College of Medicine, Hershey, PA

Disclosures: Fengming Chen: None; Yongjun Liu: None; Francesca Ruggiero: None; Bryan Tsao: None; MaryElizabeth Stein: None; Suzanne Hile: None; Kristin Eckert: None

Background: Chronic inflammation is one of the hallmarks of cancer; however, the global gene expression changes caused by chronic inflammation that impact malignant progression are poorly understood. The goals of this study are to 1) evaluate the alteration of histological inflammation in ulcerative colitis (UC) associated with colon cancer progression; and 2) examine differential gene expression signatures in response to inflammatory changes.

Design: We examined non-malignant colon tissues in 9 UC (non-progressors), 9 UC with high grade dysplasia/cancer (progressors), and 8 control patients. To examine the extent of inflammatory injury, morphology was evaluated using Geboes histological score system at three sites (left, transverse and right colon) for each patient. Then RNA-seq analyses were performed using Lexogen Quantseq expression profiling.

Results: Histological inflammatory score is significantly higher at the entire colon and left colon in non-progressors than that in progressors ($p<0.05$, Figure 1A-1B). There is no difference at the transverse and right colon (Figure 1C-1D). In an accompanied pilot study, we are analyzing genome-wide differential gene expression. We identified 1,266 differentially expressed genes (DEGs) in progressor vs. controls and 1799 DEGs in non-progressors vs. controls, with 716 DEGs overlapping (FDR $p < 0.05$). The data was then analyzed according to different sites of colon. Interestingly, we only detected DEGs (171 DEGs in progressors vs control, 157 DEGs in nonprogressors vs control and 1 DEGs in progressors vs non-progressors) at the left colon, but almost none at the transverse and right colon. Those DEGs with log fold change >2 and FDR-adjusted q value< 0.05 are further shown in Volcano plots (Figure 2). Using Gene Ontology Enrichment analysis, we found that both progressors and nonprogressors show enrichment of inflammation-related processes. However, DEGs from progressors were also enriched in cell proliferation and differentiation pathways (such as REG3A, SFRP2, VEGF-A), suggesting an underlying neoplastic gene expression.

Figure 1 - 636

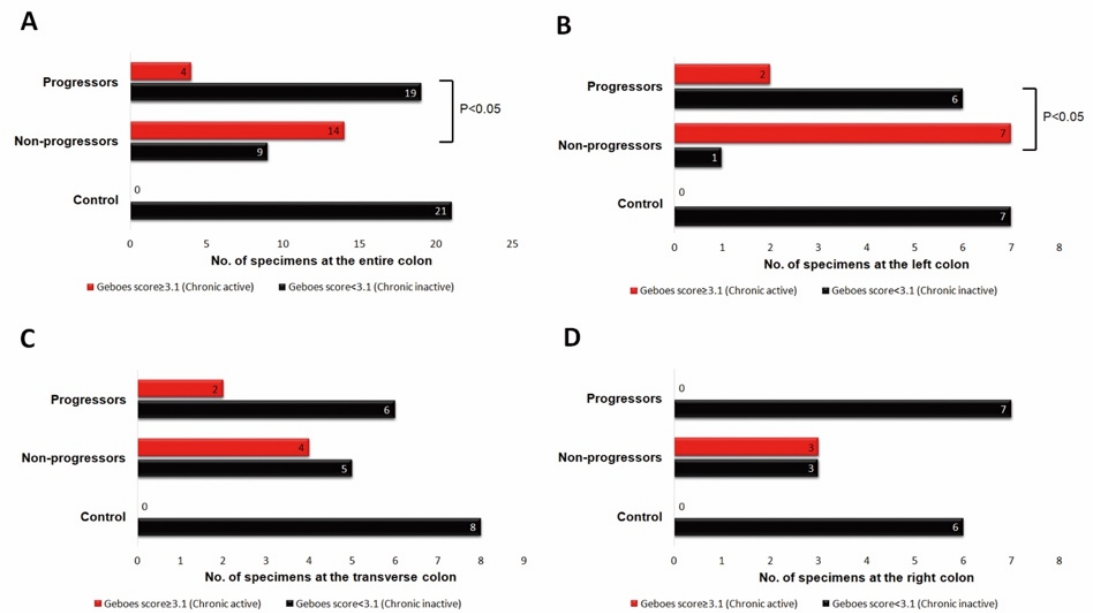

Figure 1. Association of disease severity with the status of histological activity (active disease defined as a Geboes' score ≥ 3.1) at the entire colon (A), left colon (B), transverse colon (C) and right colon (D). P: calculated by Fisher's exact for qualitative variables.

Figure 2 - 636

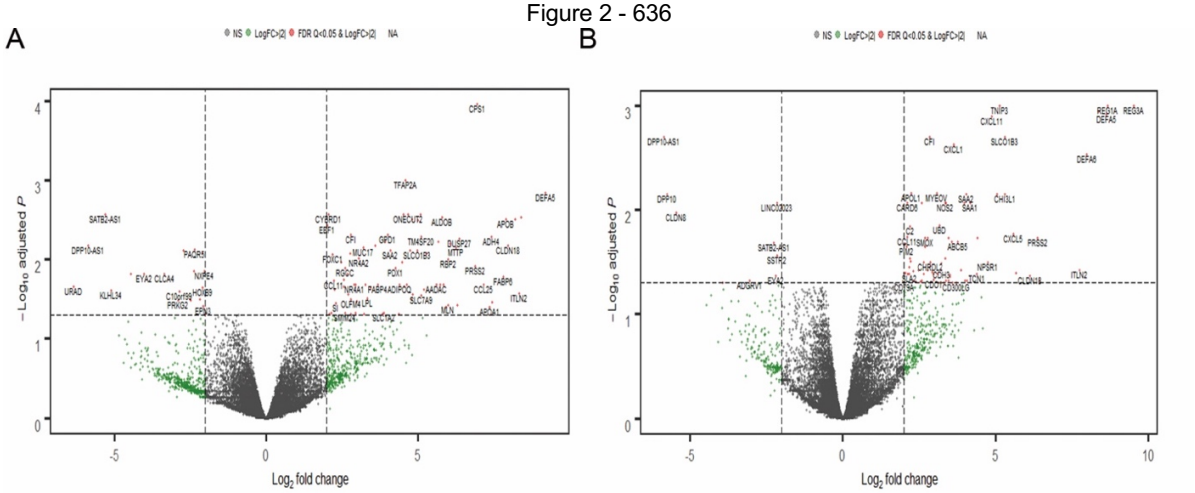

Figure 2. Volcano plots showing the global transcriptional changes in progressors vs. control (A) and non-progressors vs. control (B) at the left colon.

Conclusions: As compared to UC non-progressors, histological inflammatory injury for non-malignant colon tissues is lessened in UC progressors, especially at the left colon. RNA-seq analysis shows DEGs in progressors and non-progressors at the left colon may be involved in different pathways. Those findings suggest inflammatory changes may be the result of differential gene expression between progressors and nonprogressors.

637 Improved Interobserver Agreement in Keratin Immunohistochemistry-Assisted Diagnosis of Peritoneal Membrane Invasion by Colorectal Adenocarcinoma

Jey-Hsin Chen[1], Vikram Deshpande[2], Rajen Goyal[3], Donald Guinee[4], Gabriel Sica[5], Lisa Thomassen[6], Maria Westerhoff[7]
[1]Seattle, WA, [2]Massachusetts General Hospital, Boston, MA, [3]CellNetix Pathology and Laboratories, Seattle, WA, [4]Virginia Mason Medical Center, Seattle, WA, [5]Emory University Hospital, Atlanta, GA, [6]CellNetix Pathology and Laboratories, Issaquah, WA, [7]University of Michigan, Ann Arbor, MI

Disclosures: Jey-Hsin Chen: None; Vikram Deshpande: *Grant or Research Support*, Advanced Cell Diagnostics; *Advisory Board Member*, Viela; *Grant or Research Support*, Agios pharmaceuticals; Rajen Goyal: None; Donald Guinee: *Speaker*, Astra Zeneca; Gabriel Sica: None; Lisa Thomassen: None; Maria Westerhoff: None

Background: pT3 colorectal adenocarcinoma is clinicopathologically heterogeneous and associated with widely varying outcomes. Deeply invasive tumors, such as those that partially invade the peritoneal membrane, behave more aggressively than shallower tumors, and stratification of the pT3 category may more accurately reflect these differing risks. Evaluating tumor invasion of the peritoneal elastic lamina can be diagnostically difficult, which limits its reliability in clinical practice. Because there are localized keratin-expressing stromal cells in injured peritoneum associated with tumor invasion, we examined whether an immunostain for keratin along with an elastic stain can reliably improve the diagnosis of peritoneal membrane invasion by colorectal carcinoma.

Design: 50 cases of pT3 colorectal adenocarcinoma were analyzed for invasion of the peritoneal membrane by 6 experienced pathologists (3 GI + 3 non-GI; 3 academic + 3 non-academic) in 2 rounds separated by at least 3 months (round 1: H&E and elastic; round 2: H&E, elastic, and pan-keratin). The time to diagnosis and level of confidence (1=uncertain to 3=very confident) were also recorded. Statistical analyses were performed using R.

Results: Interobserver agreement (kappa) improved significantly from 0.435 to 0.767 with aid of a keratin immunostain. Subcategory examination also showed similar degrees of improvement among GI (0.405 to 0.706) and non-GI (0.423 to 0.865), and academic (0.479 to 0.689) and non-academic (0.373 to 0.808) pathologists. 5 of 6 observers reported significantly less time to diagnosis with the help of a keratin immunostain (overall range: round 1: 33 to 253 sec; round 2: 28 to 79 sec; mean difference: -175 to 12 sec), resulting in as much as 69% reduction in time. 5 of 6 pathologists also reported improved diagnostic confidence when aided by a keratin immunostain (round 1: 1.76 to 2.66; round 2: 2.18 to 2.96; mean difference: -0.22 to 0.94), with 4 reaching statistical significance. 1 observer felt mildly less confident with use of a keratin immunostain, but the change was not statistically significant.

Conclusions: Incorporating a keratin immunostain significantly improved the diagnostic agreement, performance, and confidence among a wide spectrum of practicing pathologists in analyzing tumor invasion of the peritoneal membrane. The reliable separation of pT3 tumors

into clear, anatomically-defined prognostic groups should aid in the oncologic management of more clinically aggressive pT3 colorectal carcinoma.

638 "Beiging" of Mesenteric Adipocytes is a Feature of Ileal Strictures of Crohn's Disease (CD)

Joyce Chen[1], Huaibin Mabel Ko[1], Hongfa Zhu[2], Alexandros Polydorides[1], Noam Harpaz[3], Qingqing Liu[1]
[1]Icahn School of Medicine at Mount Sinai, New York, NY, [2]Hackensack Pathology Associates, LLC, Hackensac, NJ, [3]Mount Sinai Medical Center, New York, NY

Disclosures: Joyce Chen: None; Huaibin Mabel Ko: None; Huaibin Mabel Ko: None; Hongfa Zhu: None; Alexandros Polydorides: None; Noam Harpaz: None; Qingqing Liu: None

Background: Based on pathological and radiological data, ileal strictures in CD have recently been subclassified into three major categories, "hypertrophic" strictures which feature fibromuscular expansion of the ileal wall layers, "constrictive" strictures which result from external narrowing that preserves the normal mural architecture, and a mixed category. The pathogenesis of constrictive stenosis is unknown. One unproven hypothesis invokes CD-related changes in the mesentery that result in fixed cocoon-like encasement of the intestine. In an effort to shed more light on these changes we evaluated the mesenteric adipocytes in all 3 stricture types by means of digital morphometry and gene expression.

Design: We studied mesenteric tissue from 21 resected ileal strictures from patients with CD, 6 hypertrophic, 7 constrictive and 8 mixed. Adipocyte area was determined by semi-automated digital image analysis of H&E sections using Image J (National Institute of Health) and Adiposoft 1.16 (University of Navarra). Gene expression analysis of paraffin-embedded mesenteric tissue was performed by quantitative PCR, focusing on genes that are involved in adipogenesis and fat metabolism such as Adp, Cebps, Pparg, Batf1 and Ucp1.

Results: Adipocyte areas were significantly decreased in all 3 stricture types compared with adipocytes in the uninvolved ileal mesentery of the same patients (Table 1); these include 4 of 6 hypertrophic strictures (4/6, 67%), 5 of 7 constrictive strictures (5/7, 71%), and 3 of 8 mixed stricture (3/8, 37.5%). In addition, we did not observe significant differences in adipocyte area among three types of strictures (one way anova, p=0.08, F ratio=2.85). Gene expression analysis revealed a trend toward upregulation of UCP1, a mitochondrial uncoupling protein, in hypertrophic and constrictive strictures (p=0.077 and p=0.070, respectively).

Table 1.

	Constrictive							
		Uninvolved			**Stricture**			
Cases	**Adipocyte number**	**Adipocyte mean area (um^2)**	**SD**	**Adipocyte number**	**Adipocyte mean area (um^2)**	**SD**	**Adipocyte area stricture/uninvolved ratio**	**P value**
1	857	1465.91	1682.56	633	1487.39	1749.26	1.01	0.81
2	583	2876.31	5894.12	659	1847.24	1949.05	0.64	<0.0001
3	840	1838.22	1756.97	498	763.19	2572.27	0.42	<0.0001
4	877	5653.86	4386.17	905	4480.77	4643.67	0.79	<0.0001
5	1136	3391.38	6886.44	2127	2151.20	1607.30	0.63	<0.0001
6	1351	2434.03	2280.07	1658	1908.15	1777.31	0.78	<0.0001
7	444	3345.40	7482.28	796	2758.41	4067.96	0.82	0.07
	Hypertrophic							
1	1365	2949.20	3425.34	1300	2787.76	3223.33	0.95	0.21
2	911	4718.06	4924.36	1497	2754.68	3103.88	0.58	<0.0001
3	726	3672.98	8590.04	1437	1928.34	1792.29	0.53	<0.0001
4	933	3072.47	2732.68	1896	2671.64	2510.24	0.87	<0.0001
5	1182	2630.28	4053.22	1357	2210.53	1895.59	0.84	<0.0001
6	768	2688.81	5879.29	343	2118.14	1751.68	0.79	0.078
	Mixed							
1	811	1481.76	1182.54	1444	1154.03	715.49	0.78	<0.0001
2	704	1726.28	1460.24	593	3427.93	2542.61	1.99	<0.0001
3	704	1726.28	1460.24	697	1662.92	1346.73	0.96	0.4
4	575	2110.46	2925.65	1126	1552.97	1002.48	0.74	<0.0001
5	639	2179.88	2775.45	951	1985.96	1342.95	0.91	0.06
6	639	2179.88	2775.45	864	1802.81	1507.45	0.83	<0.001
7	515	2140.52	2321.89	600	2356.37	2214.66	1.10	0.11
8	684	1529.27	1496.14	606	1654.18	1413.17	0.82	0.12

Conclusions: Reductions in adipocyte size and upregulation of UCP1 are features of "beiging," i.e., the assumption by white fat of brown fat characteristics. Our findings suggest that beiging of mesenteric adipocytes is a feature of ileal strictures of CD. The presence of beiging in all types of strictures, implying the phenomenon correlates with the disease status rather than specific stricture type. In addition, in view of the otherwise normal architecture and histology of constrictive strictures in CD, the presence of these morphological and potential metabolic changes implies a key role for the mesentery in producing intestinal stenosis.

639 Histologic Patterns of Treatment Response in Esophageal Squamous Cell Carcinoma - Does Granulomatous Response to Keratin Mean Anything?

Wei Chen[1], Lei Zhao[2], Agoston (Tony) Agoston[3], Abby White[3], Raphael Bueno[3], Emanuele Mazzola[4], Vikram Deshpande[5], Adam Bass[4], Mark Redston[3], Deepa Patil[3]
[1]Brigham and Women's Hospital and Harvard Medical, Boston, MA, [2]Brigham and Women's Hospital, Harvard Medical School, Boston, MA, [3]Brigham and Women's Hospital, Boston, MA, [4]Dana-Farber Cancer Institute, Boston, MA, [5]Massachusetts General Hospital, Boston, MA

Disclosures: Wei Chen: None; Lei Zhao: None; Agoston (Tony) Agoston: None; Abby White: None; Raphael Bueno: *Grant or Research Support*, Genentech;Roche;Merck;Siemens;Gritsone;Epizyme;Verastem; *Stock Ownership*, Navigation Sciences; *Speaker*, IASLC; Imig;AATS;Johnson and Johnson; Emanuele Mazzola: None; Vikram Deshpande: *Grant or Research Support*, Advanced Cell Diagnostics; *Advisory Board Member*, Viela; *Grant or Research Support*, Agios Pharmaceuticals; Adam Bass: None; Mark Redston: None; Deepa Patil: None

Background: Esophageal squamous cell carcinomas (ESCC) post-neoadjuvant therapy elicit a spectrum of histologic changes in resection specimens, including fibrosis, inflammation and granulomatous response to keratin. A detailed clinicopathologic evaluation of therapy-related changes with regards to type of response, treatment regimen and patient outcome has never been performed, and forms the basis of this study.

Design: Sixty-five cases of treated ESCC were collated from 2000 - 2012. Type of therapy, follow-up status, and the following pathologic features were recorded and analyzed: pre-treatment grade (cG) and stage (cTNM), resection G and stage, Modified Ryan Scheme for Tumor Regression Score (TRS), type and depth of histologic response.

Results: The mean age was 63y (range: 33-77); M:F ratio was 0.9:1. The cG distribution was: G1- 6%, G2- 31%, G3-26% and unknown-37%. Residual neoplasia was seen in 26% cases and the TRS was 0 - 75%, 1 - 6%, and 2 - 19%. The yTNM stage distribution was I-83%, II-5%, III-12%, IV-0%. The depth of response was T1-29%, T2-31%, T3-31%, T4-3%, and unknown-6%. (Table 1) Two major types of histologic responses were seen: inflammatory (lymphoplasmacytic infiltrate; 65%) and granulomatous [foreign-body type giant cells surrounding keratin debris; 35%)] (Fig 1). Granulomatous response was predominantly noted deep within the esophageal wall (69%), regardless of the cG or cTNM stage; while inflammatory response was usually limited to the submucosa (76%), and predominantly observed in cT1/T2 tumors (p=0.02). Platinum+5-FU therapy was more likely to elicit granulomatous response compared to non-5-FU therapy (31% vs 14%; p=0.07). Compared to inflammatory response, patients with granulomatous response were more likely to show longer overall survival (median survival: 8.4 vs 7.0 years); however, this association was of borderline significance (Fig 1).

Parameter	Inflammation response (n=42)	Granulomatous response (n=23)	P value
Pre-op Biopsy Grade (n=41)			0.307
G1	2 (5%)	2 (9%)	
G2	10 (24%)	10 (44%)	
G3	14 (33%)	3 (13%)	
Unknown	16 (38%)	8 (35%)	
Residual cancer present	9 (21%)	8 (35%)	0.255
Residual dysplasia present	3 (7%)	2 (9%)	1.000
TRS			0.412
0	33 (79%)	16 (70%)	
1	1 (2%)	3 (13%)	
2	8 (19%)	4 (17%)	
ypTNM			0.373
I	35 (83%)	19 (83%)	
II	3 (7%)	0 (0%)	
III	4 (10%)	4 (17%)	
IV	0 (0%)	0 (0%)	
Depth of response			<0.001
T1	16 (38%)	3 (13%)	
T2	16 (38%)	4 (17%)	
T3	5 (12%)	15 (65%)	
T4	1 (2%)	1 (4%)	
Could not be assessed	4 (9%)	0 (0%)	
Neoadjuvant regimen			0.07
Platinum with 5-FU	13(31%)	2(9%)	
Non 5-FU	6(14%)	7(30%)	
Unknown	23(55%)	14(61%)	

Figure 1 - 639

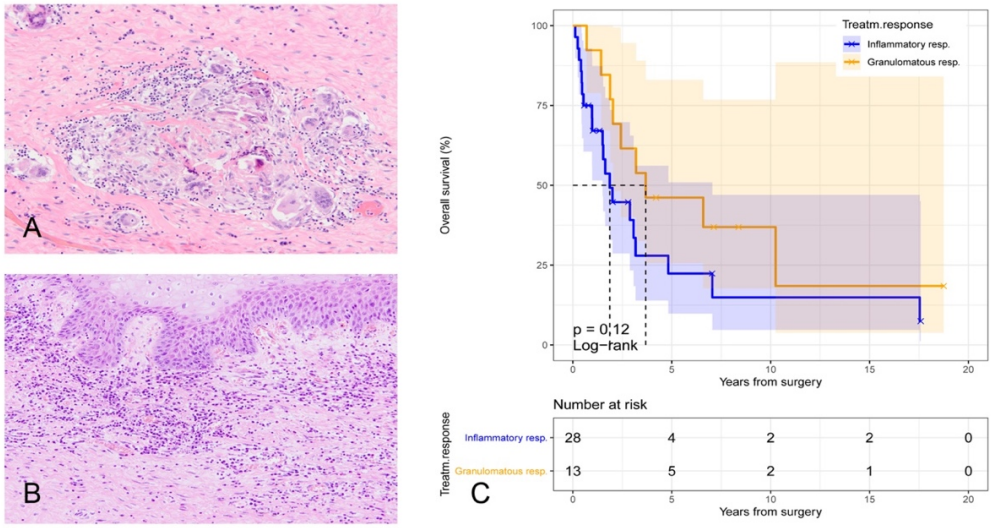

Figure 1. A. Granulomatous response (H&E, 100X). B. Inflammatory response (H&E, 100X). C. Kaplan-Meier survival curve to show differences in overall survival between patients with and without granulomatous response.

Conclusions: Up to 2/3rd of patients with treated ESCC show response to standardized therapy in the form of superficial chronic inflammation, while 1/3rd show transmural granulomatous response to keratin, regardless of the pre-operative stage, grade or amount of residual tumor. Granulomatous response is more likely to occur with 5-FU based regimen. Given the differences in patient outcome, reporting the histologic subtype of response may serve as a useful tool to guide further patient management.

640 Aberrant p53 Expression Predicts Neoplastic Progression in Barrett's Esophagus Diagnosed as Indefinite for Dysplasia

Xiuxu Chen[1], Sun A Kim[2], John Paulsen[2], Huaibin Mabel Ko[3], Hongfa Zhu[4], Alexandros Polydorides[3], Noam Harpaz[2], Qingqing Liu[3]
[1]Mount Sinai Hospital Icahn School of Medicine, New York, NY, [2]Mount Sinai Medical Center, New York, NY, [3]Icahn School of Medicine at Mount Sinai, New York, NY, [4]Hackensack Pathology Associates, LLC, Hackensac, NJ

Disclosures: Xiuxu Chen: None; Sun A Kim: None; John Paulsen: None; Huaibin Mabel Ko: None; Huaibin Mabel Ko: None; Hongfa Zhu: None; Alexandros Polydorides: None; Noam Harpaz: None; Qingqing Liu: None

Background: Aberrant p53 expression is known to correlate with neoplastic progression in Barrett's esophagus (BE) with low-grade (LGD) or high-grade dysplasia (HGD). It remains unclear whether this is also true for BE diagnosed as indefinite for dysplasia (IND).

Design: The study included all patients at our institution with established BE of any extent who underwent one index and at least one follow-up endoscopic examination between 2000 and 2019 in which the index biopsy diagnosis of IND was rendered and was accompanied by p53 immunohistochemical stain. Exclusion criteria included patients with prior LGD, HGD or adenocarcinoma (ACA) or with interval to follow-up examination of less than 1 year. Diagnoses of dysplasia were all rendered by subspecialized gastrointestinal pathologists and were routinely reviewed in a daily consensus conference supervised by a senior pathologist. p53 expression was classified as wild-type or aberrant, including overexpression or complete silencing. Median follow-up was 2.0 years (range, 1.0 to 6.5 years). Cross-sectional risks of progression from index IND to LGD, HGD or ACA in each p53 category were analyzed using Chi square test ($P<0.05$ considered significant).

Results: One hundred ten patients (71 males; median age 63, range 35-89) with index IND and concurrent p53 IHC were included. Nine patients (8.2%, 2 females, 7 males) had aberrant p53 expression and 101 patients (91.8%, 37 females, 64 males) had wild-type p53 expression. Four of nine patients with aberrant p53 expression (44.4%, 1 female, 3 males) progressed to higher grade lesions including one LGD, two HGD, and one ACA, whereas 11 of 101 (10.9%) patients with wild-type p53 expression progressed to higher grade lesions including 9 LGD and 2 HGD, but none developed ACA ($P=0.005$).

Conclusions: Aberrant p53 expression in patients with BE and IND correlates with neoplastic progression and may serve as a risk factor for purposes of clinical stratification.

641 Histopathological Analysis of 225 Gastric Biopsies with Lymphocytic Gastritis

Zongming Eric Chen[1], Hee Eun Lee[1], Thomas Smyrk[1]
[1]*Mayo Clinic, Rochester, MN*

Disclosures: Zongming Eric Chen: None; Hee Eun Lee: None; Thomas Smyrk: None

Background: Lymphocytic gastritis is a pattern of mucosa injury characterized by intraepithelial lymphocytosis (IEL) and increased lamina propria chronic inflammation. Reported associations include celiac disease, H. pylori and HIV infections, Crohn's disease, common variable immunodeficiency, collagenous colitis and certain medications. To better understand the histopathological spectrum of this entity, we conducted a comprehensive analysis of in house biopsies with the diagnosis in a single institution for a period of 20 years.

Design: Cases with a diagnosis of lymphocytic gastritis in a period of 20 years were retrieved and reviewed. Basic demographic information and detailed histopathological features are recorded and analyzed.

Results: A total of 225 biopsies (61 antral mucosa only, 53 fundic mucosa only, and 111 with both types) were analyzedfrom 222 patients (108 men and 114 women, M:F=1:1). with a mean age of 51.6±25 years (range 1 to 87). IEL was observed in all, with a mean count of 53+19.4 (range25-120) lymphocytes per 100 enterocytes. While chronic gastritis was also universal, 65 (28%) cases also showed acute inflammation. All samples were tested for H. pylori and organisms were found in 21 cases, all of which exhibited acute inflammation. Other distinct mucosal changes included erosion in 5 cases, intestinal metaplasia in 8 cases and glandular atrophy in 10 cases, respectively. In addition, 2 lymphomas (1 B-cell and 1 T-cell) were noted. No biopsy showed epithelial dysplasia or malignancy. Topology of lymphocytosis was analyzed in 111 biopsies which had both antral and fundic mucosa. A total of 21 (19%) cases showed site-specific differences including 11 with antrum and 10 with fundic predominance, respectively. Of all specimens, 132 cases had concurrent duodenal biopsies. Only 36 (27%) cases exhibited normal histology. The remaining 96 (73%) cases all showed IEL in duodenum. Furthermore, 41 of 96 (43%) cases also exhibited total villous atrophy, 34 (35%) cases with partially villous atrophy and 21 (22%) cases without villous architectural change.

Conclusions: Lymphocytic gastritis is relatively rare and current dataset represents one of the largest collections. The results highlight some new perspectives: 1. about 25% cases show concurrent acute inflammation, of which only 30% have detectable H. pylori; 2. Topological difference of lymphocytosis is only prominent in <30% cases; 3. Most cases show concurrent duodenal mucosal abnormalities.

642 Which Criteria Do Pathologists Use to Establish a Diagnosis of Chronic Ileitis?

Kenrry Chiu[1], Jose Jessurun[1], Rhonda Yantiss[1]
[1]*Weill Cornell Medicine, New York, NY*

Disclosures: Kenrry Chiu: None; Jose Jessurun: None; Rhonda Yantiss: None

Background: Recognizing chronic ileitis in mucosal biopsy samples is straightforward when pyloric metaplasia is present, but diagnostic criteria in the absence of pyloric metaplasia are not well defined. Features such as architectural changes and cellular changes are variably used, but studies validating specific histologic patterns as chronic are lacking. The purpose of this study was to gauge criteria used by pathologists to establish a diagnosis of chronic ileitis in their clinical practice.

Design: We invited pathologists with interest in gastrointestinal pathology to complete an online survey regarding their use of various criteria for a diagnosis of chronic ileitis including pyloric metaplasia, villous architectural abnormalities, plasma cell-rich infiltrates, the number and distribution of goblet cells and Paneth cells, and alterations in the muscularis mucosae, and to state their years of practice. We asked whether they would classify 9 images of ileal biopsy samples as chronic to gauge application of these criteria, without confirming that biopsies were obtained from patients with Crohn ileitis.

Results: There were 217 respondents with near equal numbers of participants having less than 5 years, 5-10 years, and >10 years of clinical experience. Seventy-two (33%) considered pyloric metaplasia a necessary requirement for a diagnosis of chronic ileitis, particularly those with <5 years of practice (48%, p=0.01 vs those with more years of experience). Other criteria considered important by most pathologists included abnormal crypt architecture (80%), variable villous shape (63%), and plasma cell expansion of the lamina propria (61%). Fewer utilized as indicative of chronicity increased plasma cells distant from lymphoid aggregates (48%), granulomata (39%), Paneth cell hyperplasia (29%), Paneth cell misplacement (32%), splayed and/or thickened muscularis mucosae (25%), goblet cell hyperplasia (19%), and patchy mononuclear inflammation (14%). An image depicting pyloric metaplasia was classified as chronic ileitis by 96% of participants, but those depicting the aforementioned features unaccompanied by pyloric metaplasia were classified as chronic ileitis at rates ranging from 20-78%.

Conclusions: One-third of gastrointestinal pathologists require pyloric metaplasia to diagnose chronic ileitis, particularly those recently out of training. Other common criteria include mucosal architectural abnormalities and plasma cell-rich infiltrates, whereas few utilized Paneth and goblet cell abnormalities.

643 Histologic Features of Chronic Ileitis in Biopsy Samples: Beyond Pyloric Metaplasia

Kenrry Chiu[1], Cindy Wang[2], Jerome Cheng[3], Maria Westerhoff[3], Lindsay Alpert[2], Jose Jessurun[1], Rhonda Yantiss[1]
[1]Weill Cornell Medicine, New York, NY, [2]The University of Chicago, Chicago, IL, [3]University of Michigan, Ann Arbor, MI

Disclosures: Kenrry Chiu: None; Cindy Wang: None; Jerome Cheng: None; Maria Westerhoff: None; Lindsay Alpert: None; Jose Jessurun: None; Rhonda Yantiss: None

Background: Chronic ileitis is a feature seen in Crohn disease. Pathologists often rely on pyloric metaplasia to diagnose chronic ileitis, even though Crohn disease causes other abnormalities, the predictive value of which is not clear. The purpose of this study was to better delineate histologic criteria for chronic ileitis that distinguish it from other causes of ileitis.

Design: We evaluated 20 resection and 20 biopsy specimens from 40 patients with Crohn ileitis in order to define architectural and inflammatory features of chronic ileitis, as well as their frequencies in biopsy material. We then assessed 110 study patients with active ileitis, none of whom had established Crohn disease prior to colonoscopy. Clinical characteristics and histologic features of ileal biopsy samples from patients who ultimately proved to have Crohn disease were compared with those of patients who did not develop Crohn disease in at least 10 months of follow-up.

Results: The resection specimens and biopsy samples from Crohn disease patients showed villus-to-villus variability and plasma cell-rich infiltrates with frequent crypt architectural abnormalities (100% and 70%), Paneth cell hyperplasia and/or Paneth cells on lateral aspects of crypts (100% and 90%), goblet cell hyperplasia (100% and 90%), splayed or thickened muscularis mucosae (100% and 65%), pyloric metaplasia (100% and 50%), and aphthous ulcers (95% and 30%). 54 study patients developed Crohn disease and 56 did not (Table 1). Those with Crohn disease were significantly younger (mean: 37 vs 51 years, p<0.01) with gastrointestinal symptoms (89% vs 57%, p<0.01), endoscopic ileitis (93% vs 74%, p=0.01) or colitis (44% vs 4%, p<0.01), inflamed colonic biopsies (43% vs 11%, p<0.01), and less frequent NSAID use (7% vs 36%, p<0.01). Their ileal biopsies showed more frequent variation in villous (83% vs 66%, p=0.05) and crypt architecture (57% vs 18%, p<0.01), splayed muscularis mucosae (45% vs 23%, p=0.02), pyloric metaplasia (39% vs 11%, p<0.01), and granulomata (9% vs 0%, p=0.03).

Histologic Feature	Crohn Ileitis n=54	Ileitis without Crohn Disease n=56	P value
Patchy chronic inflammation	36 (67%)	32 (57%)	0.33
Villus-to-villus variability	45 (83%)	37 (66%)	**0.05**
Crypt architectural distortion	31 (57%)	10 (18%)	**<0.0001**
Pyloric metaplasia	21 (39%)	6 (11%)	**0.0008**
Paneth cell hyperplasia	29 (54%)	41 (73%)	**0.05**
Paneth cells beyond crypt bases	31 (57%)	34 (61%)	0.84
Goblet cell hyperplasia	41 (76%)	38 (68%)	0.40
Plasma cells expanding villi	27 (50%)	30 (54%)	0.85
Plasma cells expanding mucosa	40 (74%)	34 (61%)	0.16
Splayed muscularis mucosae	23 (45%)	13 (23%)	**0.02**
Granulomas	5 (9%)	0	**0.03**
Aphthous ulcers	13 (24%)	8 (14%)	0.23

Conclusions: Ileal biopsy samples from patients who present with, or ultimately develop, Crohn disease show a variety of histologic abnormalities, many of which can be seen in NSAID-related injury and other types of ileitis. Architectural abnormalities of villi, crypts, and the muscularis mucosae, pyloric metaplasia, and granulomata are significantly more common in patients with ileitis who ultimately prove to have Crohn disease than patients with ileitis due to other causes.

644 Autoimmune Gastritis can be Prospectively Identified in a Background of Active Helicobacter pylori Infection

Jui Choudhuri[1], Carlos Castrodad-Rodriguez[1], Tony El Jabbour[2], Sara Hall[3], Maria Westerhoff[4], Nicole Panarelli[5]
[1]Montefiore Medical Center, Bronx, NY, [2]Tony El Jabbour, Bronx, NY, [3]Michigan Medicine, Ann Arbor, MI, [4]University of Michigan, Ann Arbor, MI, [5]Montefiore Medical Center, Scarsdale, NY

Disclosures: Jui Choudhuri: None; Carlos Castrodad-Rodriguez: None; Tony El Jabbour: None; Sara Hall: None; Maria Westerhoff: None; Nicole Panarelli: None

Background: *Helicobacter pylori* infection triggers development of autoimmune gastritis (AIG) in some genetically predisposed patients. Patients who develop AIG after *H. pylori* eradication may have persistently elevated risk of AIG-related complications. Features of early

AIG are described, but findings that confirm its presence in the background of *H. pylori*-associated gastritis have not been systematically evaluated. We performed this study to determine whether any features reliably identify AIG in biopsy samples with active *H. pylori* infection.

Design: We searched the pathology databases of two institutions between 2013-2019 for 1) cases of *H. pylori*-associated gastritis wherein pathologists prospectively noted features of AIG and 2) patients with *H. pylori*-associated gastritis who had successful eradication therapy and subsequent biopsies diagnostic of AIG. Patients who had successful *H. pylori* eradication, but no AIG after 10 years of follow-up served as controls. Cases were evaluated for features associated with AIG. Enterochromaffin-like (ECL) cell hyperplasia was detected with chromogranin immunostains.

Results: Pathologists prospectively raised the possibility of AIG in the setting of *H. pylori* infection in eight study subjects. These displayed full-thickness inflammation of oxyntic mucosa (88%), partial loss of oxyntic glands (88%), pyloric metaplasia (38%), ECL cell hyperplasia (100% of tested cases), and intestinal metaplasia (IM) (25%) (Table 1). Eight study subjects had *H. pylori*-associated gastritis followed by *H. pylori*-negative sampling that showed well-developed AIG in biopsies taken 6-144 months later (Figure 1). Retrospective review of their original biopsies displayed similar rates of full-thickness inflammation of oxyntic mucosa (100%) (Figure 2A), oxyntic gland loss (88%), pyloric metaplasia (38%) (Figure 2B), ECL cell hyperplasia (100% of tested cases) (Figure 2C), and IM (38%) in the presence of *H. pylori* (Figure 2D). Except for IM, these features were absent in all 18 control cases.

Table 1. Features of Study and Control Cases

Features	Prospective Study Cases (n=8) No (%)		Retrospective Study Cases (n=8) No (%)	Follow-up Biopsies of Retrospective Cases (n=7)* No (%)	Controls (n=18) No (%)
M:F, Mean age (years)	2:6, 67		1:7, 57	N/A	4:5, 65
Full thickness inflammation of oxyntic mucosa	7 (88)		8 (100)	7 (100)	0
Oxyntic gland loss					
None	1 (13)		1 (13)	0	18 (100)
<50%	2 (25)		4 (50)	1 (14)	0
>50%	5 (63)		3 (38)	6 (94)	0
Pyloric metaplasia	3 (38)		3 (38)	7 (100)	0
ECL cell hyperplasia					
Unknown	3 (38)		3 (38)	0	0
Absent	0		0	1 (14)	18 (100)
Linear	0		4 (50)	3 (43)	0
Linear and nodular	5 (63)		1 (13)	3 (43)	0
Intestinal metaplasia	2 (25)		3 (38)	5 (71)	2 (11)
Pancreatic metaplasia	0		0	1 (14)	0

*One follow-up biopsy was not available for review

Figure 1 - 644

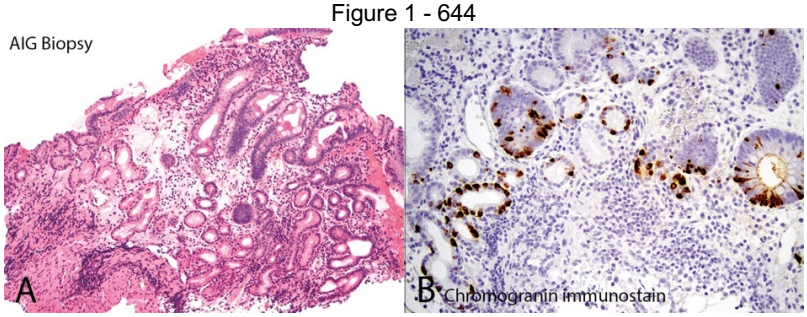

Figure 2 - 644

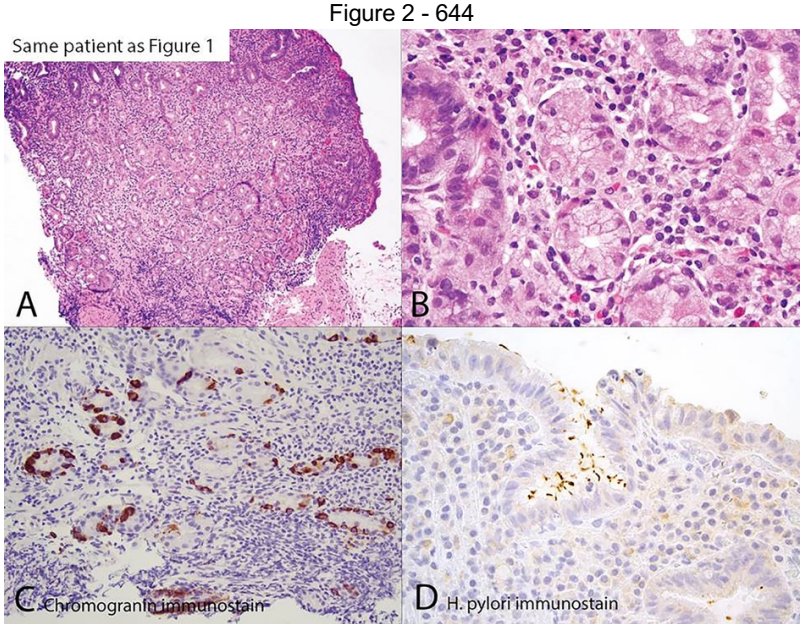

Conclusions: Findings in *H. pylori* gastritis from patients with subsequent biopsy-proven AIG support raising the possibility of AIG, even in a background of *H. pylori* infection, if typical features are present. Full thickness inflammation with oxyntic gland loss, pyloric metaplasia, and ECL cell hyperplasia may help to identify patients with persistently elevated risk of developing AIG-related complications, such as adenocarcinoma and Vitamin B12 deficiency, after *H. pylori* eradication.

645 Deconstructing the Diagnosis of Upper Gastrointestinal Dysplasia: An Analysis of 60 Cases and Evaluation of Cyto-Architectural Features

Till Clauditz[1], Gustavo Baretton[2], Ian Brown[3], David Boulware[4], Franziska Büscheck[5], Won-Tak Choi[6], Till Krech[7], Rish Pai[8], Kieran Sheahan[9], Tomas Slavik[10], Gregory Lauwers[11]
[1]Hamburg University, Hamburg, Hamburg, Germany, [2]Dresden, Saxony, Germany, [3]Brisbane, QLD, Australia, [4]H. Lee Moffitt Cancer Center, [5]Universitätsklinikum Hamburg Eppendorf, Hamburg, Germany, [6]University of California San Francisco, San Francisco, CA, [7]Pathocom, Osnabrück, Germany, [8]Mayo Clinic Arizona, Scottsdale, AZ, [9]St Vincent's University Hospital, Dublin, Dublin, Ireland, [10]Ampath Pathology Laboratories and University of Pretoria, Pretoria, South Africa, [11]H. Lee Moffitt Cancer Center & Research Institute, University of South Florida, Tampa, FL

Disclosures: Till Clauditz: None; Gustavo Baretton: None; Ian Brown: None; Franziska Büscheck: None; Won-Tak Choi: None; Till Krech: None; Rish Pai: None; Kieran Sheahan: None; Tomas Slavik: None; Gregory Lauwers: None

Background: The diagnosis of gastrointestinal dysplasia is based on the evaluation of widely accepted cyto-architectural criteria. Yet, inter observer agreement (IOV) is only fair to good in distinguishing high-grade dysplasia [HGD] / intramucosal carcinoma [IMC] from normal and poor for low grade dysplasia [LGD] vs reactive/normal. Interestingly, the relative weight of each independent criterion used in reaching the diagnosis has not been fully evaluated.

Design: A series of 60 digital slides of gastro-esophageal biopsies corresponding to all diagnostic possibilities (normal, reactive, indeterminate, LGD, HGD/IMC) were circulated among 8 pathologists. In addition to diagnostic concordance, cytologic [including hyperchromatic nuclei, nuclear (bolder-like) irregularity, chromatin clearing, prominent nucleoli, N/C ratio, nuclear stratification, lack of cell maturation, increased mitoses] and architectural features [such as villiform surface, bridging, back to back/cribriforming, budding] were evaluated. Acute epithelial inflammation and chronic stromal inflammation were also assessed.

Results: The overall kappa value (*K)* for the entire cohort was 0.268 confirming a fair agreement when considering all diagnoses. Of the 15 morphologic features evaluated, 9 were recognized with a $K > 0.250$ [fair agreement] including acute intraepithelial inflammation, villiform surface, bridging, round (bolder-like) irregular nuclei, prominent nucleoli, high N/C ratio, increased mitoses (epithelial surface & pits) and two > 0.4 [moderate agreement] , i.e., lack of maturation and back to back/cribriforming. Using a formula [by simply adding 8 of the 9 features but subtracting acute inflammation], a fair to good level of agreement was reached among the 8 raters [intraclass correlation coefficient (ICC]) of 0.531]. There was a near perfect segregation of IMC & HGD from LGD. (Fig. 1: scores of each diagnostic categories using 9 histologic features)

Figure 1 - 645

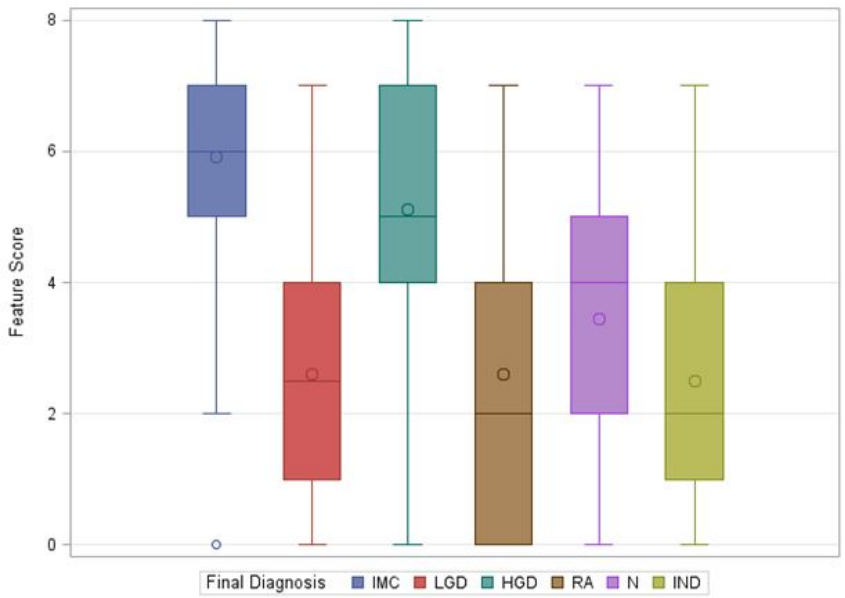

Conclusions: Our study demonstrates that some histologic features included in the traditional definition of dysplasia are not uniformly recognized and agreed upon by pathologists. By only focusing on the cyto-architectual features with fair to moderate IOV, we were able to achieve a better agreement among the 8 pathologists and to better segregate IMC/HGD from LGD. This method may help refining the diagnostic criteria and allow to develop a scoring system. Follow up studies will also help to determine if the methodology is a better predictor of progression.

646 Prognosis in Colorectal Adenocarcinomas with a Mucinous Component

Andrew Crabbe[1], Azfar Neyaz[2], Vikram Deshpande[1]
[1]Massachusetts General Hospital, Boston, MA, [2]Massachusetts General Hospital, Malden, MA

Disclosures: Andrew Crabbe: None; Azfar Neyaz: None; Vikram Deshpande: *Grant or Research Support*, Advanced Cell Diagnostics; *Advisory Board Member*, Viela; *Grant or Research Support*, Agios Pharmaceuticals

Background: Mucinous colorectal adenocarcinomas have been defined to be those tumors for which greater than 50% of the lesion is comprised of extracellular pools of mucin. It is the most commonly reported subtype of colorectal adenocarcinoma; however, the prognostic significance of this histologic phenotype has been much debated. Further, it is even less clear whether having a mucinous component that falls short of the 50% threshold has an impact on prognosis.

Design: We evaluated 813 cases of untreated colorectal adenocarcinomas resected between 2004 and 2015. The percentage of mucinous component in each primary tumor was evaluated by two pathologists. We recorded the following histologic features: pTNM stage, tumor grade, small vessel, extramural venous and perineural invasion. Mismatch repair protein status and survival data was recorded. We correlated the these features along with survival using univariate (Log Rank test) analysis. X-Tile software was used to determine optimal cut-points for overall survival.

Results: In this cohort of 813 cases (mean age: 67.8 yrs, M:F = 0.96), there were 60 cases (7.4% of total) that met conventional criteria for mucinous adenocarcinoma and 243 cases (29.9% of total) that had a percentage of mucinous component of at least 5% (mean percentage of mucinous component = 36%, ranging from 5 to 95%). Mucinous adenocarcinomas were associated with decreased overall survival ($p < 0.001$), but further, there was decreased overall survival in carcinomas with mucinous components of only greater than 10% ($p = 0.010$). This threshold of 10% was confirmed as the optimal cut-point for differentiating based on overall survival using X-Tile software. Interestingly, mucinous differentiation (defined at greater than 10%) correlated with decreased survival in patients with mismatch repair (MMR) proficient tumors ($p < 0.001$), though did not correlate with survival in those with MMR deficient tumors ($p = 0.132$).

	% of cases (n)	Mean survival in months	P value
Gender Male Female	49.2% (400) 50.8% (413)	132.0 ± 3.8 130.2 ± 3.7	0.831
T stage: T1 T2 T3 T4	7.7% (63) 15.4% (126) 51.6% (420) 25.1% (204)	167.3 ± 3.0 154.6 ± 4.6 137.9 ± 3.5 91.9 ± 6.0	< 0.001
N stage: N0 N1 N2	56.2% (457) 25.7% (209) 18.0% (147)	152.8 ± 2.7 129.6 ± 5.2 67.4 ± 6.6	< 0.001
M stage: M0 M1	88.3% (715) 11.6% (94)	146.0 ± 2.5 39.1 ± 4.4	< 0.001
Tumor grade: Low (well to mod) High (poor)	80.2% (640) 19.8% (158)	137.7 ± 2.8 102.0 ± 7.1	< 0.001
Small vessel invasion: No Yes	59.2% (453) 40.8% (312)	150.5 ± 2.8 102.5 ± 4.7	< 0.001
Extramural venous invasion: No Yes	67.3% (547) 32.7% (266)	152.0 ± 2.4 86.9 ± 5.4	< 0.001
Perineural invasion: No Yes	74.4% (601) 25.6% (207)	146.5 ± 2.6 90.6 ± 5.8	< 0.001
Mucinous differentiation > 50%: No Yes	92.6% (753) 7.4% (60)	134.0 ± 2.7 103.0 ± 10.8	< 0.001
Mucinous differentiation > 25%: No Yes	85.4% (695) 14.5% (118)	134.7 ± 2.8 114.5 ± 7.3	0.002
Mucinous differentiation > 10%: No Yes	80.0% (650) 20.0% (163)	134.9 ± 2.9 118.6 ± 6.3	0.010

Conclusions: Colorectal adenocarcinomas with a mucinous component greater than 10% of total tumor are associated with decreased overall survival. The current threshold for diagnosis of mucinous colorectal adenocarcinoma may require reevaluation.

647 A Specific Lobulated Growth Pattern Identifies Syndromic Gastric Polyps

Rory Crotty[1], Azfar Neyaz[2], Julie Tse[3], Vikram Deshpande[1]
[1]Massachusetts General Hospital, Boston, MA, [2]Massachusetts General Hospital, Malden, MA, [3]Boston, MA

Disclosures: Rory Crotty: None; Azfar Neyaz: None; Julie Tse: *Employee*, Foundation Medicine, Inc.; *Consultant*, Pathology Watch, LLC.; Vikram Deshpande: *Grant or Research Support*, Advanced Cell Diagnostics; *Advisory Board Member*, Viela; *Grant or Research Support*, Agios Pharmaceuticals

Background: Gastric polyps are often sporadic and reactive in nature, commonly occurring in the setting of gastritis. However, gastric polyps may also be a manifestation of a polyposis syndrome, such as Peutz-Jeghers polyposis (PJP), juvenile polyposis syndrome (JPS), or tuberous sclerosis (TS). These polyps are important to identify, as the patient may be at a significantly increased risk of malignancy.

As the morphologic spectrum of sporadic hyperplastic polyps in the stomach overlaps significantly with syndromic gastric polyps, identifying syndromic polyps may be challenging, and no consistent differentiating histologic features have been identified. However, in our practice, we have found that a lobulated growth pattern is often present in syndromic polyps. We aimed to evaluate whether this pattern could be used as a reliable marker of systemic polyposis.

Design: We searched our records for patients with a diagnosis of PJP, JPS, or TS, who had undergone biopsy of a stomach polyp. A control cohort of gastric polyps from patients with no documented polyposis syndrome was selected randomly from our records. For each case, H&E and desmin slides were reviewed by two pathologists, including one gastrointestinal pathology expert. Histologic details, including lobulated growth, were evaluated and compared between the two groups.

Results: We identified 16 patients with a polyposis syndrome (8 PJP, 5 JPS, 2 TS, 1 undetermined), and 23 control patients. 27 syndromic polyps (16 PJP, 5 JPS, 5 TS, 1 UD) and 25 sporadic polyps were reviewed.

We identified two patterns of lobular growth. The first, defined by lobules of foveolar epithelium at least 50% surrounded by curvilinear desmin-positive muscle fibers, did not distinguish between syndromic and sporadic polyps (82% vs. 76%, p>0.05). However, the second pattern, defined by lobules with a dilated central gland surrounded by hyperplastic foveolar epithelium and at least a partial rim of pyloric glands, resembling invaginated gastric mucosa, was significantly different between syndromic and sporadic polyps (48% vs. 8%, p<0.05). This pattern was most common in PJP (11/16 cases), and was seen in 1/5 cases of TS and JPS.

Other factors, such as polyp size, the extent of foveolar hyperplasia, or the amount of muscle splaying, did not distinguish between groups.

Conclusions: We have identified a specific pattern of lobular growth that aids in distinguishing syndromic gastric polyps, especially those of PJP, from sporadic gastric polyps.

648 Confocal Microscopy of Colorectal Polyps as an Alternative Fast and Unexpensive Microscopic Diagnosis

Miriam Cuatrecasas Freixas[1], Jose Guerrero[2], Javiera Perez-Anker[3], Henry Cordova[4], Ivan Archilla[2], Adriana Garcia Herrera[4], María Teresa Rodrigo[5], Maria Pellise[4], Gloria Fernandez-Esparrach[4]
[1]Hospital Clinic, Universitat de Barcelona, Barcelona, Spain, [2]Hospital Clinic, University of Barcelona, Barcelona, Spain, [3]Hospital Clinic de Barcelona, Barcelona, Spain, [4]Hospital Clinic, Barcelona, Spain, [5]Department of Pathology, Hospital Clinic, Barcelona, Spain

Disclosures: Miriam Cuatrecasas Freixas: None; Jose Guerrero: None; Javiera Perez-Anker: None; Henry Cordova: None; Ivan Archilla: None; Adriana Garcia Herrera: None; María Teresa Rodrigo: None; Maria Pellise: None; Gloria Fernandez-Esparrach: None

Background: Colorectal cancer (CRC) screening programmes have accomplished a significant reduction in mortality caused by this disease. Colonoscopy, as an early cancer detection procedure, allows the identification and removal of polyps for the gold-standard histological analysis. The increasing number of colonoscopies has created bottlenecks in pathology departments due to the huge number of samples to be analysed. We aimed to use alternative ways of diagnosis to overcome such bottlenecks.

Design: Thirty-eight polyps obtained through colonoscopy from twenty-two patients were assessed by conventional histology and confocal microscopy. Real time scanning of the fresh tissue was made with the confocal microscope in fusion mode (fluorescence plus reflectance) VivaScope® 2500M-G4TM. Afterwards, conventional histopathologic process of the tissue was performed. After making a consensus meeting to establish a list of the microscopic features to be evaluated, confocal images were reviewed by four pathologists blind to the haematoxylin and eosin (H&E) results. Histologic features were recorded on a data sheet by all pathologists. Diagnosis with both methods H&E and confocal were compared.

Results: Twenty polyps (52,6%) were diagnosed as tubular adenomas, fourteen (36,8%) as sessile-serrated adenomas/polyps, two (5,3%) as hyperplastic polyps, one (2,6%) as normal colonic mucosa, and one (2,6%) was not assessable. Full consensus of all features with confocal diagnoses was achieved in twenty-four cases (63,2%), with minor discrepancies in 10/38 (26,3%) and major discrepancies in 4/38 (10,5%) cases. When comparing with the H&E, confocal diagnosis was reliable and concordant in 79,2%, with minor discrepancies in the rest. Tubular adenomas were the easiest to recognise with confocal microscopy (93,3%), whilst high-grade dysplasia was the hardest feature to assess.

Conclusions: Confocal microscopy allows whole scanning of the tissue in real time and does not interfere with a subsequent pathological analysis. It is a promising tool with high reliability and reproducibility compared to gold standard diagnostics. Its main advantages are the time saving (2-5 minutes processing per sample) compared to conventional histopathology analysis, and limited required personnel. This alternative morphology-based diagnostic method may contribute to reduce the rising workload in pathology departments and bring significant economic savings in a scenario of CRC screening programmes.

649 Heterogeneity of Signet Ring Cell Carcinoma at Different Primary Sites - Human Observation Precedes Artificial Intelligence

Wissam Dahoud[1], Rami Imam[1], Laura Tang[1]
[1]Memorial Sloan Kettering Cancer Center, New York, NY

Disclosures: Wissam Dahoud: None; Rami Imam: None; Laura Tang: None

Background: Signet ring cell morphology is a distinct feature in adenocarcinomas commonly arising from the gastrointestinal tract, pancreatobiliary system, and other anatomical sites. Elucidating unknow primary sites from signet ring cell morphology in metastases presents a diagnostic challenge and requires ancillary studies such as immunohistochemistry or molecular tests. This study examines histologic patterns and cytologic features in adenocarcinomas with signet ring cell features from established primary sites to describe objective criteria which can aid in identifying the primary site of these tumors.

Design: Cases of primary and metastatic adenocarcinomas with signet ring cell features were identified from the pathology database at our institution (n=40). The primary sites included GEJ, stomach, colorectum, appendix, pancreatobiliary system, breast, and lung. H&E sections were scored using architectural and cytologic criteria. The architectures included infiltrative, gland formation, confluence, dis-cohesive, extracellular mucin, and single file pattern. The cytologic criteria included nuclear/cytoplasmic ratio (>25% vs. <25%), percent of signet ring cells within the tumor (<50% vs. >50%), and nature of cytoplasmic mucin (vesicular vs. clear).

Results: The cohort consisted of 40 cases of adenocarcinoma from the following sites: 5 breast, 5 lung, 5 GEJ, 9 stomach, 5 appendix, 5 colon, and 6 pancreatobiliary. Our study revealed the presence of extracellular mucin was significantly associated with primary adenocarcinomas of GEJ, colon, appendix, and pancreatobiliary system ($p< 0.001$). The single file formation was significantly associated with breast and gastric primaries ($P<0.001$). Predominant percentage of signet ring cell was associated with GEJ, gastric, appendix, and breast tumors ($p=0.005$). Cytoplasmic mucin/vacuole were smaller in gastric and breast primaries with associated higher nuclear to cytoplasmic ratios. Vesicular mucin was less commonly observed in breast primary.

Conclusions: While adenocarcinoma with signet ring cell features share morphologic similarities, some architectural and cytologic characteristics can provide guidance for more efficient ancillary studies leading to differentiation of their primary sites. Establishment of conventional histologic criteria can facilitate learnings for pathology trainees as well as precede forthcoming applications of artificial intelligence in pathology. Additional larger validation cohort will be performed.

650 Amyloidosis Derived from Epidermal Growth Factor-Containing Fibulin-Like Extracellular Matrix Protein 1 (EFEMP1/FBLN3) Preferentially Affects the Lower Gastrointestinal Tract of Elderly Females

Linda Dao[1], Paul Kurtin[1], Thomas Smyrk[1], Jason Theis[1], Surendra Dasari[1], Ellen Mcphail[1]
[1]Mayo Clinic, Rochester, MN

Disclosures: Linda Dao: None; Paul Kurtin: None; Thomas Smyrk: None; Jason Theis: None; Surendra Dasari: None; Ellen Mcphail: None

Background: Amyloidosis is characterized by extracellular deposits of protein fibrils aligned in cross beta-sheets. There are currently 36 human amyloid proteins recognized. Amyloid derived from epidermal growth factor-containing fibulin-like extracellular matrix protein 1 (EFEMP1), also known as fibulin-3 (FBLN3), is a proposed novel amyloid type.

Design: We reviewed the scaffolds on all tissue specimens from our liquid chromatography and tandem mass spectrometry (LC-MS/MS) amyloid typing database from 2010 to 2019 (20,612 specimens) in which there were ≥10 spectral counts for EFEMP1. EFEMP1 amyloid cases were defined as having elevated levels of EFEMP1 along with proteins commonly deposited with amyloids of all types but without proteins indicative of a separate canonical amyloid type. Clinical data were available on all cases. Histologic examination with hematoxylin and eosin and Congo red stained slides were evaluated on 25 cases. Immunohistochemistry (IHC) for EFEMP1 (clone sc-33722, Santa Cruz Biotechnology, Santa Cruz, CA) was performed on 12 cases. The Congo red and EFEMP1 stains were evaluated for intensity of staining. We compared findings to 12 colon specimens involved by amyloid (10 AL and 2 ATTR) that were previously evaluated by LC-MS/MS as controls.

Results: We identified 33 specimens involved by EFEMP1 amyloid from 32 patients. There were 3 males and 29 females with a mean age at diagnosis of 75 years (range 49-92 years). Involved sites included colon (n=26), small bowel (n=3), peritoneum (n=3) and stomach (n=1). One patient had colon and small bowel involvement. The gastrointestinal amyloid involved the submucosal veins and interstitium, lamina propria and/or muscularis propria. The amyloid deposits were very weakly Congo red positive with subtle birefringence under polarized light in most cases. EFEMP1 IHC showed high sensitivity for the amyloid deposits but also showed nonspecific weak staining predominantly in the lamina propria and muscularis mucosa in a subset of the control cases.

Conclusions: A previously unrecognized form of amyloidosis derived from EFEMP1 appears to preferentially affect the lower gastrointestinal tract of elderly females. The amyloid deposits tend to show very weak Congo red positivity and are highlighted with high

sensitivity but lower specificity by EFEMP1 IHC. LC-MS/MS is the gold standard for detection of EFEMP1-associated amyloidosis. Due to its subtle morphologic features and weak Congo red positivity, this form of amyloid may be under-recognized.

651 The Ability of Duodenal Endoscopic Abnormalities to Predict Histopathology

Debasmita Das[1], Jayalakshmi Venkateswaran[2], Kaitlyn Williams[2], Ramapriya Vidhun[1], Joseph Fiorito[2], Stephanie Stroever[2], Jessica Dodge[2]
[1]Western Connecticut Health Network, Danbury Hospital, Danbury, CT, [2]Danbury Hospital, Danbury, CT

Disclosures: Debasmita Das: None; Jayalakshmi Venkateswaran: None; Kaitlyn Williams: None; Ramapriya Vidhun: None; Joseph Fiorito: None; Stephanie Stroever: None; Jessica Dodge: None

Background: During upper endoscopy, routine biopsies are often taken from the duodenum, even if it appears normal endoscopically. The importance of histologic examination of biopsies from endoscopically normal duodenums is not well established. The abnormality rate of biopsies from endoscopically abnormal duodenums is also not well established.

Design: The laboratory information system was searched for patients who had duodenal biopsies between January 2018 and April 2019. The upper endoscopy reports were reviewed chronologically and biopsies from 500 endoscopically normal and 500 endoscopically abnormal duodenums were included. The number of patients whose duodenal biopsies showed histopathology were determined and the types of histopathology were recorded. Cost saving analysis for patients and for our laboratory was performed.

Results: Of 500 patients with endoscopically normal duodenums, 27 (5.4%) had abnormal histopathology. Of 500 patients with endoscopically abnormal duodenums, 376 (75.2%) had abnormal histopathology (Table 1).

The sensitivity of endoscopy to detect a duodenal abnormality (as defined by abnormal histopathology) was 93.3%. The specificity of endoscopy to identify normal duodenums (as defined by normal histopathology) was 79.2%. The positive and negative predictive values of duodenal endoscopy were 75.2% and 94.6%, respectively. An average of 125 patients with endoscopically normal and 35 patients with endoscopically abnormal duodenums were biopsied per month. Our charge to the patient for one duodenal biopsy was $601.00. Our laboratory's cost to process one duodenal biopsy was $55.00. If only 20% of the patients with endoscopically normal duodenums had been biopsied, $721,200 of patient charges and $66,000 costs to our lab would have been avoided per year.

Table 1.

Endoscopic Findings	Abnormal Histopathology	Normal Histology	Total
Normal Endoscopy[a]	27	473	500
Abormal Endoscopy[b]	376	124	500
Total	403	597	1000

[a]Most common histopathology was peptic duodenitis (51.9%)

[b]Most common histopathology was peptic duodenitis (39.4%); Most common endoscopic finding was polyp (22.2%)

Conclusions: The yield of biopsying endoscopically normal duodenal mucosa is very low (5.4%) and it is unlikely to find a treatable diagnosis unless there is a concern for celiac disease. In contrast, the yield of biopsying endoscopically abnormal duodenal mucosa is high (75.2%). More selective biopsying would result in significant cost savings to patients and have minimal clinical impact.

652 Exploration of Intestinal Stem Cell Niche in Duodenal Biopsies of Patients with Celiac Disease

Prasenjit Das[1], Sudha Battu[2], Alka Singh[2], Govind Makharia[2], Siddhartha Datta Gupta[2]
[1]New Delhi, India, [2]All India Institute of Medical Sciences, New Delhi, India

Disclosures: Prasenjit Das: None

Background: Crypt failure possibly results in villous flattening of duodenal mucosa in patients with celiac disease (CeD). In this study, we investigated the components of the adult intestinal stem cell (ISC) niche in patients with CeD.

Design: In total 92 duodenal biopsies (D2 & D3) from patients with CeD and 37 control biopsies were included. In 49 patients follow up duodenal biopsies were available, taken 6 months post- gluten-free diet (GFD). In all serological screening was done for anti-tissue

transglutaminase (anti-tTG) antibody and histological evaluation was performed as per the modified Marsh classification system. Immunohistochemical stains for the following ISC components were used: Lgr5+ CBC and Bmi 1+ position 4+ TA cells, β-Defensin- paneth cell, R- spondine-1- Wnt pathway activator, transcription factor 4 (TCF4)- transcription factor, BMP receptor1A (BMPR1A)- negative regulator, Fibronectin L1 receptor as extracellular matrix marker, H2AX- marker of apoptosis, and Ki67- proliferative marker. The stains were interpreted by calculating H scores (area of positivity x stain intensity) and were compared among the groups.

Results: Though in biopsies from patients with CeD, H2AX was significantly upregulated and the number of LGR5+ crypt basal cells were increased than in controls, the Bmi 1+ position 4+ TA cells, nuclear TCF4 expression and Ki67 proliferation index were significantly downregulated in crypts in biopsies from treatment naïve CeD patients than in controls. The Wnt activator RSPO1 and BMPRA1 were also markedly reduced in the former group (both P <0.001). Defensin positive Paneth cell numbers did not differ between the groups. Fibronectin expression was significantly downregulated in periepithelial stromal cells in villous and crypts in CeD than in controls. In biopsies taken after 6 months of GFD, apart from reduced H2AX expression, the other markers did not differ significantly. We also identified deposition of IgA anti-tTG antibodies in the periepithelial stromal cells with dual confocal microscopy.

Figure 1 - 652

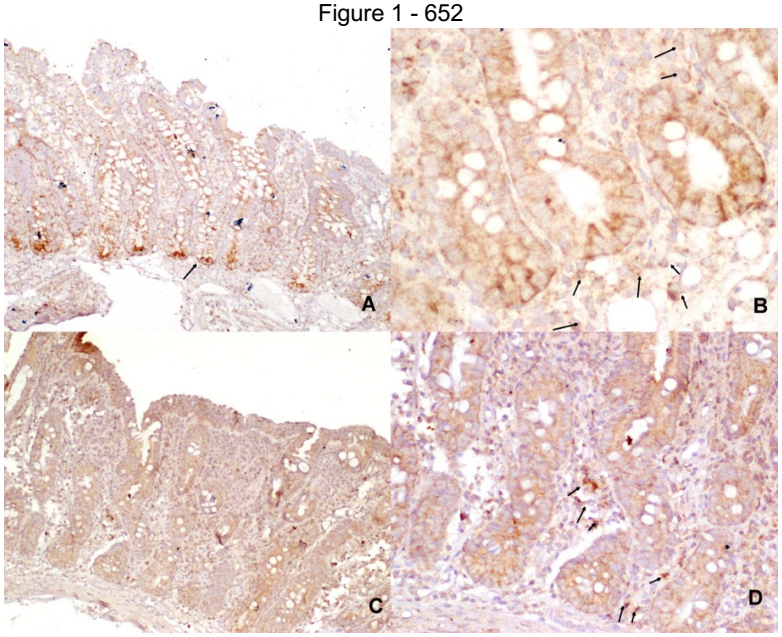

Figure Legend:

In comparison to controls (A & B), in biopsies from CeD reduced fibronectin expression noted in pericrypt stromal cells (C & D)

Conclusions: This study brings out an important observation that the integrity of the extra-cellular matrix around the ISC niche is vital to support the Stemness of crypt adult stem cells. Remodeling of the extracellular matrix by IgA anti-tTG deposits and possible loss of Foxl1+ telocytes possibly results in crypt failure in CeD.

653 Spatial Characterization of p53 and p16 Expression in Barret's Esophagus, Dysplasia and Adenocarcinoma with Quantitative Multiplex Immunofluorescence Image Analysis

Simona De Michele[1], Sonya Purushothaman[2], Caitlin Hills[3], Elena Komissarova[3], Armando Del Portillo[2], Jorge Sepulveda[3], Antonia Sepulveda[4]

[1]Columbia University Medical Center/New York Presbyterian Hospital, New York, NY, [2]New York, NY, [3]Columbia University Medical Center, New York, NY, [4]George Washington University, New York, NY

Disclosures: Simona De Michele: None; Sonya Purushothaman: None; Caitlin Hills: None; Elena Komissarova: None; Armando Del Portillo: None; Jorge Sepulveda: None; Antonia Sepulveda: None

Background: Esophageal adenocarcinoma (EAC) develops through progression of the pre-malignant lesions intestinal metaplasia (IM, Barrett esophagus/BE) and dysplasia (DYS). Alterations in tumor suppressor genes such as p16 and p53 are critical for EAC development and progression. There is limited knowledge of the spatial interactions between p16 and p53 in esophageal pre-cancer and cancer lesions. Multiplexed quantitative multispectral immunofluorescence (qMIF) provides the opportunity to characterize the temporo-spatial alterations

in biomarker expression in pre-cancer and cancer lesions. The aim of our study is to better understand the biology and to identify biomarkers underlying the progression from BE to EAC.

Design: Tissue microarrays (TMA) were constructed from FFPE resection specimens of IM (26), DYS (28), and EAC (29) from 52 patients with concurrent BE and DYS or EAC (mean 65.8 years, range 33-80 years, 44 male). TMA sections were immunostained with Opal multiplex kits and antibodies for p53, p16, pan-cytokeratin and DAPI. Multispectral images were captured with a Vectra platform and regions of interest (ROI) were identified within each core of the TMA for qMIF analysis. Custom algorithms were developed with inForm Tissue Finder software (Akoya Biosciences) to identify and quantitate nuclear p16 positive (p16Nuc+) and p53 positive (p53Nuc+) epithelial cells within BE, DYS and EAC. The proportions of positive epithelial cells for each marker and marker combinations were captured and the results for each ROI and lesion groups were analyzed using R custom algorithms.

Results: There were 826 ROI analyzed: 208 IM, 272 DYS, 346 EAC. The median % of p53Nuc+ epithelial cells in IM, DYS, and EAC was 3, 29, and 30, respectively; while for p16Nuc+ it was 4, 14, and 9, in IM, DYS and EAC, respectively. The % of p16Nuc+ epithelial cells per ROI was significantly decreased from DYS to EAC (p=0.006), whereas the % of p53Nuc+ cells increased from IM to DYS and EAC (p=0.001). Co-expression % of p53Nuc and p16Nuc was 0.0 in IM, 11 in DYS and 5 in EAC. There was a decrease in correlation of co-expression of p53Nuc and p16Nuc from IM R=.22 and DYS R=.23 to EAC R=.14 (p=0.001).

Conclusions: The decrease in co-expression and correlation of p16Nuc and p53Nuc expression, combined with a reduction in the % of p16Nuc+ and increase in p53Nuc+ epithelial cells suggests clonal evolution from DYS to EAC following two separate molecular pathways, and a potential role as biomarkers of progression from DYS to EAC.

654 Gastrointestinal Inflammation and Neoplasia in Adults with Cystic Fibrosis: The Toronto Experience

Benjamin DeKoven[1], Katherine Griffin[1], Elizabeth Tullis[1], Samir Grover[1], Tanja Gonska[2], Liron Birimberg Schwartz[2], Catherine Streutker[1]
[1]Unity Health Toronto, Toronto, ON, [2]Hospital for Sick Children, Toronto, ON

Disclosures: Benjamin DeKoven: None; Katherine Griffin: None; Tanja Gonska: None; Liron Birimberg Schwartz: None; Catherine Streutker: None

Background: The risk of gastrointestinal malignancy in patients with cystic fibrosis (CF) is increased; the cause is unknown but may be secondary to persistent inflammation, bacterial dysbiosis or the potential action of the CFTR gene as a tumour suppressor. Most cohort studies have focussed on the overall rate of malignancy, without correlation with gastrointestinal (GI) inflammation. We investigated the Adult Cystic Fibrosis registry at Unity Health Toronto (UHT) for patients with gastrointestinal pathology specimens and evaluated for the presence of inflammation and/or neoplasia.

Design: The Toronto Adult CF clinic has been existence since 1992. The patient registry (n=900) was queried for gastrointestinal biopsies or resections. GI pathology specimens were present in 154/900 (17.1%) patients. The pathology reports were reviewed to determine presence of inflammation, dysplasia or malignancy.

Results: A total of 271 procedures were performed on the 154 patients. Of these, 39/154 patients (25.3%) had normal pathology (esophagus (2), stomach (22), small bowel (18) and colon (14)). 62/154 patients had at least one specimen demonstrating GI inflammation (40.3%, average age 32.7 years. M/F 28/34) with no evidence of neoplasia. Neoplastic lesions, predominantly colonic adenomas, were identified in 41/154 patients (26.6%, average age 45 years, M/F 25/16). There were 4 colonic adenocarcinomas (ave age 41 years). Twelve patients (12/154, 7.8%, ave age 42.7 years, all female) had neoplastic lesions as well as biopsies showing inflammation in the GI tract. Of these, 3/12 had inflammation in the area of the neoplastic lesion. Overall, 34.4% of those with GI Pathology specimens had neoplasia, and 22.6% demonstrated GI inflammation.

Conclusions: While this study is limited by the absence of true screening for inflammation in these patients, the results suggest that a significant proportion of CF patients with GI neoplasia have underlying inflammation in at least one part of the GI tract. Further investigation is required to determine the relationship between inflammation and neoplasia in these patients.

655 Intestinal Spirochetosis (IS): Spectrum of Clinicopathological Correlations

Pooja Dhorajiya[1], Rifat Mannan[2], Abdelsalam Sharabi[3], Sun A Kim[4]
[1]Mount Sinai Health System, New York, NY, [2]Perelman School of Medicine at the University of Pennsylvania, Philadelphia, PA, [3]Icahn School of Medicine at Mount Sinai, New York, NY, [4]Mount Sinai Medical Center, New York, NY

Disclosures: Pooja Dhorajiya: None; Rifat Mannan: None; Abdelsalam Sharabi: None; Sun A Kim: None

Background: Human IS is infrequently identified in about 1% colonic biopsies. On routine sections it is diagnosed by identification of a thick band of basophilia on the apical surface of colonic mucosa. IS is caused by Brachyspira species, *B. aalborgi* and *B. pilosicoli.* But whether it represents a commensalism or a pathogenic process remains debated.

Design: A pathology database search was performed to retrieve the cases of IS diagnosed during last 10 years. Clinicopathologic features, H&E diagnosis and available special stains/immunohistochemistry (IHC) results were reviewed.

Results: 175 cases of IS were identified: 167 Males, 8 Females, with a median age of 52 years (range, 23 - 83). All cases were diagnosed on colonoscopic biopsy, except when IS was an incidental finding in a colectomy specimen performed for retroperitoneal liposarcoma. Indications for colonoscopy were: colorectal cancer screening (n=63), unexplained diarrhea (n=85), rectal bleeding (n=11), abdominal pain (n=7), follow up for ulcerative colitis (n=7), Crohn disease (n=1), and constipation (n=1). Associated significant clinical conditions included: HIV positive status (n=25), diabetes mellitus (n=3), post-liver transplant (n=1), retroperitoneal liposarcoma (n=1), prostate cancer (n=1), and kaposi sarcoma (n=1). Pathologic changes in background colonic mucosa included: unremarkable (n=156), active inflammation (n=12), hyperplastic polyp (n=3), tubular adenoma (n=3), trichuris trichura infestation (n=1). On H&E, all cases had the characteristic basophilic hue on the epithelial surface of colonic mucosa. Silver stains and/or IHC for spirochetes were positive in all 27 cases where performed.

Conclusions: IS in our study had a male predominance, and affected both immunocompetent and immunosuppressed individuals. Nearly two-third of the patients were symptomatic, indicating IS is likely a pathogenic infection of low virulence. Histologically IS can involve normal, inflamed as well as dysplastic epithelium. Although predominantly an H&E diagnosis, special stain /IHC can be a useful adjunct in identifying the organism.

656 Mucin Mimic: New Pitfall in Barrett's Adenocarcinoma Diagnosis and Staging

Zachary Dong[1], John Fang[2], Mary Bronner[3], Gillian Hale[3]
[1]University of Utah, Herriman, UT, [2]University of Utah Health Sciences Center, Salt Lake City, UT, [3]University of Utah, Salt Lake City, UT

Disclosures: Zachary Dong: None; John Fang: None; Mary Bronner: None; Gillian Hale: None

Background: New proprietary endoscopically injectable lifting media are being used increasingly instead of saline in endoscopic mucosal resections (EMR) of Barrett's esophagus. This foreign gel material histologically mimics mucin pools and presents a new pitfall for the overdiagnosis and staging of Barrett's adenocarcinoma. Available media in clinical use include ORISE gel (Boston Scientific) and Eleview® (Aries Pharmaceuticals). The characteristics of the media and implications for tumor diagnosis and staging have not been well described.

Design: Endoscopic reports for all patients undergoing esophageal endoscopic mucosal resection were reviewed from 2017-2019. All slides in cases using ORISE gel and Eleview® lifting media were reviewed. PAS/Alcian blue staining at pH 2.5 for all mucins, including neutral and acid mucins, which are both common in Barrett's adenocarcinoma, was performed on cases where mucin-like material was identified. Cases were also compared to true mucinous adenocarcinoma.

Results: A total of 41 EMR cases were analyzed. 90% of the patients were male. Eleview® was used in 4, ORISE gel in 2, and traditional saline in 35. The history provided to the pathologist did not indicate the type of injected lifting material in any case. Of the total EMRs, 13 of 41 (31.7%) had adenocarcinoma. Of these, 10 were staged as pT1a, 2 were pT1b, and 1 was recurrent. Lifting media was identified histologically in 2 cases of Barrett's esophagus with pT1a adenocarcinoma and both were ORISE gel. The diagnosis and staging of Barrett's adenocarcinoma was confounded in both cases: one had pools of mucin-like material associated with the carcinoma that extended to the base, and the second had mucin-like material in deeper areas not associated with malignant cells. Fortunately, PAS/Alcian blue staining for mucin was negative on the foreign media in these cases, in comparison to mucin staining in true mucinous adenocarcinoma. No mucin-like material was identified in the Eleview® or saline only cases.

Conclusions: ORISE gel lifting media mimics mucin on H&E sections from endoscopic mucosal resections but can readily be distinguished from mucin using a PAS/Alcian blue stain. As lifting media can distort tissue and microscopically resemble mucin, care must be taken to recognize and differentiate these new lifting medias from mucin to prevent the over diagnosis and overstaging of Barrett's adenocarcinoma in EMR specimens.

657 A Novel Presentation of Eosinophilic Gastrointestinal Disorders in Post-Intestinal Transplant Recipients: A Pediatric Case Series

Kayvon Dowlatshahi[1], Hanh Vo[1], Stanley Radio[1], Benjamin Swanson[1]
[1]University of Nebraska Medical Center, Omaha, NE

Disclosures: Kayvon Dowlatshahi: None; Hanh Vo: None; Stanley Radio: None; Benjamin Swanson: None

Background: Eosinophilic gastrointestinal disorders (EGID) are a group of inflammatory conditions characterized by increased eosinophils in one or more sites of the gastrointestinal tract without any other known cause of tissue eosinophilia.[1]

EGID has been described in post-liver transplant patients.[2] The mechanism of this is not known but could be due to immune dysregulation. We report a case series of seven children who presented with EGID post-intestinal transplant.

Design: A search of pathology reports from 1/1/2000 to 8/1/2019 was performed with 10 cases discussing intestinal allografts with increased eosinophilic infiltrate. Only 7 were identified after re-review to have increased eosinophils (using criteria from DeBrosse et al) [3]. Cases were examined for maximum eosinophil counts in the highest density high power field (HPF) (400x), eosinophil location, eosinophilic micro-abscesses, acute inflammation and cellular rejection. (Figure 1) The medical record was also reviewed for relevant clinical information.

Results: Median patient age at diagnosis is 12.2 years (range: 2-14). Median time from transplant to diagnosis was 2.6 years (range: 1-13). Three children had a history of food allergies or asthma, and none had eczema. Peripheral eosinophilia (> 500/mm^3) was present in 5/7 patients. All children had negative screen for ova and parasites.

The biopsies show all seven small bowel allografts with a minimum of 79 eosinophils/HPF, ranging from 79-154 eosinophils/HPF, and a median count of 119 eosinophils/HPF. (Table 1) In addition, 4/7 cases show increased eosinophils in the native gastrointestinal tract. Eosinophilic micro-abscesses are rare (1/7 cases) but 4/7 cases show crypt involvement. Acute inflammation is a consistent feature (6/7 cases). No cases have concurrent acute cellular rejection of the allograft.

Four patients required a short course of corticosteroids or budesonide in addition to targeted elimination diet; the others improved with no intervention.

Histologic Features of Eosinophilic Gastrointestinal Disorders in Intestinal Transplant Recipients

Case	Site with Eosinophils/HPF	Location of eosinophils	Eosinophilic Micro-abscesses	Acute Inflammation	Rejection
1	Small Bowel Allograft: 126	LP	No	Yes	No
	Native Stomach: NI	N/A	N/A	N/A	N/A
	Native Colon: NI	N/A	N/A	N/A	N/A
2	Small Bowel Allograft, Anastomosis: 119	LP	No	Yes	No
	Native Colon: 125	LP, BC, CS	No	Yes	N/A
3	Small Bowel Allograft: 133	LP, BC, CS	No	Yes	No
	Native Stomach: 101	LP,C, S	Yes	Yes	N/A
	Native Distal Esophagus: 62	IES	Yes	Yes	N/A
4	Small Bowel Allograft: 79	LP	No	Yes	No
5	Native Distal Esophagus: 12	IES	No	No	No
	Small Bowel Allograft- 154	LP, BC	No	Yes	No
	Native Colon: NI	N/A	N/A	N/A	N/A
6	Small Bowel Allograft: 117	LP, BC	No	No	No
	Native Colon: 86	LP	No	No	N/A
	Native Stomach: NI	N/A	N/A	N/A	N/A
7	Small Bowel Allograft: 87	LP, BC, V	No	Yes	No

Abbreviations: Lamina propria (LP), Base of crypts (BC), Crypt surface (CS), Venulitis (V), Intra-epithelial, squamous (IES), High-power Field (HPF), Not increased (NI)

Figure 1 - 657

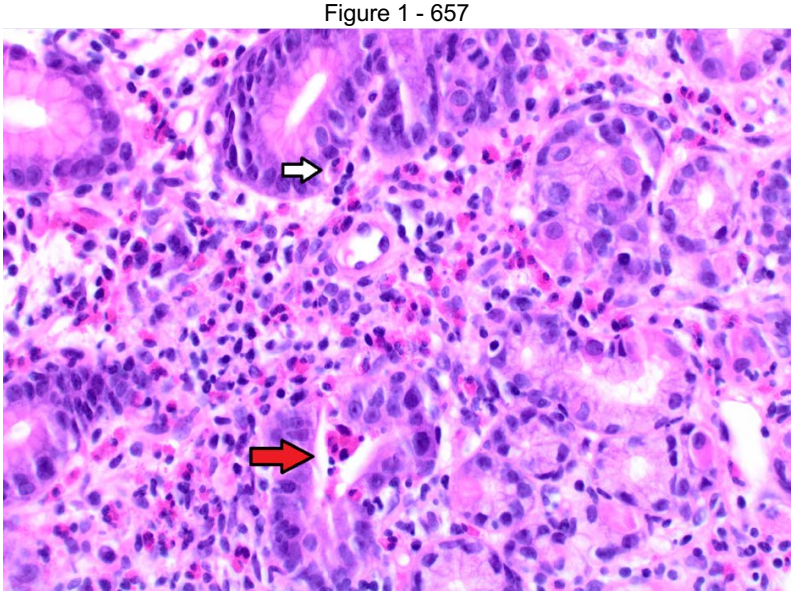

Conclusions: EGID is a potentially treatable complication of intestinal transplants and should enter the differential diagnosis for both the clinician and pathologist in the appropriate setting. While there are studies detailing normal eosinophil counts for various gastrointestinal sites, one limitation of our study is the absence of a defined criteria for eosinophil counts in the post-transplant setting. Further study of the incidence, risk factors, potential allograft complications and mechanism merits further evaluation.

658 Histologic Characterization of Gastrointestinal Mucosal Biopsy Samples in Multiple Myeloma Patients on Daratumumab

Sarah Elsoukkary[1], Jorge Monge[2], David Jayabalan[3], Ruben Niesvizky[3], Melanie Johncilla[4], Meredith Pittman[1]
[1]New York-Presbyterian/Weill Cornell Medical Center, New York, NY, [2]New York-Presbyterian Hospital/Weill Cornell Medicine, New York, NY, [3]Division of Hematology & Medical Oncology, New York-Presbyterian Hospital/Weill Cornell Medicine, New York, NY, [4]New York-Presbyterian Hospital/Weill Cornell Medical Center, Petit Valley, Trinidad and Tobago

Disclosures: Sarah Elsoukkary: None; Jorge Monge: None; David Jayabalan: None; Ruben Niesvizky: *Consultant*, Janssen; *Consultant*, Celgene; *Consultant*, Takeda; *Consultant*, BMS; Melanie Johncilla: None; Meredith Pittman: None

Background: Daratumumab is a CD38 monoclonal antibody commonly used in multiple myeloma (MM), the second most common hematologic malignancy in the United States. Although CD38 is highly expressed on myeloma cells, making it an optimal target antigen, it is also expressed on non-neoplastic hematopoietic and epithelial cells. Patients with MM often present with gastrointestinal (GI) symptoms warranting endoscopic evaluation, but the effect of daratumumab on the GI tract has not been well described. The aim of this study is to investigate the histologic changes seen in the GI tract of patients taking daratumumab.

Design: The clinical database was queried for patients with MM who had received daratumumab and undergone biopsy sampling of the GI tract. Clinical information, including GI symptoms, history of hematopoietic stem cell transplant (SCT) or other adjuvant therapy, and dates of daratumumab treatment were obtained from the electronic medical record. Cases were evaluated for intraepithelial lymphocytosis, lamina propria infiltrate, cryptitis, and epithelial apoptosis. Patients were excluded if the tissue sample showed active infection (*e.g* CMV, *H. pylori*).

Results: We reviewed tissue from 18 patients: 6 with GI biopsies prior to the initiation of daratumumab, 7 with biopsies post initiation, and 5 with both pre- and post-therapy biopsy samples. The average age was 67 years, and most patients were men (61%). Presenting symptoms did not significantly differ between pre- and post-groups, with diarrhea and abdominal pain being the most common (39% and 28%, respectively). All but one (94%) had undergone SCT prior to biopsy. The average time from SCT to biopsy was 416 days (range: 15 to 3492) and the mean duration of daratumumab treatment was 466 days (range: 1 to 1494). Patients receiving daratumumab were more likely to have intraepithelial lymphocytosis and prominent lamina propria eosinophils compared to patients who were not receiving the drug (Table 1). There was also a higher incidence of active enterocolitis in the daratumumab population. In patients with paired samples, there was an overall increase in epithelial apoptotic bodies in colonic samples, from 1 to 5 per tissue fragment.

Table 1. GI Biopsy Findings in Patients Pre- and Post-Daratumumab Therapy

	Colon		Ileum		Duodenum		Stomach	
	Pre (n=22)	Post (n=19)	Pre (n=4)	Post (n=4)	Pre (n=6)	Post (n=6)	Pre (n=15)	Post (n=12)
Intraepithelial Lymphocytosis	1 (5%)	11 (57%)	0	1 (25%)	2 (33%)	5 (83%)	1 (7%)	2 (17%)
Lamina Propria Eosinophils	5 (23%)	13 (68%)	0	4 (100%)	0	4 (67%)	1 (7%)	0
Lamina Propria Neutrophils	0	4 (21%)	0	1 (25%)	0	0	2 (14%)	0
Cryptitis	0	4 (21%)	0	1 (25%)	0	0	2 (14%)	1 (8%)
Crypt Abscess	0	3 (16%)	0	0	0	0	0	0
Apoptotic Epithelial Cells, All Cases (average/tissue fragment)	3	4	6	2	1.5	1.5	0.5	0.67
Apoptotic Epithelial Cells, Paired Samples (average/tissue fragment)	1	5	6	3	<1	1	<1	<1

Figure 1 - 658

Figure 2 - 658

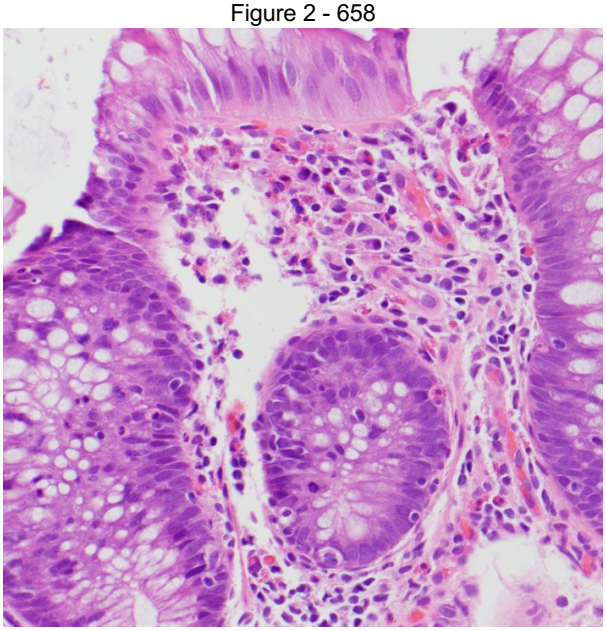

Conclusions: Although daratumumab is not associated with specific gastrointestinal symptoms in MM patients, the drug can cause a pattern of injury characterized by intraepithelial lymphocytosis, lamina propria eosinophilia, and active crypt injury. Epithelial cell apoptosis is also a feature of daratumumab therapy.

659 The Significance of Focally Enhanced Gastritis in Hematopoietic Stem Cell Transplant Recipients

Sarah Elsoukkary[1], Jose Jessurun[2], Meredith Pittman[1], Rhonda Yantiss[2], Melanie Johncilla[3]
[1]New York-Presbyterian/Weill Cornell Medical Center, New York, NY, [2]Weill Cornell Medicine, New York, NY, [3]New York-Presbyterian Hospital/Weill Cornell Medical Center, Petit Valley, Trinidad and Tobago

Disclosures: Sarah Elsoukkary: None; Jose Jessurun: None; Meredith Pittman: None; Rhonda Yantiss: None; Melanie Johncilla: None

Background: The histologic diagnosis of acute gastric graft versus host disease (aGVHD) in patients with a history of hematopoietic stem cell transplant (HSCT) is based on the presence of epithelial apoptosis. Focally enhanced gastritis (FEG), defined by the presence of focal periglandular lymphohistiocytic inflammation with associated intraepithelial involvement of gastric glands, is a known inflammatory lesion in patients with inflammatory bowel disease and is frequently encountered in HSCT patients. Interestingly, this inflammatory pattern closely resembles the focal periductal inflammation and lymphocytic exocytosis seen in chronic GVHD of the salivary gland. The aim of this study was to evaluate the significance of FEG in HSCT patients.

Design: Gastric biopsies from HSCT patients who underwent endoscopies for GVHD-like symptoms were identified. Patients with serologic or culture evidence of active infection at biopsy were excluded. Time from transplant to biopsy, presence of histologically proven extra-gastric GVHD, medications and outcome were noted. 150 biopsies were reviewed. Biopsies with FEG were evaluated for the number of foci of FEG, inflammatory infiltrates and epithelial apoptosis/10 HPF. IHC for adenovirus, CMV, *H. pylori*, CD4 and CD8 and EBER (ISH) were performed. Prior or subsequent gastric biopsies of 14 patients in the cohort were evaluated.

Results: 35 biopsies showed FEG, 21 showed aGVHD, 12 were normal and 82 showed non-specific epithelial changes. 21 (60%) FEG patients had concurrent extra-gastric GVHD. The median time to biopsy in FEG patients was significantly longer than in aGVHD patients (162 vs 57 days, p<0.01) (Table 1). Of the 14 prior or subsequent biopsies from FEG patients, 6 showed aGVHD while 1 showed persistent FEG. 97% of FEG cases showed a CD4+ lymphocyte-predominant intraepithelial and periglandular inflammatory infiltrate with minimal epithelial apoptosis (Figure 1). Adenovirus, CMV, EBER and H. pylori stains were all negative.

Table 1: Clinical Features of HSCT Patients with Gastric Biopsy Samples Showing FEG, aGVHD and Normal Findings

	FEG (n=35)	Acute GVHD (n=21)	NDA (n=12)	p-Value (FEG vs AGVHD)
Mean Age (range)	58 (28-73)	54 (37-71)	56 (19-69)	
Female: Male Ratio	0.9	1.6	1.4	0.42
Median Time to Biopsy (days)	162	57	105	<0.01
Extra-gastric GVHD (Skin, Liver, Colon)	21 (60%)	20 (95%)	1 (8%)	<0.01
Outcome				
Alive, NED	15 (42%)	2 (10%)	3 (25%)	<0.01
Alive with Hematopoetic disease	3 (9%)	5 (24%)	1 (8%)	0.70
Died of Hematopoetic disease	14 (40%)	9 (43%)	8 (67%)	0.99
Died of GVHD	3 (9%)	5 (23%)	0 (0%)	<0.01

FEG: Focal enhancing gastritis, GVHD: Graft versus host disease, NDA: No diagnostic abnormality, NED: No evidence of hematopoetic disease or GVHD.

Figure 1 - 659

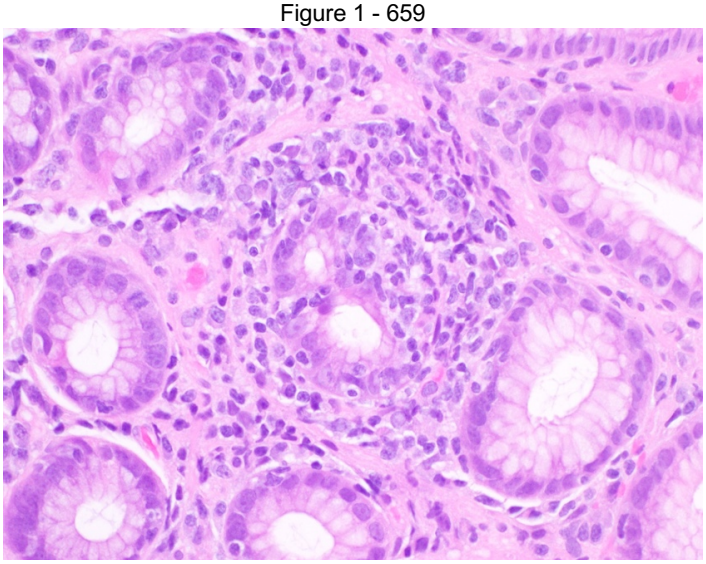

Conclusions: Nearly two-thirds of the patients with FEG had biopsy-proven, extra-gastric GVHD. Acute gastric GVHD was also present in prior or subsequent biopsies from a subset of FEG patients. These findings suggest that FEG is likely a form of GVHD. Given that the median length of time from transplant to biopsy in the FEG cohort was significantly longer than that in the aGVHD cohort, we further suggest that, like in the salivary gland, this inflammatory pattern may represent a form of chronic GVHD.

660 Unique Clinicopathologic and Genetic Alteration Features in Early Onset Colorectal Carcinoma (CRC) Compared to Age-Related CRC: A Large Cohort Next Generation Sequence Analysis

David Escobar[1], Ryan Jones[2], Juehua Gao[3], Guang-Yu Yang[2]
[1]McGaw Medical Center of Northwestern University, Chicago, IL, [2]Northwestern University, Chicago, IL, [3]Northwestern Memorial Hospital, Chicago, IL

Disclosures: David Escobar: None; Ryan Jones: None; Juehua Gao: None; Guang-Yu Yang: None

Background: It has been particularly alarming that the incidence of CRC among those under 50 years of age has increased, especially in individuals < 40 years, as the overall CRC frequency has decreased. These tumors tend to exhibit a relatively higher stage, aggressive histologic features, or metastatic disease at presentation. Comprehensive molecular characterization of early-onset CRC is currently under-reported in the literature. In the present study, we analyzed the unique clinicopathologic and genetic features in early onset CRC in a single institution cohort using next generation sequencing (NGS) approach.

Design: From our pathology database for CRC cases from 2016 to 2018 (large cohort of 635 cases with comprehensive NGS 22 panel analysis), 42 patients under 40 years old ("young cohort,") and 164 patients over 70 years old ("elderly cohort,") were collected for this study. The expression of hMLH1, hMSH2, hMSH6, and hPMS2 was reported as intact (stable, MSS) or lost (unstable, MSI). Ion AmpliSeq second generation sequencing (22 genes including *KRAS, EGFR, BRAF, PIK3CA, AKT1, ERBB2, PTEN, NRAS, STK11, MAP2K1, ALK, DDR2, CTNNB1, MET, TP53, SMAD4, FBX7, FGFR3, NOTCH1, ERBB4, FGFR1* and *FGFR2)* was performed. Student's t-test, chi-square, and Fischer's exact tests were calculated, as appropriate.

Results: CRC in the young cohort (see table) were significantly more likely to present with higher clinical stage showing positive lymph node and distant metastases, (p=0.013 and 0.025, respectively) and had aggressive histologic subtypes (micropapillary and signet ring, overall p=0.001), in contrast to CRC in the elderly cohort (see table). In the young cohort, MSS tumors showed significantly lower incidence of *PIK3CA* in comparison to the elderly cohort (p=0.010) (fig. 1 versus fig. 2). In MSI tumors of the young cohort (7/42, 16.7%), no BRAF mutations were identified. These tumors were more likely to harbor *KRAS* or *CTNNB1* mutations (p=0.0049 and 0.0025, respectively), compared to MSI tumors in the elderly cohort (9/164, 5.5%). One patient in the young cohort underwent germline testing which confirmed Lynch syndrome; this tumor harbored two point mutations in *KRAS* and *CTNNB1*.

		Total Cases		
		<40 years	> 70 years	p values
Cases		42	164	
Age		35 (19 - 40)	77 (70 - 95)	
Sex				
	Male	21 (50%)	83 (50.6%)	-
	Female	21 (50%)	81 (49.4%)	-
Location				
	Right	7 (16.7%)	73 (44.5%)	0.0007
	Left	19 (45.2%)	47 (28.7%)	0.0438
	Transverse	2 (4.8%)	12 (7.3%)	0.7396
	Rectum	13 (31.0%)	27 (16.5%)	0.0478
	Appendix	0 (0%)	1 (0.6%)	1.0000
	Unlabeled	1 (2.4%)	4 (2.4%)	-
		Overall p value	0.0093	
Tumor size		4.6 (0.2 - 11.5)	4.7 (0.2 - 14.5)	0.8870
Histologic grade				
	Low/Mod	32 (76.2%)	113 (68.9%)	0.4496
	High	10 (23.8%)	38 (23.2%)	1.0000
	Not resected/Not reported	0 (0%)	13 (7.9%)	-
pN				
	pNX	12 (28.6%)	40 (24.4%)	0.5573
	pN0	10 (23.8%)	88 (53.7)	0.0013
	pN1	7 (16.7%)	23 (14.0%)	0.6307
	pN2	10 (23.8%)	13 (7.9%)	0.0103
Tumor Stage				
	0	1 (2.4%)	4 (2.4%)	1.0000
	I	4 (9.5%)	31 (18.9%)	0.1735
	II	6 (14.3%)	51 (31.1%)	0.0334
	III	12 (28.6%)	26 (15.9%)	0.0739
	IV	15 (35.7%)	34 (20.7%)	0.0658
	Not Resected	4 (9.5%)	18 (11.0%)	-
		Overall P value	0.0253	
Tumor subtype				
	Adenocarcinoma NOS	33 (78.6%)	139 (84.8%)	0.3544
	Mucinous	1 (2.4%)	12 (7.3%)	0.4743
	Micropapillary	6 (14.3%)	2 (1.2%)	0.0011
	Signet Ring	2 (4.8%)	10 (6.1%)	1.0000
	Adenosquamous	-	1 (0.6%)	-
	Enteroblastic	-	1 (0.6%)	-
		Overall P value	0.001039	
Tumor Budding				
	None	3 (7.1%)	10 (6.1%)	0.7331
	Low	7 (16.7%)	22 (13.4%)	0.6205
	Intermediate	1 (2.4%)	4 (2.4%)	1.0000
	High	2 (4.8%)	26 (15.9%)	0.0766
	Not reported	29 (69.0%)	102 (62.2%)	-
Crohn's-like reaction				
	Present	1 (2.4%)	9 (5.5%)	0.6907
	Absent	-	2 (1.2%)	-
	Not reported	41 (97.6%)	153 (93.3%)	-
Precursor lesion				
	Adenoma	18 (42.9%)	84 (51.2%)	0.3886
	Serrated	0 (0%)	5 (3.0%)	0.5855
Lynch				
	Present	1 (2.4%)	0 (0%)	0.2039
	Possible	6 (14.0%)	9 (5.5%)	0.0874
	Absent	35 (83.3%)	155 (94.5%)	0.0242
MSI				
	Intact - Stable	35 (83.3%)	129 (78.7%)	0.6681
	Absent - Unstable	7 (16.7%)	30 (18.3%)	1.0000
	Unknown	0 (0%)	5 (3.0%)	-
No. of genes mutated				
	0	4 (9.5%)	15 (9.1%)	1.0000
	1	13 (31.0%)	43 (26.2%)	0.5625
	2	13 (31.0%)	61 (37.2%)	0.4778
	3	11 (26.2%)	37 (22.6%)	0.6830
	4	1 (2.4%)	5 (3.0%)	1.0000
	5	-	2 (1.2%)	-

	6	-	1 (0.6%)	-
Genes mutated				
	KRAS	19 (45.2%)	70 (42.6%)	0.8617
	EGFR	1 (2.4%)	4 (2.4%)	1.0000
	BRAF	2 (4.8%)	32 (19.5%)	0.0198
	PIK3CA	4 (9.5%)	48 (29.3%)	0.0089
	AKT1	1 (2.4%)	2 (1.2%)	0.4973
	ERBB2	0 (0%)	3 (1.8%)	1.0000
	PTEN	3 (7.1%)	9 (5.5%)	0.7130
	NRAS	1 (2.4%)	4 (2.4%)	1.0000
	STK11	0 (0%)	2 (1.2%)	1.0000
	MAP2K1	0 (0%)	0 (0%)	1.0000
	ALK	0 (0%)	1 (0.6%)	1.0000
	DDR2	1 (2.4%)	1 (0.6%)	0.3731
	CTNNB1	5 (11.9%)	4 (2.4%)	0.0187
	MET	3 (7.1%)	7 (4.3%)	0.4292
	TP53	27 (64.3%)	97 (59.1%)	0.5990
	SMAD4	4 (9.5%)	18 (11.0%)	1.0000
	FBX7	2 (4.8%)	16 (9.8%)	0.5388
	FGFR3	1 (2.4%)	2 (1.2%)	0.4973
	NOTCH1	0 (0%)	2 (1.2%)	1.0000
	ERBB4	2 (4.8%)	2 (1.2%)	0.1853
	FGFR1	1 (2.4%)	0 (0%)	0.2039
	FGFR2	0 (0%)	1 (0.6%)	1.0000

Figure 1 - 660

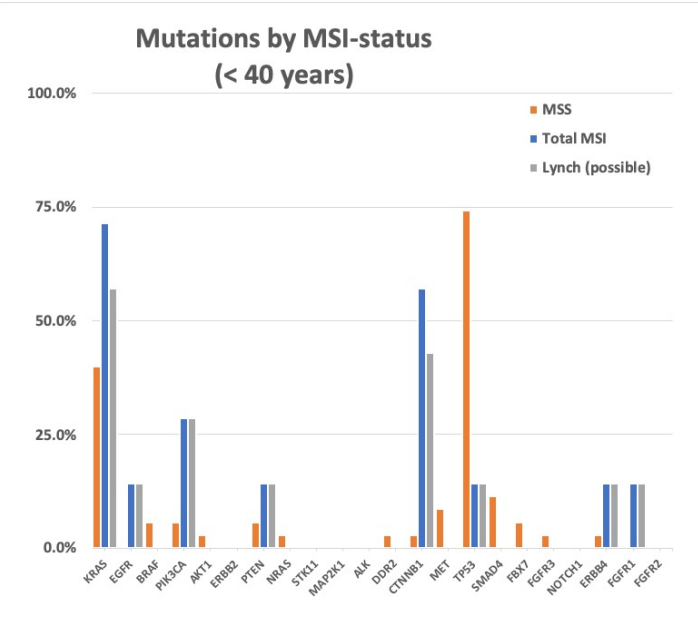

Figure 2 - 660

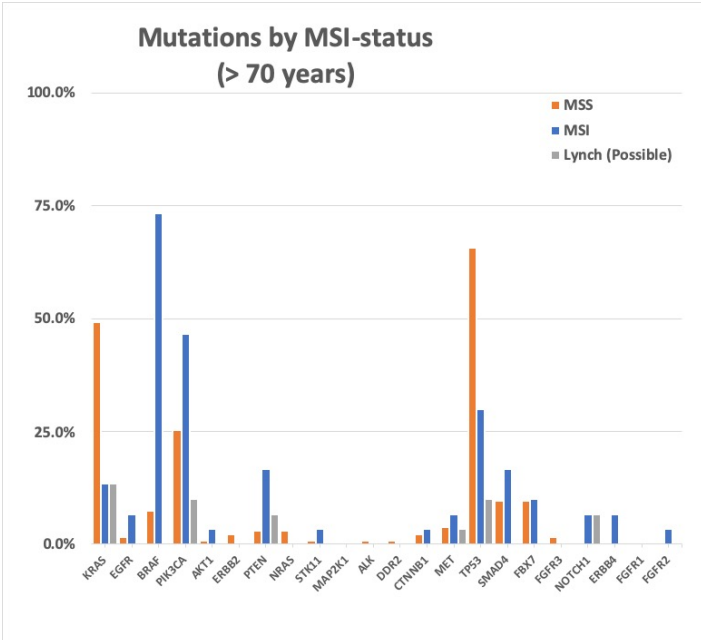

Conclusions: Early-onset CRC shows distinct molecular features with more frequent *KRAS* or *CTNNB1* mutation and less *PIK3CA* or *BRAF*. Early-onset CRC is more likely to show aggressive clinicopathologic features and to show a distinct molecular mutational profile when compared to CRC in the elderly.

661 Microsatellite Instability Screening in a Canadian Cohort of Esophageal Adenocarcinomas

Gertruda Evaristo[1], Amit Katz[2], Duc-Vinh Thai[1], Veena Sangwan[1], Jose Ramirez-GarciaLuna[1], Carmen Mueller[2], Jonathan Cools-Lartigue[2], Victoria Marcus[3], Lorenzo Ferri[1], Pierre Fiset[2]
[1]McGill University, Montreal, QC, [2]McGill University Health Center, Montreal, QC, [3]MUHC, Mont-Royal, QC

Disclosures: Gertruda Evaristo: None; Amit Katz: None; Duc-Vinh Thai: None; Veena Sangwan: None; Jose Ramirez-GarciaLuna: None; Carmen Mueller: None; Jonathan Cools-Lartigue: None; Victoria Marcus: None; Lorenzo Ferri: None; Pierre Fiset: *Consultant*, Pfizer Canada; *Speaker*, Merck Serono Canada

Background: Reported prevalence of microsatellite instability (MSI) varies between 0-8.3% for esophageal cancers. Most series have focused on Eastern Asian and European populations, which showed inter-country variability. Recent reports show that MSI status in upper GI cancers has important prognostic influence on surgical, chemotherapeutic and immunotherapeutic outcomes. It is therefore critical to define population-specific prevalence and evaluate the need for routine screening. We thus sought to characterize a Canadian cohort of patients in urban Quebec with respect to MSI status and clinicopathologic correlates.

Design: We performed IHC for MLH1, MSH2, MSH6, PMS2 and BRAF V600E on tissue microarrays constructed from 109 cases of esophageal (4) and esophagogastric junction (105) adenocarcinomas resected at our institution from 2011-2018. Mismatch repair (MMR) IHC was repeated on full section tumors for cases showing MMR-deficient (MMR-D) immunophenotype. Patterns of MMR expression were correlated with overall survival (OS) using Cox proportional-hazards modeling.

Results: MMR-D immunophenotype was identified in 11 out of 109 tumors (10.1%). The majority (54.5%) were junctional (Siewert II), with remainder corresponding to Siewert III. Ten cases showed a combined loss of MLH1/PMS2, but none of these were positive for BRAF V600E. A single case with isolated MSH6 loss was identified. Review of patient's file revealed a synchronous squamous cell carcinoma of the lung. MSH6 loss was confirmed on whole sections of the esophageal tumor while the lung cancer was MMR-proficient (MMR-P). Overall, MMR-D tumors showed a poor pathologic response to preoperative therapy in 82.8% of cases. Nevertheless, compared with MMR-P patients, MMR-D immunophenotype was associated with a trend for longer median OS of 64 versus 27 months (p=0.08).

Conclusions: The significant proportion of MMR-D esophageal cancers identified in our Canadian cohort along with the associated increased OS trend highlight the importance of MSI status determination and the potential of IHC as a viable screening tool for assessment of patients for therapy and prognostic features within a public system. Further molecular characterization of identified cases could additionally allow better understanding of the mechanisms of MSI in upper GI cancers.

662 Chronic Bowel Ischemia due to Mesenteric Vascular Fibromuscular Dysplasia Mimicking Crohn Disease

Lifang Fan[1], Yanyan Chen[2], Shu-Yuan Xiao[3], Jun Luo[4]
[1]Hubei Cancer Hospital, Wuhan, Hubei, China, [2]Department of Pathology, Zhongnan Hospital of Wuhan University; and Wuhan University Center for Pathology and Molecular Diagnostics, Wuhan, Hubei, China, [3]Department of Pathology, Zhongnan Hospital of Wuhan University, Wuhan, Hubei, China, [4]Wuhan University Zhongnan Hospital, Wuhan, Hubei, China

Disclosures: Lifang Fan: None; Yanyan Chen: None; Shu-Yuan Xiao: None

Background: Fibromuscular dysplasia (FMD) is a non-inflammatory, non-atherosclerotic vascular disease that usually involves medium-sized arteries. Involvement of the mesenteric arteries is uncommon and may be overlooked during the diagnostic work-up for gastrointestinal symptoms. Abnormal proliferation of fibromuscular tissue causes vessel wall thickening and partial or complete obliteration, leading to chronic bowel ischemic injury with ulcerations and strictures, mimicking Crohn disease. We aimed to analyze the clinicopathological features of mesenteric FMD in recent cases to shed light on clues that may help in differential diagnosis.

Design: 8 surgically resected cases of mesenteric FMD were collected with detailed clinical data. H&E, Verhoff Von Geason and Masson trichrome stains were used, the latter to highlight arterial internal elastic lamina and arterial fibrosis, respectively. The cases were classified into three types: intimal, medial and perimedial.

Results: The study includes 5 male and 3 female patients, between 14 and 72 years of age. All patients had intermittent abdominal pain and/or distension, for 2 weeks to 16 years. Of the 8 patients, 5 (62.5%) had abdominal pain, 2 (25%) abdominal pain and bloating, 1 (25%) bloating, 3 (37.5%) intestinal obstruction. All patients had at least one set of biopsies and diagnosed as either “chronic mucosal inflammatory”(CMI) or CD. The pre-operative clinical diagnosis included 7(87.5%) as or suspicious for CD, 1 as suspicious for tumor. The procedures included 4 (50%) partial resection of small intestine, 3 (37.5%) right hemicolectomy and 1(12.5%) total colectomy. Ulcers and strictures were observed in all cases; 6 (75%) had one stenotic segment, 2 (25%) multifocal stenoses. Microscopical findings included chromic mucosal ischemia, ulceration, fibrosis and muscular hyperplasia at the base of ulcers. Medium-sized arteries and arterioles within submucosa or subserosa exhibited focal narrowing or completely obliteration by intimal or intimal-medial fibrosis. No granulomas were identified in these cases.

Case Number	Age	Gender	Presentation	Endoscopy	Clinical Diagnosis	Biopsy Diagnosis	Surgical procedure	Microscopy View	FMD Type
1	44	M	Intermittent AP for 10 ys	Ulcer and strictures in ielium	Ulceration suspicious for CD	MCI	Partial resection of SB	5 cm stricture	Intimal
2	42	F	AP+ bloating + diarrhea for 4ys	Multiple ulcers and strictures in SB and sigmoid colon; SB internal fistula	CD	MCI with ulceration	Partial resection of SB+ total colectomy	Multiple ulcerations and strictures	Intimal
3	31	M	Intermittent AP for 10 ys	Stricture and ulcer in SB	CD	MCI	Partial resection of SB	3cm segmental stricture with 1.2*1.0cm ulcer	Medial
4	14	F	Intermittent AP for 2 ys	Multiple ulcers, segmental intestinal strictures and dilation	Incomplete intestinal Obstruction; diagnosed as CD intraoperatively	Chronic Enteritis	Partial resection of SB	Multiple segmental strictures	Medial
5	36	M	Bloating for 4months	Ulcer and stricture in jejunum and SB-bladder fistula	Suspicious for CD	MCI	Partial resection of SB	Ulcers and strictures	Intimal+ medial
6	72	F	Right lower AP for 2 weeks	Terminal ileum ulcer and stricture	Suspicious for carcinoma	MIC	Right hemicolectomy	2*0.6cm ulceration	Intimal
7	54	M	Intermittent AP for 6ys	Multiple ulcer in SB and colon	CD; intestinal obstruction	Chronic enteritis	Right hemicolectomy	10cm segmental stricture and proximal intestinal dilation	Intimal
8	61	M	Intermittent AP for 16ys	Ulcer and stricture in SB	Suspicious for carcinoma; incomplete intestinal obstruction	Chronic enteritis	Right hemicolectomy	stricture and proximal intestinal dilation	Intimal +medial

AP indicates abdominal pain; MCI indicates mucosal chronic inflammation; SB indicates small bowel; CD indicates Crohn disease

Figure 1 - 662

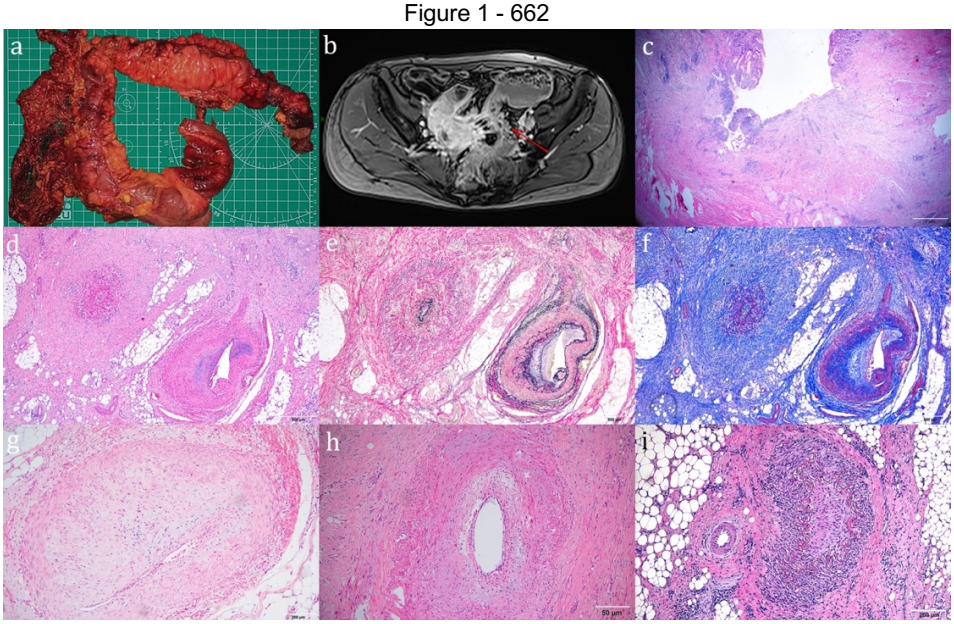

Conclusions: Patients with mesenteric FMD have long-term intermittent digestive symptoms, similar to Crohn disease clinically. Small intestine is involved more often than colon. Most cases showed intimal proliferation. All diagnoses were made based on resected specimens. It is not possible to find diagnostic features of FMD in mucosal biopsies.

663 Intestinal Inflammation Induces Cytoplasmic Expression of NUR77 in Enteric Epithelial Cells with Accentuation in Mucin-Producing Compartments

Karen Fang[1], Subrata Ghosh[2], Xianyong Gui[3]
[1]University of Washington, Seattle, WA, [2]University of Birmingham, Birmingham, United Kingdom, [3]University of Washington Medical Center, Seattle, WA

Disclosures: Xianyong Gui: None

Background: Nuclear receptors (NRs) have been found to be physiologic protective factors of intestinal epithelial integrity, partly through enhancing epithelial mucus production by binding to the promoter region of *Muc* genes and regulating goblet cell maturation. Nuclear expressions of some NRs in enteric epithelial cells in IBD have been reported to be decreased. We recently for the first time observed a different and interesting expression pattern of NUR77 (NR4A1), a member of the NRs, in Crohn's bowel inflammation.

Design: 20 full-thickness section samples of ileum and colon with active Crohn's disease (CD) were retrieved from ileocolectomy specimens of CD patients treated by surgical resection. Adjacent uninflamed bowel samples were paired as controls. Expression of NUR77 was studied by immunohistochemistry, focusing exclusively on the surface and cryptal epithelial cells.

Results: Normal enteric epithelial cells showed no or minimal NUR77 expression within the cytoplasm, usually confined to the subapical portion. In comparison, in mucosa with mild active inflammation, a mildly increased cytoplasmic expression of NUR77 appeared, which was in some cases accentuated in the enterocytes around goblet cells. In cases with severe active inflammation, *e.g.,* in areas adjacent to ulceration, the NUR77 expression was further increased and was primarily seen within the cytoplasm of goblet cells in a concentrated manner. In some cases, NUR77 was seen admixed with the excreted mucin on the mucosal surface. No nuclear expression was seen in either inflamed or normal epithelial cells, although it was present in lamina propria mononuclear cells.

Conclusions: Our observation about NUR77 expression in enteric epithelial cells in CD is an unreported new finding. First, NUR77 expression occurs in cytoplasm but not in nuclei, which is suggestive of extranuclear translocation of this NR, as previously reported in some cancer cells. Second, NUR77 expression in IBD is higher rather than lower compared to normal condition, and it is increasingly higher with the severity of active inflammation. Third, in the high end of mucosal inflammation, NUR77 expression is relocated into the goblet cells and is rich in mucin products. Our findings demonstrate both the upregulation of epithelial cytoplasmic NUR77 expression in bowel mucosal inflammation and its association with epithelial mucin production, which may be at least one of the protective roles of NUR77 in enteric mucosa.

664 Quantitative CD8-Positive T-cell Density and Intratumoral Budding in Pre-Treatment Biopsies Can Predict Response to Neoadjuvant Chemoradiotherapy and Tumor Recurrence in Rectal Adenocarcinoma

Lama Farhat[1], Douglas Hartman[1], David Medich[1], James Celebrezze[1], Liron Pantanowitz[2], Madison Frank[1], Reetesh Pai[3]
[1]University of Pittsburgh Medical Center, Pittsburgh, PA, [2]University of Pittsburgh, Wexford, PA, [3]UPMC-Presbyterian Hospital, Pittsburgh, PA

Disclosures: Lama Farhat: None; Douglas Hartman: None; David Medich: None; James Celebrezze: None; Liron Pantanowitz: *Advisory Board Member*, Leica; Madison Frank: None; Reetesh Pai: None

Background: Tumor budding and infiltrating CD8 positive (+) T-cells (TIL) are recognized prognostic factors in colorectal adenocarcinoma. The aim of this study was to correlate quantitative CD8+TIL density and intratumoral budding in pre-treatment rectal cancer biopsies with pathological response to neoadjuvant chemoradiotherapy (CRT) and recurrence-free survival following surgical resection.

Design: Pre-treatment rectal biopsies and resection specimens of patients with rectal adenocarcinoma who underwent preoperative CRT were retrospectively reviewed (n=101). Quantification of CD8+TIL was assessed using automated image analysis, and the number of intratumoral buds per 0.785 mm^2 were recorded for each biopsy and correlated with clinicopathological variables in resection specimens. ROC analysis was used to determine the optimal cutoff for CD8+TIL density in predicting tumor regression following CRT. Univariate and multivariate logistic regression models were used to assess the associations between intratumoral budding and CD8+TIL density and tumor regression. The effect of CD8+TIL and intratumoral budding in predicting recurrence-free survival following resection was evaluated by Kaplan-Meier survival functions.

Results: Increased CD8+TIL density in pre-treatment biopsies was significantly associated with complete/near complete response (TRG 0-1) to CRT, low tumor stage, mid rectal tumor site, and MMR deficiency (all with $p<0.05$). Multivariate analysis demonstrated that CD8+TIL density ≥157/mm^2 and ≥2 intratumoral buds per 0.785 mm^2 on pre-treatment biopsies were the only variables that independently predicted complete/near complete response to CRT (CD8+TIL OR 0.27, 0.12-0.66 95% CI, p=0.004; intratumoral budding OR 3.60, 1.03-12.80 95% CI, p=0.04). Patients were stratified into low-risk (CD8+TIL density ≥157/mm^2 and <2 intratumoral buds per 0.785 mm^2) and high-risk groups (CD8+TIL density <157/mm^2 or ≥2 intratumoral buds per 0.785 mm^2) for recurrence-free survival analysis. Patients in the low-risk

category had significantly improved recurrence-free survival following surgical resection compared to patients in the high-risk category (log-rank p=0.04).

Conclusions: A high CD8+TIL density and low intratumoral budding in pre-treatment biopsies of rectal adenocarcinoma are independent predictors of complete/near complete response to chemoradiotherapy and identify patients with a low recurrence risk following surgical resection.

665 A Single Institution Experience in EBV Positive Mucocutaneous Ulcer: A New Entity of 2017 WHO

Fei Fei[1], Vishnu Reddy[2], Deniz Peker[3], Chirag Patel[1], Deepti Dhall[1], Goo Lee[2], Sameer Al Diffalha[1]
[1]The University of Alabama at Birmingham, Birmingham, AL, [2]UAB Hospital, Birmingham, AL, [3]Emory University, Atlanta, GA

Disclosures: Fei Fei: None; Vishnu Reddy: None; Deniz Peker: None; Chirag Patel: None; Deepti Dhall: None; Goo Lee: None; Sameer Al Diffalha: None

Background: EBV positive mucocutaneous ulcer (EBVMCU) is a newly recognized clinicopathologic entity in the 2017 World Health Organization (WHO) classification. EBVMCU is characterized by occurring in patients with age-related or iatrogenic immunosuppression, which is a main risk factor for EBVMCU. Patients usually present with an isolated ulcerative lesion in oral mucosa, skin and gastrointestinal tract. The disease typically follows an indolent clinical course and stopping the immunosuppressive factor is a crucial part of the treatment. The aim of the study is to highlight the pathology, diagnosis and clinical features of patients with EBVMCU.

Design: A retrospective chart review identified was performed for patients diagnosed with EBVMCU from January 2009 through June 2019. Data regarding age, sex, ethnicity, clinical presentation, risk factors, treatment, patients' outcome, and pathologic features were reviewed.

Results: Four patients diagnosed with EBVMCU were identified. Mean age of the study was 60 years (range: 37–70 years) with male predominance. The lesional sites involved in oral mucosa, esophagus mucosa, nasopharyngeal mucosa and rectal mucosa. Two patients had immunosuppression due to long-term azathioprine usage for Crohn's disease and HIV positive status respectively, one patient had no evidence of immunosuppression other than advanced age, and one patient had unknown risk factor. The pathologic features show ulceration in mucosal or cutaneous surface with a substantial number of large atypical transformed cells, either atypical immunoblasts or Hodgkin/Reed-Sternberg (HRS)-like cells in the background of dense polymorphous infiltrate. These large atypical cells are positive for EBER and CD30 with variable expression of CD20 (Figure 1). Two patients regressed spontaneously with no treatment, one age-related patient needed Rituximab, and one patient developed EBV positive diffuse large B cell lymphoma in the setting of Crohn's disease within a 6-year period after cessation of azathioprine and Rituximab therapy. The clinical and pathologic features of the four patients are summarized in Table 1.

Table 1. Clinical features, treatment, and prognosis in patients with EBV positive mucocutaneous ulcer (EBVMCU).

Case No.	Age	Sex	Ethnicity	Clinical Presentation	Lesion Site	Immunosuppression	Treatment	Patient Outcome	Morphology	IHC staining pattern
1	69	M	White	2013, Perianal abscess 2015, Persistent perineal wound 2018, Persistent rectal mucosal ulceration	Skin Rectum	Crohn's disease Azathioprine x 8 years	2013, Azathioprine was stopped. 2015, Treated with Rituximab x 4 doses.	2019, Patient had ileocecal resection and proctectomy. 2019, diagnosed with large B-cell lymphoma transformation. Planned for 3 cycles of RCVP regimen (Rituximab, Cyclophosphamide, Vincristine, Prednisone).	Skin with infiltration of the dermis with scattered large, pleomorphic lymphocytes in a background of acute and chronic inflammation.	Positive:EBER, CD20, CD30 Negative: CD15
2	37	M	White	Ulcerated maxillary palatal lesion x 2 month	Oral mucosa	N/A	None	After the biopsy, the lesion completely healed well.	Marked surface ulceration with necrosis and bacterial colonization. The lamina propria shows a marked lymphoma proliferation process with necrosis.	Positive:EBER, CD30, CD45, CD3, Granzyme B Negative: CD15, CD5, CD7, CD8 Ki-67: 90%
3	70	M	White	Epigastric abdominal pain, difficulty with poor oral intake, Shingles and weight loss. Upper GI endoscopy showed a 4 cm, cratered esophageal ulcer.	Esophagus mucosa	Old age	Rituximab x 4 doses	Symptoms improved. Upper GI endoscopy showed a superficial esophageal ulcer with no bleeding and no stigmata of recent bleeding were found in the lower third of the esophagus. Biopsy showed resolving prior biopsy-proven EBV-positive mucocutaneous ulcer. Follow-up every 3 months.	Areas of acute and chronic inflammation forming ulcers. Clusters of large atypical lymphoid cells were also identified.	Positive: EBER, CD20, CD30, CD45, MUM1 Negative: BCL6
4	63	M	Black	Left-sided hearing loss and further workup were found to have a nasopharyngeal mass occluding bilateral eustachian tube opening and bilateral bulky cervical lymphadenopathy.	Nasopharyngeal mucosa	HIV	N/A	Follow-up every 6 months.	Reactive mixed lymphoplasmacytic infiltrate.	Positive: EBER

Note: N/A, Not applicable.

Figure 1 - 665

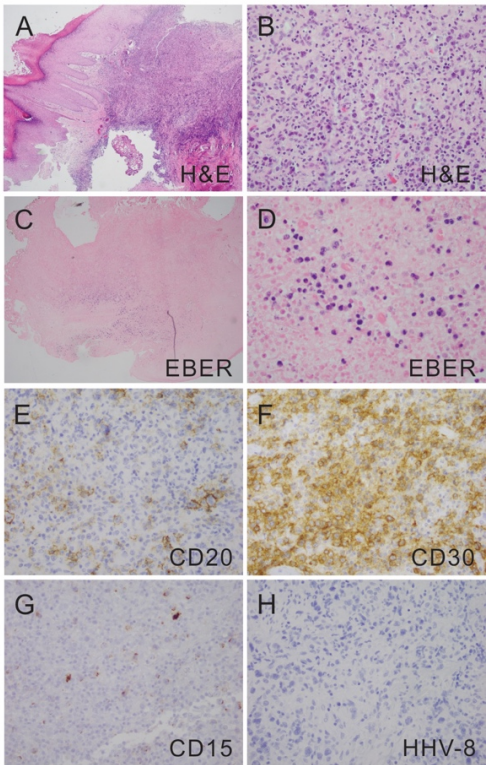

Conclusions: EBVMCU is a rare EBV-related lymphoproliferative disorder. So far only a small number of case reports have been discussed. In general, patient with EBVMCU typically has an indolent clinical course. Rare cases of relapse or progression to more widespread disease has been observed. This case series highlights the importance of clinical and pathologic features of EBVMCU.

666 Pan-Trk Immunoexpression Occurs in a Subset of Gastrointestinal Stromal Tumors (GIST) but is not Specific for NTRK Rearrangement

Daffolyn Rachael Fels Elliott[1], Walter Devine[2], Sanjay Kakar[1], Joseph Rabban[1]
[1]University of California San Francisco, San Francisco, CA, [2]University of California San Francisco, Berkeley, CA

Disclosures: Daffolyn Rachael Fels Elliott: None; Walter Devine: None; Sanjay Kakar: None; Joseph Rabban: *Employee*, Spouse is an employee of Merck & Co.

Background: Rearrangement or mutation of the neurotrophic receptor tyrosine kinase genes *NTRK1* and *NTRK3* has been described in a rare subset of wild-type GISTs that lack mutations in *KIT*, *PDGFRA*, *SDH* or *RAS* pathway components. Response to *NTRK* targeted therapy has been reported in these rare GISTs. In other types of neoplasms that harbor an *NTRK* rearrangement, pan-Trk immunohistochemistry is a sensitive and specific marker for the rearrangement. The prevalence of pan-Trk immunoexpression and its correlation with *NTRK* rearrangement has not been evaluated in GIST.

Design: Immunohistochemistry for pan-Trk, DOG-1, CD117, and SDHB was performed on tissue microarrays (triplicate 2 mm cores) of resected GISTs (median age 64 y; 55% female; 6% advanced stage; 17% with metastasis or recurrence). Any cytoplasmic staining for pan-Trk was defined as positive. S100 was also performed as some forms of *NTRK* neoplasms are known to be strongly diffusely S100 positive. Tumors with the strongest degree of pan-Trk staining were evaluated by next generation sequencing (NGS) using a 500 gene panel.

Results: 143 GISTs were evaluated (83% primary, 17% metastatic/recurrent). The most common sites were stomach (62%), duodenum (15%) and small intestine (12%). All were positive for DOG-1 and/or CD117. Pan-Trk was positive in 17% (24/143) of GISTs. The staining was moderate-strong in 2/24; moderate in 2/24; weak-moderate in 8/24; weak in 8/24; and faint in 4/24. Loss of SDHB staining occurred in 6% (9/143). None showed diffuse strong S100 staining but 11% had focal-patchy staining. No rearrangements of *NTRK1, NTRK2,* or *NTRK3* were detected by NGS testing of the 3 strongest pan-Trk staining GIST (all duodenal origin); however, 2 cases had deleterious alterations in *NF1* (nonsense mutation and deep deletion) and the third had a *KIT* mutation (activating in-frame deletion). No mutations in *PDFGRA* or *SDH* were detected. Besides the 2 patients for whom NGS testing revealed *NF1* mutation, 6 others had a

previously known diagnosis of NF1; pan-Trk was moderate-strong (1/6); weak-moderate (1/6); weak (2/6) or negative (2/6); none were tested for *NTRK* rearrangement.

Conclusions: pan-Trk staining may be detected in a minority of GISTs, and can be strong in rare cases. This appears to be a non-specific finding as it does not correlate with the presence of an *NTRK* rearrangement. The finding of *NF1* mutation in 3 of 4 moderate-strong pan-Trk positive GISTs raises the possibility of relationship between these alterations and merits further inquiry.

667 Processing Rectal Cancer Resection Specimens: A Comparative Evaluation of a Cross Sectioning Approach with Wholemount Blocks and Slides versus the Regular Approach

Canan Firat[1], Mithat Gonen[1], Peter Ntiamoah[2], Efsevia Vakiani[1], Julio Garcia-Aguilar[1], Jinru Shia[1]
[1]Memorial Sloan Kettering Cancer Center, New York, NY, [2]New York, NY

Disclosures: Canan Firat: None; Mithat Gonen: None; Peter Ntiamoah: None; Efsevia Vakiani: None; Julio Garcia-Aguilar: *Speaker*, Intuitive Surgical, Medtronic, Johnson and Johnson; Jinru Shia: None

Background: In rectal cancer management, thorough pathological assessment of histologic features such as mesorectum intactness, circumferential margin(CRM), lymphovascular invasion(LVI) including extra-mural large venous invasion(EMVI), and lymph node(LN) status, has contributed significantly to the marked improvement in clinical outcome in recent years. It has been proposed that, for rectal cancer resection specimens, a cross-sectioning approach(CSA) may allow more accurate pathological evaluation. In this analysis, we employed CSA in a series of rectal cancer resections, and compared the pathological parameters in these cases with that of comparable cases that were processed by the regular-approach(RA).

Design: CSA included 1)fixing the rectal specimen with tumor region intact/not-opened for >= 48hours, 2)cross sectioning at 4mm-interval of the entire tumor region and the portion distal to it, 3)wholemount blocks and slides of each cross section, and 4)digitization of both gross and microscopic wholemounts. RA was according to routine protocol with regular-size sections of the entire tumor region upon visualization of the opened specimen. The 2 groups were comparable with regard to clinical features (including treatment modalities) and operating surgeons.

Results: Sixty-three primary rectal cancer resections within a one-year period were evaluated, 28 by CSA and 35 by RA. No difference was detected between the 2 groups in mesorectal intactness (89% complete in CSA vs 94% in RA, p=0.5), distal margin-clearance (median, 31 vs 35mm, p=0.7), greatest-tumor-dimension (median, 25 vs 30mm, p=0.4), and rates of LVI/EMVI (any LVI, 64% vs 40%, p=0.08; EMVI, 14% vs 26%, p=0.35). Of the tumors treated with neoadjuvant-therapy, no difference was detected between treatment responses (32% grade-3 vs 34%, p=0.7); however, CSA detected a significantly closer CRM-clearance (mean/median, 7.8mm/7mm vs 14.4mm/12mm, p<0.0001), although the rates of CRM-involvement did not differ significantly (CRM<=1mm, 5/28[18%] in CSA vs 2/35[6%] in RA, p=0.23). CSA yielded a higher LN-count than RA (median, 23 vs 15, p=0.03), but no difference was detected in the number of positive LNs (mean, 2 vs 0.8, p=0.3) or pN stage (pN+: 29% vs 37%, p=0.5). pT stage was similarly not different (p=0.3).

Conclusions: The CSA-approach with wholemount-sections detected a closer CRM-clearance in rectal cancer resections when compared to the regular-approach. Further studies are underway to determine the clinical significance of such findings.

668 Whole Block Imaging (WBI) Utilizing Micro-Computed Tomography (Micro-CT) Reveals Pathological Information Not Detected on Regular Histology: A Pilot Study of Rectal Cancer Resection Specimens

Canan Firat[1], Alexei Teplov[1], Noboru Kawata[1], Kareem Ibrahim[1], Peter Ntiamoah[2], Meera Hameed[1], Efsevia Vakiani[1], Julio Garcia-Aguilar[1], Yukako Yagi[1], Jinru Shia[1]
[1]Memorial Sloan Kettering Cancer Center, New York, NY, [2]New York, NY

Disclosures: Canan Firat: None; Alexei Teplov: None; Noboru Kawata: None; Kareem Ibrahim: None; Peter Ntiamoah: None; Meera Hameed: None; Efsevia Vakiani: None; Julio Garcia-Aguilar: *Speaker*, Intuitive Surgical, Medtronic, Johnson and Johnson; Yukako Yagi: None; Jinru Shia: None

Background: The continued improvement in pathological evaluation of rectal-cancer-resection specimens (including increasingly more-detailed assessment of mesorectum, circumferential-margin, tumor-deposits[TDs] and lymph nodes[LNs]) has been contributary to the continuing improvement of clinical outcome. Micro-CT-WBI is a newly emerged 3-dimensional-modality that can assess the paraffin-tissue's microarchitecture. This pilot-study aimed at exploring whether there was additive utility of this modality to the current approach in assessing rectal-cancer-resection specimens.

Design: Micro-CT-WBI of wholemount-blocks and whole-slide-imaging(WSI) of the corresponding-wholemount-H&E-sections of rectal-cancer specimens were evaluated. Detailed annotations on the WSI served as training tools for the recognition of the histologic patterns on

WBI. Comparative analyses were performed to determine whether WBI revealed additional information beyond what was ascertained from H&E.

Results: Eighty wholemount-blocks and H&E-sections from 7 rectal-cancer-resections were evaluated. Major histological features(tumor, mucin, LNs, TDs) were readily recognizable on WBI, at a resolution = 1-10x magnification(~1um/pixel). WBI recognized viable-carcinoma in 3/3 cases(31/31 blocks) that contained viable-tumor, and predicted lack of viable-carcinoma in 2/2 cases(11/11 blocks) that showed 100% treatment response. In the remining 2 cases, WBI did not reveal evidence of tumor while H&E identified small foci of tumor in <=2 slides. Similar accuracy-rates were achieved with mucin, LNs with or without macroscopic metastasis and TDs. WBI recognized large-venous-invasion 50% of the time. WBI could not recognize perineural invasion(0/3 cases). Complementing the conventional-histology, WBI allowed visualization of the evolution of the histologic features both within the same block and through the entire tumor via contiguous blocks. This was particularly informative on the origin of TDs: WBI detected TDs in 3/3 cases; in 1, the origin of TD was traced to large-venous-invasion, and in another, to the primary-cancer. No origin could be detected in the 3rd case.

Conclusions: Micro-CT-WBI provided a 3rd-dimension that complemented conventional histology. It revealed evidence indicating varied origins of tumor deposits in rectal cancers. Studies are ongoing to further address the clinical/biological implication of such findings.

669 H. pylori Negative Primary Gastric Mucosa-Associated Lymphoma (MALToma) More Often Associated with Obesity, a Single-Institution Study

Michaelangelo Friscia[1], Brenda Mai[2], Jaiyeola Thomas[2], Mamoun Younes[3], Md Amer Wahed[2], Zhihong Hu[4], Xiaohong Iris Wang[5], Nghia Nguyen[2], Lei Chen[6]
[1]Houston, TX, [2]The University of Texas Health Science Center at Houston, Houston, TX, [3]UTHealth McGovern Medical School, Houston, TX, [4]The University of Texas Health Science Center at Houston, Sugar Land, TX, [5]Bellaire, TX, [6]University of Texas Houston, Houston, TX

Disclosures: Michaelangelo Friscia: None; Brenda Mai: None; Md Amer Wahed: None; Zhihong Hu: None; Xiaohong Iris Wang: None; Xiaohong Iris Wang: None; Xiaohong Iris Wang: None; Xiaohong Iris Wang: None; Nghia Nguyen: None; Lei Chen: None

Background: More than 90% of gastric mucosa-associated lymphoid tissue (MALT) lymphomas can be associated with Helicobacter pylori infection (H. pylori). However, the pathogenesis of H. pylori-negative MALT lymphomas is still controversial. Some experts have argued that the H. pylori negativity is a false negative, whereas others suggest that additional etiologies should be investigated.

Design: An archival search from our institutions for gastric MALT lymphoma cases over an interval of 15 years was performed. The height and weight of the patients were collected. If the H. pylori stain was negative, results from the urea breath test, serology, stool antigen, and previous biopsy results were also reviewed.

Results: There were 56 patients identified; 21 patients positive for H. pylori (Positive group; 37.5%) and 35 patients negative for H. pylori (negative group; 62.5%). The mean BMI of the positive group was 27.36 kg/m2 (range, 17.96-47.25) with a SD of 7.81 and a SEM as 1.70. The mean BMI of the negative group was 31.90 kg/m2 (range, 18.17-49.77) with a SD of 7.78 and a SEM as 1.31. A Fisher's exact test comparing the frequency of patients that were obese versus non-obese in relation to their H. pylori status resulted in a two-tailed *p*-value of 0.0255 and this was deemed to be statistically significant. In addition, an unpaired t-test comparing the mean BMIs in relationship to their H. pylori status revealed a two-tailed *p*-value of 0.0396 and this was also deemed to be statistically significant.

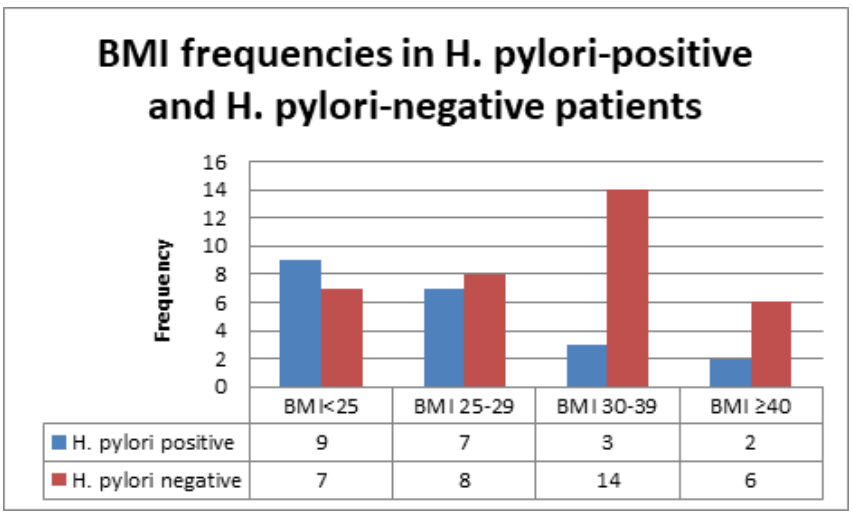

Conclusions: Obesity is associated with an increased risk of several malignancies and higher mortality rates in patients with cancers in some body sites. However, there is no report to link obesity in patients with gastric MALT lymphoma. Our study is the first to reveal a potential correlation between obesity and the risk of development of H. pylori-negative primary gastric MALT lymphoma.

670 Lymphocytic Colitis- Pattern Injury Presenting as Endoscopic Polyps: Case Series

Zhiyan Fu[1], Mahmoud Aldyab[1], Mustafa E Arslan[1], Ann Boguniewicz[2], HwaJeong Lee[3]
[1]Albany Medical Center, Albany, NY, [2]Loudonville, NY, [3]Albany Medical Center, Guilderland, NY

Disclosures: Zhiyan Fu: None; Mahmoud Aldyab: None; Mustafa E Arslan: None; Ann Boguniewicz: None; HwaJeong Lee: None

Background: Lymphocytic colitis (LC) is characterized by chronic watery diarrhea and unremarkable endoscopic findings. Only one case of LC presenting as multiple colonic polyps has been reported. Having encountered cases of endoscopic “polyps” with histologic LC-pattern injury (LCPI), we examined such cases and evaluated their presentation and associated risk factors in comparison to conventional non-polypoid LC.

Design: Archived (2009 – 2019) polypoid LCPI were retrieved. Polypoid LCPI with superimposed histologic features accountable for a polyp other than LCPI, such as adenoma, hyperplastic change or lymphoid aggregate, was excluded. Indication for the colonoscopy, endoscopic findings and clinical history including medication history were obtained from the electronic medical records. 40 cases of conventional LC were used as a control. Fisher’s exact test was performed to evaluate associations between two variables. $P<0.05$ was considered statistically significant.

Results: A total of 19 polypoid LCPI cases were retrieved from 18 (12 female, 6 male) patients. The mean age of the patients was 60.5 years (range 25-84). The indication for colonoscopy was chronic watery diarrhea (10/19; 53%), screening/surveillance (7/19; 37%), and rectal bleeding (2/19; 11%). The mean number of the polyps was 1.7 (range 1-6) with the mean size 2.9 mm (range 1-6). 56% (18/32) of the polyps were located in the right colon and 44% (14/32) were sessile. Endoscopically, the background non-polypoid mucosa appeared normal in 17 cases and erythematous/friable in two. When biopsied (14/19; 74%), all non-polypoid colonic mucosa showed LCPI. Between the polypoid LCPI vs. conventional LC, there was no difference in the mean age, gender, and the average number of lymphocytes/100 epithelial cells (37 vs 41; $p>0.05$). Hypertension, peripheral vascular disease and history of malignancy were more common in polypoid LCPI group compared to the control LC group ($p<0.05$). Frequencies of other comorbidities and risk factors for LC, including autoimmune disease and medication history, were similar between the two groups.

Conclusions: LCPI may present as endoscopic polyps, frequently in patients with hypertension, peripheral vascular disease and history of malignancy. Polypoid LCPI may be a harbinger of LCPI in the background non-polypoid colonic mucosa. A subset (53%) of polypoid LCPI represents LC.

671 Detection and Immunosurveillance of Senescent Cells in Colorectal Carcinoma – Evaluation of Senescence-Associated Biomarkers and Analysis of the Interactions between Senescent Tumor Cells and Immune Cells

Franziska Gach[1], Aurélie Fernandez[1], Katrin Tagscherer[1], Sabrina Schecher[1], Esther Huettermann[2], Achim Heintz[2], Wilfried Roth[1], Sebastian Foersch[3]
[1]University Medical Center Mainz, Mainz, Rhineland Palatinate, Germany, [2]Department of General, Visceral and Vascular Surgery, Catholic Hospital Mainz, Mainz, Rhineland Palatinate, Germany, [3]University Medical Center Mainz, Mainz, Germany

Disclosures: Franziska Gach: None; Aurélie Fernandez: None; Sebastian Foersch: None

Background: Permanent cell cycle arrest following the initiation of senescence in (pre)malignant cells counteracts progression. Apart from ceasing proliferation, cells entering senescence adopt a characteristic secretory phenotype (SASP). This results in potentially pro-tumorigenic alterations to the microenvironment and affects the immunosurveillance of the tumor. To understand the role of senescence in a clinical context of carcinogenesis, specific immunohistochemistry (IHC) biomarkers are required. Our aim is to investigate the clinical implications of senescence in colorectal carcinoma (CRC) and to analyse the interactions of immune cells and senescent tumor cells.

Design: Senescence was induced in CRC cell lines by low-dose etoposide treatment. Using this cell culture system, Western Blotting and FACS analysis, different markers were validated. A TMA containing tissue of 598 CRC patients was generated and IHC for senescence-associated molecules and markers of immune cell subtypes was carried out. Comprehensive digital image analysis of the TMA sections was performed. Results were correlated to overall survival (OS) and progression-free survival (PFS). Co-cultures of senescent Caco-2 cells and immune cell populations were established, and effects were studied using white-light microscopy, electron microscopy, live cell imaging and multiple cell viability assays.

Results: Addition of immune cell lines NK92 or TALL104 to Caco-2 colon cancer cells leads to dose-dependent cell death in >75% of senescent Caco-2 cells but less than 20% of proliferating control cells. This specific cytotoxicity is a result of direct cell-cell-interaction and

mainly facilitated via apoptosis induction. Regarding the expression of different senescence markers, a low (<0,1), as well as an extremely high (>0.6) ratio of senescent cells are associated with a decreased OS and PFS. Proximity analysis of senescent cells and CD8+ cells allows a better discrimination regarding OS than evaluating CD8-status only.

Conclusions: Senescence-associated molecules have significant prognostic value in CRC. Absence as well as high expression of these biomarkers are associated with a poor prognosis. Arresting the cell cycle of impaired cells imposes a barrier on tumorigenesis. However, a high expression of senescence markers within the tumor does not indicate a potent tumor defence due to the importance of an effective immunosurveillance. To reflect this, proximity analyses of these cell populations might be a strong prognostic tool.

672 Pathological and Molecular Features of Mucinous Colorectal Adenocarcinoma

Roberta Gafa'[1], Giulia Galli[2], Iva Maestri[2], Lanza Giovanni[2]
[1]University of Ferrara, Ferrara, FE, Italy, [2]Division of Anatomic Pathology, University Hospital of Ferrara, Ferrara, Italy

Disclosures: Roberta Gafa': None; Giulia Galli: None; Iva Maestri: None; Lanza Giovanni: None

Background: Mucinous carcinomas (MC) account for 10-15% of colorectal carcinomas (CRC) and are considered aggressive tumors. They differ from conventional adenocarcinoma for many clinico-pathologic and molecular characteristics with implications on patient management and prognosis. Aim of the study was to compare clinical, pathological and biologic features of MC (mucin >50%) with those of conventional adenocarcinomas (AD) and of adenocarcinomas with <50% of mucin (AD-MC).

Design: The study included 1675 patients with CRC surgically resected between 2004 and 2018. Mismatch repair status (MMR) was determined in 1422 cases by immunohistochemical analysis of MLH1, MSH2, MSH6 and PMS2 expression and/or by microsatellite instability analysis using a fluorescent PCR method. Tumors with loss of MMR protein expression and/or MSI-H were classified as MMR-deficient (MMR-D) and tumors with retained MMR proteins expression and/or MSS/MSI-L as MMR-proficient (MMR-P). KRAS exon 2 and BRAF-V600E mutation were investigated by direct DNA sequencing or RT-PCR in 630 cases.

Results: Of the 1675 tumors, 1123 (67%) were classified as AD, 352 (21%) as AD-MC and 200 (12%) as MC. Comparing the three groups, MC and AD-MC occurred more frequently in the proximal colon ($p<0.001$) and more often demonstrated poor differentiation. No other significative differences were found concerning the other clinical and pathological variables examined. MC (37%) and AD-MC (34%) were more frequently MMR-D ($p<0.001$) than AD (6%). MC (36%) and AD-MC (41%) were also more often BRAF mutated than AD (12%). KRAS mutations were detected at a higher rate in AD and MC with respect to AD-MC ($p=0.01$). As a whole the proportion of KRASwt/BRAFwt AD (45%) was higher with respect to AD-MC (22%) and MC (18%). The strong association between BRAF mutation and tumor type was also observed in the group of MMR-P carcinomas.

Conclusions: MC represent a distinct but heterogeneous group of CRC, characterized by specific molecular features such as MMR deficit and BRAF mutation. Interestingly, AD-MC display a genetic pattern of alterations similar to MC, suggesting that these tumors should be classified separately from conventional adenocarcinomas.

673 High Body Mass Index (BMI) Directly Correlates with High Tumor Budding and More Aggressive Tumor Biology in Kentuckians with Colon Adenocarcinoma

Tong Gan[1], Akila Mansour[1], Daheng He[1], Chi Wang[1], Tianyan Gao[2], Therese Bocklage[3], Kurt Schaberg[4], Mark Evers[1]
[1]University of Kentucky Healthcare, Lexington, KY, [2]University of Kentucky, Lexington, KY, [3]University of Kentucky College of Medicine, Lexington, KY, [4]University of California Davis, Sacramento, CA

Disclosures: Tong Gan: None; Akila Mansour: None; Daheng He: None; Chi Wang: None; Tianyan Gao: None; Therese Bocklage: None; Kurt Schaberg: None

Background: Kentucky ranks 1st in the U.S. in colorectal cancer (CRC) incidence with particularly high rates in Appalachian Kentucky where obesity is also prevalent. Obesity has not only been recognized as a risk factor for CRC, but it has also been associated with reduced survival compared to normal weight CRC patients. An emerging histologic criterion that portends a more aggressive tumor biology and worse outcome in patients with CRC is high number of tumor buds at the invasive edge. The relationship between the BMI as an indicator for obesity and tumor budding as a marker for a more aggressive behavior in CRC has not been studied.

Design: Kentucky CRC specimens (Stages I-III) from 2008-2014 were scored by two pathologists for tumor budding, poorly differentiated tumor clusters, lymph node metastasis, and inflammation. Data was subsequently correlated with stage, patient location, and body mass index (BMI) using the Kentucky Cancer Registry and SEER registry.

Results: We reviewed 174 specimens stratified by stage: I (30%), II (37%), III (33%); and geography: Appalachian (55%) and non-Appalachian (45%). Of these, 50% had low (<5 buds), 18% had intermediate (5-9) and 32% had high (>10)tumor budding. High tumor

budding was significantly associated with more poorly differentiated tumor clusters, positive lymph nodes, higher tumor stage and poorer overall survival in both the Appalachian and non-Appalachian population (Table 1). Importantly, we found a novel significant association of high BMI with high tumor budding on both univariate and multivariate analyses.

Table 1. Clinicopathological Tumor Characteristics Associated with Tumor Budding in the Kentucky Colorectal Cancer Population

Histological Features	**Tumor Budding**			
	Univariate	*Multivariate*	*OR/HR*	*95% CI*
Poorly Diff. Tumor Clusters	< 0.001	< 0.001		
Grade 2 vs 1			10.01	(4.00 - 26.50)
Grade 3 vs 1			8.22	(3.78 - 18.61)
Positive Lymph Nodes	< 0.001	0.015	1.07	(1.01 - 1.12)
AJCC TNM Stage	< 0.001	< 0.001		
Stage II vs I			1.39	(0.67 - 2.91)
Stage III vs I			4.99	(2.33 – 10.68)
Body Mass Index (BMI)	0.018	0.029		
Obese vs Non-Obese			2.12	(1.08 - 4.16)
Overall Survival	0.008	0.012	1.48	(1.09 - 2.01)

Obese: BMI ≥ 30, Non-Obese: BMI < 30; Odds Ratio (OR)/Hazard Ratio (HR)

Multivariate Analysis Adjusted for Age, Sex, TNM Staging, Location, Appalachian Status, BMI.

Conclusions: We report, for the first time, a direct correlation between a systemic risk factor for CRC, high body mass index, and a local (histologic) marker of CRC aggressiveness, high tumor budding. Work is ongoing to identify additional possible etiologic factors related to obesity that may be driving tumor budding.

674 Prospective Testing for Loss or Over-Expression of p53 Identifies Barrett's Esophagus Patients at Increased Risk of Subsequent High Grade Dysplasia or Adenocarcinoma

Daniel Geisler[1], Minami Tokuyama[2], Kevin McGrath[3], Reetesh Pai[4], Jon Davison[3]
[1]UPMC, Pittsburgh, PA, [2]Icahn School of Medicine at Mount Sinai, New York, NY, [3]University of Pittsburgh School of Medicine, Pittsburgh, PA, [4]UPMC-Presbyterian Hospital, Pittsburgh, PA

Disclosures: Daniel Geisler: None; Minami Tokuyama: None; Kevin McGrath: None; Reetesh Pai: None; Jon Davison: None

Background: Abnormal p53 protein expression detected by immunohistochemistry (IHC) in Barrett's esophagus (BE) is reported to be a prognostic biomarker for progression to high grade dysplasia (HGD) or esophageal adenocarcinoma (EAC). One reason p53 IHC is not currently recommended as a biomarker is the paucity of prospective data supporting its use. We, therefore, sought to evaluate the ability of p53 IHC to identify patients at risk for progression in a group of patients prospectively tested during routine clinical care.

Design: We identified all cases from 2010 to 2016 in which p53 IHC was performed during routine surveillance (Figure 1). We reviewed the original diagnostic H&E and p53 IHC slides and scored the IHC for loss or overexpression of p53 protein in BE using independently validated criteria, based Kaye et al. [PMID 26918780] and Younes et al. [PMID 28226185]. A determination of either loss or overexpression of p53 required the consensus of 2 pathologists. We compared time to subsequent HGD or EAC using Kaplan Meier curves and adjusted for other known risk factors using multivariate Cox regression.

Results: We identified a total of 465 BE biopsy cases that reported p53 testing, representing 5.6% of all BE cases diagnosed during the study period. After exclusions (Figure 1), there were 94 cases of BE tested during routine surveillance, prior to a diagnosis of HGD or EAC, with subsequent clinical follow-up, and original diagnostic slides available for review. Patients (n=84) averaged 62 years old, predominantly male (71%) with short segment BE (53%), and most were originally diagnosed with indefinite (54%) or low grade dysplasia (30%). Abnormal p53 expression (loss or overexpression) was present in 49%. Eight (8) patients were upgraded to HGD on review of the tested biopsies and 11 other patients were subsequently diagnosed with HGD or EAC.

Excluding patients upgraded to HGD on review, the cumulative rate of subsequent HGD or EAC at 5 years was 43.9% in patients with aberrant loss or overexpression of p53, compared to 7.1% for patients with wild-type p53 (P=0.003, Figure 2). In multivariate analysis, overexpression or loss of p53 carried a 10.9-fold risk of subsequent HGD or EAC, independent of age, sex, BE length, ablation history and dysplasia grade (95% CI 1.5-75, P=0.016).

Figure 1 - 674

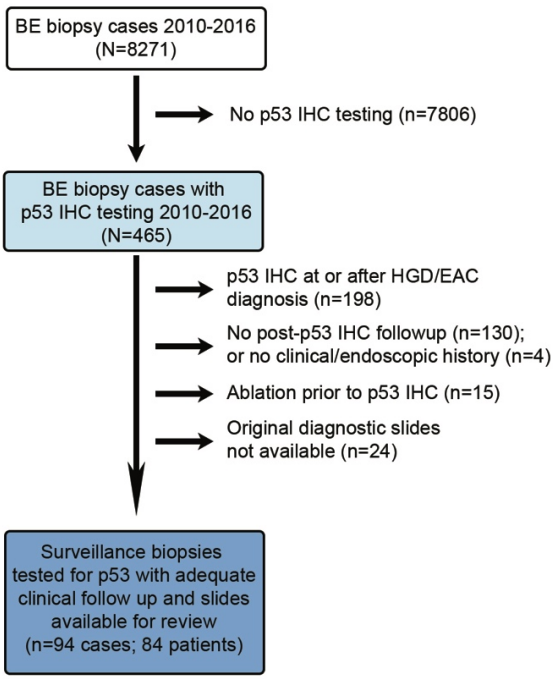

Figure 2 - 674

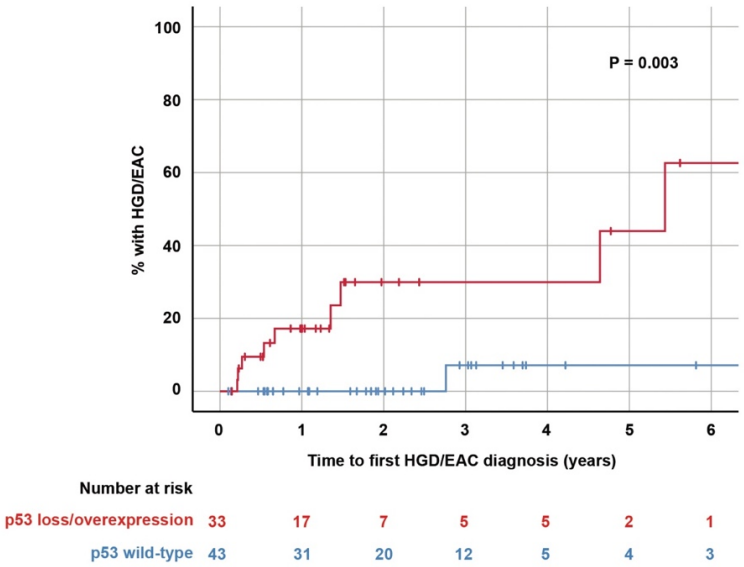

Conclusions: Selective prospective testing for aberrant loss or overexpression of p53 identified patients under surveillance for BE who were at increased risk of subsequent HGD or EAC.

675 High-Grade Appendiceal Mucinous Neoplasm: A Clinicopathologic Analysis of 22 Cases

Raul Gonzalez[1], Norman Carr[2], Haihui Liao[3], Reetesh Pai[4], Diana Agostini-Vulaj[5], Joseph Misdraji[6]
[1]Beth Israel Deaconess Medical Center, Boston, MA, [2]Basingstoke and North Hampshire Hospital, Basingstoke, United Kingdom, [3]Massachusetts General Hospital, Harvard Medical School, Boston, MA, [4]UPMC-Presbyterian Hospital, Pittsburgh, PA, [5]University of Rochester Medical Center, Rochester, NY, [6]Harvard Medical School, Boston, MA

Disclosures: Raul Gonzalez: None; Norman Carr: None; Haihui Liao: None; Reetesh Pai: None; Diana Agostini-Vulaj: None; Joseph Misdraji: None

Background: The term "high-grade appendiceal mucinous neoplasm" (HAMN) was introduced by the Peritoneal Surface Oncology Group International in 2016 for mucinous epithelial tumors of the appendix with pushing invasion similar to low-grade appendiceal neoplasms (LAMN) but with unequivocal high-grade cytology. As HAMNs are rare and poorly characterized, we assembled a multi-institutional cohort.

Design: We identified 22 HAMNs from four different institutions. Cases were centrally reviewed by two authors. For each, we recorded patient age, sex, and symptoms; tumor size, gross and microscopic appearance, and margin status; presence of extra-appendiceal disease; adjuvant therapy; and patient outcome.

Results: The 22 patients included 16 women and 6 men, with median age of 58 years (range: 23-76 years). Many (12; 55%) had abdominal/pelvic pain or symptoms of appendicitis; 3 were asymptomatic. Average tumor size was 8.1 cm (range: 3.2-19.0 cm); 7 (32%) were grossly perforated. Most appendices were entirely submitted for microscopy. Half (11) had diffuse (>75%) high-grade cytology, compared to focal in the others. The luminal epithelium was typically flat to undulating (Fig. 1A); some showed cribriform or micropapillary growth (Fig. 1B). The high-grade epithelium always at least focally displayed mucinous features, though 10 (45%) also showed more colonic-type epithelium (Fig. 1C). Only 3 cases were confined to the appendiceal mucosa; 13 (59%) demonstrated serosal epithelium and/or mucin. Pseudomyxoma peritonei (PMP) was present in 12 resection specimens (55%) (Fig. 1D), comprising 7 (58%) of the mucinous HAMN and 5 (50%) of the mixed mucinous/colonic HAMN. PMP involved ovaries in 5 (23%). No case had positive lymph nodes, and none of the patients without PMP at diagnosis developed it after resection. Postsurgical treatment included hyperthermic intraperitoneal chemotherapy (n=8), FOLFOX (n=4), and cytoreductive surgery/debulking (n=9). Follow-up on 19 patients (median length: 36 months) showed 3 with PMP died of disease, 3 with PMP alive with disease, and the rest (including 6 with PMP) alive with no evidence of disease.

Figure 1 - 675

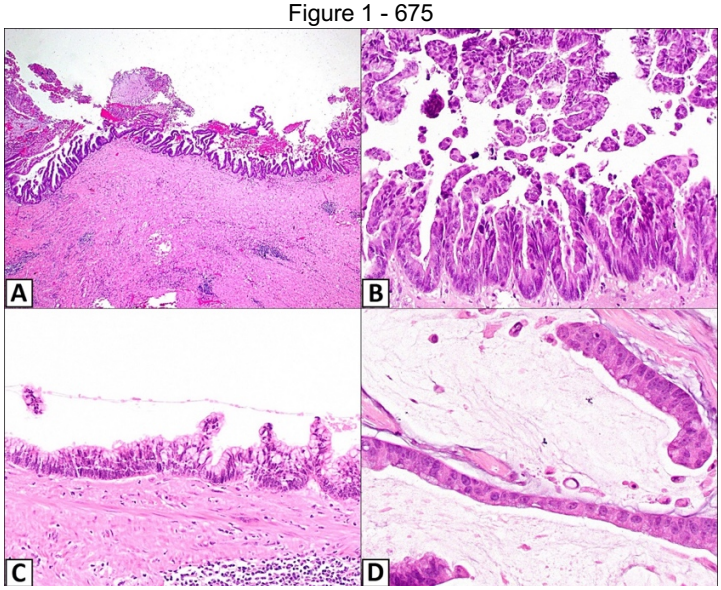

Conclusions: HAMN can be an aggressive malignancy that results in death in about 14% of patients. They are more common in women, and roughly half present with PMP. Some HAMNs show only focal high-grade cytology and are likely related to progression of LAMN. However, tumors with diffuse high-grade cytology may be biologically distinct from LAMN and arise as HAMN *de novo*.

676 Adenoma-Like Adenocarcinoma: Clinicopathologic Characterization of a Newly Recognized Subtype of Colorectal Carcinoma

Iván González[1], Philip Bauer[1], Esther Lu[2], Deyali Chatterjee[3]
[1]Washington University School of Medicine, St. Louis, MO, [2]St. Louis, MO, [3]Washington University in St. Louis, St. Louis, MO

Disclosures: Iván González: None; Philip Bauer: None; Esther Lu: None; Deyali Chatterjee: None

Background: The 2019 WHO recognizes a new subtype of colorectal adenocarcinoma (CRAC) termed adenoma-like adenocarcinoma (AA), characterized by adenoma-like morphology in at least 50% of the tumor, and associated with favorable prognosis. Not much is known about this newly recognized subtype. We sought to better characterize AA in our institutional cohort of CRAC.

Design: IRB approval was obtained. 372 cases of stage I-III CRAC without neoadjuvant therapy were identified from 2013-2016. Following 2019 WHO criteria, 91 AA cases were identified of which 67 were subclassified as pure (100%) and 24 cases were mixed (50-99%, figure 1), based on the percentage of AA-growth pattern. Other special types were excluded. Tumor budding (TB) was classified according to the recommendation by the International Tumor Budding Consensus Conference as low (TB1), intermediate (TB2), or high (TB3). Peritumoral stromal reaction was noted as no significant, collagenous, or myxoid stromal desmoplasia. Tumor infiltrating lymphocytes (TIL) was recorded as present, when >5 intratumoral lymphocytes per high-power field were identified. The clinical information was obtained from the electronic medical records.

Results: Clinicopathologic data and comparisons of AA and CRAC-NOS are shown in Table-1. AA was associated with significantly less lymphovascular invasion, perineural invasion, lymph nodal involvement, myxoid stroma, tumor deposits and tumor budding, and with significantly more TILs, higher pT- and TNM-stage (all parameters with $p<0.05$). AA (as defined by WHO) is associated with better RFS compared to CRAC-NOS ($p=0.026$; figure 2a). Although not statistically significant, the mixed group shows an intermediate survival between AA and CRAC-NOS (figure 2b). For the 24 mixed AA, a macro %findcut by the Contal and O'Quigley method gives 70% as the best cut point (figure 2c).

Table-1. Characteristic and Associations of Adenoma-Like Adenocarcinoma				
	Total	**AA (based on WHO definition)**		***P***
	N = 342	No[1] (n: 251)	Yes (n: 91)	
Age	65.2 ±12.6	64 ±12.3	68 ±13.1	
Gender				
Male	179, 52%	133, 53%	46, 51%	0.689
Female	163, 48%	118, 47%	45, 49%	
History of other cancer				
No	293, 86%	219, 87%	74, 81%	0.166
Yes	49, 14%	32, 13%	17, 19%	
Location				
Right colon	204, 60%	147, 59%	57, 63%	0.497
Left colon	138, 40%	104, 41%	34, 37%	
Tumor Grade				
Well/Moderate	294, 86%	206, 82%	88, 97%	**<0.001**
Poorly	48, 14%	45, 18%	3, 3%	
Lymphovascular invasion				
No	217, 63%	143, 57%	74, 81%	**<0.0001**
Yes	125, 37%	108, 43%	17, 19%	
Perineural invasion				
No	289, 85%	204, 81%	85, 93%	**0.006**
Yes	53, 15%	47, 19%	6, 7%	
TB				
No	239, 70%	153, 61%	86, 95%	**<0.0001**
Yes	103, 30%	98, 39%	5, 5%	
Stromal reaction				
Non-myxoid	225, 66%	145, 58%	80, 88%	**<0.0001**
Myxoid	117, 34%	106, 42%	11, 12%	
Tumor infiltrating lymphocytes				
No	228, 67%	178, 71%	50, 55%	**0.006**
Yes	114, 33%	73, 29%	41, 45%	
Tumor deposits				
No	303, 89%	217, 86%	86, 95%	**0.038**
Yes	39, 11%	34, 14%	5, 5%	
MMR status (n = 298)				
Retained	245, 82%	187, 84%	58, 77%	0.201
Lost	53, 18%	36, 16%	17, 23%	
pT stage				
pT1	25, 7%	18, 7%	7, 8%	**0.047**
pT2	71, 21%	50, 20%	21, 23%	
pT3	202, 59%	143, 57%	59, 65%	
pT4	44,13%	40, 16%	4, 4%	
pN stage				
pN0	218, 64%	145, 58%	73, 80%	**<0.001**
pN1	81, 24%	70, 28%	11, 12%	
pN2	42, 12%	36, 14%	7, 8%	
pTNM Stage				
I	79, 23%	55, 22%	24, 26%	**<0.001**
II	139, 41%	90, 36%	49, 54%	
III	124,36%	106, 42%	18, 20%	
[1]No = CRAC, NOS				

Figure 1 - 676

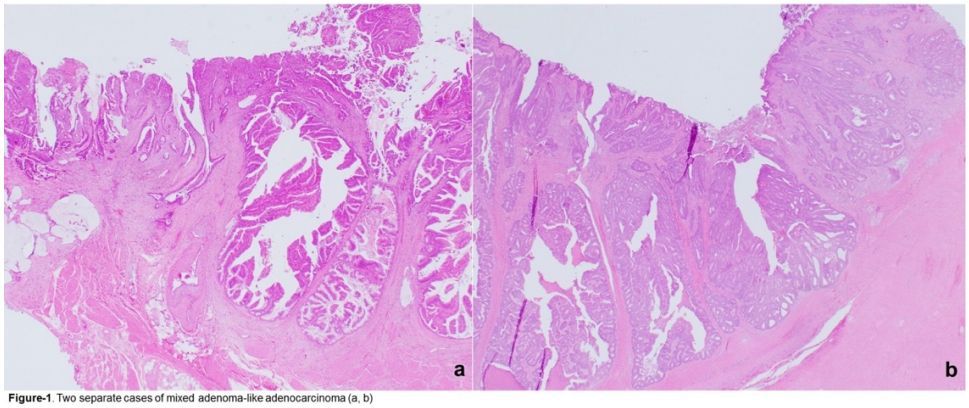

Figure-1. Two separate cases of mixed adenoma-like adenocarcinoma (a, b)

Figure 2 - 676

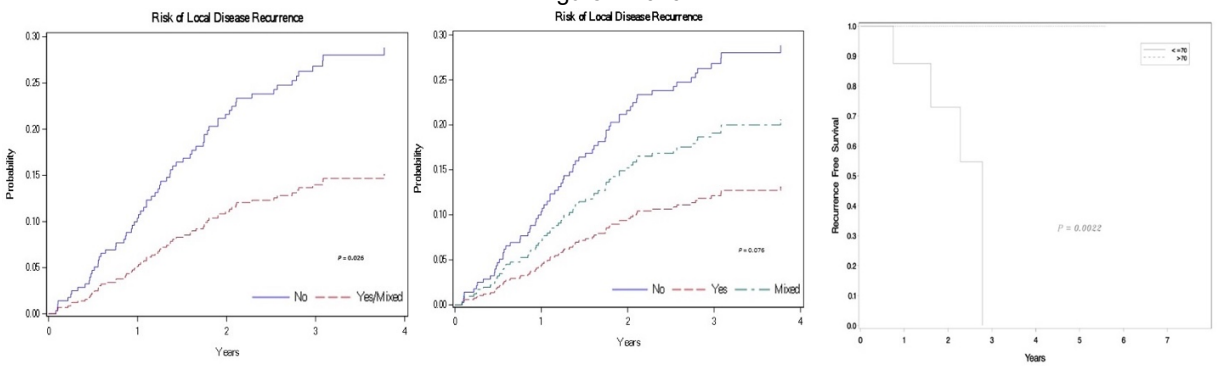

Conclusions: AA is associated with better RFS than CRAC-NOS, and show significant differences in terms of other histologic prognostic parameters. Although WHO suggests classifying this tumor subtype with a minimum 50% presence of the characteristic morphologic feature, our study suggests that tumors with mixed morphology are likely not as prognostically good as the cases with morphologically pure AA.

677 Clinicopathologic Significance of Tumor Budding, Tumor-Infiltrating Lymphocytes, and Stromal Reaction in the New 2019 WHO Colorectal Adenocarcinoma, NOS

Iván González[1], Philip Bauer[1], Esther Lu[2], Deyali Chatterjee[3]
[1]Washington University School of Medicine, St. Louis, MO, [2]St. Louis, MO, [3]Washington University in St. Louis, St. Louis, MO

Disclosures: Iván González: None; Philip Bauer: None; Esther Lu: None; Deyali Chatterjee: None

Background: Prior to the 2019 WHO classification, colorectal adenocarcinoma (CRAC), NOS included a now-recognized subtype, adenoma-like adenocarcinoma (AA). Consequently, with exclusion of this category of tumors known to have better prognosis, we sought to evaluate the significance of the already established histologic prognosticators in the new CRAC, NOS.

Design: IRB approval was obtained. 372 resected CRAC (stage I-III, without neoadjuvant treatment) were identified from 2013 to 2016. All special types (AA, mucinous, signet ring-cell, etc) were excluded. Tumor budding (TB) was assessed according to the International Tumor Budding Consensus Conference as low (TB1), intermediate (TB2) or high (TB3). Peritumoral stromal reaction was noted as no significant, collagenous, or myxoid. Tumor-infiltrating lymphocytes (TILs) was defined as >5 intratumoral lymphocytes per high-power field. The clinical information was obtained from the electronic medical records.

Results: 251 cases (mean age of 64 years, 73% women) of CRAC, NOS were included. The clinicopathologic data, histologic associations, and univariate and multivariate analyses are detailed in Table-1. All established pathologic prognosticators such as tumor and nodal stage, lymphovascular and perineural invasion, TB, and TILs, hold their significance in this cohort (all with p values < 0.05). Interestingly, the presence and absence of TB (p=0.02; fig-1), as well as TB1 versus TB2 and TB3 (p=0.02) were significant, however, not when stratified in a three-tier system. Also a significant poor prognostic parameter that was reinforced in this cohort was the presence of myxoid stroma in comparison to cases with collagenous or no significant stromal response (fig-2). On multivariate analysis, TILs (p=0.007) and pTNM stage (p<0.0001) were significant for RFS (table-1).

Table-1. Characteristic and Associations of Adenocarcinoma, NOs

	Total	Tumor budding		*P*	Stromal reaction		*P*	TILs		*P*
		No	Yes		Non-myxoid	Myxoid		No	Yes	
	N = 251									
TB										
No	153, 61%				101, 70%	52, 49%	**0.001**	99, 56%	54, 74%	**0.007**
Yes	98, 39%				44, 30%	54, 51%		79, 44%	19, 26%	
Stromal reaction										
Non-myxoid	145, 58%	101, 70%	44, 30%	**0.001**				93, 64%	52, 36%	**0.005**
Myxoid	106, 42%	52, 49%	54, 51%					85, 80%	21, 20%	
TILs										
No	178, 71%	99, 65%	79, 81%	**0.007**	93, 64%	85, 80%	**0.006**			
Yes	73, 29%	54, 35%	19, 19%		52, 36%	21, 20%				
Location										
Right colon	147, 59%	87, 29%	60, 61%	0.493	86, 59%	61, 58%	0.779	100, 56%	47, 64%	0.230
Left colon	104, 41%	66, 43%	38, 39%		59, 41%	45, 43%		78, 44%	26, 36%	
Tumor Grade										
Well/Moderate	206, 82%	118, 77%	88, 90%	**0.011**	113, 78%	93, 88%	**0.046**	156, 88%	50, 68%	**<0.0001**
Poorly	45, 18%	35, 23%	10, 23%		32, 22%	13, 12%		22, 12%	23, 32%	
LVI										
No	143, 57%	95, 62%	48, 49%	**0.041**	89, 61%	54, 51%	0.099	95, 53%	48, 66%	0.072
Yes	108, 43%	58, 38%	50, 51%		56, 39%	52, 49%		83, 47%	25, 34%	
PNI										
No	204, 81%	126, 82%	78, 80%	0.584	122, 84%	82, 77%	0.173	139, 78%	65, 89%	**0.043**
Yes	47, 19%	27, 18%	20, 20%		23, 16%	24, 22%		39, 22%	8, 11%	
Tumor deposits										
No	217, 86%	136, 89%	81, 82%	0.159	128, 88%	89, 84%	0.324	153, 86%	64, 88%	0.718
Yes	34, 14%	17, 11%	17, 17%		17, 11%	17, 16%		25, 14%	9, 12%	
MMR status										
Retained	187, 75%	110, 83%	77, 85%	0.798	102, 82%	85, 87%	0.301	15, 10%	21, 31%	**<0.0001**
Lost	36, 14%	22, 17%	14, 15%		23, 18%	13, 13%		140, 90%	47, 69%	
pT stage										
pT1	18, 7%	16, 10%	2, 2%	**0.048**	13, 9%	5, 5%	0.381	13, 7%	5, 7%	0.264
pT2	50, 20%	29, 19%	21, 21%		32, 22%	18, 17%		30, 17%	20, 27%	
pT3	143, 57%	81, 53%	62, 63%		78, 54%	65, 61%		107, 60%	36, 49%	
pT4	40, 16%	27, 18%	13, 13%		22, 15%	18, 17%		28, 16%	12, 16%	
pN stage										
pN0	145, 58%	98, 64%	47, 48%	**0.036**	93, 64%	52, 49%	0.057	98, 55%	47, 64%	0.370
pN1	70, 28%	35, 23%	35, 36%		34, 24%	36, 34%		52, 29%	18, 25%	
pN2	36, 14%	20, 13%	16, 16%		18, 12%	18, 17%		28, 16%	8, 11%	
Number of positive LNs		1.3, ±2.8	1.7, ±2.9	**0.011**	1.2, ±2.6	1.7, ±3.2	**0.010**	1.5, ±2.9	1.2, ±2.5	0.112
pTNM Stage										
I	55, 22%	37, 24%	18, 8%	**0.042**	37, 26%	18, 17%	**0.048**	35, 20%	20, 27%	0.284
II	90, 36%	61, 40%	29, 30%		56, 39%	34, 32%		63, 35%	27, 37%	
III	106, 42%	55, 36%	51, 52%		52, 36%	54, 51%		80, 45%	26, 36%	

Abbreviations: TB – tumor budding, TILs – tumor infiltrating lymphocytes, LVI – lymphovascular invasion, PNI – perineural invasion, MMR – miss-match repair; LNs – lymph nodes. *Percentage might not add to 100% due to rounding

Cox Proportional Hazard Models of Recurrence-Free Survival

	Univariate Analysis	Multivariate Analysis	
	P	HR (95% CI)	*P*
Age	0.172		
Gender	0.616		
Tumor location	0.912		
Tumor budding	**0.026**		
Tumor Infiltrating Lymphocytes	**0.007**		**0.007**
Yes		1	
No		2.681 (1.314 – 5.472)	
Lymphovascular invasion	**<0.0001**		
Perineural invasion	**0.012**		
Tumor deposits	**<0.0001**		
Myxoid stromal reaction	**0.029**		
MMR expression	0.743		
pT-stage	**<0.0001**		
pN-stage	**<0.0001**		
pTNM-stage	**<0.0001**		**<0.0001**
I		0.105 (0.033 – 0.338)	
II		0.219 (0.110 – 0.435)	
III		1	

Abbreviations: HR - Hazard ratio; CI - Confidence interval

Figure 1 - 677

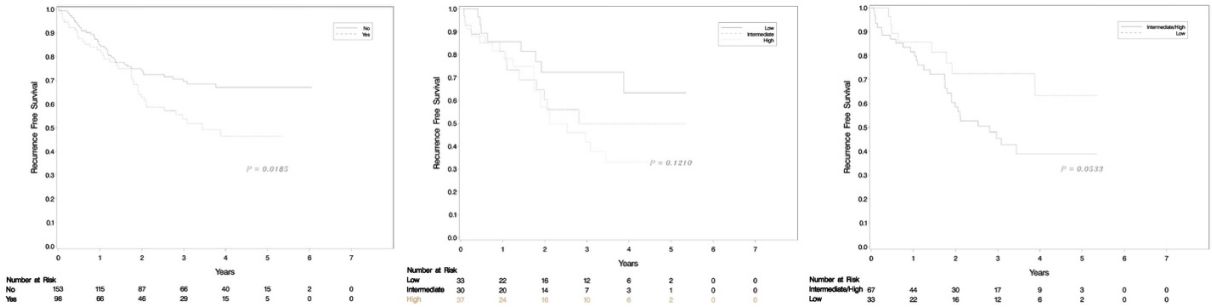

Figure 2 - 677

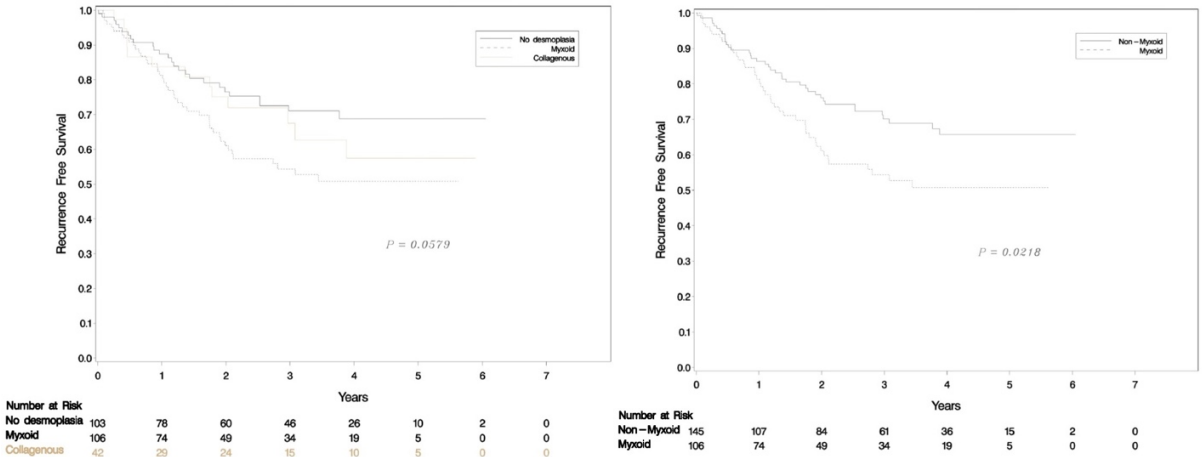

Conclusions: The prognostic significance of all established histologic parameters hold true for the newly reshuffled category of CRAC, NOS. In this cohort, a two-tier system for TB shows better correlation with RFS than the recommended 3-tier system. Only myxoid peritumor stromal response but not collagenous, is significantly associated with worse prognosis.

678 Ki-67 Proliferation Index Assessment in Gastrointestinal Neuroendocrine Tumors (GI-NET) by Digital Image Analysis (DIA) with Stringent Case- and Hotspot Level Concordance Requirements

Matthew Gosse[1], Sarag Boukhar[2], Andrew Bellizzi[2], Anand Rajan KD[2]
[1]Iowa City, IA, [2]University of Iowa Hospitals and Clinics, Iowa City, IA

Disclosures: Matthew Gosse: None; Sarag Boukhar: None; Andrew Bellizzi: None; Anand Rajan KD: *Advisory Board Member*, Roche Diagnostics Corporation

Background: Ki-67 proliferation index immunohistochemistry (IHC) assessment is an integral part of the diagnosis and prognostication of gastrointestinal (GI) neuroendocrine tumors (NET). Automated Ki-67 measurement in routine practice would greatly aid clinical workflows, reproducibility and standardization. Adoption of digital methods however have lagged owing to concerns of human-machine non-equivalency. We sought to address this in GI-NET with 2 image analysis platforms with bidirectional same case—different hotspot & same hotspot—different methodology concordance assessment with strict criteria.

Design: We assembled a cohort of GI-NET (n=20) comprising of primary and metastatic tumor from 16 patients. Ki-67 IHC slides were scanned at 20x (0.24µm/pixel resolution) by a P1000 Pannoramic scanner (3DHistech). 40x area equivalent hotspots (0.440 mm^2) known to contain ~1000 tumor cells were annotated by a pathologist (AR). The pre-chosen hotspots ('I') were manually counted by two independent observers, one of whom was an expert GI pathologist (AB), and by two DIA platforms, QuantCenter (3DHistech), and HALO (Indica Labs). A second set of hotspots ('II') were chosen by an expert GI pathologist and manually counted (SB) and analyzed by DIA (HALO). Tumor cell segmentation for both platforms was optimized by using 3 non-study cases. A per-method threshold of no greater than 20% cases outside 20% of original reported values was assessed. Concordance was assessed using ICC measures.

Results: Ki-67 measurement by both DIA platforms showed excellent correlation with their human counterparts (Pearson coefficient: 0.881 - 0.978, $p < 0.001$, all possible pairs). The intraclass correlation coefficient (ICC) was excellent in both within-hotspot (I: 0.94, II: 0.89) and

case level assessments (0.926, all $p < 0.001$). Inter-DIA reproducibility was 0.90. Among possible meaningful pairs (expert-DIA, DIA-DIA, expert-expert), none showed greater than 55% (11/20) cases with Ki-67 values within 20% of each other.

Figure 1 - 678

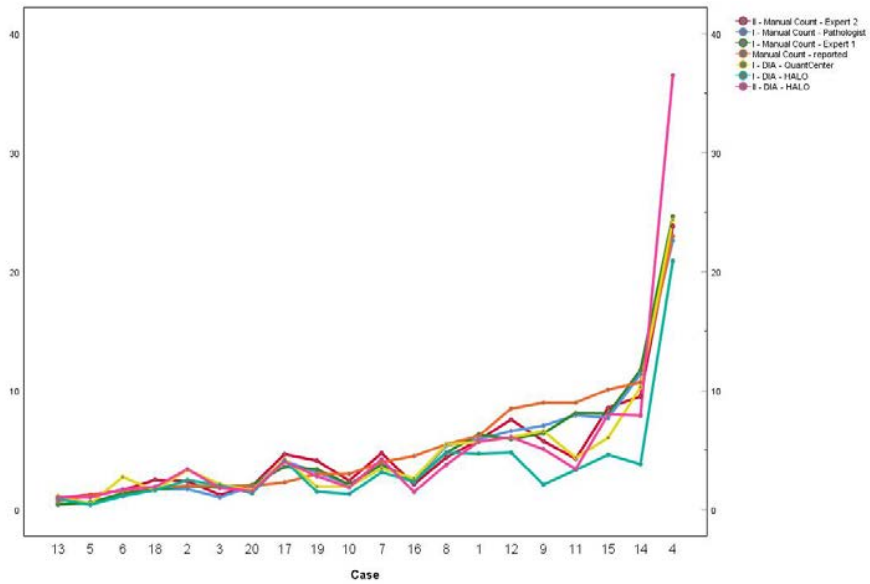

Conclusions: Ki-67 measurement by digital image analysis (DIA) shows excellent agreement with expert-assessed values and with each other. Close concordance by strict criteria (<20% cases +/- 20%) is not seen. The results show, however, that between-expert Ki-67 measurements exhibit the same property. These findings suggest the existence of a 'concordance ceiling' independent of the method of assessment and support full adoption of digital Ki-67 measurement in routine clinical practice.

679 EBV-Positivity is Rare in Gastroesophageal Adenocarcinomas and is Restricted to Gastric Tumors

Matthew Gosse[1], Robert Humble[2], Ibrahim Abukhiran[2], Jason Hornick[3], Andrew Bellizzi[2]
[1]Iowa City, IA, [2]University of Iowa Hospitals and Clinics, Iowa City, IA, [3]Brigham and Women's Hospital, Harvard Medical School, Boston, MA

Disclosures: Matthew Gosse: None; Robert Humble: None; Ibrahim Abukhiran: None; Jason Hornick: *Consultant*, Eli Lilly; *Consultant*, Epizyme; Andrew Bellizzi: None

Background: Pathologists have long recognized an association between Epstein-Barr virus (EBV) and undifferentiated carcinomas with prominent lymphoid stroma (lymphoepithelioma-like carcinoma), which arise at diverse anatomic sites but have a predilection for the stomach. A medical oncologist who recently joined our group has claimed that, in his prior post, EBV testing is performed on all esophageal, gastroesophageal junction (GEJ), and gastric cancers "enterprise-wide" (a claim not endorsed by our pathology colleagues from said enterprise). That being said, there is increased interest in identifying EBV-positive tumors, as they appear to respond favorably to anti-PD1 therapy. The current NCCN gastric cancer guideline cites a frequency of 8-10% and an association with diffuse-type histology, which is contrary to our clinical experience; there is no mention of EBV testing in the esophageal/GEJ guideline.

Design: We assembled our institutional cohort of gastroesophageal adenocarcinomas from 1991-2018 in which there was sufficient material to construct tissue microarrays. All original glass slides/pathology reports were reviewed for tumor epicenter (esophagus, GEJ, stomach), pTNM, Lauren classification, and presence of prominent lymphoid stroma or conspicuous tumor infiltrating lymphocytes (TILs); age and gender were recorded; EBV-encoded RNA (EBER) in situ hybridization and MMR and PD-L1 immunohistochemistry (IHC) were performed.

Results: We examined 349 samples (232 primaries, 86 lymph node metastases, 26 distant metastases, and 5 clinical recurrences) from 249 patients (206 M:43W), including 109 esophageal, 68 GEJ, and 72 gastric cancers. EBV-positivity was noted in 4 samples from 3 patients, each of whom were men (ages 60, 62, 76) with intestinal-type gastric cancers (4% of all gastric cancers). Esophageal and GEJ tumors were uniformly negative. EBV-positivity was noted in 1 of 3 (33%) tumors with lymphoepithelial features, 2 of 38 (5%) with conspicuous TILs (Figure), and only 1 of 230 (0.4%) with inconspicuous to absent TILs. EBV-positive cases had intact MMR and were PD-L1-positive (with combined positive scores of 50, 2, 2, and 1).

Figure 1 - 679

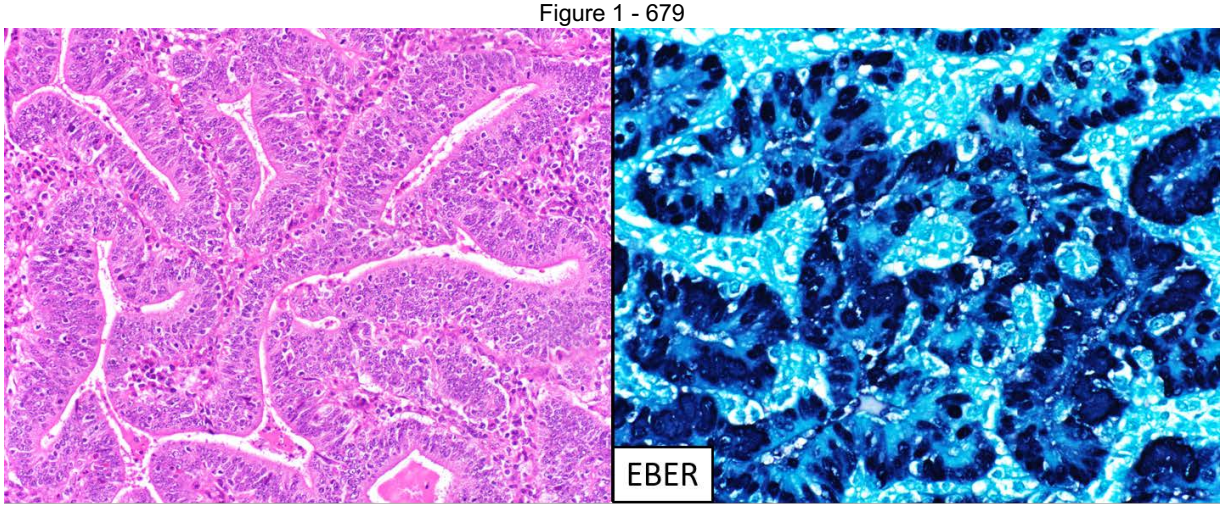

Conclusions: EBV-positivity was incredibly uncommon in our cohort and was restricted to intestinal-type gastric cancers. Universal EBV testing of esophageal/GEJ carcinomas is wasteful, and testing in gastric cancer should be guided by histology. Even if EBV-positive tumors are missed, positive PD-L1 IHC will select patients for the appropriate therapy.

680 Deep Learning-Based Tool for Automated Gastrointestinal Neuroendocrine Tumor Detection and Grading

Darshana Govind[1], Kuang-Yu Jen[2], Pinaki Sarder[1]
[1]SUNY Buffalo, Buffalo, NY, [2]University of California Davis, Sacramento, CA

Disclosures: Darshana Govind: None; Kuang-Yu Jen: None; Pinaki Sarder: None

Background: Gastrointestinal neuroendocrine tumors (GI-NETs) are graded based on mitotic count and Ki67 index (KI). The latter involves hot spot selection followed by manual count of Ki67-positive cells within 500-2000 total tumor cells, which is tedious, subjective, and error prone. Difficulty in distinguishing tumor from non-tumor cells on Ki67 immunohistochemistry (IHC)-stained slides further amplifies the problem. To overcome these limitations, we have developed a deep-learner based pipeline to grade GI-NETs from standard H&E and Ki67-only stained tissue whole slide images (WSIs).

Design: We have previously generated a computational pipeline (called SKIE) that accurately assesses KI from WSIs of synaptophysin/Ki67 double immunostains (SK). As SK is not a standard stain, we developed an algorithm to automatically grade GI-NETs using either Ki67 IHC or H&E alone. WSIs of SK for 48 GI-NETs were cropped into hot spot-sized tiles (500 x 500 μm^2) and categorized into one of four classes using SKIE, which served as ground truth: 0 (background), 1 (non-tumor), 2 (grade 1: KI <3%) or 3 (grade 2: 3> KI >20%). The corresponding tiles from the adjacent sections stained with H&E and Ki67 IHC were categorized into the same class as their SK counterparts. The Inception V3 network was trained and validated using 40 and tested on 8 cases. Three models (M_SK, M_HE, and M_K) were generated using SK, H&E, and Ki-67-only image tiles, respectively. Tumor prediction in a holdout case is shown in Fig 1.

Results: As expected, M_SK agreed with the ground truth with a substantial linear-weighted Cohen's kappa and displayed the highest accuracy (Table 1). M_K generated comparable results with high accuracy. M_HE accurately detects tumor with limitations in differentiating grade 1 from 2.

Model	Training accuracy	Validation accuracy	Testing accuracy	Observed kappa	Lower 95% CI	Upper 95% CI
M_SK	98.85	96.07	94.03	0.917	0.909	0.924
M_K	97.19	92.48	88.26	0.819	0.808	0.831
M_HE	97.11	93.30	85.86	0.515	0.500	0.529

Table 1. Performance metrics of generated models. The training, validation, and testing accuracies of each model, and the linear weighted Cohen's kappa, along with the upper and lower 95% confidence intervals (CI) are shown. M_SK refers to synaptophysin-Ki-67 model, M_K refers to Ki-67-only model and M_HE refers to H&E model.

Figure 1 - 680

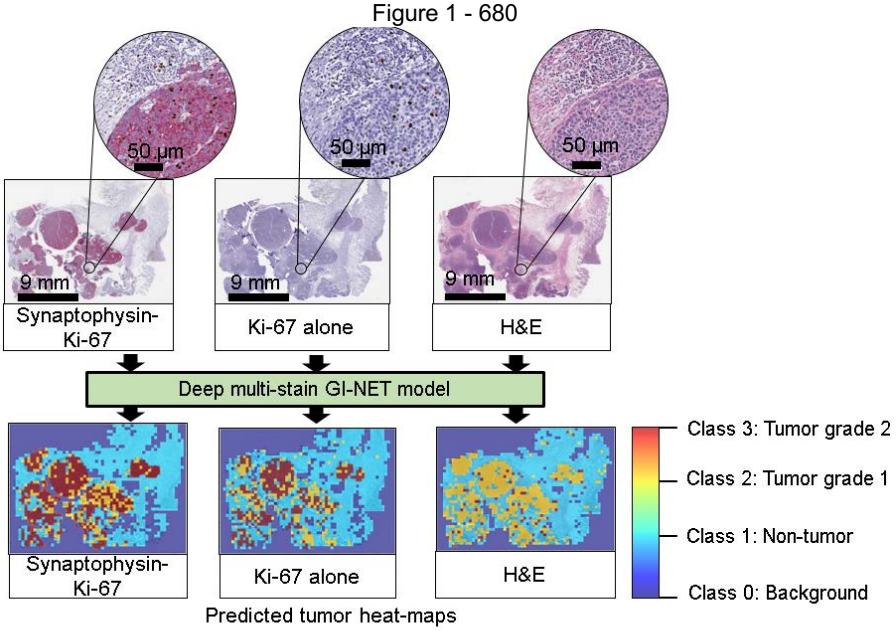

Figure 1. Predicted tumor heat-maps. A holdout slide with adjacent tissue sections stained with synaptophysin-Ki-67, Ki-67 alone and H&E, respectively, were processed by the model to generate the respective tumor heat-maps.

Conclusions: The proposed pipeline enables the accurate detection and grading of GI-NETs from standard histological GI-NET tissues. The predicted heatmap displays the region-based tumor grade, which may provide additional information, superior to single hot-spot based analysis (needs to be proven with outcome studies).

681 Intramucosal Lipoma in Gastrointestinal Biopsy is More Predictive of Cowden Syndrome than Ganglioneuroma

Hongxing Gui[1], Alice Dobi[2], Jigisha Chaudhari[2], Ihab Lamzabi[3]
[1]Philadelphia, PA, [2]Pennsylvania Hospital, Philadelphia, PA, [3]Pennsylvania Hospital, Gladwyne, PA

Disclosures: Hongxing Gui: None; Alice Dobi: None; Jigisha Chaudhari: None; Ihab Lamzabi: None

Background: Cowden syndrome (CS) is an autosomal dominant disorder with increased predisposition to colorectal cancer. Gastrointestinal (GI) polyps of various histologic types including hyperplastic polyps, ganglioneuromas and hamartomatous polyps have been reported in 35-85% CS patients, with ganglioneuromas considered the most specific GI finding. Intramucosal lipomas have been recently reported associated with CS. However, the significance of intramucosal lipomas, compared to ganglioneuromas, in predicting CS have not yet been fully characterized.

Design: We conducted a retrospective study enrolling 55 patients with either intramucosal lipomas or ganglioneuromas in GI polyps biopsied during 2010-2019 (over 70,000 cases). A total number of 190 polyps from those patients were reviewed.

Results: We identified 15 patients having germline *PTEN* mutation or clinical CS. Among those, nine patients (9/15) had 13 intramucosal lipomas and six (6/15) had 13 ganglioneuromas. Of 40 patients without CS, 12 patients (12/40) had 14 intramucosal lipomas and 22 patients (22/40) had 30 ganglioneuromas. Forty-eight percent 48% (13/27) intramucosal lipomas were associated with CS versus 30% (13/43) of ganglioneuromas. Three CS patients had both intramucosal lipoma and ganglioneuroma, which was not seen in patients without CS. In addition, four CS patients (4/15, 27%) had two intramucosal lipomas while only one patient without CS (1/40, 2.5%) had more than one lipoma.

Conclusions: Intramucosal lipoma is a rare finding of GI biopsies, but is a common finding in CS patients. It is more common in CS than ganglioneuroma and has a higher value in predicting CS in our study. Presence of both intramucosal lipomas and ganglioneuromas or

multiple intramucosal lipomas is highly specific for CS. Clinicians and pathologists should be more aware of these associations in order to screen for CS.

682 Loss of SMAD4 Protein Expression is Consistent with Fully Developed Traditional Serrated Adenoma (TSA)

Hongxing Gui[1], John Brooks[2], Zhaohai Yang[3], Franz Fogt[4], Rifat Mannan[5]
[1]Philadelphia, PA, [2]University of Pennsylvania Perelman School of Medicine, Swarthmore, PA, [3]University of Pennsylvania Perelman School of Medicine, Philadelphia, PA, [4]Hospital of the University of Pennsylvania, Gladwyne, PA, [5]Perelman School of Medicine at the University of Pennsylvania, Philadelphia, PA

Disclosures: Hongxing Gui: None; John Brooks: None; Zhaohai Yang: None; Franz Fogt: None; Rifat Mannan: None

Background: Serrated lesions(SLs) are considered to be precursors of 15-35% of colorectal cancer. TSAs are the least characterized SLs in colorectal carcinogenesis, which comprise 0.56-1.9% of all colorectal polyps. They typically show eosinophilic cytoplasm and pencillate nuclei, slit-like serration, ectopic crypt formation (ECF) and villous architecture. Although these features are well-recognized, TSAs are underdiagnosed and have considerable inter-observer variabilities. No immunohistochemical markers are available to support the diagnosis of TSA.

Design: We studied 63 colorectal polyps with serrated changes (31 previously diagnosed TSA and 32 other polyps). Three GI pathologists reviewed the slides, single-blinded. All TSAs, and 11 other polyps were stained with SMAD4 antibody. Fisher's exact test was performed for evaluating statistical significance.

Results: Forty-five percent (14/31) of previously diagnosed TSAs were confirmed as TSAs after review, the rest (17/31) were reclassified as other polyps. Among confirmed TSAs, 64% (9/14) reached complete consensus diagnosis amongst the reviewers. Eight of these (89%, 8/9) occurred in distal colon. In the control group, after review, 22% (7/32) were thought to be TSAs, but only one (14%, 1/7) reached consensus among all 3 reviewers. This made a total of 10 consensus TSAs. All consensus TSAs had villous architecture and 3 common histologic features (eosinophilic cytoplasm with pencillate nuclei, slit-like serrations and ECF). Non-consensus TSAs had at least two features, most commonly villous architecture and one of the above 3 morphologic changes. On IHC, majority of consensus TSAs (90%, 9/10) showed more than 50% loss of SMAD4, whereas the control polyps (14/20, *P*=0.0052) and non-consensus TSAs (9/11, *P*=0.002), retained SMAD4 protein expression.

Figure 1 - 682

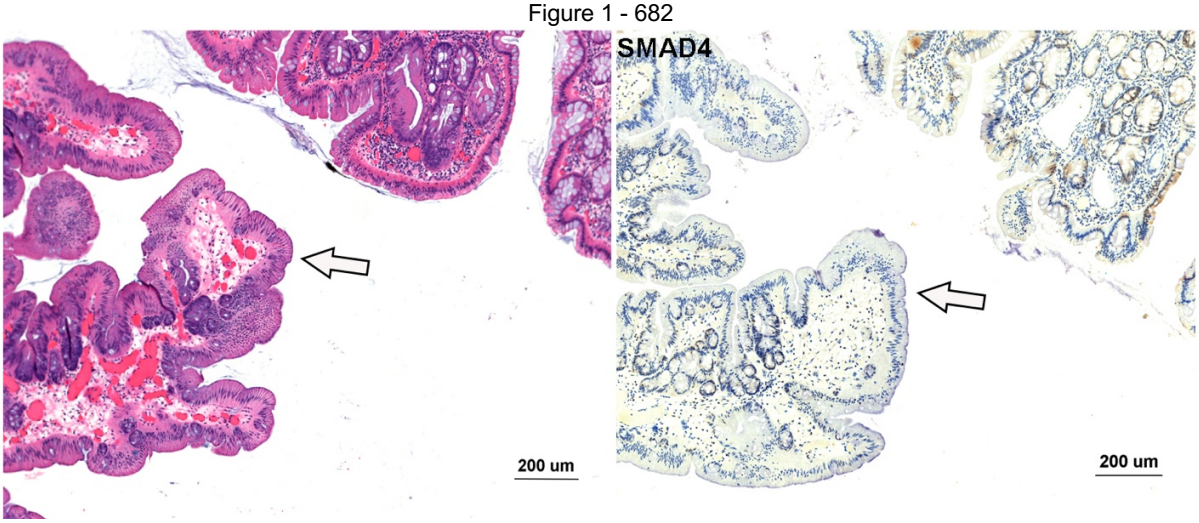

Conclusions: TSAs are underdiagnosed and have high inter observer variability, even among trained experts. Careful attention to all morphologic features are important for correct diagnosis. Loss of SMAD4 protein correlates with consensus morphologic diagnosis, suggesting involvement of SMAD4 in TSA pathogenesis. It also indicates SMAD4 as a potentially useful marker for diagnosis of TSAs.

683 High-Risk Human Papillomaviruses (HPV) and Epstein - Barr virus (EBV) are Commonly Present in Rectal Cancer

Ishita Gupta[1], Ayesha Jabeen[1], Faruk Skenderi[2], Mohammed Malki[1], Hamda Al-Thawadi[1], Ala-Eddin Al Moustafa[1], Semir Vranic[3]
[1]Qatar University, Doha, Qatar, [2]Sarajevo, FBIH, Bosnia and Herzegovina, [3]College of Medicine, Qatar University, Doha, Qatar

Disclosures: Ishita Gupta: None; Ayesha Jabeen: None; Faruk Skenderi: None; Mohammed Malki: None; Hamda Al-Thawadi: None; Ala-Eddin Al Moustafa: None; Semir Vranic: None

Background: Human papillomaviruses (HPVs) and Epstein–Barr virus (EBV) are well-established oncoviruses that can be co-present and cooperate in the initiation and/or progression of various human cancers. We recently reported their common co-expression in several cancers including cervical, breast and head and neck carcinomas. In the present study, we explored the co-presence of high-risk HPVs and EBV in a cohort of rectal cancer samples.

Design: One-hundred and eight formalin-fixed paraffin-embedded tissue samples of rectal cancer were analyzed for EBV (LMP1) and HPV (E6) using polymerase chain reaction (PCR) and immunohistochemistry (IHC) analysis. IHC assays were performed on the tissue microarray platform.

Results: All cancers were primary rectal carcinomas (intestinal type) diagnosed in 64 male (59%) and 44 female (41%) patients. Mean patient's age was 65 years (range, 41-86 years). LMP1 of EBV was detected in 25% of the samples. Various high-risk HPVs were commonly present: HPV16 (55%), HPV31 (54%), HPV18 (50%), HPV51 (47%), HPV52 and 45 (39% each) and HPV35 (26%). Co-presence of LMP1 of EBV and E6 of HPV was detected in 11% of the samples. PCR and IHC data were in a good concordance.

Conclusions: High-risk HPVs are commonly present in rectal cancers while EBV characterizes 25% of rectal cancers. A proportion of rectal cancers was infected by both EBV and high-risk HPVs. Further studies should elucidate their potential roles in the initiation and/or progression of rectal cancer.

684 Desmoplastic Reaction in Colorectal Carcinoma: An Institutional Interobserver Reliability Study of 228 Colorectal Adenocarcinoma Cases

Sean Hacking[1], Nathaniel Greenbaum[2], Mallorie Angert[3], Taisia Vitkovski[4], Rebecca Thomas[5], Cao Jin[3], Hector Chavarria Bernal[6], Nidhi Kataria[7], Mansoor Nasim[8]
[1]Northwell Health, Forest Hills, NY, [2]SUNY Downstate Health Sciences University, New York, NY, [3]Donald and Barbara Zucker School of Medicine at Hofstra/Northwell, Lake Success, NY, [4]Lake Success, NY, [5]Northwell Health System, New Hyde Park, NY, [6]Northwell Health, New Hyde Park, NY, [7]Northwell Health, Hofstra School of Medicine, Manhasset, NY, [8]Northwell Health Pathology Inc, Jericho, NY

Disclosures: Sean Hacking: None; Nathaniel Greenbaum: None; Mallorie Angert: None; Taisia Vitkovski: None; Rebecca Thomas: None; Cao Jin: None; Hector Chavarria Bernal: None; Nidhi Kataria: None; Mansoor Nasim: None

Background: Colorectal cancer is a clinically diverse disease which carries with it a spectrum of possible clinical outcomes. Importantly, an emerging body of evidence suggests that cancer associated fibroblasts can actually alter the tumoral microenvironment and effect tumor aggressiveness. Currently, research has examined different aspects of the cancer microenvironment, including stromal desmoplastic reaction. Desmoplastic reaction, or DR, is the term applied to the phenomenon of an excessive accumulation of connective tissue, usually indicative of a neoplastic process. With this in mind, research in colon cancer found that DR categorization outperformed other conventional prognostic factors including tumor budding and tumor stage in predicting disease free survival. As of yet, there are no internationally accepted guidelines for DR categorization and its reproducibility is unknown.

Design: A total of 228 cases of colorectal carcinoma diagnosed in our health system were retrospectively reviewed and routine H&E stained slides of these cases were collected. Four American board-certified pathologists were selected, supplied with current literature pertaining to the evaluation of DR and evaluated stromal maturity independently of one another. Scoring was preformed based on the 3-tier grading system as proposed by Ueno et al. (Figure.2). More specifically, this three-tier system consisted of immature, intermediate, and mature stroma (Figure.2). Statistical analysis for inter-rater reliability was computed with python 3.6 (Python Software Foundation, Delaware, USA).

Results: Four observers rated 228 cases resulting in 912 decisions. Krippendorff alpha and Fleiss kappa values for inter-rater reliability were 0.226 and 0.225 respectively (Figure. 1).

Figure 1 - 684

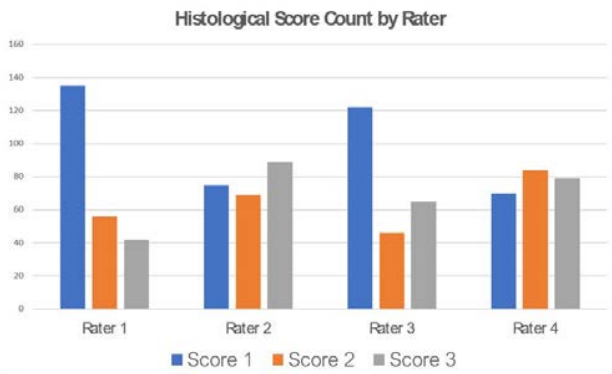

Inter-rater Krippendorff Alpha

	Rater 1	Rater 2	Rater 3	Rater 4
Rater 1	1	0.118	0.295	0.254
Rater 2		1	0.119	0.208
Rater 3			1	0.316
Rater 4				1

Figure 2 - 684

Desmoplastic Reaction Grading

Immature (A)	Intermediate	Mature (B)
DR was categorized as immature when myxoid stroma, an amorphous stromal substance comprising amphophilic or basophilic extracellular matrix, was present (usually intermingled with randomly oriented hyalinized collagen)	DR was categorized as intermediate when keloid-like collagen was intermingled with the mature stroma, typically in an orientation parallel to mature collagen fibers	DR was regarded as mature when the fibrotic stroma did not contain myxoid stroma or keloid-like collagen but typically comprised only fine mature collagen fibers stratified into multiple layers in all reactive fibrous zones

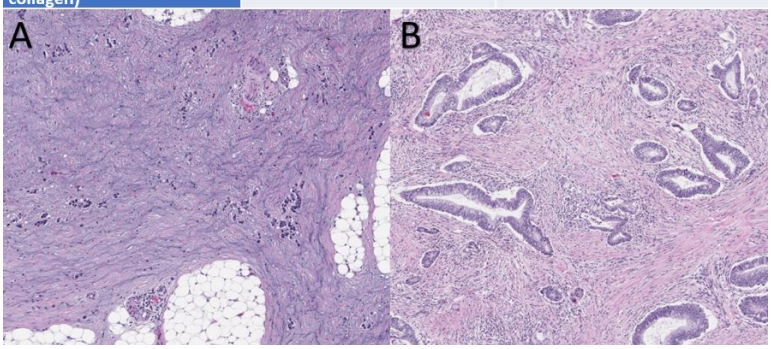

Conclusions: In summation, this is the only large study to look at the reproducibility of DR in colon cancer. Herein, the results from our study showed that agreement between observers was suboptimal (Figure. 1). There are many possible reasons for these results, including a lack of training and an absence of standardization. Many cases which resulted in high variability were ones which contained mixed components of the different stromal subtypes. Finally, the development of international guidelines, such as that proposed for tumor budding (ITBCC), have the potential to improve reproducibility.

685 Molecular Features of Unconventional Dysplastic Lesions Associated with Chronic Inflammatory Bowel Disease

Noam Harpaz[1], Wei Zhang[2], Suparna Sarkar[3]
[1]Mount Sinai Medical Center, New York, NY, [2]University of Wisconsin-Madison, Madison, WI, [3]NYU Langone Health, New York, NY

Disclosures: Noam Harpaz: None; Wei Zhang: None; Suparna Sarkar: None

Background: Colorectal carcinoma (CRC) in patients with longstanding inflammatory bowel disease (IBD) is the culmination of an inflammation-dysplasia-cancer sequence. Its molecular pathogenesis is not fully understood, because in addition to adenomatous dysplasia analogous to conventional sporadic adenomatous lesions, dysplasia in IBD can assume other distinctive phenotypically heterogeneous changes, the clinical characteristics and significance of which are largely unknown. We characterized 2 types of unconventional dysplasias; Goblet Cell Deficient (GCD) and Crypt Cell/Terminally Differentiated (CC/TD) by sequencing DNA for cancer-related hotspots.

Design: Nineteen mucosal samples of dysplasia from biopsies or resection specimens of patients with IBD, eleven ulcerative colitis, six Crohn's colitis, two indeterminate colitis) were evaluated at Mount Sinai Hospital. Fourteen as GCD featured tubular crypts lined by monotonous columnar cells with eosinophilic cytoplasm and mildly atypical nuclei and 5 as CC/TD featured tubular crypts lined by differentiated enterocytes, goblet cells, Paneth cells and/or endocrine cells with cytologically atypical nuclei as previously described (1). The slides were de-identified and the presence of dysplasia confirmed by two independent pathologist. DNA extracted from formalin-fixed, paraffin-embedded dysplastic samples containing at least 10% dysplastic cells and from adjacent non-dysplastic mucosa were analyzed for a 50-gene panel of hotspot mutation sequences on an Ion Torrent PGM sequencer with strict quality assurance (50,000 reads, 200X coverage, AQ20). Data was analyzed on Torrent Suite Analysis Software and annotated with Ion Reporter Software.

Results: Seven lesions (37%) harbored mutations that have been implicated in the development of carcinoma (GCD, n=4, CC/TD n=3) per Catalogue of Somatic Mutations in Cancer (COSMIC) database, including known mutations of KRAS, p53, IDH1 and FBXW7, however no correlations were observed between the mutations and dysplasia phenotypes or type of IBD. Two lesions contained variants of unknown significance (VUS) in addition to pathogenic mutations (GCD with IDH1, CC/TD with TP53) and two lesions harbored only VUS.

Table 1. Pathogenic mutations and VUS in 9 unconventional dysplastic lesions in IBD

Cases	Ulcerative Colitis	Crohn's Colitis	Type of Dysplasia	Molecular Alteration	Chromosome	Biological Effect	Clinical Implications
1	x		GCD	FBXW7 p.R465C	4	Loss of Function	Oncogenic
2	Indeterminate		GCD	KRAS p.G12D	12	Gain of function	Oncogenic
3	x		GCD	IDH1 p.R132C ALK p.G1184E	2	Switch of Function VUS	Oncogenic VUS
4		x	GCD	KRAS p.G12C	12	Gain of function	Oncogenic
5	x		CC/TD	FBXW7 p.R505C TP53 p.C135S	4 17	Loss of function Loss of function	Oncogenic Oncogenic
6		x	CC/TD	TP53 p.G245S	17	Loss of function	Oncogenic
7	x		CC/TD	TP53 p.R213L, p.R248Q; ERBB2 p.D769N	17	Loss of function VUS	Oncogenic VUS
8		x	GCD	TP53 p.P72R	17	VUS	VUS
9	x		GCD	ATM p.P604S	11	VUS	VUS

Conclusions: Unconventional dysplastic lesions corresponding to GCD and CC/TD harbor pathogenic mutations that are implicated in the development and progression of sporadic CRC.

Reference: Harpaz N, Goldblum J, Shepherd N, et al. Novel Classification of Dysplasia in IBD. Mod Pathol 2017;30:174A

686 Characterization of Benign Epithelial Stromal Polyps

Erika Hissong[1], Melanie Johncilla[2], Rhonda Yantiss[3]
[1]New York-Presbyterian/Weill Cornell Medical Center, New York, NY, [2]New York-Presbyterian Hospital/Weill Cornell Medical Center, Petit Valley, Trinidad and Tobago, [3]Weill Cornell Medicine, New York, NY

Disclosures: Erika Hissong: None; Melanie Johncilla: None; Rhonda Yantiss: None

Background: Some benign epithelial and stromal polyps of the colorectum contain variably dilated or serrated crypts surrounded by spindle cells that show pericryptal accentuation. These lesions have been classified as perineuriomas based on the frequent presence of spindle cell immunopositivity for EMA and/or GLUT1. Such polyps with serrated crypts harbor *BRAF* mutations at rates similar to sessile serrated polyps, whereas those without serrated crypts have not been specifically studied. We suspect that colonic perineuriomas represent a heterogeneous group of lesions with different clinicopathologic associations.

Design: We retrospectively identified 46 benign epithelial/stromal polyps (i.e. perineuriomas) that were classified based on the presence (n=21) or absence (n=25) of serrated crypts. Electronic medical records were reviewed and all cases were evaluated with EMA and BRAF V600E immunostains. Twenty normal colonic biopsy samples were also stained for EMA.

Results: There were no significant differences between the two groups with respect to sex, age, or polyp location (Table 1). Polyps with serrated crypts were significantly associated with other colonic polyps (90% vs 36%, $p<0.001$), particularly serrated lesions (38% vs 4%, $p=0.007$). They also showed significantly more common BRAF V600E staining in the epithelium (100%) than non-serrated polyps (0%) and normal colon (0%, $p<0.001$ for both comparisons). Most (95%) polyps with serrated crypts displayed strong, diffuse EMA positivity in the spindle cells. On the other hand, only 4 (16%, $p<0.001$) non-serrated polyps showed strong, pericryptal EMA positivity. The rest of these lesions were either EMA-negative or contained scattered, weakly stained cells in a non-pericryptal distribution similar to that seen in the normal colon.

	Serrated polyps (N=21)	Non-serrated polyps (N=25)	p value
Male:Female	8:13	7:18	0.54
Age (years)	58.7	57	1
Location			
Right colon	3 (14%)	3 (12%)	1
Left colon	2 (10%)	5 (20%)	0.4
Rectosigmoid colon	16 (76%)	17 (68%)	0.7
Mean size	4.6 cm	4.3 cm	0.84
Concurrent polyps	19 (90%)	9 (36%)	0.0002
Tubular adenoma	9 (43%)	7 (28%)	0.36
Sessile serrated polyp	8 (38%)	1 (4%)	0.0067
Hyperplastic polyp	6 (29%)	0	0.0058
Strong, stromal EMA staining	20 (95%)	4 (16%)	<0.001
Epithelial BRAF staining	21 (100%)	0	<0.0001

Figure 1 - 686

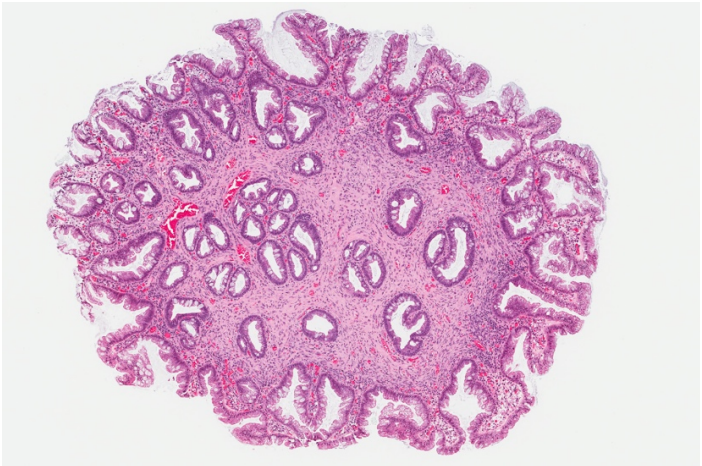

Figure 2 - 686

Conclusions: Epithelial/stromal polyps commonly termed “perineuriomas” probably include at least two separate entities. Those with serrated crypts share overlapping clinical, morphologic, and molecular features with sessile serrated polyps/adenomas, suggesting they simply represent variants of that type of lesion containing a prominent spindle cell component. Epithelial/stromal polyps without serrated crypts are non-syndromic and unassociated with other polyp types. The characteristic pericryptal accentuation of spindle cells in both types of lesion suggests they represent non-neoplastic proliferations of modified myofibroblasts that normally support the colonic crypts, similar in function to perineural cells.

687 Histologic Features of Tacrolimus-Induced Colonic Injury

Erika Hissong[1], Jose Jessurun[2], Rhonda Yantiss[2]
[1]New York-Presbyterian/Weill Cornell Medical Center, New York, NY, [2]Weill Cornell Medicine, New York, NY

Disclosures: Erika Hissong: None; Jose Jessurun: None; Rhonda Yantiss: None

Background: Tacrolimus is a common immunosuppressant used in solid organ transplant recipients. Although large trials have shown that it causes diarrhea in up to 43% of patients, many of those who undergo mucosal biopsy are also receiving mycophenolate or other drugs known to cause colitis. As a result, data regarding the histologic features of tacrolimus-induced colonic damage are limited. The aim of this study is to better characterize these changes.

Design: We retrospectively searched our database for a 20-year period to identify colonic biopsies from patients receiving tacrolimus. Most cases were from bone marrow transplant patients that we excluded to avoid the confounding effects of graft vs host disease and other medications. The remaining patient records were reviewed for medications, symptoms, endoscopic findings, and gastrointestinal infections. Ultimately, 22 patients receiving tacrolimus monotherapy comprised the study group; all had negative microbiologic studies and none had received mycophenolate within 6 months of presentation. Hematoxylin and eosin-stained slides prepared from colonic samples were evaluated for the nature and distribution of inflammation, crypt architectural distortion, crypt cell apoptosis, crypt destruction, and regenerative epithelial changes.

Results: Most study patients were adults (mean: 51 years) with a near-equal sex distribution and mean treatment duration of 63 months. Twenty (91%) were solid organ transplant recipients; 1 patient each had systemic lupus erythematosus and corticosteroid-refractory nephrotic syndrome. Seventeen (77%) had gastrointestinal symptoms, particularly diarrhea (n=16). Most (54%) patients had endoscopic colitis and 14% had ulcers/erosions. Regenerative crypt epithelial changes and scattered apoptotic crypt cells were detected in 82% and 94% of cases, respectively. Active colitis accompanied by plasma cell-rich inflammation was seen in 9 (41%) cases, including 6 (27%) with crypt destruction and 4 (18%) with crypt architectural distortion. There was no correlation between therapy duration and features of chronic injury.

Figure 1 - 687

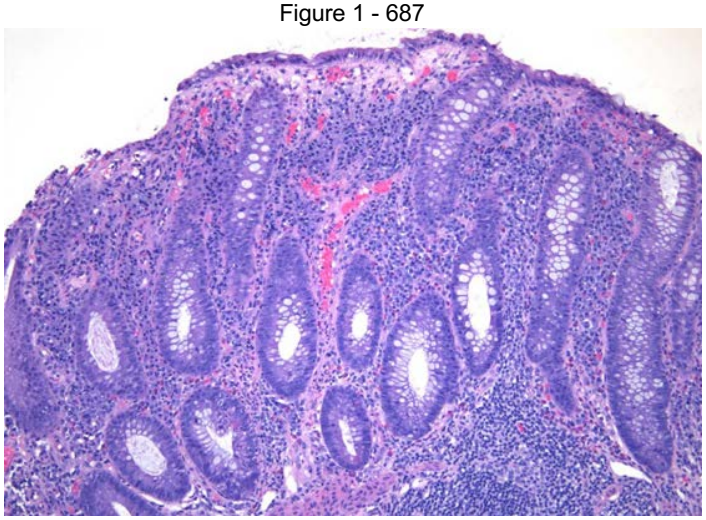

Figure 2 - 687

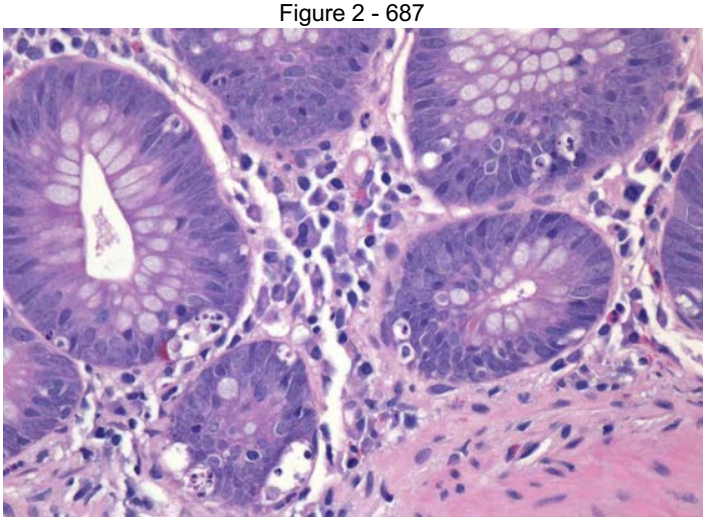

Conclusions: Tacrolimus can cause endoscopic colitis with erosions. Histologic abnormalities are often mild, featuring apoptotic debris and regenerative crypts, although approximately 40% of symptomatic patients have chronic active colitis. These findings reinforce the notion that new-onset chronic colitis in transplant patients is more likely a medication effect than new-onset idiopathic inflammatory bowel disease.

688 Is Histologic Grade Prognostically Important among Goblet Cell Neoplasms Confined to the Appendix?

Erika Hissong[1], Raul Gonzalez[2], Brandon Umphress[3], Laura Tang[3], Rhonda Yantiss[4]
[1]New York-Presbyterian/Weill Cornell Medical Center, New York, NY, [2]Beth Israel Deaconess Medical Center, Boston, MA, [3]Memorial Sloan Kettering Cancer Center, New York, NY, [4]Weill Cornell Medicine, New York, NY

Disclosures: Erika Hissong: None; Raul Gonzalez: None; Brandon Umphress: None; Laura Tang: None; Rhonda Yantiss: None

Background: Recently published WHO criteria propose a 3-tiered grading system for appendiceal goblet cell carcinomas based on extent of high-grade areas (grade 1:<25%, grade 2:25-50%, grade 3:>50%), as defined by single infiltrating cells, solid sheets, large aggregates, or foci of conventional adenocarcinoma. Most studies describing the effects of tumor grade on outcome have not controlled their data for stage. Almost all of their grade 1 tumors have been localized to the appendix (stage I/II), and a disproportionate number of grade 2 and 3 tumors have already spread beyond the appendix (stage III/IV) at presentation. It is not clear whether the proposed WHO grading scheme is predictive of behavior among tumors limited to the appendix, so we performed this study to answer this question.

Design: We reviewed histologic sections from 37 appendiceal goblet cell carcinomas graded according to WHO 5th edition criteria. There were 14 (38%) grade 1, 15 (40%) grade 2, and 8 (22%) grade 3 tumors. All cases were stained with ki-67 to determine the proliferation index. Follow-up data (mean: 63 months) were obtained from the electronic medical records.

Results: Most patients were older adults (mean: 59 years, M/F=16/21). Twenty-three (62%) cases were limited to the appendix (Stage I/II), including 11 grade 1, 11 grade 2, and 1 grade 3 tumor with a mean ki-67 labeling index of 25%(range:6-63%). There were 3 (8%) Stage III, and 11 (30%) Stage IV cases (X grade 1, Y grade 2, and Z grade 3) with a mean ki-67 labeling index of 20%(range:2-39%). There was no relationship between ki-67 staining and grade or stage; a similar extent of staining was observed in both low- and high-grade areas of the same tumor. Eleven tumors recurred or progressed during follow-up: 1 was grade 1, 4 were grade 2, and 6 were grade 3. All 11 of these cases were advanced (Stage III/IV) at the time of diagnosis. None of the Stage I/II tumors recurred (mean follow-up:66 months).

Conclusions: Similar to results of others, we identified a relationship between tumor grade and outcome among goblet cell carcinomas that have already spread beyond the appendix. However, none of our cases confined to the appendix (Stage I/II) recurred or progressed,

regardless of the presence or extent of high-grade components. Immunostain results for ki-67 did not correlate with tumor grade, stage, or outcome. We conclude that current grading criteria are probably of limited value in determining subsequent treatment of goblet cell carcinomas confined to the appendix.

689 Kras Alteration and Overall Survival of Advanced Colorectal Cancer

Kun Hu[1], Wenwei Hu[2], Yong Lin[3], Zhaohui Feng[2], Nan Gao[4], Lanjing Zhang[5]
[1]University at Buffalo, Buffalo, NY, [2]Rutgers Cancer Institute of New Jersey, New Brunswick, NJ, [3]Department of Biostatistics, Rutgers School of Public Health, New Brunswick, NJ, [4]Department of Biological Sciences, Rutgers University, Newark, NJ, [5]Princeton Medical Center, Plainsboro, NJ

Disclosures: Kun Hu: None; Wenwei Hu: None; Yong Lin: None; Zhaohui Feng: None; Nan Gao: None; Lanjing Zhang: *Employee*, Celgene; *Stock Ownership*, Celgene

Background: Kras mutation is linked to no benefits of anti-EGFR (epidermal growth factor receptor) therapy for colorectal cancer (CRC). We recently demonstrated its association with progression of CRC with recorded tumor-deposit status. However, its role in CRC progression is unclear.

Design: We analyzed the prognostic values of Kras mutation using the National Cancer Database, which is the largest cancer registry database in the U.S., with adjustment for potential confounders and time-varying covariates. We also interrogated 2 genomic databases for the prognostic values of Kras alteration and its associated genes.

Results: 1) Among 11,331 CRC in The National Cancer Database, Kras mutation (versus wildtype) was associated with worse overall survival in early and late CRC (hazard ratio=1.66, p=0.008 and HR=1.36, p=0.007, respectively). 2) Among 597 CRC in The Cancer Genome Atlas (TCGA), Kras alteration, including mutation and copy number variation, was also found associated with worse overall survival in advanced CRC (n=279, p=0.0075), but not in early CRC (n=318, p=0.43). 3) Our additional analyses on 1,099 CRC in The Metastatic Colorectal Cancer (MCC) Project of Memorial Sloan Kettering Cancer Center confirmed the link between Kras alteration and worse overall survival (P=0.0067, Figure 1). Further gene co-expression/enrichment analyses showed that PIK3CA was co-expressed with Kras alteration in advanced CRC of the TCGA database (p=0.000027, q=0.00037). We also found PIK3CA mutation co-occurred with Kras alteration in 137 (27.02%) of Kras-altered group and 92 (14.67%) of Kras-unaltered group (log-ratio=0.88, p=2.02E-07, q=2.39E-05) in the MCC project. In addition, Kras alteration was linked to AMER1 mutation in 44 (8.68%) of Kras-altered group and 21 (3.35%) of Kras-unaltered group (log-ratio=1.37, p=1.02E-04, q=9.68E-03) (Table 1).

Table 1: List of Top 10 Genes Linked to KRAS in MCC (Ranked by p Value)

Gene	Cytoband	Altered group	Unaltered group	Log Ratio	p-Value	q-Value	Tendency
TP53	17p13.1	305 (60.16%)	525 (83.73%)	-0.48	3.84E-19	1.81E-16	Mutual exclusivity
BRAF	7q34	20 (3.94%)	115 (18.34%)	-2.22	4.74E-15	1.12E-12	Mutual exclusivity
NRAS	1p13.2	4 (0.79%)	42 (6.70%)	-3.09	6.93E-08	1.09E-05	Mutual exclusivity
PIK3CA	**3q26.32**	**137 (27.02%)**	**92 (14.67%)**	**0.88**	**2.02E-07**	**2.39E-05**	**Co-occurrence**
AMER1	**Xq11.2**	**44 (8.68%)**	**21 (3.35%)**	**1.37**	**1.02E-04**	**9.68E-03**	**Co-occurrence**
SMAD2	18q21.1	32 (6.31%)	16 (2.55%)	1.31	1.45E-03	0.114	Co-occurrence
DDR2	1q23.3	13 (2.56%)	3 (0.48%)	2.42	3.04E-03	0.205	Co-occurrence
GNAS	20q13.32	20 (3.94%)	8 (1.28%)	1.63	3.52E-03	0.208	Co-occurrence
CBL	11q23.3	9 (1.78%)	1 (0.16%)	3.48	4.13E-03	0.21	Co-occurrence
FBXW7	4q31.3	80 (15.78%)	65 (10.37%)	0.61	4.43E-03	0.21	Co-occurrence

Figure 1 - 689

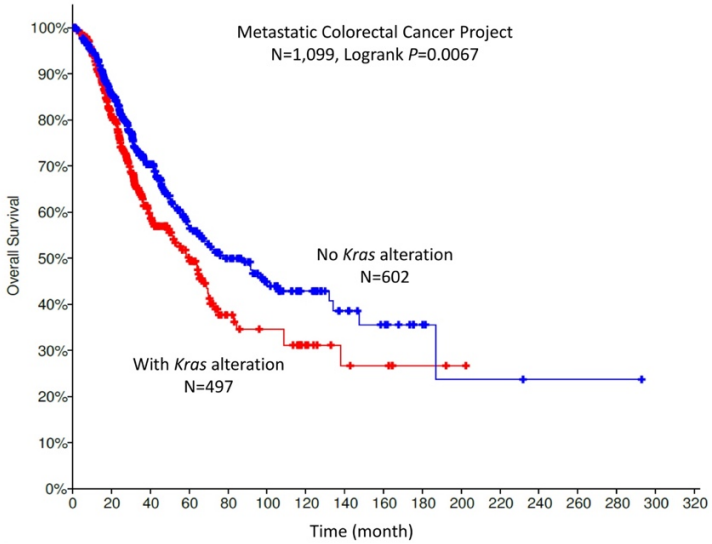

Conclusions: This study of total 13,027 CRC from 3 cohorts shows that *Kras* alteration is independently associated with a worse overall survival of advanced CRC. Its potential collaborators in advanced CRC include *PIK3CA* and possibly *AMER1*. These data suggest that *Kras* alteration may play a role in the progression of advanced CRC.

690 Gastrointestinal Stromal Tumors Arising in Uncommon Locations: Clinicopathologic Features and Risk Assessment of Esophageal, Appendiceal, and Colonic Tumors

Shaomin Hu[1], Lindsay Alpert[1], John Goldblum[2], Ahmed Bakhshwin[3], Sindhu Shetty[2], Rondell Graham[4], Hanlin Wang[5], Trang Lollie[5], Rhonda Yantiss[6], Erika Hissong[7], Ayesha Siddique[8], Murray Resnick[9], Elizabeth Wu[10], Nicole Panarelli[11], Kevin Kuan[12], Jonathan Pomper[13], Andrew Bellizzi[14], David Klimstra[15], Jinru Shia[15], Monika Vyas[16], Teri Longacre[17], Shyam Raghavan[17], Joseph Misdraji[18], Sanjay Kakar[19], Won-Tak Choi[19], Marie Robert[20], Hongjie Li[20], Michael Feely[21], Mary Bronner[22], Zachary Dong[23], Mojgan Hosseini[24], Jingjing Hu[25], Maria Westerhoff[26], Jerome Cheng[26], Harry Cooper[27], Rajeswari Nagarathinam[27], Diana Agostini-Vulaj[28], Zu-Hua Gao[29], Nadine Demko[29], Gregory Lauwers[30], Masoumeh Ghayouri[31], John Hart[1], Raul Gonzalez[32]
[1]The University of Chicago, Chicago, IL, [2]Cleveland Clinic, Cleveland, OH, [3]Robert J. Tomsich Pathology & Laboratory Medicine Institute, Cleveland Clinic, Pepper Pike, OH, [4]Mayo Clinic, Rochester, MN, [5]David Geffen School of Medicine at UCLA, Los Angeles, CA, [6]Weill Cornell Medicine, New York, NY, [7]New York-Presbyterian/Weill Cornell Medical Center, New York, NY, [8]Rocky Hill, CT, [9]Sharon, MA, [10]Rhode Island Hospital/Brown University, Providence, RI, [11]Montefiore Medical Center, Scarsdale, NY, [12]Montefiore Medical Center, Albert Einstein College of Medicine, Bronx, NY, [13]Albert Einstein College of Medicine, Bronx, NY, [14]University of Iowa Hospitals and Clinics, Iowa City, IA, [15]Memorial Sloan Kettering Cancer Center, New York, NY, [16]Beth Israel Deaconess Medical Center, Harvard Medical School, Newton MA, MA, [17]Stanford University, Stanford, CA, [18]Harvard Medical School, Boston, MA, [19]University of California San Francisco, San Francisco, CA, [20]Yale University School of Medicine, New Haven, CT, [21]University of Florida, Gainesville, FL, [22]University of Utah, Salt Lake City, UT, [23]University of Utah, Herriman, UT, [24]University of California San Diego, La Jolla, CA, [25]University of California San Diego, San Diego, CA, [26]University of Michigan, Ann Arbor, MI, [27]Fox Chase Cancer Center, Philadelphia, PA, [28]University of Rochester Medical Center, Rochester, NY, [29]McGill University, Montreal, QC, [30]H. Lee Moffitt Cancer Center & Research Institute, University of South Florida, Tampa, FL, [31]Moffitt Cancer Center, Tampa, FL, [32]Beth Israel Deaconess Medical Center, Boston, MA

Disclosures: Shaomin Hu: None; Lindsay Alpert: None; John Goldblum: None; Ahmed Bakhshwin: None; Sindhu Shetty: None; Rondell Graham: None; Hanlin Wang: None; Trang Lollie: None; Rhonda Yantiss: None; Erika Hissong: None; Ayesha Siddique: None; Murray Resnick: *Consultant*, PathAI; Elizabeth Wu: None; Nicole Panarelli: None; Kevin Kuan: None; Jonathan Pomper: None; Andrew Bellizzi: None; David Klimstra: None; Jinru Shia: None; Monika Vyas: None; Teri Longacre: None; Shyam Raghavan: None; Joseph Misdraji: None; Sanjay Kakar: None; Won-Tak Choi: None; Marie Robert: None; Hongjie Li: None; Michael Feely: None; Mary Bronner: None; Zachary Dong: None; Mojgan Hosseini: None; Mojgan Hosseini: None; Jingjing Hu: None; Maria Westerhoff: None; Jerome Cheng: None; Harry Cooper: None; Rajeswari Nagarathinam: None; Diana Agostini-Vulaj: None; Zu-Hua Gao: None; Nadine Demko: None; Gregory Lauwers: None; Masoumeh Ghayouri: None; John Hart: None; Raul Gonzalez: None

Background: Prior studies have shown that risk of progression for gastrointestinal stromal tumors (GISTs) is related to tumor size and mitotic rate. These data are largely based on experience with tumors of the stomach, small bowel, and rectum, which are far more common than GISTs from other sites. In fact, criteria for risk assessment of esophageal, colonic, and appendiceal tumors are mostly extrapolated

from outcome data for gastric, intestinal, and rectal GISTs. In this multi-institutional study, we analyzed a large cohort of GISTs arising in less common locations to evaluate their features and determine whether current criteria accurately predict their biologic behavior.

Design: We identified 158 resected GISTs of the esophagus (n=60), colon (n=83), and appendix (n=15) from 23 institutions, all of which were immunopositive for KIT and/or DOG1. Each case was evaluated for clinical manifestations, tumor size, mitotic figures/5 mm2, tumor cell morphology, and outcome by participating pathologists at each institution.

Results: Most patients were older adults (mean: 66 years) with an equal sex distribution. Overall, 105 GISTs were incidental lesions, with most measuring <2 cm. Esophageal GISTs had a mean size of 3.9 cm (range: 0.08-14) and, when symptomatic, presented with dysphagia, cough, or odynophagia. They displayed spindled (90%), epithelioid (2%), or mixed morphology (8%), with a mean mitotic rate of 3.9/5 mm2. Colonic GISTs had a mean size of 2.7 cm (range: 0.1-24.5) and, when symptomatic, presented with pain and bleeding. They were mostly composed of spindled cells (92%) with a mean mitotic rate of 4.5/5 mm2. All appendiceal tumors were incidentally discovered, measured <2 cm (mean: 0.55 cm), and were composed of spindled cells without significant mitotic activity. Follow-up data were available for 138 patients (median 40 months): 13 (8%) GISTs metastasized, including 6 (11%) esophageal and 7 (10%) colonic tumors (**Table**). Half of GISTs with mitotic rates >5/5 mm2 or size >5 cm progressed, whereas none of the 117 tumors with ≤5 mitotic figures/5 mm2 and size ≤5 cm progressed.

Prognostic Features		**Metastasis or Disease-Related Death**		
Mitotic Rate	Size	Esophagus (n=53)	Colon (n=71)	Appendix (n=14)
≤5 per 5 mm^2	≤2 cm	0/22 (0%)	0/46 (0%)	0/14 (0%)
	>2 - ≤5 cm	0/14 (0%)	0/11 (0%)	No cases
	>5 - ≤10 cm	1/4 (25%)	1/2 (50%)	No cases
	>10 cm	No cases	0/3 (0%)	No cases
>5 per 5 mm^2	≤2 cm	No cases	0/1 (0%)	No cases
	>2 - ≤5 cm	0/1 (0%)	1/3 (33%)	No cases
	>5 - ≤10 cm	4/9 (44%)	2/2 (100%)	No cases
	>10 cm	1/3 (33%)	3/3 (100%)	No cases

Conclusions: Similar to GISTs of the stomach, small bowel, and rectum, progression risk among esophageal and colonic GISTs is more likely to occur among those with mitotic counts >5/5 mm2 or size >5 cm. Most appendiceal GISTs are incidentally discovered small lesions cured by appendectomy alone. Our findings validate size and mitotic rate for assessing risk of disease progression among GISTs in uncommon locations.

691 H. pylori Pattern Gastritis with Negative Helicobacter Immunohistochemical Stain: A Multi-Center Study

Xiaobang Hu[1], Elena Lucas[2], Amarpreet Bhalla[3], Jerome Cheng[4], Ilke Nalbantoglu[5], Nicole Panarelli[6], Maria Westerhoff[4], Suntrea Hammer[1], Purva Gopal[1]
[1]University of Texas Southwestern Medical Center, Dallas, TX, [2]University of Texas Southwestern, Dallas, TX, [3]Albert Einstein/Montefiore Medical Center, Bronx, NY, [4]University of Michigan, Ann Arbor, MI, [5]Yale University School of Medicine, Woodbridge, CT, [6]Montefiore Medical Center, Scarsdale, NY

Disclosures: Xiaobang Hu: None; Elena Lucas: None; Amarpreet Bhalla: None; Jerome Cheng: None; Ilke Nalbantoglu: None; Nicole Panarelli: None; Maria Westerhoff: None; Suntrea Hammer: None; Purva Gopal: None

Background: The clinical significance of H. pylori (HP) pattern of gastritis with a negative immunohistochemical (IHC) stain on gastric biopsy is unclear. Some pathologists report this pattern with a comment raising the possibility of HP infection, stating the negative IHC could be due to prior/ partial treatment or patchy organism distribution; however, the subsequent clinical management of these patients has not been well described. Our study aim was to investigate the clinical management of patients with HP pattern gastritis with negative IHC.

Design: We conducted a multi-center retrospective cohort study including patients from four academic centers who underwent gastric biopsy between 2016 and 2019. We included patients with reported chronic active or chronic inactive gastritis, suggestive of HP infection, with negative Helicobacter IHC (Figure 1). Patients were required to have a comment in their report stating the inflammation pattern was suggestive of H. pylori infection. We reviewed clinical data including history of HP prior to biopsy, HP treatment prior to biopsy, NSAID and proton pump inhibitor (PPI) use prior to biopsy, HP laboratory testing after biopsy, and HP treatment after biopsy.

Results: We identified 59 patients eligible for inclusion. Mean age was 56 (range 12-89) and 33 patients (55.9%) were male. 19 patients were on NSAIDs and 27 on PPI at time of biopsy. No patients received HP laboratory testing (stool antigen, breath test, or serology) immediately post-biopsy. However, 14 (50.0%) of 28 patients with a history of previously treated HP underwent retreatment despite negative IHC, while 16 (51.6%) of 31 patients without prior HP infection received subsequent treatment (p=0.90). We observed significant

regional differences, with 67.5% of the 37 patients from institutions in the South undergoing HP treatment post-biopsy, compared to only 27.2% of the 22 patients from Midwest or Northeast institutions (p=0.003). Following post-biopsy HP treatment, 7 patients with a history of HP and 6 patients without prior HP underwent stool antigen testing and none were positive.

Figure 1 - 691

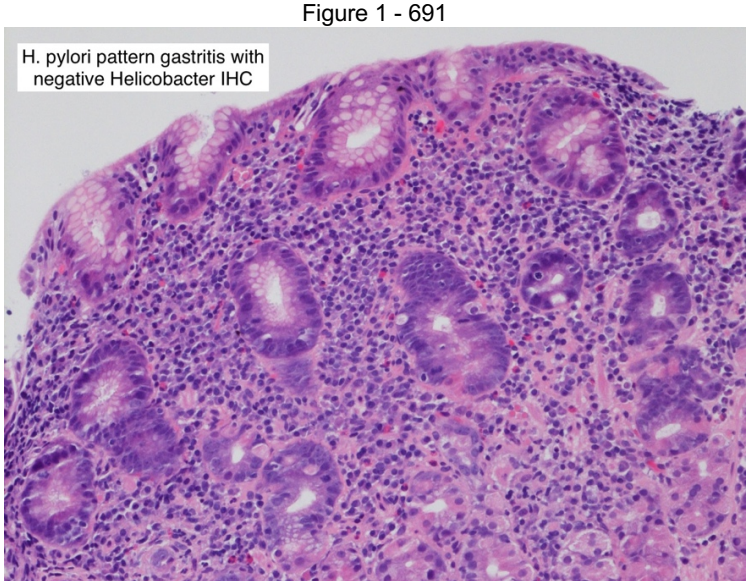

Conclusions: Including a comment to distinguish HP pattern gastritis from other gastritis patterns in patients with negative IHC can change clinical management. Nearly half of patients with HP pattern gastritis and negative IHC received HP treatment, independent of prior HP history. This was more likely in institutions in the South, which may reflect HP prevalence and pre-test suspicion in those populations.

692 Secondary Perianal Paget's Disease as Spread from Non-Invasive Colorectal Adenomas: A Series of Four Cases

Danielle Hutchings[1], Annika Windon[2], Kevan Salimian[3], Naziheh Assarzadegan[4], Elizabeth Montgomery[5]
[1]Johns Hopkins Medicine, Baltimore, MD, [2]Johns Hopkins Hospital, Baltimore, MD, [3]Johns Hopkins, Baltimore, MD, [4]Department of Pathology, The Johns Hopkins Medical Institutions, Baltimore, MD, [5]Johns Hopkins Medical Institutions, Baltimore, MD

Disclosures: Danielle Hutchings: None; Annika Windon: None; Kevan Salimian: None; Naziheh Assarzadegan: None; Elizabeth Montgomery: None

Background: Paget's disease of the perianal skin can be of primary intraepithelial adnexal-type or secondary due to spread from a colorectal lesion, nearly always colorectal adenocarcinoma. Secondary perianal Paget's disease (PPD) arising in association with non-invasive precursor colorectal lesions is exceedingly rare with only a few cases documented previously. In this study, we present the clinical and pathologic features of four cases of secondary PPD associated with colorectal adenomas.

Design: Two cases were identified from our consultation service. Two additional cases were found through a search of our pathology database. Pathology reports and all available slides, including immunohistochemical studies, were reviewed for each case. Follow-up information for each patient was obtained from the referring pathologist or clinician.

Results: All patients (2 women, 2 men) were adults, with a median age of 72 years (range 68-76 years). In all cases, PPD was associated with colorectal adenomas, including three (75%) conventional tubular adenomas and one (25%) tubulovillous adenoma with serrated foci. All adenomas had high-grade dysplasia and one had intramucosal adenocarcinoma (lamina propria invasion), but all lacked submucosal invasion. PPD showed a colorectal phenotype by immunohistochemistry in all cases. Specifically, PPD was positive for CK20 in all cases, CK7 in 3/3 cases, CDX2 in 1/1 case, p16 in 1/1 case, BER-EP4 in 1/1 case and CEA in 1/1 case. PPD was negative for GCDFP in 2/2 cases, S100 protein in 2/2 case, SOX10 in 1/1 case and CK903 in 1/1 case. PPD was associated with pseudoepitheliomatous hyperplasia of the squamous mucosa in one case. Follow-up information was available for three patients. One patient developed invasive mucinous adenocarcinoma of the perianal tissue 36 months after initial presentation. One patient had no evidence of disease at 87 months. One patient has no clinical evidence of disease but is scheduled for re-excision due to positive margins at the time of this writing; 6 months after presentation.

Conclusions: We present the largest series (4 cases) of secondary PPD associated with non-invasive colorectal adenomas. Although it is rare, knowledge of this entity is important to forestall overdiagnosis of invasion and potential overtreatment. However, clinical course following excision is variable and close long-term follow-up for patients is essential.

693 Mismatch Repair Deficiency in Squamous Cell Carcinoma of the Gastrointestinal Tract: Frequency and Clinical Implication

Rami Imam[1], Irene Gullo[2], Wissam Dahoud[1], Mahra Nourbakhsh[1], Canan Firat[1], Zalak Patel[1], Efsevia Vakiani[1], Jaclyn Hechtman[1], Laura Tang[1], David Klimstra[1], Zsofia Stadler[1], Jinru Shia[1]
[1]Memorial Sloan Kettering Cancer Center, New York, NY, [2]University of Porto/IPATIMUP, Porto, Portugal

Disclosures: Rami Imam: None; Wissam Dahoud: None; Mahra Nourbakhsh: None; Canan Firat: None; Zalak Patel: None; Efsevia Vakiani: None; Jaclyn Hechtman: *Speaker*, WebMD; Jaclyn Hechtman: *Speaker*, WebMD; Laura Tang: None; David Klimstra: None; Zsofia Stadler: None; Jinru Shia: None

Background: Currently, routine mismatch repair (MMR)-deficiency testing for tumors of the gastrointestinal tract (GIT) is mostly applied to adenocarcinomas. The frequency and clinical implication of MMR-deficiency in GIT squamous cell carcinoma remain to be defined.

Design: GIT squamous cell carcinomas evaluated by Next Generation Sequencing via MSK-IMPACT (n=125) were queried for MMR-deficiency. A separate series of germline mutation proven Lynch syndrome (LS) patients who presented with non-colorectal-/non-endometrial-adenocarcinomas (n=49) were also queried for GIT squamous cell tumors. All tumors found to be MMR-deficient were further evaluated for clinico-pathological and molecular characteristics with a focus on the underlying etiology for the MMR-deficiency.

Results: In total, 2 of 125 (1.6%) GIT squamous cell carcinomas from the IMPACT series exhibited MMR-deficiency: 1/45 (2%) in esophageal tumors, and 1/80 (1.3%) in anal tumors. Additionally, 2 GIT squamous tumors were identified from the LS series (2/49, 4%). The specific characteristics of the 4 cases are outlined in the Table. All 3 tumors in LS (including 1 with germline *MLH1* epimutation) were esophageal. One esophageal tumor in an MSH6 LS patient exhibited loss of MLH1 and PMS2 with retained MSH2 and MSH6, and with no evidence of *MLH1* methylation. The etiology of the MMR-deficiency in this case remained unclear. The one non-LS associated tumor occurred in the anal canal and was associated with HPV infection. This case was negative for MMR germline mutation, and the MMR-deficiency was likely caused by somatic *MLH1* mutation.

Case ID	Age/Sex	Tumor	HR HPV	MMR IHC	MSI	Pathogenic germline mutation	Additional testing
From IMPACT series							
1	44/M	Esophageal SCC	Not tested	MLH1/PMS2 loss	MSI-H	*MSH6*	Tumor *MLH1* methylation negative
2	69/M	Anal SCC	Present	MLH1/PMS2 loss	MSI-H	Negative	Tumor with *MLH1* E600*
From LS series							
3	69/F	Esophageal SCC in situ	Not tested	MLH1/PMS2 loss	MSI-H	*MLH1* (epimutation)	
4	53/M	Esophageal SCC	Not tested	MLH1/PMS2 loss	MSI-H	*MLH1*	

Conclusions: In our series, MMR-deficiency occurred in only 1.6% of the GIT squamous cell carcinomas, and among the LS patients who presented with non-colorectal-/non-endometrial-adenocarcinomas, only 4% manifested GIT squamous cell tumors. Of the MMR-deficient GIT squamous cell tumors detected, 3 of 4 were LS associated, and 1 was likely related to somatic *MLH1* mutation/inactivation. Our results suggest that the frequency of MMR-deficiency in GIT squamous lesions may be too low to justify routine MMR testing for LS screening; nonetheless, this tumor type may show MMR-deficiency in LS patients and can serve as a useful test sample in the LS work-up for high risk families.

694 Esophageal Verrucous Carcinoma Is Molecularly Distinct from Conventional Esophageal Squamous Cell Carcinoma

Raymond Isidro[1], Fei Dong[2], Jason Hornick[3], Jon Wee[3], Agoston (Tony) Agoston[2], Deepa Patil[2], Vikram Desphande[4], Lei Zhao[3]
[1]Brigham and Women's Hospital, Harvard Medical School, Brookline, MA, [2]Brigham and Women's Hospital, Boston, MA, [3]Brigham and Women's Hospital, Harvard Medical School, Boston, MA, [4]Massachusetts General Hospital, Harvard Medical School, Boston, MA

Disclosures: Raymond Isidro: None; Fei Dong: None; Jason Hornick: *Consultant*, Eli Lilly; *Consultant*, Epizyme; Jon Wee: None; Agoston (Tony) Agoston: None; Deepa Patil: None; Lei Zhao: None

Background: While verrucous carcinoma of the esophagus is morphologically distinct from conventional squamous cell carcinoma (SCC) of the esophagus, it is unclear whether there are significantly difference at the molecular level. Previous studies have suggested that HPV infection is not involved in carcinogenesis. In this study, we set out to characterize the genomic landscape of esophageal verrucous carcinoma.

Design: Three cases of esophageal verrucous carcinoma were retrieved from our pathology archive. Clinical information was collected by reviewing electronic medical records. Pathologic features were evaluated by reviewing pathology reports and examination of all slides. HPV infection status was tested by p16 immunohistochemistry and high-risk HPV mRNA ISH. Genetic alterations were analyzed by targeted massively parallel sequencing. Four additional verrucous carcinoma cases were identified by reviewing digital images of the esophageal SCC TCGA cohort (95 cases in total).

Results: The clinical findings for all 7 cases of esophageal verrucous carcinoma are summarized in Table 1. None of the 3 in-house cases were positive for P16 or HPV. None of the 7 cases showed *TP53*gene alterations. Recurrent potential driver mutations were identified in the following genes: *FBXW7*(3/7 cases), *GNAS*(3/7 cases) and *PIK3CA*(2/7 cases) [full list of genes with recurrent mutations in Figure 1].

	Source	Sex	Age (years)	Relevant history	Tumor site	T stage	p16 IHC	HPV ISH
1	In house	male	65	GERD/peptic ulcer	Distal esophagus	3	negative	negative
2	In house	male	58	Longstanding Barrett's esophagus, alcohol	Distal esophagus	1	negative	negative
3	In house	male	57	Smoking, alcohol, GERD	Distal esophagus	2	negative	negative
4	TCGA-L5-A88W	male	67	Alcohol	Distal esophagus	Clinical stage 2a	NA	NA
5	TCGA-IC-A6RF	female	69	Alcohol	Mid esophagus	Clinical stage 1a	NA	NA
6	TCGA-JY-A93F	female	58	Alcohol	Distal esophagus	Clinical stage 1b	NA	NA
7	TCGA-IG-A4QT	male	56	Alcohol	Distal esophagus	Clinical stage 2a	NA	NA

Figure 1 - 694

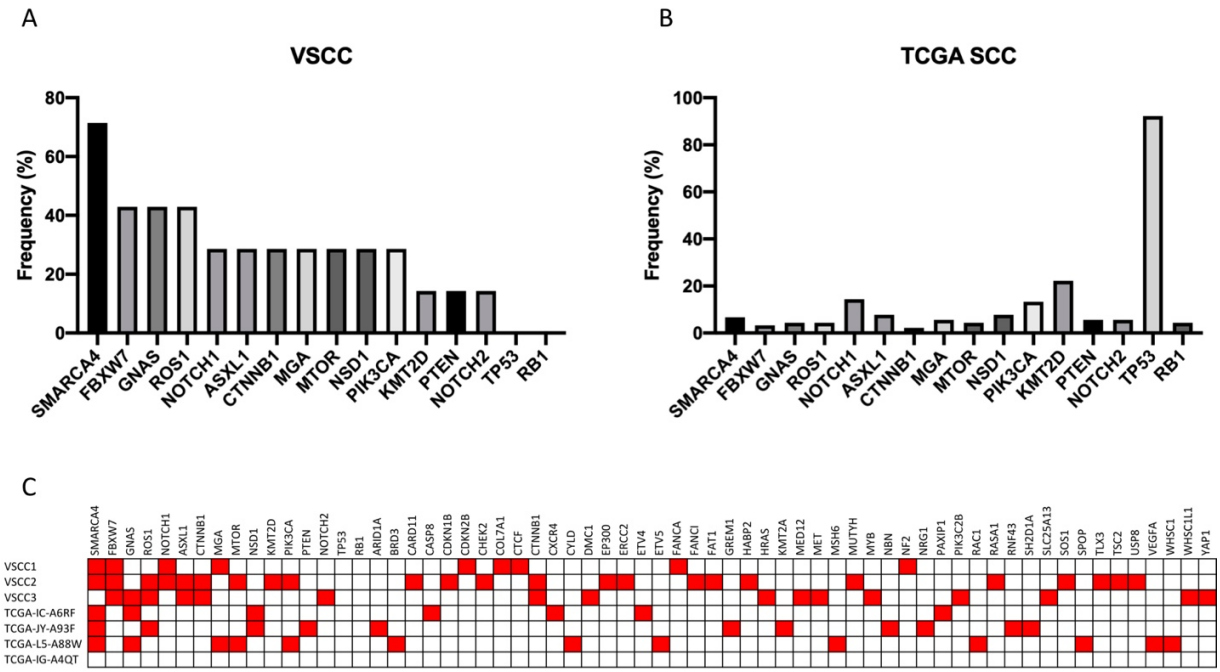

Conclusions: This study confirms that HPV is not involved in the tumorigenesis of esophageal verrucous carcinoma. The mutational profile of esophageal verrucous carcinoma is different from conventional SCC. *TP53*gene alterations, which are present in more than 90%

of conventional SCC, are not identified in esophageal verrucous carcinomas. Some of the molecular pathways involved in esophageal verrucous carcinoma, such as PIK3CA, are potential therapeutic actionable targets.

695 Medication-Specific Differences in Morphological Patterns of Injury in Immune Checkpoint Inhibitor-Associated Colitis

Raymond Isidro[1], Alex Ruan[2], Osama Rahma[3], Shilpa Grover[4], Amitabh Srivastava[4]
[1]Brigham and Women's Hospital, Harvard Medical School, Brookline, MA, [2]Harvard Medical School, Philadelphia, PA, [3]Dana-Farber Cancer Institute, Boston, MA, [4]Brigham and Women's Hospital, Harvard Medical School, Boston, MA

Disclosures: Raymond Isidro: None; Alex Ruan: None; Osama Rahma: *Advisory Board Member*, Merck; *Speaker*, BMS; Shilpa Grover: *Employee*, UpToDate Inc (Editor for Gastroenterology); Amitabh Srivastava: None

Background: Immune checkpoint inhibitor-associated (ICI) colitis typically manifests as a variably active colitis with increased intraepithelial lymphocytes (IELs) and prominent apoptosis. However, there is a paucity of data regarding possible variations in morphological patterns of injury between the commonly used ICIs (ipilimumab, Ipi; nivolumab, Nivo; Pembrolizumab; Pembro).

Design: Symptomatic patients on ICI therapy who were diagnosed with histologically confirmed colitis were retrospectively identified. All index biopsies were reviewed blindly using the Geboes score, commonly used in IBD studies, to quantitate architectural and inflammatory changes and the degree of tissue destruction. Also recorded for each biopsy were presence of Paneth cells in left colon, IELs, abnormal subepithelial collagen and degree of crypt epithelial apoptosis. A predominant pattern of colitis was recorded for each patient.

Results: A total of 99 biopsies from 57 patients with ICI colitis: Ipi, n=12; Nivo, n=15; Ipi and Nivo, n=19; and Pembro, n=11) formed the final study group. Crypt architecture was maintained in most biopsies (88/99; 89%) and Paneth cell metaplasia was uncommon (13/82; 16%). An active neutrophilic infiltrate within lamina propria or epithelium was present in 74.7% of all biopsies. Compared to Ipi alone, patients treated with other ICIs more frequently demonstrated increased IELs (69/79, 87% vs 8/20, 40%; p<0.001) and apoptosis (38/79, 48% vs 3/20, 15%; p=0.01). Geboes chronic inflammation Grades 2-3 were more common in Nivo patients (14/22, 63%) compared to other ICIs (27/77, 35%, p=0.011). Pembro was less frequently associated with features of crypt destruction (6/25, 24% vs 36/74, 48%; p=0.04) and of erosion/ulceration (1/25, 4% vs 25/74, 33%; p=0.003) when compared to other ICIs.

Compared to those on other ICIs, patients on Ipi alone more frequently demonstrated a diffusely active colitis without features of chronicity (7/12, 58% vs 6/45, 13%; p=0.02) and manifested less frequently with a microscopic colitis pattern of injury (lymphocytic or collagenous; 20/45, 44% vs 0/12; p=0.03). An IBD-like pattern of injury was seen in a subset of Nivo patients but not in Pembro patients (8/34 vs 0/11; ns).

Pattern	Ipi (n=12)	Ipi+Nivo (n=19)	Nivo (n=15)	Pembro (n=11)
Diffuse active	7	4	1	1
Chronic active	3	2	6	0
Lymphocytic	0	4	2	4
Collagenous	0	2	5	3
GVHD	1	4	0	2
Mixed	1	2	1	1
Eosinophilic	0	1	0	0

Conclusions: Our findings suggest that there are medication-specific differences in mucosal injury patterns in ICI colitis. This may be clinically useful when trying to distinguish entities in the differential diagnosis of ICI colitis and when ICI agents are given along with conventional chemotherapy.

696 Programmed Death-Ligand 1 (PD-L1) Expression in Anal Squamous Cell Carcinoma Used in Combination with HPV Status Further Stratifies Clinical Outcome

Sarah Jamshed[1], Xiaoqin Zhu[2], Karen Dresser[3], Jacob Bledsoe[3]
[1]University of Massachusetts Medical School, Worcester, MA, [2]Brigham and Women's Hospital, Shrewsbury, MA, [3]UMass Memorial Health Care, Worcester, MA

Disclosures: Sarah Jamshed: None; Xiaoqin Zhu: None; Karen Dresser: None; Jacob Bledsoe: None

Background: Immunotherapy is emerging as a fundamental pillar in the management of many solid organ tumors. Little is known about the PD-L1 profile of anal squamous cell carcinoma (ASCC) and its clinicopathologic associations. Studies have shown an adverse clinical

outcome in ASCC that express PD-L1 but correlation with HPV status is not well-defined. We investigated the correlation of PD-L1 expression in ASCC with patient characteristics, pathologic features, and clinical outcome in order to ascertain whether a prognostic value of PD-L1 exists in ASCC.

Design: Sixty-two cases of ASCC were identified from 2000 to 2018. FFPE tissue from biopsy and resection samples was tested for HPV16/18 by Cervista Invader Assay (Hologic) and mutation status by a 50 gene NGS platform using the Ampliseq Cancer Hotspot Panel v2. Cases were stained with PD-L1 IHC (E1L3N, Cell Signaling), scored using the Combined Positive Score by two pathologists, and reported as positive (≥1) or negative (<1). Correlation between PD-L1 status and pathologic features was analyzed using the two-tailed Fischer's exact test. Survival outcome was performed using the Kaplan-Meier method and log-rank test.

Results: Forty-seven HPV+ and 15 HPV- cases were identified. PD-L1 was positive in 32% of cases and was not significantly associated with HPV status (HPV+: 30%; HPV-: 40%; p=0.53). HPV negativity was associated with worse OS (median survival: HPV-: 35.8 mos; HPV+: median not reached; p=0.008; Figure 1). Within the HPV- group, PD-L1+ cases showed a trend towards worse OS (median survival: 9.8 vs. 40.6 mos; p=0.064). Considering HPV negativity and PD-L1 positivity together improved risk stratification when compared with HPV status alone (p=0.0008; Figure 2). No association was found with PDL1 and OS in HPV+ cases (p=0.237) or in the entire cohort (p=0.905). There was no significant correlation between PDL1 expression and sex, pathologic stage, TP53 mutation, mutation status or morphology (keratinizing vs. non-keratinizing types).

Figure 1 - 696

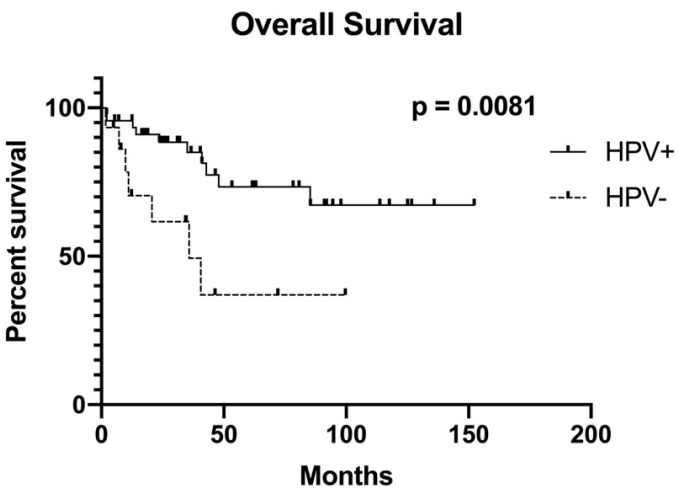

Figure 1: Overall survival between HPV+ and HPV- ASCC

Figure 2 - 696

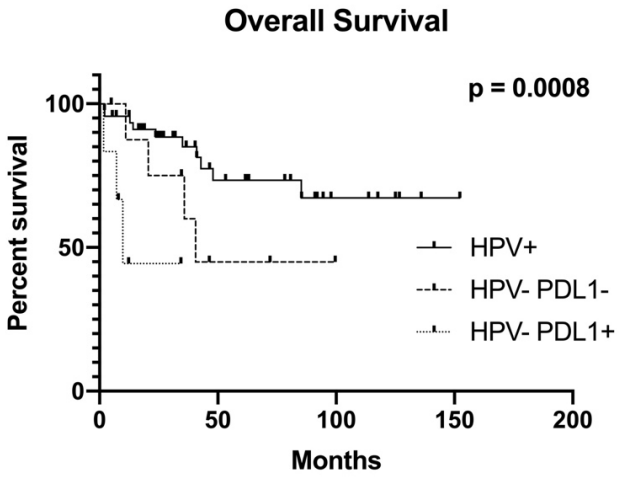

Figure 2: The addition of PD-L1 further stratifies outcome in the HPV-, but not HPV+ cases, with PD-L1 expression associated with worse survival.

Conclusions: PD-L1 expression is frequent in both HPV+ and HPV- ASCC and may indicate susceptibility to immune checkpoint blockade. PD-L1 assessment may be particularly informative in HPV- ASCC as it infers a poor prognosis in this group, and may aid in risk stratification. Our results suggest that the previously reported poor prognosis associated with PD-L1 positivity may be driven by HPV- PD-L1+ cases. Further studies with a larger HPV- sample size are needed to support these novel findings.

697 Mouse Double Minute 2 Amplification in Esophageal Squamous Cell Carcinoma Associated with Better Outcome

Dongxian Jiang[1], Yingyong Hou[2]
[1]Zhongshan Hospital of Fudan University, Shanghai, China, [2]Zhongshan Hospital, Fudan University, Shanghai, China

Disclosures: Dongxian Jiang: None; Yingyong Hou: None

Background: The study aimed to determine the frequency of *Mouse Double Minute 2* (*MDM2*) amplification in esophageal squamous cell carcinoma (ESCC), and to clarify its prognostic significance.

Design: In this study, we investigated *MDM2* amplification on tissue microarray, using fluorescence in situ hybridization and analyzed the correlations with clinicopathological features and outcome in 515 Chinese ESCC patients.

Results: *MDM2* amplifications were found in 37 of 515 ESCC (7.2%). They were significantly negative correlation to tumor size (*P*=0.045) and disease progression (*P*=0.002) or death (*P*=0.003). In univariate Cox regression analysis, differentiation, vessel invasion, nerve invasion, clinical stage, and *MDM2* amplification were associated with disease free survival (DFS) and overall survival (OS). In multivariate Cox regression analysis, *MDM2* amplification was found to be an independent prognostic factor for improved outcomes (*P*=0.023 for DFS, *P*=0.027 for OS), and clinical stage was an independent prognostic factor for worsened outcomes (*P*<0.001). When survival analyses were conducted in different clinical stage, *MDM2* amplification was associated with longer DFS and OS in stage I-II ESCC (*P*=0.003 for DFS and 0.003 for OS).

Table Univariate and Multivariate Analyses of Prognostic Factors for Survival

	DFS			OS	
Univariate factor analyses					
Sex	0.185	1.232 (0.905-1.678)		0.183	1.236 (0.905-1.687)
Age	0.981	1.003 (0.791-1.272)		0.735	1.042 (0.821-1.323)
Smoking	0.294	1.138 (0.894-1.448)		0.208	1.168 (0.917-1.486)
Tumor Size	0.111	1.213 (0.957-1.538)		0.048	1.271 (1.002-1.612)
Tumor Location	0.949	0.993 (0.810-1.219)		0.894	1.014 (0.825-1.247)
Differentiation	0.025	1.283 (1.032-1.594)		0.061	1.231 (0.990-1.532)
Vessel invasion	0.001	1.550 (1.193-2.015)		0.002	1.512 (1.159-1.972)
Nerve invasion	0.009	1.382 (1.085-1.759)		0.001	1.488 (1.169-1.895)
Clinical stage	<0..001	2.832 (2.220-3.611)		<0.001	2.873 (2.251-3.667)
MDM2 amplification	0.012	0.460 (0.252-0.841)		0.014	0.469 (0.256-0.857)
Type of surgery	0.585	0.969 (0.868-1.083)		0.761	0.983 (0.879-1.099)
Charlson index	0.416	1.113 (0.860-1.439)		0.292	1.149 (0.887-1.488)
Postoperative complications	0.065	0.734 (0.529-1.020)		0.031	0.691 (0.494-0.967)
Adjuvant therapy	0.059	1.186 (0.993-1.417)		0.178	1.133 (0.945-1.360)
Multivariate factor analyses					
Tumor Size	-	-		0.447	1.101 (0.859-1.413)
Differention	0.491	1.082 (0.865-1.352)		-	-
Vessel invasion	0.555	1.087 (0.824-1.435)		0.769	1.043 (0.788-1.380)
Nerve invasion	0.308	1.138 (0.888-1.458)		0.226	1.173 (0.906-1.518)
Clinical stage	<0.001	2.653 (2.051-3.430)		<0.001	2.695 (2.082-3.488)
MDM2 amplification	0.023	0.494 (0.270-0.906)		0.027	0.504 (0.275-0.923)
Postoperative complications	-	-		0.046	0.707 (0.504-0.994)

Figure 1 - 697

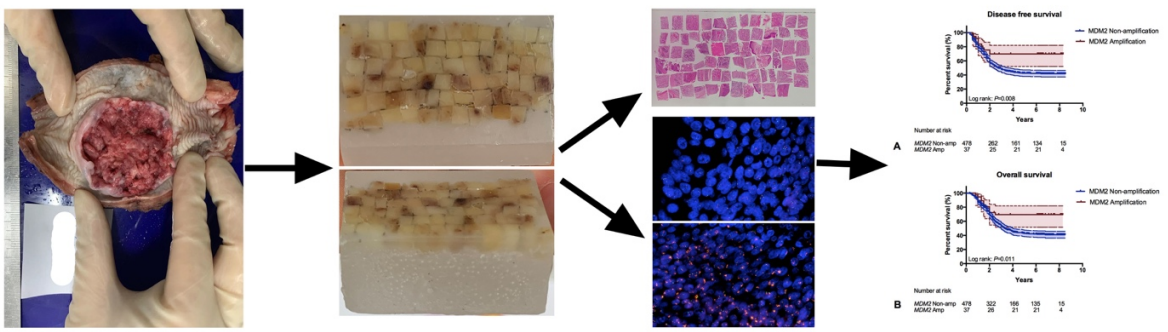

Figure 2 - 697

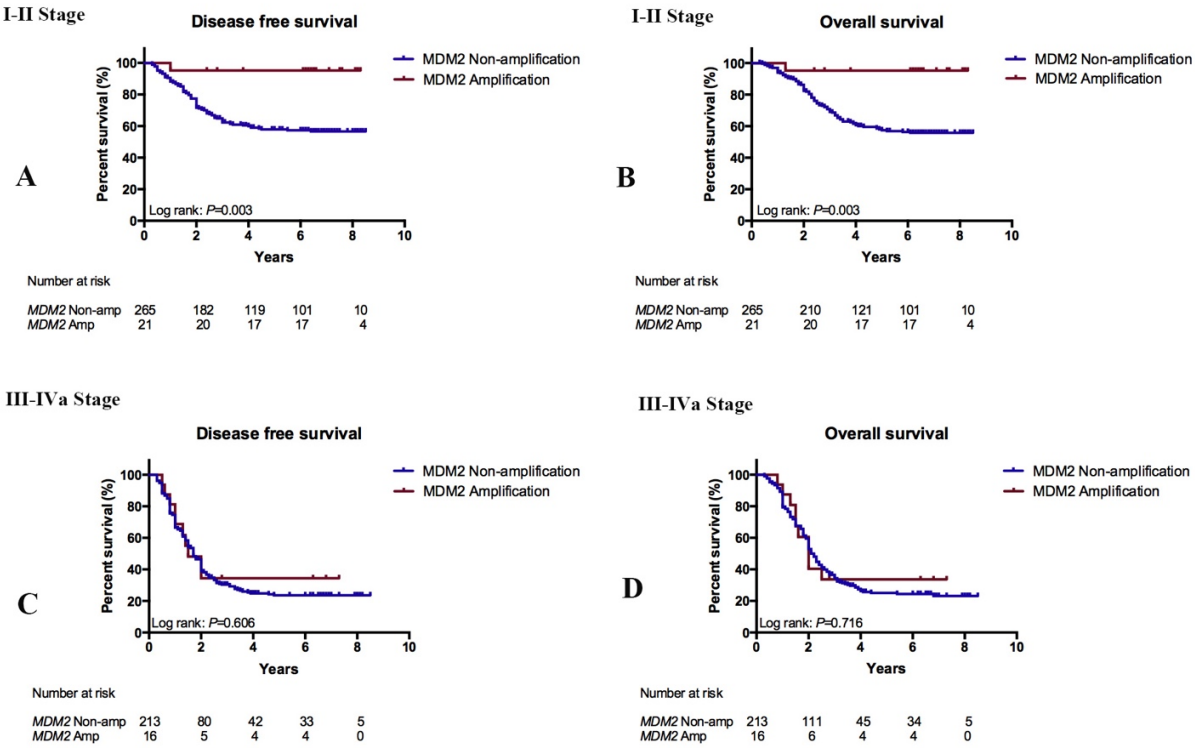

Conclusions: *MDM2* amplification was significantly correlated with an improved outcome, especially in stage I-II diseases and verified as an independent prognostic factor in our patients. Therefore, *MDM2* amplification might be a potential biomarker for risk stratification of lower stage of ESCC.

698 Tumor Budding and Poorly Differentiated Clusters in Small Intestinal Adenocarcinoma

Sun-Young Jun[1], Nara Yoon[2], Seung-Mo Hong[3]
[1]Incheon St. Mary's Hospital, Incheon, Korea, Republic of South Korea, [2]Incheon St. Mary's Hospital, College of Medicine, The Catholic University of Korea, Incheon, Korea, Republic of South Korea, [3]Asan Medical Center, Songpa-gu, Seoul, Korea, Republic of South Korea

Disclosures: Sun-Young Jun: None; Nara Yoon: None; Seung-Mo Hong: None

Background: Tumor budding (TB) and poorly differentiated clusters (PDC) are well-established independent prognostic factors in gastrointestinal malignancies, but their clinicopathologic and prognostic significances have not been investigated in small intestinal adenocarcinomas (SIACs).

Design: TB and PDC were assessed in 236 surgically-resected SIACs and analyzed their association with clinicopathologic variables, including and overall survival. TB (a single tumor cell or a tumor cell cluster ≤ 4 cells) and PDC (a tumor cell cluster ≥ 5 tumor cells) at the invasive front (p) and in intratumoral area (i) were independently counted in one hotspot of x200 magnification, and they were graded as grade-1 (0 to 4), grade-2 (5 to 9), or grade-3 (≥10). Consequently, SIACs with grade-2 or -3 were categorized high level of TB or PDC.

Results: High levels of pTB, pPDC, iTB, and iPDC were observed in 73.7% (174/236), 50.0% (118/236), 54.7% (129/236), and 36.0% (85/236), respectively. High TB or PDC was associated with nodular or infiltrative growth pattern (P<0.001 in pTB, pPDC, and iTB, all; P=0.002 in iPDC) and non-intestinal type (P<0.001 in pTB and iTB, both; P=0.029 in pPDC; P=0.018 in iPDC). In addition, SIACs with high TB or PDC were related with aggressive behaviors, including higher grade of tumor (P<0.001 in pTB, iTB, and iPDC, all; P=0.002 in pPDC), higher T- and N-categories (P<0.001 in pTB and pPDC, all; P<0.001 and P=0.006 in iTB, respectively; P=0.001 and P=0.003 in iPDC, respectively) and stage grouping (P<0.001 in pTB and pPDC, both; P=0.002 in iTB; P=0.001 in iPDC), and more frequent perineural (P<0.001 in pTB and iTB, both; P=0.008 in pPDC; P=0.003 in iPDC) or lymphovascular (P<0.001 in pTB, iTB, and iPDC, all; P=0.004 in pPDC) invasion. Patients with high levels of TB or PDC had significantly shorter survival times than those with low levels (median, 23.3 *vs.* 133.7 months in pTB, P<0.001; 24.9 *vs.* 47.4 months in pPDC, P=0.023; 23.3 *vs.* 50.1 months in iTB, P=0.001; 23.0 *vs.* 44.4

months in iPDC, *P*=0.043). On multivariate analysis, high pTB (*P*=0.003), distal tumor location and non-intestinal type (*P*<0.001, both), high N-category (*P*=0.001), and the presence of lymphovascular invasion (*P*=0.021) remained as worse independent prognostic predictors.

Conclusions: TB and PDC, both in peritumoral and intratumoral regions, are associated with aggressive behaviors in SIACs. Among them, high pTB can be used as an important worse prognostic indicator in SIAC patients.

699 Application of Whole Block Imaging (WBI) by Micro-Computed Tomography for the Evaluation of Endoscopic Submucosal Dissection Specimens

Noboru Kawata[1], Alexei Teplov[1], Takashi Ohnishi[1], Kareem Ibrahim[1], Masao Yoshida[2], Takashi Sugino[3], Hiroyuki Ono[3], Tadakazu Shimoda[3], Yukako Yagi[1]
[1]Memorial Sloan Kettering Cancer Center, New York, NY, [2]Shizuoka Cancer Center, Nagaizumi, Shizuoka, Japan, [3]Shizuoka Cancer Center, Nagaizumi-Cho, Shizuoka, Japan

Disclosures: Noboru Kawata: None; Alexei Teplov: None; Takashi Ohnishi: None; Kareem Ibrahim: None; Masao Yoshida: None; Takashi Sugino: None; Hiroyuki Ono: None; Tadakazu Shimoda: None; Yukako Yagi: None

Background: The precise pathological diagnosis of endoscopic submucosal dissection (ESD) specimens is essential, because the criteria for determining subsequent therapeutic steps is the presence or absence of risk factors for lymph node metastasis. However, the current diagnosis technique involves the evaluation of two-dimensional images of cross-sections of resected specimens, which only evaluates a small part of the tumor. Micro-computed tomography (micro-CT) can non-destructively provide three-dimensional (3D) reconstructed whole block imaging (WBI) at a high resolution. Therefore, the aim of this study was to determine whether micro-CT was able to provide further pathological information in addition to conventional diagnosis methods in the evaluation of ESD specimens.

Design: We scanned formalin-fixed paraffin-embedded (FFPE) tissue blocks of ESD specimens using a custom-built micro-CT scanner. Reconstructed imaging data were visualized and analyzed using commercially available software, Dragonfly 4.1. Finally, we evaluated tumor invasion depth, lymphovascular invasion (LVI), and resected margin status by correlating the reconstructed images obtained by micro-CT with those from whole slide imaging (WSI) of hematoxylin and eosin (H&E)-stained slides.

Results: A total of 8 FFPE tissue blocks of 3 ESD specimens (2 gastric cancer and 1 colon cancer) were scanned by micro-CT. The matching cross-section slices between WSIs of H&E-stained slides and micro-CT images are shown in Figure 1. All reconstructed images with high resolution allowed for clear visualization of tissue structure and differentiation between tumor and non-tumor tissue. In the micro-CT images, we were able to determine tumor invasion depth, LVI, and resected margin status by correlating them with WSI images. In addition, micro-CT images revealed that the actual tumor invasion depth was deeper than the conventional pathological diagnosis in 2 cases of gastric cancer. 3D reconstruction provided a cross-sectional image at any location and increased the ease of identifying the running direction of blood vessels and the horizontal tumor spread pattern, which were difficult to identify using conventional slide images.

Figure 1 - 699

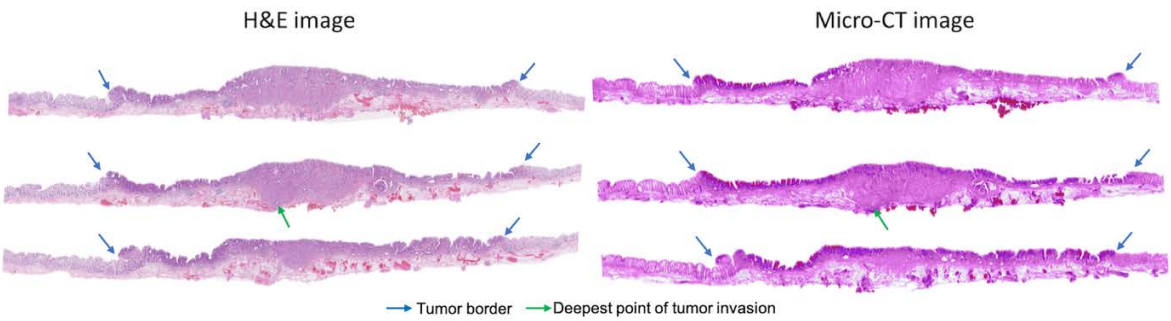

Conclusions: Our results showed that WBI by micro-CT has the potential to provide further pathological information related to the treatment strategy after ESD in addition to conventional methods. Further studies in additional cases are needed to confirm this.

700 Review of Pathology and Cost Benefit Analysis of Hernia Sacs Processed over a 19-Year Period

Arshia Kazerouni[1], Klaudia Nowak[2], Kenny Chieu[3], Tao Wang[4], Runjan Chetty[3], Rajkumar Vajpeyi[3], Stefano Serra[5]
[1]University Health Network, Hamilton, ON, [2]Toronto General University Health Network, Toronto, ON, [3]University Health Network, Toronto, ON, [4]Queen's University/Kingston Health Sciences Centre, Kingston, ON, [5]University Health Network, University of Toronto, Toronto, ON

Disclosures: Arshia Kazerouni: None; Klaudia Nowak: None; Kenny Chieu: None; Tao Wang: None; Runjan Chetty: None; Rajkumar Vajpeyi: None; Stefano Serra: None

Background: Herniorrhaphy is relatively common surgical procedure. As such, the excised hernia sacs are sent for pathological evaluation. Practice varies from a gross only examination to submission for microscopic evaluation. The purpose of this study was to analyze the pathological findings and the cost benefit of undertaking gross and microscopic evaluation of the tissue removed at hernia surgery.

Design: A retrospective search of the digital records for all hernia sacs received in the Division of Anatomical Pathology, Laboratory Medicine Program, University Health Network, Toronto from 2001-2019 (inclusive) was undertaken. The pathology reports were reviewed looking specifically at: the number of sections taken in each case, the gross descriptions and the final diagnosis. The cost of each block sampled was based on the average time (15-20 minutes per case) for a pathologists' assistant to examine the gross specimen (including patient chart review for indication of the surgery and dictation of the gross) as well as the cost of processing, cutting and staining a routine block. This was averaged out to $15 per block based on the hourly rates of pay and cost of consumables. The average time taken by the reporting pathologist was 5 minutes per case to look at the slides, occasionally access the patient's electronic records, and generate a report. The hourly rate of payment for pathologists is $135 per hour.

Results: In total, 3655 cases of hernias were reviewed. An average of 2 blocks per case were taken amounting to a total technical cost of approximately $109 000. The total Pathologist cost in reporting these cases was approximately $41 000. Thus, the overall cost of processing and examining hernia sacs of over a 19-year period amounted to $150 000.Of the 3655 hernia cases a specific diagnosis (benign or malignant) was made in 157 cases (4.3%). 43 cases required follow up. 3 of these cases consisted of a new diagnosis malignancy and 7 contained vas deferens. One vas deferens was part of a larger orchiectomy specimen. Thus, a total of 9 out of 3655 (0.25%) hernia sacs analyzed microscopically demonstrated unexpected findings only 3 cases were deemed clinically significant.

Table 2. Clinical characteristics of malignancies in hernias

Age	Sex	Diagnosis	Lesion seen Grossly	Clinical comment
Abdominal				
78	F	Neuroendocrine tumor	Yes	Clinically known or suspicious of malignancy
68	F	Poorly differentiated carcinoma	Yes	Clinically known or suspicious of malignancy
79	M	Prostate adenocarcinoma	Yes	Clinically was initially thought to be bladder carcarcinoma
60	F	Primary peritoneal carcinoma	Yes	Further workup revealed it to be primary peritoneal in origin
71	M	Pleomorphic sarcoma	Yes	Clinically was initially thought to be hepatocellular carcarcinoma (HCC) due to history of HCC
74	F	Serous ovarian carcinoma	Yes	Clinically known or suspicious of malignancy
63	F	Serous ovarian carcinoma	Yes	Clinically known or suspicious of malignancy
56	F	Serous ovarian carcinoma	Yes	Clinically known or suspicious of malignancy
67	F	Serous ovarian carcinoma	Yes	Clinically known or suspicious of malignancy
82	F	Serous ovarian carcinoma	Yes	Clinically known or suspicious of malignancy
73	M	Adenocarcinoma, colorectal	No	Clinically known or suspicious of malignancy
68	M	Adenocarcinoma, NOS	No	Clinically known or suspicious of malignancy
53	F	Mixed carcinoma, clear cell and endometrioid adenocarcinoma	No	Clinically known or suspicious of malignancy
64	M	Neuroendocrine tumor	No	Clinically known or suspicious of malignancy
49	M	Neuroendocrine tumor	No	Clinically known or suspicious of malignancy
87	F	Pancreatic ductal carcinoma	No	Subsequently confirmed pancreatic carcinoma
74	F	Serous ovarian carcinoma	No	Clinically known or suspicious of malignancy
64	F	Serous endometrial carcinoma	No	Clinically known or suspicious of malignancy
57	F	Small B Cell Lymphoma	No	Clinically known or suspicious of malignancy
Inguinal				
79	M	Cholangiocarcinoma	Yes	Clinically known or suspicious of malignancy
47	F	Serous ovarian carcinoma	Yes	Clinically known or suspicious of malignancy
56	M	Chronic lymphocytic leukemia	No	Clinically known or suspicious of malignancy
90	M	Chronic lymphocytic leukemia	No	Clinically known or suspicious of malignancy
53	M	Liposarcoma	No	New diagnosis
72	M	Neuroendocrine tumor	No	Clinically known or suspicious of malignancy
Site not specified				
66	F	Granulosa cell tumor	Y	Clinically known or suspicious of malignancy
47	F	Serous ovarian carcinoma	Y	Clinically known or suspicious of malignancy
39	F	Choriocarcinoma	N	Clinically known or suspicious of malignancy
69	F	Clear cell renal cell cell carcinoma	N	Clinically known or suspicious of malignancy
88	F	Endometrial carcinoma	N	Clinically known or suspicious of malignancy
69	F	Granulosa cell tumor*	N	Clinically known or suspicious of malignancy
69	F	Granulosa cell tumor*	N	Clinically known or suspicious of malignancy
65	M	Hepatocellular carcinoma	N	Clinically known or suspicious of malignancy
67	F	Serous ovarian carcinoma	N	Clinically known or suspicious of malignancy
73	F	Serous ovarian carcinoma	N	Clinically known or suspicious of malignancy
* Same patient with two hernia sacs				

Conclusions: Over a 19-year period a total of 3655 hernia sac were examined yielding an unexpected findings rate of 0.25% at a cost of $150,000. Our findings suggest that hernia sac specimens should be a gross only specimen. However, sections should be submitted for microscopic analysis if grossly evident lesions are present.

701 Reappraisal of HER2 FISH Interpretation Guidelines in Gastroesophageal Adenocarcinoma Based on an 8 Year Experience at a Referral Institution

Rhett Ketterling[1], Kathryn Pearce[1], William Sukov[1]
[1]*Mayo Clinic, Rochester, MN*

Disclosures: Rhett Ketterling: None; William Sukov: None

Background: The current standard of practice in gastroesophageal adenocarcinoma (GEA) includes testing for HER2 status. Guidelines for HER2 testing in GEA were released by ASCO/CAP in 2013. These mirrored the HER2 testing guidelines for breast cancer in place at

that time. Based on the breast carcinoma guidelines, GEA samples with an initial equivocal result by FISH were retested by using an alternative control probe. In 2018 HER2 FISH guidelines for breast cancer for were changed dramatically, largely due to high equivocal rates. Based on these changes, our institution discontinued using an alternative control probe for equivocal cases, including for GEA samples. The guidelines for HER2 FISH testing in GEA have not been revised to date.

Design: IRB approval was granted. Results for GEA HER2 FISH testing performed at Mayo Clinic from 01/2011 until 07/2019 were compiled.

Results: HER2 FISH testing in GEA samples was successful in 3422 cases with 772 (23%) positive for HER2 amplification, 234 (7%) equivocal, and 2416 (71%) negative. A total of 972 results were obtained prior to implementation of GEA HER2 guidelines (01/2011-11/2013). Of those, HER2 was amplified in 182 (18%) and 24 (2%) were equivocal. During this time no equivocal cases were reflexed to an alternative control probe. A total of 2020 cases were tested from implementation of GEA HER2 guidelines (11/2013) to implementation of revised HER2 guidelines for breast carcinoma (07/2018) with 518 (25%) HER2 amplified and 139 (7%) equivocal. Of 518 positive cases, 141 (27%) had initial equivocal results, were retested with an alternative control probe and a final positive result was obtained. From implementation of revised HER2 guidelines for breast carcinoma (07/2018) until 07/2019, 438 specimens were tested with HER2 amplification in 72 (16%) and 71 (16%) showing equivocal results. Only 1 (2%) equivocal case showed a HER2:CEP17 ratio greater than 2. During this time, no cases were retested with an alternative control probe.

Conclusions: Using current guidelines, HER2 FISH testing in GEA specimens results in a high equivocal rate. Prior to new HER2 breast cancer guidelines, equivocal FISH cases were resolved using an alternative control probe. With implementation of new HER2 guidelines for breast cancer and discontinuation of retesting with an alternative control probe, GEA HER2 equivocal rates are high and these cases remain unresolved. Therefore, reevaluation of current GEA HER2 interpretation guidelines may be warranted.

702 Checkpoint Inhibitor Induced Colitis: A Comparative Analysis of 25 Colonic Specimens

Nigar Khurram[1], Rifat Mannan[2], Danielle Fortuna[1], Emma Furth[3], Rashmi Tondon[1]
[1]Hospital of the University of Pennsylvania, Philadelphia, PA, [2]Perelman School of Medicine at the University of Pennsylvania, Philadelphia, PA, [3]University of Pennsylvania, Philadelphia, PA

Disclosures: Nigar Khurram: None; Rifat Mannan: None; Danielle Fortuna: None; Emma Furth: None; Rashmi Tondon: None

Background: Immune checkpoint inhibitor agents pose significant risk for colonic mucosal injury, which often mimic other disease processes. Limited data is available regarding the histopathological findings in this group of patients. We evaluated colonic mucosal changes in patients presenting with checkpoint inhibitor induced colitis (CIC) due to different classes of such agents (antiCTLA-4 and antiPD-1/PDL-1) and compared the histopathological similarities and differences.

Design: A 10-year retrospective database search was performed to identify specimens from patients with CIC. Slides were reviewed and evaluated for presence of apoptosis, neutrophilic abscesses, lamina propria (LP) expansion, architectural changes, basal plasmacytosis, crypt drop out, intraepithelial lymphocytosis (IEL) and inflammatory pseudo polyps.

Results: We identified 25 colonic specimens (20 biopsies and 5 resections) from 16 patients with CIC (Figure 1). Of these, 9 were treated with anti-CTLA-4 (Ipilimumab), 5 with anti-PD-1 ((Nivolumab (2), Pembrolizumab (3)), one patient was treated with combination anti-CTLA4/anti-PD-1 (Ipilimumab/Nivolimumab (1) and one with sequential use of Ipilimumab/Pembrolizumab (1). Average age was 61 (range 44-81; M: 9, F: 7).

Apoptosis (Figure 2) was the most consistent finding seen with all classes of checkpoint inhibitor colitis. IEL was seen in 78% of anti-CTLA-4 and 28% of anti PD-1. Crypt architectural distortion was observed in 85% of anti-CTLA-4 and 71% of anti-PD-1 cases respectively. Acute colitis pattern was seen in 100% of anti-PD-1 but was observed in 42% of anti-CTLA-4. Both patients on combination therapy showed intense apoptosis along with neutrophilic abscesses, crypt drop out, and LP expansion. Additionally, biopsy from Ipilimumab/Nivolimumab combination drug showed pseudo polyps.

Figure 1 - 702

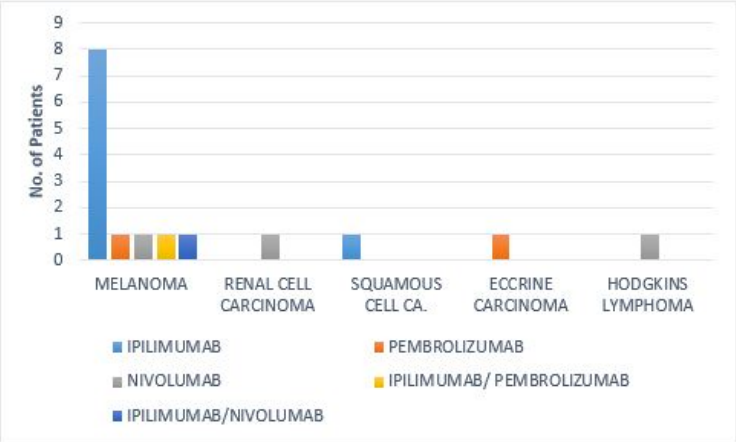

Fig 1: Malignancies with their respective treatment drug regimen

Figure 2 - 702

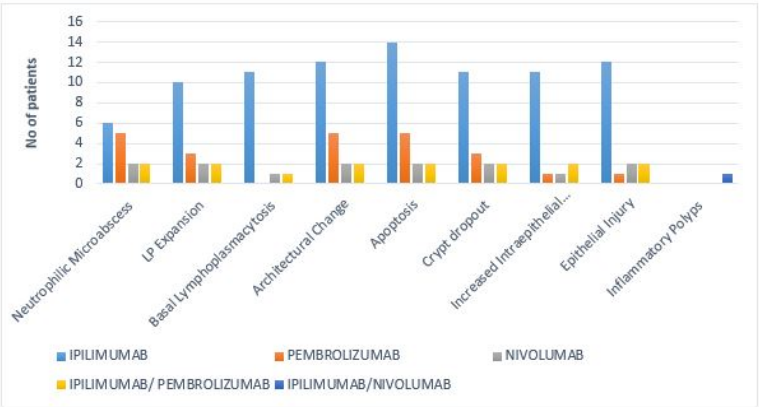

Fig 2: Comparative analysis of different immunomodulatory drugs

Conclusions: Increased crypt epithelial apoptosis is a consistent finding amongst all classes of CIC. IEL is more often observed with anti-CTLA-4, while acute colitis is a prominent feature with anti-PD-1 agents. Pseudopolyps were only seen with combination therapy. Despite a trend, different drug classes cannot be differentiated based on histology alone.

703 VGLL4 with Low YAP Expression is Associated with Favorable Prognosis in Colorectal Cancer

Joo Young Kim[1], Eun Kyung Kim[2], Won Mi Lee[2], Young Ok Hong[2], Hojung Lee[2]
[1]Nowon Eulji Medical Center, Eulji University, Seoul, Korea, Republic of South Korea, [2]Department of Pathology, Nowon Eulji Medical Center, Eulji University, Seoul, Korea, Republic of South Korea

Disclosures: Joo Young Kim: None; Eun Kyung Kim: None; Won Mi Lee: None; Young Ok Hong: None; Hojung Lee: None

Background: The Hippo pathway is a tumor suppressive pathway regulating cellular apoptosis and proliferation via YAP (Yes-associated protein)-TEAD (TEA domain-containing sequence-specific transcription factor) complex. VGLL (Vestigial-like) proteins are recently introduced transcriptional cofactors competing with YAP for TEAD binding and interfering oncogenic transcription activity of YAP-TEAD complex. We evaluated the expression of VGLL4, YAP, and TEAD4 and assessed their correlations and prognostic effects in colorectal cancers.

Design: A total of 295 colorectal carcinomas were retrieved with immunolabeling for VGLL4, YAP and TEAD4. Expression profiles were compared with each other and clinicopathologic factors.

Results: VGLL4 was positive in 164 (55.6%) cases and correlated with small tumor size (p=0.005), low pT classification (p=0.002), and absence of lymph node metastasis (p=0.024). YAP and TEAD4 were highly expressed in 138 (46.8%) cases and 144 (48.8%) cases,

respectively. High YAP expression was associated with presence of lymphovascular invasion (p=0.001) and lymph node metastasis (p=0.044), and high TEAD4 expression was associated with presence of lymphovascular invasion (p=0.001), and distant metastasis (p=0.045). VGLL4 expression was significantly correlated with low YAP expression (p<0.001), and high YAP expression was significantly associated with high TEAD4 expression (p<0.001). VGLL4 expression had significantly better overall survival than negative expression (p<0.001). High YAP and TEAD4 expressions were significantly associated with poor overall survivals (p=0.006, and p=0.042, respectively). The combined VGLL4^{pos}YAP^{low} expression showed the best overall survival than other groups (p<0.001). VGLL4 expression (HR=0.381; 95% CI, 0.212-0.683; p=0.001) and combined VGLL4^{pos}YAP^{low} expression (HR=0.227; 95% CI, 0.108-0.475; p<0.001) were independent good prognostic factors in colorectal cancers.

Figure 1 - 703

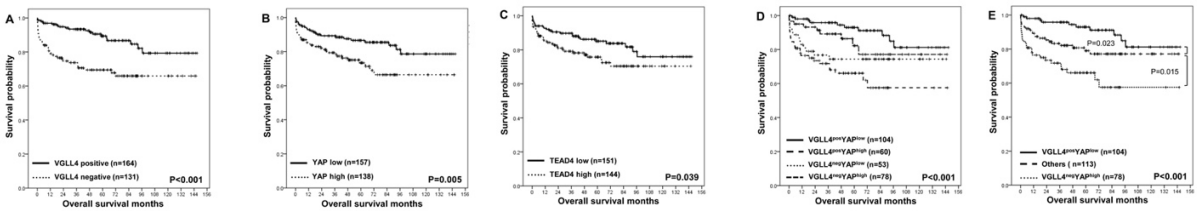

Conclusions: VGLL4^{pos}YAP^{low} expression is correlated with favorable prognosis and expression of VGLL4, YAP, and TEAD4 can be used as prognostic markers in colorectal cancer patients.

704 Segmental Absence of Intestinal Musculature in Adults: A Rare and Clinically Consequential but Easily Misdiagnosed Entity

Sun A Kim[1], Xiuxu Chen[2], Huaibin Mabel Ko[3], Qingqing Liu[3], John Paulsen[1], Alexandros Polydorides[3], Hongfa Zhu[4], Noam Harpaz[1]
[1]Mount Sinai Medical Center, New York, NY, [2]Mount Sinai Hospital Icahn School of Medicine, New York, NY, [3]Icahn School of Medicine at Mount Sinai, New York, NY, [4]Hackensack Pathology Associates, LLC, Hackensac, NJ

Disclosures: Sun A Kim: None; Xiuxu Chen: None; Huaibin Mabel Ko: None; Qingqing Liu: None; John Paulsen: None; Alexandros Polydorides: None; Hongfa Zhu: None; Noam Harpaz: None

Background: Segmental absence of intestinal musculature (SAIM) is a rare idiopathic entity that can cause spontaneous perforation or dysmotility in low-birth-weight infants. SAIM in adults is extremely rare with only 15 cases reported hitherto, and is easily misdiagnosed clinically and pathologically. We describe 3 cases to highlight the entity and its salient clinical and pathological features.

Design: Slides of resected intestinal specimens diagnosed with SAIM were identified in our departmental gastrointestinal pathology and consultation databases. The referral diagnoses and all available patient and specimen data were compiled from the clinical records.

Results: The patients, 2 males and 1 female of ages 46–93 years, each underwent an emergent segmental intestinal resection for management of spontaneous intestinal perforation involving the proximal jejunum, ascending colon or sigmoid colon. Referral diagnoses included Crohn's disease, diverticulosis and idiopathic perforation. Microscopically, all 3 specimens exhibited multiple discrete gaps in the muscularis propria, 0.3 to 2.5 cm, or replacement by wisps of attenuated myocytes and connective tissue. The defects were present both near to and remote from the perforation sites. The uninvolved muscularis propria and all other intestinal layers were histologically unremarkable on careful review. The defects in the patient with colonic diverticulosis involved the inter-diverticular colon. No recurrent perforations or deaths were reported during follow-up periods ranging from 2 months to 5 years.

Table 1. Clinicopathologic features of three patients with SAIM

Patient	Gender	Age	Chronic GI symptoms	Anatomical site	Synchronous conditions	SAIM remote from perforation site	Follow-up
1	Male	46	Yes	Proximal jejunum	None	Yes	8 months No recurrence
2	Female	93	No	Ascending colon	Cardiovascular disease	Yes	2 months No recurrences
3	Male	62	No	Sigmoid colon	Colonoscopy (5 days before), diverticulosis	Yes	5 years No recurrences

Abbreviations: GI, Gastrointestinal; SAIM, Segmental absence of intestinal musculature

Figure 1 - 704

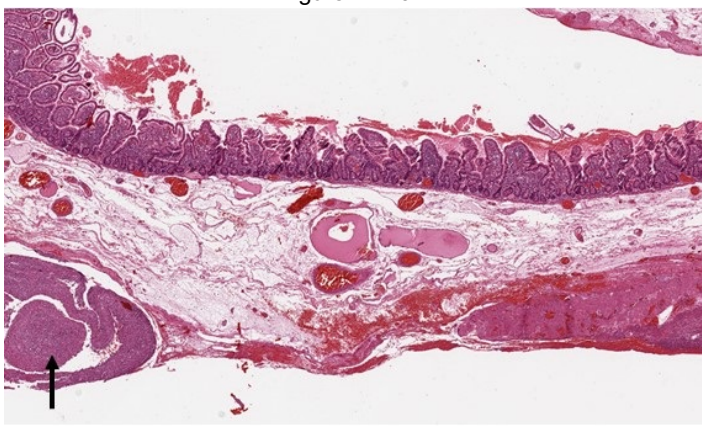

Figure 1. Jejunal section featuring discrete gap in the muscularis propria remote from perforation site. Arrow designates adherent serosal exudate.

Figure 2 - 704

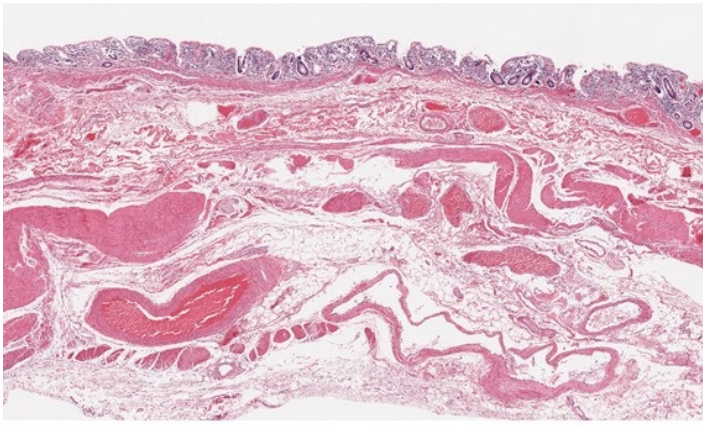

Figure 2. Discontinuous ascending colon muscularis propria with intervening wisps of connective tissue

Conclusions: SAIM is an extremely rare cause of clinically unexplained spontaneous intestinal perforation in adults. The pathological diagnosis is based on specific histological characteristics but may be missed due to their multifocality, remoteness from the perforation site, and the potential co-existence of other lesions such as diverticular disease. Clinicians and pathologists should be aware of this entity. The pathological examination of intestinal resection specimens performed for spontaneous perforation should include extensive sectioning, including sites away from the perforation site, even when diverticula are present.

705 Eosinophil Blockade in Drug-Induced Remission of Ulcerative Colitis

Sun A Kim[1], Minami Tokuyama[2], Saurabh Mehandru[2], John Paulsen[1], Xiuxu Chen[3], Hongfa Zhu[4], Qingqing Liu[2], Alexandros Polydorides[2], Noam Harpaz[1], Jean-Frederic Colombel[2], Huaibin Mabel Ko[2]
[1]Mount Sinai Medical Center, New York, NY, [2]Icahn School of Medicine at Mount Sinai, New York, NY, [3]Mount Sinai Hospital Icahn School of Medicine, New York, NY, [4]Hackensack Pathology Associates, LLC, Hackensac, NJ

Disclosures: Sun A Kim: None; Minami Tokuyama: None; Saurabh Mehandru: None; John Paulsen: None; Xiuxu Chen: None; Hongfa Zhu: None; Qingqing Liu: None; Alexandros Polydorides: None; Noam Harpaz: None; Jean-Frederic Colombel: *Grant or Research Support*, AbbVie, Janssen Pharmaceuticals and Takeda; *Grant or Research Support*, AbbVie, Janssen Pharmaceuticals and Takeda; *Stock Ownership*, Intestinal Biotech Development and Genfit; *Consultant*, AbbVie, Amgen, Allergan, Inc. Ferring Pharmaceuticals, Shire, Takeda, Arena Pharmaceuticals, Boehringer Ingelheim, Celgene Corporation, Celltrion, Eli Lilly, Enterome, Genentech; Huaibin Mabel Ko: None

Background: The role of eosinophils in the pathogenesis of inflammatory bowel disease (IBD) is controversial, with some studies reporting correlations between disease activity and eosinophil density in intestinal mucosa and others reporting no correlation. Vedolizumab, a monoclonal antibody approved for the treatment of IBD, is an anti-α4β7 integrin whose therapeutic effect has been attributed to selective blockade of gut-homing lymphocytes. We evaluated its effects on mucosal eosinophil density in a cohort of ulcerative colitis (UC) patients.

Design: We evaluated the biopsies obtained over a 2-year interval from pre- and post-treatment colonic examinations of 9 patients with UC following vedolizumab therapy. The corresponding changes in endoscopic inflammation score (Mayo scale) and patient-reported symptoms were recorded. Hematoxylin and eosin-stained slides were evaluated to determine peak eosinophil densities (count/0.237mm^2) by a pathologist who was blinded to clinical data. Paired student's t-test was used to assess pre- and post-treatment changes.

Results: The cohort comprised 5 males and 4 females with the median age 29 years (range 24 to 69 years) at initiation of therapy. Biopsies were obtained a median 2.5 weeks (range 0.4 to 6.6 weeks) prior to and 22.0 weeks (range 12.7 to 130.6 weeks) following initiation of treatment. The number of sites biopsied in pre- and post-treatment endoscopies was similar (median 7 and 7, p=0.594). The mean of peak eosinophil densities in all sets of post-treatment biopsies was significantly lower compared to pretreatment biopsies (mean 18/HPF [range 3-36] vs. 38/HPF [range 8-65], p= 0.001) and achieved pair-wise significance in 7 of 9 patients. The 2 patients whose reduction in eosinophil density failed to reach significance were the only ones whose endoscopic scores did not diminish in response to therapy, although one of them reported symptom improvement (Table 1). Interestingly, the uninvolved mucosa also showed a significant decrease in post-treatment eosinophil count (mean 13/HPF [range 3-42] vs. 24/HPF [range 6-46], p=0.011).

Table 1. Clinicopathological characteristics in UC patients treated with vedolizumab

Case	Age (year)	Sex	Time to post-Tx biopsy (weeks)	Mean eosinophil #/HPF		# of matched biopsy sites pre- & post-Tx	p-value	Endoscopic score*		Clinical response
				Pre-Tx	Post-Tx			Pre-Tx	Post-Tx	
1	60	M	21.4	40	21	8	0.006	2, 1	2	Improved
2	30	M	26.9	46	28	7	0.015	2, 3	1	Improved
3	69	F	22.1	34	19	5	0.016	1	0	In remission
4	25	M	19.1	16	8	3	0.094	3	3	No response
5	40	M	21.9	42	36	7	0.118	2	2	Improved
6	29	F	15.1	26	9	7	0.019	1, 2	0	In remission
7	24	F	12.7	8	3	6	0.046	2, 1	0	In remission
8	28	M	130.6	65	31	4	0.046	3	1	Improved
9	28	F	95.1	16	5	5	0.043	2	0	In remission
				Overall						
	Median		Median	mean eosinophil #		Mean	Overall			
	29		21.9	33	18	6	p=0.001			

Abbreviations: HPF, high power field; Tx, Treatment; UC, Ulcerative colitis

*Endoscopic subscore of Mayo score for ulcerative colitis (0, normal or inactive disease; 1, mild disease; 2, moderate disease; 3, severe disease)

Figure 1 - 705

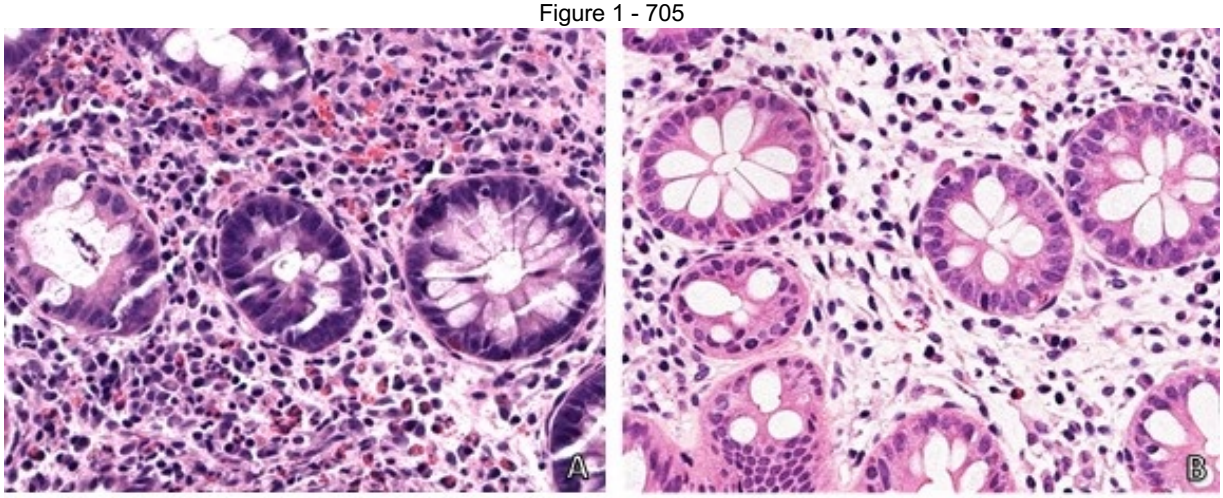

Figure 1. Intestinal eosinophils decrease in UC patients after anti-α4β7 therapy. Pre-treatment transverse colon biopsy (A) demonstrating mildly active colitis with a dense eosinophilic infiltrate in the lamina propria. Post-treatment biopsy in the same patient (B) shows significantly decreased numbers of eosinophils as well as resolution of active inflammation. (Hematoxylin and Eosin stain, x200).

Conclusions: Eosinophil density is decreased following anti-α4β7 integrin (Vedolizumab) therapy in patients with UC and correlates with endoscopic improvement. The post-treatment change of eosinophil density may be attributable to an effect of vedolizumab.

706 The Use of a Novel Histologic Score to Predict Recurrence of Barrett's Esophagus in High-Risk/Uncontrolled Reflux Patients After RFA Eradication

Katrina Krogh[1], Joseph Triggs[2], Sri Komanduri[3], Guang-Yu Yang[4]
[1]McGaw Medical Center of Northwestern University, Chicago, IL, [2]University of Pennsylvania Health System, Philadelphia, PA, [3]Northwestern Memorial Hospital, Chicago, IL, [4]Northwestern University, Chicago, IL

Disclosures: Katrina Krogh: None; Joseph Triggs: None; Guang-Yu Yang: None

Background: Radiofrequency ablation (RFA) of Barrett's esophagus (BE) is an efficient treatment for eradication of this precancerous lesion. However, treated patients with uncontrolled reflux are at higher risk of recurrent BE. Currently, there are no qualitative or quantitative studies examining histologic changes in the neosquamous epithelium available, particularly in conjunction with clinical reflux

testing or outcomes data. In the present study, a unique scoring system was proposed and evaluated based on well-established nonerosive reflux disease (NERD) and gastrointestinal reflux disease (GERD) histologic findings and surveillance biopsies were retrospectively scored to predict BE recurrence.

Design: An initial cohort of BE patients who underwent RFA followed by 24-hour pH-impedance testing to detect occult reflux was identified (n=41). A second cohort (n=64) of patients with known BE recurrence was identified and matched to controls (n=72). Slides from surveillance biopsies were scored blindly using a newly-designed score: "RECUR" (Recurrent Epithelial Changes from Uncontrolled Reflux). The scoring system (Fig. 1) includes four morphologic features of esophageal squamous epithelium, each with subscores of 0–2, with a maximum total RECUR score of 8: dilated intercellular spaces (Fig. 2A), parakeratosis (Fig. 2B), epithelial ballooning degeneration (Fig. 2C), and basal cell hyperplasia (Fig. 2D). Scores were compared in the first cohort for normal vs. abnormal reflux, and in the second cohort for recurrence vs. no recurrence. Univariate and multivariate logistic regression analyses were performed.

Results: In the first cohort, the average RECUR score in patients with normal reflux was 4.0 (±1.6) and with abnormal reflux was 5.9 (±0.9) (*P*=0.015). In the second cohort, univariate analysis showed an average RECUR score of 4.1 (±2.0) in patients without recurrence and 5.2 (±1.7) in patients with recurrence (*P*=0.001). Importantly, when compared with other clinical parameters (age, sex, BE length, hiatal hernia length, anti-reflux surgery, RFA sessions, endoscopic mucosal resection), multivariate regression analysis identified the RECUR score as the only significant predictor of recurrence, even after controlling for highest histologic grade (odds ratio 1.360, 95% confidence interval 1.097–1.686, *P*=0.005).

Figure 1 - 706

Histologic Criteria	Score	Definition
Dilated intercellular spaces	0	none
	0.5	intercellular spaces seen at 40x; focal
	1	intercellular spaces seen at 40x; diffuse
	1.5	intercellular spaces seen at 10x; focal
	2	intercellular spaces seen at 10x; diffuse
Parakeratosis	0	absent
	2	present
Ballooning degeneration	0	none
	1	focal
	2	extensive
Basal cell hyperplasia	0	<15% of total thickness
	1	15%–33% of total thickness
	1.5	33%–66% of total thickness
	2	>66% of total thickness
RECUR Score	_/8	

Figure 2 - 706

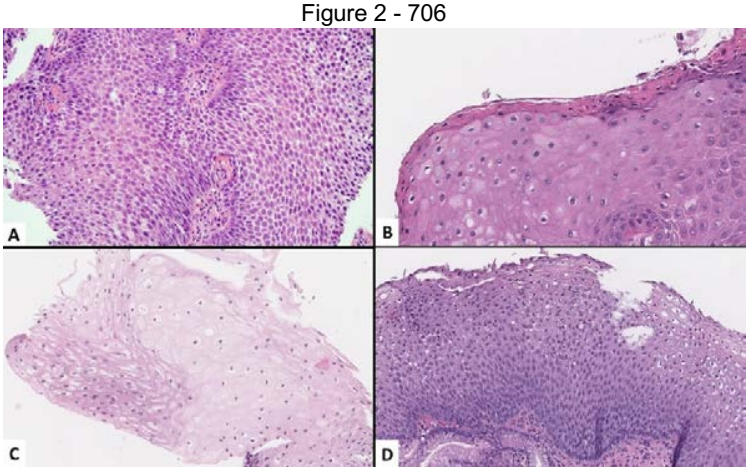

Conclusions: Use of our validated histologic scoring system (RECUR) on routine neosquamous samples obtained after BE treatment can be used to identify uncontrolled reflux and predict BE recurrence.

707 Computationally Derived Morphological Features of Cancer Nuclei from Colon Whole Slide Images Can Distinguish Stage 2 from Stage 4 Colon Cancers

Neeraj Kumar[1], Cheng Lu[1], Kate Butler[2], Hannah Gilmore[3], Joseph Willis[4], Anant Madabhushi[1]
[1]Case Western Reserve University, Cleveland, OH, [2]Case Western Reserve University/University Hospitals Cleveland Medical Center, Cleveland, OH, [3]University Hospitals Case Medical Center, Case Western Reserve University, Cleveland, OH, [4]University Hospitals Cleveland Medical Center, Cleveland, OH

Disclosures: Neeraj Kumar: None; Cheng Lu: None; Kate Butler: None; Hannah Gilmore: None; Joseph Willis: *Consultant*, Lucid Diagnostics; Anant Madabhushi: *Consultant*, Inspirata Inc; *Stock Ownership*, Inspirata Inc

Background: Machine learning analysis of digital whole slide images (WSI) has immense promise to affect how anatomic pathology is practiced. Computerized processing of these gigapixel images has the potential to facilitate a variety of clinical scenarios – including standardization of tumor morphological classifications, identification of unique intra-tumor regions of potential biological significance; and identification of important sub-visual features not currently appreciated by standard light microscopy techniques. In this work we employed computational image analysis to evaluate the role of shape and texture features of nuclei of colon cancer from WSIs to distinguish between Stage 2 from Stage 4 cancers.

Design: One representative H&E stained digital WSI was obtained from 20 Stage 2 and 33 Stage 4 colon cancers. A fully-convolutional deep neural network with VGG-18 architecture was trained to first identify the cancer extent on the WSIs. Another deep learning (DL) model based on Mask-RCNN with Resnet-50 architecture was used to segment out all nuclei from within the identified cancer region.

These two DL models were validated on publically available datasets. Subsequently, a total of 146 shape, size and texture features were extracted from the tumor nuclei and Wilcoxon rank-sum test was used to select the most discriminatory features between Stage 2 and Stage 4 tumors. The selected features were then employed in a Random Forest classifier to distinguish Stage 2 and Stage 4 colon tumors.

Results: Only five out of the 146 nuclear features were found to be useful for discerning between Stage 2 and Stage 4 colon cancers. The classifier trained in a cross-validation setting using these five features yielded an average AUC of 0.78±0.09. The five discriminative features related to first order statistics of nuclear area, perimeter and length are described in Table 1.

Table 1: Top discriminative nuclear features between Stage 2 and Stage 4 colon cancers

Feature	Stage 2 vs. Stage 4 Classification AUC±STD.	p-value
Standard deviation of nuclei area	0.74±0.10	<0.001
Average nuclei area	0.63±0.13	0.015
Average major axis length	0.63±0.11	0.001
Average nuclei perimeter	0.67±0.10	<0.001
Kurtosis of nuclei area	0.60±0.10	0.012
All features combined	**0.78±0.09**	-

Conclusions: The results of our preliminary study suggest that nuclei of Stage 4 colon cancers tend to have a higher area, perimeter and length as well as more variance in nuclear area compared to Stage 2 tumors. These findings will be validated in an independent test set.

708 A SEER Study: Incidence of Localized, Regional, and Distant Cancer in Young-Onset (Aged Under 45 Year) Patients with Rectal Cancer

Jonathan Lai[1], Daryl Ramai[2], Andrew Ofosu[2], Douglas Adler[3]
[1]McGill University Health Centre, Montreal, QC, [2]The Brooklyn Hospital Center, Brooklyn, NY, [3]Huntsman Cancer Center, Salt Lake City, UT

Disclosures: Jonathan Lai: None

Background: According to evidence, the incidence of colorectal cancer (CRC) appears to be increasing among adults younger than 50 years in the United States. The objective of this study was to investigate the incidence, demographics, tumor characteristics, treatment, and survival of rectal cancer in patients under 45 years of age.

Design: Data on young-onset (ages under 45 years) rectal cancer between 2000 and 2016 was extracted from the Surveillance, Epidemiology and End Results Registry.

Results: A total of 10,375 patients with young-onset rectal cancer were identified where 54.7% were male. Median age at diagnosis was 40 ± 5.7 years. The overall age-adjusted incidence of rectal cancer between 2000 and 2016 was 1.24 per 100,000 per year. Incidence increased with age, with the highest incidence occurring in the 40-44 year age group. Over the 16-year study period, the annual incidence of rectal cancer increased by approximately 3.0% in a given year. Most tumors on presentation were moderately differentiated (30.8%) while the most common stage at presentation was Stage 4 (48.3%). One- and 5-year cause-specific survival for rectal cancer was 92.7% and 70.8% respectively. On Cox proportional hazard regression analysis, worse outcomes were noted with males (HR:1.16; CI:1.07-1.25; p= 0.000), increasing cancer stage (regional cancer HR: 2.26; CI:1.95-2.63; p=0.000 and distant cancer HR: 5.57; CI:4.80-6.46; p=0.000), and patients who did not undergo surgery (HR: 2.53; CI:2.12-3.03; p=0.000).

Conclusions: In patients under 45-years of age, our study highlights an increasing incidence of rectal cancer, specifically regional and distant cancer stages. Further research is needed to understand factors leading to this alarming increase and help guide screening in efforts to decrease the incidence and mortality of this potentially curable disease in this young population.

709 Comparative Molecular Subtypes of Initial and Metachronous Gastric Adenocarcinomas

Gregory Lauwers[1], Baek-Hui Kim[2], Hayeon Kim[3]
[1]H. Lee Moffitt Cancer Center & Research Institute, University of South Florida, Tampa, FL, [2]Korea University Guro Hospital, Seoul, Korea, Republic of South Korea, [3]Korea University, Seoul, Korea, Republic of South Korea

Disclosures: Gregory Lauwers: None; Baek-Hui Kim: None; Hayeon Kim: None

Background: The incidence of metachronous gastric cancer (MGC) is reported between 2.8% and 30%. While molecular subtyping of gastric cancer (GC) is available, there is no study comparing the molecular subtypes of initial gastric cancers (IGCs) and MGCs

Design: We evaluated a cohort of 42 patients with 43 IGCs and 45 MGCs. Molecular subtyping was performed by IHC of MMR proteins, E-cadherin, p53 and EBV -ISH. GCs were classified into 5 subtypes: EBV GCs, MMR deficient (MMRD), E-cadherin aberrant, p53 aberrant (p53+), and p53 non-aberrant tumors [p53 (neg)].

Results: All IGCs had been successfully treated by either surgery [19%] or endoscopic resection [81%]. The M:F ratio was 6:1. The mean interval between IGC and MGC was 85 months (48-199 months). H. pylori infection was present in 62% of IGCs and 14% of MGCs. IGCs were located in the upper [7% (n=3)], middle [44% (n=19)], and lower third [49% (n=21)] of stomach. MGCs, were located in the upper [10 (22%)], middle [17 (38%)], and lower third [18 (40%)]. Most cases were well to moderately differentiated. There was only 7 (15%) and 9 (20%) poorly differentiated carcinoma and 2 (4%) and 1(2%) of poorly cohesive carcinomas in IGCs and MGCs, respectively.

Among IGCs, EBV, MMRD, E-cadherin, p53(+) and p53(neg) represented 2 (5%), 4 (9%), 2 (5%), 21 (49%), and 14 (32%) of the cases. Two case had concomitant p53(+) and aberrant E-cadherin. Among MGCs, EBV, MMRD, E-cadherin, p53(+) and p53(neg) represented 3 (7%), 11 (24%), 0 (0%), 22 (49%), and 9 (20%) of the cases. Concomitant p53(+) was observed in 1 EBV, 2 MMRD in MGCs. Molecular subtypes of MGCs may be affected by IGC subtypes with 50% of later presenting a similar subtype. All 4 MMRD IGC patients developed MMRD MGCs. The interval between the development of IGC and MGC was significantly longer when the molecular subtypes were different (p=0.013).

Figure 1 - 709

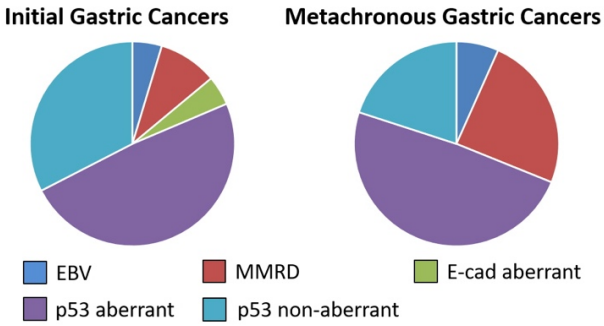

Molecular subtype	Initial GC	Metachronous GC
EBV	2 (5%)	3 (7%)
MMRD	4 (9%)	11 (24%)
E-cad aberrant	2 (5%)	0 (0%)
p53 aberrant	21 (49%)	22 (49%)
p53 non-aberrant	14 (32%)	9 (20%)

Figure 1. Molecular subtypes of initial and metachronous gastric cancers.

Figure 2 - 709

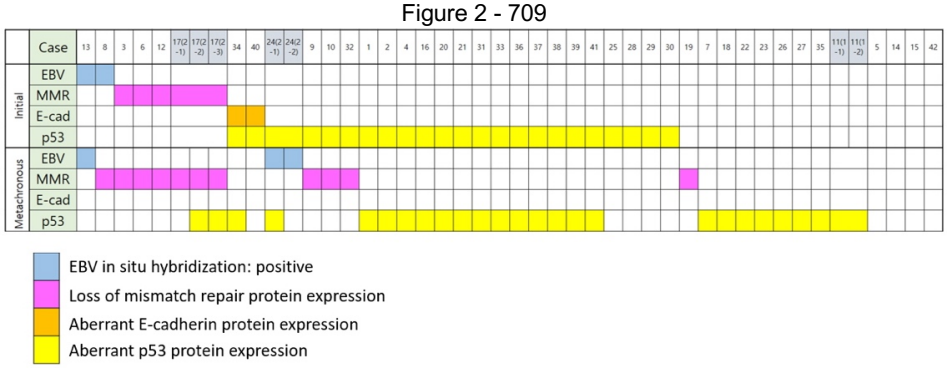

Figure 2. Protein expression pattern of initial and metachronous gastric cancers.

Conclusions: The frequency of each molecular subtypes was similar in IGCs and MGCs, but for MMRD which showed an increased trend in frequency in MGCs (*p*=0.134). E-cadherin aberrant subtype was rare [because of selection bias (81% of IGCs treated by ESD/EMR)]. 50% of MGCs showed different molecular subtypes than IGCs, but patients with MMRD IGCs showed the same subtype in MGCs. Concurrent molecular subtypes in IGCs & early developing MGCs appear to confirm the concept of mucosal field cancerization. Divergent subtypes in late occurring MGCs suggest a *de novo* carcinogenic mechanism affecting the residual mucosa possibly related to *H.pylori* eradication.

710 DNA Flow Cytometric and Clinicopathologic Analysis of Non-Conventional Dysplasia and Serrated Lesions in Inflammatory Bowel Disease

Hannah Lee[1], Peter Rabinovitch[2], Aras Mattis[1], Gregory Lauwers[3], Won-Tak Choi[1]
[1]University of California San Francisco, San Francisco, CA, [2]University of Washington, Seattle, WA, [3]H. Lee Moffitt Cancer Center & Research Institute, University of South Florida, Tampa, FL

Disclosures: Hannah Lee: None; Peter Rabinovitch: None; Aras Mattis: None; Gregory Lauwers: None; Won-Tak Choi: None

Background: There is limited information regarding the molecular and clinicopathologic features of non-conventional dysplasia and serrated lesions in inflammatory bowel disease (IBD).

Design: A total of 565 dysplastic and serrated lesions from 264 IBD patients were analyzed and subtyped as: conventional dysplasia (including tubular adenoma-like [n = 282] and tubulovillous/villous adenoma-like [n = 62]), non-conventional dysplasia (including hypermucinous [n = 7], goblet cell deficient [GCD, n = 10], and dysplasia with increased Paneth cell differentiation [DPD, n = 56]), and serrated lesions (including sessile serrated adenoma-like [n = 44], traditional serrated adenoma-like [n = 3], and serrated lesion, not otherwise specified [n = 101]). Since the presence of aneuploidy is known to be a significant predictor of high-grade dysplasia (HGD) or colorectal cancer (CRC), DNA flow cytometry was performed on 65 low-grade conventional (n = 36) and non-conventional (n = 29) dysplastic samples as well as 26 serrated lesions to determine their malignant potential.

Results: 73 (13%) non-conventional dysplastic lesions were identified in 57 (22%) of the 264 patients, whereas 344 (61%) conventional dysplastic and 148 (26%) serrated lesions were identified in 212 (80%) and 100 (38%) patients, respectively. Non-conventional dysplastic lesions occurred more frequently in men (72%), with a mean age of 53 years and a long history of IBD (mean: 19 years). They usually appeared as a polypoid lesion (77%) in the right colon. Among non-conventional dysplasia, DPD was the most common (77%), followed by GCD (14%) and hypermucinous dysplasia (10%). HGD was more frequently associated with hypermucinous (n = 3; 43%) and GCD dysplasia (n = 4; 40%) than DPD (n = 6; 11%) ($p = 0.016$). The rate of aneuploidy was also significantly higher in hypermucinous (80%) and GCD (25%) dysplasia than DPD (10%) ($p < 0.005$). Overall, 24% of non-conventional dysplasia showed aneuploidy, while only 8% of conventional dysplasia and none of the serrated lesions demonstrated aneuploidy ($p = 0.043$).

Conclusions: Non-conventional dysplasia is not uncommon in IBD patients. The higher frequency of aneuploidy in low-grade non-conventional dysplasia suggests that they may have a higher malignant potential than conventional dysplasia. While conventional and non-conventional dysplastic lesions develop dysplasia or CRC via the chromosomal instability pathway, an alternative serrated pathway is responsible for the development of dysplasia or CRC in serrated lesions.

711 Low Grade Appendiceal Mucinous Neoplasm: Correlation of AJCC Stage with Long Term Clinical Outcomes

Hee Eun Lee[1], Thomas Smyrk[1]
[1]Mayo Clinic, Rochester, MN

Disclosures: Hee Eun Lee: None; Thomas Smyrk: None

Background: A TNM classification system for low grade appendiceal mucinous neoplasm (LAMN) was recently revised. Its relevance to prognosis is not yet clear, particularly for patients with subserosal or mesoappendiceal involvement (T3). We assessed outcomes for patients with LAMN classified according to the updated AJCC TNM staging system.

Design: The institutional pathology file at Mayo Clinic was searched for mucocele, mucinous cystadenoma, LAMN, and adenoma between 2000 and 2015. All available H&E slides were reviewed and cases with diagnostic features of LAMN, based on a recent consensus statement published in 2016 by PSOGI, were selected. Medical record and pathology reports were reviewed. Kaplan-Meyer survival analyses for overall survival (OS) and recurrence-free survival (RFS) were performed.

Results: 75 LAMNs were identified, including 33 men and 42 women with median age of 54 (range 18-88) years. 48 patients (64%) had LAMN confined to the appendix (Tis). 9 (12%) had acellular mucin in the subserosa or mesoappendix (T3) and 18 (24%) had involvement of the visceral peritoneum but not adjacent organs (T4a). 20 (27%) patients had pseudomyxoma peritonei (PMP); 10 had acellular mucin only (M1a) and the remaining 10 had involvement by dysplastic epithelium (M1b). M stage was significantly associated with T stage ($p<0.001$); 3 (6%) cases with Tis, 5 (56%) with pT3, and 12 (67%) with T4b showed M1a or M1b. 3 patients (1 with Tis M1b and 2 with T3 M1b) had disease recurrence or progression at 6, 8, and 15 months of follow-up per each. Cases with T3 had a significantly shorter DFS time than the rest (median 30 vs 73 mo; $p=0.012$). Only patients with M1b suffered disease recurrence; they had significantly shorter DFS than the rest of the study group (median 8 vs 73 mo; $p<0.001$). 16 (21%) patients died during the follow-up period, 2 of disease and the rest of other disease or unknown causes. T4a conferred a shorter OS than other T stages, with marginal significance (median 140 vs 112 mo; $p=0.089$). Patients with M1 tended to have a shorter OS than those without PMP (median 111 vs 115 mo; $p=0.081$).

Conclusions: Tis LAMN may not exclude the possibility of developing PMP and even recurrence. A significant number of T3 LAMNs were associated with PMP. Disease recurrence was seen only in patients with peritoneal involvement by dysplastic epithelium, regardless of T stage, indicating M stage is a significant predictive factor of disease recurrence. Cases with advanced T or M stage tended to have worse OS.

712 The Proliferative Indices of the Primary Ileal Well Differentiated Neuroendocrine Tumors, Corresponding Lymph Nodes/Mesenteric Deposits, and Distant Metastatic Sites Show Poor Correlation

Jane Lee[1], Deyali Chatterjee[2]
[1]Washington University, St. Louis, MO, [2]Washington University in St. Louis, St. Louis, MO

Disclosures: Jane Lee: None; Deyali Chatterjee: None

Background: Gastrointestinal well differentiated neuroendocrine tumors (NETs) have an unpredictable biologic behavior. WHO-recommended grading using Ki-67 proliferative index (PI) is considered as one of the most important prognostic parameters. There is a common notion that metastatic sites often show a higher PI as compared to the primary tumor. We wanted to see if there is a true difference in the PI of the primary tumors versus metastases. If identified, since tumors usually metastasize via regional lymph nodes, we then looked to see if this lack of correlation occurs at the mesenteric lymph node/ tumor deposit (LN/TD) stage.

Design: 23 patients were identified who underwent resection for a primary NET of the ileum at our institution, with concurrently identified positive LN/TD, who also had at least one tissue diagnosis in-house for distant metastasis. PI of the primary tumor, LN/TD, and metastatic tumor, were systematically determined using the CAP recommended method of assessment. PI which were less than 1% were rounded up to 1% in order to be able to perform statistical correlation. A linear regression model followed by a Pearson correlation coefficient was calculated using standard statistical software.

Results: First, we tested to see if the PI of the primary NETs correlated with those seen in the corresponding metastases. Using the linear regression model, the coefficient of determination or R^2 value was only 0.22 (Fig 1). The Pearson correlation coefficient, an index of the strength and direction of a linear relationship between two interval level variables, was 0.47, indicating a weak positive correlation between the data sets. Similar statistical correlation methods for the primary NET and LN/TD showed R^2 of 0.3 (Fig.2) and a Pearson coefficient of 0.55. The Pearson coefficient between nodes and metastasis was 0.58. In terms of WHO grading, 17 of 23 cases had concordant grades between primary and metastasis, but of the discordant cases, 3 of them had a lower PI at the metastatic site, and 3 had a higher PI at the metastatic site, compared to the primary. The PI of the LN/TD did not correlate well either with the primary or with the metastasis.

Figure 1 - 712

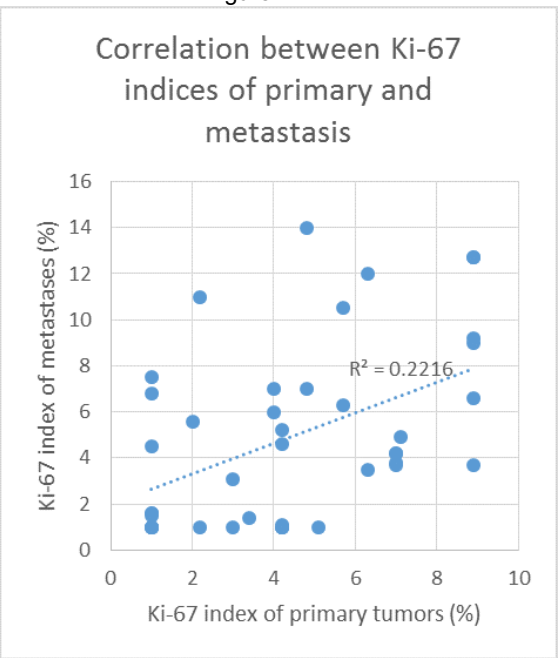

Figure 2 - 712

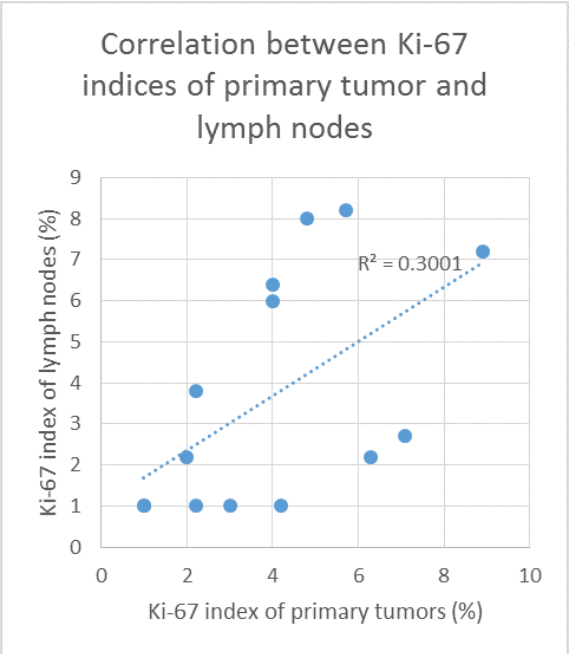

Conclusions: The unpredictable biologic behavior of ileal NETs reflect in the variability of PI at the primary, LN/TD, and metastatic sites. For predictive purposes, PI should ideally be assessed from every metastatic site, as assumption of the primary tumor grade is often not reflective of the biologic behavior.

713 Implications of FOXP3+ T Cells in the Immune Microenvironmental Context of Colorectal Carcinomas with Microsatellite Instability

Ji Ae Lee[1], Seung-Yeon Yoo[1], Nam-Yun Cho[2], Gyeong Hoon Kang[1], Jung Ho Kim[1]
[1]Seoul National University Hospital, Seoul, Korea, Republic of South Korea, [2]Cancer Research Institute, Seoul National University College of Medicine, Seoul, Korea, Republic of South Korea

Disclosures: Ji Ae Lee: None; Seung-Yeon Yoo: None; Gyeong Hoon Kang: None; Jung Ho Kim: None

Background: In contrast to other malignancies, in colorectal carcinomas (CRCs), FOXP3+ T cells have frequently been reported to be associated with a favorable prognosis. Moreover, a previous study revealed two distinct subpopulations of FOXP3+ T cells, immunosuppressive Fr-II regulatory T (T_{reg}) cells and pro-inflammatory Fr-III non-T_{reg} cells, in CRCs. Based on the controversial role of FOXP3+ T cells in tumors, we aimed to investigate the detailed clinicopathologic and immunologic implications of FOXP3+ T cells in CRCs with microsatellite instability-high (MSI-high).

Design: A total of 128 MSI-high CRCs were retrospectively collected. Whole-slide-based quantitative analysis of tumor-infiltrating lymphocytes, including CD3+ T cells, CD8+ T cells, and FOXP3+ T cells, was conducted using immunohistochemistry and computer-assisted image analysis. Activity of Crohn-like lymphoid reaction was assessed by measuring the size of the largest peritumoral lymphoid aggregate (Ueno's criteria).

Results: In contrast to MSI-high CRCs with a low density of FOXP3+ T cells (FOXP3-low), MSI-high CRCs with a high density of FOXP3+ T cells (FOXP3-high) were significantly associated with high densities of both CD3+ T cells and CD8+ T cells ($P < 0.001$ and $P = 0.003$, respectively) and active Crohn-like lymphoid reaction ($P = 0.001$). In addition, FOXP3-high status was inversely correlated with mucinous histology ($P = 0.017$), signet ring cell histology ($P = 0.049$), depth of tumor invasion (pT3 or pT4; $P = 0.001$), nodal metastasis (pN1 or pN2; $P = 0.025$), and distant metastasis (pM1 or cM1; $P = 0.013$) in MSI-high CRCs. There was no significant association between FOXP3+ T cells and major molecular factors, including CpG island methylator phenotype, *KRAS*/*BRAF* mutations, and MLH1/MSH2/MSH6/PMS2 expression status, in MSI-high CRCs.

Conclusions: The high density of FOXP3+ T cells correlates with increased anti-tumor lymphocytic responses and decreased tumor aggressiveness in MSI-high CRCs. Our findings suggest that the majority of tumor-infiltrating FOXP3+ T cells in MSI-high CRCs may represent pro-inflammatory non-T_{reg} cells.

714 Pseudoinvasion or Invasive Adenocarcinoma? Interobserver Variability in the Assessment of Left Sided Colon Polyps

Michael Lee[1], Satoru Kudose[2], Armando Del Portillo[2], Huaibin Mabel Ko[3], HwaJeong Lee[4], Meredith Pittman[5], Marcela Salomao[6], Antonia Sepulveda[7], Stephen Lagana[8]
[1]Columbia University, Long Island City, NY, [2]New York, NY, [3]Icahn School of Medicine at Mount Sinai, New York, NY, [4]Albany Medical Center, Guilderland, NY, [5]New York-Presbyterian/Weill Cornell Medical Center, New York, NY, [6]Mayo Clinic, Scottsdale, AZ, [7]George Washington University, New York, NY, [8]New York-Presbyterian/Columbia University Medical Center, New York, NY

Disclosures: Michael Lee: None; Satoru Kudose: None; Armando Del Portillo: None; Huaibin Mabel Ko: None; HwaJeong Lee: None; Meredith Pittman: None; Marcela Salomao: None; Antonia Sepulveda: None; Stephen Lagana: None

Background: Misplaced epithelium in tubular adenomas can be misdiagnosed as invasive adenocarcinoma. Histologic features that help in distinguishing pseudoinvasion from invasive adenocarcinoma include hemosiderin, lamina propria surrounding the crypts, desmoplasia and degree of dysplasia. However, this is a challenging differential and microscopic assessment varies between pathologists. This study evaluated the interobserver variability in the assessment of left sided colon polypectomies for pseudoinvasion versus invasive adenocarcinoma.

Design: 28 patients with left sided colon polyps were diagnosed as either tubular adenomas with pseudoinvasion or invasive adenocarcinoma. These slides were retrospectively reviewed by 8 experienced gastrointestinal pathologists across multiple medical institutions. We examined the presence or absence of hemosiderin in the stroma, lamina propria/eosinophils surrounding the glands, desmoplasia, high grade dysplasia/intramucosal adenocarcinoma, and whether this represented pseudoinvasion or invasive adenocarcinoma. All statistical analysis was performed using R (version 3.6.1). Fleiss' Kappa statistics were computed to evaluate interobserver reliability among the eight pathologists.

Results: Agreement among pathologists was substantial for desmoplasia (κ = 0.701), there was moderate agreement for high grade dysplasia/intramucosal adenocarcinoma (κ = 0.67) and invasive adenocarcinoma (κ = 0.631), fair agreement for hemosiderin in stroma (κ = 0.528) and prolapse/pseudoinvasion (κ = 0.502). Agreement was low for lamina propria/eosinophils around glands with slight agreement (κ = 0.116). In 25 of 28 cases (89%), 6 or more pathologists agreed as to whether invasive adenocarcinoma was present. In 24 of 28 cases (86%), 6 or more pathologists agreed as to whether pseudoinvasion was present.

Kappa statistics were interpreted with the Landis and Koch scale (κ values: <0: poor agreement, 0.01-0.20: slight agreement, 0.21-0.40: fair agreement, 0.41-0.60: moderate agreement, 0.61-0.80: substantial agreement, >0.80: nearly perfect agreement).

Conclusions: Pathological assessment of left sided colon polyps for pseudoinvasion versus invasive adenocarcinoma is a challenging differential with fair to moderate agreement among experienced gastrointestinal pathologists. This stems from interobserver variability seen in the interpretation of histologic features (desmoplasia, lamina propria surrounding glands, hemosiderin in stroma, etc.) that distinguish these diagnostic considerations.

715 Clinicopathologic Characteristics of de novo Crohn's Disease (CD) Following Ileo Pouch-Anal Anastomosis (IPAA) for Ulcerative Colitis (UC) and Indeterminate Colitis (IC): A Single Center Study

Hua Li[1], Mustafa E Arslan[1], Michael Mikula[1], Zhiyan Fu[1], Edward Lee[2], Cary Qualia[1], HwaJeong Lee[3]
[1]Albany Medical Center, Albany, NY, [2]AMC, Albany, NY, [3]Albany Medical Center, Guilderland, NY

Disclosures: Hua Li: None; Mustafa E Arslan: None; Michael Mikula: None; Zhiyan Fu: None; Edward Lee: None; Cary Qualia: None; HwaJeong Lee: None

Background: Diagnostic criteria for de novo CD following IPAA are not well defined. We studied clinicopathologic characteristics of UC/IC patients who developed CD following IPAA.

Design: Patients with an original diagnosis of UC/IC that underwent IPAA (1996 to 2018) with at least 12 months of follow-up after the proctocolectomy were identified. Electronic medical records were reviewed and patients with a new diagnosis of CD during the follow-up period were further identified. Archived total proctocolectomy slides from this group were reviewed, when available. Cases with deep ulceration associated with transmural inflammation/lymphoid aggregates were considered fulminant colitis.

Results: Out of 163 (original diagnosis UC-160, IC-3), new CD diagnosis was made in 32 patients (19.6%; male-16, female-16; original diagnosis UC-30, IC-2) during the mean follow-up of 118 (range 40 to 240) months. In these, the mean age at the proctocolectomy was 28 (range 10 to 58) years. The mean duration of UC/IC prior to proctocolectomy was 53 (range 1 to 132) months. Indications for proctocolectomy were refractoriness to medical therapy (n=14), UC flare (n=4), and UC, NOS (n=14). The signs and symptoms that initially raised concern for the patients having CD at a mean follow-up of 56 (range 0 to 192) months following IPAA were: perianal fistula/fissure (12), severe/segmental pouchitis (11), ileal inflammation (6), pouch/ileal stricture (5), pathologic finding (ileal granuloma, features of IC on proctocolectomy, and duodenal inflammation) (3), small bowel obstruction (3), duodenal inflammation (3), chronic watery diarrhea (1) and extraintestinal manifestations (1). The diagnosis of CD was made 15 (range 0 to 84) months after the initial signs and symptoms. Of the 22 proctocolectomy specimens retrieved, 14 (64%) showed fulminant colitis. No granulomas were found. The ileoanal J-pouch was excised in 7 (21.9%) of the 32 patients diagnosed with CD following IPAA and in 3 (2.3%) of 131 (130-UC, 1-IC) patients without CD, for pouch dysfunction.

Conclusions: The diagnosis of de novo CD following IPAA is made for a variety of reasons. The diagnosis may be delayed due to nonspecific clinical pictures and lack of standardized diagnostic criteria. In a subset, pathologic findings may lead to the diagnosis of de novo CD. A significant portion of patients who have de novo CD will have fulminant colitis at the time of proctocolectomy.

716 Prevalence of Pyloric Gland Metaplasia (PGM) in De Novo Crohn's Disease (CD) Following Ileal Pouch-Anal Anastomosis (IPAA) for Ulcerative Colitis (UC)

Hua Li[1], Mustafa E Arslan[1], Michael Mikula[1], Zhiyan Fu[1], Edward Lee[2], Cary Qualia[1], Ann Boguniewicz[3], HwaJeong Lee[4]
[1]Albany Medical Center, Albany, NY, [2]AMC, Albany, NY, [3]Loudonville, NY, [4]Albany Medical Center, Guilderland, NY

Disclosures: Hua Li: None; Mustafa E Arslan: None; Michael Mikula: None; Zhiyan Fu: None; Edward Lee: None; Cary Qualia: None; Ann Boguniewicz: None; HwaJeong Lee: None

Background: PGM is commonly found in CD. It is less common in UC. A subset of patients thought to have UC develops signs of CD following IPAA (de novo CD). PGM may be more common in de novo CD compared to UC, and may be useful in identifying patients suspected of having UC who require close follow-up for the potential development of de novo CD following IPAA.

Design: Patients who underwent IPAA for UC and had at least 1 year of post-surgery follow-up (1996 to 2018) were identified (n=160). In this cohort, patients diagnosed with de novo CD, and those without signs of CD (remained as UC) were further identified by reviewing the medical records. Ileocolonic resection cases for CD were used as a control. Archived pathology specimens including ileocolonic resection, colectomy, ileostomy, and follow-up ileal, pouch, and rectal cuff biopsies were reviewed. The presence of PGM and granulomas in the specimens was assessed. In paired ileal and pouch biopsies, the degrees of activity in two biopsies were compared. Chi square test was performed to compare the frequencies of the above findings between groups. $P<0.05$ was considered statistically significant.

Results: 30 de novo CD, 33 UC, and 22 CD patients were identified. In de novo CD, PGM was more common compared to UC [15/30 (50%) vs. 5/33 (15.2%); p=0.003] and less common than CD [15/30 (50%) vs. 17/22 (77.3%); p=0.046]. In the de novo CD group, PGM was found in the resected colon (n=3), neo-terminal ileum (n=16), pouch (n=20), ileoanal anastomosis (n=1), ileostomy (n=1), and rectum (n=1). PGM was found prior to (n=6, up to 56.4 months prior), simultaneously (n=2), and following (n=7, up to 14 years later) the first signs of CD. In the UC group, PGM was found in the resected colon (n=1), neo-terminal ileum (n=1), pouch (n=3), and rectum (n=1). No statistically significant difference was found in presence of granulomas between the 3 groups [de novo CD 7/30 (23.3%), UC 3/33 (9.1%), CD 6/22 (27.3%); p>0.05]. There was no consistent pattern in the degree of activity in the paired ileal/pouch biopsies in both de novo CD and UC groups.

Conclusions: PGM is a more common finding in de novo CD than it is in UC. Finding PGM in biopsy specimens of patients suspected of having UC may warrant close follow up for the potential development of de novo CD. PGM may be found in a minor subset of UC patients, despite signs of CD not being seen in either their colectomy or follow-up biopsy specimens.

717 Integrin β4 is an Effective and Efficient Marker in Synchronously Highlighting Lymphatic and Blood Vascular Invasion, as well as Perineural Aggression in Malignancy

Jian Li[1], Weihua Yin[2]
[1]Peking University Shenzhen Hospital, Shenzhen, Guangdong Province, China, [2]Peking University Shenzhen Hospital, Shenzhen, Guangdong, China

Disclosures: Jian Li: None; Weihua Yin: None

Background: Lymphovascular invasion (LVI) and perineural invasion (PNI) are two important pathological parameters for their well-established correlations with unfavorable prognosis in various malignancies. Searching for LVI and PNI on hematoxylin and eosin stained sections is a time-consuming work for pathologists. Immunohistochemical stains are commonly used to highlight the lymphatic, vascular, and perineural aggression. Integrin β4 has been reported to be positively expressed in vascular endothelia, peripheral nerves, and a collection of epithelia. However, little is known about the effectiveness of β4 in highlighting LVI and PNI.

Design: We first explored the immunoreactive features of β4 in lymphatic and vascular endothelia, and peripheral nerves in normal stomach, thyroid, and breast. Second, the immunohistological features of LVI and PNI labeled by β4 were evaluated in gastric adenocarcinoma (GA), papillary thyroid carcinoma (PTC) and invasive breast carcinoma of no special type (IBC). Third, a diagnostic test was performed to explore the detective efficiency of β4 on LVI and PNI. Fourth, the detective application of β4 on LVI and PNI was further assessed on extended nine types of malignancies, including cancers of the colon, prostate, bladder, tongue, esophagus, liver, lung, kidney, and uterus. The labeling of D2-40, CD34, and S-100 was used as controls for lymphatic and vascular endothelia, and neural fibers, respectively.

Results: The results demonstrated that β4 could concurrently stain with lymphatic and vascular endothelia, as well as peripheral nerves in normal stomach, thyroid, and breast. LVI and PNI were clearly and synchronously outlined by the staining of β4 in GA (Figure 1), PTC, and IBC . Specifically, β4 was also expressed in majority of tumor cells, and, thus, greatly favored the detection of LVI and PNI invaded by small tumor clusters. In addition, in contrast to that of D2-40 and CD34, β4 stains were not observed in stromal cells and, therefore, facilitated the differentiation between shrinkage cleft and LVI (Figure 2). Diagnostic tests revealed that β4 labeling overtly increased the diagnostic accuracy and interobserver concordance on LVI and PNI in comparison with H&E staining alone (Table). Finally, the usefulness of β4 was further confirmed on 9 other types of malignancies as listed above.

TABLE. The Efficiency of β4 Staining on the Detection of LVI and PNI in Malignancies of Stomach, Thyroid, and Breast

Tumor type	n	Category	Diagnostic accuracy (mean [range]) (%)				Kappa value (95% CI)	
			H&E slides	H&E and β4-stained slides	*P* value		H&E slides	H&E and β4-stained slides
GA	15	LVI	78.67±5.59	89.33±3.65	**0.04**		0.44 (0.26-0.63)	0.65 (0.35-0.95)
		PNI	82.68±3.67	92.00±5.58	**0.03**		0.54 (0.17-0.92)	0.73 (0.40-1.00)
PTC	15	LVI	76.00±7.60	96.00±3.65	**0.01**		0.28 (0.07-0.65)	0.86 (0.65-1.00)
		PNI	96.00±5.95	98.67±2.98	0.43		0.78 (0.38-1.00)	0.87 (0.32-1.00)
IBC	16	LVI	72.50±7.13	87.50±4.45	**0.01**		0.26 (0.09-0.43)	0.59 (0.42-0.76)
		PNI	93.75±4.42	97.50±3.42	0.70		0.65 (0.25-1.00)	0.86 (0.43-1.00)

LVI, lymphovascular invasion; PNI, perineural invasion; GA, gastric adenocarcinoma; PTC, papillary thyroid carcinoma; IBC, invasive breast carcinoma of no special type.

Figure 1 - 717

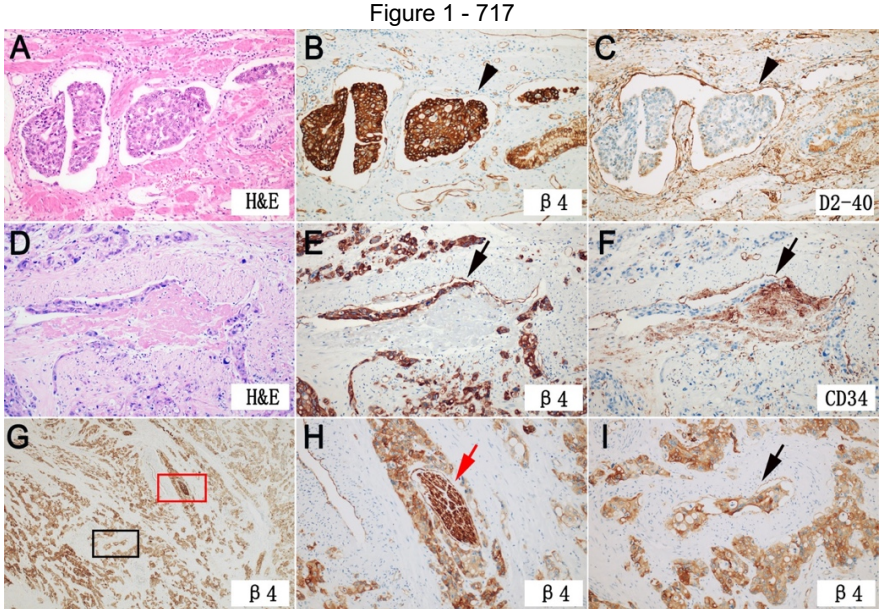

Figure 2 - 717

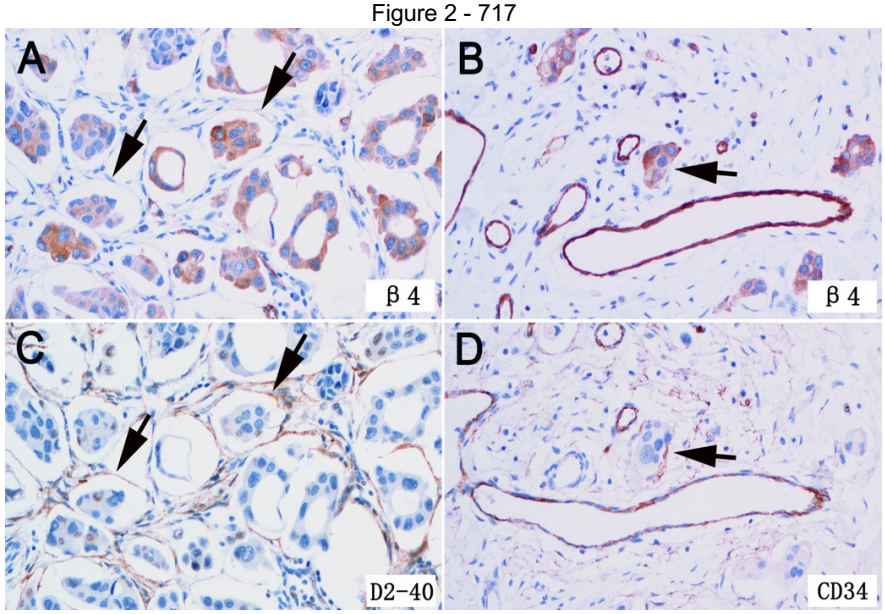

Conclusions: Based on its satisfactory immunostaining performance, integrin β4 is a reliable marker for convenient and accurate detection of LVI and PNI in diagnostic practice.

718 Comparative Studies of Pyloric Gland Adenomas in Gallbladder vs. Stomach and Duodenum Reveal Distinct Clinicopathologic Features

Xiaoyan Liao[1], Qi Yang[2], Dongwei Zhang[1]
[1]University of Rochester Medical Center, Rochester, NY, [2]Pittsford, NY

Disclosures: Xiaoyan Liao: None; Qi Yang: None; Dongwei Zhang: None

Background: Pyloric gland adenomas (PGA) are rare non-invasive polypoid neoplasms of the gallbladder and gastrointestinal tract. Recent studies demonstrated high frequency of β-catenin mutation in gallbladder PGAs (GB-PGA) which is different than gastric or duodenum PGAs (G/D-PGA). The aim of this study is to compare the clinicopathologic features of GB-PGAs and G/D-PGAs that are small in size and low-grade in cytology.

Design: GB-PGAs and G/D-PGAs diagnosed between 2000 and 2019 were identified retrospectively from our institution. Available slides were reviewed by two gastrointestinal pathologists. Relevant clinical information was collected and immunohistochemical studies were performed.

Results: Eight GB-PGAs were identified from 6 cholecystectomy specimens in 1 male and 5 female patients, with a median age of 80 years (range 46-85). Eleven G/D-PGAs, each biopsied at different times, were retrieved from 5 patients (2 males and 3 females), with a median age of 70 years (range 59-85). The average size of GB-PGAs was 0.5 cm (range 0.1-1.5 cm), while the average size of G/D-PGAs was 0.8 cm (range 0.2-2.5 cm, $P>0.05$). Histologically, all polyps demonstrated uniform back-to-back mucinous glands arranged in a tubular configuration with minimal cytologic atypia and no invasive growth. Immunostains showed strong and diffuse expression of MUC6 in all polyps. MUC5AC was co-expressed in the mucinous glands in most G/D-PGAs, while in GB-PGAs, MUC5AC was only seen in superficial epithelial cells. CDX2 was negative or only focally expressed in all polyps. P53 overexpression was focally detected in one large G/D-PGA (2.5 cm), where Ki67 labeling index was focally increased to >70%. The rest of polyps, both GB-PGA and G/D-PGAs, showed normal wild-type expression of p53 and low Ki67 labeling index. Interestingly, nuclear β-catenin was detected in 7 of 8 (87.5%) GB-PGAs, even when sub centimeter in size. In contrast, none of the G/D-PGAs demonstrated nuclear β-catenin expression (0/11, $P<0.0001$).

Conclusions: This study cohort, composed of PGAs that were mostly small in size and low-grade in cytology, demonstrated different expression profiles of MUC6, MUC5AC, and β-catenin in GB-PGAs compared to G/D-PGAs, suggesting different pathogenesis. While a size cut off of 0.2 cm was suggested by new WHO classification to distinguish PGAs from pyloric gland metaplasia in gallbladder, our results showed aberrant nuclear β-catenin expression in GB-PGAs, regardless of size.

719 Increased T Regulatory Cells can Help Differentiate Active Ulcerative Colitis from Other Acute Colitis in Colon Biopsies

Bo Lin[1], Constantine Axiotis[2]
[1]SUNY Downstate Medical Center, Brooklyn, NY, [2]SUNY/KCHC, Fairfield, CT

Disclosures: Bo Lin: None

Background: Ulcerative colitis (UC) is characterized by a chronic relapsing and remitting inflammatory condition of the gastrointestinal tract. Accumulating evidences indicate that the pathogenesis of UC is caused by the imbalance of immunity, which includes an excess of inflammatory stimuli and the downregulation of self-tolerance. The regulatory T (Treg) cell is a lymphocyte subset that is involved in immunosuppression and immunological tolerance. Functional Treg cells are characterized by the expression of the transcription factor FOXP3 and are effective in the prevention and downregulation of UC in animal models. The aim of this study was to determine whether the frequency of Treg cells and their distribution in the intestinal mucosa can differentiate UC from other acute colitis.

Design: Three cohorts of colon biopsies were reviewed: normal colonic mucosa (n=10), non-UC acute colitis (including ischemic colitis, infectious colitis) excluding ulcerative colitis (n=10), and active ulcerative colitis (n=40). Foxp3 immunohistochemistry stain was used to identify Treg cells in the biopsies, and Foxp3+ Treg cells in the lamina propria excluding areas of lymphoid follicles were counted in each biopsy as maximum Treg cells per high power field.

Results: In normal colon biopsies, there were only rare Treg cells in the lamina propria excluding areas of lymphoid follicles. Median max Treg cells was 1.5/HPF. In acute colitis including ischemic colitis and infectious colitis, median max Treg cells was increased compared to normal colon (16.5/HPF vs 1.5/HPF, $p<0.05$). However, in active ulcerative colitis, there was a marked increase in Treg cells compared to other acute colitis or normal colon (both $p<0.05$). The median max Treg cells was 42.5/HPF, and the Treg cells were diffusely distributed in the lamina propria.

Figure 1 - 719

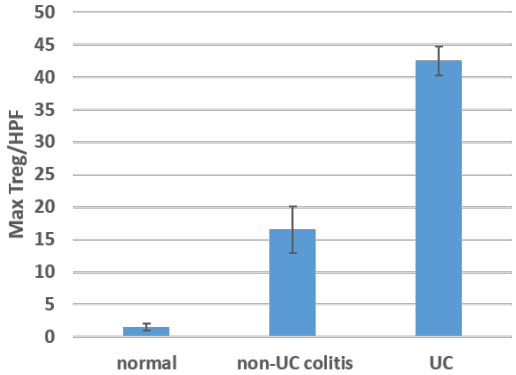

Conclusions: In active ulcerative colitis, there is a marked increase in Treg cells in lamina propria compared to other acute colitis and normal colonic mucosa. The max Treg cell count/HPF can help differentiate active ulcerative colitis from other acute colitis in colon biopsies, and it is especially useful in first time diagnosis with limited clinical information.

720 DSPP/αvβ3 Axis Induce Colorectal Cancer Metastasis and Chemoresistant by Suppression of Tumor Vessel Normalization

Chaoqun Liu[1], Liang Zhao[1], Hui Wang[2], Rui Zhou[3], Wanqi Zhan[1]
[1]Department of Pathology, School of Basic Medical Sciences, Southern Medical University, Guangzhou, Guangdong, China, [2]Department of Medical Oncology, Affiliated Tumor Hospital of Guangzhou Medical University, Guangzhou, Guangdong, China, [3]School of Basic Medical Sciences, Southern Medical University, Guangzhou, Guangdong, China

Disclosures: Chaoqun Liu: None; Liang Zhao: None; Hui Wang: None; Rui Zhou: None; Wanqi Zhan: None

Background: Pathological angiogenesis is one of the hallmarks of cancer. Compared with normal vessels, tumor vessels are structurally and functionally abnormal, which have been demonstrated contributing to tumor metastasis and chemotherapy resistance. Abnormal blood vessels have also been detected in primary colorectal cancer (CRC), especially in those undergone lymph node metastasis,by analyzing paraffin specimens from 152 CRC patients. Secreted protein Dentin Sialophsphp- protein (DSPP), was identified as a prometastatic protein in CRC. DSPP is highly expressed in metastatic CRC patients, and it specifically binds to the endothelial alphavbeta3 (αvβ3) integrin at RGD sequence to increase the formation of tumor vessels and stimulate colorectal cancer metastasis and chemoresistant.

Design: Immunofluorescence (IF) assays were carried out to detect the interaction between DSPP and αvβ3 in cancer cells and Endothelial cells. The expression of proteins CRC tissues was detected by immunohistochemistry (IHC) staining. Immunohistochmical labeling of Pimonidazole was used to test hypoxia level in the tumor tissue. Chicken chorioallantoic membrane (CAM) assay was used for in vivo angiogenesis study. A nude mice model of subcutaneous transplantation was adopted to study the effects of DSPP on oxaliplatin sensitivity in CRC.

Results: IHC results characterized the metastatic CRC (mCRC) patients with DSPP overexpression. Microvessels in mCRC tissues are cystic, pedantic, and branched. The vessel walls become thinner and cracked, with endothelial cells overlapped and protruded into the lumen. IF indicated a co-localization of DSPP and αvβ3 in SW620 cells and HUVECs. The tumor cell-derived DSPP might contributes mostly to the vascular changes. DSPP dramatically promoted tumor angiogenesis. PIMO staining of subcutaneous tumors indicated that silencing DSPP significantly alleviated the hypoxia in tumor tissues, whereas increased the coverage of pericytes in tumor tissues. This was consistent in the *in vitro* and *in vivo* experiments using Cyclo, the αvβ3 specific inhibitor. The tumor-bearing nude mice model indicates that DSPP antibody combined with Oxaliplatin could enhance the sensitivity to chemotherapy in colorectal cancer.

Figure 1 - 720

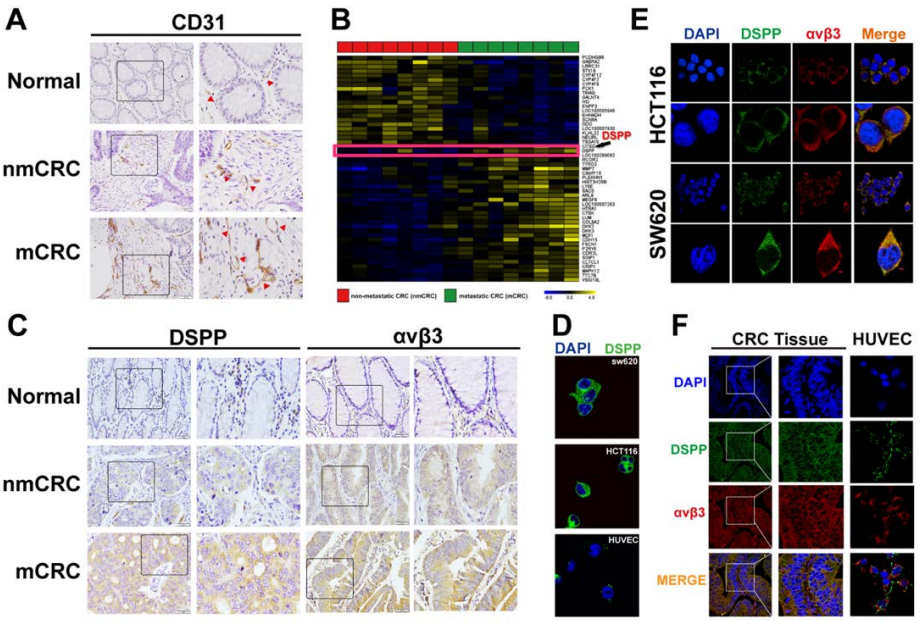

Figure 2 - 720

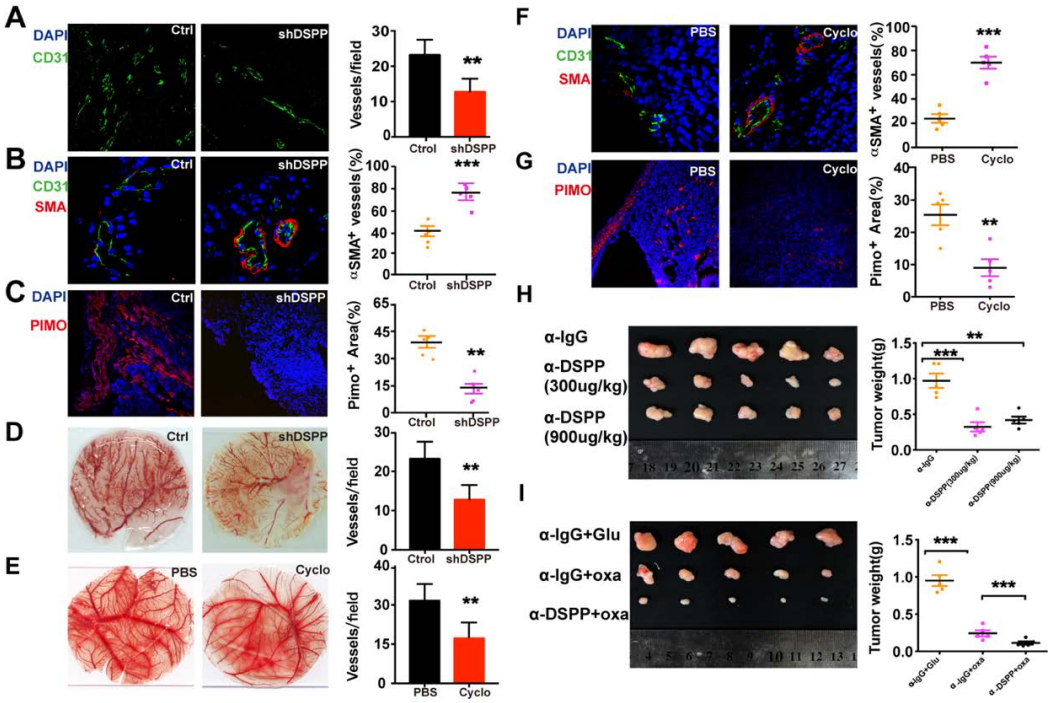

Conclusions: DSPP induces colorectal cancer metastasis and chemoresistant through suppressing the normalization of tumor vascular system via activating DSPP/αvβ3 axis. DSPP might be a potential metastatic biomarker and therapeutic target for the advanced CRC patients.

721 WNT/β-catenin Signaling Pathway Regulating PD-L1 Expression by CMTM6 in Colorectal Cancer

Kunping Liu[1], Jinbang Li[1]
[1]Department of Pathology, the Sixth Affiliated Hospital of Guangzhou Medical University, Qingyuan People's Hospital, Qingyuan, Guangdong, China

Disclosures: Kunping Liu: None; Jinbang Li: None

Background: Aberrant WNT pathway signaling occurs in most sporadic colorectal cancers (CRC) and plays an important role in the regulation of immunotherapy. Recent research indicates that CMTM6 is a major regulator of PD-L1 expression. However, the significance, correlation and underlying mechanism of β-catenin, CMTM6 and PD-L1 expression in CRC still unknown and need to be further determined.

Design: The expression of β-catenin, CMTM6 and PD-L1 proteins in 771 CRC patients were detected by immunohistochemistry. The CMTM6 and PD-L1 expressions were evaluated after activation/inhibition of WNT signaling pathway by small molecule compounds BIO/XAV939 treatment and WNT3a/si-CTNNB1 transfection in CRC cells. The expression of β-catenin and PD-L1 were evaluated after overexpression/inhibition of CMTM6. Bioinformatics predicts the molecular mechanism of WNT/β-catenin regulates the expression of CMTM6 and PD-L1.

Results: The expression level of β-catenin protein in CRC tissues was positively correlated with CMTM6 and PD-L1 proteins. Activation/inhibition of WNT signaling activity increased/decreased CMTM6 and PD-L1 proteins expression in CRC cells. Overexpression/inhibition of CMTM6 significantly increased/decreased the PD-L1 protein expression in CRC cells. However, CMTM6 has slight effect on β-catenin expression. Bioinformatics analyses suggest that β-catenin regulate the expression of PD-L1 by targeting CMTM6.

Figure 1 - 721

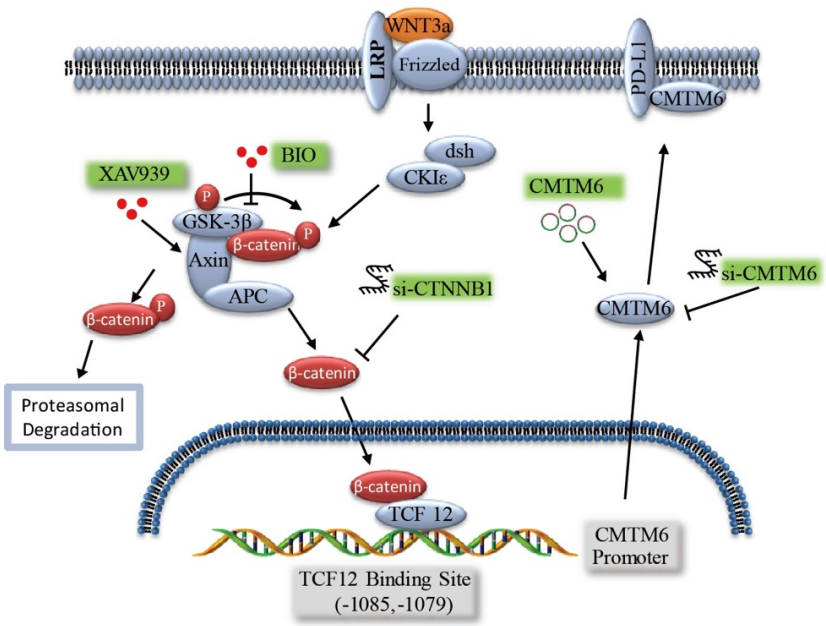

Conclusions: Our experimental results suggest that the WNT signaling pathway may affect PD-L1 expression by targeting CMTM6. The inhibition of β-catenin/ CMTM6/PD-L1 provides a new promising strategy for CRC treatment.

722 Prevalence and Patterns of p16 Expression in Esophageal Squamous Cell Carcinoma

Laura Malone[1], William Twaddell[2]
[1]*University of Maryland Medical Center, Columbia, MD,* [2]*Baltimore, MD*

Disclosures: Laura Malone: None; William Twaddell: None

Background: Human Papilloma Virus (HPV)-related squamous cell carcinoma (SCC) of the head and neck is biologically distinct from non-HPV related SCC and has a better prognosis and treatment response.

HPV positivity has been seen in esophageal SCC (eSCC). Previous studies demonstrate significant geographical differences in the proportion of HPV-related eSCC. Prevalence up to 60% has been reported in Asia and South America. In North America, studies have shown a prevalence between 2 and 33%; this range may be due in part to geographic variation in HPV infection.

A surrogate marker used to identify HPV-related SCC is the p16 immunohistochemical (IHC) stain. There are differing thresholds for positivity in the head and neck region versus other organs, with no commonly accepted threshold defined in the esophagus.

We aim to define the prevalence of HPV-related eSCC in our region, assess for outcome differences, and set a meaningful cutoff for p16 positivity in the esophagus.

Design: 45 cases of eSCC (34) and/or high grade dysplasia (HGD, 33) were found in the surgical pathology archives of our institution. A p16 IHC was performed on each case and assessed in normal (NM), HGD, and eSCC components. Age, sex, and location in the esophagus were enumerated. 10 demographically matched control cases were identified and stained for p16.

Results: NM in control cases was significantly more likely to show no p16 staining compared to NM in cases with associated eSCC/HGD (p=0.03). There were no significant differences in p16 positivity by region of the esophagus, sex, or age. Additional findings shown in Table 1.

Total Cases	45		
Invasive component	34		
P16+	8	8/34	24%
Associated Dysplasia	5	5/8	63%
P16+	3	3/5	60%
P16-	2	2/5	40%
P16-	26	26/34	76%
Dysplasia	17	17/26	65%
P16+	3	3/17	18%
P16-	14	14/17	82%
No invasion	11		
Dysplasia P16+	3	3/11	27%
Dysplasia P16 -	8	8/11	73%

Figure 1 - 722

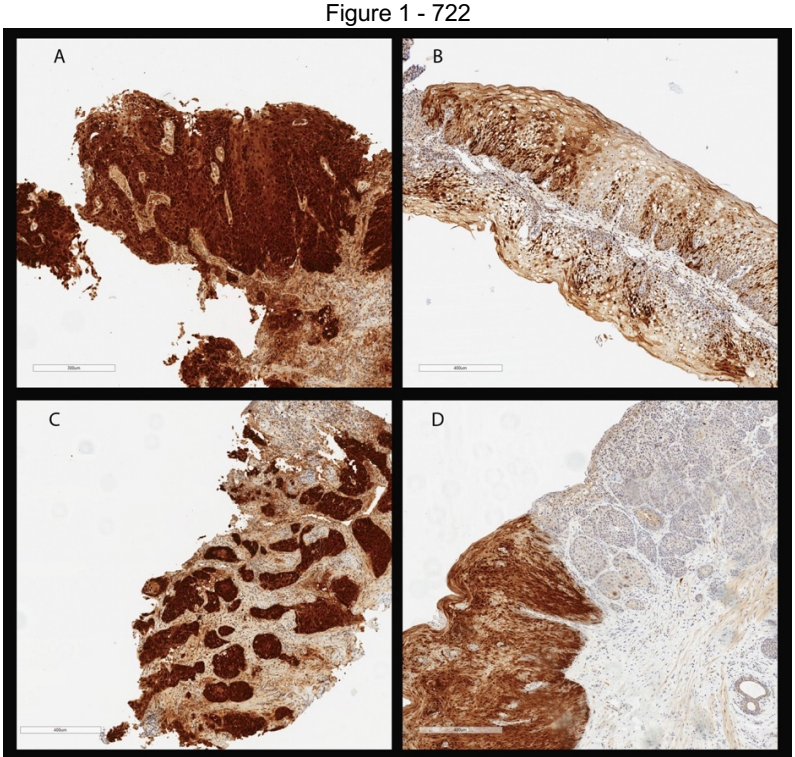

Figure 1: A. Positive staining in HGD. B. Borderline staining in HGD.
C. Positive staining in eSCC. D. Positive staining in HGD with no staining in eSCC.

Conclusions: The majority of lesions were p16-negative (62%, n=28). However, a p16 positivity rate of 38% (n=17) is higher than most previously reported rates within the USA.

Several unexpected patterns of p16 positivity emerged. Of p16-positive eSCC, HGD was also positive in 60% (n=3) of cases; however, the adjacent HGD in the remaining 40% (n=2) of cases showed staining without a block-like distribution (borderline staining). In 18% (n=3) of p16-negative eSCC the adjacent HGD was strongly and diffusely positive.

To set a meaningful threshold for p16 positivity in the esophagus, a selection of cases showing differing strengths of p16 staining will be assessed using digital image analysis. In situ hybridization will be performed on a subset of cases to correlate p16 positivity patterns with the presence or absence of viral DNA. Outcome data will be compared between the HPV-related and non-related cases.

723 Histopathologic Comparison of Acute and Interval Appendicitis

Grace Malvar[1], Pooja Navale[1], Raul Gonzalez[1]
[1]*Beth Israel Deaconess Medical Center, Boston, MA*

Disclosures: Grace Malvar: None; Pooja Navale: None; Raul Gonzalez: None

Background: While patients presenting with clinical signs and symptoms of acute appendicitis (AA) often receive swift surgical intervention, certain patients may instead receive nonoperative management initially, with appendectomy later. The histology of such interval appendicitis (IA) has been described in small series, often focusing on one or a few changes. We have noticed a recent increase in the incidence of IA specimens at our institution. This study aims to characterize the findings in IA, distinguishing it from AA and highlighting potential diagnostic pitfalls.

Design: We identified appendectomy specimens received by our department during the year 2018 with available H&E slides and clinical data. We divided cases into AA and IA (with the cutoff being one week between presentation and appendectomy). For each, we recorded patient age and sex, and we evaluated slides for multiple histologic findings. Cases of "AA" with no histologic changes were excluded, as were cases demonstrating an appendiceal neoplasm. Changes between groups were compared using Fisher's exact test, with statistical significance set at $P<0.05$.

Results: The cohort included 112 cases (76 AA, 36 IA). There were 58 males and 54 females, with a median age of 38 years; age and sex distribution were similar in the two groups. Median length of time from presentation to surgery for the IA patients was 75 days (range: 15-347 days). Histologic changes are summarized in the **Table**. Findings significantly more common in AA than IA included mucosal acute inflammation, mural acute inflammation, acute serositis, perforation, and fat necrosis of the mesoappendix. Findings significantly more common in IA than AA included mural fibrosis, granulomas **(Fig. 1)**, xanthogranulomas, chronic serositis, serosal adhesions, hemosiderin-laden macrophages **(Fig. 2)**, and granulation tissue. Crohn-like chronic mural inflammation (any amount) was more common in IA than AA, though this did not quite reach statistical significance.

Table: Histologic Changes in Acute and Interval Appendicitis

	Acute appendicitis (n=76)	Interval appendicitis (n=36)	*P*-value
Mucosal acute inflammation	75 (99%)	14 (39%)	<0.0001 *
Mural acute inflammation	75 (99%)	15 (42%)	<0.0001 *
Mural chronic inflammation	62 (82%)	30 (83%)	1.0
Crohn-like mural inflammation	19 (25%)	16 (44%)	0.050
Mural fibrosis	26 (34%)	34 (94%)	<0.0001 *
Granulomas	1 (1%)	5 (19%)	0.013 *
Xanthogranulomas	0 (0%)	3 (8%)	0.031 *
Acute serositis	69 (91%)	13 (36%)	<0.0001 *
Chronic serositis	19 (25%)	19 (53%)	0.0054 *
Serosal adhesions	27 (36%)	23 (64%)	0.0077 *
Perforation	14 (18%)	1 (3%)	0.034 *
Hemosiderin-laden macrophages	0 (0%)	13 (36%)	<0.0001 *
Mural edema	33 (43%)	15 (42%)	1.0
Mesoappendix fat necrosis	47 (62%)	14 (39%)	0.027 *
Granulation tissue	1 (1%)	5 (14%)	0.013 *

Figure 1 - 723

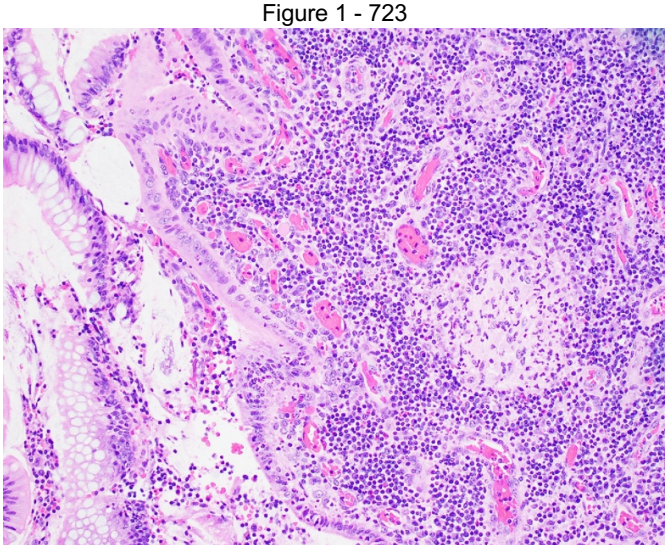

Figure 2 - 723

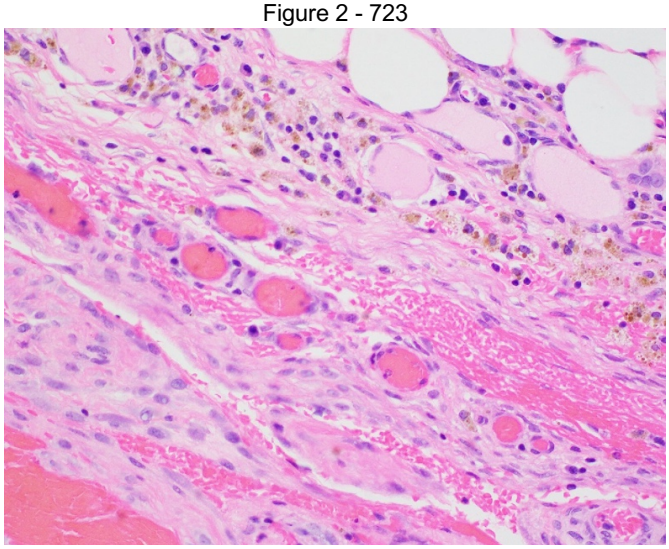

Conclusions: Acute inflammatory changes are more common in AA but can remain present in IA. Mural fibrosis, serosal adhesions, hemosiderin-laden macrophages, and granulation tissue suggest IA. Granulomas and xanthogranulomas can also be seen in IA and do not necessarily point to a persistent infectious cause. Similarly, Crohn-like inflammation is not uncommon in appendicitis. Knowledge of these histologic patterns can guide signout, particularly when clinical information is unavailable.

724 Immune Infiltrates Associated with Tumor Budding in Gastric Adenocarcinoma: A Histopathological Characterization

Mario Marques-Piubelli[1], Rossana Lazcano Segura[2], Debora Ledesma[1], Carmelia Noia Barreto[1], Patricio Weber[3], Edinson Bravo[4], Miguel Villaseca[5], Ignacio Wistuba[1], Juan Araya[6], Luisa Solis Soto[1]
[1]The University of Texas MD Anderson Cancer Center, Houston, TX, [2]Hospital Nacional Arzobispo Loayza, Lima, Peru, [3]Universidad de La Frontera, Temuco, IX Region, Chile, [4]Universidad de La Frontera, Temuco, Chile, [5]Universidad de La Frontera, Temuco, Araucania, Chile, [6]Temuco, Cautin, Chile

Disclosures: Mario Marques-Piubelli: None; Rossana Lazcano Segura: None; Debora Ledesma: None; Carmelia Noia Barreto: None; Patricio Weber: None; Edinson Bravo: None; Miguel Villaseca: None; Ignacio Wistuba: None; Juan Araya: None; Luisa Solis Soto: None

Background: Gastric carcinoma (GC) is the fifth most incident cancer worldwide and the third in lethality. With the current advances in targeted therapy and immunotherapy, there is a need to understand the tumor immune landscape and its histological associations to better classify tumors. Tumor budding (TB) and immune infiltrate at the invasive front are an adverse prognostic factor in several types of cancer including GC. We aim to study the associations of tumor budding and its surrounding stromal infiltrating lymphocytes (SIL) and determine correlations with histopathological characteristics.

Design: We used a retrospective cohort of patients (n = 136) that underwent partial or total gastrectomy without neoadjuvant treatment. We reviewed whole section H&E slides from a representative tumor block. All selected H&E slides were scanned using *Aperio AT2* software (Leica Biosystems). We used the criteria stated by the International Consensus Conference on Tumor Budding (ITBCC) to quantify TB and divided into groups according to the median number. We estimated the percentage of lymphoid cells surrounding the tumor budding, to quantify SIL in the same selected hotspot budding field. We correlated these findings with annotated histopathological data: number of lesions, tumor size, vertical location, macroscopic type (B1, B2, B3, B4 or B5), histologic grade (G1, G2, and G3), histologic classification (Lauren and WHO), and TNM pathological staging.

Results: From the 136 cases, we successfully evaluated TB and SIL in 94 cases. We excluded 42 cases: 27 cases with positive margins, and 15 cases, which the distinction of malignant cells and lymphoid cells was not possible. The distribution of TB number, SIL%, and histopathological features are summarized in Table 1. Based on a combination of TB and SIL, we created four groups (Figure 1). In our series, a high TB number correlated with lower SIL% ($r = -0.4536$, $p < 0.0001$) (Figure 2). This correlation was also observed when we used categorical variables ($p = 0.008$). High tumor budding group correlated with more aggressive pathologic features such as diffuse type of Lauren Classification ($p = 0.0495$), histologic Grade 3 ($p= 0.0450$) and pT4 staging ($p = 0.0081$). No significant associations were found with SIL and histopathological features.

Histopathological data (n = 77)*	Low Budding (0-3); (n, %)	High Budding (≥4); (n, %)
Lauren Classification (*p = 0.0495*)**		
Diffuse	19 (25%)	25 (32%)
Intestinal Type	20 (26%)	13 (17%)
Histologic grade *(p = 0.0450)***		
G1 and G2	21 (28%)	12 (15%)
G3	18 (23%)	26 (34%)
pT *(p = 0.0081)***		
pT1, pT2 and pT3	36 (47%)	26 (34%)
pT4	3 (4%)	12 (15%)

*Histopathological data was not available in 17 cases.

**Chi-square test.

Figure 1 - 724

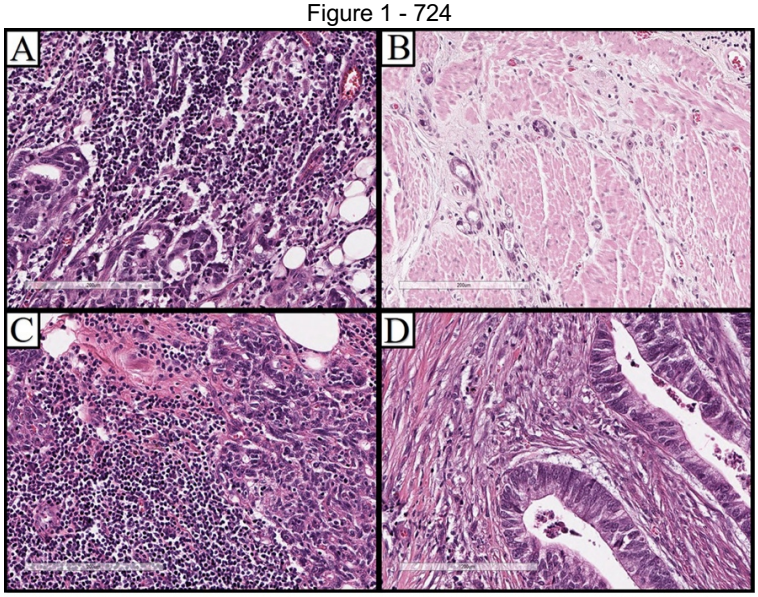

Figure 1. Histological characterization according to tumor budding number and stromal infiltrating lymphocytes in front of invasion. A) high tumor budding/high stromal infiltrating lymphocytes (HTB/HSIL); B) high tumor budding/low stromal infiltrating lymphocytes (HTB/LSIL); C) low tumor budding/high stromal infiltrating lymphocytes (LTB/HSIL); D) low tumor budding/low stromal infiltrating lymphocytes (LTB/LSIL). H&E, 200x.

Figure 2 - 724

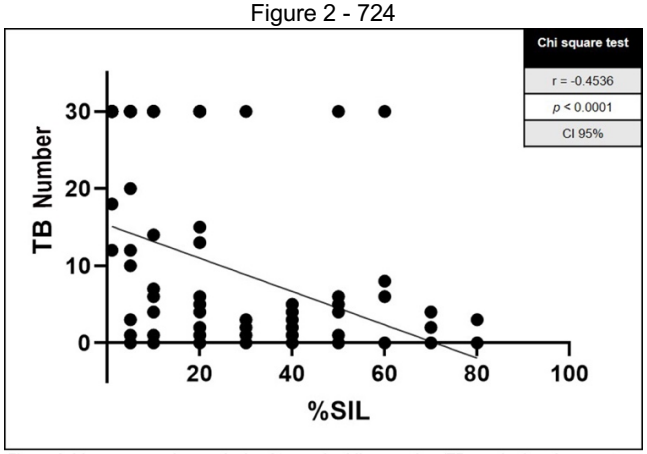

Figure 2. Linear regression analysis of tumor budding number (TB number) and percentage of stromal infiltrating lymphocytes (%SIL).

Conclusions: We characterized TB and SIL at the invasive front of gastric adenocarcinoma. We found an inverse correlation between TB and SIL, as well as association with histologic type, high histologic grade, and pT4 staging.

725 Patients with 22q11.2 Deletion Syndrome (DiGeorge Syndrome) Have a Significant Decrease in Lamina Propria Plasma Cells in the Gastro-intestinal Tract: Morphologic Description of a Unique Cohort

Jake Maule[1], Jadee Neff[2], Shannon Mccall[2], Avani Pendse[2]
[1]Duke University Health System, Durham, NC, [2]Duke University Medical Center, Durham, NC

Disclosures: Jake Maule: None; Jadee Neff: None; Shannon Mccall: None; Avani Pendse: None

Background: The aim of this study is to perform a comprehensive morphologic evaluation of the luminal gastro-intestinal (GI) tract in pre-thymus transplant 22q11.2 deletion syndrome (DiGeorge syndrome or DGS) patients. Along with the well documented cardiac abnormality and immunodeficiency, GI symptoms are a common feature in these patients. But, very limited literature is available describing the specific histo-pathologic changes in the GI tract.

Design: Cytogenetically confirmed DGS patients from 1990 till 2018 were identified and GI biopsies prior to thymus transplant were retrospectively reviewed. Clinical and laboratory data were analyzed to determine the severity of immunodeficiency and stratified into mildly immunocompromised (DGS) or severely immunosuppressed (DGS-I) groups. H&E slides were reviewed for evaluation of epithelial cell abnormalities, composition of lamina propria inflammatory infiltrate and morphologic changes suggestive of infections. Immunohistochemistry (IHC) for CD138 was performed on duodenum and colon to highlight plasma cells (PCs). Five immunocompetent non-DGS pediatric patients with abdominal symptoms but normal GI tract endoscopic biopsies were used as controls.

Results: DGS-I patients showed a near complete absence of PCs in the duodenum and colon lamina propria (Fig 1B). This finding was confirmed by immunohistochemistry for CD138 which showed an average of 1.17 (n=5) and 0.8 (n=12) plasma cells per 40X high power field (HPF) in the duodenum and colon respectively. Average plasma cells per HPF in control cases were 64.56 (n=4) and 74.11 (n=6), and in mildly immunocompromised DGS patients were 116.07 (n=4) and 62.84 (n=4) in the duodenum and colon, respectively (Fig 1A, 2). Additionally, DGS patients' colon biopsies showed a mild increase in epithelial cell apoptosis regardless of the immune status. On average, a maximum of 3.67 (n=23) apoptotic cells were noted per biopsy fragment when compared to 1.34 (n=12) in the controls.

Figure 1 - 725

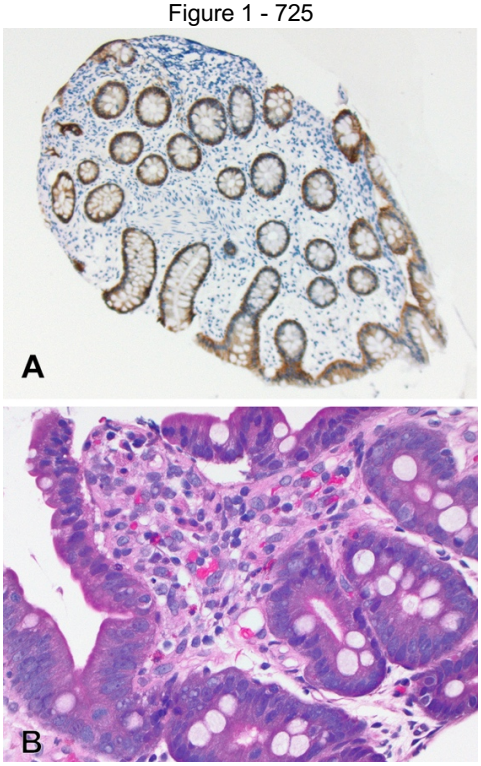

Figure 2 - 725

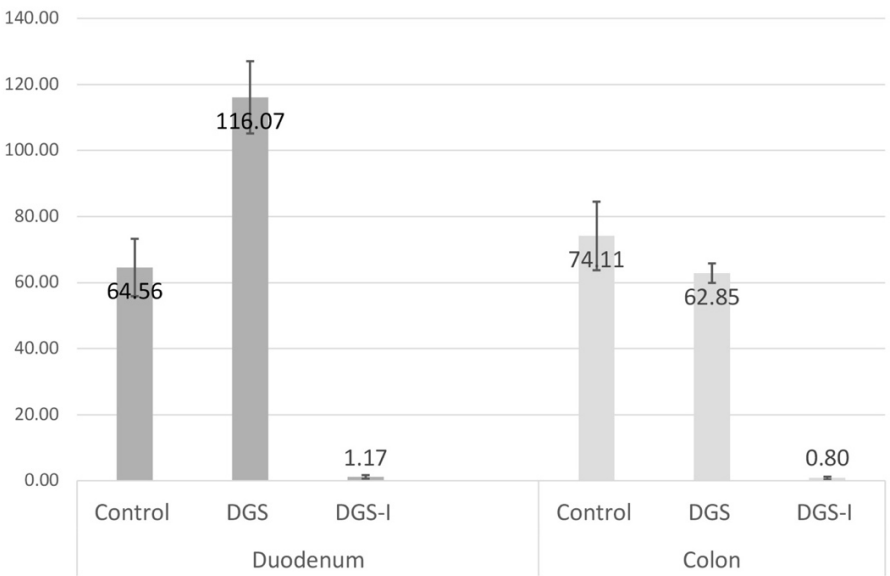

Conclusions: To our knowledge, this is the first comprehensive morphologic description of gastrointestinal tract changes in DGS patients prior to thymus transplantation. The near complete absence of plasma cells correlates with the immune status and can potentially be a useful marker of immunodeficiency/T-cell dysfunction before it clinically manifests. The mild increase in the colonic epithelial cell apoptosis prior to thymus transplant warrants caution while interpreting post-transplant GI biopsies for monitoring graft-versus-host-disease.

726 Heterogeneity and Geographical Patterns of PD-L1 Expression in Colonic Adenocarcinoma with Discordant PD-L1 Status

Lynn Messersmith[1], Grant Williams[2], Phillip Kemp Bohan[3], Robert Chick[3], Devin Broadwater[4], Jamie Lombardo[5], Annelies Hickerson[1], Jessica Cindass[1], Robert Brady[1], George Peoples[6], Guy Clifton[7]
[1]SAMMC, Fort Sam Houston, TX, [2]SAMMC, Schertz, TX, [3]BAMC, Ft. Sam Houston, TX, [4]USAF, San Antonio, TX, [5]The University of Texas MD Anderson Cancer Center, Cibolo, TX, [6]Spring Branch, TX, [7]San Antonio Uniformed Services Health Education Consortium, San Antonio, TX

Disclosures: Lynn Messersmith: None; Grant Williams: None; Phillip Kemp Bohan: None; Robert Chick: None; Devin Broadwater: None; Jamie Lombardo: None; Robert Brady: None; George Peoples: None

Background: Expression of programmed death-ligand 1 (PD-L1) on tumor cells is highly predictive of response to checkpoint inhibitor therapy. PD-L1 expression within the tumor is heterogeneous, potentially hindering accurate reporting of PD-L1 status. Cases of colonic

adenocarcinoma with discordant PD-L1 staining between biopsy and resection were evaluated for heterogeneity and geographical patterns of PD-L1 expression.

Design: 96 patients with matched biopsies and colonic adenocarcinoma resection specimens from a single institution between 2006-2016 were selected for review. Neoadjuvant therapy cases were excluded. PD-L1 immunohistochemical staining was performed on the biopsy and one block of resection. PD-L1 was interpreted as negative, low, or high. 20 cases with a PD-L1 negative biopsy and positive resection were identified. From these discordant cases, 104 additional resection tumor blocks were stained for PD-L1 in order to evaluate heterogeneity and characterize geographical patterns of expression. Patterns of PD-L1 were recorded as expression at the surface, center of tumor, and invasive margin.

Results: 17/96 (18%) cases were true positives with concordant PD-L1 status between biopsy and resection. 46/96 (48%) cases were true negatives. The false negative rate of PD-L1 expression was 30%. In discordant cases, an average of 5 additional blocks were stained per resection specimen (range 1- 12). 74/104 (71%) of additional sections were positive for PD-L1 and 30/104 (29%) were negative. 9/20 (45%) cases showed PD-L1 positivity in all additional blocks stained. 20/20 (100%) cases had at least one block with PD-L1 expression at the invasive margin. In 29/74 (39%) positive additional blocks, PD-L1 was exclusively expressed at the invasive margin. 33/74 (45%) positive additional blocks lacked surface expression. When present, surface expression was focal. Staining at the invasive margin was more consistent and intense compared to surface staining. 10/74 (14%) positive additional blocks expressed PD-L1 at the center of the tumor.

Conclusions: PD-L1 status on biopsy has a false negative rate of 30% and can be explained by tumor heterogeneity and geographical patterns of PD-L1 expression, primarily lack of surface expression in superficial biopsies. PD-L1 status should be confirmed on multiple blocks of resection specimens. The invasive margin should be adequately evaluated, reducing the likelihood that tumor heterogeneity affects PD-L1 status and affects eligibility for checkpoint inhibitor therapy.

727 Serrated Epithelial Change in Inflammatory Bowel Disease Frequently Harbor KRAS Mutation and are Not Associated with an Increased Risk of Dysplasia or Malignancy

Gregory Miller[1], Cheng Liu[2], Mark Bettington[1], Christophe Rosty[1]
[1]Envoi Specialist Pathologists, Brisbane, QLD, Australia, [2]Highgate Hill, QLD, Australia

Disclosures: Gregory Miller: None; Cheng Liu: None; Christophe Rosty: None

Background: Serrated epithelial change (SEC) is an underappreciated lesion of the colon diagnosed in some IBD patients. It characteristically shows subtle serration limited to the upper half of the crypts, without cytological atypia. Previous studies on the neoplastic potential of SEC provided conflicting results, making management of patients difficult. Moreover, the molecular characteristics of SEC have not been well studied.

Design: The pathology database was searched for diagnosis of SEC or “hyperplastic-like change” in IBD patients, from 2010 to 2019. All cases were reviewed by 3 pathologists to exclude typical hyperplastic polyp (HP) or sessile serrated lesion (SSL). The following features were recorded: patient demographics, characteristics of IBD and associated colorectal lesions. Clinical follow-up was measured from time of index SEC lesion to most recent colonoscopy. Immunohistochemistry for p53 and Ki67, and mutation analysis for *BRAF* and *KRAS* were performed on each SEC.

Results: Eighty-one SEC lesions were identified in 26 patients (16 females) with a median age of 54 years (range 27-76). There were 20 patients with ulcerative colitis and 6 patients with Crohn’s colitis. The extension of the disease was the entire large bowel for 20 patients, left colon for 5 and the rectum for 1.

The distribution of SEC was the right colon for 38 lesions, left colon for 27 and rectum for 14 (unknown for 2). The background colorectal mucosa showed features of quiescent IBD in all but 1 case. Six patients had 1-3 synchronous sporadic-type lesions (5 SSLs and 4 TAs). Immunohistochemistry showed no abnormal p53 expression and no proliferation above the basal half of the crypts using Ki67 in any SEC. *KRAS* mutation was present in 43/73 analysed cases (59%). A single case showed *BRAF* mutation; however, on deeper levels features of SSL were evident.

Median follow-up was 65 months (range 0-135) with a median number of 5 surveillance colonoscopies per patient. One patient had an invisible lesion at 50 months classified as indefinite for dysplasia, with no dysplasia found on a subsequent colonoscopy. Metachronous sporadic-type TAs and SSLs were resected in 7 patients. No IBD-related dysplasia or malignancy was identified.

Conclusions: SEC in IBD patients can occur in any part of the large bowel. Most SECs harbor a *KRAS* mutation suggesting that they may be related to goblet cell-rich HP. Our follow-up study does not provide evidence for an increased risk of advanced colorectal neoplasia associated with SEC.

728 Colonic Malakoplakia: A Rare and Largely Incidental Entity

Fatima Mir[1], Prih Rohra[1], Lindsay Yassan[1], Shriram Jakate[1]
[1]Rush University Medical Center, Chicago, IL

Disclosures: Fatima Mir: None; Prih Rohra: None; Lindsay Yassan: None; Shriram Jakate: None

Background: Malakoplakia is an uncommon chronic granulomatous disease which mainly affects the genitourinary(GU) tract and is associated with immunosuppressive states such as transplantation, chemotherapy, HIV, diabetes and autoimmune disorders. Pathophysiologically, there is decrease in bactericidal action of the macrophages and granulomatous reaction contains characteristic calcium deposit granules("Michaelis Gutman bodies"). Clinically, most patients are symptomatic and show abnormalities on gross examination or imaging that may be mistaken for a tumor. While isolated case reports are described in gastrointestinal(GI) tract and other organs, the overwhelming majority of patients have GU tract involvement and common clinical profile. We studied cases of GI malakoplakia for their frequency, clinical features and distribution.

Design: Our surgical pathology database was reviewed from January 2000 to August 2019 to identify cases of malakoplakia involving GI tract. Clinical and pathological data was reviewed.

Results: A total of only 5 cases of malakoplakia were identified in approximately 140,000 GI biopsies and resections(3 females, ages 46, 58 and 60 and 2 males, ages 63 and 71). All 5 cases involved the colon, showed characteristic granulomatous collection of macrophages(CD68+) and Michaelis Gutman bodies highlighted by von Kossa stain. None of the cases showed association with GU malakoplakia. 3/5 cases were identified as 'cecal polyp' in asymptomatic patients during routine screening colonoscopy and measured between 4-7 mm. Fourth case showed an incidental patch(grossly plaque) of rectal malakoplakia adjacent to a residual rectal adenocarcinoma resected after chemoradiotherapy. Fifth case showed a small 5 mm 'rectal polyp' with malakoplakia in a patient with long-standing ulcerative colitis during routine surveillance colonoscopy. No specific treatment for malakoplakia was administered in any of the 5 cases and followup endoscopy performed in 3/5 cases showed no recurrent or residual malakoplakia.

Conclusions: Malakoplakia affecting GI tract is extremely rare and colon appears to be the favored location. Within the colon, cecum and rectum are the most commonly affected sites. Colonic malakoplakia is not associated with concurrent GU malacoplakia and is often incidentally detected as a small 4-7 mm polyp during screening or surveillance colonoscopy. No therapeutic intervention appears to be necessary and followup endoscopies are negative for residual or recurrent colonic malakoplakia.

729 Lichenoid Esophagitis Pattern (LEP) of Esophageal Injury: Overlapping Clinicopathologic and Endoscopic Findings with Lichen Planus (LP) and Other Clinical Conditions

Mitul Modi[1], Rifat Mannan[2]
[1]Pennsylvania Hospital of University of Pennsylvania Health System, Philadelphia, PA, [2]Perelman School of Medicine at the University of Pennsylvania, Philadelphia, PA

Disclosures: Mitul Modi: None; Rifat Mannan: None

Background: LP is known to involve mucosal surface, including esophagus and is characterized by intraepithelial and lamina propria lymphocytosis and Civatte bodies. However, LEP histology is not specific, being reported with unrelated clinical conditions, medications and esophageal squamous dysplasia/carcinoma. We sought to study clinical, endoscopic and pathologic features LEP diagnosed at our institution.

Design: We identified 45 specimens of LEP from 29 patients (2009-2019). Clinical details and endoscopic findings were obtained from available records. Histology was reviewed for confirmation of diagnosis and associated pathology.

Results: Detailed results are summarized in table 1. Mean age was 62.1 years (range 21 -89); 19 (65%) were female. Seven patients (24%) had a diagnosis of LP. Dysphagia was the most common indication for endoscopy (90%, 26/29). On endoscopy, LEP appeared as luminal stenosis (28%, 8/29), followed by mucosal scarring (14%, 4/29). When specified (n=15), mucosal changes were variably distributed, most commonly involving distal esophagus (27%, 4/15). All patients had classic LEP histology. None of them had associated squamous dysplasia or malignancy. Four patients had associated candida esophagitis. Significant comorbidities included gastroesophageal reflux (n=6), rheumatologic diseases (n=4), Crohn disease (n=3; all were adults), HIV, Hepatitis B and Hepatitis C (n=1 each). Polypharmacy (patient taking $\geq$ 3 medications) was observed in 86 % (n=25) patients. When available (n=21), patients were managed with endoscopic dilation (95%, 20/21) or medications (5%, 1/21) with a favorable outcome.

Table 1: Clinical characteristics of the patients with lichenoid esophagitis pattern (n=29)

No. of patients	29
Average age (years)	62.1 (range 21-89)
Gender	
Female	19 (65%)
Male	10 (35%)
Presenting symptoms	
Dysphagia	26 (90%)
Heartburn	1 (3%)
Anemia	1 (3%)
Not specified	1 (3%)
Distribution	
Proximal	2 (13%)
Middle	1 (7%)
Distal	4 (26%)
GE junction	1 (7%)
Proximal, mid, distal	2 (13%)
Proximal and distal	3 (20%)
Mid and distal	1 (7%)
Diffuse	1 (7%)
Not specified	14
Endoscopic appearance	
Stenosis	8 (28%)
Scarring, sclerosis	4 (14%)
Rings	3 (11%)
Feline appearance	2 (7%)
Linear ulcer	2 (7%)
White plaque	2 (7%)
Erosion	1 (3%)
Mucosal tear	1 (3%)
Web	1 (3%)
Sloughing	1 (3%)
Diverticulum	1 (3%)
Unremarkable	3 (11%)
Associated Lichen Planus	
Total	7 (24%)
Cutaneous	6
Mucocutaneous	1
Direct immunofluorescence positive	3 (43%)
Associated other clinical conditions	
Rheumatologic disorders SLE Sjogren syndrome Autoimmune hepatitis	4 2 1 1
Crohn disease	3
Candida esophagitis	4
GE refllux	6
HIV	1
Hepatitis B	1
Hepatitis C	1
Malignancy (non esophageal)	4
Other diseases	13
Polypharmacy ≥3	25 (86%)
Management	
Dilation	20 (95%)
Medications	1 (5%)
Not specified	8

Conclusions: LEP of injury can be observed in association with LP as well as unrelated clinical conditions, including candida esophagitis, rheumatologic disorders, Crohn disease, HIV, viral hepatitis and use of multiple medications. Common in adult female, majority present with dysphagia due to stricture formation. Endoscopic features are variable (stenosis being the most common), can involve different regions of esophagus, and often mimic other mucosal pathologies. Endoscopic dilation is a reasonable treatment option, with favorable outcome. Though previously reported, none of our patients had associated squamous neoplasia. It is important to be aware of this uncommon pattern of esophageal mucosal injury such that symptomatic patients can be appropriately managed and followed up as needed.

730 Her2 Detection in Gastric and Gastroesophageal Adenocarcinomas: IHC, FISH, or Both? A Single Institution's Experience

Jeremy Molligan[1], Paul Zhang[2], Emma Furth[1]
[1]University of Pennsylvania, Philadelphia, PA, [2]Hospital of the University of Pennsylvania, Media, PA

Disclosures: Jeremy Molligan: None; Paul Zhang: None; Emma Furth: None

Background: Trastuzumab has been used to treat patients with HER2 positive gastric and GEJ adenocarcinomas (G-GJE Ad) since 2010. The FDA approved IHC and FISH Her2 tests are both wildly used clinically to evaluate patient eligibility for the drug. Many institutions have borrowed the testing algorithm for breast cancer and used IHC as first line test with a modified scoring system and reflex to FISH on 2+ cases. Some studies have shown a greater degree of tumor heterogeneity and higher incidence of discordance between IHC and FISH Her2 results compared to breast cancer. In our institution, since 2009, both IHC and FISH were performed on all the requested G-GEJ Ad. The aim of this study is to evaluate the concordance between IHC and FISH Her2 tests and subsequently a better testing strategy in G-GEJ Ad in a larger series from a single institution.

Design: From 2009 and 2019, Her2 was tested in 283 G-GEJ Ad, among these, both IHC and FISH were simultaneous performed in 219 cases. Commercially available FDA approved Her2 tests were used and IHC scoring for HER2 was conducted in accordance to the standards proposed by Hofmann et al. Vysis PathVysion Dual Her2 DNA probe kit was used, manual signal enumeration was performed, and a ratio of Her2/CEP17 >2.0 or Her2/cell >6 was reported as positive for amplification.

Results: Of the 219 G-GEJ Ad, the IHC score was 0/1+ in 176 (80% of 219); 2+ in 23 (10.5% of 219); and 3+ in 20 (9%) cases; FISH results were positive in 40 (18%) and negative in 179 (82%) cases. Concordance between IHC and FISH is 83.6% (183 out of 219). Of the IHC negative cases (0/1+) (n=176), 11 were positive by FISH corresponding to a "false negative rate" of 5.0%. Of the IHC positive (3+) (n=20), 2 were FISH negative corresponding to a "false positive rate" of 0.9%. Of the IHC 2+ cases (n=23), 11 cases were positive by FISH (5%) and 12 cases were negative by FISH (5.5%).

Conclusions: This study found an overall concordance rate between IHC and FISH for HER2 overexpression of 83.6% in accordance to what has previously been reported in the literature (Hofmann 2008). This concordance rate in G-GEJ Ad is lower than that of breast cancer and reflects the higher incidence of FISH positive/IHC negative or 2+ cases. FISH seems to be significantly more sensitive (18%) to detect Her2 positive status than IHC (9%) in this series. Although less sensitive, IHC has many other obvious advantages over FISH. We recommend that both IHC and FISH should be performed on G-GJE adenocarcinomas.

731 Do Tumor Budding and Inflammatory Response Have Prognostic Significance in Neoadjuvant Treated Colorectal Cancer?

Gustavo Moreno[1], Catherine Hagen[2], Christopher Hartley[3], Mohamed Mostafa[4]
[1]Medical College of Wisconsin, Brookfield, WI, [2]Mayo Clinic, Rochester, MN, [3]Medical College of Wisconsin, Milwaukee, WI, [4]Medical College of Wisconsin, Wauwatosa, WI

Disclosures: Gustavo Moreno: None; Catherine Hagen: None; Christopher Hartley: None; Mohamed Mostafa: None

Background: Several independent histologic prognostic factors in colorectal cancer have emerged with two of the most studied being tumor budding (TB) and inflammatory response. The majority of prior studies have focused on evaluating these factors in treatment naive patients and therefore the significance in neoadjuvant treated colorectal cancer is largely unknown. The goal of our study was to evaluate the significance of TB and inflammatory response in post-neoadjuvant therapy colorectal resections.

Design: Our pathology database was retrospectively searched from 2015-2019 for cases of colorectal cancer resected after neoadjuvant therapy. TB was evaluated at the leading edge of the tumor according to the 2016 ITBCC guidelines. The Klintrup system was used to score peritumoral and intratumoral inflammatory response. The peak intratumoral tumor-infiltrating lymphocyte (TIL) count in a single 40x HPF was assessed as well as the presence of a Crohn's-like response. Clinicopathologic and survival data were collected from chart review.

Results: The study group consisted of 121 colorectal resections from an equal number of patients (M:F 1.4:1, mean age 56.8). 14 patients had complete treatment response and were excluded from further analysis. In 17 patients TB could not be assessed because of presence of tumor regression with large pools of extracellular mucin. 63 patients had low TB, 15 intermediate, and 12 high TB. Patients with intermediate/high TB showed a trend of worse overall survival (p=0.14, HR 3.6, CI 0.5-24.4) (Figure 1). In 3 patients with poorly differentiated carcinoma Klintrup score could not be assessed. 90 patients had a Klintrup score of 0/1 and 14 a score of 2/3. Patients with a Klintrup score of 0/1 showed a trend of worse overall survival compared to those with a score of 2/3 (p=0.50, HR 3.1, CI 0.1-68.2) (Figure 2). There was no significant difference in overall survival for patients with and without a Crohns-like response (p=0.99) or patients with any TILs vs those with none (p=0.91).

Figure 1 - 731

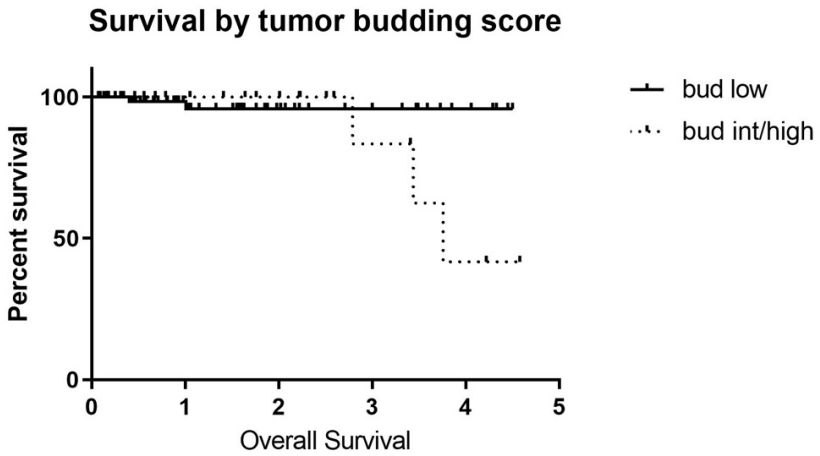

Figure 2 - 731

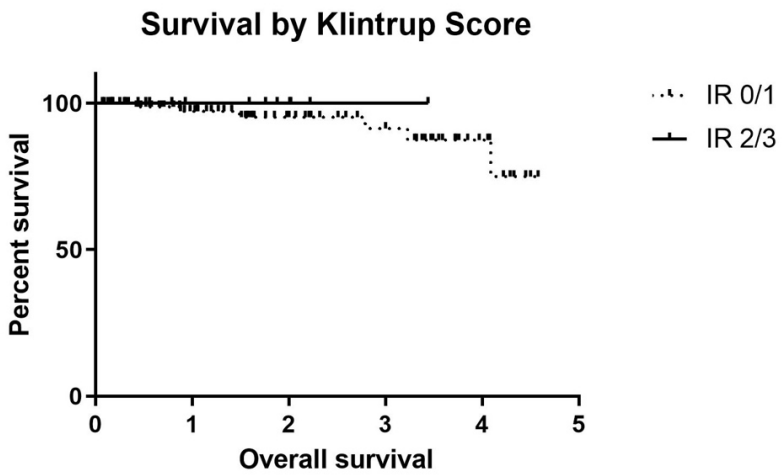

Conclusions: TB is more difficult to assess in the neoadjuvant setting because of extracellular mucin pools but may be of prognostic significance in cases where it can be assessed. Klintrup score may be significant in neoadjuvant treated rectal cancer but larger studies with longer follow up are needed to explore the trends noted here.

732 Histopathologic Findings are Similar in Cirrotic Patients with and without Endoscopic Portal Hypertensive Gastropathy

Matthew Morrow[1], Raul Gonzalez[1]
[1]*Beth Israel Deaconess Medical Center, Boston, MA*

Disclosures: Matthew Morrow: None; Raul Gonzalez: None

Background: Portal hypertensive gastropathy (PHG) is caused by portal hypertension and is endoscopically characterized by mucosal hyperemia, friability, and dilated submucosal vessels, creating a mucosal "mosaic" pattern. It is commonly seen in cirrhosis and is associated with esophageal varices. PHG changes on histology can be nonspecific and often require correlation with endoscopic findings. We undertook this study to evaluate the contexts in which a histologic diagnosis of PHG might be rendered.

Design: We searched gastric biopsies from 2010 to 2019 to establish two cohorts. The first included cases obtained during screening for clinically suspected or established esophageal varices, and the second included cases described in the pathology report as having histopathologic changes of PHG. Chart review was performed to assess for endoscopic PHG, varices, and clinical cirrhosis. H&E slides on all cases were assessed for pathologic findings (see **Table**), which were correlated with the presence of endoscopic PHG and clinical cirrhosis. Hepatic venous pressure gradient and Model for End-Stage Liver Disease scores were not recorded, as they were available for few patients. Histologic changes were compared between groups using Fisher's exact test in a 2x2 contingency table, with significance set at $P<0.05$.

Results: The first cohort contained 188 patients undergoing screening for varices. Forty (27%) had an endoscopic appearance indicative of PHG. Cases with and without endoscopic PHG were histologically similar, though cases with endoscopic PHG tended to more commonly show acute inflammation (4/40 [10%] vs. 4/148 [3%], $P=0.06$). Cases from patients with clinical cirrhosis were more likely to show reactive-type gastropathy than those without (42/139 [30%] vs. 7/49 [15%], $P=0.037$). The second cohort contained 29 patients whose pathology reports indicated PHG. Sixteen demonstrated endoscopic PHG. The most common histologic changes were capillary dilation, reactive-type gastropathy, lamina propria fibrosis, and smooth muscle hyperplasia. In this cohort, there were no significant histologic differences between cases with and without endoscopic PHG.

	Cohort 1 (n=188)	Cohort 2 (n=29)
Male:female ratio	120 male:68 female	17 male:12 female
Median age	59 years	59 years
Endoscopic PHG	40 (21%)	15 (52%)
Clinical cirrhosis	139 (74%)	24 (83%)
Histologic erosion	6 (3%)	6 (21%)
Foveolar hyperplasia	15 (8%)	7 (24%)
Lamina propria edema	18 (10%)	1 (3%)
Lamina propria fibrosis	29 (15%)	11 (38%)
Smooth muscle hyperplasia	20 (11%)	11 (38%)
Lamina propria acute inflammation	8 (4%)	4 (14%)
Lamina propria chronic inflammation	56 (30%)	2 (7%)
Reactive-type gastropathy	49 (26%)	14 (48%)
Capillary dilation (measured as having a diameter >5 lymphocytes across)	61 (32%)	23 (79%)
Fibrin thrombi	0 (0%)	0 (0%)
Lamina propria thick-walled blood vessels	3 (2%)	4 (14%)
Extravasated red blood cells	9 (5%)	2 (7%)

Conclusions: In patients undergoing screening for esophageal varices, histologic changes in the stomach are generally similar in patients with and without clinical cirrhosis, and with and without endoscopic PHG. Other than perhaps confirming a clinical impression, rendering a pathologic diagnosis of PHG appears nonspecific and may have little meaning for the patient.

733 Evaluation of Tumor Stroma in Neoadjuvant Treated Colorectal Cancer

Mohamed Mostafa[1], Catherine Hagen[2], Gustavo Moreno[3], Christopher Hartley[4]
[1]*Medical College of Wisconsin, Wauwatosa, WI,* [2]*Mayo Clinic, Rochester, MN,* [3]*Medical College of Wisconsin, Brookfield, WI,* [4]*Medical College of Wisconsin, Milwaukee, WI*

Disclosures: Mohamed Mostafa: None; Catherine Hagen: None; Gustavo Moreno: None; Christopher Hartley: None

Background: The interaction between tumor cells and fibroblasts in colorectal carcinoma results in high turnover and remodeling of the adjacent extracellular matrix producing what is commonly referred to as desmoplastic stroma. Emerging studies have shown that the type

of stroma has prognostic implications. However, these studies utilized cohorts of patients who did not receive neoadjuvant treatment. The goal of this study was to evaluate the prognostic significance of tumor stroma in neoadjuvant treated colorectal cancer.

Design: Our surgical pathology database was retrospectively searched from 2015-2019 for cases of colorectal cancer resected following neoadjuvant therapy. H&E stained slides were evaluated at the invasive edge of the tumor for stroma type. Stroma was categorized as mature when only parallel collagen fibers were present, intermediate when keloidal collagen was identified, and immature when myxoid stroma was seen spanning at least one 40x field. Clinicopathologic information and survival data were gathered from chart review.

Results: The study group consisted of 121 colorectal resections from an equal number of patients (M:F 1.4:1; mean age 56.8). The average follow-up for all patients was 1.8 years. Fourteen patients had complete treatment response and were excluded from further analysis. 82 patients (76.6%) demonstrated mature tumor stroma, 14 (13.1%) intermediate stroma, and 11 (10.3%) immature stroma. Patients with immature stroma had significantly worse overall survival (p=0.033) and progression free survival (p=0.010) (Figures 1 and 2). Other pathologic variables did not significantly correlate with overall survival (ypT3/T4 vs. ypT1/pT2 (p=0.71), presence of lymph node metastases (p=0.65), tumor regression grade (p=0.73), presence of lymphovascular invasion (p=0.27), or presence of venous invasion (p=0.38)).

Figure 1 - 733

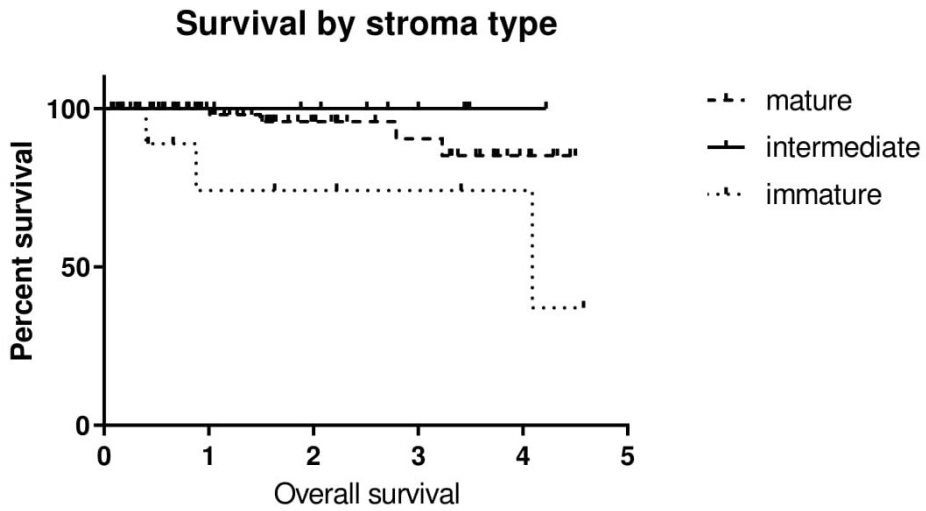

Figure 2 - 733

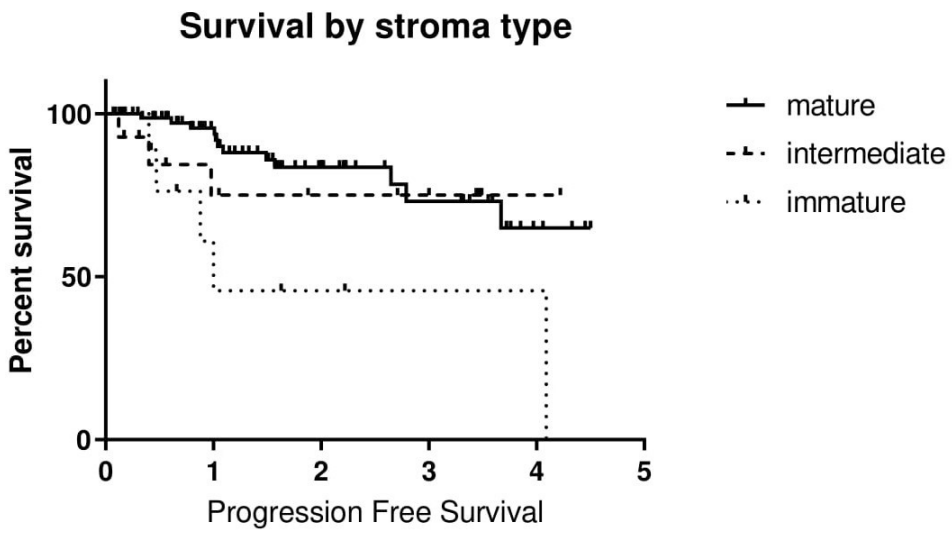

Conclusions: Our preliminary findings suggest that tumor stroma may be an important prognostic factor in neoadjuvant treated colorectal cancer and may more significantly be associated with survival than other traditional pathologic features. Further studies are necessary to explore the findings presented here.

734 Clinicopathologic Features of Varicella Zoster Virus Infection of the Upper Gastrointestinal Tract

Maria Mostyka[1], Jinru Shia[2], William Neumann[3], Christa Whitney-Miller[4], Rhonda Yantiss[5]
[1]New York-Presbyterian Weill Cornell, New York, NY, [2]Memorial Sloan Kettering Cancer Center, New York, NY, [3]Mid-Valley Pathology, Weslaco, TX, [4]University of Rochester Medical Center, Rochester, NY, [5]Weill Cornell Medicine, New York, NY

Disclosures: Maria Mostyka: None; Jinru Shia: None; William Neumann: None; Christa Whitney-Miller: None; Rhonda Yantiss: None

Background: Reactivation of latent varicella zoster virus (VZV) can lead to disseminated disease among immunocompromised patients. Upper gastrointestinal tract involvement rarely occurs in this situation and may precede onset of cutaneous manifestations. The purpose of this study is to describe the clinicopathologic features of VZV-related gastrointestinal injury to determine whether any findings facilitate its recognition.

Design: We identified 5 patients with VZV infection of the upper gastrointestinal tract: 3 had esophagitis, 1 had gastritis, and 1 had infection of both sites. Study cases were evaluated for endoscopic findings, nature of exudates, distribution of infected cells in the epithelium, and viral cytopathic features. Confirmatory VZV immunostains were performed in all cases. The features of VZV-associated esophagitis were compared with those of 18 cases of herpes simplex virus (HSV)-associated esophagitis, all of which were immunohistochemically confirmed.

Results: All patients were immunocompromised adults (mean age: 59.8 years) with hematologic malignancies, four of which were treated with stem cell transplant. Four patients presented with cutaneous disease and gastrointestinal symptoms or developed rashes following onset of gastrointestinal symptoms. All had multi-organ involvement that led to death of two patients. Endoscopic features included diffuse mucosal erythema and serpiginous ulcers; punched-out shallow ulcers typical of HSV infection were not identified in any cases. Esophageal ulcers featured fibrin-rich, pauci-inflammatory exudates, and necrotic keratinocytes. Viral cytopathic changes were present at all levels in the mucosa, especially in a peripapillary distribution (Fig. 1). In contrast, HSV-associated exudates were rich in macrophages and neutrophils ($p<0.0001$); viral cytopathic changes were most pronounced in the superficial epithelium ($p=0.003$). Hemorrhagic exudates, glandular apoptosis, and drop-out characterized VZV-related gastritis (Fig. 2).

Figure 1 - 734

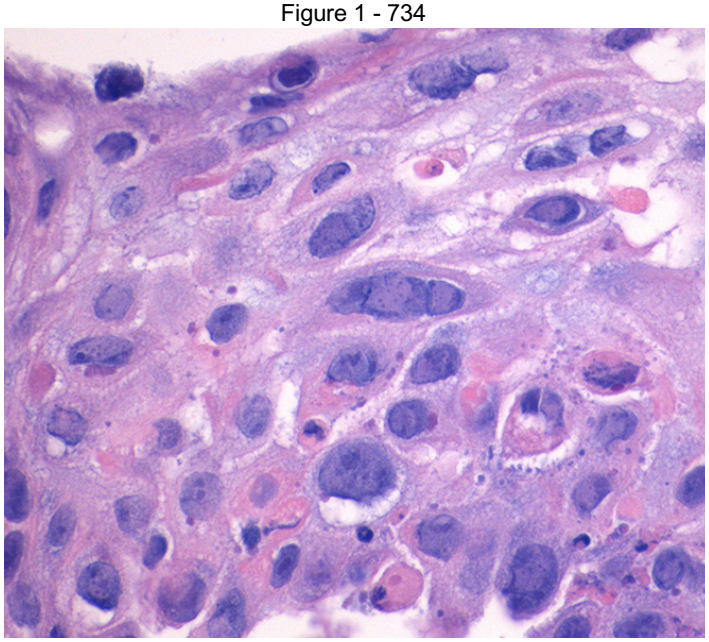

Figure 2 - 734

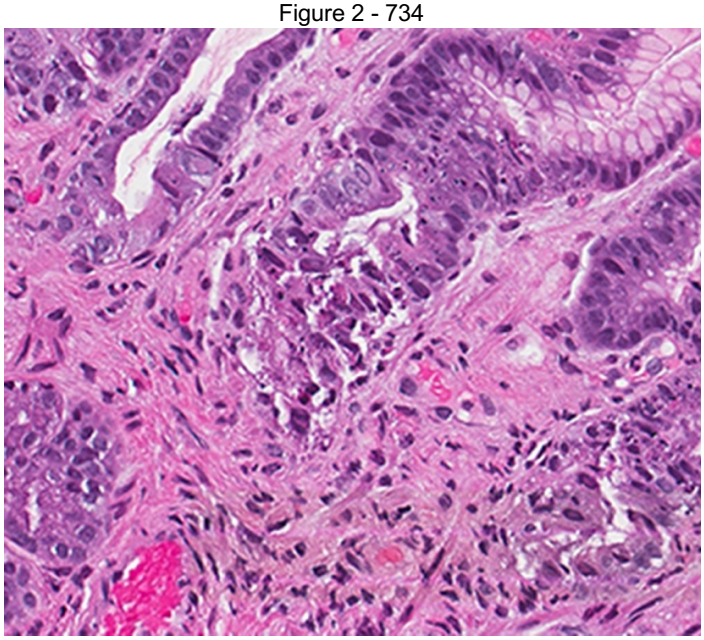

Conclusions: Gastrointestinal VZV infection produces histologic changes that simulate HSV infection and/or graft *versus* host disease. Pauci-inflammatory, hemorrhagic exudates containing necrotic epithelial cells are helpful diagnostic clues. Viral cytopathic changes occur at all levels in the squamous epithelium with a striking peripapillary distribution not seen in HSV infection. Recognition of VZV infection is important because gastrointestinal manifestations often herald potentially life-threatening disseminated disease.

735 Crohn Disease Infrequently Affects the Appendix and is a Rare Cause of Granulomatous Appendicitis

Maria Mostyka[1], Clifton Fulmer[2], Erika Hissong[3], Rhonda Yantiss[4]
[1]New York-Presbyterian Weill Cornell, New York, NY, [2]Cleveland Clinic Foundation, Cleveland, OH, [3]New York-Presbyterian/Weill Cornell Medical Center, New York, NY, [4]Weill Cornell Medicine, New York, NY

Disclosures: Maria Mostyka: None; Clifton Fulmer: None; Erika Hissong: None; Rhonda Yantiss: None

Background: Historical data suggest that approximately 10% of granulomatous appendicitis cases are due to Crohn disease. In fact, many pathologists raise the possibility of Crohn disease as a serious consideration whenever they encounter granulomatous inflammation in appendectomy specimens. We suspect that involvement of the appendiceal mucosa by Crohn disease is uncommon. Most examples of idiopathic granulomatous appendicitis occurring in the modern era are likely related to organizing inflammation in the setting of delayed (*i.e.* interval) appendectomy. The purpose of this study is to determine the prevalence of appendiceal involvement by Crohn disease among patients with established ileocolic inflammation.

Design: We reviewed 200 resection specimens, including 100 ileocolic specimens with strictured/fistulizing Crohn disease and 100 ulcerative colitis colectomy specimens. All cases were evaluated for the presence and nature of inflammatory changes in the appendix. Appendiceal findings were classified as normal, fibrous obliteration, active appendicitis (i.e. neutrophils in mucosa), chronic active appendicitis, and periappendicitis. Mural changes (e.g. lymphoid aggregates, fibrosis, sinus tracts) and granulomata were noted when present.

Results: There were no significant differences between patients with Crohn disease and ulcerative colitis with respect to patient age or sex. Involvement of the appendiceal mucosa was more common among patients with ulcerative colitis compared with Crohn disease patients (28% vs 5%, $p<0.001$). In fact, the appendix was usually normal (n=26, 26%) or showed fibrous obliteration (n=50, 50%) in Crohn disease patients. Only five (5%) cases contained epithelioid granulomata, three of which were associated with mural fibrosis and lymphoid aggregates. Eight (8%) cases with ileocolic adhesions showed only periappendiceal inflammation with sparing of the inner appendiceal layers.

Conclusions: Although the appendix may be adherent to the inflamed ileum or cecum, involvement of the appendix proper by Crohn disease occurs in only 5% of cases, always in patients with ileocolonic disease. We conclude that granulomatous inflammation in appendectomy specimens rarely reflects underlying inflammatory bowel disease, especially when patients do not have a history of Crohn disease. Interval appendectomy and infection are more important considerations when appendectomy specimens feature granulomatous and/or mural inflammation with lymphoid aggregates.

736 Incidental Tumors in Appendices and Their Outcomes: A Clinico-Pathologic Study on 1870 Appendectomies

Aysha Mubeen[1], Amal Shukri[1], Civan Altunkaynak[1], Jaime Morel[2]
[1]University of Florida College of Medicine, Jacksonville, FL, [2]University of Florida, Jacksonville, FL

Disclosures: Aysha Mubeen: None; Amal Shukri: None; Civan Altunkaynak: None; Jaime Morel: None

Background: Appendicitis is the most common cause of acute abdomen seen in the emergency room, as well as the most common reason to have an emergency surgical procedure. Although fecoliths and lymphoid hyperplasia constitute majority of causes of acute appendicitis, unusual histopathologic findings are sometimes encountered on pathologic examination of these appendices. These findings may be infections like *Enterobius vermicularis*, granulomatous inflammation, endometriosis etc. However, the more significant are the incidentally discovered tumors in appendix as these can affect the long term outcome for the patients and have potential treatment implications. Well differentiated neuroendocrine tumors(WDNET), low grade appendiceal mucinous neoplasms(LAMN) and serrated polyps are just some of the common neoplasms in appendix. Our study aims to identify the frequency of these incidentally discovered tumors in our patient population, their clinico-pathologic features and outcome.

Design: A total of 1870 consecutive appendectomies done for presumed acute appendicitis were studied. The cases with incidental tumors discovered on pathologic examination were examined in detail with regard to demographic data and pathologic findings. Follow up data were recorded whenever available. Appendectomies done as part of other surgical procedures (incidentally) were excluded.

Results: Out of 1870 appendectomies studied, 43 incidental tumors were identified (2.3% of appendectomies). WDNETs (34.9% of tumors, 0.8% of appendectomies) and LAMN had a similar frequency (**Table 1, Fig. 1 & 2**).

No residual tumor or lymph node involvement was identified in any of the follow up hemicolectomy specimens. All patients were disease free till their last follow up. The average follow up was 26 months. Twenty cases with insufficient follow up were excluded from the calculation.

Other worth noting non-neoplastic incidental findings were *Enterobius vermicularis* infections (0.3%), endometriosis (0.1%) and granulomatous appendicitis (0.1%).

PARAMETER	TOTAL NUMBER OF INCIDENTAL APPENDICEAL TUMORS (n=43)
Gender Males Females	**23/43** **20/43**
Average Age (yrs)	**58.3**
Positive Margins	**3/43 (2 WDNET and 1 Adenocarcinoma)**
Follow up Right Hemicolectomy	**5/43 (11.6%)**
Mortality rate (Dead of intercurrent disease with no recurrence of appendiceal tumor)	**2/43 (4.6%)**

Figure 1 - 736

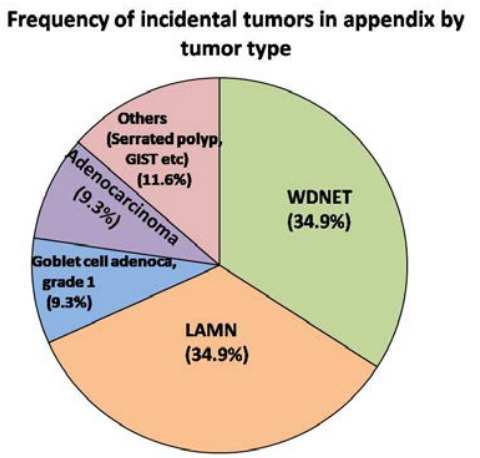

Figure 2 - 736

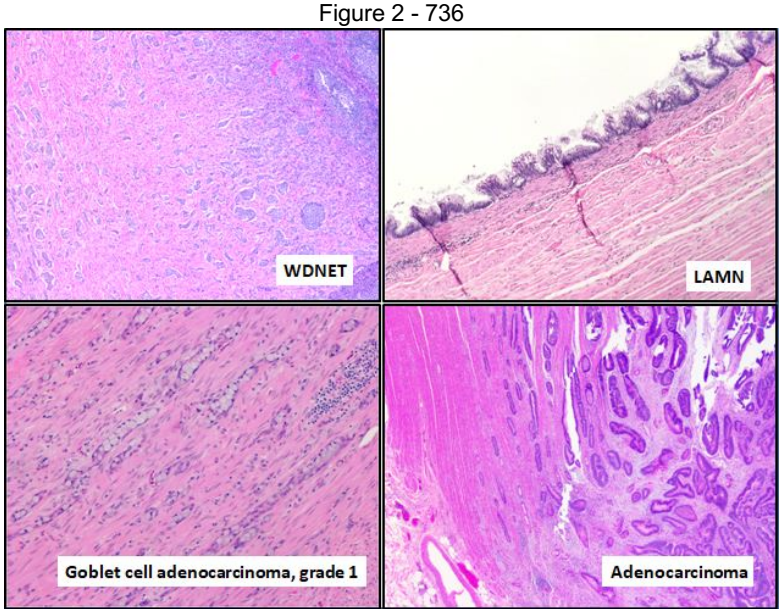

Conclusions: Appendix is a common surgical specimen whose histopathologic examination sometimes reveals a variety of tumors and non-neoplastic conditions. Appendiceal tumors are frequently recognized only on pathologic examination and may be devoid of clinical manifestations. This highlights the importance of careful sampling and pathologic examination of appendix specimens. The frequency of incidentally discovered tumors seems to be low in our patient population and the long term outcome appears good.

737 The Expression of Human Leukocyte Antigen Class I and β2-Microglobulin in Colorectal Cancer and its Prognostic Impact

Hee Young Na[1], Park Yujun[2], Hwang Hye Jung[2], Nam Soo Kyung[3], Woo Ho Kim[4], Hye Seung Lee[5]
[1]Seoul National University Bundang Hospital, Seongnam-si, Gyeonggi-do, Korea, Republic of South Korea, [2]Seoul National University Bundang Hospital, SeongNam, Gyeonggi-do, Korea, Republic of South Korea, [3]Seoul National University Bundang Hospital, SeongNam, Gyeonggi, Korea, Republic of South Korea, [4]Seoul National University Hospital, Seoul, Korea, Republic of South Korea, [5]Seoungnam-Si, Gyeonggi-do, Korea, Republic of South Korea

Disclosures: Hee Young Na: None; Park Yujun: None; Hwang Hye Jung: None; Nam Soo Kyung: None; Woo Ho Kim: None; Hye Seung Lee: None

Background: Human leukocyte antigen (HLA) class I is crucial in anti-tumoral immune responses of cancer. Impaired of HLA class I function has been postulated to be a mechanism of adaptive immune escape in various tumors, especially microsatellite instability (MSI)-high colorectal cancer (CRC). However, the frequency and prognostic impact of HLA class I and β2-microglobulin (β2M) protein expression varies among previous studies. In this study, we aimed to investigate HLA class I and β2-microglobulin (β2M) expression in MSI-high and microsatellite stable (MSS) CRCs and evaluate its prognostic impact.

Design: The representative areas from tumor center (TC) and tumor periphery (TP) from a total of 300 CRCs, including 161 MSI-high and 139 MSS cases, were chosen to construct tissue microarray. Immunohistochemistry for HLA class I, β2M, CD3, and CD8 was performed and correlation with clinicopathologic parameters was analyzed.

Results: Reduced HLA class I expression was detected in 127 (78.9%), and 120 (74.5%) at TC and TP, respectively. Reduced β2M expression was found in 81 (50.3%) at TC, and 77 (47.8%) at TP. Intact HLA class I and β2M expression was correlated with higher CD3 and CD8 positive lymphocytes infiltration (all p<0.05). Compared with MSS CRCs, MSI-high tumors were more frequently associated with downregulated HLA class I and β2M. Although reduced β2M expression was associated with higher pT stage in MSI-high CRC, there was no significant association with HLA class I and β2M expression with survival. Interestingly, reduced HLA class I and β2M expression in MSS were associated with higher stage, and reduced β2M expression remained to be an independent prognostic factor in multivariate analysis.

Table 1. Univariate and multivariated analyses in MSS colorectal cancer patients

Clinicopathologic variables	DFS			OS		
	Univariate	Multivariate		Univariate	Multivariate	
	p-value	p-value	HR (95% CI)	p-value	p-value	HR (95% CI)
Sex	0.282			0.1		
Location	0.216			0.089		
Differentiation	<0.001*	0.008*	4.472 (1.477-13.541)	<0.001*	0.022*	3.622 (1.207-10.868)
Mucin	0.591			0.978		
Lymphatic invasion	0.01*			0.005*		
Perineural invasion	0.001*			0.004*		
Venous invasion	0.001*	0.004*	2.526 (1.340-4.760)	<0.001*	<0.001*	3.162 (1.662-6.017)
pT stage	0.046*			0.068		
pN stage	0.001*			0.001*		
pM stage	<0.001*			<0.001*		
Stage	0.001*	0.003*	2.726 (1.398-5.315)	0.001*	0.014*	2.414 (1.195-4.877)
HLA class I-TC	0.028*			0.041*		
HLA class I-TP	0.005*			0.015*		
B2M-TC	0.001*			0.001*	0.015*	0.469 (0.255-0.866)
B2M-TP	<0.001*	<0.001*	0.334 (0.181-0.614)	0.004*		

Figure 1 - 737

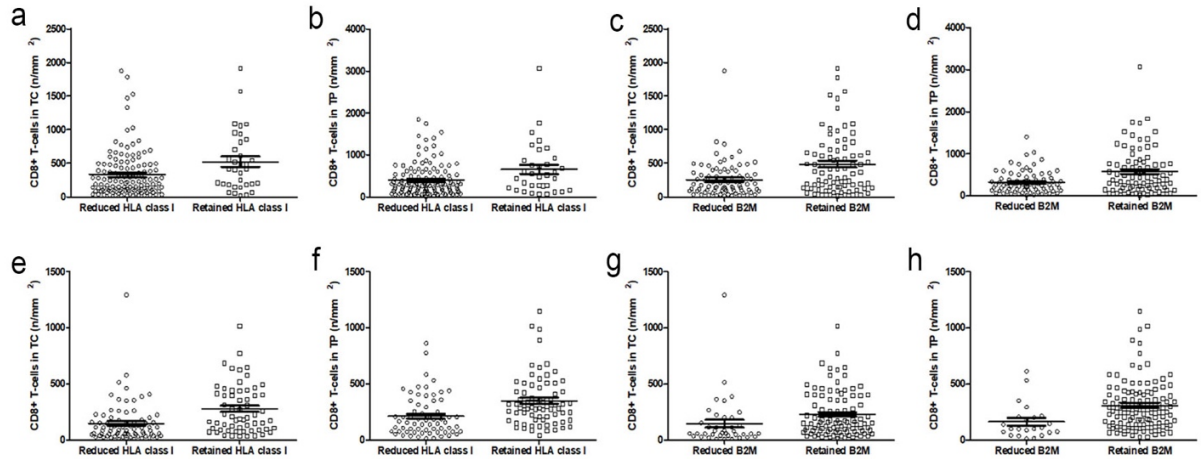

Figure 2 - 737

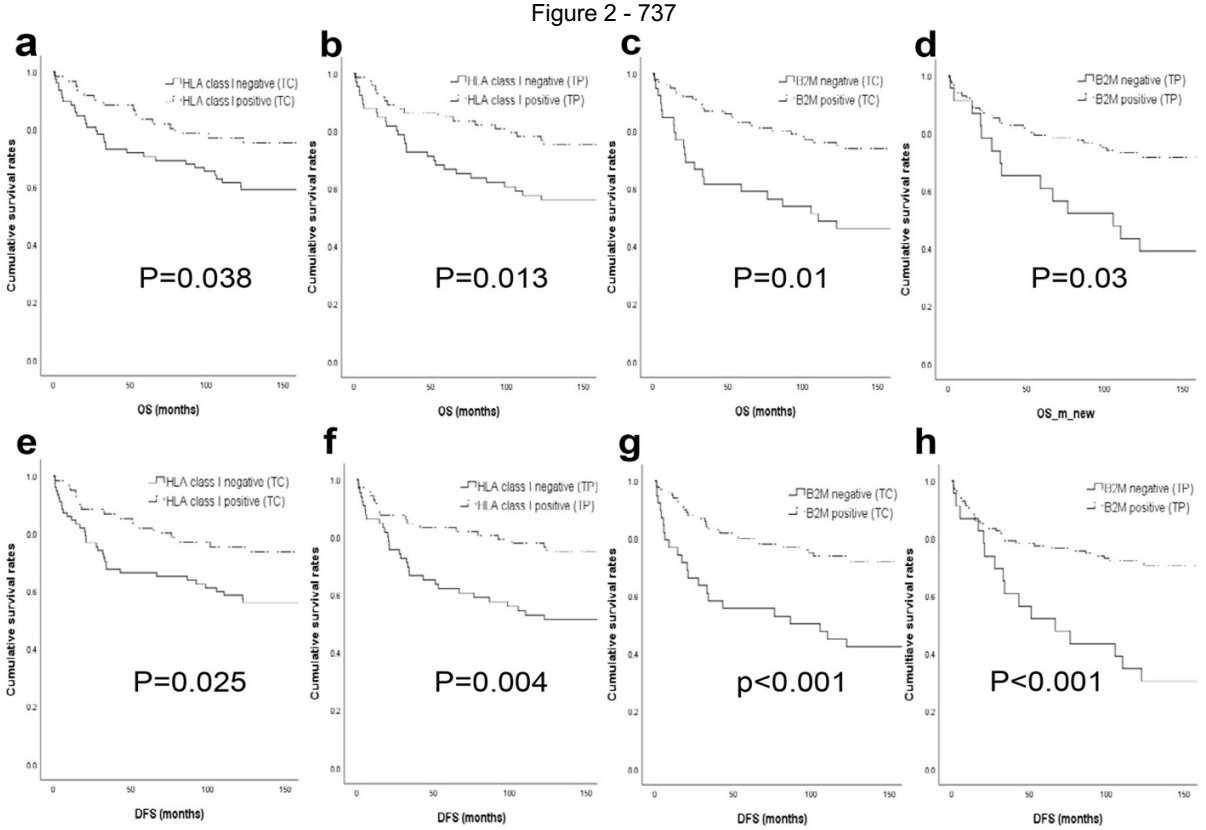

Conclusions: Reduced β2M was proved to be a reliable prognostic factor in MSS CRCs, suggesting that cell-mediated anti-tumor immune responses might play a role in MSS tumors as well as in MSI-high tumors. Further investigation on clinical responses of immunotherapy in MSI-high CRC with reduced HLA class I and β2M is needed.

738 Mcl-1 as a Potential Prognostic Biomarker in Gastric Adenocarcinoma

Teddy Nagaria[1], Jamie Lombardo[2], Wenyi Luo[1], Junsheng Ma[1], Roland Bassett[1], Dipen Maru[1], Dongfeng Tan[1]
[1]The University of Texas MD Anderson Cancer Center, Houston, TX, [2]The University of Texas MD Anderson Cancer Center, Cibolo, TX

Disclosures: Teddy Nagaria: None; Jamie Lombardo: None; Wenyi Luo: None; Junsheng Ma: None; Roland Bassett: None

Background: Gastric cancer is one of the leading causes of cancer-related deaths. Due to its heterogenous genetic profiles, treatment resistance and tumor progression remain major clinical challenges. One potent driver of tumor progression is the anti-apoptotic protein myeloid cell leukemia (Mcl-1), which regulates apoptosis by modulating mitochondrial membrane integrity. Mcl-1 has been shown to be upregulated in various cancers and is associated with tumor progression and invasion. However, systematic investigation of Mcl-1 expression in gastric adenocarcinoma is still lacking. The aim of our study is to assess Mcl-1 expression in gastric adenocarcinoma and its potential use as a prognostic biomarker.

Design: The study included 184 cases of primary gastric adenocarcinoma that were treated with surgical resection without neoadjuvant therapy at our institution between 1987 and 2006. High-density formalin-fixed paraffin-embedded tissue microarrays (TMAs) were constructed from surgical specimens. TMAs were stained for Mcl-1 by immunohistochemistry. Mcl-1 expression was assessed independently based on the intensity and extent of staining by two observers without prior knowledge of clinicopathological information. Clinicopathologic parameters in this study include age, race, gender, tumor differentiation, HER-2 expression, pathologic stage of the tumor, and survival.

Results: The median age of this study at initial diagnosis was 63.6 years (range 28.4-89.6), with the majority of patients being male (63.6%) and Caucasians (57.6%). Our data showed cases with high Mcl-1 expression level (50.4% of positive cases) were associated with worse overall survival (HR=1.47, 95%, CI: 1.02-2.11, p-value=0.038). Mcl-1 expression is also associated with advanced disease stage at initial presentation. There was no direct correlation between Mcl-1 and HER-2 expression or other clinicopathological parameters in our study. A brief summary of results is listed in Table 1.

Table 1. Multivariate Cox Analysis for Overall Survival

Variable	Category	Reference	HR	95% CI for HR	p-value
Race	Asian	Caucasian	0.70	(0.41, 1.14)	0.162
Race	Black	Caucasian	0.89	(0.48, 1,53)	0.696
Race	Hispanic	Caucasian	0.96	(0.56, 1.56)	0.863
M stage	M1	M0	4.28	(2.59, 6.93)	<0.001
Tumor diff.	Signet ring	Poor diff. (intestinal)	1.17	(0.73, 1.84)	0.512
Tumor diff.	Well/Mod. Diff.	Poor diff. (intestinal)	0.56	(0.38, 0.84)	0.004
Mcl-1 median	40-300	0-39	1.47	(1.02, 2.11)	0.038

Conclusions: Our study showed Mcl-1 is associated with shorter survival in gastric adenocarcinoma. Mcl-1 expression is also associated with advanced disease stage at initial presentation. This preliminary data underlines the role of anti-apoptotic signaling in gastric adenocarcinoma, and suggests the expression of Mcl-1 may be a prognostic biomarker. Our data also indicates the potential identification of a subset of gastric adenocarcinoma patients that may benefit from targeted Mcl-1 therapy.

739 The Prevalence and Distribution of Serrated Colorectal Polyps in Patients with Bona Fide Lynch Syndrome

Aqsa Nasir[1], Saba Yasir[2], Samar Said[2], Kandelaria Rumilla[3], Myra Wick[2], Kevin Halling[3], Katelyn Reed[2], Christopher Hartley[4], Sarah Kerr[5], Rondell Graham[2]
[1]Emory University, Atlanta, GA, [2]Mayo Clinic, Rochester, MN, [3]Mayo Clinic Rochester, Rochester, MN, [4]Medical College of Wisconsin, Milwaukee, WI, [5]Hospital Pathology Associates, PA, Minneapolis, MN

Disclosures: Aqsa Nasir: None; Saba Yasir: None; Samar Said: None; Kandelaria Rumilla: None; Myra Wick: None; Kevin Halling: None; Katelyn Reed: None; Christopher Hartley: None; Sarah Kerr: None; Rondell Graham: None

Background: Lynch syndrome (LS) is an inherited cancer syndrome characterized by tumors which display microsatellite instability. Affected individuals have an increased frequency of adenomatous polyps which are the precursors to microsatellite unstable colorectal cancer. There are very limited data on polyps with a serrated architecture in LS. The frequencies and anatomic distribution of sessile

serrated adenomas (SSA) and hyperplastic polyps (HPP) in patients with LS are unknown. It is also unknown how often patients meet diagnostic criteria for serrated polyposis syndrome and over what time period do most patients with LS develop SSA.

Design: We reviewed all of the colonoscopic biopsies from consecutive patients with bona fide LS confirmed by germline genetic testing from January 1992 - June 2018. For polyps which were not clearly SSA or HPP, they were classified as serrated polyp not otherwise specified (SP-NOS).

Results: We identified 148 patients (M:F =1:1) with a median age of 58 (range 28-89 years) who had 735 colonoscopic biopsies.

There were 187 polyps with a serrated architecture including 132 HPP, 50 SSA, and 5 SP-NOS compared to 338 adenomas and 38 adenocarcinomas. 4% of SSA showed cytologic dysplasia.70 (47%) patients had at least 1 polyp with a serrated architecture (CI 39.0%-55.7%). SSA was diagnosed in 13.5% of patients (CI 8.5%-20.1%) and HPP in 40% of the patients.

The prevalence of LS patients with at least 1 SSA reached 50% at 20 years (Fig 1) after their first colonoscopy at our institution (median age at SSA diagnosis = 63 (range 39-80)). The prevalence of any polyp with serrated architecture (HPP or SSA) reached 50% at 10 years after their first colonoscopy (Fig 2).

HPP showed a left-sided predominance (L:R = 4.5:1) while a greater proportion of SSA were right-sided (L:R = 2:1). SP-NOS were all right-sided, where that information was available.

One patient (0.4%) met the criteria for the serrated polyposis syndrome (SPS) while another patient had >5 SSA proximal to the sigmoid colon but the endoscopic sizes were unavailable.

Figure 1 - 739

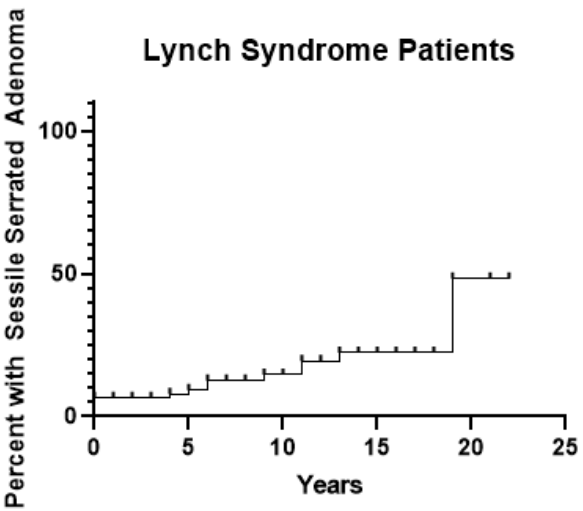

Figure 2 - 739

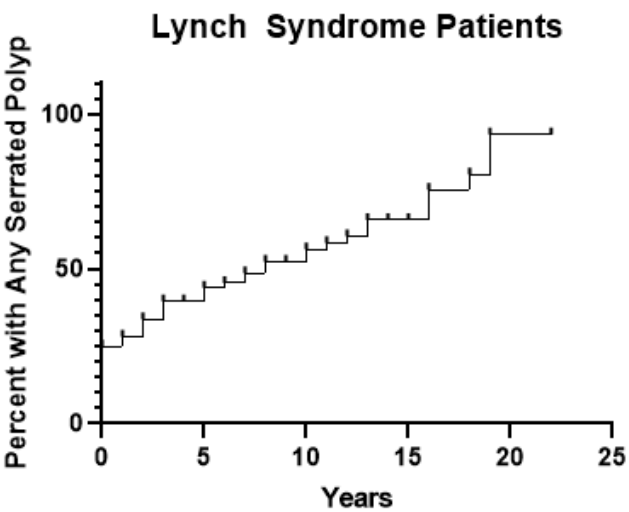

Conclusions: Our data from a large consecutive series of patients with LS show that the prevalence of SSA is greater than 2-8% quoted for the average-risk population. Also, our data show that half of LS patients will develop an SSA by 20 years post index colonoscopy and if total colectomy is not performed, patients with LS can expect to develop SSA at a median age of 63. These data are relevant for counseling patients and relatives with LS.

740 Incidental Findings in Hemorrhoidectomy Specimens: What to Expect When You are Not Expecting!

Pooja Navale[1], Raul Gonzalez[1], Monika Vyas[2]
[1]Beth Israel Deaconess Medical Center, Boston, MA, [2]Beth Israel Deaconess Medical Center, Harvard Medical School, Newton MA, MA

Disclosures: Pooja Navale: None; Raul Gonzalez: None; Monika Vyas: None

Background: Hemorrhoidectomy specimens serve as an excellent resource for study of incidental anal pathology. The likelihood of detection of certain incidental findings, such as anal intraepithelial neoplasia (AIN) and associated malignancy, largely depends on the

patient population. The aim of this study was to describe the spectrum of incidental findings in hemorrhoidectomy specimens and recognize the likelihood of AIN detection in the patient population served at a large academic center.

Design: Our departmental pathology database was queried for all hemorrhoidectomy specimens received over a 16-year period (2003-2019). All cases with incidental clinically significant diagnoses, in addition to hemorrhoids, were included. Patient demographic data (age and sex) and significant clinical history (HIV status; presence of warts, squamous intraepithelial neoplasia, or malignancy) were recorded from clinical notes.

Results: We identified incidental clinically significant findings in 74/1612 (4.5%) specimens, from 44 males and 30 females (average age: 46.7 years). Most (58, 78%) were squamous lesions (56 AIN, 1 invasive squamous cell carcinoma, 1 verrucous carcinoma). The rest included 5 non-squamous malignancies and 11 benign findings (details in Table, examples in Fig. 1). Analyzing trends over time, while the detection of LSIL (low-grade squamous intraepithelial lesion, including AIN1 and condyloma) remained steady, there was a recent, sustained spurt in detection of HSIL (high-grade squamous intraepithelial lesion, AIN2/3) (Fig. 2). There were more cases with HSIL (2.6% of total) than cases only with LSIL (0.8%). The HSIL group consisted of 30 males and 12 females. Of the 58 patients with squamous lesions, 22 (21 males, 1 female) were known to be HIV-positive, while 15 (11 males, 4 females) were HIV- negative; HIV status was unknown in 21. Two males with squamous lesions had a history of penile warts, and 5 females had history of gynecologic squamous lesions. P16 and/or Ki67 immunohistochemistry aided in the diagnosis of incidental AINs in 17/56 cases (30%).

Incidental histologic finding	Females (n=30)	Males (n=44)	Total (n=74)
LSIL (AIN-1/condyloma)	7	7	14 (18.9%)
HSIL (AIN2/3)	12	30	42 (56.7%)
Squamous cell carcinoma	0	1	1 (1.3%)
Verrucous carcinoma	0	1	1 (1.3%)
Adenocarcinoma	1	1	2 (2.7%)
Poorly differentiated neuroendocrine carcinoma	0	1	1 (1.3%)
Poorly differentiated adenocarcinoma with neuroendocrine features	1	0	1 (1.3%)
Melanoma	1	0	1 (1.3%)
Melanocytic nevi	2	2	4 (5.4%)
Genital lentiginosis	1	0	1 (1.3%)
Sessile serrated adenoma	1	0	1 (1.3%)
Tubular adenoma	1	0	1 (1.3%)
Angiokeratoma	1	0	1 (1.3%)
Granulomas	1	0	1 (1.3%)
Sexually transmitted infectious colitis (Chlamydia-associated)	0	1	1 (1.3%)
Hypersensitivity reaction	1	0	1 (1.3%)

Figure 1 - 740

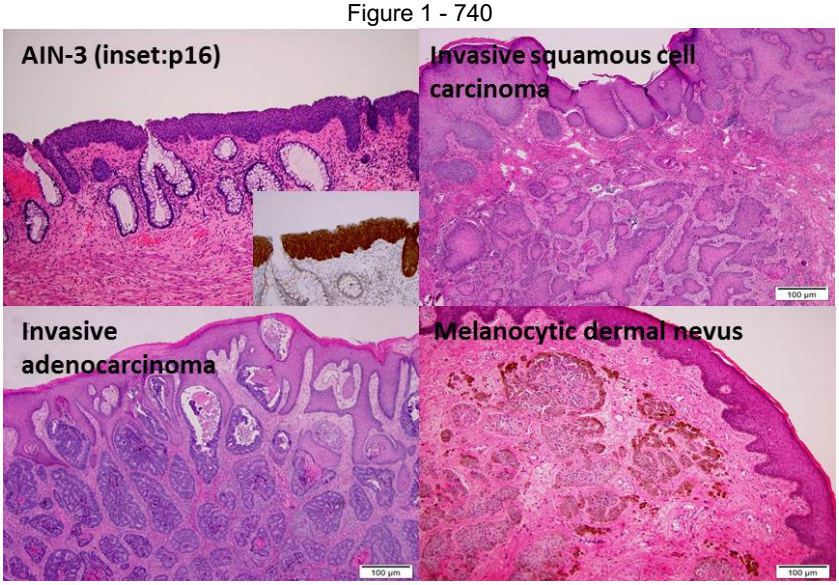

Figure 2 - 740

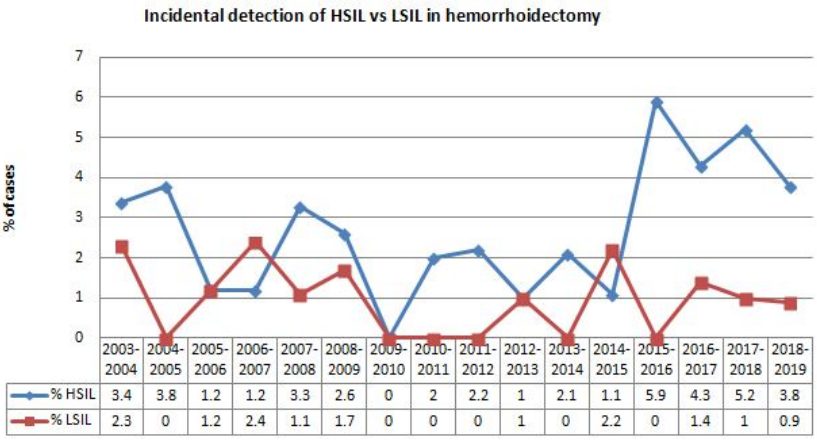

	2003-2004	2004-2005	2005-2006	2006-2007	2007-2008	2008-2009	2009-2010	2010-2011	2011-2012	2012-2013	2013-2014	2014-2015	2015-2016	2016-2017	2017-2018	2018-2019
% HSIL	3.4	3.8	1.2	1.2	3.3	2.6	0	2	2.2	1	2.1	1.1	5.9	4.3	5.2	3.8
% LSIL	2.3	0	1.2	2.4	1.1	1.7	0	0	0	1	0	2.2	0	1.4	1	0.9

Conclusions: Significant incidental findings were detected in 4.5% of the hemorrhoidectomy specimens examined at our institution, supporting routine histological examination of all such cases. While our overall incidence of incidental AIN detection is similar to prior studies, we noted a recent surge of HSIL at our institution. Pathologists need to be cognizant of such trends, especially if their patient population includes high-risk groups.

741 LGR5 in Barrett's Esophagus and its Utility in Predicting Patients at Increased Risk of Advanced Neoplasia

Azfar Neyaz[1], Robert Odze[2], Deepa Patil[3], Vikram Deshpande[4]
[1]Massachusetts General Hospital, Malden, MA, [2]Boston, MA, [3]Brigham and Women's Hospital, Boston, MA, [4]Massachusetts General Hospital, Boston, MA

Disclosures: Azfar Neyaz: None; Robert Odze: None; Deepa Patil: None; Vikram Deshpande: *Grant or Research Support*, Advanced Cell Diagnostics; *Advisory Board Member*, Viela; *Grant or Research Support*, Agios pharmaceuticals

Background: Leucine-rich repeat-containing G-protein-coupled receptor 5 (LGR5) is a known intestinal stem cell marker. LGR5 is overexpressed in Barrett's esophagus and related neoplasia. There is a growing interest in identifying patients with Barrett's esophagus with a high risk of advanced neoplasia. We evaluated the value of LGR5 in predicting dysplasia in patients with BE.

Design: We analysed 131 patients including biopsies from normal gastroesophageal mucosa, BE with or without dysplasia and invasive adenocarcinomas for LGR5 using RNA in situ hybridization. This included patients who progress to high-grade dysplasia or

adenocarcinoma (progressor group) and those that did not progress (non-progressor group) (mean follow-up of 13.2 years). The LGR5 stain was evaluated qualitatively, semi-quantitatively and quantitatively on an automated platform.

Results: Aberrant surface LGR5 expression was exclusively seen in dysplastic BE (66.7%). In contrast to non-dysplastic BE, low-grade (LGD) and high-grade dysplasia (HGD) showed significantly higher percentage of LGR5-positive crypts (p=0.0001) and increased LGR5 transcripts per cell (p=0.0001). The percentage of positive crypts and LGR5 transcripts/cells was also significantly higher in non-dysplastic BE from progressors as compared to non-progressors (p<0.0001 and p=0.014). The sensitivity and specificity of LGR5 in distinguishing non-dysplastic progressor from non-progressor biopsies were 50% and 87%, respectively (table 1).

LGR5 Parameters	Benign vs Dysplasia/Adenocarcinoma			
	Sensitivity	Specificity	PPV	NPV
LGR5 positive crypts per HPF ≥50%	84%	94%	97%	73%
LGR5 transcripts per cell ≥6	73%	87%	92%	59%
LGR5 surface involvement	63%	100%	100%	55%
LGR5 positive crypts per HPF (>50%) OR LGR5 transcripts per cell =>6 OR LGR5 surface involvement	95%	82%	92%	88%

Conclusions: BE-related neoplasia shows an expansion of the LGR5 positive cellular compartment, supporting its role as a stem cell marker in this context. Increased LGR5 expression and surface reactivity: 1) are objective tools in the diagnosis of BE-related neoplasia and, 2) predict risk for progression to advanced neoplasia.

742 Automated Analysis of p53 Immunohistochemistry in Patients with Barrett's Esophagus Predicts Disease Progression to Advanced Neoplasia

Azfar Neyaz[1], Robert Odze[2], Deepa Patil[3], Vikram Deshpande[4]
[1]Massachusetts General Hospital, Malden, MA, [2]Boston, MA, [3]Brigham and Women's Hospital, Boston, MA, [4]Massachusetts General Hospital, Boston, MA

Disclosures: Azfar Neyaz: None; Robert Odze: None; Deepa Patil: None; Vikram Deshpande: *Grant or Research Support*, Advanced Cell Diagnostics; *Advisory Board Member*, Viela; *Grant or Research Support*, Agios Pharmaceuticals

Background: There are currently no validated markers to predict Barrett's esophagus (BE) patients at a high risk of progressing to advanced neoplasia (high-grade dysplasia and adenocarcinoma). *TP53* mutation is highly recurrent in esophageal adenocarcinomas and is also detected in patients with non-dysplastic BE, predominantly those that progress to advanced neoplasia. We investigated the utility of p53 immunohistochemistry in predicting advanced neoplasia in patients with BE. To circumvent the challenges associated with manual assessment we performed automated image analysis.

Design: The progressor cohort was comprised of 89 patients, 43 (48%) progressed to high-grade dysplasia and 46 (52%) to adenocarcinoma. We evaluated 106 non-dysplastic biopsies from this group; the mean duration between the non-dysplastic biopsy and the biopsy with dysplasia/adenocarcinoma was 3.4 years. The control cohort (non-progressor) was comprised of 129 patients with a mean follow-up of 9.6 years. The absence of dysplasia in both the progressor and non-progressor cohorts was confirmed by 3 experienced gastrointestinal pathologists that were blinded to the immunohistochemistry results. p53 immunohistochemistry was performed (DAKO, clone D019, 1:250). Regions of interest were annotated, and the nuclear staining was categorized using the Visiopharm automated image analysis platform into 3 classes: 1+, 2+ and 3+. 3+ reactivity mirrored the reactivity seen in the basal portion of squamous epithelium. Receiver Operating Characteristics (ROC) curve was used to identify optimal cut-points between the progressor and non-progressor cohort.

Results: p53 nuclear reactivity was noted in both the progressor and non-progressor groups, however, there were significant differences in numbers of 3+ and 2+ p53 positive epithelial cells between the two cohorts (p <0.0001) (table1). At a cut point of ≥10 cells 3+ cells, p53 immunohistochemistry predicted progression to advanced neoplasia with a sensitivity and specificity of 49% and 92%, respectively.

Clinical and p53 scoring parameters	BE Non-progressor biopsies (n=129)	BE Progressor biopsies (n=106)
Male/Female ratio	1.6:1	6.4:1
Mean age in years	56.1	62.8
Mean Length of Barrett's epithelium in cm	3.6	5.0
Mean follow-up	9.6 years	3.4 years
Mean 3+ positive p53 epithelial cells (SD, Median, Range)	5.0 (21.3, 1, 0-238)	290.8 (844.5, 9, 0-7189)
3+ positive p53 epithelial cells < 5 cells ≥ 5 cells	102 (79.1 %) 27 (20.9 %)	42 (39.6 %) 64 (60.4 %)
3+ positive p53 epithelial cells < 10 cells ≥ 10 cells	119 (92.2%) 10 (7.8%)	54 (50.9%) 52 (49.1%)
Mean 2+ positive p53 epithelial cells (SD, Median, Range)	122.6 (176.9, 68, 0-962)	747.8 (1028.6, 339, 0-4999)
2+ positive p53 epithelial cells < 50 cells ≥ 50 cells	58 (45.0%) 71 (55.0%)	15 (14.2%) 91 (85.8%)
2+ positive p53 epithelial cells < 150 cells ≥ 150 cells	96 (74.4%) 33 (25.6%)	30 (28.3%) 76 (71.7%)
P53 3+ positive cells (≥ 10 cells) OR 2+ positive cells (≥ 150 cells) No Yes	94 (72.9%) 35 (27.1%)	29 (27.4%) 77 (72.6%)

Conclusions: Quantitative analysis of p53 immunohistochemistry in non-dysplastic BE biopsies can help identify patients at a high risk of advanced neoplasia. Patients with Barrett's esophagus showing strong reactivity for p53 in the glandular compartment should be placed in an accelerated screening program.

743 Over-expression of Programmed Death Ligand 1 (PD-L1) in Refractory Inflammatory Bowel Disease (IBD): Implication in Pathogenesis

Jessica Nguyen[1], Brian Finkelman[1], Yue Xue[1], Guang-Yu Yang[2], Kristy Wolniak[3], Maryam Pezhouh[1]
[1]Northwestern University Feinberg School of Medicine, Chicago, IL, [2]Northwestern University, Chicago, IL, [3]Northwestern University, Evanston, IL

Disclosures: Jessica Nguyen: None; Brian Finkelman: None; Yue Xue: None; Guang-Yu Yang: None; Kristy Wolniak: None; Maryam Pezhouh: None

Background: PD-L1 is critical in suppression of activated T cell responses and immune homeostasis. PD-L1 dysregulation has been implicated in chronic inflammatory diseases, but the role of PD-L1 in regulation of intestinal mucosa inflammation is unclear. The aim of this study was to assess PD-L1 expression in patients with refractory IBD compared to controls.

Design: Our cohort includes surgically resected colonic specimens from 30 patients with refractory ulcerative colitis (UC) and 30 patients with refractory Crohn's disease (CD). Representative sections of 25 colectomy specimens from patients with no history of IBD were included as controls. PD-L1 expression was assessed in both inflammatory cells and colonic epithelium on a representative block from each specimen using anti-PD-L1 antibody (E1L3N®) XP® Rabbit mAb (Cell Signaling Technology Inc). Inflammatory activity was scored as none, mild <50% of crypts involved, moderate = >50% of crypts involved and severe when ulcerated. PD-L1 expression was scored as a percentage and categorized as follows: 0 = 0%, 1 = ≥1%, 2 = ≥10%, 3 = ≥25%, and 4 = ≥50%. The location of the inflammatory infiltrate expressing PD-L1 was scored as either subepithelial or throughout the lamina propria.

Results: Refractory UC cases showed significantly higher PD-L1 expression in the colonic epithelium (mean 22%, 70% score 2+) compared to CD (mean 5%, 23% score 2+) and controls (mean <1%, 0% score 2+; both P<0.001). Refractory UC group showed similar PD-L1 expression in the inflammatory infiltrate (mean 29%, 90% score 2+) to CD (mean 27%, 87% score 2+), and both showed higher expression than controls (mean 7%, 32% score 2+; both P<0.001). Location of inflammatory infiltrate expressing PD-L1 was more commonly dispersed throughout the lamina propria in UC (83%) compared to CD (57%) or the control group (4%; overall P<0.001). Among IBD cases of either type, higher activity scores were associated with higher levels of PD-L1 expression in both the colonic epithelium (P<0.001) and the inflammatory infiltrate (P<0.05).

Conclusions: Interestingly, PD-L1 was upregulated in colonic epithelium of UC patients as compared to CD or control group and in the inflammatory infiltrate of both UC and CD. These findings implicate a role for PD-L1 in the dysregulation of the immune response in refractory IBD. Further studies are warranted to better understand the role of immune regulatory pathways in refractory IBD. Further studies are warranted to better understand the role of immune regulatory pathways in refractory IBD.

744 Distinct Metabolic Signatures in Colonic Serrated Lesions and Adenoma

Recep Nigdelioglu[1], Shaun Boyes[1], Robert Hamanaka[2], Gokhan Mutlu[3], Yihong Ma[4], Stefan Pambuccian[1], Xianzhong Ding[5]
[1]Loyola University Medical Center, Maywood, IL, [2]The University of Chicago Medicine, Chicago, IL, [3]The University of Chicago, Chicago, IL, [4]Loyola University Medical Center, Hinsdale, IL, [5]Loyola University Medical Center, Northbrook, IL

Disclosures: Recep Nigdelioglu: None; Shaun Boyes: None; Robert Hamanaka: None; Gokhan Mutlu: None; Yihong Ma: None; Stefan Pambuccian: None; Xianzhong Ding: None

Background: Colorectal cancer is a rather heterogeneous disorder. The two main carcinogenic pathways, the conventional adenoma-carcinoma pathway involving tubular adenomas and the serrated pathways involving serrated precursor lesions, result in colorectal cancers with distinct molecular background and clinicopathological manifestations. In addition to molecular alterations, cellular metabolism can also be reprogrammed in neoplasms. While it is known that glycolytic genes, including branching serine and glycine *de novo* biosynthetic pathways, are upregulated in a variety of human cancers, cellular metabolism alterations have not been previously studied in precursor lesions of colorectal cancer. Phosphoglycerate dehydrogenase (PHGDH), the first enzyme in the serine glycine *de novo* pathway has been found to be upregulated in various cancers. Here, we investigated the potential diagnostic value of alterations in PHGDH protein expression in colorectal polyps.

Design: We retrieved 56 cases of colorectal polyp specimens diagnosed from January 2018 to June 2019, including 6 hyperplastic polyps (HP), 13 tubular adenomas (TA), 12 sessile serrated lesions/polyps (SSL), 11 sessile serrated lesions with cytological dysplasia (SSL-D), 9 traditional serrated adenomas (TSA), and 5 colorectal adenocarcinomas (CRA). Immunohistochemical staining for PHGDH was performed and the expression intensities were scored as 0, 1+, 2+ and 3+ along with percentage of positive cells. The results were analyzed by one-way ANOVA and $p<0.05$ was considered significant.

Results: PHGDH was not or only minimally expressed (0-1+) in normal colonic mucosa, HP, TSA and SSL (Figure 1A). PHGDH was markedly upregulated in TA (Figure 1C), SSL-D (Figure 1B) and CRA ($p<0.0001$) (Figure 1A and 1D). The differences in PHGDH expression between SSL and SSL-D were statistically significant ($p<0.0001$) (Figure 1A). Additionally, PHGDH protein was highly expressed in desmoplastic stromal fibroblasts.

Figure 1 - 744

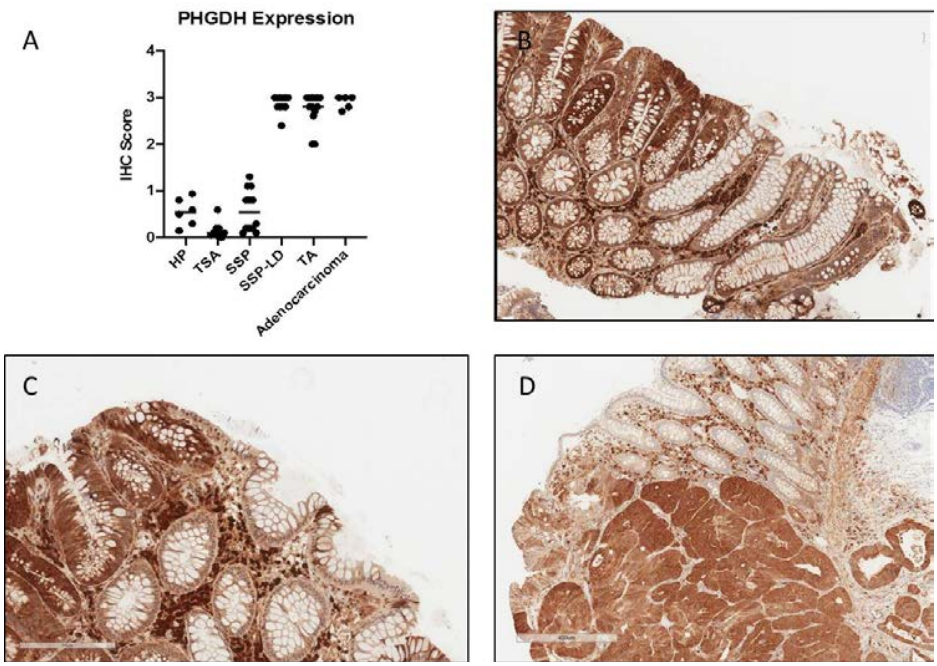

Conclusions: We found significant differences in metabolic alternations of different precursor lesions of colorectal cancer. PHGDH can be a valuable marker for diagnosing cytological dysplasia in sessile serrated lesion/polyp. More importantly, PHGDH can be a potential new therapeutic target for prevention of colorectal adenoma-carcinoma progression.

745 A Histological Analysis of Laparoscopic Sleeve Gastrectomy Specimens and a Cost Benefit Analysis of Microscopic Examination

Klaudia Nowak[1], Kenny Chieu[2], Runjan Chetty[2], Stefano Serra[3], Adam Di Palma[2], Fayez Quereshy[2], Timothy Jackson[2], Allan Okrainec[2]

[1]Toronto General University Health Network, Toronto, ON, [2]University Health Network, Toronto, ON, [3]University Health Network, University of Toronto, Toronto, ON

Disclosures: Klaudia Nowak: None; Kenny Chieu: None; Runjan Chetty: None; Stefano Serra: None; Adam Di Palma: None; Fayez Quereshy: None; Timothy Jackson: None; Allan Okrainec: *Speaker*, Ethicon; *Speaker*, Medtronic; *Speaker*, Merck

Background: In 2016 the WHO reported more than 1.9 billion adults, 18 years and older, were overweight and of these over 650 million were obese. Alternatives to medical management of obesity include a Roux-en-Y gastric bypass and laparoscopic sleeve gastrectomy (LSG). LSG represents one of the most commonly performed bariatric procedures and, in contrast to the Roux-en-Y gastric bypass, produces a specimen for pathologic examination. The aim of the study is to provide the range of pathology seen and determine the cost benefit analysis of histological examination of sleeve gastrectomy specimens.

Design: All LSG cases performed at an academic centre in Toronto, Ontario between 2010 and 2019 were reviewed. All pathology reports were reviewed, and the number of sections taken in each case, the gross descriptions, and the final diagnosis were noted. The cost of each block sampled was based on the average time (approximately 15-20 minutes per case) for a pathologists' assistant to examine the gross specimen (including patient chart review for indication of the surgery and to exclude co-morbidity, inspection, measurement, dictation of the gross report and sampling) as well as the cost of processing, cutting and staining a routine block. This was averaged out to $15.50 per block based on the hourly rates of pay and cost of consumables. The hourly rate for pathologists is $135 per hour.

Results: 558 patients, (females n= 426, males n= 132) with an average age of 48.4 years, underwent LSG from 2010 to 2019. Specimens often demonstrated more than one histological diagnosis. The most common histopathological diagnoses included no abnormal findings (45.9 %), proton pump inhibitor related changes (24.0%), and gastritis (18.5%). Abnormal findings warranting a change in postoperative management or follow-up were discovered in 4.7 % of specimens. An overall total of 6 out of 558 cases (1.1 %) were not identified on gross and warranted a change in post-operative management. The overall cost of processing (2648 blocks*) and examining LSG specimens amounted to $59, 877.

*excludes signet ring adenocarcinoma (72 blocks)

Table 1. Summary of Demographics and Findings

Diagnosis*	Number of Females	Number of Males	Average age	Number of Specimens	Percentage of Specimens
No significant abnormalities	201	55	46.8	256	45.9%
PPI related change	107	41	50.1	148	26.5%
Gastritis	80	23	48.5	103	18.5%
Lymphoid aggregates	30	13	46.9	43	7.7%
Fundic gland polyps	18	5	53.9	23	4.1%
GIST	6	3	55.4	9	1.6%
Other	14	2	48.6	16	2.9%
Helicobacter pylori	6	1	46.3	7	1.3%
Intestinal metaplasia	4	3	54.1	7	1.3%
ECL hyperplasia	5	1	56.3	6	1.1%
Neuroendocrine Tumor	1	0	56	1	0.2%
Signet ring carcinoma	1	0	50	1	0.2%

*Specimens often had more than one diagnosis; ECL= Enterochromaffin like cells; GIST = gastrointestinal stromal tumor; PPI = proton pump inhibitor; Other= reactive gastropathy, reactive changes, foreign body reaction, and ischemic changes

Conclusions: 4.7 % of LSG specimens had findings requiring a change in postoperative management. This dropped to 1. 1% when diagnoses were known preoperatively and grossly identified lesions were excluded. Our findings suggest that LSG specimens should be a gross only specimen. However, sections should be submitted for microscopic analysis if grossly evident lesions are present.

746 The Prevalence of Defective Mismatch Repair Proteins (MLH1, MSH2) Positivity Expression in Colorectal Carcinoma Patients at Federal Medical Centre Owerri, Nigeria: A Five Year Retrospective Study (2010-2014)

Juliet Nwokorie[1], Fatimah Abdulkareem[2], Nicholas Awolola[3]
[1]Federal Medical Center, Owerri, imo, Nigeria, [2]Lagos University Teaching Hospital, Surulere, Lagos, Nigeria, [3]Lagos University Teaching Hospital, Lagos, Nigeria

Disclosures: Juliet Nwokorie: None

Background: Colorectal cancer results from accumulation of genetic and epigenetic alterations that lead to uncontrolled growth of colonocytes, the cells linning the colon and rectum. Several pathways have been studied about the molecular pathogenesis of colorectal carcinoma which include Chromosomal Instability (CIN) Pathway, CpG island methylated phenotype (CIMP), Landscaper Pathway, and microsatellite instability pathway. Microsatellite instability (MSI) is a molecular fingerprint of a deficient mismatch repair system with about 15% of colorectal cancers being characterized by genomic microsatellite instability. A clinical and molecular profile of MSI tumours have been described, leading to concept of an MSI phenotype in colorectal carcinoma with studies confirming that MSI tumors have a better than microsatellite stable CRC.

Design: This is a retrospective study of all histologically diagnosed colorectal carcinoma cases diagnosed in the department of pathology at Federal Medical Center Owerri Imo Nigeria, it included referral of tissue blocks sent to our department for second opinion. Biodata and information about patients were extracted from the referral forms. Genetic testing was not done and as such patients consent was not gotten. Tissue blocks were sectioned at 3 microns, stained with H&E and subjected to Immunohistochemistry using MLH1 and MSH2 antibodies using Thermor - Fisher Scientific Ultra and Quanto Detection Kit. Nuclear MLH1/MSH2 immunostaining of tumour cells were considered positive and microsatellite stable (MSS), whereas tumour negative for both or either MLH1 /MSH2 were considered as microsatellite unstable. Positive nuclear staining of lymphocytes served as internal control.

Results: sixty (60) tissue blocks met the inclusion criteria. biopsy constituted 37 (62%) while resections were 23 (38%). Age range was 27 to 89 years, a male to female ratio of 1.4:1, mean age of 54.2 years and median of 54.2 years. adenocarcinoma was the most predominant histological type 43/60 (72%). 23/60 (38%) of the tumour showed microsatellite instability. 63% of the MSI cases were seen in age less than 50 years, 8/23 (78%) were located on the right side of the colon and were mainly of mucinous carcinoma.

Conclusions: microsatellite instability accounted for 38% of our cases. this is almost in keeping with the values gotten from other parts of Nigeria 43%; 34.5% and in Ghana 41% an African -American 30.5%. testing for MSI status should be made a routine.

747 Pattern of INSM1 Expression Distinguishes Well-Differentiated Neuroendocrine Tumors of the Terminal Ileum

Nkechi Okonkwo[1], Allison Zemek[2], Teri Longacre[3], Gregory Charville[4]
[1]Stanford Hospital and Clinics, Mountain View, CA, [2]SCPMG, Downey, CA, [3]Stanford University, Stanford, CA, [4]Stanford University School of Medicine, Stanford, CA

Disclosures: Nkechi Okonkwo: None; Allison Zemek: None; Teri Longacre: None; Gregory Charville: None

Background: Insulinoma-associated protein 1 (INSM1) is a transcription factor involved in the development of diverse neuroepithelial tissues. INSM1 has been fairly recently described as a marker of neuroendocrine differentiation in a broad spectrum of malignancies. Given fairly limited data on the characteristics of INSM1 expression in well-differentiated neuroendocrine tumors (WD-NETs) of gastroenteropancreatic origin, we applied anti-INSM1 immunostaining to a large cohort of such cases from a single institution.

Design: INSM1 expression was analyzed in a total of 268 WD-NETs of pancreatic (153), gastric (25), terminal ileum (TI; 66), and duodenal (24) origin. Tumors were represented as triplicate, duplicate, or single 1-mm cores. Immunohistochemistry (IHC) for INSM1 (Clone A-8, Santa Cruz Biotechnology) was performed on a Leica BOND platform at 1:200 dilution following antigen retrieval with BOND Epitope Retrieval Solution 2. IHC studies were reviewed and scored by 2 gastrointestinal pathologists. Intensity of anti-INSM1 staining was approximated semi-quantitatively using a scale akin to that used for estimation of estrogen receptor expression in breast carcinoma: 1+ (weak but detectable above control), 2+ (distinct), and 3+ (strong). The percentage of neoplastic cells with nuclear immunoreactivity was also recorded. Tumors were considered “positive” for INSM1 expression if there was >5% immunoreactivity of any intensity.

Results: INSM1 expression was positive in 73% of TI NETs (48/66), 93% of pancreatic NETs (142/153; $P < 0.001$ vs. TI), 96% of gastric NETs (24/25; $P = 0.019$ vs. TI), and 92% of duodenal NETs (22/24, $P = 0.084$ vs. TI). Among TI cases positive for INSM1 expression, 77% (37/48) showed no more than 1+ immunoreactivity, while only 24% of pancreatic (34/142; $P < 0.001$), 17% of gastric (4/24; $P < 0.001$), and 5% of duodenal tumors (1/22; $P < 0.001$) exhibited staining at the 1+ threshold. By Ki67 immunohistochemistry, Grade 2 NETs accounted 6% of INSM1-negative and 10% of INSM1-positive TI cases.

Figure 1 - 747

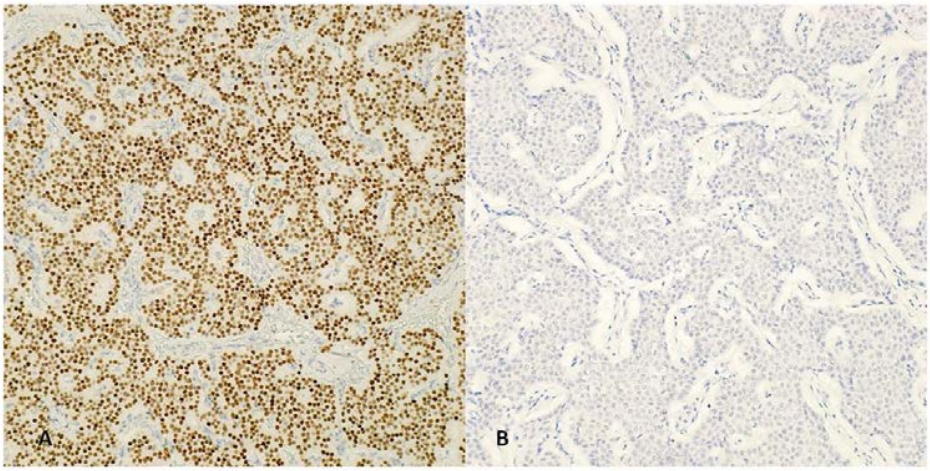

Figure 1. Representative immunohistochemical examination of well-differentiated neuroendocrine tumors (A, INSM1-positive; B, INSM1-negative;) original magnification X 200.

Conclusions: Our findings from a large cohort of gastroenteropancreatic WD-NETs confirm that identification of INSM1 expression by IHC is a sensitive marker of neuroendocrine differentiation. Surprisingly, WD-NETs arising in the TI exhibited a distinctive pattern of generally diffuse but weak immunoreactivity that largely distinguished these tumors from their counterparts arising in the stomach and pancreas. A substantial minority of TI NETs is negative for INSM1 expression, making this a somewhat less<

748 Histomorphologic and Clinical Features of Syphilitic and Chlamydia Proctitis

Maria C. Olave[1], Andrea Barbieri[1]
[1]*Yale University, New Haven, CT*

Disclosures: Maria C. Olave: None; Andrea Barbieri: None

Background: A reemergence of syphilis and chlamydia with a global increase in the incidence of sexually transmitted infections (STI) has been reported in the last decades. Syphilitic and chlamydia proctitis are relatively uncommon manifestations, with most cases reported in HIV positive men who practice receptive anal intercourse. Given the importance of recognizing and excluding STI as an etiology of proctitis, the aim of this study was to compare the histomorphologic features of syphilitic and chlamydia proctitis and inflammatory bowel disease (IBD).

Design: The syphilitic/chlamydia proctitis group included 8 patients with confirmed diagnoses of syphilis (n=6), chlamydia (n=1) and syphilis and chlamydia co-infection (n=1) with positive immunostains (*T. pallidum* and/or *Chlamydia*). All patients had clinical confirmation of the disease and follow up. All infectious cases were compared with patients matched for age, sex and site with diagnosis of established IBD and with negative infectious workup. Clinical, endoscopic and histopathologic features were recorded and statistically analyzed with Fisher's exact test.

Results: The mean age in our study group was 44 years old, and 42.75 years old for the control group. All patients were males, and 37.5% of patients (3/8) were positive for HIV. Distinguishing histopathological features for syphilis and chlamydia proctitis included: focal lymphoid aggregates (*P* 0.04), moderate or marked superficial mucosal acute inflammation, (*P* 0.001) and poorly formed granulomas (*P* 0.02). Distinguishing histopathological features for IBD included frequent lymphoid aggregates (*P* 0.04) and moderate or marked architectural distortion, (*P* 0.02) (Table 1).

Histopathological feature	All confirmed Syphilis/Chlamydia Patients (n=8)	All Control patients (IBD) (n=8)	Fisher Test (Two-sided) P-value
Ulceration	3	1	>.05
Aphthous lesion	1	1	>.05
Mucosal plasma cells > 50%	4	6	>.05
Mucosal plasma cells < 50%	4	2	>.05
Expansion of lamina propria by chronic inflammatory cells	6	5	>0.99
Basal lymphoplasmacytosis moderate or marked	5	1	0.11
Lymphoid aggregates, focal	6	1	**0.04**
Lymphoid aggregates, frequent	1	6	**0.04**
Cryptitis, mild	4	4	0.13
Cryptitis, moderate or marked	4	2	0.60
Crypt abscess, focal	2	2	>0.99
Crypt abscess, frequent	3	2	0.56
Superficial mucosal acute inflammation, moderate or marked	7	0	**0.001**
Architectural distortion, mild	5	4	>0.99
Architectural distortion, moderate or marked	0	5	**0.02**
Crypt shortfall	3	2	>0.99
Crypt dropout	4	3	>0.99
Lymphocytes within epithelium	5	2	0.15
Granulomas, poorly formed	5	0	**0.02**
Granulomas, well formed	0	1	>0.99
Paneth cell metaplasia	0	1	>0.99
Mucosal eosinophils, > 50 hpf	4	3	>0.99
Mucosal eosinophils, < 50 hpf	2	5	0.31
Perivascular plasma cell cuffing	2	0	0.46
Histiocytic inflammation	4	0	0.07
Fibrosis	1	0	>0.99

Conclusions: Syphilitic and chlamydia proctitis show significant histomorphologic overlap with IBD. Potentially distinguishing histopathological features depend on the presence and degree of disease activity and chronicity, which may limit their utility. Previously reported case series have shown the vast majority of STI proctocolitis in HIV positive patients. Fewer than 50% of the patients in our series were HIV positive. Our study demonstrates that syphilitic/chlamydia proctitis also occurs in HIV negative individuals, which reinforces the importance of a thorough sexual history to screen for anal receptive intercourse. Our findings further support that pathologists should employ a very low threshold for performing ancillary testing and suggesting clinical laboratory testing in patients with proctocolitis.

749 Histologic Changes Caused by ORISE Gel Injection in Gastrointestinal Specimens

Andrea Olivas[1], Namrata Setia[2], Christopher Weber[3], Shu-Yuan Xiao[4], Villa Edward[2], Christopher Chapman[2], Uzma Siddiqui[2], Irving Waxman[2], John Hart[2], Lindsay Alpert[2]
[1]University of Chicago Medical Center, Chicago, IL, [2]The University of Chicago, Chicago, IL, [3]Oak Park, IL, [4]Department of Pathology, Zhongnan Hospital of Wuhan University, Wuhan, Hubei, China

Disclosures: Andrea Olivas: None; Namrata Setia: None; Christopher Weber: None; Shu-Yuan Xiao: None; John Hart: None; Lindsay Alpert: None

Background: ORISE Gel is a recently-introduced, FDA-approved submucosal lifting agent used in endoscopic resection of gastrointestinal mucosal lesions. The histologic changes seen in pathology specimens following injection of this gel have not been previously reported in the literature.

Design: 54 specimens from 39 patients who underwent endoscopic mucosal resection (EMR) or endoscopic submucosal dissection (ESD) with ORISE Gel injection, as well as 3 surgical resection specimens from 3 patients who previously underwent EMR with ORISE Gel injection, were included in the study. Patient demographics and details of the endoscopy procedure were obtained. H&E-stained slides from all cases were reviewed. Periodic acid-Schiff (PAS) and mucicarmine stains were performed on select cases.

Results: A total of 48 EMR and 6 ESD specimens were identified: 2 from the duodenum and the rest from the colorectum. Lesions resected included tubular/tubulovillous adenomas (33/54), sessile serrated polyps (15/54), invasive colorectal adenocarcinomas

(2/54), duodenal adenomas (2/54), a hyperplastic polyp (1/54), and a healing polypectomy site (1/54). In 48 of 54 (89%) EMR/ESD specimens, an amorphous, pale-blue to gray, finely granular material was evident in the submucosa; this material was also detected within the mucosa in 3 cases. Two patterns of deposition were observed: most cases showed the material nearly completely filling the submucosa in a homogenous manner (Fig 1A), while in some cases areas of condensation and retraction were seen (Fig 1B). Mucicarmine and PAS stains were negative for mucin (Fig 1C & 1D). Histologic review of the 3 surgical resections, performed 1-2 months following ORISE Gel injection, revealed extensive deposition of dense, eosinophilic material with associated multinucleated giant cells and a variably-dense mixed inflammatory infiltrate (Fig 2). This material was seen in the submucosa in all cases, with transmural extension into the pericolonic adipose tissue in 2 cases.

Figure 1 - 749

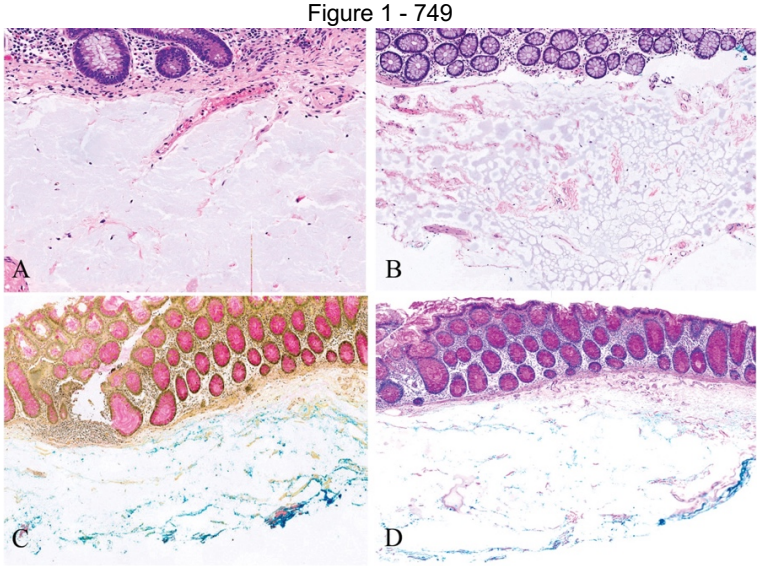

Figure 1. Endoscopic resection with ORISE Gel injection. On H&E sections, ORISE Gel is identified as an amorphous, pale-blue to gray material within submucosal spaces. Either a homogeneous pattern (A) or areas of condensation and retraction (B) can be seen. The material is negative for mucin on mucicarmine (C) and PAS (D) special stains.

Figure 2 - 749

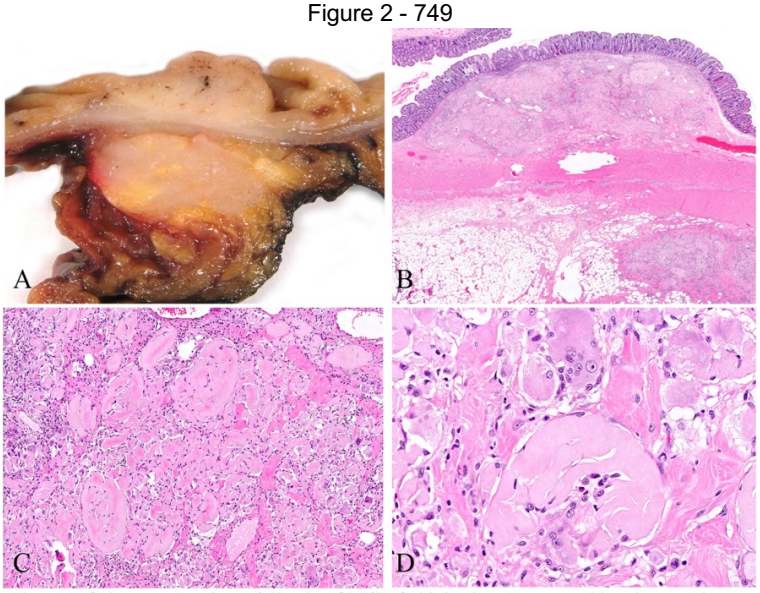

Figure 2. Colectomy specimen following ORISE Gel injection. Transmural involvement by nodular, white-tan to yellow material is grossly evident (A). Histologically, dense eosinophilic material is present, with an associated multinucleated giant cell reaction (B-D).

Conclusions: ORISE Gel injection during endoscopic resection of GI lesions often results in submucosal deposition of amorphous, blue-gray material seen in histologic sections. Resections from areas previously injected with this material demonstrate abundant dense, eosinophilic material with an associated giant cell reaction. Awareness of these procedure-related artifacts among pathologists will help avoid misinterpretation of their presence as a pathologic finding.

750 Analysis of Risk Factors for Local Recurrence of Colon Polyps Removed by Endoscopic Mucosal Resection

Yuho Ono[1], Justin Cates[2], Douglas Pleskow[1], Raul Gonzalez[1]
[1]Beth Israel Deaconess Medical Center, Boston, MA, [2]Vanderbilt University Medical Center, Nashville, TN

Disclosures: Yuho Ono: None; Justin Cates: None; Douglas Pleskow: *Consultant*, Boston Scientific; *Consultant*, Medtronic; *Consultant*, Olympus; *Consultant*, Fujifilm; *Consultant*, Ninepoint medical; Raul Gonzalez: None

Background: Endoscopic mucosal resection (EMR) is standard management for colon polyps difficult to remove by simple polypectomy. Previous clinical studies have reported post-EMR local recurrence to be associated with piecemeal resection, larger size, villous features, ileocecal or perianal location, and prior resection attempts. However, no large-cohort pathology study has correlated confirmed histologic features of EMR specimens with recurrence risk.

Design: We retrospectively identified 623 colon polyps removed by EMR with at least one follow-up colonoscopy. H&E slides were reviewed for diagnosis, fragmentation (large and loose fragments, per gross description), high-grade dysplasia (HGD), and positive fragment edge (lesion seen at cauterized edge of a tissue fragment) or distance to negative edge. Records were reviewed for polyp site and size, presence of synchronous adenomas, and subsequent local recurrence or most recent negative colonoscopy and/or EMR site biopsy. Clinicopathologic features were compared to risk of recurrence by univariate and multivariate analyses, with statistical significance set at $P<0.05$.

Results: The 623 polyps included 299 tubular adenomas, 87 tubulovillous adenomas (TVA), 211 sessile serrated adenomas (SSA), and 26 dysplastic SSA. They came from 255 men and 368 women (median age: 65 years). 272 had one large fragment, 262 had at least two large fragments, and the remaining 89 consisted of loose fragments. On univariate analysis (Table), increasing age, diagnosis of TVA, HGD, increasing polyp size, increasing number of large fragments, and positive tissue edges (primarily in large fragments) significantly increased recurrence risk. Other findings, including polyp site, did not. Additional adenomas indicated a lower recurrence risk. On multivariable analysis (Table), only increasing age, increasing polyp size, and HGD increased the risk of recurrence. The validity of the findings regarding HGD were dubious, however, as diagnostic assessments suggested violation of the proportional hazards assumption for this variable. In contrast, non-linear regression for polyp size showed no evidence of non-linearity for this variable.

Variable	Hazard Ratio	95% Confidence Interval	*P*-Value
Univariate analysis			
Age (per 1 year increase)	1.02	1.00-1.04	0.036
Diagnosis			
Tubular adenoma	1 (baseline)	N/A	
Sessile serrated adenoma	1.05	0.66-1.68	0.83
Tubulovillous adenoma	1.84	1.04-3.28	0.037
Dysplastic sessile serrated adenoma	1.64	0.65-4.14	0.30
Presence of high-grade dysplasia	2.25	1.33-3.80	0.0025
Polyp size (per 1 mm increase)	1.03	1.02-1.04	<0.0001
Number of large fragments (per 1 increase)	1.13	1.06-1.21	0.0003
Number of large fragments with positive edge (per 1 increase)	1.17	1.07-1.28	0.0009
Presence of other adenomas	0.65	0.43-0.98	0.042
Multivariate analysis			
Age (per 1 year increase)	1.02	1.00-1.04	0.042
Polyp size (per 1 mm increase)	1.03	1.01-1.04	0.0002
Presence of high-grade dysplasia	1.89	1.11-3.24	0.020

Conclusions: By multivariate analysis, larger polyp size and possibly the presence of HGD (components of “advanced adenomas”) increased recurrence risk for colonic polyps removed by EMR. Specimen fragmentation often precludes accurate evaluation of EMR margins, and reporting positive edges does not appear to have clinical utility in this setting.

751 Attitudes Regarding the World Health Organization-Recommended Term "Sessile Serrated Lesion": Results from an International Survey

Yuho Ono[1], Kenrry Chiu[2], Rhonda Yantiss[2], Raul Gonzalez[1]
[1]Beth Israel Deaconess Medical Center, Boston, MA, [2]Weill Cornell Medicine, New York, NY

Disclosures: Yuho Ono: None; Kenrry Chiu: None; Rhonda Yantiss: None; Raul Gonzalez: None

Background: Several names have been proposed for non-dysplastic serrated colorectal polyps that contain elongated, dilated crypts with abnormal maturation at the bases. The 4th edition World Health Organization (WHO) Classification of Tumors of the Digestive System recommended the term "sessile serrated adenoma/polyp" for these polyps. The recent 5th edition classification changed the recommendation to "sessile serrated lesion," a term previously endorsed by the British Society of Gastroenterology. We sought to assess attitudes and opinions regarding this change in terminology.

Design: We created a brief, five-question survey focused on use of, and preferences for, the term "sessile serrated lesion." It also included an opportunity for respondents to provide open commentary. We circulated this survey online via email and social media, soliciting responses from practicing pathologists with interest in gastrointestinal pathology. We analyzed the survey results for overall findings and for trends based on practice location.

Results: The questions and tabulated responses of the 358 survey respondents are shown in the Table. "Sessile serrated adenoma," "sessile serrated polyp," or similar terms were previously in use by >95% of respondents across all regions except Europe, where 28% already used "sessile serrated lesion." Most (71%) North American pathologists expressed disinterest in adopting the new terminology, most commonly to prevent confusing or frustrating gastroenterologists. However, most pathologists in Europe and Asia (>70%) planned to adopt "sessile serrated lesion," often stating the term seemed more accurate (Figure). Open commentary elicited some positive comments, often stating "adenoma" is misleading for these polyps, as well as many negative, sometimes forceful, opinions regarding the change, as well as frustration with the WHO for changing nomenclature seemingly without rationale.

Survey Questions	Responses (n=358)	
1. Where do you practice?		
North America	275	(77%)
Europe	40	(11%)
Asia	30	(8%)
Australia / New Zealand	7	(2%)
South America	5	(1%)
Africa	0	(0%)
No response	1	(<1%)
2. Prior to mid-2019, what term did you use to diagnose the entity designated by the 2010 (4th Edition) WHO digestive tumors classification as "sessile serrated adenoma/polyp"?		
Sessile serrated adenoma	143	(40%)
Sessile serrated adenoma/polyp	89	(25%)
Sessile serrated polyp	74	(21%)
Sessile serrated polyp/adenoma	37	(10%)
Sessile serrated lesion	13	(4%)
Other	2	(<1%)
3. The newly released 2019 (5th Edition) WHO classification now recommends the term "sessile serrated lesion" to diagnose the entity. Do you plan to use this term going forward?		
Yes	138	(39%)
No	219	(61%)
No response	1	(<1%)
4. If you plan to use "sessile serrated lesion", why? (n=138)		
Term seems more accurate based on my understanding of the entity	71	(51%)
Term seems more accurate based on new evidence	31	(22%)
Was already using "sessile serrated lesion"	20	(14%)
My pathologist colleagues appear to prefer "sessile serrated lesion"	15	(11%)
My gastroenterologist colleagues have requested/encouraged the change	1	(<1%)
Other (e.g., to standardize terminology, because the WHO says so, etc.)	32	(23%)
5. If you do not plan to use "sessile serrated lesion", why not? (n=219)		
Might confuse/frustrate my gastroenterologist colleagues	186	(85%)
Term seems less accurate than the term I currently use	119	(54%)
Insufficient evidence to justify new term	70	(32%)
My pathologist colleagues appear hesitant to use "sessile serrated lesion"	55	(25%)
My gastroenterologist colleagues have specifically asked me not to change terms	12	(5%)
Other (e.g., simply dislike the term, prefer the status quo, etc.)	22	(10%)

Figure 1 - 751

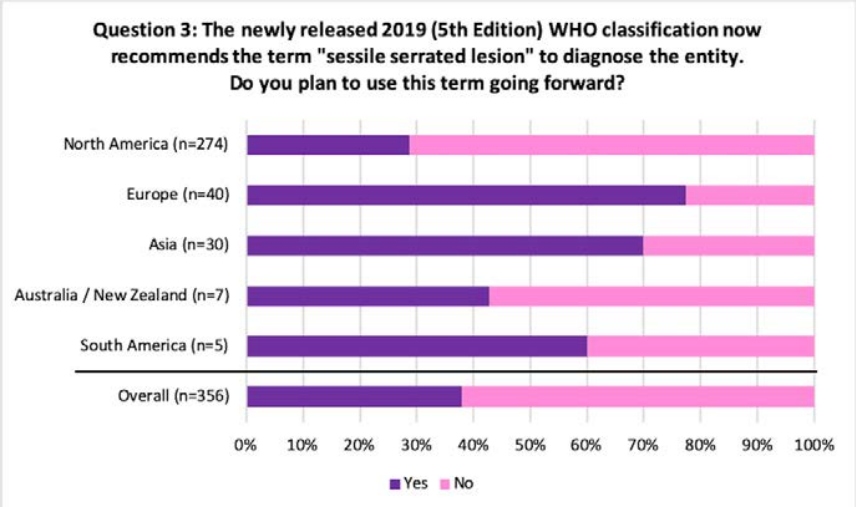

Conclusions: Attitudes regarding the WHO recommendation to abandon “sessile serrated adenoma/polyp” in favor of “sessile serrated lesion” vary with geography. Although standardized terminology can facilitate communication among pathologists from different countries, many North American pathologists do not intend to change their practice in a way that might confuse clinical colleagues and potentially prevent patients from receiving appropriate treatment and follow-up. Our findings point to a potential larger problem regarding the value of “consensus” recommendations that do not truly reflect global opinion.

752 Treatment Naïve Colonic Adenocarcinomas Close to the Serosal Surface: Challenges with T3 versus T4a Staging and Correlation with Clinical Outcomes

Robert Pantaleon Vasquez[1], Tonya King[2], Mustafa E Arslan[3], HwaJeong Lee[4], Dipti Karamchandani[1]
[1]Penn State Health Milton S. Hershey Medical Center, Hershey, PA, [2]Pennsylvania State University College of Medicine, Hershey, PA, [3]Albany Medical Center, Albany, NY, [4]Albany Medical Center, Guilderland, NY

Disclosures: Robert Pantaleon Vasquez: None; Tonya King: None; Mustafa E Arslan: None; HwaJeong Lee: None; Dipti Karamchandani: None

Background: Per American Joint Committee on Cancer Staging Manual 8th edition, pT4 colonic adenocarcinoma is defined as “tumor that invades through the visceral peritoneum (including continuous invasion of tumor through areas of inflammation to the surface of the visceral peritoneum).” Still, disagreement exists amongst pathologists on staging tumors in which carcinoma is close (within 1 mm) to the serosal surface, with some staging this as T3 and others as T4a, the latter especially when there is intervening contiguous inflammation.

Design: In this retrospective study, 159 untreated colonic adenocarcinoma originally staged as either pT3 or pT4 were retrieved from pathology database of two academic institutions, and re-classified into one of three groups- *Group 1(40 cases)*: unequivocal pT4a wherein tumor is seen at the serosal surface; *Group2 (67 cases)*: pT3 with tumor more than 1 mm from the serosal surface; *Group 3(52 cases)*: Tumor less than 1 mm from the serosal surface (initially staged as either T3 or T4a), separated by fibrosis (43 of 52 cases) or contiguous inflammation (9 of 52 cases). Five-year follow-up data and clinical outcomes were analyzed for each group.

Results: There was a significant difference amongst the 3 groups in 5-year recurrence free rates (Group 1: 0.58, Group 2: 0.87, Group 3: 0.62, p<0.001; *Fig 1*), as well as 5-year survival (Group 1: 0.20, Group 2: 0.81, Group 3: 0.29, p<0.001; *Fig 2*). Even after adjusting for adjuvant therapy as a confounding factor, the risk of death (p<0.001) and risk of recurrence (p=0.003) were significantly greater in Group 1 (7.6 times and 4.2 times, respectively) and Group 3 (6.3 times and 3.6 times, respectively) as compared to Group 2. Nodal metastases were also significantly greater in Groups 1 and 3 as compared to Group 2 (p=0.006), as was distant metastases (Group 1: 35%, Group 2: 10.5%, Group 3: 31%, p=0.004). There was no significant difference for tumor differentiation, lymphovascular or big vessel invasion, amongst the 3 groups.

Figure 1 - 752

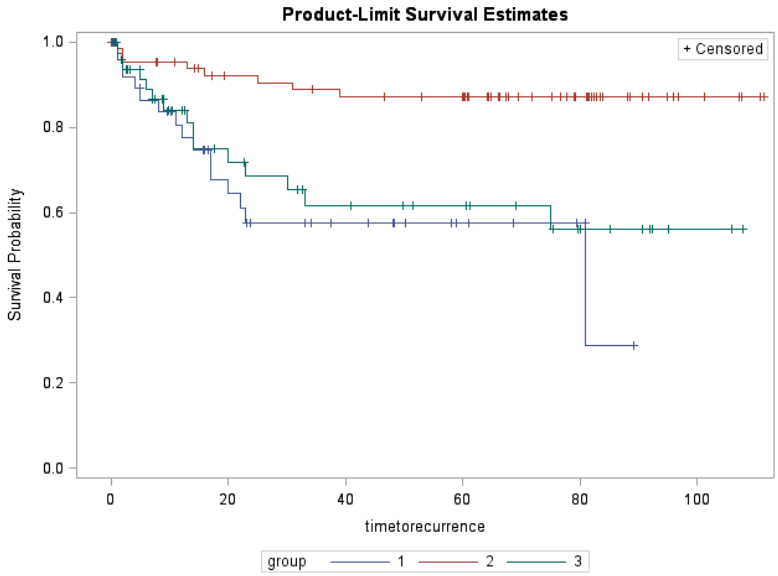

Figure 2 - 752

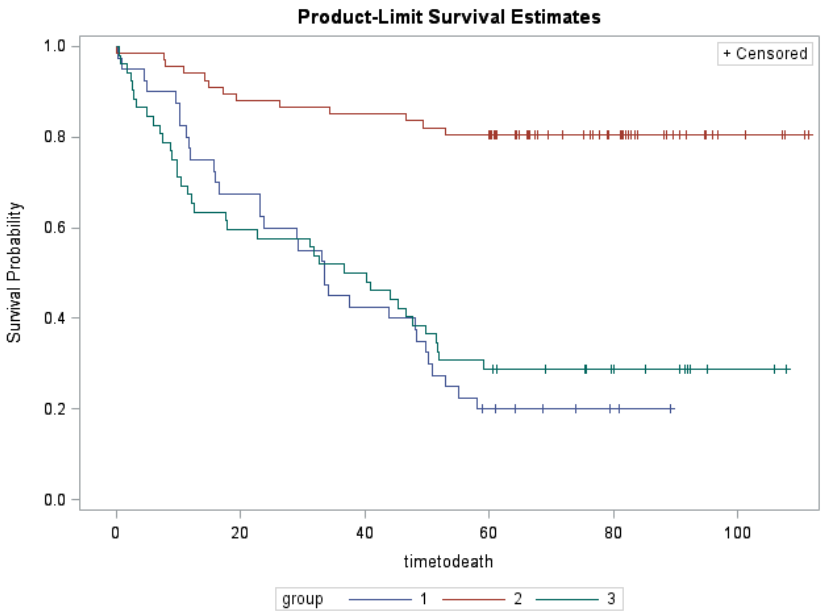

Conclusions: Our study shows that colonic adenocarcinomas wherein tumor is less than 1 mm from the serosal surface (Group 3) behave similar to “bonafide” pT4a adenocarcinomas (Group 1). Although the numbers in this study are small; the above data preliminary supports that tumors less than 1 mm from the serosal surface may better be staged as pT4a, rather than pT3 tumor with regards to clinical outcomes.

753 Hermansky-Pudlak Syndrome in the Gastrointestinal Tract: A Cohort Study for the Histopathological Characterization of a Monogenic, Inflammatory Bowel Disease Entity

Xenia Parisi[1], Nathan Shelman[2], Kevin O'Brien[3], William Gahl[3], May Christine Malicdan[3], Bernadette Gochuico[3]
[1]Beth Israel Deaconess Medical Center, Harvard Medical School, Boston, MA, [2]Indiana University School of Medicine, Indianapolis, IN, [3]National Institutes of Health, Bethesda, MD

Disclosures: Xenia Parisi: None; Nathan Shelman: None; Kevin O'Brien: None; William Gahl: None; May Christine Malicdan: None; Bernadette Gochuico: None

Background: Hermansky-Pudlak Syndrome (HPS) is an autosomal recessive condition classically characterized by oculocutaneous albinism with a bleeding diathesis and systemic intracellular accumulation of ceroid lipofuscin. Pulmonary fibrosis, neutropenia, and inflammatory bowel disease (IBD) are major contributors to disease morbidity and mortality; however, information on the histopathology and clinical course of the attendant IBD is scant.

Design: All adult and pediatric patients with HPS evaluated at the National Institutes of Health Clinical Center between 1995 and 2018 were included in this cohort study. Patients were enrolled in 95-HG-0193 (Clinical and Basic Investigations of HPS) and 04-HG-0211 (Procurement and Analysis of Specimens from Individuals with Pulmonary Fibrosis), approved by the institutional review board of the National Human Genome Research Institute. Data were obtained from retrospective review of medical records and donated colectomy specimens.

Results: IBD affected 35 of 259 patients (13.5%). Mean age at onset was 20 years (range: 1-52) with six having infantile-onset disease. Affected patients had HPS-1, HPS-3, HPS-4, or HPS-6 subtypes. Of note, HPS-3 was associated with more mild symptoms. Seventy-four percent of IBD patients sought medical treatment. Seven of 13 patients trialed on anti-tumor necrosis factor alpha (TNF-alpha) therapy achieved sustained response. Colectomy was clinically indicated in 37% of IBD. Donated specimen demonstrated a spectrum of disease burden from minimally active colitis with edema to frank ulceration. Poorly-formed, non-necrotizing, granulomas and ceroid-laden macrophages were identified in the submucosa and lamina propria of all specimens but not commonly within the mucosa. Notably however, numbers of CD63+ macrophages and intensity of TNF-alpha positive epithelial cells generally correlated with severity of disease.

Conclusions: Inflammatory bowel disease resembling Crohn's disease affects children and adults with HPS. Here we describe previously uncharacterized histopathologic findings and recommend careful pathologic examination of biopsy specimen with special attention to the numbers of CD63+ macrophages and TNF-alpha positive epithelial cells within the mucosa to track disease activity and response to therapy.

754 Nrf2/Keap1 as a Predictor of Prognosis and Radiotherapy Resistance in Rectal Cancer Patient: A Prospective Analysis

Ji Min Park[1], Kangkook Lee[2], Sung Uk Bae[3], Sang Jun Byun[4], Shin Kim[5], Hyunseung Oh[6], Hyeong Chan Shin[1], Ilseon Hwang[5], Hye Ra Jung[1], Sun Young Kwon[5], Misun Choe[5], Yu Na Kang[1], Sang Pyo Kim[5], Hye Won Lee[1]
[1]Department of Pathology, School of Medicine, Keimyung University and Dongsan Medical Center, Daegu, Korea, Republic of South Korea, [2]Division of Hematology and Oncology, Department of Internal Medicine, Keimyung University Dongsan Medical Center, Daegu, Korea, Daegu, Korea, Republic of South Korea, [3]Keimyung University and Dongsan Medical Center, Daegu, Korea, Republic of South Korea, [4]Keimyung University Dongsan Hospital, Daegu, Korea, Republic of South Korea, [5]Keimyung University School of Medicine, Daegu, Korea, Republic of South Korea, [6]Department of Pathology, School of Medicine, Keimyung University and Dongsan Medical Center, Dalseo-gu, Daegu, Korea, Republic of South Korea

Disclosures: Ji Min Park: None; Kangkook Lee: None; Sung Uk Bae: None; Sang Jun Byun: None; Shin Kim: None; Hyeong Chan Shin: None; Ilseon Hwang: None; Hye Ra Jung: None; Sun Young Kwon: None; Misun Choe: None; Yu Na Kang: None; Sang Pyo Kim: None; Hye Won Lee: None

Background: Nrf2-Keap1 signaling pathway plays a crucial role in regulating cell responses against oxidative stress. Nrf2 acts as a cell protector from inflammation, cellular damage, as well as from cancer, while Keap1 is a negative-regulator of Nrf2. Dysregulation of Nrf2/Keap1 causes tumor proliferation and active metabolism which finally leads to high resistance on radiotherapy. The aim of this study was to evaluate the predictive role of Nrf2 and Keap1.

Design: Before preoperative radiotherapy, total 72 rectal cancer patients were staged and endoscopic biopsies from the tumor were taken. Expression of Nrf2 and Keap1 was assessed by immunohistochemistry both pre- and postoperative specimens. Response to therapy was evaluated after surgery by pathologic tumor regression grade. And the association between Nrf2 and Keap1 immunoreactivity levels and clinicopathologic factors was evaluated. Functional studies for tumor proliferation and migration were performed in cell line models.

Results: High-expression of Keap1 in pre-radiotherapy specimen is significantly correlated with better overall and disease-free survival. And aberrant expression of Nrf2 was associated with poor prognostic parameters. This result corresponded with analysis of both in vitro

study and large cohort public data. Additionally, the patients with high Nrf2 expression level also showed high tumor regression grade, interpreted as having radioresistance.

Conclusions: Radioresistance is an important issue in rectal cancer and a major aspect of treatment. Nrf2/Keap1 expression can be suggested as a potential predictor of preoperative radiotherapy resistance. Also Nrf2-Keap1 modulators that interact with each other would also be effectively applicable to radioresistant locally advanced rectal cancer.

755 Molecular Stratification and Gene Profiling in 138 Microsatellite Unstable Colonic Adenocarcinomas: Optimizating Patient Management and Clinical Courses

Archi Patel[1], Kun Jiang[1]
[1]Moffitt Cancer Center, Tampa, FL

Disclosures: Archi Patel: None; Kun Jiang: None

Background: Microsatellite instability (MSI) impacts the outcome of patients with colorectal cancers (CRCs) and is associated with an improved efficacy of immuno-checkpoint inhibitors and favorable prognoses. However, comprehensive molecular and mutational profiling of MSI CRCs has not been completely established. Such knowledge is pivotal for patient stratification and therapeutic optimization.

Design: We retrospectively analyzed 138 MSI CRCs including 17 Lynch syndrome cases. Clinical history, next generation sequencing, histomorphology, immunohistochemistry and follow-up were reviewed.

Results: Our study uncovered significant mutational complex involving oncogenes and antioncogenes in MSI CRCs, highlighting novel mutational percentage/distributions distinct from the literature. Importantly, multiple clinically unsuspected mutations have been detected, such as those involving CDH1, AKT1, BRCA2, and KIT genes. In particular, novel CDH1 mutations were uncovered in 4/138 (2.9%); AKT1 mutations were detected in 3/138 (2.2%); BRCA2 mutations in 2/138 (1.5%); KIT mutations in 3/138 cases (2.2%). Additional mutations involving EGFR and HER2 oncogenes were also uncovered. Furthermore, FBXW7 mutations were detected in 7/138 cases (5.1%), which is significantly lower than the published data. These molecules have been known to play key roles in tumor behavior, metastasis, recurrence and patient prognoses.

Conclusions: This investigation has illustrated high mutational frequencies and distinct gene profiles in MSI CRCs that have not been clarified previously and indicates that early molecular testing with multigene analysis encompassing MSI should be considered for all CRC patients, especially in advanced tumors. In additional to well-recognized immunotherapy, gene-targeting strategy and precision medicine should also be utilized to improve patient management and optimize clinical course.

756 Prognosis of Colorectal Mucinous Adenocarcinomas is Dependent on Anatomic Location

Chirag Patel[1], Michael Behring[1], Sameer Al Diffalha[1], Nirag Jhala[2], Deepti Dhall[1], Upender Manne[1]
[1]The University of Alabama at Birmingham, Birmingham, AL, [2]Temple University Hospital, Philadelphia, PA

Disclosures: Chirag Patel: None; Michael Behring: None; Sameer Al Diffalha: None; Nirag Jhala: None; Deepti Dhall: None; Upender Manne: None

Background: Mucinous adenocarcinoma (MCA) is a subtype of colorectal adenocarcinoma characterized by abundant extracellular mucin (>50% of the lesion). Older literature suggests that MCAs have a worse prognosis, but recent studies indicate that stage-matched MCAs are not prognostically different from non-mucinous adenocarcinomas (NMCAs).

Design: We collected tissues of 175 MCAs and 1,015 NMCAs. Sections were immunostained for molecular markers (Muc1, Muc2, Bcl-2, and p53), and extracted DNA was analyzed for microsatellite instability (MSI) status at five NIH consensus polymorphic loci; they were scored as MSI-H if there was instability at two or more loci. We compared MCAs to NMCAs for baseline characteristics by chi-square tests, and outcomes by univariate Kaplan-Meyer and multivariate Cox methods. The IHC markers were binarized into positive and negative categories and were evaluated according to the histologic type and/or the tumor site.

Results: MCAs were more commonly found in the right colon (86 of 175, 50%), were high-grade (26% MCAs vs. 17% NMCAs), were more prevalent in younger patients (<40 years, MCAs 8% vs. NMCAs 4%), exhibited strong expression of Muc2 (76 of 77, 99%) and Bcl-2 (49 of 165, 30% vs. NMCAs 220 of 962, 23%), and had less aberrant p53 staining (MCAs 33 of 90, 37% vs. NMCAs 266 of 496, 54%). In contrast, most NMCAs were low-grade tumors positive for Muc1 (NMCAs 148 of 250, 51%, vs. MCAs 29 of 80, 36%). There were no differences in relation to gender, race, older age, or MSI. The incidence of cancer deaths was marginally higher for patients with MCAs compared to those with NMCAs (52% vs. 45%). However, in univariate analyses, there was no difference in overall survival between those with MCAs and NMCAs (P =0.12) when all anatomic locations were grouped together. Interestingly, MCAs in the rectum showed poor outcomes in comparison to NMCAs (log rank, P= 0.0017), even though the distributions of advanced staged tumors were similar (x^2,

P=0.787). In multivariate analyses, for MCAs, late-stage disease (III and IV) (2.9 HR, CI=1.9-4.5) and the site (rectum) (1.6 HR, CI=0.95-2.73), and, for NMACs, late-stage disease (3.8 HR, CI=3.1-4.6) were independent prognostic indicators of cancer-specific deaths. Marker data (IHC and MSI) was not included in these models because they were not evaluated on all cases.

Demographic	Mucin (N=175)	Non-Mucinous (N=1015)	P
Ages (years)	64.1 +/- 14.4	64.2 +/- 12.5	0.919
Age (0-40)	14 (8.1%)	39 (3.9%)	0.077
Pathology			
Tumor Location			0.151
Proximal	86 (49.7%)	424 (41.8%)	
Distal	50 (28.9%)	344 (33.9%)	
Rectum	37 (21.4%)	246 (24.3%)	
AJCC Stage			0.428
I	27 (15.5%)	210 (20.9%)	
II	66 (37.9%)	252 (35.0%)	
III	57 (32.8%)	305 (30.3%)	
IV	24 (13.8%)	140 (13.9)	
Grade			0.008
Low	126 (73.6%)	836 (83.1%)	
High	45 (26.3%)	170 (16.9%)	
MUC1			0.027
Negative	51 (63.8%)	142 (49.0%)	
Positive	29 (36.2%)	148 (51.0%)	
MUC2			0.000
Negative	1 (1.3%)	105 (42.5%)	
Positive	76 (98.7%)	142 (57.5%)	
p53			0.004
Negative	57 (63.3%)	230 (46.4%)	
Positive	33 (36.7%)	266 (53.6%)	
Bcl-2			0.072
Negative	116 (70.3%)	742 (77.1%)	
Positive	49 (29.7%)	220 (22.9%)	

Figure 1 - 756

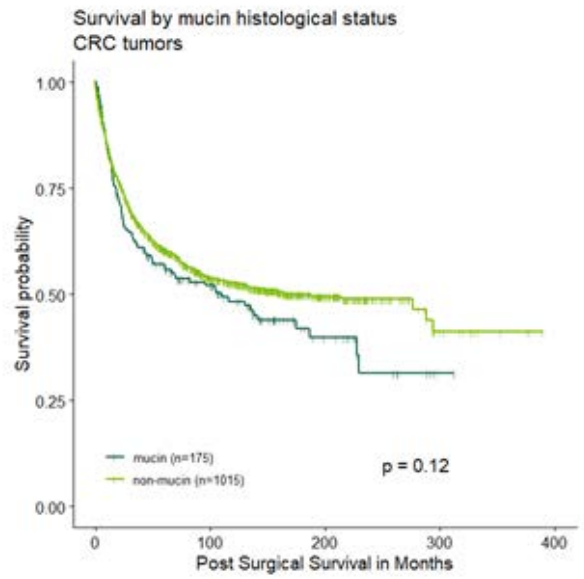

Figure 2 - 756

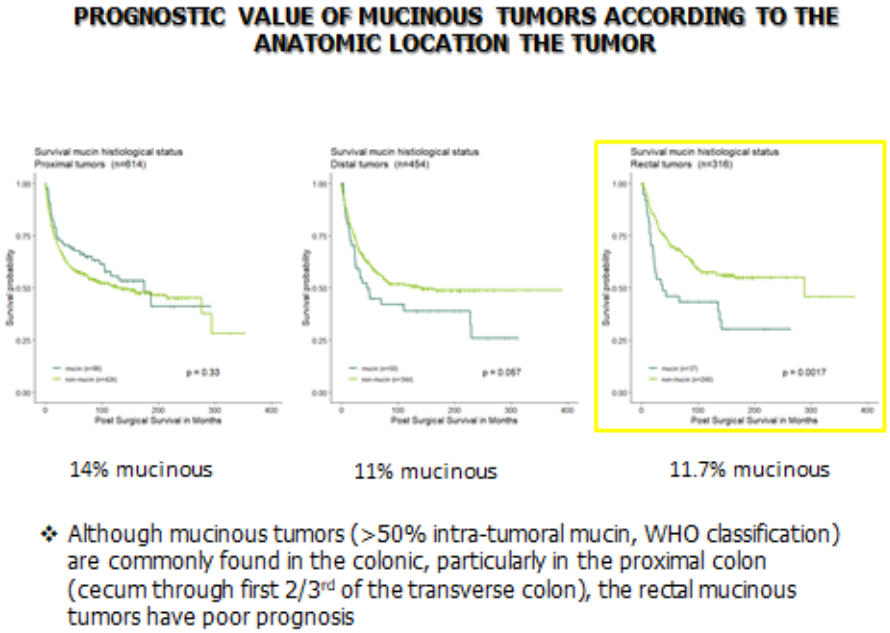

Conclusions: These findings indicate that almost all MCAs exhibit Muc2 expression and that, when they are located in the rectum, the patients have a poor prognosis.

757 Non-Celiac Non-Helicobacter Associated Lymphocytic Gastritis is Characterized by Increased Intraepithelial CD4 and Gamma-Delta Lymphocytes

Priyanka Patil[1], Ashlee Sturtevant[2], Sonja Chen[3], Murray Resnick[4], Elizabeth Wu[5]
[1]Montefiore Medical Center, Bronx, NY, [2]Brown University, Providence, RI, [3]Rhode Island Hospital, Providence, RI, [4]Sharon, MA, [5]Rhode Island Hospital/Brown University, Providence, RI

Disclosures: Priyanka Patil: None; Ashlee Sturtevant: None; Sonja Chen: None; Murray Resnick: *Consultant*, Pathai; Elizabeth Wu: None

Background: Lymphocytic gastritis (LyG; ≥25 intraepithelial lymphocytes (IELs) per 100 epithelial cells) is associated with celiac disease (CeD) and Helicobacter pylori (HP). Duodenal intraepithelial gamma-delta (γ-δ) T cells are increased in CeD, but are not well-studied at other tubal gut sites. The aim of this study is to compare degree of intraepithelial γ-δ lymphocytosis in CeD-associated LyG compared to patients with HP LyG and non-CeD/non-HP LyG.

Design: We included LyG cases with both duodenal and gastric biopsies, and relevant clinical history. None of the patients had inflammatory bowel disease or immune checkpoint inhibitor therapy. Demographic, endoscopic findings and medications were reviewed. Confirmed CeD patients had compatible duodenal histology (increased IELs and moderate to severe villous blunting) and positive anti-tissue transglutaminase antibodies (TTG), while suspected CeD patients had either compatible histology with no recorded TTG, or normal TTG responding to a gluten free diet. HP-negative cases had confirmatory negative Giemsa stain and immunohistochemistry (IHC). γ-δ, CD3, CD4, and CD8 IHC were evaluated in LyG biopsies.

Results: Thirty-two patients with gastric and duodenal biopsies were evaluated (Table 1). Sixteen patients had LyG and confirmed or suspected CeD with negative HP. Four patients had LyG and HP, with normal duodenal biopsies (n=2) or isolated increased IELs (n=2). Twelve patients were negative for both CeD (TTG negative, normal duodenal biopsy) and HP (by IHC and/or Giemsa); of these, two patients with increased IELs and normal villous architecture in the duodenum had normal TTG. CeD patients were more likely to have increased IELs and moderate to severe villous blunting in the duodenum ($p<0.0001$). There was no significant difference in symptoms, endoscopic findings, or use of medications associated with CeD-like enteropathy or lymphocytic colitis among groups.

Histologically, IELs of all LyG cases were CD8 predominant. Non-CeD/non-HP LyG cases were characterized by increased intraepithelial CD4 and γ-δ T cells compared to CeD and HP LyG cases ($p=0.04$ and 0.03). There was no difference in number of gastric biopsies or documented prior HP gastritis among groups.

Table 1. Demographic and endoscopic features and intraepithelial lymphocyte subsets in celiac-associated, Helicobacter-associated, and non-celiac/non-Helicobacter associated lymphocytic gastritis	Celiac (confirmed and suspected; n=16)	Helicobacter (confirmed; n=4)	Non-celiac, non-Helicobacter (n=12)	p-value
Age (median, range, yrs)	44.5 (2-69)	62.5 (45-83)	48 (10-75)	NS
Male/Female (M/F)				NS
M	7	2	5	
F	9	2	7	
TTG				0.001
Positive (>20 U)	10	0	0	
Negative (<20 U)	1	2	5	
Not documented	5	2	7	
Duodenal biopsy findings				<0.0001
Normal or peptic duodenitis	0	2	10	
Increased intraepithelial lymphocytes with no or mild villous blunting	1	2	2	
Increased intraepithelial lymphocytes with moderate to severe villous blunting	15	0	0	
Presenting symptoms (number, %)				NS
Abdominal pain	5	0	5	
Diarrhea	3	0	2	
Iron deficiency anemia, hematochezia, melena	3	3	3	
Weight loss	2	0	1	
Not documented	1	0	0	
Other	2	1	1	
Endoscopic findings (stomach)				NS
Normal	6	0	4	
Erythema, congestion	5	3	7	
Nodularity	1	1	0	
Other	0	0	1	
Not documented	4	0	0	
Medications (taking one of: angiotensin receptor blockers/ARBs, proton pump inhibitors/PPIs, non-steroidal anti-inflammatory drugs/NSAIDs, statins, selective serotonin reuptake inhibitors/SSRIs at the time of biopsy)				NS
Yes	3	3	6	
No	6	1	4	
Not documented	7	0	2	
CD4 count (median, range)	0	0	0 (0-16)	0.04
Gamma-delta T cell count	3 (0-21)	2.5 (0-14)	14.5 (0-52)	0.03

Conclusions: Non-CeD/non-HP LyG is characterized by increased intraepithelial γ-δ and CD4 IELs compared to CeD LyG and HP LyG; as the non-CeD/non-HP group is likely heterogeneous, further work is needed to investigate the etiologic associations of intraepithelial γ-δ and CD4 IELs in this group.

758 Interobserver Agreement Among Gastrointestinal Pathologists Using the Updated Sydney System for Gastric Biopsy Interpretation

Michael Pepper[1], Alaleh Esmaeili Shandiz[2], Gregory Charville[3], John Higgins[4], Teri Longacre[2], Brock Martin[3]
[1]Palo Alto, CA, [2]Stanford University, Stanford, CA, [3]Stanford University School of Medicine, Stanford, CA, [4]Stanford University Hospital, Stanford, CA

Disclosures: Michael Pepper: None; Gregory Charville: None; John Higgins: None; Teri Longacre: None; Brock Martin: None

Background: The updated Sydney system for the classification of gastritis is widely used in clinical practice and in research settings for stratification of gastric cancer risk. Accurate grading of morphologic variables is important for informing the clinical decision to offer endoscopic follow-up and surveillance. This study was conducted to investigate the interobserver agreement for graded morphologic variables in the updated Sydney system.

Design: Gastric biopsy specimens from patients in a gastric intestinal metaplasia (GIM) endoscopic surveillance program were independently evaluated by five gastrointestinal pathologists according to the updated Sydney classification system. Morphologic grading was performed for GIM, mucosal atrophy, chronic inflammation (CI), acute inflammation (AI), and dysplasia. Biopsies with GIM were subclassified as complete, incomplete, or mixed types on the basis of morphology. Inter-rater reliability was determined using Fleiss' kappa (κ) and Krippendorff's alpha (α) coefficients for categorical and weighted ordinal (graded) variables, respectively.

Results: H&E sections of 104 gastric biopsies from 27 endoscopy procedures (24 patients) were evaluated. Mucosa from the gastric antrum and body was sampled from each patient, and GIM was present in at least one biopsy per case. Interobserver agreement was

highest for the detection of Helicobacter (κ=1), GIM (κ=0.95), and AI (κ =0.88); whereas, there was moderate agreement on the presence of CI (κ=0.59). Agreement was lower for the detection of atrophy (κ=0.43) and for subtyping GIM (κ=0.37). Among the variables graded by study pathologists, GIM and CI were assessed more consistently than atrophy, which exhibited poor inter-rater reliability (α=0.54, 0.52, 0.13, respectively). One adenocarcinoma with associated high-grade dysplasia was detected by all study participants.

Conclusions: While there is high interobserver agreement for the detection of Helicobacter, GIM, and gastric inflammation, inter-rater reliability is lower for the detection and grading of mucosal atrophy and for subclassification of GIM, even among subspecialized gastrointestinal pathologists. This study highlights the need for continued investigation into objective and reproducible strategies, such as a two-tiered grading system, well-defined histologic criteria, and/or judicious use of biomarkers (e.g. mucin stains), for evaluating and reporting prognostic variables in stomach biopsies from patients at risk for gastric cancer.

759 The Elusive Sarcina Ventriculi, Infectious Pathogen or Innocent Bystander in the Esophagus

Florence Perrault[1], Philippe Echelard[2], Jean-Daniel Baillargeon[1], Sameh Geha[3]
[1]Sherbrooke University, Sherbrooke, QC, [2]Université de Sherbrooke, Sherbrooke, QC, [3]University of Sherbrooke, Sherbrooke, QC

Disclosures: Florence Perrault: None; Philippe Echelard: None; Jean-Daniel Baillargeon: None; Sameh Geha: None

Background: *Sarcina ventriculi* (SV) is an anaerobic gram-positive coccus occurring in tetrads. It's role as a human pathogen in the stomach has been partially elucidated. A current hypothesis is that SV is not inherently pathogenic but rather puts patients with gastric ulcers and delayed gastric emptying at increased risk for serious complications. SV's signification in the esophagus is yet to be resolved.

Design: We performed a review of the literature in order to concentrate all reported cases of SV in the esophagus. We obtained the clinical history, endoscopic results, microscopic diagnosis and treatment plan for those cases when available. We added to this list a case that we encountered in our institution. We reviewed all the biopsies of the case found at our institution and reviewed the clinical history of the patient. Pictures of SV on the H&E and histochemical slides were taken using Q-Color 5 Imaging System-Olympus.

Results: We were able to isolate 8 other reported SV cases in esophageal biopsy and 1 case from a fine needle aspiration (FNA). 6 patients showed either delayed gastric emptying or esophageal stasis. 5 cases were associated with concomitant or previous gastritis showing SV. All 9 patients were symptomatic with either dysphagia, abdominal pain, emesis, diarrhea, hematemesis or anemia. 6 cases showed acute esophagitis on histological examination. Our case was associated with distal esophageal stasis with sacculation and gastric stasis. Our patient was subjected to 6 esophageal biopsies over the course of a 10 years follow-up. We reviewed the histological slides of 5 of biopsies and the pathological reports of all 6. Of note, SV was present in every biopsy but had only been reported in 2 of them. The 5 first biopsies were only significant for mild chronic inflammation while the most recent was associated with concomitant Candida infection and lymphocytic esophagitis.

Table 1. Clinico-pathological characteristics of 10 *Sarcina ventriculi* cases identified in the esophagus.

Study	Age (years)	Sex	Medical history	Presentation	Endoscopy	Microscopy	Treatment and follow up
Lam-Himlin et al. (2011)	12	F	Esophageal atresia Status post gastric pull-through with anastomotic narrowing	Dysphagia	Stricture at anastomosis. Retained food	Reflux esophagitis. SV	No therapy initiated, follow up not specified
Sauter et al. (2013)	12	M	None	Emesis and abdominal pain	Erosive esophagitis (distal third). Erythematous gastric mucosa. Highly edematous, tight pylorus	Active erosive esophagitis with SV. Chronic active H. pylori gastritis with SV. H. pylori duodenitis with SV. In all 3 locations, SV was present in ulcer bed and erosion areas	No therapy initiated, follow up not specified
Sauter et al. (2013)	16	F	GERD controlled with medication. Normal EGD one year prior. (sibling of case #2)	Emesis and abdominal pain	Severe erosive esophagitis. Highly edematous pylorus.	Same as above	No therapy initiated, follow up not specified

					Stomach markedly inflamed with food debris.		
Carrigan S. et al. (2015)	70	M	COPD Type II diabetes Hypertension CANCA+ granulomatous vasculitis with polyangitis	Drop of hemoglobin (131 to 106 g/l in one month)	White plaques in oesophagus and 1,5 cm subepithelial bleb. Erosion of gastric antrum. Patchy villous loss in duodenum.	Superficial acute oesophagitis with SV in anucleate squamous cell. Reactive gastropathy. Villous blunting, ulceration and inflammation in duodenum.	No therapy initiated. No endoscopic or histologic change after one year (untreated)
De Meij T GJ et al. (2017)	12	F	West syndrome (psychomotor retardation and refractory epilepsy) Percutaneous endoscopic gastrostomy 2 episodes of H.pylori associated gastritis (eradicated both times)	Emesis and hematemesis	Severe distal erosive esophagitis. Multifocal hemorrhagic gastritis with ulcers. Large amount of stomach retention (delayed gastric emptying)	Ulcerative oesophagitis and gastritis, both with SV in mucus surface	10 days of Ciprofloxacin and Metronidazole. Symptom resolution. Control EGD and biopsy at 6 weeks shows complete resolution, no more SV.
Behzadi et al. (2017)	65	F	Metastatic breast cancer Schatzki ring	Progressive dysphagia over two months	Short segment stricture in mid-distal esophagus with 7mm nodule at GEJ Gastric ulcer with residual food in stomach.	Chronic active oesophagitis and gastritis with SV	Dilatation of stricture and stent. 7 days of IPP, ciprofloxacin and metronidazole. Patient died during hospital stay of hemorrhagic gastropathy secondary to therapeutic heparin in the setting of pulmonary embolism.
Dolganiuc A. et al. (2017)	49	F	Environmental allergy and asthma	Fatigue and dysphagia (3 months), nausea, abdominal pain and diarrhea (3 weeks)	Punctuate white spotted mucosa in the entire esophagus. Normal stomach and duodenum	Mild parakeratosis of oesophagus forming plaque-like structure with SV but without inflammation.	No therapy initiated, follow up not specified
U. Shetty et al. (2018)	48	F	COPD Type II diabetes with diabetic enteropathy Hypertension Polysubstance abuse 4 months prior to this episode, endoscopy showed oesophagitis, phytobezoar and gastric biopsy shows SV (retrospectively identified)	Acute epigastric and left upper quadrant pain, nausea and emesis	Oesophagitis	Cytology (brushings) shows reactive squamous and glandular cells and SV	No therapy initiated, follow up not specified
Sinhg et al. (2019)	14	F	Esophageal atresia Status post gastric pull up and fundoplication Recurrent esophageal strictures	Not specified	Oesophageal stricture with inflammation 5cm below stricture.	SV	Ciprofloxacin and metronidazole. Follow up gastroscopy shows resolution of inflammation, no more SV.
Our case	58	F	Status post myotomy and fundoplication Oesophageal hypomotility with oesophageal dilatation	Asymptomatic	Distal esophageal stasis with sacculation associated with gastric stasis	SV Mild chronic inflammation	No therapy initiated. 10 years follow up with persistence of SV in biopsies

Figure 1 - 759

Figure 1. *Sarcina ventriculi* as seen on H&E and special stains (picture taken using Q-Color 5 Imaging System- Olympus).

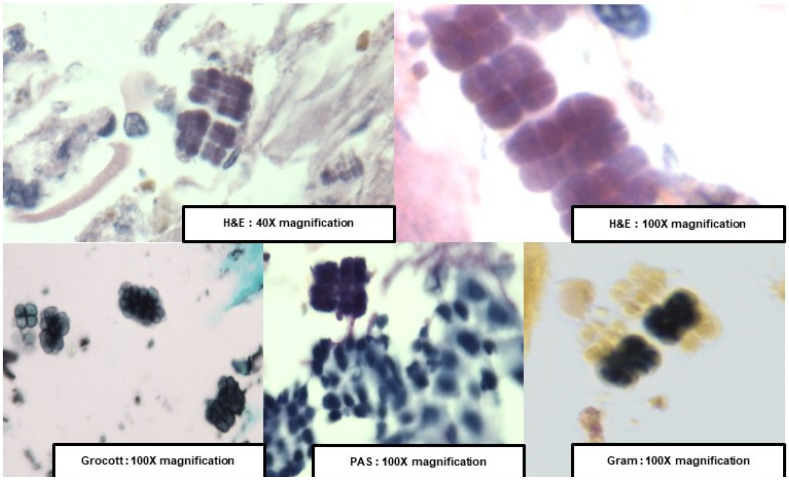

Figure 2 - 759

Figure 2. *Sarcina ventriculi*, Micrococci and miscellaneous cocci as seen on a Gram stain (picture taken using Q-Color 5 Imaging System- Olympus).

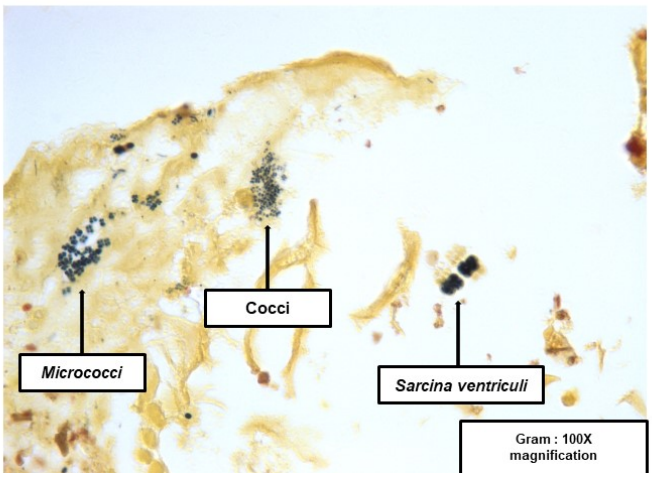

Conclusions: While most publications associate SV's presence to bio-mechanical anomaly of the gastro-esophageal tracts, there is a discordance concerning the pathogenic potential of the micro-organism. Our findings are concordant with the literature on SV, showing the association between the organism and gastro-intestinal stasis. While 6 of the 9 reported cases were associated with acute esophagitis, the 10 years follow-up of our case which was associated with a benign course suggest that SV can, at least in some cases, be an innocent bystander in the esophagus.

760 Characterization of Injectable Agents for Colonic Polyp Removal: A New Amyloid Mimic

Maryam Pezhouh[1], Lawrence Burgart[2], Kenrry Chiu[3], David Cohen[4], Danielle Hutchings[5], Schuyler Sanderson[6], Maryam Shirazi[1], Peter Stanich[7], Lysandra Voltaggio[8], Ellen Willhoit[9], Christina Arnold[10]
[1]Northwestern University Feinberg School of Medicine, Chicago, IL, [2]Abbott Northwestern Hospital, Saint Paul, MN, [3]Weill Cornell Medicine, New York, NY, [4]Atlanta, GA, [5]Johns Hopkins Medicine, Baltimore, MD, [6]Stillwater, MN, [7]The Ohio State University Medical Center, Columbus, OH, [8]Baltimore, MD, [9]Abbott Northwestern Hospital, Minneapolis, MN, [10]The University of Colorado, Denver, CO

Disclosures: Maryam Pezhouh: None; Lawrence Burgart: None; Kenrry Chiu: None; David Cohen: None; Danielle Hutchings: None; Schuyler Sanderson: None; Maryam Shirazi: None; Peter Stanich: *Primary Investigator*, Janssen Pharmaceuticals; Lysandra Voltaggio: None; Ellen Willhoit: None; Christina Arnold: None

Background: Complete polypectomy can require injection of a lifting agent to fully visualize and completely resect a large or flat polyp. Eleview® (Cosmo Technologies, 2015) and Orise® (Boston Scientific, 2018) are relatively new lifting agents that offer the advantage of immediate availability without requiring media preparation during the procedure. To the best of our knowledge, this is the first morphologic description of these lifting agents.

Design: Eleven specimens from 9 patients were collected between 02/2019 to 09/2019 (6 men, mean age=69 years old). All specimens were for polypectomy completion (biopsies=4, resections=7), and all but two patients had documented Eleview® (n=2) or Orise® (n=5) (injection at time of biopsy=4, resection status post prior injection=7).

Results: All resection specimens displayed prominent hyalinized, pink-amorphous ribbons with a foreign body giant cell reaction. The epicenter of the lesion was in the submucosa, and the lesions ranged in size from 11 to 35mm (mean=18 mm). All five cases stained with Congo Red were negative. One case was extensively stained and demonstrated the following phenotype: trichrome (light blue), PAS/PASD (pink), Alcian blue 2.5 (pale blue), AFB (blue/purple); non-reactive for Movat, mucicarmine, GMS, iron, von Kossa, colloidal iron. The material from the resection specimens was neither refractile nor polarizable. In contrast, the four biopsies procured at the time of injection showed focal deposits of colorless linear foreign material that was brightly refractile and polarizable, and elicited no tissue reaction (mean size = 3.2 mm). This material was too scanty for additional studies. Pathologic diagnoses of the index polyp included tubular adenoma (n=5), tubulovillous adenoma (TVA, n=1), TVA with high grade dysplasia (HGD, n=3), sessile serrated adenoma/polyp (n=1), and at least intramucosal carcinoma arising in a TVA with HGD (n=1).

Conclusions: Awareness of the morphology of these new injectable agents is important for accurate diagnosis and to avoid the diagnostic pitfall of amyloid. These lesions can be definitively distinguished from amyloid by their non-reactivity on Congo Red. Based on the altered morphology of the foreign material with time, we propose that the hyalinized material represents a tissue reaction to the injectable agents, similar to that described in pulse granulomata.

761 Tumour Budding and Tumor Stroma are Correlated with Prognosis in Intestinal-Type Gastric Adenocarcinoma

Cherry Pun[1], Shelly Luu[1], Carol Swallow[2], Richard Kirsch[2], James Conner[2]
[1]University of Toronto, Toronto, ON, [2]Mount Sinai Hospital, Toronto, ON

Disclosures: Cherry Pun: None; Shelly Luu: None; Carol Swallow: None; Richard Kirsch: None; James Conner: None

Background: Tumour budding (TB) and peritumoral stroma (TS) morphology are features of the tumor microenvironment that have been linked to colorectal cancer (CRC) prognosis. Their significance in other gastrointestinal tumors, including gastric adenocarcinoma (GAC), has not been as thoroughly studied. In this study, we examined the prognostic role of TB and TS in intestinal-type GAC.

Design: 76 gastrectomies for intestinal-type GAC from were identified. Patients with at least 100 days of follow-up were included to exclude those with poor outcome related to surgery. TB was defined and graded (Bd1, Bd2, Bd3) based on International Tumour Budding Consensus Conference 2016 recommendations. TS was evaluated as described by Ueno et al (Am J Surg Pathol 2017;41:1506-1512). Cases were classified as mature (fine collagen fibers, densely packed layers), intermediate (keloid-like collagen), or immature (myxoid stroma). Classification as intermediate or immature required that the respective features fill a 40x field. TB and TS were evaluated for association with pathologic risk factors and clinical outcome: stage, lymphovascular invasion (LVI), perineural invasion (PNI), overall survival (OS), and recurrence.

Results: 22%, 24%, and 53% of cases were classified as Bd1, Bd2, and Bd3, respectively and 26%, 28%, and 46% had mature, intermediate and immature stroma, respectively. TB was associated with pT ($p<0.001$), pN ($p=0.001$), overall stage ($p<0.001$), LVI ($p=0.002$) and PNI ($p=0.03$). TS was associated with pT ($p<0.001$), pN ($p=0.01$), overall stage ($p=0.007$) and PNI ($p=0.001$), but not LVI. There was correlation between TB and TS ($p<0.001$). Kaplan-Meier survival analysis showed decreased OS ($p=0.05$) and increased recurrence for high TB ($p=0.01$). Outcomes in patients with immature stroma were poorer, but not significantly ($p=0.09$ for survival and $p=0.11$ for recurrence). Statistical significance of TB and TS in survival analysis was not stage independent, however, this may be a function of sample size and data collection is ongoing.

Conclusions: In intestinal-type GAC, TB and TS were associated with known pathologic risk factors and TB was associated with OS and recurrence. This expands on current data suggesting that features of the tumor microenvironment have prognostic value in intestinal-type GAC, analogous to CRC. Larger cohorts are needed to determine if these are stage independent and worth reporting in routine clinical practice.

762 Validation of Histopathology Activity Indices in Pediatric Ulcerative Colitis

Juan Putra[1], Amanda Ricciuto[1], Nicholas Carman[2], Thomas Walters[1], Anne Griffiths[1], Eric Benchimol[3], Peter Church[1], Iram Siddiqui[4]
[1]The Hospital for Sick Children, Toronto, ON, [2]The Children's Hospital of Eastern Ontario, Ottawa, ON, [3]Children's Hospital of Eastern Ontario, Ottawa, ON, [4]Toronto, ON

Disclosures: Juan Putra: None; Amanda Ricciuto: None; Nicholas Carman: None; Eric Benchimol: None

Background: The Robarts Histopathology Index (RHI) and the Nancy Index (NI) have been developed and validated in adult ulcerative colitis (UC), primarily applied to the rectosigmoid region. Both indices have not been formally assessed in the pediatric population. This study aimed to validate the RHI and NI applied to pancolonic biopsies in a pediatric UC cohort by comparing them to endoscopic, clinical, and biochemical activity markers.

Design: Pediatric patients ($\leq$18 years old) with UC were recruited consecutively during diagnostic or follow-up procedures (n=60). Colonoscopies were recorded, and each colonic segment was scored by 4 blinded pediatric gastroenterologists using the UC Endoscopic Index of Severity (UCEIS; score 0-8). Histologic slides of all colonic segments (cecum to rectum) were prospectively reviewed by 2 pediatric gastrointestinal pathologists and each segment was scored using the RHI and NI. The Pediatric UC Activity Index (PUCAI; score 0-85) was utilized to determine clinical activity. Fecal calprotectin (FCP) and CRP were documented to evaluate biochemical activity. Endoscopic and histologic activity scores were assigned to individual segments and the rectosigmoid region, and pancolonic scores were calculated by averaging scores from all segments. Validity was assessed using Spearman's correlation. The data is presented as median (IQR).

Results: The cohort comprised of 35% diagnostic and 65% follow-up procedures (53% male) with a median age of 13.4 (9.8-16.1) years at the time of procedure. Median UCEIS scores for rectosigmoid and pancolonic variations were 4.0 (2.0-5.0) and 2.6 (0.7-4.2), respectively. Both histologic indices demonstrated a very strong correlation with each other ($r \geq 0.90$, $p<0.001$, whether considered by segment, pancolonic or rectosigmoid). The pancolonic RHI (6.3; 1.2-9.5) and NI (1.7; 0.7-2.0) correlated better with endoscopic and clinical activities compared to rectosigmoid RHI (7.0; 1.0-12.0) and NI (2.0; 1.0-2.0) (Table 1). In a fifth of cases, the most severe histologic activity was proximal to the rectosigmoid.

Table 1. Correlation between the histology indices with endoscopic, clinical, and biochemical activity (r values using Spearman's correlation; all $p<0.001$)

	Rectosigmoid UCEIS	Pancolonic UCEIS	PUCAI	FCP	CRP
Rectosigmoid RHI	0.69	-	0.56	0.55	0.47
Rectosigmoid NI	0.71	-	0.55	0.61	0.53
Pancolonic RHI	-	0.84	0.67	0.52	0.61
Pancolonic NI	-	0.82	0.71	0.52	0.66

Conclusions: The RHI and NI appear to be valid histologic activity measures in pediatric UC when applied to the rectosigmoid region alone and when averaged over the entire colon, showing strong correlations with endoscopic activity and moderate correlations with clinical and biochemical activities. Slightly stronger correlations were seen for the pancolonic variations. The RHI and NI correlate very strongly and demonstrate comparable performance.

763 Unexpected High Prevalence of Myenteric Lymphocytic Ganglionitis in Intestinal Inertia

Rehan Rais[1], Jiani Chai[2], Elizabeth Blaney[3], Ta-Chiang Liu[1]
[1]Washington University School of Medicine, St. Louis, MO, [2]Washington University School of Medicine in St. Louis, St. Louis, MO, [3]Washington University in St. Louis, St. Louis, MO

Disclosures: Rehan Rais: None; Jiani Chai: None; Elizabeth Blaney: None; Ta-Chiang Liu: None

Background: Intestinal inertia is a form of gut dysmotility disorder requiring colectomy in severe cases. Loss of ganglion cells in the myenteric plexus has been proposed as a possible etiology. More recently, a preclinical model of virus infection-induced gut dysmotility has suggested that ganglionitis may be an alternative pathogenic factor. The goal of this study was to determine if intestinal inertia is associated with the absence of myenteric ganglion cells or ganglionitis.

Design: Colectomy specimens from 27 patients with intestinal inertia (from 2014-2019) were retrospectively reviewed to determine the presence of myenteric ganglion cells, and the extent of associated inflammatory cell infiltration. Specimens from 28 colon cancer patients (from 2018-2019) without history of gut dysmotility served as controls. A hot spot approach with 5 high-power fields (HPF) was used for quantifying inflammatory cells (lymphocytes, eosinophils, neutrophils, and plasma cells). CD3 and CD20 immunohistochemistry was used to quantify T and B lymphocytes, respectively. Statistical analysis was performed using Fisher's exact test.

Results: None of the intestinal inertia or control cases showed absence of myenteric ganglion cells. A total of 15 (55.6%) of the 27 intestinal inertia cases showed inflammatory cell infiltration in the myenteric ganglion cells, compared to only 1 of 28 (3.6%) control cases (P<0.0001). The intestinal inertia cases with inflammatory infiltrates were associated predominantly with lymphocytes (n=15), including 3 cases (11.1%) with concurrent eosinophil infiltration, and 1 case (3.7%) with concurrent neutrophil infiltration. All 15 inertia cases with myenteric lymphocytic ganglionitis were associated with T lymphocytes (100%), including 1 case with a subset of concurrent B lymphocytes. The CD3 count ranged from 1-15 cells/HPF (average 3.8 cells/HPF). In contrast, the only control case with lymphocytic ganglionitis showed a mixed B and T lymphocytes (9 cells combined/HPF) and eosinophils.

Conclusions: In this study, a significantly high percentage of intestinal inertia specimens possess T lymphocyte infiltration in the myenteric ganglion cells. Myenteric lymphocytic ganglionitis could be the underling pathogenic process of a subset of cases with intestinal inertia.

764 Deep Learning for Computer Assisted Diagnosis of Hereditary Diffuse Gastric Cancer

Sean Rasmussen[1], Thomas Arnason[2], Weei-Yuarn Huang[3]
[1]Dalhousie University, Halifax, NS, [2]Halifax, NS, [3]QE2 Health Sciences Centre, Halifax, NS

Disclosures: Sean Rasmussen: None; Weei-Yuarn Huang: None

Background: Patients with germline mutations in the *CDH1* gene are at high risk for gastric signet ring cell carcinoma, referred to as hereditary diffuse gastric cancer. These patients often undergo prophylactic gastrectomy to minimize their cancer risk. Because the lesions are typically not grossly visible, many pathologists assess the entire gastrectomy microscopically. With 150 or more slides per case, this is a major pathologist time burden. This study utilizes deep learning methods to automatically analyze digitized slides from prophylactic gastrectomy specimens and detect regions suspicious for signet ring cell carcinoma.

Design: We identified prophylactic gastrectomy specimens from 5 patients with hereditary diffuse gastric cancer. All slides (62 in total) containing carcinoma were scanned at 200x magnification. Of these, 9 slides were randomly selected to be used as test data. From the remaining 53 slides, patches of size 256x256 pixels were randomly extracted from areas containing carcinoma (4653 patches) or areas of normal background tissue (4325 patches). Training data was augmented by rotating the patches 90, 180, and 270 degrees. We trained a convolutional neural network using Densenet-121 architecture for 60 epochs. The trained network was assessed on a test set of 1138 patches randomly extracted from the test slides. As well, whole-slide images from the test set were analyzed to determine the network's sensitivity and false positive rate in a realistic use situation.

Results: On patches randomly extracted from test slides, the trained network achieved an ROC AUC of 0.997. This enabled it to maintain a sensitivity for carcinoma patches of 95% with a false positive rate of 0.4%. On whole slide images, the network detected 100% of lesions and correctly eliminated an average of 99.8% of the whole-slide image from consideration.

Figure 1 - 764

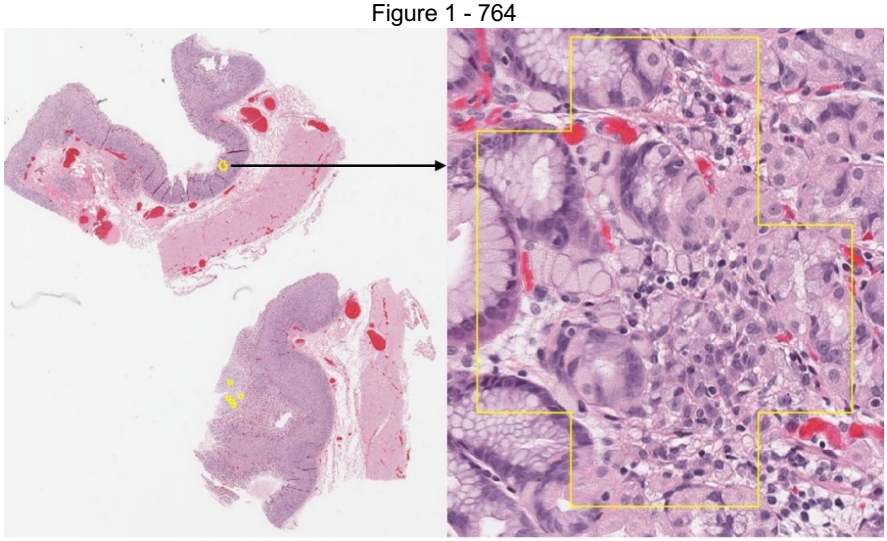

Figure 1. A representative whole-slide image is shown on the left with regions identified as suspicious for carcinoma outlined in yellow. A correctly identified lesion is magnified on the right. Several false positive regions can be seen in the lower half of the whole-slide image.

Conclusions: This network, trained on a relatively small set of images, shows encouraging progress towards computer-assisted diagnosis of hereditary diffuse gastric cancer. This approach could allow pathologists to focus their attention on only a small fraction the tissue from gastrectomy specimens with minimal loss of sensitivity.

765 Concordance Analysis between Microsatellite Instability Status and Tumor Mutational Burden in Colorectal Cancer Patients: A Nested Case-Control Study

Natalia Rodon Font[1], Yessica Anahi No Garbarino[1], Olga Díaz Castello[1], Xavier Puig Torrus[2]
[1]BIOPAT. Biopatologia Molecular SL., Barcelona, Spain, [2]Barcelona, Spain

Disclosures: Natalia Rodon Font: None; Yessica Anahi No Garbarino: None; Olga Díaz Castello: None; Xavier Puig Torrus: None

Background: Mismatch repair (MMR) deficiency and microsatellite instability (MSI) are approved predictive biomarkers of PD1/PD-L1 therapy in colorectal cancer (CRC) patients. Tumor Mutational Burden (TMB) quantifies the number of somatic mutations in tumoral DNA and is reported as number of mutations per DNA Megabase (mut/Mb). TMB is being investigated as a novel predictive biomarker for immune checkpoint inhibitors. In this study we explore the feasibility and potential utility of calculating TMB with a next-generation sequencing (NGS) based panel and its correlation with MMR and MSI.

Design: We designed a nested case-control study in our cohort of CRC patients with complete morpho-molecular characterization since 2009. All patients had previous MSI assessment with a 5 microsatellites panel kit (MSI Analysis System, Promega) and immunohistochemical analysis of MMR proteins (MLH1, MSH2, MSH6 and PMS2). Cases (high-MSI) were defined as CRC patients with MSI. Controls (MSS, 1:1) were selected among CRC patients without high-MSI. Genomic DNA was extracted from paired FFPE normal and malignant tissue sections (RecoverAll Kit for FFPE, ThermoFisher). TMB was assessed with a targeted NGS assay detecting somatic mutations and Indels from 409 genes, spanning 1.7 Mb of genomic space (Oncomine TMB. Thermofisher). High-TMB was defined as ≥ 10 mut/Mb. Analysis was performed using SSPS v20.

Results: Sixty CRC patients were included: 30 high-MSI and 30 MSS without differences regarding age or gender (68% females, median age 68 years). The concordance rate between MSI status and MMR expression was 97.7%. All but one TMB studies were informative. Median TMB was higher in the high-MSI group compared to the MSS group [28.1 (15.2-50.2) vs 5.3 (1.7-18.5) Mut/Mb respectively, p=0.000]. A TMB threshold ≥ 10 mut/Mb was associated with a high-MSI status in 98.3%. One (3.4%) MSS tumor with no MMR deficiency showed an unexpected high-TMB (18.48mut/Mb) (Figure 1).

Figure 1 - 765

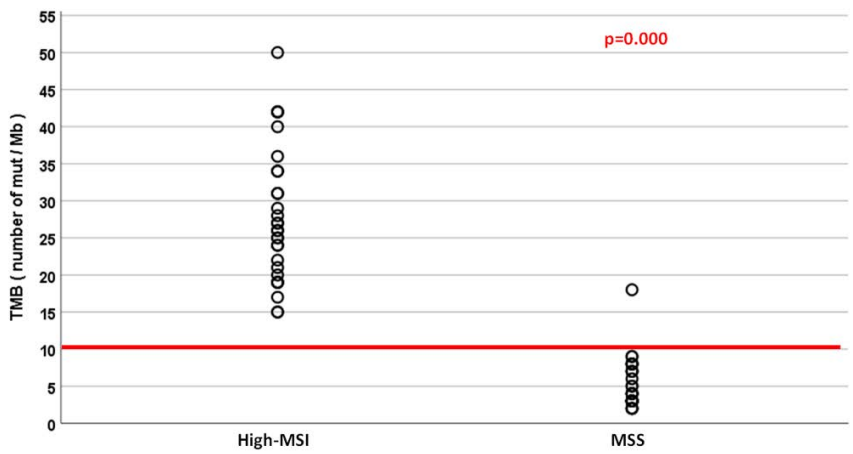

Conclusions: The concordance rate between MSI status and TMB in CRC is excellent. A TMB threshold ≥ 10mut/Mb accurately identifies CRC patients with high-MSI. TMB is able to identify 1 in 30 patients suitable to respond to immunotherapy not previously detected by MSI or MMR studies.

766 Genomic Alterations in Anal Carcinoma Subtypes

Jeffrey Ross[1], James Corines[1], Jo-Anne Vergilio[2], Keith Killian[2], Douglas Lin[2], Erik Williams[3], Natalie Danziger[4], James Haberberger[5], Julie Tse[3], Shakti Ramkissoon[5], Amanda Hemmerich[5], Naomi Lynn Ferguson[5], Claire Edgerly[5], Daniel Duncan[5], Richard Huang[6], Jon Chung[2], Russell Madison[2], Kimberly McGregor[2], Julia Elvin[2]
[1]Upstate Medical University, Syracuse, NY, [2]Foundation Medicine, Inc., Cambridge, MA, [3]Boston, MA, [4]Foundation Medicine, Inc., Somerville, MA, [5]Foundation Medicine, Inc., Morrisville, NC, [6]Foundation Medicine, Inc., Cary, NC

Disclosures: Jeffrey Ross: *Employee*, Foundation Medicine; James Corines: None; Jo-Anne Vergilio: *Employee*, Foundation Medicine, Inc; *Employee*, Foundation Medicine, Inc; Keith Killian: *Employee*, FMI; Douglas Lin: *Employee*, Foundation Medicine; Erik Williams: *Stock Ownership*, F. HoffmanLa Roche, Ltd.; *Employee*, Foundation Medicine, Inc.; Natalie Danziger: *Employee*, Foundation Medicine Incorporated; James Haberberger: *Employee*, Foundation Medicine Inc.; Julie Tse: *Employee*, Foundation Medicine, Inc.; *Consultant*, Pathology Watch, LLC.; Shakti Ramkissoon: *Employee*, Foundation Medicine/Roche; Amanda Hemmerich: *Employee*, Foundation Medicine, Inc; Naomi Lynn Ferguson: *Employee*, Foundation Medicine; Claire Edgerly: *Employee*, Foundation Medicine, Inc.; Daniel Duncan: *Employee*, Foundation Medicine; Richard Huang: *Employee*, Roche/Foundation Medicine; Jon Chung: *Employee*, Foundation Medicine; *Stock Ownership*, Roche; Russell Madison: *Employee*, Foundation Medicine Inc.; *Stock Ownership*, Roche; Kimberly McGregor: *Employee*, Foundation Medicine; Julia Elvin: *Employee*, Foundation Medicine, Inc.; *Employee*, Hoffman La Roche

Background: Basaloid squamous (BSCC), conventional squamous (CSCC) and adenosquamous (ASCC) carcinomas of the anus are aggressive malignancies that can cause life-threatening local and systemic disease. We used comprehensive genomic profiling (GCP) to evaluate the genomic alterations (GA) of the three subtypes of anal carcinomas.

Design: FFPE tissues from clinically advanced BSCC (31 cases), CSCC (442 cases) and ASCC (8 cases) underwent hybrid-capture based comprehensive genomic profiling (CGP) to evaluate all classes of genomic alterations. Tumor mutational burden (TMB) was determined on up to 1.1 Mbp of sequenced DNA and microsatellite instability (MSI) was determined on 114 loci. PD-L1 expression in tumor cells (Dako 22C3) was measured by IHC.

Results: BSCC, CSCC and ASCC patients had a similar median age (59-63 years) and female preponderance (Table). BSCC and CSCC tumors were more often HPV16 positive compared to ASCC tumors. GA per tumor was highest in ASCC followed by CSCC. BSCC had the lowest GA/tumor frequency. Non-clinically relevant (CR) GAs were similar in BSCC and CSCC but were different in ASCC. The 50% *TP53* GA frequency in ASCC was significantly higher than that seen in either BSCC or CSCC. CR GA in BSCC and CSCC were most frequent in the PI3KCA/mTOR pathway with only rare kinase gene targets identified (*ERBB2* in BSCC and *FGFR3* in CSCC, both at 4%). In ASCC, kinase targets were more frequent including *ERBB2*, *EGFR* and *BRAF* all at 13%. Alterations in APC were not identified in the ASCC cases. Using various metrics, TMB was highest in ASCC which also featured the only MSI-high sample in this study followed by CSCC and BSCC samples. HPV+ status and *TERT* mutations were strongly anti-correlated in the CSCC.

	Basaloid Carcinoma (BSCC)	Conventional Squamous Cell Carcinoma (CSCC)	Adenosquamous Carcinoma (ASCC)
Number of Cases	31	442	8
Males/Females	M 16% F 84%	M 31% F 69%	M 25% F 75%
Median age (range)	59 (46-80)	59 (25-88)	63 (33-89)
HPV16	90%	79%	25%
HPV18	6%	4%	13%
HPV6/11	3%	<1%	13%
HHV8	3%	3%	0%
HHV4	<1%	<1%	0%
GA/tumor	2.45	4.6	6.9
Top Non-CR GA	*CYLD* 35% *KMT2D* 20% *SOX2* 10% *CTNNB1* 10% *KMT2C* 8% *MSH2* 7% *TP53* 7% *RB1* 7%	*KMT2D* 20% *FBXW7* 17% *KMT2C* 14% *SOX2* 10% *TP53* 10% *CYLD* 10% *FAT1* 10%	*TP53* 50% *RB1* 25% *PIK3R1* 25% *CREBBP* 25% *CDKN2A* 25%
Top CRGA	*PIK3CA* 23% *NF1* 4% *ERBB2* 4%	*PIK3CA* 33% *PTEN* 16% *STK11* 4% *FGFR3* 4%	*BRCA2* 13% *NF1* 13% *ERBB2* 13% *EGFR* 13% *BRAF* 13% *PIK3CA* 13%
MSI-High	0%	1%	13%
Mean TMB	4.8	6.8	10.6
Median TMB	3.6	5.2	3.5
TMB>10 mut/Mb	13%	19%	38%
TMB>20 mut/Mb	3%	5%	25%
PD-L1 IHC Positive	NA	29%	NA

Conclusions: Although clinically advanced BSCC, CSCC and ASCC have similar age and gender distributions, HPV infection is less often associated with ASCC. BSCC and CSCC feature a similar distribution of both non-CR and CR GA, while ASCC features more GA in targetable kinase genes and significantly higher TMB indicating potential for immunotherapy benefit. Based on these findings, CGP shows promise for personalizing therapies for anal carcinoma patients and improving their clinical outcomes.

767 Secondary Carcinomas Involving the Mucosa of the Gastrointestinal Tract: A Series of 201 Cases

Christophe Rosty[1], Rondell Graham[2], Rish Pai[3]
[1]Envoi Specialist Pathologists, Brisbane, QLD, Australia, [2]Mayo Clinic, Rochester, MN, [3]Mayo Clinic Arizona, Scottsdale, AZ

Disclosures: Christophe Rosty: None; Rondell Graham: None; Rish Pai: None

Background: Secondary carcinomas involving the gastrointestinal tract are relatively rare, except in the small bowel where metastatic disease outnumbers primary carcinomas. Secondary tumors can involve the gastrointestinal tract by direct extension, peritoneal seeding or by hematogenous spread. The distinction between secondary and primary carcinomas can be challenging on biopsy specimens. In this study, we report the clinical and histopathologic features of a large series of secondary carcinomas involving the mucosa of the gastrointestinal tract.

Design: The pathology databases of 3 institutions were searched for reports of metastatic or secondary tumors involving any part of the gastrointestinal tract (from the esophagus to the anus), over a 10-year period of time (2009-2018). Non-carcinomatous tumors and direct extension of pancreatic carcinoma to the duodenum were excluded. All endoscopic biopsy specimens and surgical resection specimens with mucosal involvement were reviewed. The following parameters were recorded: patient demographics, patient clinical history, tumor site, histologic type and other pathology in the gastrointestinal tract.

Results: The study group consisted of 201 cases from 198 patients (112 females, 86 males) with a median age at diagnosis of 68 years (range 33-89). Most specimens were endoscopic biopsy specimens (n = 184, 92%). The most common primary sites were breast (n = 68), lung (n = 25, including 13 adenocarcinomas, 7 non-small cell carcinomas, 3 squamous cell carcinomas and 2 small cell carcinomas), kidney (n = 27, all clear cell renal cell carcinoma), gynecologic tract (n = 22, including 16 ovarian, 4 endometrial and 2 cervical carcinomas), prostate (n = 17), and genitourinary tract (n = 12). The table below shows the distribution of primary tumors by gastrointestinal site. An example of squamous cell carcinoma involving the entire wall of the small bowel is illustrated in figures 1 (gross image) and 2 (corresponding microscopic image).

Metastatic site	Primary tumor
Esophagus (n = 10)	Kidney (4), Breast (3), Prostate (2), Thyroid (1)
Stomach (n = 61)	Breast (33), Kidney (12), Lung (8), Pancreas (3), Colon (1), Gynecological tract (1), Thyroid (1), Salivary gland (1), Unknown (1)
Duodenum (n = 24)	Breast (8), Kidney (5), Esophagus (2), Lung (1), Genitourinary tract (1), Gynecological tract (1), Head and neck (1), Testis (1), Adrenocortical (1), Gallbladder (1), Liver (1), Unknown (1)
Small bowel (n = 9)	Lung (3), Kidney (2), Stomach (2), Breast (1), Genitourinary tract (1)
Terminal ileum (n = 2)	Pancreas (1), Gynecological tract (1)
Colon (n = 65)	Breast (19), Gynecological tract (15), Lung (11), Genitourinary tract (4), Kidney (4), Prostate (2), Stomach (2), Peritoneal (2), Appendix (1) Liver (1), Unknown (4)
Rectum (n = 29)	Prostate (13), Genitourinary tract (6), Gynecological tract (4), Breast (3), Lung (2), Pancreas (1)
Anus (n = 1)	Breast (1)

Figure 1 - 767

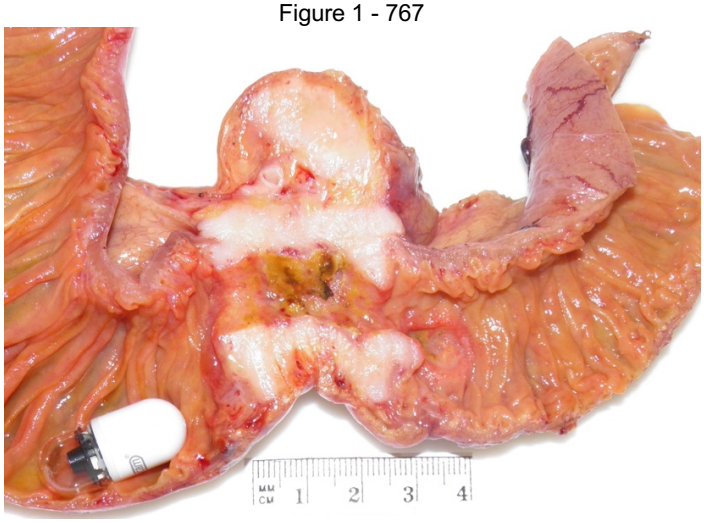

Figure 2 - 767

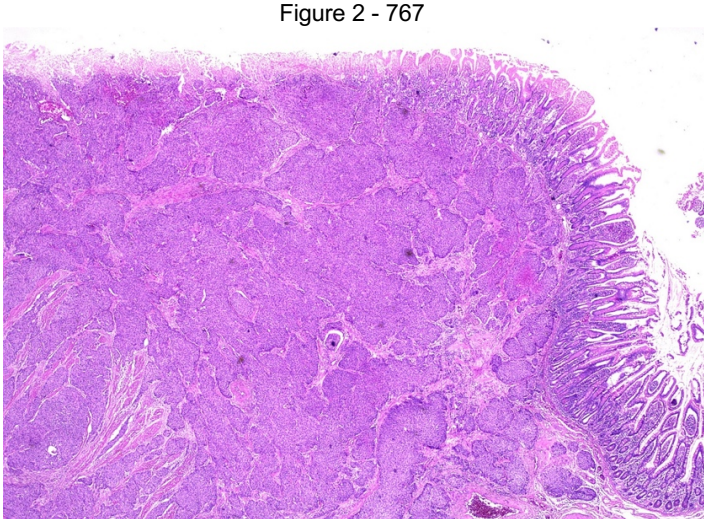

Conclusions: The most common sites for secondary carcinoma involving the mucosa of the gastrointestinal tract are the large bowel and the stomach. Metastatic carcinoma from the breast, lung and kidney can be identified in any part of the gastrointestinal tract mucosa. Metastatic carcinoma from the genitourinary tract and the gynecological tract are more commonly found in the large bowel while prostate carcinoma is predominant in rectal biopsies.

768 Glycogenic Acanthosis of the Esophagus: Clinical, Endoscopic and Histologic Correlation

Miguel Rufail[1], Rashmi Tondon[2], Franz Fogt[3], Rifat Mannan[4]
[1]Pennsylvania Hospital of University of Pennsylvania Health System, Philadelphia, PA, [2]Hospital of the University of Pennsylvania, Philadelphia, PA, [3]Hospital of the University of Pennsylvania, Gladwyne, PA, [4]Perelman School of Medicine at the University of Pennsylvania, Philadelphia, PA

Disclosures: Miguel Rufail: None; Rashmi Tondon: None; Franz Fogt: None; Rifat Mannan: None

Background: Glycogenic acanthosis (GA) is characterized by single or multifocal plaques of hyperplastic squamous epithelium with abundant intracellular glycogen. Although mostly benign, diffuse forms are known to be associated with Cowden syndrome (CS). Endoscopic appearance is nonspecific and is commonly mistaken for candida esophagitis. We sought to analyze clinical, endoscopic and histologic features of GA diagnosed at our institution and also study its association with CS.

Design: We identified 48 cases of GA, over a 10-year period. Clinical details, with endoscopic findings were obtained from available records. Histology was reviewed for confirmation of diagnosis and associated pathology.

Results: Average age was 60 years (range, 31-81; M: 23, F: 25). Indications for endoscopy included heartburn (n=12), dysphagia (n=9), surveillance of Barrett esophagus (n=7), abdominal pain (n=5), follow up of previous esophageal neoplasia (n=2) and non-specific GI symptoms, including dyspepsia (n=13). On endoscopy, GA appeared as solitary (n=14), or multiple (n=18) whitish nodules, solitary white patch (n=4), diffuse white plaques (n=4), erythema (n=1), ring (n=1), or unremarkable mucosa (n=6). Most solitary lesions were described as “small” and ranged from 1mm to 2cm in diameter. Within the esophagus, the lesion(s) were located in distal (n=13), mid (n= 8), proximal (n= 4), multiple areas (n = 6), diffuse (n=12), or unspecified (n= 5). In 10 cases (21%) an endoscopic diagnosis of GA was entertained.

There was coexistent reflux esophagitis (25%, 12/48) and hiatal hernia (21%, 10/48). None of the cases of GA were associated with CS. All cases were confirmed to be GA on re-review. Adjoining uninvolved epithelium was remarkable for low grade squamous dysplasia (n=1), and squamous cell carcinoma (n=1). None of the cases had associated infective organisms, including candida.

Conclusions: GA is most often an incidental endoscopic finding with variable appearance, more commonly involving distal esophagus. It is not typically associated with candida esophagitis. Reflux esophagitis and hiatus hernia can be common associations. Presence of squamous neoplasia in 2 of our patients was likely coincidental. Interestingly, none of our cases (including the diffuse examples) were associated with CS, emphasizing that GA is primarily a benign sporadic occurrence. Awareness of the entity can help provide the endoscopists an explanation for the abnormal endoscopic appearance.

769 Psammomatous Melanotic Schwannoma of the Lower Gastrointestinal Tract

Kevan Salimian[1], Naziheh Assarzadegan[2], Danielle Hutchings[3], Annika Windon[4], Elizabeth Montgomery[5]
[1]Johns Hopkins, Baltimore, MD, [2]Department of Pathology, The Johns Hopkins Medical Institutions, Baltimore, MD, [3]Johns Hopkins Medicine, Baltimore, MD, [4]Johns Hopkins Hospital, Baltimore, MD, [5]Johns Hopkins Medical Institutions, Baltimore, MD

Disclosures: Kevan Salimian: None; Naziheh Assarzadegan: None; Danielle Hutchings: None; Annika Windon: None; Elizabeth Montgomery: None

Background: Psammomatous melanotic schwannomas (PMSs), also referred to as malignant melanotic schwannian tumor (MMST), are rare tumors with a variable association with Carney complex. They classically arise adjoining spinal nerve roots. Extremely rare examples have been reported in the gastrointestinal (GI) tract (most commonly esophageal and gastric). Whereas a subset of soft tissue examples can metastasize; malignant behavior has not been reported in the GI tract to date. Herein, we describe the clinicopathologic findings and follow-up data for the largest case series of PMSs of the lower GI tract.

Design: A search of our pathology database from 1985 to 2019 identified four PMSs of the GI tract. Patient demographics, clinical history and follow-up data were collected for each case.

Results: PMSs were discovered at a median age of 46 years (range: 28-67 yrs.) with gender parity. The lesions were based in the rectosigmoid (n=1), sigmoid (n=2) and an unspecified site in the colon (n=1). Three of the tumors were incidentally discovered as polyps during colonoscopy. One tumor resulted in colonic obstruction resulting in segmental resection. Follow-up data showed no tumor recurrence or metastasis in all cases (mean follow-up length: 79 months; range: 48-143 months). None of the patients had other stigmata associated with Carney complex. Microscopically, these tumors displayed solid sheets of spindled and epithelioid cells with fusiform to round nuclei with occasional pseudoinclusions. These tumors lacked the nuclear atypia, necrosis, and spindle cell features encountered in classic PMSs/MMSTs. Mitoses were rare. Prominent melanin and psammomatous calcifications were present in all cases. All of the tumors were based in the submucosa with extension into the mucosa in two cases and full-thickness involvement of the colon in one case. By immunohistochemistry (IHC), these lesions all labeled with S100 protein and other melanoma markers.

Conclusions: We report the largest series of PMSs in the lower GI tract. While malignant soft tissue counterparts have been described, PMSs of the GI tract have not been shown to have metastatic potential and have distinct morphologic features. The presence of melanin in the tumor cells, as well as the IHC profile, places melanoma in the differential diagnosis of these lesions; however, the bland cytology allows for distinction between the two entities based on morphology. The outcome and distinct morphology makes the term PMS (rather than MMST) applicable at this site.

770 NSAID-Induced Diaphragm Disease: Distinctive Diagnostic Features of an Under-Recognized Cause of Small Bowel Strictures

Marcela Salomao[1], Dora Lam-Himlin[1]
[1]Mayo Clinic, Scottsdale, AZ

Disclosures: Marcela Salomao: None; Dora Lam-Himlin: None

Background: Diaphragm disease (DD) is an unusual NSAID-induced disorder characterized by circumferential web-like strictures affecting the small bowel. Distinguishing DD from other stricturing diseases is critical for proper treatment, but pathologic features are often under-recognized. This study seeks to identify distinctive gross and histologic features of DD to improve diagnostic accuracy.

Design: The pathology database was queried for DD (2009-2018). Inclusion criteria required documented NSAID use and imaging/surgical findings suggestive of DD. Cases with clinical concern for Crohn disease or known infection were excluded. Ten patients (8M:2F, mean age 65±7 yrs; 8 resections, 6 biopsies) met criteria, and clinicopathologic features were evaluated by 2 GI pathologists.

Results: Seventy strictures (range 3-13 per patient) were documented in the medical records, involving the ileum in all cases, and jejunum in 2 cases. Gross photos were available for 5 resections, all of which show a distinctive circumferential mucosal furrow with raised edges at strictured areas (Fig 1 arrows). All sections of strictures (n=27) have a characteristic 1x finding, consisting of an elongated and widened plicae circularis with a bulbous apex containing a central depression (Fig 2) imparting a “double promontory” sign visible by the naked eye. Histologically, the depressions contain erosions and ischemic-like changes with small fibro-inflammatory eruptions. Among resections, crypt distortion and pyloric metaplasia are in 6 (75%) and 3 (38%) cases, respectively, but isolated to areas directly flanking the erosion. The adjacent raised mucosa shows only crypt shortfall and edema. Twenty-three (85%) central depressions contain an oblong fibromuscular nodule (Fig 2 arrowhead) centered on the muscularis mucosae and superficial submucosa. Below this, submucosal strands of smooth muscle are oriented perpendicular to the lumen. Small superficial lymphoid aggregates are present (88%), but 2 cases show deep/transmural lymphoid nodules. Biopsies are unremarkable (33%) or show acute erosion/ulceration (50%), crypt distortion (50%) and pyloric metaplasia (33%), but no distinctive features.

Figure 1 - 770

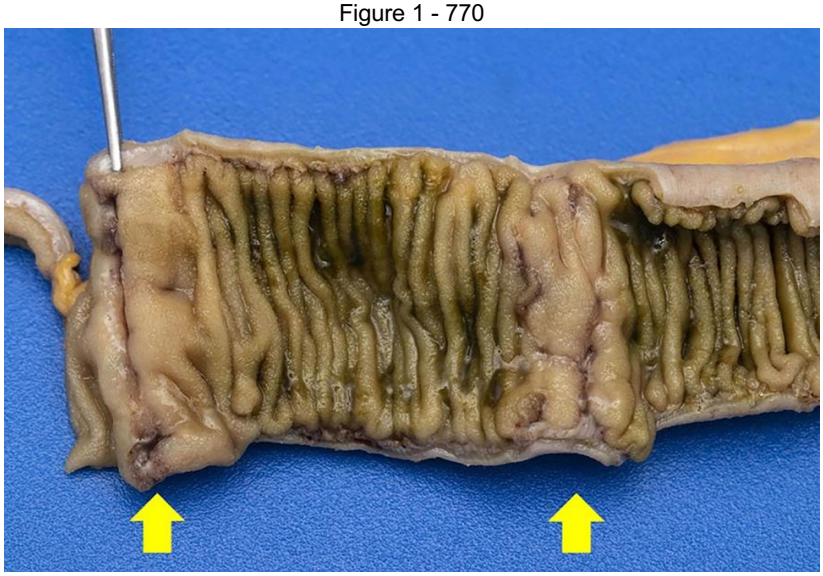

Figure 2 - 770

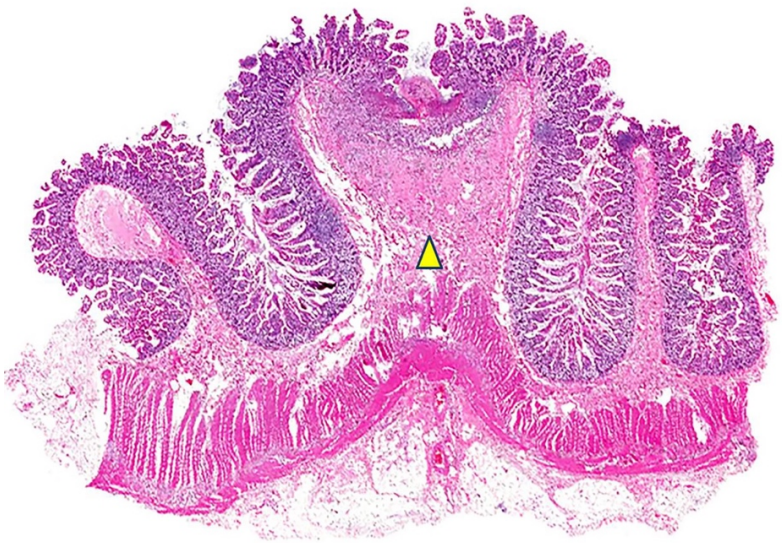

Conclusions: NSAID-induced diaphragm disease can be identified in 100% of cases by a grossly distinctive circumferential linear furrow with raised edges and a double promontory sign at 1x magnification. Histologic features include a central erosion with underlying fibromuscular nodule and negligible crypt distortion or metaplasia.

771 Goblet Cell Rich Hyperplastic Polyps of the Right Colon: A Common but Previously Underreported Entity of Uncertain Clinical Significance

Monica Sanchez-Avila[1], Aastha Chauhan[2], Dale Snover[1]
[1]University of Minnesota, Minneapolis, MN, [2]University of Minnesota, Saint Paul, MN

Disclosures: Monica Sanchez-Avila: None; Aastha Chauhan: None; Dale Snover: None

Background: Goblet cell-rich hyperplastic polyps (GCHP) are characterized by minimal serration and abundant goblet cells without microvesicular mucin. They are reported to occur almost exclusively in the left colon and have no known risk of malignant transformation. Recently, however, these lesions are being increasingly identified in the right colon. The purpose of this study is to evaluate GCHPs of the right colon.

Design: We queried the University of Minnesota database for the years 2016 - 2018 for endoscopic polyps from the right colon with the word “hyperplastic” in the final diagnosis. These were reviewed to determine how many were GCHP. Age, gender, polyp location and size were obtained from the medical record. We randomly selected 22 left-sided lesions originally diagnosed as GCHP for comparison.

Results: There were 187 polyps from the right colon that fulfilled our criteria and had evaluable tissue. Of these, 95 (51%) were reclassified as GCHP, 42 (22%) MVHP,12 (6%) SSA, 9 (5%) tubular adenoma, 2 (1%) inflammatory polyp,1 (0.5%) traditional serrated adenoma. In 26 (14%) cases no epithelial polyp was identified. GCHP was the initial diagnosis in 11 of 95 cases (11%). The most common initial diagnosis assigned to these polyps was uncategorized hyperplastic polyp (n=48, 51%), followed by "colonic mucosa with surface hyperplastic change" (n=36, 38%).

Of the 95 right-sided GCHP, 42 (44%) occurred in females and 53 (56%) in males. Mean age for women and men was 63 and 60 years. Mean size of the polyps was 0.42 cm (range of 0.1 – 1.0 cm). Location of the polyps: cecum, 35 (37%); ascending colon16 (17%); hepatic flexure 20(21%); transverse colon 24(25%).

Of the 22 left sided polyps 14 (64%) were in females and 8 (36%) males. The mean age for females and males was 61 and 54 years. Mean size was 0.35 cm with a range of 0.1 – 0.6 cm.

Conclusions: GCHPs of the right colon are common but often diagnosed as colonic mucosa with surface hyperplastic change. These polyps occur most frequently at approximately 60 years of age and have no difference by gender, and are most frequently located in the cecum. Although the histological appearance of these lesions is similar to GCHP in the left colon, they tend to be larger and are often sometimes exuberant and serrated, suggesting the possibility of 2 different lesions. Their natural history and clinical significance is unknown. Long-term follow-up data will be needed to determine if these lesions can safely be treated as hyperplastic polyps.

772 Well-Differentiated Rectal Neuroendocrine Tumors: Analysis of Biologic Behavior and INSM1 Expression in 94 Cases

Ryan Sappenfield[1], Iván González[2], Dengfeng Cao[3], Deyali Chatterjee[1]
[1]Washington University in St. Louis, St. Louis, MO, [2]Washington University School of Medicine, St. Louis, MO, [3]Barnes Jewish Hospital/Washington University, St. Louis, MO

Disclosures: Ryan Sappenfield: None; Iván González: None; Dengfeng Cao: None; Deyali Chatterjee: None

Background: Rectal well-differentiated neuroendocrine tumors (R-NET) are usually indolent neoplasms that are increasingly being detected by screening colonoscopy, commonly manifesting as small submucosal polyps. Although the histologic diagnosis of NET relies on the confirmation with neuroendocrine (NE) markers, chromogranin is frequently negative in R-NETs. Insulinoma-associated protein 1 (INSM1) is a novel transcription factor that has recently shown excellent sensitivity and specificity for NE differentiation in various anatomic sites, but has not been evaluated in R-NETs.

Design: A retrospective review of all available archival slides of R-NETs excised at our institution was performed. INSM1 immunohistochemistry was performed on all cases for which blocks were also available. Ki-67 and chromogranin stains were performed on all cases which did not have those stains already available for review. Clinical and follow-up information was obtained from the medical chart.

Results: A total of 94 patients with R-NET were included in our cohort. Of these, 84 (89%) had tumors ≤ 10 mm in diameter and submucosal involvement was noted in 70 patients (74%). The majority of the tumors showed a nested pattern (70 cases, 74%); however, the histologic patterns varied widely with 46 tumors (49%) showing multiple histologic subtypes. The majority of the cases had intratumoral fibrosis (57 cases, 61%). Synaptophysin was reactive in 100% (66 of 66 cases) of cases with a mean reactivity of 99% (range: 90-100%) of the tumour cells. Chromogranin A was reactive in 45% (41 of 92 cases) of cases and showed a mean reactivity of 57% (range: 2-100%). INSM1 was reactive in 100% (89 of 89 cases) of cases with a mean reactivity of 96% (range: 70-100%). The mean Ki-67 proliferative index

was 1.6% (range: 0.5-5%). 83 cases (88%) were classified according to the WHO criteria as grade 1 and 11 cases (12%) as grade 2. Median follow-up of the cohort was 30 months (80 cases, range: 3-226 months). Overall, three patients (3%) were identified with lymph node or distant metastasis, all of which showed tumor size ≥ 11 mm and had lymphovascular invasion (LVI).

Conclusions: R-NETs in our fairly large cohort display similar biologic behavior as has been reported in literature. Metastatic behavior was associated with tumor size and the presence of LVI, but not with Ki-67 proliferative index. This is also the first study documenting that INSM1 is a highly sensitive NE marker in this group of neoplasms.

773 Characterization of LGR5 Expression in Tumor Budding of Colorectal Carcinoma with PD-L1 Expression

Koichi Sato[1], Takeshi Uehara[1], Tomoyuki Nakajima[2], Mai Iwaya[3], Hiroyoshi Ota[4]
[1]Shinshu University School of Medicine, Matsumoto, Japan, [2]Shinshu University Hospital, Matsumoto, Japan, [3]Shinshu University Hospital, Matsumoto, Nagano, Japan, [4]Shinshu University School of Health Sciences, Matsumoto, Japan

Disclosures: Koichi Sato: None; Takeshi Uehara: None; Tomoyuki Nakajima: None; Mai Iwaya: None; Hiroyoshi Ota: None

Background: We investigated expression of *LGR5,* the most robust and reliable cancer stem cell (CSC) marker of colorectal cancer, and PD-L1 in tumor budding (TB) of colorectal adenocarcinoma, and clinicopathological features.

Design: Tissue microarrays (TMAs) were generated from TB of 55 colorectal adenocarcinoma patient samples, and *LGR5* expression in TMAs was evaluated by RNAscope, a highly sensitive RNA *in situ* hybridization technique. Patients were stratified into negative and positive *LGR5* expression groups. PD-L1 expression was classified into PD-L1 positive (1%) with positive expression of 1% or more and PD-L1 positive (5%) with positive expression of 5% or more in TB.

Results: In the PD-L1-positive (5%) group, *LGR5* expression was significantly lower than in the PD-L1-negative (5%) group (P=0.0183). In the PD-L1-positive (1%) group, inflammatory cell infiltration was weaker, and the stage was higher in the *LGR5*-positive group compared with the *LGR5*-negative group (P=0.0017 and P=0.0332, respectively). In both PD-L1-negative (1%) and PD-L1-negative (5%) groups, there was a significant difference in OS between *LGR5*-positive and *LGR5*-negative groups (log-rank test, P=0.0011 and P=0.0351, respectively). In both PD-L1-negative (1%) and PD-L1-negative (5%) groups, cox proportional hazards models revealed that the *LGR5*-positive group had better OS (P= 0.0011 and P= 0.0424 respectively).

Conclusions: This study showed that the PD-L1-positive group is a unique population with low *LGR5* expression, and that *LGR5*-positive cells may be a promising therapeutic target in the PD-L1-negative group.

774 Hypertrophic Lesions of Chronic Herpes Simplex Virus Infection: Clinicopathologic Features of Anal and Perianal Disease

David Saulino[1], Rhonda Yantiss[2], Xuefeng Zhang[3], Maria Westerhoff[4], Jerome Cheng[4], Xuchen Zhang[5], Xiuli Liu[6], Michael Feely[6]
[1]Immunology and Lab Medicine, University of Florida, Gainesville, FL, [2]Weill Cornell Medicine, New York, NY, [3]Cleveland Clinic, Beachwood, OH, [4]University of Michigan, Ann Arbor, MI, [5]Yale University School of Medicine, Orange, CT, [6]University of Florida, Gainesville, FL

Disclosures: David Saulino: None; Rhonda Yantiss: None; Xuefeng Zhang: None; Maria Westerhoff: None; Jerome Cheng: None; Xuchen Zhang: None; Xiuli Liu: None; Michael Feely: None

Background: Although small series have been reported in the clinical literature, the clinicopathologic features of chronic herpes simplex virus (HSV) infection are not well-defined, particularly when infection causes hypertrophic lesions that simulate condylomata or carcinoma. The purpose of this study is to evaluate the clinicopathologic features of chronic HSV infections that produce mass-like lesions rather than typical ulcers.

Design: We identified 13 cases of hypertrophic HSV-related lesions from 6 patients at 5 institutions, all of which were immunohistochemically confirmed. Clinical features regarding HIV status, lesion location, and outcome were recorded. Cases were assessed for squamous hyperplasia, nature and distribution of inflammation, and ulcers. These features were compared with those of acute HSV infection (n=2) and condyloma latum (n=2).

Results: All study patients were HIV-infected adults (mean age: 49) with an equal sex distribution. Concurrent CD4 counts were available in 7 cases; 5 (71%) were >200 cells/mm3. Lesions involved the perianal skin (n=8), anal canal (n=4), or both (n=1).
Ten of 13 (77%) were multifocal at presentation, ranging from 1-10 cm in size (Fig. 1). Three patients were clinically suspected to have condylomata at initial presentation; HSV infection was not originally considered in any patient. Three patients suffered recurrent disease with multiple excisions despite extended antiviral therapy. All cases displayed notable squamous hyperplasia with dense

lymphoplasmacytic infiltrates; 11 (85%) showed perivascular inflammation (Fig. 2). Viral cytopathic changes were limited to epithelium adjacent to ulcers. In contrast, acute HSV infection featured minimally expanded squamous epithelium with neutrophil-rich inflammation and a paucity of plasma cells. Condylomata lata exhibited squamous hyperplasia and dense lymphoplasmacytic infiltrates associated with nerves and vessels similar to chronic HSV infection.

Figure 1 - 774

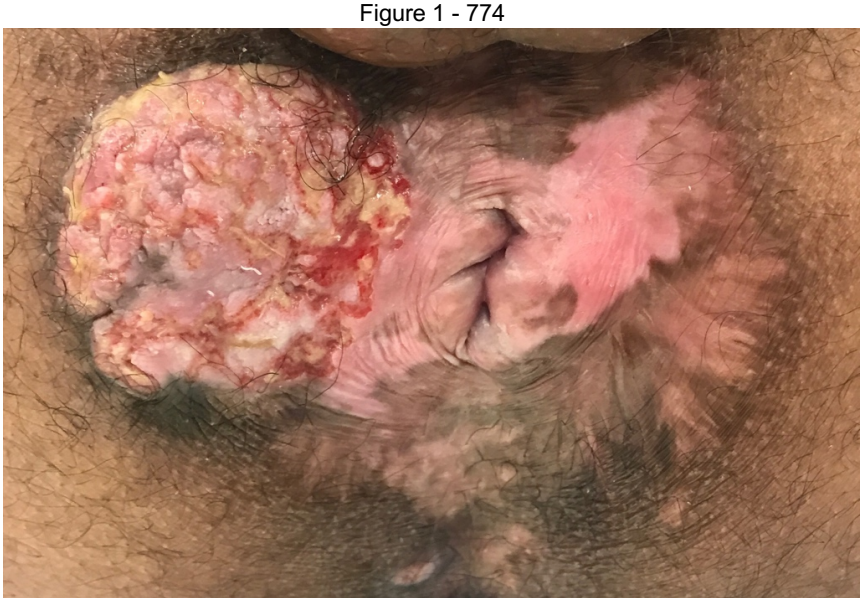

Figure 2 - 774

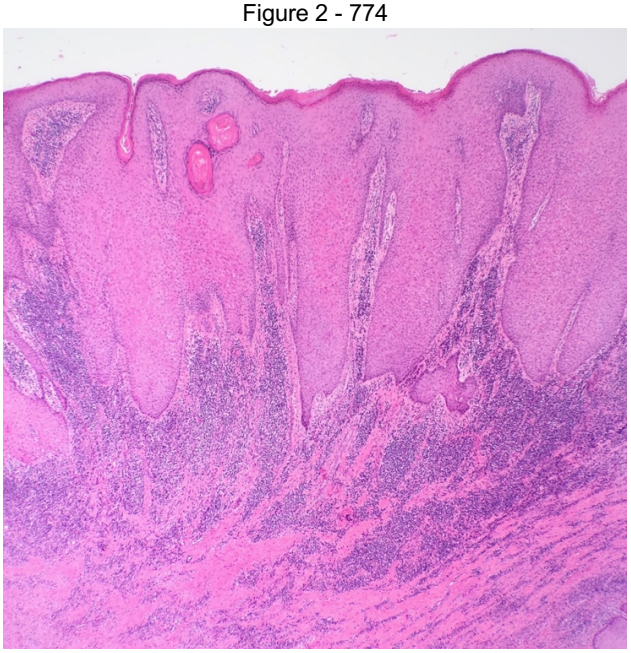

Conclusions: Chronic HSV infection can cause hypertrophic lesions with striking epithelial hyperplasia and dense lymphoplasmacytic inflammation that contain only occasional HSV-positive cells in close proximity to ulcers. While they bear little histologic resemblance to ulcers of acute HSV infection, hypertrophic HSV-related lesions closely mimic condylomata lata. Pathologists should be aware of this differential diagnosis, particularly when dealing with samples from HIV-infected patients that show squamous hyperplasia and dense lymphoplasmacytic inflammation.

775 Characterization of Chronic Gastritis Underlying Lynch Syndrome-Associated Gastric Cancer

David Saulino[1], Minqian (Jasmine) Shen[2], Xuefeng Zhang[3], Maria Westerhoff[4], Jerome Cheng[4], Jingmei Lin[5], Xuchen Zhang[6], Michael Feely[7], Xiuli Liu[7]
[1]Immunology and Lab Medicine, University of Florida, Gainesville, FL, [2]Cleveland Clinic Foundation, Cleveland, OH, [3]Cleveland Clinic, Beachwood, OH, [4]University of Michigan, Ann Arbor, MI, [5]Indiana University, Indianapolis, IN, [6]Yale University School of Medicine, Orange, CT, [7]University of Florida, Gainesville, FL

Disclosures: David Saulino: None; Minqian (Jasmine) Shen: None; Xuefeng Zhang: None; Maria Westerhoff: None; Jerome Cheng: None; Jingmei Lin: None; Xuchen Zhang: None; Michael Feely: None; Xiuli Liu: None

Background: Gastric cancer is a Lynch syndrome (LS) associated malignancy. Recent studies have attempted to identify the clinical risk factors for LS-associated gastric cancer. Additionally, a few previous studies suggest that there may be underlying immune gastritis in some LS-associated gastric cancers. However, histology of this potential underlying immune gastritis is not well defined. This study aims to characterize the underlying gastritis in LS patients with gastric cancer.

Design: A cohort of 12 LS-associated gastric cancer cases were collected via a multicenter collaboration. Our study includes patients diagnosed with LS using clinical criteria and/or genetic confirmation. Clinicodemographics and pathology material were reviewed. The frequency of chronic gastritis and intestinal metaplasia was then compared to a cohort of LS patients without gastric cancer in a previously published study [Renkonen-Sinisalo L et al., 2002].

Results: A cohort of 12 LS patients (4 male and 8 female, mean age 62 years) with gastric cancer were included in this study. Seven of the patients had gastrointestinal symptoms and 5 were evaluated as part of a surveillance program. All patients had a background gastric biopsy available for review and 9 had chronic gastritis. The gastric body was biopsied in 9 cases and 7 had at least moderate chronic gastritis. Additionally, 6 of these cases had atrophy, 5 had multifocal intestinal metaplasia, and 5 had pseudopyloric gland metaplasia. Eight cases had gastric antral biopsies; 2 of these cases had moderate chronic gastritis, 3 had mild chronic gastritis, 1 had reactive gastropathy, and 2 had intestinal metaplasia. Of the 5 cases that had both antral and body biopsies 4 had body predominant gastritis and 1 had similar inflammation in both. H. pylori gastritis was noted in 2 of the 11. Activity was noted in 3 cases including those two with H. pylori infection. Compared to LS patients without gastric cancer from a previously published study; LS patients with gastritis cancer had a higher rate of chronic gastritis (p=0.006), atrophy (p=0.009), and intestinal metaplasia (p=0.038). [Table 1]

Table 1. Comparison of gastric findings between lynch patients with gastric cancer (current study) and without gastric cancer [[Renkonen-Sinisalo L et al., 2002].

	Chronic gastritis, N (%)	*H. pylori* infection, N (%)	Atrophy, N (%)	IM, N (%)
Current study N=12	9 (75)	2 (16.7)	6 (50)	5 (41.6)
Previous study N=73	23 (31.5)	19 (26.0)	10 (13.7)	10 (13.7)
P value	0.006	0.52	0.009	0.038

Note: IM: intestinal metaplasia

Conclusions: LS patients with gastric cancer had higher rate of chronic gastritis, atrophy, and intestinal metaplasia compared to a previously published group of LS without gastric cancer. The presence of gastritis may help risk stratify LS patients for gastric cancer. Therefore, future studies are needed to examine the mechanisms of chronic gastritis in LS patients.

776 Gastric Cancer in the Setting of Intestinal Metaplasia and Surveillance in a Low-Risk Population: Does the End Justify the Means?

Namrata Setia[1], Jerome Cheng[2], Rachel Horton[3], Maria Westerhoff[2], Won-Tak Choi[4], Suntrea Hammer[5], Stuti Shroff[6], Rondell Graham[3], John Hart[1]
[1]The University of Chicago, Chicago, IL, [2]University of Michigan, Ann Arbor, MI, [3]Mayo Clinic, Rochester, MN, [4]University of California San Francisco, San Francisco, CA, [5]University of Texas Southwestern Medical Center, Dallas, TX, [6]Massachusetts General Hospital, Watertown, MA

Disclosures: Namrata Setia: None; Jerome Cheng: None; Rachel Horton: None; Maria Westerhoff: None; Won-Tak Choi: None; Suntrea Hammer: None; Stuti Shroff: None; Rondell Graham: None; John Hart: None

Background: The goal of endoscopic gastric intestinal metaplasia surveillance is to prevent incident gastric cancers. In this study, we reviewed clinicopathologic features of gastric cancers in the setting of gastric intestinal metaplasia to determine if surveillance of gastric intestinal metaplasia is justified in a low-risk population.

Design: Gastric cancers with at least one prior endoscopy with intestinal metaplasia, performed >30 days before cancer diagnosis were included in the study. A total of 25 gastric cancers in the setting of intestinal metaplasia were retrospectively identified from six academic institutions after review of 5,771 resected gastric cancers. Carcinomas arising in the setting of Barrett esophagus were excluded.

Results: The median age at the diagnosis of gastric intestinal metaplasia was 64 years (range 9-90, +/-17.4), and the median age at the diagnosis of gastric cancer was 72 years (range 16-90, +/-15.9). About 56% (14/25) of patients were male. Race/ethnicity distribution of the cohort was 4: 3.5: 2: 1 - Caucasians: African Americans: Asians: Hispanics. A family history of gastric cancer was present in 15% (3/20) patients, H. pylori gastritis in 27.3% (6/22) patients, and autoimmune gastritis in 22.7% (5/22) patients. The median duration between prior endoscopy and subsequent endoscopic diagnosis of gastric cancer was 18 months (1-125, +/-31). Of all gastric cancers, 72% (18/25) were diagnosed within 3 years of the last endoscopy. Gastric cancers in the setting of gastric intestinal metaplasia were preceded by endoscopic biopsy detection of dysplasia in only 13.6% (3/22) cases. About half of the gastric cancers (45.4%, 10/22) were non-intestinal Lauren type.

Conclusions: The extremely low incidence of gastric cancer in the setting of gastric intestinal metaplasia does not support universal (non-risk adapted) endoscopic surveillance of gastric intestinal metaplasia in a low-risk population. Even targeted endoscopic surveillance in certain high risk racial/ethnic groups may not be justified; however, the cost-effectiveness of these type of surveillance programs needs to be determined. If performed, a surveillance interval of 3 years may be associated with an unacceptable rate of interval gastric cancer.

777 Clinical Significance of Inactive Antral Gastritis

Namrata Setia[1], Andrea Olivas[2], Katherine Boylan[1], John Hart[1]
[1]The University of Chicago, Chicago, IL, [2]University of Chicago Medical Center, Chicago, IL

Disclosures: Namrata Setia: None; Andrea Olivas: None; Katherine Boylan: None; John Hart: None

Background: Inactive gastritis constitutes 10-25% of all diagnoses rendered on gastric biopsies in clinical practice, and often prompts pathologists to order ancillary stains for *H. pylori* organisms. The disease states other than *H. pylori* infection that are associated with inactive gastritis are not delineated and the clinical significance of a diagnosis of inactive gastritis on patient management is not well studied.

Design: A retrospective study was performed that included 65 randomly selected biopsy cases diagnosed with inactive antral gastritis (IAG) and normal gastric body mucosa. These were compared with 68 site- and age-matched histologically normal antral biopsies. Information regarding indication for endoscopy, past medical history, medication use, and treatment following endoscopy was obtained. H&E-stained slides were reviewed, and the use of *H. pylori* immunostain was recorded. Of note, upfront universal *H. pylori* testing is not performed at our institution.

Results: The median age of the cohort was 42 years (8-80 years, +/-23). The results are summarized in Figure 1. A plausible disease association could be established in only 53.8% of cases which were constituted by *H. pylori* infection and inflammatory bowel disease. An immunostain for *H. pylori* was ordered in 55% (36/65) of cases, but organisms were seen only in 1.5% (1/65) cases. Endoscopic abnormalities were more commonly seen in patients with IAG when compared with normal antral mucosa. The diagnosis of IAG affected clinical management in the one patient with *H. pylori* infection. The clinical management was symptom-based in the remaining patients in both groups. Abdominal pain and gastroesophageal reflux were the most common symptoms and anti-reflux medications were the most commonly prescribed treatment after endoscopy in both groups.

Figure 1 - 777

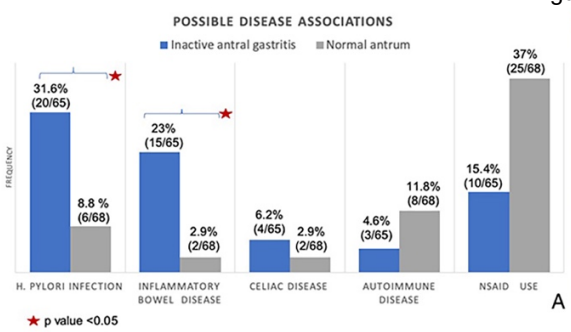

	INACTIVE ANTRAL GASTRITIS	NORMAL ANTRAL MUCOSA	p value
CLINICAL DISEASE			
Untreated *H. pylori* infection	4.6% (3/65)	None (0/68)	0.11
Prior *H. pylori* infection	26% (17/65)	8.8% (6/68)	**0.01**
Inflammatory bowel disease	23% (15/65)	2.9% (2/68)	**0.0001**
Celiac disease	6.2% (4/65)	2.9% (2/68)	0.43
Autoimmune disease	4.6% (3/65)	11.8% (8/68)	not applicable
MEDICATION USE			
NSAID use	15.4% (10/65)	37% (25/68)	not applicable
CLINICAL INDICATION			
Abdominal pain and/or gastroesophageal reflux	57% (37/65)	63% (43/68)	0.48
ENDOSCOPIC FINDINGS			
None or normal	44.6% (29/65)	67.6% (46/68)	**0.007**
TREATMENT AFTER ENDOSCOPY			
PPIs and/or H2 antagonists	47.7% (31/65)	58.8% (40/68)	0.22

B

Figure 1: A) Histogram showing frequency of clinical disease and medication use in patients with inactive antral gastritis (blue) and normal antral mucosa (grey). B) Distribution of clinical and endoscopic variables in inactive antral gastritis and normal antral mucosa with corresponding p values (Fisher Exact Probability Test, http://vassarstats.net).

Conclusions: Biopsy diagnosis of inactive gastritis does not prompt treatment that differs from when a diagnosis of normal antrum is made. In both cases the treatment is instead based on the symptoms that prompted the endoscopy. In about half of cases inactive antral

gastritis could be a result of underlying inflammatory bowel disease or prior *H. pylori* infection. Routine ordering of *H. pylori* immunostain is not justified in biopsies with inactive antral gastritis.

778 Clinicopathologic Features of Checkpoint Inhibitor-Induced Enteritis: A Single Institution Experience

Nima Sharifai[1], Kathleen Byrnes[2]
[1]Washington University in St. Louis, Brentwood, MO, [2]Washington University in St. Louis, St. Louis, MO

Disclosures: Nima Sharifai: None; Kathleen Byrnes: None

Background: Immune checkpoint inhibitor (ICI) induced-enteritis is a severe side effect of ICIs. Given the relative recent use of ICIs, and the heterogeneity of histologic features, we aimed to characterize the clinicopathologic features of ICI-induced enteritis at our institution.

Design: Cases of patients (pts) with ICI use from 2011-2019 were retrieved from our files. The pathology report and the electronic medical record were reviewed for: type of inflammation, specific histologic features, endoscopic findings, and pertinent clinical information.

Results: Of the 46 cases available, 65% (n=30) of pts were treated with ipilimumab (IPI). The rest were treated with nivolumab (nivo; n=3), pembrolizumab (pembro; n=5), and IPI plus nivo (n=8). 67% (n=31) were men and the mean age was 58 years (range, 22-80). Most were being treated for melanoma (78%) and presented with diarrhea (85%). Most of the injury involved the colon, either isolated (43%, n=20) or multisite (48%, n=22). Histologically, the presence of apoptosis (n=20), granulomata (n=8), and intraepithelial lymphocytes (n=9) were noted. Granulomata were only seen in pts on IPI. Chronic active inflammation (80%, n=37) was the most common pattern of injury. There were two cases of chronic inactive inflammation in pts on nivo or pembro. Of the 25 small intestine biopsies, 7% (n=3) showed isolated involvement. Chronic active inflammation was the most common pattern (64%, n=16). In four cases, there was only active inflammation in the small intestine, while the colon had chronic active inflammation. Pts with small intestine involvement were mostly on IPI or nivo, with one pt on pembro.

Conclusions: The majority of our cases were associated with IPI. While ICI-induced enteritis has been described as an active colitis with minimal chronicity, we found that most had chronic active colitis. Nivo and pembro each had a case of chronic inactive enteritis, while IPI was always associated with some activity and was the only ICI with granulomata. Finally, most cases of IPI or nivo involved the small intestine, whereas only one case of pembro involved the upper GI tract. The pattern of injury can mimic inflammatory bowel disease, especially with granulomata. Presence of apoptosis and a history of prior malignancy should raise suspicion for ICI-induced enteritis. Our findings highlight the importance of appreciating the spectrum of histopathologic presentations of ICI-induced enteritis, including small intestinal involvement and varying levels of inflammation.

779 Immune Checkpoint Inhibitor-Associated Celiac Disease

Angela Shih[1], Yousef Badran[1], Alexandra Coromilas[2], Jonathan Chen[3], Marina Kem[1], Jennifer Borowsky[4], Joseph Misdraji[5], Michael Dougan[1], Mari Mino-Kenudson[1]
[1]Massachusetts General Hospital, Boston, MA, [2]Columbia University, New York, NY, [3]Cambridge, MA, [4]The Royal Brisbane & Women's Hospital, Brisbane, QLD, Australia, [5]Harvard Medical School, Boston, MA

Disclosures: Angela Shih: None; Yousef Badran: None; Alexandra Coromilas: None; Jonathan Chen: None; Marina Kem: None; Jennifer Borowsky: None; Joseph Misdraji: None; Michael Dougan: *Consultant*, Genentech; *Consultant*, Tillotts; *Consultant*, Partners Therapeutics; *Grant or Research Support*, Novartis; Mari Mino-Kenudson: None

Background: Immune checkpoint inhibitor associated duodenitis (ICI-D) has been frequently reported in the literature. Rarely, patients may develop TTG IgA antibodies presenting with a phenotype of immune checkpoint inhibitor associated celiac disease (ICI-CD). This study characterizes clinicopathologic and immunophenotypic features of ICI-CD in comparison to ICI-associated duodenitis (ICI-D) and conventional celiac disease (CD).

Design: A medical records search between 2015-2019 identified 8 cases of ICI-CD, confirmed by TTG IgA. Ten cases each of ICI-D and at least moderate CD as well as 5 normal controls were used for comparison. Clinical information was collected from the electronic medical record. IHC for CD3, CD8, TCR gamma/delta (γδ), PDL1, PD1, and CD68 were performed, with quantification of intraepithelial lymphocyte (IEL) subsets in 3 villi. PDL1 and PD1 were assessed by H scores. Statistical significance was calculated by Mann-Whitney U tests.

Results: Eight ICI-CD patients (M:F = 3:1) and ten ICI-D patients (M:F = 2:3) presented similarly with diarrhea (n=14/18) and abdominal pain (n=7/18) after an average of 4 months on immunotherapy (anti-PD(L)1, anti-CTLA4, or combined). In ICI-CD patients, TTG IgA ranged from 104 to > 300 IU/mL. Histologic findings in ICI-CD and ICI-D were similar and included expansion of the lamina propria (n=16/16), active neutrophilic duodenitis (n=13/16), increased IELs (n=13/16), and villous blunting (n=6/16). IHC showed that in ICI-CD and ICI-D, average IELs per 100 enterocytes for CD3, CD8, and γδ were similar (p=0.4 to 1). ICI-CD and ICI-D also had increased CD3 and CD8 and decreased γδ IELs compared to CD (p =0.001 to 0.04) and increased CD3 and CD8 compared to normal duodenum (p=0.008 to 0.1).

Lamina propria showed aggregates of CD68 macrophages in ICI-CD and ICI-D, but only scattered macrophages in CD and normal. Average H score for PD1 was 0 in all cases; average H score for PDL1 was 0.2 in CPI-CD and 0.5 in ICI-D, in comparison to 0.01 in CD and normal (p=0.001 to 0.04). Of ICI-CD, 6 patients were initiated on gluten free diet with adequate response, and 2 patients required steroids. ICI-D patients invariably required steroids and/or anti-TNF therapy.

		Mean Cell Counts (Per 100 Enterocytes)	Comparison with ICI-D (p value)	Comparison with CD (p value)	Comparison with Normal (p value)
CD3	ICI-CD	25 cells (SD 11 cells)	0.96	0.026 *	0.023 *
	ICI-D	28 cells (SD 14 cells)	X	0.017 *	0.0085 *
	CD	48 cells (SD 19 cells)	X	X	0.0027 *
	Normal	7.8 cells (SD 4.3 cells)	X	X	X
CD8	ICI-CD	20 cells (SD 18 cells)	0.48	0.044 *	0.12
	ICI-D	23 cells (SD 14 cells)	X	0.046 *	0.0085 *
	CD	33 cells (SD 7.5 cells)	X	X	0.0027 *
	Normal	5.9 cells (SD 3.0 cells)	X	X	X
TCR γδ	ICI-CD	0.3 cells (SD 0.6 cells)	0.42	0.0048 *	0.41
	ICI-D	1.2 cells (SD 1.8 cells)	X	0.0013 *	0.95
	CD	16 cells (SD 11 cells)	X	X	0.012 *
	Normal	0.5 cells (SD 0.5 cells)	X	X	X

* statistically significant by Mann-Whitney U test

Conclusions: ICI-CD resembles ICI-D clinically and histologically but shares serologic features and response to gluten elimination with CD. IEL immunophenotyping showed similar CD3, CD8, and γδ T cell subsets, macrophage counts, and PDL1 scores in ICI-CD and ICI-D, all of which differed from standard CD.

780 Interobserver Variability in Tumour Budding Assessment among Experienced General Surgical Pathologists: Association with "Hotspot" Selection

Sameer Shivji[1], Kai Duan[1], James Conner[2], Richard Kirsch[2]
[1]Toronto, ON, [2]Mount Sinai Hospital, Toronto, ON

Disclosures: Sameer Shivji: None; Kai Duan: None; James Conner: None; Richard Kirsch: None

Background: High grade tumour budding (TB) is a well-established prognostic factor in colorectal cancer (CRC). Despite its prognostic significance, challenges related to interobserver variability (IOV) persist. A majority of CRC resections are reported by general surgical pathologists, yet IOV has not been well studied in this group. Moreover, the relationship between "hotspot" selection for TB assessment and IOV has not been previously assessed. We therefore evaluated IOV among 9 experienced general surgical pathologists and evaluated the relationship between "hotspot" selection and IOV.

Design: A representative H&E slide was selected from 50 consecutive CRC resections to generate a study set. Two observers, experienced in TB assessment (SS, KD), evaluated TB in all slides using ITBCC criteria. Consensus TB grades served as the "gold standard" against which accuracy was measured. Nine general surgical pathologists then evaluated TB on each slide, using ITBCC criteria. Observers could designate a case non-evaluable (NE) if obscuring inflammation or glandular fragmentation precluded their assessment. Based on clinical relevance in surgical resections, Bd3 and non-Bd3 were the two categories used for Fleiss kappa analysis. For each slide, observers were provided with a corresponding digital image on which they annotated their selected 'hotspots' using a standard movable circular marker. Observer indicated 'hotspots' were digitally compiled, generating an average region of interest (ROI) for each case. The average distance between each individual hotspot and the ROI was then determined for each case, and used as a descriptive measure of degree of spread.

Results: Based on the "gold standard" assessment, the study set included 33 Bd1/2 and 17 Bd3 cases. Measured against this standard, average accuracy among observers was 74%. The Fleiss kappa value was 0.38 (fair agreement). Cases with unanimous agreement in TB grade (n=31) were associated with less spread in 'hotspot' selection compared to cases with one or more discordance (n=19) (mean spread distance of 2.4 mm vs 3.6 mm, respectively).

Conclusions: This is the largest study to date evaluating IOV in TB assessment by general surgical pathologists. Our findings suggest that IOV remains a challenge in this group. In addition, this is the first study to demonstrate that variation in 'hotspot' selection is associated with IOV. Educational initiatives focused on this aspect of TB assessment may prove helpful in reducing IOV.

781 Loss of ARID1A Expression is Associated with Poor Prognosis in EBV-Negative and Mismatch Repair Protein Proficient Gastric Carcinomas

Susan Shyu[1], Reetesh Pai[2], Changqing Ma[3]
[1]University of Pittsburgh Medical Center, Columbia, MD, [2]UPMC-Presbyterian Hospital, Pittsburgh, PA, [3]University of Pittsburgh, Pittsburgh, PA

Disclosures: Susan Shyu: None; Reetesh Pai: None; Changqing Ma: None

Background: *ARID1A* has been implicated as tumor suppressor gene in gastric carcinoma. ARID1A loss has been found in nearly 20% of gastric carcinomas and associated with Epstein-Barr virus (EBV) positivity and microsatellite instability/DNA mismatch repair (MMR) protein deficiency. The prognostic significance of ARID1A loss in gastric carcinoma has not been well-defined, particularly in EBV-negative, DNA MMR protein proficient gastric carcinoma.

Design: In this study we retrospectively evaluated 184 surgically resected gastric carcinomas for ARID1A and DNA MMR proteins by immunohistochemistry and EBV infection by EBER in-situ hybridization.

Results: Loss of ARID1A expression was detected in 32 (17%) of 184 gastric carcinomas. DNA MMR protein deficiency was identified in 12% (22/184) carcinomas while 8 (4%) carcinomas were EBV-positive. Consistent with literature, EBV-positive carcinomas more frequently demonstrated ARID1A loss (4/8, 50%) than EBV-negative carcinomas (28/176, 15%, $P = 0.03$). MMR deficiency was also more frequently detected in ARID1A loss carcinomas (11/32, 34%) than in ARID1A retained carcinomas (11/152, 7%; $P < 0.001$). ARID1A loss was not associated with survival in the entire cohort. In the subset of 154 MMR protein proficient, EBV-negative gastric carcinomas, 17 (11%) demonstrated loss of ARID1A expression. ARID1A loss was more frequently identified in carcinomas of female patients (13/68, 19%) than those of male patients (4/86, 5%, $P = 0.008$) and more frequent in diffuse-type than in intestinal-type carcinomas (14/68, 21% vs. 1/63, 2%, $P = 0.003$). Furthermore, in this subset, patients with ARID1A loss carcinomas had significantly decreased overall survival (OS) and disease-free survival (DFS) compared to patients with ARID1A retained carcinomas (mean [month]: OS: 19 vs. 34, $P = 0.01$; DFS: 13 vs. 29, $P = 0.0498$, respectively). On multivariate analysis, ARID1A loss was associated with poor OS and DFS independent of other prognostic factors including R0 resection, clinical stage and angiolymphatic invasion (hazard ratio and 95% confidence interval: OS 2.3, 1.1-4.6, $P = 0.02$; DFS 2.3, 1.1-4.8, $P = 0.036$, respectively).

Conclusions: In summary, in MMR protein proficient, EBV-negative gastric carcinomas, loss of ARID1A expression is associated with diffuse-type histology and high prevalence in carcinomas of female patients. Furthermore in these patients, ARID1A loss in gastric carcinoma is independently associated with a poor prognosis.

782 Clinicopathologic Analysis of Appendiceal Goblet Cell Adenocarcinoma with Peritoneal Metastasis: WHO Grade Predicts Survival Following Cytoreductive Surgery with Intraperitoneal Chemotherapy

Susan Shyu[1], Lauren Hall[2], Reetesh Pai[3]
[1]University of Pittsburgh Medical Center, Columbia, MD, [2]University of Pittsburgh Medical Center, Pittsburgh, PA, [3]UPMC-Presbyterian Hospital, Pittsburgh, PA

Disclosures: Susan Shyu: None; Lauren Hall: None; Reetesh Pai: None

Background: Pathologic classification and prediction of clinical behavior of appendiceal goblet cell adenocarcinoma (GCA) remains a challenge. While most studies have focused on the grading and evaluation of the primary appendiceal tumor, the utility of applying the same grading schemes to peritoneal metastases is unknown.

Design: We compared the clinicopathologic features and overall survival (OS) of 63 patients with peritoneal metastasis of GCA who underwent cytoreductive surgery with hyperthermic intraperitoneal chemoperfusion (CRS-HIPEC). The tumors were graded using both the WHO 5th edition criteria and the criteria proposed by Tang et al. The GCA patients were also compared to 120 patients with appendiceal mucinous neoplasia (59 G1, 41 G2, and 20 G3) treated with CRS-HIPEC.

Results: The peritoneal metastasis of 46 GCA (73%) were WHO G3, 10 (16%) were G2, and 7 (11%) were G1. G3 GCA more frequently demonstrated areas of gland-forming adenocarcinoma or undifferentiated carcinoma (71%) compared to G2 GCA (40%) and G1 GCA (0%) (p=0.04). Patients with G3 GCA were less likely to achieve a completeness of cytoreduction (CC) score of 0 (49%) compared to patients with G2 (60%) and G1 GCA (100%) (p=0.04).

G3 GCA demonstrated significantly decreased OS compared to G1/G2 GCA (median survival: 33 months vs 98 months, p=0.01). On univariate analysis, factors associated with reduced survival were WHO G3 grade (hazard ratio (HR) 3.2, 95% CI 1.2-8.3, p=0.02) and CC score ≥1 (HR 2.2, 95% CI 1.1-4.2, p=0.02). In the multivariable model, only WHO G3 grade was associated with reduced survival (HR 2.5, 95% CI 0.9-7.0, p=0.05). There was no significant difference in OS between the Tang A/B (median: 34 months) and Tang C groups (median: 35 months).

In comparison to appendiceal mucinous neoplasia, G1/G2 GCA had reduced survival compared to G1 mucinous neoplasms (median 204 months, p=0.001) but a similar survival to G2 mucinous adenocarcinoma (median 80 months, p=0.9). Patients with G3 GCA demonstrated significantly reduced OS compared to patients with G2 mucinous adenocarcinoma (p<0.001) but a similar survival to G3 mucinous adenocarcinoma.

Conclusions: The WHO 5th edition grading scheme is better at predicting survival in patients with peritoneal GCA compared to the Tang scheme. Patients with G3 GCA have reduced survival compared to G1/G2 GCA. Compared to appendiceal mucinous neoplasia, G1/G2 GCA have significantly reduced survival compared to G1 but a similar survival to G2 mucinous adenocarcinoma.

783 Immunohistochemical Staining for PTEN in Gastrointestinal Lesions/Polyps Can Be Used to Identify Patients with Cowden Syndrome

Faiza Siddiqui[1], Shruti Patrey[2], Jessica Stoll[1], Sonia Kupfer[1], John Hart[2], Namrata Setia[2]
[1]The University of Chicago Medicine, Chicago, IL, [2]The University of Chicago, Chicago, IL

Disclosures: Faiza Siddiqui: None; Shruti Patrey: None; Jessica Stoll: *Advisory Board Member*, Invitae; Sonia Kupfer: None; John Hart: None; Namrata Setia: None

Background: Gastrointestinal lesions in Cowden syndrome (CS) are present in over 90% of affected individuals and include a variety of mucosal mesenchymal polyps, as well as epithelial polyps such as tubular adenomas (TAs) and sessile serrated polyps (SSPs). Recognition of these polyps as markers of CS is challenging in the absence of a clinical history of CS, as the mesenchymal polyps may be morphologically underwhelming and TAs/SSPs may be regarded as sporadic. The aim of our study was to determine if the use of immunohistochemical staining for PTEN can facilitate the recognition of these gastrointestinal lesions/polyps as markers of CS.

Design: Immunohistochemistry for PTEN was performed using a rabbit anti-PTEN monoclonal antibody (1:200 dilution; Cell Signaling Technology, Danvers, MA). The case group was formed by 111 polyps/lesions from 8 individuals with a confirmed germline diagnosis of CS. Appropriate site-matched sporadic polyps of the same type formed the control group. PTEN expression was recorded as follows: retained, complete loss, or heterogeneous loss of expression. Heterogenous loss was defined as loss of expression in some components and retained expression in other components of the polyp.

Results: Representative examples of PTEN expression in gastrointestinal lesions/polyps are shown in Figure 1. Heterogenous loss of PTEN expression was seen in the ganglion cells in 100% (11/11) of ganglioneuromas, the myofibroblasts in 92.8% (52/56) of mesenchymal polyps, in the epithelium of 80% (4/5) of sessile serrated polyps, in the epithelium of 62% (15/24) of tubular adenomas, and in all the upper tract lesions (100%, 9/9- 2/2 glycogenic acanthosis, 3/3 fundic gland polyps, 2/2 gastric stromal polyps, and 2/2 duodenal polyps). Retained expression of PTEN was seen in the epithelial and stromal cells of 100% (6/6) of inflammatory-type polyps. The sensitivity of PTEN expression for CS-related mesenchymal polyps, SSPs, TAs, and upper tract lesions was 92.8%, 80%, 62.5%, and 100%, respectively. The specificity of PTEN expression for CS-related mesenchymal polyps, SSPs, TAs, and upper tract lesions was 100%, 57.1%, 77%, and 100%, respectively.

Figure 1 - 783

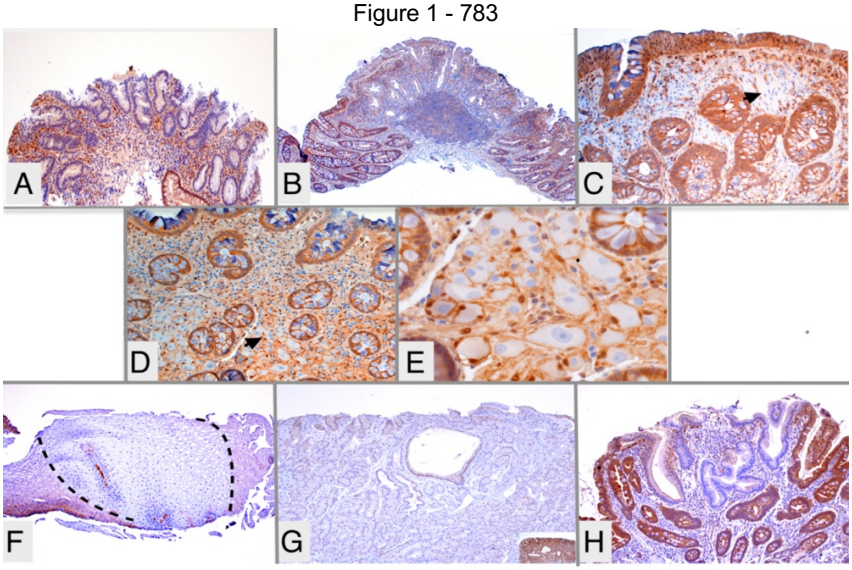

Representative images showing heterogenous loss of PTEN expression in Cowden syndrome associated gastrointestinal polyps/lesions.
No PTEN expression is seen in the epithelium of a tubular adenoma (A), epithelium of a sessile serrated polyp (B), myofibroblasts of a mesenchymal polyp (C, arrow), ganglion cells of a ganglioneuroma [D (arrow, 100x) and E (400x)], epithelium of glycogenic acanthosis (F, dashed lines), parietal/chief cells in a fundic gland polyp (G, inset- bottom right- PTEN expression in a sporadic fundic gland polyp), and epithelium of a duodenal polyp (H).

Conclusions: Heterogenous loss of PTEN expression, especially in mesenchymal polyps and upper gastrointestinal tract lesions, is both sensitive and specific for CS.

784 Serrated Epithelial Change in Long-Standing Inflammatory Bowel Disease (IBD) - A Precursor Lesion Morphologically and Genetically Distinct from Sporadic Serrated Polyps Arising in IBD Patients

Aatur Singhi[1], Elizabeth Montgomery[2]
[1]University of Pittsburgh Medical Center, Sewickley, PA, [2]Johns Hopkins Medical Institutions, Baltimore, MD

Disclosures: Aatur Singhi: None; Elizabeth Montgomery: None

Background: Serrated epithelial change (SEC), characterized by strikingly distorted architecture and crypt serrations without dysplasia arises in patients with longstanding inflammatory bowel disease (IBD). Although SEC is histologically readily distinguished from sessile serrated adenomas (SSAs) and hyperplastic polyps (HPs), whether SEC is a distinct precursor to IBD-associated colorectal neoplasia is incompletely established. We attempted to molecularly profile a series of SEC specimens and associated dysplasia/adenocarcinoma from the same patients for genes frequently altered in sporadic serrated lesions and colorectal cancer.

Design: The study cohort consisted of 10 patients with SEC and associated dysplasia/cancer that included 14 specimens (6 resections and 8 biopsies): 8 cases of SEC without dysplasia, 5 low-grade dysplasia (LGD), 4 high-grade dysplasia (HGD) and 5 adenocarcinomas. Targeted next-generation sequencing (NGS) was performed for 22 genes implicated in colorectal neoplasia with an average depth of coverage >1000X.

Results: Targeted NGS detected genomic alterations in 3 of 8 (38%) cases of SEC without dysplasia, 3 of 5 (60%) LGD, 4 of 4 (100%) HGD and 5 of 5 (100%) adenocarcinomas. The most frequently altered gene was *TP53* (14 of 22, 64%), followed by *KRAS* (n=2, 9%), *PIK3CA* (n=2, 9%), *RNF43* (n=2, 9%), *SMAD4* (n=2, 9%) and *BRAF* (n=1, 5%). Mutations in *TP53* were detected in 3 (38%) cases of SEC without dysplasia, 3 (60%) LGD, 3 (75%) HGD and 5 (100%) adenocarcinomas. However, *KRAS* mutations were only detected in SEC without dysplasia and a *BRAF* mutation was found only in a case of associated HGD. Paired specimens from the same patients were available to compare SEC without dysplasia to associated dysplasia (n=5) and adenocarcinoma (n=3), and associated LGD to adenocarcinoma (n=1). Among these 6 patients, 4 pairs of specimens harbored *TP53* mutations and the same alteration was conserved between them. Of note, a *KRAS* mutation was also present in a case of SEC without dysplasia, but absent in associated areas of LGD, HGD and adenocarcinoma.

Conclusions: In contrast to SSAs and HPs arising in patients with IBD, SEC is not only morphologically distinct from them but generally lacks mutations in *BRAF* and *KRAS*. Instead mutations in *TP53* are the most prevalent alteration in not only SEC, but associated dysplasia and adenocarcinoma. These *TP53* alterations are conserved between SEC and associated neoplastic specimens thereby implicating SEC in the pathogenesis of IBD-associated colorectal cancer.

785 Tailgut Cyst (Retrorectal Cystic Hamartoma): A Pathological Review of 70 Cases

Anna Sokolova[1], Ian Brown[2], Christophe Rosty[3], Rondell Graham[4]
[1]Queensland Health, Herston, QLD, Australia, [2]Brisbane, QLD, Australia, [3]Envoi Specialist Pathologists, Brisbane, QLD, Australia, [4]Mayo Clinic, Rochester, MN

Disclosures: Anna Sokolova: None; Ian Brown: None; Christophe Rosty: None; Rondell Graham: None

Background: Tailgut cyst (retrorectal cystic hamartoma) is one of several cystic lesions that may be encountered in the retrorectal/presacral space. Their histogenesis is unknown, possibly representing a subtype of teratoma or vestigial remnant of the hindgut. To date the limited published data comprises single case reports or small series, with a bias to cases associated with neoplasia, resulting in a published rate of neoplastic transformation of 26.6%. This study was undertaken to review the pathological findings of an unselected large series of tailgut cysts.

Design: All cases of histologically confirmed tailgut cyst from a retrospective database search of two institutions were retrieved and re-reviewed. Demographic data (age and gender), cyst size, multiloculation, types of epithelium present (squamous, columnar, transitional between squamous and columnar), presence and type of neoplasia, presence of cyst rupture, and features in the cyst wall (smooth muscle, inflammation, calcification, heterotopic bone) were recorded.

Results: 70 cases were identified. The median age was 53 years (range 12-77) and 74% were female. Mean cyst diameter was 5.4cm (range 0.2-20cm) and 46% were larger than 5cm. The majority were multiloculated (figure 1). Epithelial types included transitional (71%), ciliated (7%) and non-ciliated (24%) columnar epithelium and keratinizing (27%) and non-keratinizing (37%) squamous epithelium. 57% of cases had more than one epithelial type. 12 cases had evidence of rupture with an associated inflammatory response. Smooth muscle was present in the wall in all cases. Two (3%) case had bone and two (3%) had dystrophic calcification in the wall. Six cases (9%) were associated with neoplasia arising directly from the cyst (3 mucinous adenocarcinoma, 1 adenocarcinoma, NOS and 2 neuroendocrine tumors (figure 2)). Three of the four adenocarcinomas were associated with dysplasia in the epithelial lining of the cyst.

Figure 1 - 785

Figure 2 - 785

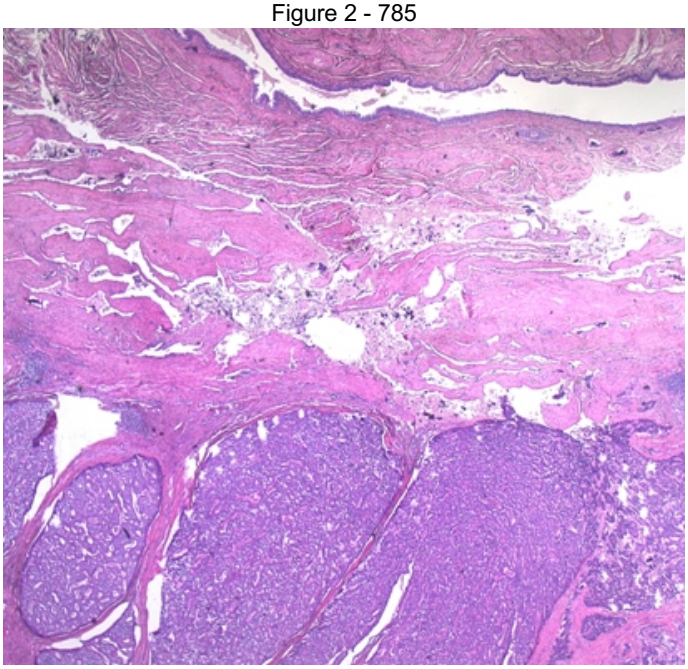

Conclusions: Tailgut cyst was more common in females and typically presented in middle age. Many were large with a mean cyst diameter of 5.4cm, the largest cyst measuring 20cm. The cysts were predominantly multiloculated, demonstrated multiple epithelial types and had smooth muscle in the wall. 9% of cases demonstrated associated neoplasia which is a lower prevalence than reported in the literature, however, sufficient to justify close examination and complete embedding of all cases received with a clinical diagnosis of tailgut cyst.

786 Colorectal Adenocarcinomas Missed by Screening Show High Risk Pathologic Features

Michael Steel[1], Hussam Bukhari[2], Laura Gentile[3], Jennifer Telford[4], David Schaeffer[1]
[1]Vancouver General Hospital, Vancouver, BC, [2]Vancouver, BC, [3]BC Cancer Agency, Vancouver, BC, [4]St Paul's Hospital, Vancouver, BC

Disclosures: Michael Steel: None; Hussam Bukhari: None; Laura Gentile: None; Jennifer Telford: None; David Schaeffer: None

Background: The fecal immunochemical test (FIT) is used to screen average-risk individuals age 50 to 74 years every two years with a follow-up colonoscopy for positive results. The sensitivity for the detection of colorectal adenocarcinoma is over 80% in meta-analysis for a one-time test. Nonetheless, a proportion of colorectal adenocarcinoma is diagnosed following a negative FIT; the biology of these malignancies requires further investigation.

Design: A retrospective pathology review of colorectal malignancies from 926 individuals who completed FIT in the British Columbia Colon Screening Program in 2014 and whose pathology was available to review, was conducted. This cohort was divided into two groups: individuals with colorectal adenocarcinomas diagnosed following a positive FIT (screen detected), and individuals with colorectal adenocarcinoma diagnosed within 25 months following a negative FIT (interval cancers). Rates of pertinent pathologic parameters were compared between the screen detected and interval cancer groups: histotype, T-stage, tumor size, grade, mismatch repair (MMR) deficiency, BRAFV600E mutational status, and additional prognostic considerations as outlined in the American Joint Committee on Cancer 8th Edition.

Results: 876 screen detected and 50 interval cancers were identified. The average ages were 67.1 and 68.2 years for screen detected and interval cancer groups, respectively. Male sex accounted for 58.0% and 52.0% of the screen detected and interval cancer groups, respectively. Interval cancers exhibited higher rates of high-grade differentiation (including poorly and un-differentiated cases), aggressive histotype (signet ring and mucinous carcinoma), and lymphovascular invasion than did the screen detected cancers (Table 1).

Table 1. Relative risk of pertinent pathologic parameters seen in interval cancers, compared to those seen in screen detected colorectal cancers.

Pathologic Parameter	Interval Cancer %	Screen Detected Cancer %	Relative Risk (RR)
Aggressive histotype	**14.0%** (7/50)	**3.1%** (28/876)	**4.4** (2.01 – 9.53)
High-grade	**34.8%** (16/46)	**8.2%** (65/792)	**4.2** (2.68 – 6.71)
Lymphovascular invasion	**35.6%** (16/45)	**21.6 %** (165/765)	**1.6** (1.09 – 2.50)
Rightsidedness	**36.0%** (18/50)	**24.5%** (215/876)	**1.5** (1.00 – 2.16)
Perineural invasion	**21.7%** (5/23)	**14.3%** (71/495)	**1.5** (0.68 – 3.39)
BRAFV600E Mutation	**16.7%** (3/18)	**10.9%** (20/184)	**1.5** (0.50 – 4.67)
High-grade tumor budding	**23.1%** (3/10)	**15.1%** (30/199)	**1.5** (0.54 – 4.36)
Extramural venous invasion	**27.3%** (3/11)	**19.4%** (53/273)	**1.4** (0.52 – 3.80)
Regional lymph node involvement	**38.3%** (18/47)	**32.7%** (243/744)	**1.2** (0.80 – 1.71)
Metastasis	**4.3%** (2/46)	**5.4%** (40/743)	**0.8** (0.20 – 3.24)
Tumor deposit(s)	**42.8%** (9/21)	**53.4%** (70/131)	**0.8** (0.47 – 1.35)
MMR deficiency	**8.7%** (2/23)	**11.1%** (29/261)	**0.8** (0.20 – 3.07)

The associated ranges accompanying relative risks represent 95% confidence intervals. The designation of “high-grade” includes “poorly-differentiated” and “undifferentiated” cases. “Rightsidedness” was attributed to any tumor that involved the cecum, ascending colon, hepatic flexure or transverse colon. Aggressive histotype was denoted by cases of both mucinous and signet-ring carcinoma. MMR: mismatch repair.

Conclusions: Colorectal adenocarcinoma diagnosed after a negative FIT may be associated with worse prognostic determinants than screen detected cancers. Further study of a larger cohort of interval cancers controlling for interaction amongst the different pathologic parameters will be undertaken.

787 Appendiceal Neuroendocrine Hyperplasia: Proposed Terminology for Small Appendiceal Neuroendocrine Tumors Based on Long-Term Follow-Up and Review of the Literature

Yvelisse Suarez[1], Qing Chang[2], Odise Cenaj[3]
[1]NYU Medical Center, New York, NY, [2]NYU Langone Health, Staten Island, NY, [3]New York University Langone Health, New York, NY

Disclosures: Yvelisse Suarez: None; Qing Chang: None; Odise Cenaj: None

Background: Neuroendocrine tumors (NETs) have been well studied and most organs have criteria which allow for neuroendocrine hyperplasia (NH) or a preneoplastic state before a neuroendocrine proliferation is defined a neuroendocrine tumor. In the lung, neuroendocrine proliferations <5mm are designated tumorlets. In the stomach, neuroendocrine proliferations range from NH to neuroendocrine dysplasia, and the designation of NET does not occur unless the proliferation is >5mm. In the pancreas, neuroendocrine proliferations with a diameter of <5 mm are termed neuroendocrine microadenomas. However in the appendix, there is no provision for NH and there are no established minimal size criteria for appendiceal NETs in the current 5th edition WHO book, which considers all NETs to have malignant potential. Also the current CAP protocol applies to all appendiceal NETs regardless of size, forcing pathologists to diagnose NETs despite studies demonstrating small appendiceal NETs (<1cm) to be indolent.

Design: A single institution database of adult patients with appendectomies containing the word “neuroendocrine” and “carcinoid” was queried from January 2004 to December 2012. Patients with neuroendocrine carcinoma, goblet cell carcinoid, and patients without follow up were excluded.

Results: 32 patients were included in the study. The mean age at diagnosis was 40.3 years (18-79). Females represented 59.3 % (19/32) of all patients. All appendiceal NETs were incidentally identified in a background of acute appendicitis. Tumor size ranged from 1 mm to 17 mm and the depth of extension ranged from submucosa to mesoappendix. One patient underwent a right hemicolectomy because of tumor size > 1cm. In long term follow up (7-15 years), none of these patients had disease recurrence.

Depth of invasion	Number of cases	5-year survival rate	10-year survival rate
Mucosa	2	100%	100%
Submucosa	5	100%	100%
Muscularis propria	6	100%	100%
Subserosa	6	100%	100%
Serosa and mesoappendix	11	100%	100%
Distant metastasis	0	N/A	N/A
Unspecified	2	100%	100%
Tumor Size	Number of cases	5-year survival rate	10-year survival rate
<=5 mm	17	100 % (17/17)	100 % (17/17)
>5 mm	15	100 % (15/15)	100 % (15/15)
Tumor Grade	Number of cases	5-year survival rate	10-year survival rate
G1	11	100%	100%
G2	1	100%	100%
Unspecified	20	100%	100%

Conclusions: The majority of appendiceal NETs are small incidental findings associated with acute appendicitis. In this setting, neural proliferation and mucosal expansion can often be seen and it is reasonable for NH to also represent inflammatory/reactive changes rather than a neoplastic process given their indolent behavior and long term survival rate (100%). In the appendix, we propose NH is part of the inflammatory process and should not be classified as a NET unless it is >5mm. We advocate the terminology of appendiceal NH in neuroendocrine proliferations <5mm in keeping with size criteria in other organs. This change in terminology from NET to NH may reduce unnecessary medical surveillance, overtreatment, and patient anxiety.

788 p4EBP1 and PTEN Expression in Advanced Colorectal Cancer: Relation to Predictive Markers for Chemotherapy

Oksana Sulaieva[1], Dmytro Shapochka[1]
[1]*Laboratory of Pathology CSD Health Care, Kyiv, Ukraine*

Disclosures: Oksana Sulaieva: None; Dmytro Shapochka: None

Background: Metabolic reprogramming is a key factor driving secondary mutagenesis and tumor resistance to therapy in colorectal cancer (CKC). Tumor biological behavior and metabolism are based on tight cooperation between MAPK signaling and PI3K/AKT/mTOR pathways that are affected by different mutations. The PI3K/AKT/mTOR pathway and its inhibitor PTEN aberrations are common in CRC. However, it is still unclear how their interplay related with other predictive markers expression. The aim of this study was to investigate the relationship of mTOR and PTEN expression with mutations, tumor microenvironment and theranostic markers in advanced CRC.

Design: We retrospectively collected clinical and pathological records as well as molecular profiling data of 51 patients with advanced CRC (30 men and 21 women – 59,23±1,85 and 60,65±2,0 years old respectively). Molecular profiling was performed by NGS with either 65- or 313-gene panel, MSI-testing and 8 immunohistochemical (IHC) markers, including DNA repair-associated enzymes (ERCC1, TOPO1, TS) and tumor immune status (CD8+ and PD-L1). Evaluation of mTOR activation was performed by IHC detection of its effector – p4EBP1. The expression of p4EBP1 and PTEN were assessed by IHC.

Results: Expression of p4EBP1 and PTEN was not related with patients age, sex, tumor location and size. We found loss of PTEN expression in 20 tumors (39,2%), however only 8 of them were p4EBP1 positive. Among 31 p4EBP1 positive tumors (60,8%) there were 8 cases with loss of PTEN, and 23 tumors demonstrated PTEN and p4EBP1 co-expression. PIK3CA mutations were found in 5 (10%) patients, all of them were PTEN positive, but only 3 of 5 demonstrated p4EBP1 expression. We did not find significant relationship between RAS, BRAF, P53, APC mutations and PTEN or p4EBP1 expression. Loss of PTEN was associated with low CD8+ cells infiltration whereas PTEN+ tumors demonstrated high number of CD8+ lymphocytes (OR=3,15; p=0,05) regardless of MSI and PD-L1 status. Evaluating the expression of enzymes responding to DNA damage, we found that most of observed tumors expressed TOPO1. TS expression was higher in p4EBP1+ tumors (p=0,006). PTEN+/p4EBP1- tumors showed lower expression of ERCC1 (p=0,0289) and TS (p=0,0285). However, the highest rate of ERCC1 and TS expression was found in PTEN-/p4EBP1- tumors (p=0,015).

Conclusions: Changes in balance between p4EBP1 and PTEN affect tumor sensitivity to chemotherapy, associated with alternative expression of ERCC1 and TS, and alter tumor immune status.

789 Histologic Features of Clostridioides difficile Colitis in Patients with Inflammatory Bowel Disease

Jacob Sweeney[1], Carl Crawford[2], Zhengming Chen[1], Jose Jessurun[1], Rhonda Yantiss[1]
[1]*Weill Cornell Medicine, New York, NY,* [2]*Weill Cornell Medical Center, New York City, NY*

Disclosures: Jacob Sweeney: None; Carl Crawford: *Speaker*, Merck; *Primary Investigator*, Finch; *Primary Investigator*, Summit; *Speaker*, RedHill; Zhengming Chen: None; Jose Jessurun: None; Rhonda Yantiss: None

Background: Distinguishing *Clostridioides difficile* infection from active colitis in patients with inflammatory bowel disease (IBD) poses several challenges because their clinical presentations, endoscopic appearances, and histopathologic inflammatory patterns can be similar, especially when pseudomembranes and other classic features of *C. difficile* infection are lacking. Distinction between infection and a colitic flare is potentially important to the gastroenterologist who may be contemplating escalation of therapy. The aim of this study was to identify histopathologic lesions that favor the diagnosis of *C. difficile*-related colitis over active inflammatory bowel disease.

Design: The study group included 22 patients with IBD (15 with ulcerative colitis and 9 with Crohn disease) and with worsening diarrhea; all underwent colonoscopy with biopsies, had concurrent positive PCR assays for *C. difficile* toxin, and were subsequently treated for this infection. None received antibiotic therapy prior to colonoscopy or had other enteric infections. Routinely stained histologic sections from biopsy material were evaluated for the distribution of neutrophils in the lamina propria, crypts and surface epithelium, location of plasma cell-rich infiltrates relative to epithelial injury, necrosis, ischemic changes, and pseudomembranes. The features were compared with those of 28 IBD controls with similar symptoms and negative *C. difficile* toxin assays.

Results: Although all patients in the study group had endoscopic colitis, only 2 (9%) had pseudomembranes. Lamina propria neutrophils distant from inflamed crypts (Figure 1) and a scarcity of plasma cells in close proximity to actively inflamed surface epithelium and crypts (Figure 2) were significantly more common among *C. difficile*-infected patients than controls (32% vs 4%, p=0.02; 41% vs 4%, p=0.003; 18% vs 0%, p=0.03, respectively). However, crypt abscesses were more common among *C. difficile*-negative patients than the study group (68% vs 36%, p=0.04). None of the other features evaluated distinguished superimposed infection from an IBD flare.

Figure 1 - 789

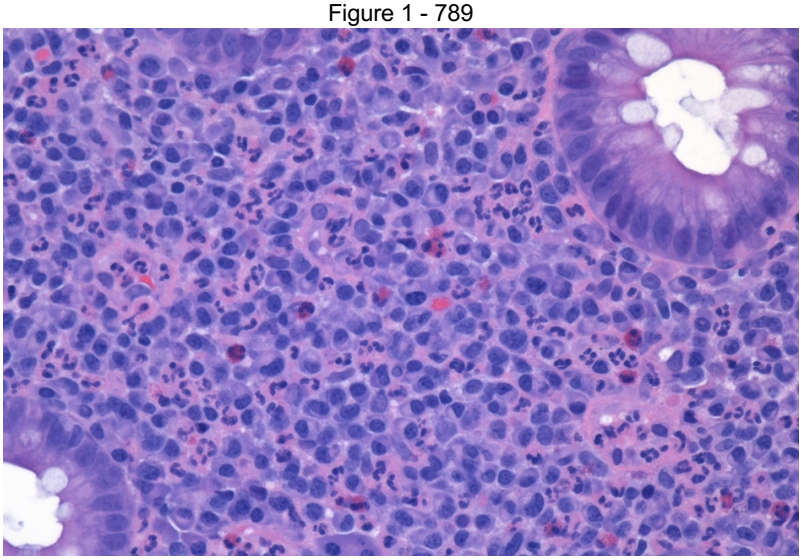

Figure 2 - 789

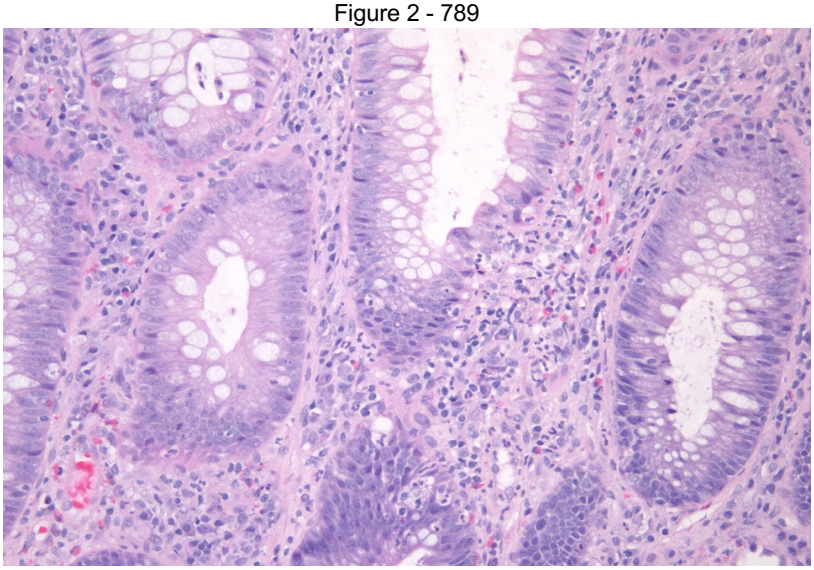

Conclusions: Epithelial cell necrosis, mucosal ischemia, and pseudomembranes are generally lacking in *C. difficile*-infected IBD patients. However, neutrophil-rich lamina propria infiltrates distant from areas of cryptitis and neutrophilic infiltration of the epithelium unaccompanied by nearby plasma cells are significantly more common among *C. difficile*-infected IBD patients than those with worsening IBD.

790 Deep Proteomics of Diffuse-Type Gastric Cancer Uncovers New Therapeutic Targets and Accelerates Drug Repositioning

Atsushi Tanaka[1], Makiko Ogawa[1], Julia Wang[1], Ronald Hendrickson[1], David Klimstra[1], Michael Roehrl[1]
[1]Memorial Sloan Kettering Cancer Center, New York, NY

Disclosures: David Klimstra: None; Michael Roehrl: None

Background: Genomics and transcriptomics of diffuse-type gastric cancer (DGC) have discovered many oncogenic mutations and activated signaling pathways. However, there have only been few new therapeutic strategies for DGC, and these have not yielded significant improvement in patient outcome. To date, there are only few studies that have applied deep pan-proteomics to DGC. Especially lacking is the use of proteomics for therapeutic target discovery. Moreover, previous transcriptome studies likely missed targetable proteins because large-scale correlation between mRNA abundance and quantitative protein expression is generally low. This encouraged us to perform a pan-proteomic analysis of DGC and to identify protein biomarkers and therapeutic targets.

Design: We obtained raw proteome data and annotation for 80 DGCs matched with normal mucosa from the ProteomeExchange data repository. First, we re-analyzed semi-quantitative protein expression data to discover differentially expressed proteins in tumor by using Perseus informatics. Next, to uncover therapeutic targets that have already been targeted in other organ cancers, we used the list of DGC-upregulated proteins and searched for drug-protein interactions by using the Drug-Gene Interaction database (DGIdb). In addition, to discover specific neoantigens of DGC, which might provide new biomarkers/therapeutic targets, we analyzed mass-spectrometric raw data by our in-house mutant peptide detection pipeline.

Results: We found and quantified over 10,000 proteins with 1% FDR in these samples. In differential analyses, we detected 347 up-regulated proteins and 283 down-regulated proteins in DGC compared to adjacent normal mucosa with 5% FDR and an 8-fold change threshold. Based on a DGIdb search of 347 up-regulated proteins, 138 proteins (40%) had 687 drugs with interactions. Of these, 95 proteins (69%) had FDA-approved drugs, suggesting possible avenues for therapeutic repurposing in clinical practice. Furthermore, integrating proteome data with the human SNP and COSMIC databases, we discovered DGC-specific neoantigens. Some of these showed high antigenicity scores based on MHC class I binding prediction algorithms, such as NetMHCpan, suggesting new immunotherapy targets.

Conclusions: Global deep proteomics by mass spectrometry can discover promising therapeutic targets and potential biomarkers that are specific for DGC. Pan-proteomic testing of cancers may enable us to tailor the treatment of DGC and provide powerful solutions for other cancers.

791 Deep Proteomics of Colorectal Cancer Liver Metastases Uncovers New Tumor Subtypes and Therapeutic Targets

Atsushi Tanaka[1], Makiko Ogawa[1], Julia Wang[1], Ronald Hendrickson[1], David Klimstra[1], Michael Roehrl[1]
[1]Memorial Sloan Kettering Cancer Center, New York, NY

Disclosures: David Klimstra: None; Michael Roehrl: None

Background: Approximately 20% of patients with colorectal carcinoma (CRC) present with distant metastases at the time of diagnosis, most often in the liver. To date, there are few studies of metastatic CRC (mCRC) using deep pan-proteomic approaches. Moreover, previous transcriptome studies likely missed targetable proteins because large-scale correlation between mRNA abundance and quantitative protein expression is generally low. This encouraged us to perform mass spectrometric pan-proteomic analyses of mCRC and to identify protein biomarkers that are specific to metastatic lesions.

Design: We selected 25 matched triplet sample sets of primary CRC, liver metastasis, and normal mucosa. Total proteomes were extracted from fresh frozen tissue and analyzed by liquid chromatography tandem mass spectrometry using a high-end Orbitrap Fourier transform instrument. Protein identification and expression profiling were performed with MaxQuant software using label-free quantification. We performed differential expression analyses and protein pathway enrichment analyses. To uncover potential therapeutic targets, we searched for drug-protein interactions by using the drug-gene interaction database (DGIdb).

Results: We detected 7,574 proteins in these samples. Of these proteins, 4,751 proteins were shared by both primary and metastatic lesions. 1,145 proteins were only detected in metastases. Unsupervised clustering of primary and metastatic lesions discovered 4 distinct proteomic subtypes in primary and metastatic lesions. In differential analyses, we found 165 up-regulated proteins and 121 down-regulated proteins in metastatic CRC that distinguished metastases from primary CRC. Among metastasis-upregulated differentially expressed proteins (DEPs), 36 proteins (22%) were unfavorable outcome factors in the TCGA CRC dataset, suggesting selected DEPs in metastatic lesions may provide potential prognostic biomarkers. Based on a DGIdb search, 79 mCRC-specific proteins have FDA-approved drug interaction partners, suggesting possible new avenues for targeting metastases specifically. A KEGG pathway analysis found enrichment of metastasis-specific metabolic pathways that may represent additional therapeutic vulnerabilities.

Conclusions: Global deep proteomics by mass spectrometry can uncover new proteome-based CRC subtypes of primary and metastatic lesions. Our approach provides promising therapeutic protein targets and proof-of-principle for new diagnostic proteomic tests that are specific for mCRC.

792 Measuring Submucosal Depth of Invasion in Endoscopic Mucosal Resections for Barrett's Adenocarcinoma Would Only Rarely Impact the Decision for Esophagectomy

Alexander Taylor[1], Jerome Cheng[1], Maria Westerhoff[1]
[1]University of Michigan, Ann Arbor, MI

Disclosures: Alexander Taylor: None; Jerome Cheng: None; Maria Westerhoff: None

Background: Endoscopic mucosal resection (EMR) has made it possible for Barrett's (BE) patients with superficial cancers to be treated without esophagectomy. Recent pathology society guidelines recommend measuring depth of invasion in submucosal cancers (SM-CA). This is based on reports that, in low risk cancers, SM-CA invasion ≤500 µm from the deepest aspect of muscularis mucosa is associated

with low nodal metastasis rates and good outcomes similar to intramucosal cancer. Thus, low risk, SM-CA ≤500 µm pts can potentially be spared surgery. The AJCC & CAP do not require measurements. Moreover, a recent study indicates that pathologists' measurements of SM-CA invasion are not reproducible. Hence, we sought to determine how often low risk, SM-CA occurs, and the impact that depth measurement could have on the decision for esophagectomy.

Design: Our database was searched for all BE-cancer EMRs from 2013-2019. Cancer differentiation, lymphovascular invasion (LVI), deep margin status, and outcomes were assessed. Low risk SM-CAs were defined as in the literature: negative deep margin, no high grade histology (G3), no LVI. These cancers were measured for invasion depth to determine ≤500 µm or >500 µm SM-CA invasion from the deepest aspect of muscularis mucosa.

Results: Of 165 EMRs from 81 BE-cancer pts, 8.5% (n=14) were SM-CA. All SM-CA pts were offered esophagectomy according to ACG guidelines. Overall, 78% SM-CAs had high risk features, including positive deep margins (57%), G3, or LVI (21%) (FIG 1). Three (1.8% of all EMRs) had low risk SM-CA, meaning the next step, treatment decision point could potentially be affected by depth measurements. Of these, 1 had >500 µm and the other 2 had ≤500 µm (FIG 2). One pt with ≤500 µm SM-CA refused esophagectomy; the other received it. All with low risk SM-CA regardless of depth are alive without disease, including the pt who refused surgery, on 2 year follow up.

Figure 1 - 792

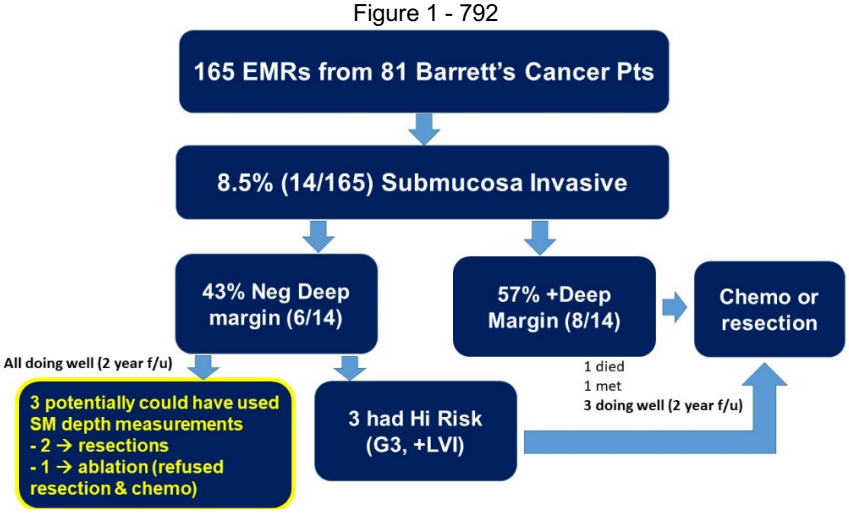

Figure 2 - 792

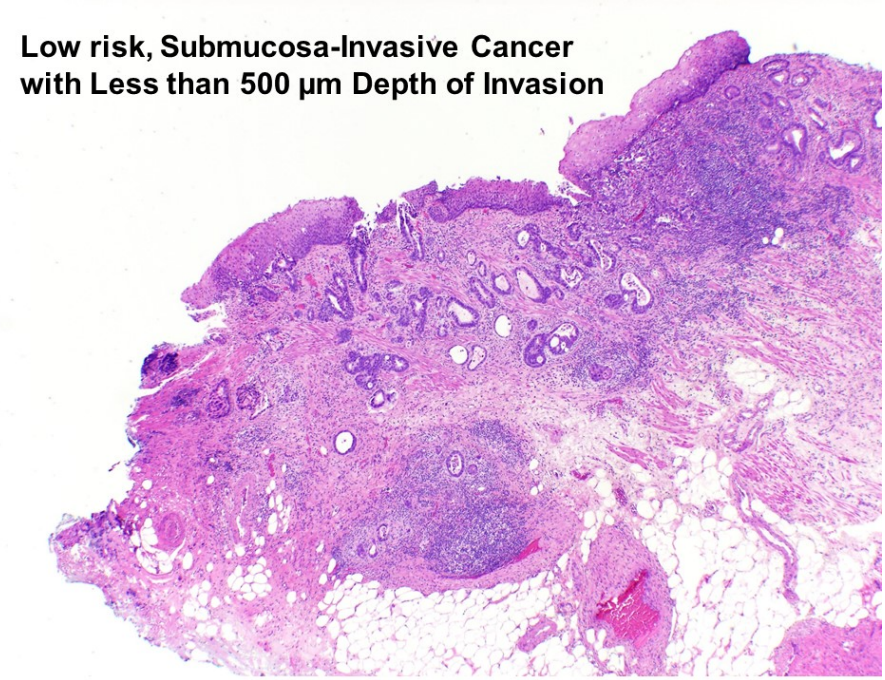

Conclusions: EMR is an attractive alternative to surgery for low risk, ≤500 µm SM-CAs. Given the published lack of reproducibility in measurements, basing a decision for esophagectomy on SM-CA depth is of concern. Our study shows, however, that most SM-invasive CAs already have high risk features warranting esophagectomy; the decision for surgery would hinge solely on measurement in only 1.8% of EMRs. This suggests that measurement (perhaps by >1 pathologist for consensus) may only need to be performed in the rare situation of a low risk, SM-CA, where ≤500 µm could give a pt the option of declining surgery.

793 Should Cribriform Colon Cancer Have Been Taken out of the WHO?

Alexander Taylor[1], Natalia Liu[2], Jiayun Fang[3], Nicole Panarelli[4], Jerome Cheng[1], Purva Gopal[5], Suntrea Hammer[5], Jing Sun[5], Henry Appelman[1], Maria Westerhoff[1]

[1]University of Michigan, Ann Arbor, MI, [2]Department of Pathology and Laboratory Medicine, David Geffen School of Medicine at UCLA, Los Angeles, CA, [3]University of Michigan Hospitals, Ann Arbor, MI, [4]Montefiore Medical Center, Scarsdale, NY, [5]University of Texas Southwestern Medical Center, Dallas, TX

Disclosures: Alexander Taylor: None; Natalia Liu: None; Jiayun Fang: None; Nicole Panarelli: None; Jerome Cheng: None; Purva Gopal: None; Suntrea Hammer: None; Jing Sun: None; Henry Appelman: None; Maria Westerhoff: None

Background: Cribriform colon adenocarcinoma (CRIB) was a subtype recognized in the previous WHO classification of tumors of the colon that is no longer included in the recent edition. Previous reports have described these tumors as having poor cancer-related outcomes, worse overall survival, and being microsatellite stable. We sought to validate whether CRIB is a distinct morphologic subtype with clinical relevance in the context of modern colon cancer (CA) diagnosis.

Design: Consecutive cases of resected colon CA over a 5-year period were identified; neoadjuvantly treated CAs (i.e. rectal) were excluded. Tumor slides of all cases (n=191) were reviewed and evaluated for morphology (including whether the CA was conventional adenoCA NOS, mucinous, medullary, cribriform, etc), extramural venous invasion (EVI), infiltrative vs. nodular/pushing architecture, prominent desmoplasia, lymph node positivity, tumor infiltrating lymphocytes, high tumor budding (>10), and MSI status. Patient outcome and other clinical data were gathered from the electronic medical record.

Results: CRIB was defined as solid nests of CA with round, "punched out" spaces, growing in expansile nodules that seem to mold to each other in a "jigsaw puzzle" fashion; the nodules were separated from each other by fibrous septa (see figure 1). Overall, CRIB represented 16.2% of all cases. There was no statistically significant difference in overall survival (p=0.19; see figure 2). pT3-pT4 stage, positive lymph nodes, microsatellite stability, lack of desmoplasia, and EVI occurred more often in CRIB than conventional CA (p=0.0145, 0.0037, 0.0060, 0.0001, and 0.0027, respectively; see table). Cribriform appearance (without the other defining features of CRIB) did occur in 42.2% of all other colon cancer cases.

		CRIB	Conventional	p value
n		31 (16.2%)	90 (47.1%)	
Stage	pT1-pT2	4 (12.9%)	30 (33.3%)	0.0145
	pT3-pT4	27 (87.1%)	60 (66.7%)	
Node status	N0	9 (29.0%)	53 (58.9%)	0.0037
	Positive nodes	22 (71.0%)	37 (41.1%)	
Metastasis		8 (25.8%)	16 (17.8%)	0.4332
Microsatellite status	Stable	30 (100%)	72 (81.8%)	0.0060
	Unstable	0 (0%)	16 (18.2%)	
High tumor budding (>10)		19 (61.3%)	41 (45.6%)	0.0961
Prominent desmoplasia		22 (70.1%)	26 (30.9%)	0.0001
Extravenous extension		9 (29.0%)	6 (6.7%)	0.0027
Developed recurrence		5 (16.7%)	11 (12.2%)	0.5433

Figure 1 - 793

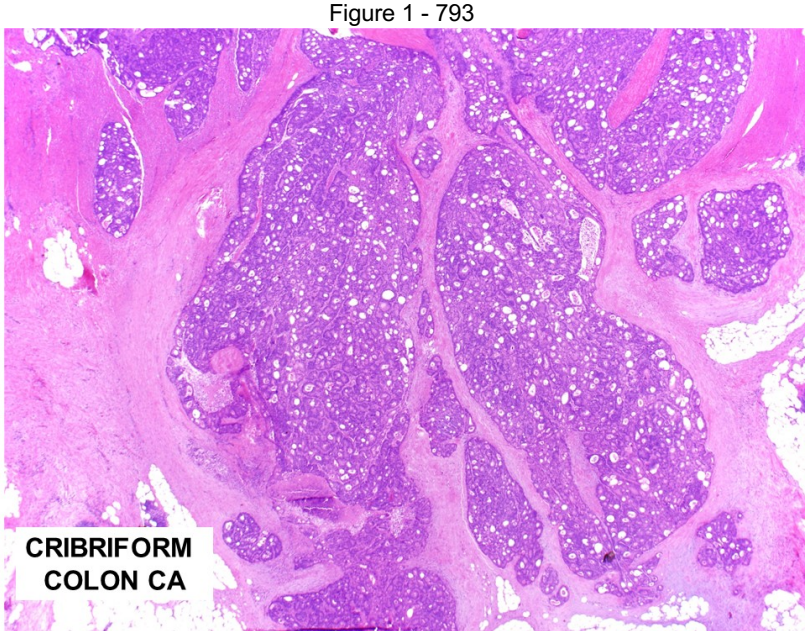

Figure 2 - 793

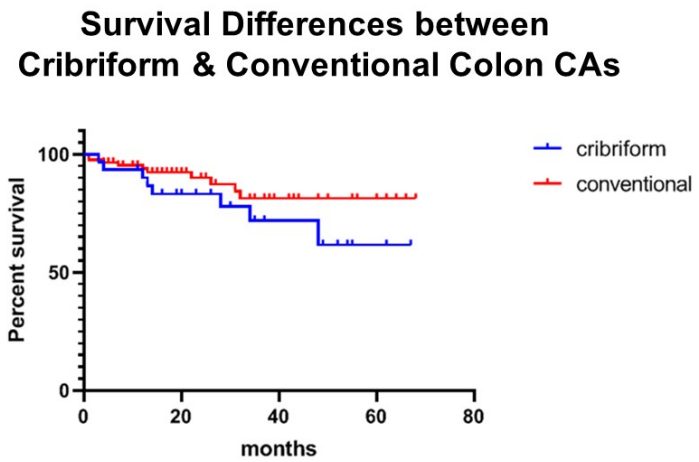

Conclusions: In contrast to previous reports, we did not find significantly worse survival for CRIB vs. conventional colon CA. CRIB was more likely to have EVI and positive lymph nodes, which are known adverse features. Identifying CRIB in a biopsy may be useful due to these important clinical aspects, but given that cribriforming appearance without the other distinct, expansile architectural features may be found in conventional colon CA, CRIB may not be easily distinguished with certainty.

794 Crosstalks of PXR, Autophagy and Drug Resistance in Colorectal Cancer

Stamatios Theocharis[1], Evangelos Koustas[2], Panagiotis Sarantis[2], Gerasimos Tsourouflis[3], Michalis Karamouzis[4]
[1]National and Kapodistrian University of Athens, Medical School, Athens, Greece, [2]Department of Biological Chemistry, Medical School, National and Kapodistrian University of Athens, Athens, GR, Greece, [3]Athens Medial School, Athens, Greece, [4]National and Kapodistrian University of Athens, Laikon General Hospital, Athens, Greece

Disclosures: Stamatios Theocharis: None; Evangelos Koustas: None; Panagiotis Sarantis: None; Gerasimos Tsourouflis: None

Background: Colorectal cancer (CRC) is one of the most frequently diagnosed malignancies worldwide. Although chemotherapy represents an effective anti-tumor therapeutic approach for CRC, drug treatment efficacy is often limited due to the development of resistant cancer cells. Several studies associate the pregnane X receptor (PXR) with resistance to chemotherapeutic drugs by regulating drug metabolism and transportation. Autophagy represents another well-known resistance mechanism against chemotherapy, which is closely associated with tumor development.

Design: In the current study, the impact of PXR link with mtKRAS-depended autophagy in CRC post-irinotecan treatment was investigated. The mtKRAS CRC cell lines, DLD-1, HCT116 and SW480 exposed in 10 μM irinotecan and 80nM PXR-siRNA for 48hrs. In addition, the same cell lines were exposed in 5mM 3-MA (3-Methyladenine), 10μM HCQ (Hydroxychloroquine) and 1μM of PI-103 for 24 hrs. The viability of cells was measured through MTT analysis and the protein levels of p62, LC3, PARP, and PXR were detected by Western blotting. The sub-cellular localization of PXR was detected with confocal microscopy. The expression levels of different genes were tested by RT-PCR after the silence of PXR with siRNA in mtKRAS CRC cell lines.

Results: Irinotecan activated autophagy in all CRC cell lines used, as it was identified through the reduction of p62 and increasing ratio of LC3II/I. Besides, PXR protein levels were increased. After knockdown of PXR with siRNA, the activation of autophagy was not affected and apoptotic cell death was triggered. In order to investigate the role of autophagy in PXR activation, the mtKRAS CRC cell lines were treated with two autophagy inhibitors (3-MA/HCQ) and with the dual inhibitor of AKT/mTOR (PI-103). Inhibition of autophagy (HCQ) appeared to decrease the PXR protein levels. On the contrary, increasing autophagy (PI-103) reduced PXR expression. Furthermore, PXR nuclear distribution was increased post-autophagy induction, evident by confocal microscopy. Alterations of several genes' expression levels, such as MDR1, CYP3A4, and GADD45B, were noted by RT-PCR in mtKRAS CRC cell lines after the silence of PXR.

Conclusions: Collectively, these results support the hypothesis that autophagy acts as a cytoprotective mechanism against irinotecan, possibly through the induction and subcellular trafficking of PXR in mtKRAS CRC models.

795 Clinical Associations of Pyloric Gland Metaplasia in Intestinal Specimens

Minami Tokuyama[1], Qingqing Liu[1], Huaibin Mabel Ko[1], Hongfa Zhu[2], Noam Harpaz[3], Alexandros Polydorides[1]
[1]Icahn School of Medicine at Mount Sinai, New York, NY, [2]Hackensack Pathology Associates, LLC, Hackensac, NJ, [3]Mount Sinai Medical Center, New York, NY

Disclosures: Minami Tokuyama: None; Qingqing Liu: None; Huaibin Mabel Ko: None; Hongfa Zhu: None; Noam Harpaz: None; Alexandros Polydorides: None

Background: Pyloric gland metaplasia (PGM) is a histopathologic change in intestinal mucosa seen in the setting of chronic injury. Although often described in association with inflammatory bowel disease (IBD), and particularly Crohn disease (CD), the significance and specificity of this finding in IBD diagnosis is debated. We aimed to evaluate the long-term clinical correlates of PGM in a large cohort of small and large bowel specimens.

Design: We performed a retrospective search for PGM and equivalent terms in our pathology reports (2002-2012), which routinely include comments on the histological features of chronic injury (such as PGM) in most cases. Biopsies and resections from mid/distal small bowel (jejunum and ileum, including pouches) and colorectum were included, but duodenum, pancreas, and gallbladder were excluded. Electronic medical records were extensively reviewed for clinical information before and after PGM diagnosis. Nine patients could not be reliably characterized as having IBD or not and were excluded. Statistical significance ($P<0.05$) was determined with chi square test for categorical the student's t-test for continuous variables.

Results: We identified 532 cases (198 [37%] biopsies, 334 [63%] resections) of PGM from 504 patients (293 [58%] male, 211 [42%] female). During an average follow-up time of 4.63 years, 453 patients (90%) had or were subsequently diagnosed with IBD and of these, 410 (91%) had CD. In 51 non-IBD patients, the most common etiology for PGM was prior colectomy for a non-IBD cause (29%), followed by unclear etiology (16%) and NSAID use (12%). IBD patients with PGM were younger than non-IBD patients (mean age 42.1 vs. 53.3 years respectively, $p<0.0001$), but did not differ with respect to sex or follow-up time. Specimens with PGM from non-IBD patients were more likely to be biopsies (66%), while those from IBD patients were more likely to be resections (66%) ($p<0.0001$). PGM was more frequently found in the small bowel in both IBD and non-IBD patients, but it was seen at a higher rate in colonic specimens from non-IBD patients (11% vs. 5% in IBD patients, $P<0.05$). PGM with concurrent active inflammation was seen more frequently in specimens from IBD patients (98% vs. 89% in non-IBD patients, $P<0.001$).

Conclusions: The presence of PGM in intestinal specimens warrants a high suspicion for IBD and particularly CD, however it should be interpreted with caution, especially in older patients and in biopsy specimens from the colon, or those lacking active inflammation.

796 p53 Immunostaining Characteristics in the Diagnosis of Barrett's Esophagus-Associated Dysplasia

Kristen Tomaszewski[1], Azfar Neyaz[2], Deepa Patil[3], Vikram Deshpande[1]
[1]Massachusetts General Hospital, Boston, MA, [2]Massachusetts General Hospital, Malden, MA, [3]Brigham and Women's Hospital, Boston, MA

Disclosures: Kristen Tomaszewski: None; Azfar Neyaz: None; Deepa Patil: None; Vikram Deshpande: *Grant or Research Support*, Advanced Cell Diagnostics; *Advisory Board Member*, Viela; *Grant or Research Support*, Agios Pharmaceuticals

Background: The development of dysplasia in cases of Barrett's esophagus (BE) has significant implications for patient management, but determining whether dysplasia is present on biopsy H&Es is subjective. Immunostaining for tumor protein p53 expression has been used to predict or diagnose dysplasia or malignancy in BE biopsies; however, precise guidelines for interpreting p53 are currently unavailable.

Design: We identified a cohort of biopsies with low grade dysplasia (LGD), high grade dysplasia (HGD), or adenocarcinoma (ADCA) in the setting of BE (n=81). We studied two biopsies (n=308) (the initial and last biopsy) from a control cohort of 154 patients that on mean followup of 9 years did not develop dysplasia. The diagnoses were validated by 3 gastrointestinal pathologists. Biopsies from both cohorts were stained for p53 (DAKO, clone D019, 1:250) and semiquantitatively analyzed for the number and percentage of crypts with strong p53 staining (a positive crypt defined as 5 cells with reactivity similar to basal squamous cells). We also noted the presence of strong p53 staining on the columnar epithelial surface. On an automated platform, the nuclear staining was categorized into 3 classes: 1+, 2+ and 3+. A Receiver Operating Characteristics (ROC) curve was used to identify optimal cut-points between the progressor and non-progressor cohort.

Results: Of 81 biopsies showing dysplasia or adenocarcinoma, 6 (7.4%) demonstrated null phenotype including 3 ADCAs, 2 HGD and 1 LGD. The remaining cohort included 75 patients with neoplastic biopsies, including LGD n=10, HGD n= 38, and ADCA n= 27. Strong surface p53 reactivity was absent in biopsies negative for dysplasia, but was seen in 33.3% of LGD, 28.6% of HGD, and 61.5% of ADCA cases. The semiquantitative analysis predicted neoplasia with sensitivity and specificity equivalent to an automated approach (Table).

p53 Results	Sensitivity (%)	Specificity (%)	Area Under Curve
Semiquantitative: >25 strongly positive crypts	91	84	0.92
Semiquantitative: 2% strongly positive crypts	69	99	0.94
Automated: 10 cells 3+ positive	91	84	0.92

Conclusions: BE-associated dysplasia is associated with increased p53 expression and a semiquantitative analysis is a sensitive and specific means for the diagnosis of dysplasia. A significant proportion of dysplastic biopsies do not show p53 reactivity on the surface epithelium.

797 Proton Pump Inhibitors-Associated Well-Differentiated Gastric Neuroendocrine Tumors

Vincent Quoc-Huy Trinh[1], Chanjuan Shi[1], Changqing Ma[2]
[1]Vanderbilt University Medical Center, Nashville, TN, [2]University of Pittsburgh, Pittsburgh, PA

Disclosures: Vincent Quoc-Huy Trinh: None; Chanjuan Shi: None; Changqing Ma: None

Background: The WHO classification has divided well-differentiated gastric neuroendocrine tumors (GNETs) into type I seen in patients with atrophic gastritis, type II associated with gastrinoma, and type III for the remaining cases. The incidence of well-differentiated gastric neuroendocrine tumors (GNETS) has increased significantly in the last decades. The increase has paralleled the widespread use of proton pump inhibitors (PPIs) since the 90s, although no study has shown direct association between these two events. Biologically, PPIs increase circulating gastrin levels, which might result in GNETs in a similar mechanism to Type 1 and 2 GNET. In this study, we examined clinicopathological features of GNETs arising in patients without atrophic gastritis or gastrinomas.

Design: We identified 103 (center 1) and 150 (center 2) GNET cases from 2002-2019 in two high-volume institutions. Patient's clinical history (especially PPI-use), gastric levels, imaging studies, pathology report, and H&E slides from both tumor and background gastric mucosa were reviewed to excluded GNETs that were associated with gastrinoma or atrophic gastritis. Background gastric mucosa was also reviewed for PPI effect.

Results: Sixty-six cases (66/253, %) were identified that were not associated with atrophic gastric or gastrinoma. These cases were grouped according to the use of PPIs for >1 year prior to the diagnosis (Table 1). Thirty-eight patients (58%) were on chronic PPI use (>1 year) and 28 (42%) patients were not. PPI effect (P=0.034) and presence of fundic gland polyps (P=0.040) were significantly more common in the chronic PPI use group. Metastasis-free survival analysis (Figure 1) showed that chronic PPI use (log-rank P=0.151), elevated gastrin levels (P=0.111), and presence of PPI effect (P=0.022) tended to be associated with better prognosis. Notably, none of GNET patients with PPI effect developed a metastasis (median follow-up 31 months).

Factor	**Chronic PPI use (n=38)**	**No Chronic PPI use (n=28)**	**Total (n=66)**	**P-value**
Clinical factors				
Mean age (S.D.)	57.0 (13.2)	57.2 (13.4)	57.1 (13.1)	0.984
Gender	16 (42.1%)	18 (64.3%)	32 (48.5%)	0.087

Female Male	22 (57.9%)	(10 (35.7%)	34 (51.5%)	
Race White Black Other	35 (92.1%) 3 (7.9%) 0 (0.0%)	22 (78.6%) 5 (17.9%) 1 (3.6%)	57 (86.4%) 8 (12.1%) 1 (1.5%)	0.221
Cause of endoscopy Incidental/Unrelated cause Melena/Bleeding/Anemia Reflux/Nausea/Pain/Dysphagia Carcinoid syndrome	7 (18.4%) 9 (23.7%) 20 (52.6%) 2 (5.3%)	8 (28.6%) 6 (21.4%) 14 (50.0%) 0 (0.0%)	15 (22.7%) 15 ((22.7%) 34 (51.5%) 2 (3.0%)	0.520
Circulating gastrin levels Normal at diagnosis Elevated at diagnosis Not tested	12 (31.6%) 15 (39.5%) 11 (28.9%)	10 (35.7%) 14 (50.0%) 4 (14.3%)	22 (33.3%) 29 (43.9%) 15 (22.7%)	0.365
Median follow-up (IQR)	31 (13.75-59.5)	53 (24-89.75)	38.0 (16-67.3)	0.121
Background histology				
Largest specimen type Biopsy Polypectomy Endoscopic mucosal resection Gastrectomy (partial/wedge)	11 (28.9%) 9 (23.7%) 8 (21.1%) 10 (26.3%)	5 (17.9%) 8 (28.6%) 3 (10.7%) 12 (42.9%)	16 (24.2%) 17 (25.8%) 11 (16.7%) 22 (33.3%)	0.344
PPI effect	5 (17.9%)	17 (44.7%)	22 (33.3%)	**0.034**
Fundic gland polyp or large fundic gland dilation	6 (21.4%)	18 (47.4%)	24 (36.4%)	**0.040**
Focal intestinal metaplasia	1 (2.6%)	2 (7.1%)	3 (4.5%)	0.570
Focal ECL-cell hyperplasia	5 (13.2%)	0 (0.0%)	5 (7.6%)	0.067
Chronic gastritis	7 (18.4%)	5 (17.9%)	12 (18.2%)	1.000
Active gastritis	1 (2.6%)	1 (3.6%)	2 (3.0%)	1.000
Tumor characteristics				
Location Body/Fundus Antrum/Pyloric region	34 (89.5%) 4 (10.5%)	22 (78.6%) 6 (21.4%)	56 (84.8%) 10 (15.2%)	0.302
Focality Unifocal Multifocal	33 (89.2%) 4 (10.8%)	26 (92.9%) 2 (7.1%)	59 (90.8%) 6 (9.2%)	0.692
Endoscopic appearance (terminology used on report) Nodule/Polyp Mass Ulcer Scar	27 (71.1%) 7 (18.4%) 3 (7.9%) 1 (2.6%)	23 (82.1%) 2 (7.1%) 2 (7.1%) 1 (3.6%)	50 (75.8%) 9 (13.6%) 5 (7.6%) 2 (3.0%)	0.610
Mean largest size in centimeter (S.D.) Minimum size in centimeter Maximum size in centimeter	1.54 (1.72) 0.10 2.98	2.10 (2.65) 0.30 12.3	1.72 (2.12)	0.404
Mitosis G1 G2 G3 GX (less than 2 mm2)	20 (52.6%) 12 (31.6%) 1 (2.6%) 5 (13.2%)	13 (46.4%) 9 (32.1%) 0 (0.0%) 6 (21.4%)	33 (50.0%) 21 (31.8%) 1 (1.5%) 11 (16.7%)	0.677
Ki-67 G1 G2 G3 GX (not performed, inadequate surface)	12 (31.6%) 15 (39.5%) 2 (5.3%) 9 (23.7%)	9 (32.1%) 9 (32.1%) 1 (3.6%) 9 (32.1%)	21 (31.8%) 24 (36.4%) 3 (4.5%) 18 (27.3%)	0.858
T stage T1 T2 T3 T4 TX	14 (36.8%) 11 (28.9%) 0 (0.0%) 2 (5.3%) 7 (25.0%)	7 (25.0%) 5 (17.9%) 1 (3.6%) 5 (17.9%) 10 (35.7%)	21 (31.8%) 16 (24.2%) 1 (1.5%) 7 (10.6%) 21 (31.8%)	0.237
N stage N0 N1 MX	30 (78.9%) 7 (18.4%) 1 (2.6%)	17 (60.7%) 7 (25.0%) 4 (14.3%)	47 (71.2%) 14 (21.2%) 5 (7.6%)	0.137
M stage M0 M1 MX	34 (89.5%) 3 (7.9%) 1 (2.6%)	20 (71.4%) 4 (14.3%) 4 (14.3%)	54 (81.8%) 7 (10.6%) 5 (7.5%)	0.125

Figure 1 - 797

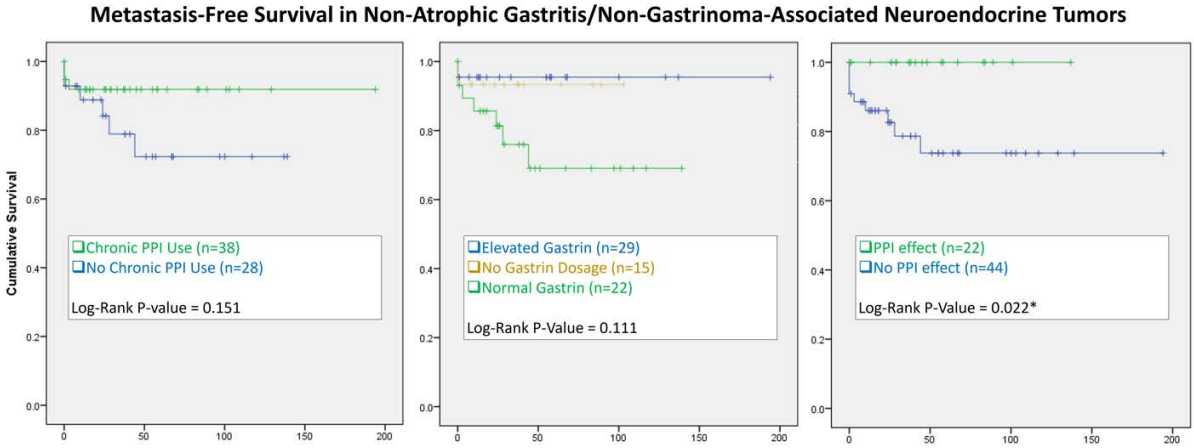

Figure 1. Metastasis-free survival curves according to features associated to PPI intake.

Conclusions: GNETS arising in patients with chronic PPI use and with PPI effect may have an indolent clinical course and a better prognosis compared to typical type III GNETs. This study suggests classification of these tumors into type I GNETs.

798 Colorectal Cancer Arising in Polyps. Watchful Waiting versus Surgical Removal, What to do Next? Our 21-Year's Experience

Maria Trujillo[1], Elena Garcia-Garcia[1], Grevelyn Sosa[1], Ester Martínez Negro[1], Federico Ochando[1], Sirio Melone[1], Jose Fernandez-Cebrian[1]
[1]HUFA, Alcorcón, Madrid, Spain

Disclosures: Maria Trujillo: None; Elena Garcia-Garcia: None; Grevelyn Sosa: None; Ester Martínez Negro: None; Federico Ochando: None; Jose Fernandez-Cebrian: None

Background: Colorectal cancer (CRC) is the second most common cause of cancer-related death in women and the third in men in the world. Faecal occult blood (FOB) testing is the screening strategy recommended. Colonoscopy is the diagnostic procedure in patients with anaemia, abdominal pain and colorectal symtomathology and positive FOB test. Screening campains implementation has increased the detection of early stage CRC.

Design: We performed a retrospective study of patients diagnosed of levels 3 and 4 Haggitt CRC on endoscopic polypectomy between 1998 and 2019 in Hospital Universitario Fundación Alcorcón (Spain), including more than 150 patients. The aim of our study is to figure out the management, surveillance and follow-up of these cohort in order to select the patients who could benefit a conservative management instead of undergo surgery according to pathological features of endoscopic resection. First step pilot study was performed with a cohort diagnosed between 2017-2019. Statistical studies were analyzed using SPSS software.

Results: The following results belong to the pilot study we studied 48 patients, 29 males (60%) and 19 females (40%). The most frequent localization of polyps was sigmoid colon (73%). The frequency of fragmented specimens was 17% and of intact polyps was 83%. Sessile configuration was present in 69% and pedunculated with stalk in 31% of total. Haggitt 3 level tumors were diagnosed in 31% of polyps, level 4 in 65% and unknown level in 4%. Using Kikuchi classification, 10% were stratified as SM1,13% as SM2 and 73% SM3, 4% couldn't be evaluated. Positive margins were detected in 44%, negative margins in 48% and unknown margins in 8%. Lymphovascular invasion was identified in 10% and perineural invasion in 6% of the patients. 46% of the patients underwent surgical resection, 81% of those showed no residual disease and 91% with no lymph node metastases. Only SM3 tumors in polypectomy showed residual disease and regional lymph node metastases. None of the tumors arised on pedunculated polyps showed residual disease in surgical specimen.

Conclusions: Pilot study results reveal that conservative management could be recommended as a valid alternative in non-SM3 Kikuchi patients.

799 Comprehensive Analysis of the Molecular and Clinicopathological Characteristics in Primary Malignant Melanoma of the Esophagus by Next Generation Sequencing

Sho Tsuyama[1], Shinji Kohsaka[2], Takuo Hayashi[3], Yoshiyuki Suehara[4], Takashi Yao[5], Tsuyoshi Saito[4]
[1]Juntendo University Graduate School of Medicine, Bunkyo-ku, Tokyo, Japan, [2]Division of Cellular Signaling, National Cancer Center Research Institute, Tokyo, Japan, [3]Juntendo University Graduate School of Medicine, Tokyo, Japan, [4]Juntendo University, School of Medicine, Tokyo, Japan, [5]Juntendo University, Tokyo, Japan

Disclosures: Sho Tsuyama: None; Shinji Kohsaka: None; Takuo Hayashi: None; Yoshiyuki Suehara: None; Takashi Yao: None; Tsuyoshi Saito: None

Background: Primary malignant melanoma of the esophagus (PMME) is extremely rare entity, accounting for 0.1-0.5% of esophageal cancers and <0.05% of all melanoma subtypes. Molecular pathogenesis of PMME have not been fully elucidated and there is no well-established treatment for PMME.

Design: Thirteen cases of PMME and ten cases of skin melanoma (SKMM) were collected from pathological files at Juntendo University Hospital from 2003 to 2016. In addition to the clinicopathological analysis, all cases were analyzed by Todai OncoPanel (TOP) testing, i.e. DNA and RNA hybridization capture-based next-generation sequencing panels, which can detect MSI status, fusion gene, and copy number status.

Results: The male-to-female ratio was 11:2 and age ranged 47-74 years (mean: 63.2). All cases were protruded tumor and most cases (9/13 cases 69.2%) were located at the lower third portion or esophago-gastric junction. Three-year overall survival rate was 23.1% (median survival: 1.42 year). Lymph node metastasis was observed in 8 out of 13 cases (61.5%). Nine tumors were composed of epithelioid cells, and 6 of which showed rhabdoid feature. Two tumor showed spindle cell morphology, and 3 cases had papillary structure. NGS revealed *NF1* as the most frequently mutated gene (4/10 cases). *NF1* mutation was also detected frequently in SKMM (3/10 cases). Other PMME cases had mutations such as *KRAS, BRCA2, SF3B1, KIT, TP53*, some of which were concordant with the immunohistochemical staining. Focal PD-L1 expression was observed in tumor cells in one PMME and one SKME, respectively. Tumor mutation burden in PMME was significantly lower than SKMM. No case showed microsatellite instability (MSI) high, and no fusion gene was detected. RNA sequencing revealed distinctive expression pattern in PMME compared to SKMM.

Conclusions: The prognosis of PMME was extremely poor. It is noteworthy that *BRAF/RAS* mutations commonly observed in skin malignant melanoma were not detected in PMME. This study suggests that PMME is a molecular pathologically distinctive tumor and provides us important information to establish the therapeutic strategy in PMME; i.e. immune check point inhibitors and *BRAF* inhibitors are less likely effective. A few possible targets such as *KIT* mutation were detected.

Acknowledgements

We thank Dr. Toshihide Ueno and Dr. Hiroyuki Mano at Division of Cellular Signaling, National Cancer Center Research Institute, Tokyo, Japan for their excellent technical assistances and advice.

800 Do Pathologists Agree on P53 Labelling Pattern in Barrett's Dysplasia? Added Value of P53 Labelled Slide Assessment within a Large International Consensus Study

Myrtle van der Wel[1], Helen Coleman[2], Marnix Jansen[3], Sybren Meijer[4]
[1]University Medical Center Utrecht, Utrecht, Utrecht, Netherlands, [2]Queen's University Belfast, Belfast, Down, United Kingdom, [3]UCL Cancer Institute, London, United Kingdom, [4]Amsterdam University Medical Center, Amsterdam, North-Holland, Netherlands

Disclosures: Myrtle van der Wel: None; Helen Coleman: None; Marnix Jansen: None; Sybren Meijer: None

Background: Assessment of Barrett's esophagus (BE) biopsies is associated with significant interpathologist variability. Efforts to decrease this variability include expert review and implementation of adjunct biomarkers. Immunohistochemical labelling for P53 protein expression has been variably recommended as a diagnostic tool by major international societies. Our large scale international consensus study revealed that inclusion of P53 labelled slides significantly reduces major diagnostic errors for pathologists working in non-teaching hospitals (OR 1.76, 95%CI 1.15-2.69). Here we investigate concordance of P53 labelling assessment and effects on diagnostic concordance amongst our international sample of pathologists diagnosing Barrett's dysplasia.

Design: Participating pathologists (n=51) from over 20 countries assessed 55 digitized H&E BE biopsies from across the diagnostic spectrum, before and after viewing consecutive P53 labelled slides. They also completed a demographic questionnaire covering professional background and diagnostic practice. Reference assessment for P53 labelled slides (wild-type, overexpression, or null) were obtained from expert panel review. Concordance was determined by comparing participating pathologists' majority assessment of P53 labelled slides with the consensus diagnosis.

Results: We recorded over 6,000 case diagnoses total and 3,025 assessments of P53 labelling pattern. A two-thirds majority assessment for P53 labelling pattern was obtained in 50/55 cases (2,371 of 3,019 assessments, 91%, missings n=6, Figure 1). Overall concordance with gold standard assessment was 87% (48/55 cases, 2,274 of 3,019 assessments). Disagreements encompassed lack of majority assessment amongst participating pathologists (5/55, 9%) and assessment of overexpression versus either wild-type or null (2/55, 4%). Discordant P53 labelled slides also lacked diagnostic concordance on HE in 6/7 cases. Addition of P53 triggered a change in diagnostic assessment in 419 diagnoses (14%, Figure 2). 76.5% of participants did not report routine use of P53 as an adjunct diagnostic tool.

Figure 1 - 800

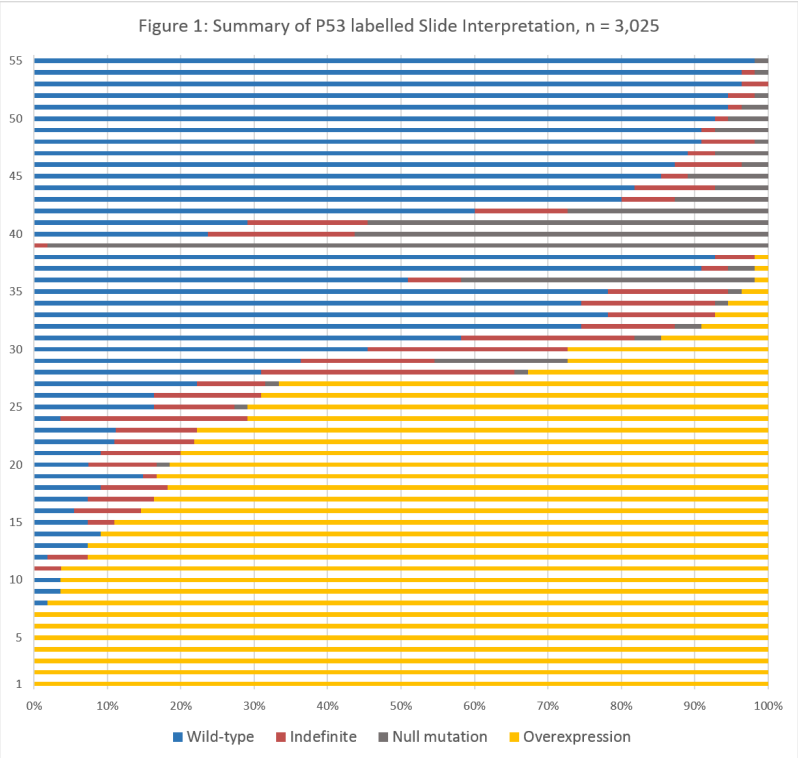

Figure 2 - 800

Figure 2: Stage migration per diagnostic category after P53 labelled slide assessment, n = 3,025

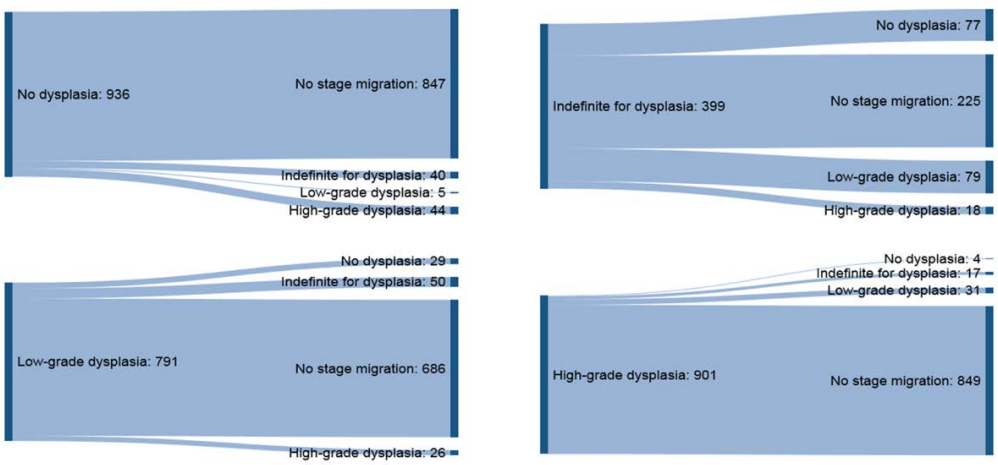

Conclusions: Accuracy for P53 labelled slide interpretation is high amongst a large international sample of pathologists, even amongst pathologists who do not routinely use it. Our results support routine use of P53 immunohistochemistry as a diagnostic tool to decrease interobserver variability for Barrett's signout.

801 Prognostic Significance of Immune Cells and Their Spatial Distribution in Colorectal Cancer Determined by Computational Pathology Using Hematoxylin & Eosin Stained Sections

Juha Väyrynen[1], Mai Chan Lau[2], Koichiro Haruki[2], Sara Väyrynen[1], Andressa Dias Costa[1], Jennifer Borowsky[3], Melissa Zhao[2], Junko Kishikawa[4], Simeng Gu[2], Annacarolina Fabiana Lucia Da Silva[2], Charles Fuchs[5], Jeffrey Meyerhardt[1], Marios Giannakis[1], Shuji Ogino[2], Jonathan Nowak[2]
[1]Dana-Farber Cancer Institute, Boston, MA, [2]Brigham and Women's Hospital, Boston, MA, [3]The Royal Brisbane & Women's Hospital, Brisbane, QLD, Australia, [4]Brigham and Women's Hospital, Brookline, MA, [5]Yale Cancer Center, New Haven, CT

Disclosures: Juha Väyrynen: None; Mai Chan Lau: None; Koichiro Haruki: None; Sara Väyrynen: None; Andressa Dias Costa: None; Jennifer Borowsky: None; Melissa Zhao: None; Junko Kishikawa: None; Simeng Gu: None; Annacarolina Fabiana Lucia Da Silva: None; Charles Fuchs: *Stock Ownership*, CytomX Therapeutics; *Consultant*, Eli Lilly; *Consultant*, Agios; *Consultant*, Bain Capital; *Consultant*, Bayer; Jeffrey Meyerhardt: *Consultant*, Ignyta; *Consultant*, Taiho Pharmaceutical; *Consultant*, COTA Healthcare; Marios Giannakis: *Grant or Research Support*, Bristol Myers-Squibb; *Grant or Research Support*, Merck; Shuji Ogino: None; Jonathan Nowak: None

Background: The colorectal cancer (CRC) microenvironment is composed of a mixture of interacting cell types including tumor cells, fibroblasts, endothelial cells, and adaptive and innate immune cells. High T cell density is a well-established marker of favorable clinical outcome, but the prognostic significance of tumor-associated plasma cells, neutrophils, and eosinophils is less well-defined.

Design: We computationally processed digital images of hematoxylin & eosin stained tumor sections from 934 CRC patients to identify and quantify intraepithelial and stromal lymphocytes, plasma cells, neutrophils, and eosinophils. Cox proportional hazard models were used to compute hazard ratios (HRs) and confidence intervals (CIs) of cancer-specific survival (CSS) according to ordinal quartiles (C1-C4) of immune cell density, controlling for potential confounders, including microsatellite instability, *KRAS, BRAF*, and *PIK3CA* mutation status, and LINE-1 methylation. Spatial patterns of immune cell infiltration were studied using the tumor:immune cell G-cross function which estimates the likelihood of any tumor cell in a sample having at least one immune cell of the specified type within a certain radius.

Results: Immune cell densities measured by the automated classifier demonstrated strong to very strong Spearman rank correlation (0.71-0.96 depending on the cell type) with densities both from manual counts and those obtained from an independently trained automated classifier. In multivariable-adjusted Cox regression models, high densities of stromal eosinophils (C1 vs. C4: HR 0.51, 95% CI 0.35-0.74), lymphocytes (C1 vs. C4: HR 0.51, 95% CI 0.36-0.71), and plasma cells (C1 vs. C4: HR 0.61, 95% CI 0.43-0.86) were associated with better CSS (P_{trend}<0.001 for all). Higher areas under the curve for G-cross functions testing eosinophil and lymphocyte proximity to tumor cells were also associated with better CSS ($G_{Tumor:Eosinophil}$ C1 vs. C4: 0.45, 95% CI 0.30-0.68, P_{trend}=0.005; $G_{Tumor:Lymphocyte}$ C1 vs. C4: HR 0.60, 95% CI 0.41-0.87, P_{trend}=0.002).

Conclusions: Machine learning-based immune cell characterization in CRC using standard H&E-stained sections identified lymphocyte, plasma cell, and eosinophil densities within tumor stroma as relevant prognostic parameters. The results also suggest that the spatial patterns of immune cell infiltrates in relation to tumor cells harbor prognostic information, underscoring the biologic potential of certain immune cell types to drive tumor-directed cytotoxicity.

802 Defining the Prognostic Significance of Macrophages in the Colorectal Cancer Microenvironment via Multimarker Measurement of the Macrophage Polarization Spectrum

Juha Väyrynen[1], Koichiro Haruki[2], Mai Chan Lau[2], Sara Väyrynen[1], Andressa Dias Costa[1], Jennifer Borowsky[3], Melissa Zhao[2], Junko Kishikawa[4], Simeng Gu[2], Annacarolina Fabiana Lucia Da Silva[2], Charles Fuchs[5], Jeffrey Meyerhardt[1], Marios Giannakis[1], Shuji Ogino[2], Jonathan Nowak[2]
[1]Dana-Farber Cancer Institute, Boston, MA, [2]Brigham and Women's Hospital, Boston, MA, [3]The Royal Brisbane & Women's Hospital, Brisbane, QLD, Australia, [4]Brigham and Women's Hospital, Brookline, MA, [5]Yale Cancer Center, New Haven, CT

Disclosures: Juha Väyrynen: None; Koichiro Haruki: None; Mai Chan Lau: None; Sara Väyrynen: None; Andressa Dias Costa: None; Jennifer Borowsky: None; Melissa Zhao: None; Junko Kishikawa: None; Simeng Gu: None; Annacarolina Fabiana Lucia Da Silva: None; Charles Fuchs: *Consultant*, CytomX Therapeutics; *Consultant*, Eli Lilly; *Consultant*, Agios; *Consultant*, Merck; *Consultant*, Bayer; Jeffrey Meyerhardt: *Consultant*, Ignyta; *Consultant*, Taiho Pharmaceutical; *Consultant*, COTA Healthcare; Marios Giannakis: *Grant or Research Support*, Bristol Myers-Squibb; *Grant or Research Support*, Merck; Shuji Ogino: None; Jonathan Nowak: None

Background: Macrophages are among the most common cells in the colorectal cancer (CRC) microenvironment, although their significance is less well understood than other immune cell types. Macrophage polarization, defined as the type of activation state at a given point in time and space, can be viewed as a phenotypic continuum spanning the extreme pro-inflammatory M1 and anti-inflammatory M2 states.

Design: To elucidate the role of macrophage polarization in CRC, we identified and quantified intraepithelial and stromal macrophages and estimated their polarization state across a continuous M1:M2 spectrum in 931 stage I-IV CRCs with a multiplexed immunofluorescence assay containing pan-macrophage marker CD68, two M1 phenotype markers (CD86, IRF5), two M2 phenotype markers (MRC1, MAF), and cytokeratin. We used Cox proportional hazards models to compute hazard ratios (HRs) and confidence intervals (CIs) of cancer-

specific survival (CSS) according to ordinal quartiles (Q1-Q4) of densities of M1-polarized and M2-polarized macrophages, as well as the M1:M2 density ratio, controlling for potential confounders, including tumor stage, microsatellite instability, *KRAS, BRAF*, and *PIK3CA* mutation status, and LINE-1 methylation.

Results: In multivariable-adjusted Cox regression models, overall macrophage densities in tumor intraepithelial regions (Q1 vs. Q4: HR 0.81, 95% CI 0.54-1.22, P_{trend}=0.28) or in tumor stroma (Q1 vs. Q4: HR 0.78, 95% CI 0.52-1.17, P_{trend}=0.23) were not significantly associated with CSS. However, when macrophages representing the extreme 30% ends of the macrophage M1-M2 polarization spectrum were examined, a high density of M1-polarized macrophages in tumor stroma was associated with better CSS (Q1 vs. Q4: HR 0.68, 95% CI 0.46-0.99, P_{trend}=0.014), while, conversely, a high density of M2-polarized macrophages in tumor stroma was associated with worse CSS (Q1 vs. Q4: HR 1.46, 95% CI 1.00-2.13, P_{trend}=0.006). High M1:M2 density ratio in tumor stroma was associated with better CSS (Q1 vs. Q4: HR 0.57, 95% CI 0.38-0.84, P_{trend}=0.004).

Conclusions: Macrophage polarization state, rather than absolute density, is associated with CRC-specific survival, with M1- and M2-polarized macrophage phenotypes exhibiting opposite effects. These results underscore the role of macrophages in shaping the CRC tumor-immune microenvironment and highlight the utility of using a multimarker strategy to establish a macrophage polarization spectrum.

803 SWI/SNF Complex-Deficient Colorectal Adenocarcinoma is Frequently Associated with DNA Mismatch Repair Protein Deficiency and Medullary Differentiation

Tatiana Villatoro[1], Changqing Ma[2], Reetesh Pai[3]
[1]University of Pittsburgh Medical Center, Pittsburgh, PA, [2]University of Pittsburgh, Pittsburgh, PA, [3]UPMC-Presbyterian Hospital, Pittsburgh, PA

Disclosures: Tatiana Villatoro: None; Changqing Ma: None; Reetesh Pai: None

Background: The switch/sucrose-nonfermenting (SWI/SNF) complex is composed of several subunits (SMARCA2, ARID1A, INI1, and BRG1) that are involved in cellular proliferation and differentiation. The aim of this study was to correlate the expression of SWI/SNF complex subunits in colorectal adenocarcinoma with clinicopathologic and molecular features and patient survival.

Design: The immunohistochemical expression of SMARCA2, ARID1A, INI1, and BRG1 was evaluated by tissue microarray in 338 patients with colorectal adenocarcinoma and correlated with histopathologic features, DNA mismatch repair protein (MMR) expression, CDX2 and SATB2 expression, *KRAS* and *BRAF* mutations, and patient survival.

Results: 23 (7%) colorectal adenocarcinomas demonstrated deficient SWI/SNF expression: 7 SMARCA2 deficient, 12 ARID1A deficient, and 4 with both SMARCA2 and ARID1A deficiency. No cases were INI1 or BRG1 deficient. Compared to SWI/SNF complex-proficient tumors, SWI/SNF complex-deficient tumors more frequently demonstrated MMR deficiency (52% vs. 30%, p=0.02), medullary differentiation (26% vs. 7%, p=0.001), and negative CDX2 expression (39% vs. 8%, p<0.001). Of the 12 MMR deficient SWI/SNF complex-deficient tumors, 8 were sporadic MLH1 deficient, and 4 were seen in Lynch syndrome patients (2 with germline *MSH2* mutation and 2 with germline *MLH1* mutation). Notably, compared to ARID1A-only deficient tumors (n=12), SMARCA2 deficient tumors (n=11) were less likely to exhibit MMR deficiency (27% vs. 75%, p=0.02) and medullary differentiation (0% vs. 50%, p=0.006). There was no difference in *KRAS* mutation, *BRAF* mutation, stage, disease-specific survival, or disease-free survival for patients stratified by SWI/SNF expression (all with p>0.05).

Clinical and Pathologic Features	SWI/SNF Complex Deficient Colorectal Adenocarcinoma N (%)	SWI/SNF Complex Proficient Colorectal Adenocarcinoma N (%)	*p*-value
No. of Patients	23	315	NA
Gender, Male/Female	10 (43) / 13 (57)	146 (46) / 169 (54)	0.8
Median Age in Years (range)	65 (30-87)	70 (21-93)	0.2
Grade **Low** **High**	15 (65) 8 (35)	263 (75) 52 (25)	0.03
Overall Stage **I** **II** **III** **IV**	1 (4) 10 (43) 9 (39) 3 (13)	49 (16) 115 (37) 87 (28) 62 (20)	0.3
Location **Right Colon** **Left Colon / Rectum**	14 (61) 9 (39)	166 (53) 147 (47)	0.6
Mucinous Differentiation	10 (43)	112 (36)	0.5
Signet Ring Cell Differentiation	1 (4)	12 (4)	0.9
Medullary Differentiation	6 (26)	21 (7)	0.001
Angiolymphatic Invasion	16 (70)	185 (59)	0.3

Perineural Invasion	10 (43)	85 (27)	0.09
High Tumor Budding	5 ()	66 ()	0.9
CDX2 Positive Expression	14 (61)	284/310 (92)	<0.001
SATB2 Positive Expression	20 (87)	276/307 (90)	0.7
MMR Protein Status **MMR deficient** **MMR proficient**	12 (52) 11 (48)	95 (30) 220 (70)	0.02
***KRAS* exon 2 or 3 mutation present**	6/14 (43)	96/262 (37)	0.6
***BRAF* V600E mutation present**	8/21 (38)	66/304 (22)	0.08

Conclusions: SWI/SNF-deficient colorectal adenocarcinomas are frequently MMR deficient and can be identified in patients with sporadic MLH1 deficiency and Lynch syndrome. Loss of CDX2 expression is common in SWI/SNF-deficient colorectal adenocarcinoma. ARID1A-deficient colorectal adenocarcinoma is more often MMR deficient and more frequently demonstrates medullary differentiation. In contrast, SMARCA2-deficient colorectal adenocarcinoma is gland-forming without medullary differentiation. Patients with SWI/SNF-deficient colorectal adenocarcinomas have similar survival compared to patients with SWI/SNF-proficient colorectal adenocarcinomas.

804 Clinicopathologic Features of Extra-Pancreatic Gastrointestinal Grade 3 Well-Differentiated Neuroendocrine Tumors

Monika Vyas[1], Andrew Bellizzi[2], Kelsey McHugh[3], Daniela Allende[4], Chanjuan Shi[5], Changqing Ma[6], Stuti Shroff[7], Raul Gonzalez[8]
[1]Beth Israel Deaconess Medical Center, Harvard Medical School, Newton MA, MA, [2]University of Iowa Hospitals and Clinics, Iowa City, IA, [3]Cleveland Clinic, Lakewood, OH, [4]Cleveland Clinic, Lerner College of Medicine of Case Western University School of Medicine, Avon Lake, OH, [5]Vanderbilt University Medical Center, Nashville, TN, [6]University of Pittsburgh, Pittsburgh, PA, [7]Massachusetts General Hospital, Watertown, MA, [8]Beth Israel Deaconess Medical Center, Boston, MA

Disclosures: Monika Vyas: None; Andrew Bellizzi: None; Kelsey McHugh: None; Daniela Allende: None; Chanjuan Shi: None; Changqing Ma: None; Stuti Shroff: None; Raul Gonzalez: None

Background: Per the 2019 gastrointestinal (GI) WHO classification, well-differentiated neuroendocrine tumors (WD-NET) with Ki67 index >20% or >20 mitoses per 10 high-power fields (HPF) are now considered grade 3 (G3) WD-NET, rather than poorly differentiated neuroendocrine carcinoma (PD-NEC). While pancreatic G3 WD-NETs are known to be morphologically and genetically distinct from NECs, there are limited data on extra-pancreatic GI G3 WD-NETs. We evaluated a cohort of such WD-NETs to define their morphologic features and behavior.

Design: We identified 23 GI G3 WD-NETs in the pathology archives of 6 institutions over a 9-year period (2011-2019). Only cases where the primary lesion showed WD-NET morphology and met G3 criteria in a “hotspot” were included. Available H&E and immunohistochemical slides were reviewed for focal PD morphology, nucleoli, necrosis, lymphovascular invasion, and perineural invasion. Patient data (age, sex, symptoms, other relevant diagnoses), radiology (focality, size, metastasis), and treatment and follow-up (FU) data (recurrence, metastasis) was recorded for each.

Results: The cohort included 7 males and 16 females (average age: 69 years). Most were symptomatic, including 3 with carcinoid syndrome at presentation; 2 WD-NET were incidentally discovered. Primary sites included stomach (n=5), small intestine (SI) (n=12), and colorectum/anus (CRA) (n= 6). Clinical and microscopic findings are listed in the Table. Microscopically, focal tumor necrosis was present in 2 cases, and nucleoli were identified in 3 cases; however, none had definitive foci of high-grade morphology. Mitotic rate varied from 0 to 22/10 HPF, and Ki67 index ranged from 10.5 to 50.2% (Fig. 1). One case with Ki67 of 10.5% was classified as G3 based on 22 mitoses in 10 HPF (Fig. 2). Nodal metastases were present in 16 cases, and distant metastases in 19 (14 of which were synchronous). Six patients received chemotherapy +/- radiation, and 8 received somatostatin analogs (SSA) (6 SI, 1 stomach, 1 CRA primary). Four patients recurred (3 to 24 months), while 7 had persistent disease. Eleven patients died of disease, 9 were alive with disease, and 3 were alive without disease (FU average, 32 months; range, 8-88 months).

Site		**Stomach (n=5)**	**Small intestine (n=12)**	**Colorectum (n=6)**
Age (average, years)		**68**	**70.3**	**66.5**
Sex (M:F)		**1:4**	**1:2**	**1:1**
Tumor size (average, cm)		**2.45**	**2.78**	**2.2**
Histology	**PD morphology**	**0**	**0**	**0**
	Prominent nucleoli	**2/5 (40%)**	**0**	**1/6 (16.6%)**
	Necrosis	**0**	**2/12 (16.6%)**	**0**
	Mitotic rate (average, range) per 10 HPF	**3.4 (0-10)**	**10.6 (0.4 to 22)**	**4.6 (<2-8)**
Ki67 % (average, range)		**32 (25-44)**	**27 (10.5-43)**	**32 (22-50.2)**
Lymphovascular invasion		**5/5 (100%)**	**12/12 (100%)**	**2/6 (33%)**
Perineural invasion		**1/5 (20%)**	**9/12 (75%)**	**2/6 (33%)**
Metastasis	**Lymph node**	**3/5 (60%)**	**10/12 (83.3%)**	**3/6 (50%)**

	Distant	4/5 (80%)	10/12 (83.3%)	5/6 (83.3%)
Treatment	Chemotherapy	2/5 (40%)	1 (20%)	3/6 (50%)
	Radiation	0	0	2/6 (33%)
	Somatostatin analogues	1/5 (20%)	5/12 (41.6%)	1/6 (16.6%)
	Embolization/RFA (for metastases)	0	2/12 (16.6%)	1/6 (16.6%)
Outcome	No evidence of disease	1/5 (20%)	2/12 (16.6%)	0
	Alive with disease	2/5 (40%)	4/12 (33.3%)	3/6 (50%)
	Died from disease	2/5 (40%)	6/12 (50%)	3/6 (50%)

Figure 1 - 804

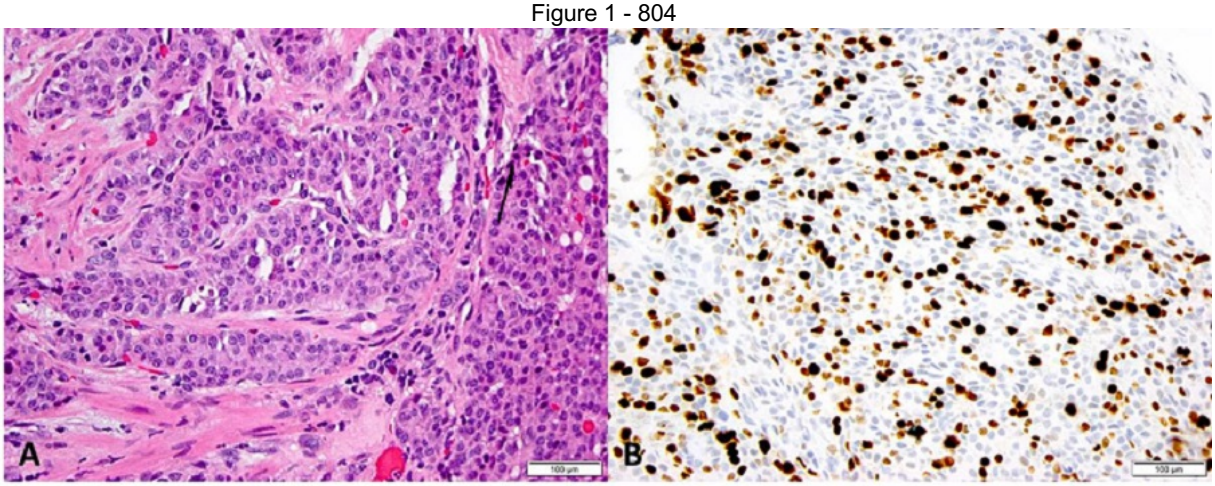

Figure 2 - 804

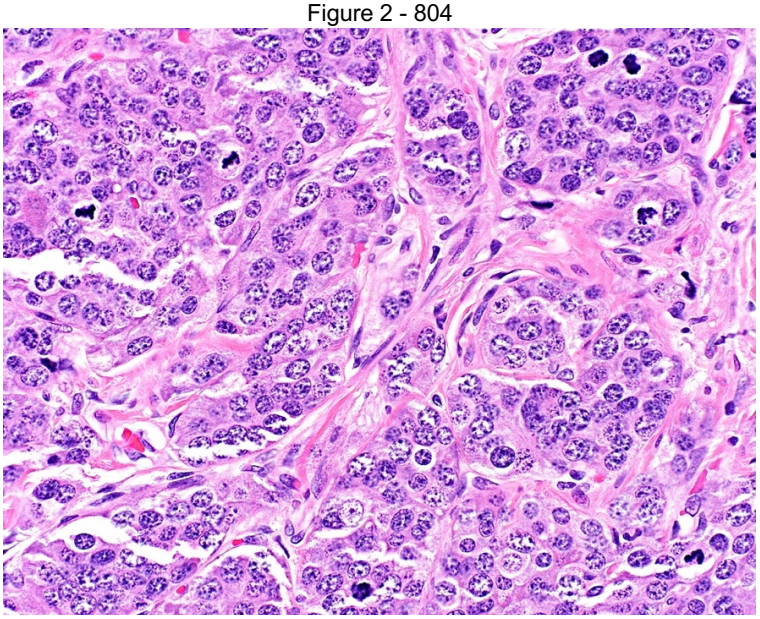

Conclusions: GI G3 WD-NETs are rare. Our data shows that G3 WD-NETs have an aggressive biologic course, with frequent nodal and distant metastases. SI G3 WD-NETs are often treated with SSA, while gastric and CRA primary sites may receive chemoradiation; however, disease-free survival remains poor.

805 Metastases to the Stomach: Frequent Fliers and Unexpected Guests

Monika Vyas[1], Erika Hissong[2], Raul Gonzalez[3], Jinru Shia[4], Jose Jessurun[5]
[1]Beth Israel Deaconess Medical Center, Harvard Medical School, Newton MA, MA, [2]New York-Presbyterian/Weill Cornell Medical Center, New York, NY, [3]Beth Israel Deaconess Medical Center, Boston, MA, [4]Memorial Sloan Kettering Cancer Center, New York, NY, [5]Weill Cornell Medicine, New York, NY

Disclosures: Monika Vyas: None; Erika Hissong: None; Raul Gonzalez: None; Jinru Shia: None; Jose Jessurun: None

Background: Metastatic tumors to the stomach can be diagnostically challenging due to their histologic resemblance to primary gastric carcinomas. They are seldom included in differential diagnosis due to their infrequent occurrence. Literature on the frequency and types of metastatic tumors involving the stomach is limited. The aim of this study was to evaluate the histologic features of such metastatic tumors which can be helpful in resolving a differential diagnosis.

Design: The pathology archives of 3 institutions were searched for all cases of metastases to the stomach, excluding those involving only the serosa. Patient demographic data and clinical information were obtained. All H&E and immunohistochemical stained slides were reviewed. We recorded segment and layers of the stomach involved by tumor, lymphovascular invasion (LVI), and appearance of the background mucosa. Tumors were grouped according to their histologic growth pattern as gland-forming and solid/diffuse. The latter were sub-classified according to cell size/type as small, medium to large, pleomorphic, clear, and spindle.

Results: The study group comprised of 150 cases; in 96, slides were available for review. There were 66 males and 84 females, with an average age of 64 years (range: 15 to 95 years). Fig 1 shows the distribution of the most common tumors by sex. In 22/150 (15%) cases (predominantly melanoma and lobular carcinoma), metastases were the first manifestation of the disease. There was no preferential involvement of a region or layer of the gastric wall. LVI were present in 27% cases. Most tumors (84%) had a homogeneous growth pattern. The most common was the solid/diffuse pattern (75%) which included predominantly large cell tumors (primarily melanomas), followed by small cell tumors (primarily lobular carcinoma), and tumors with clear cell features (primarily renal cell carcinoma). Metastatic gland-forming tumors were less frequent, mostly from Müllerian organs, colon, or pancreas/bile ducts (see Table & Fig 2). Several malignancies only represented 1 case in our series. Only in 2 cases did background mucosa show intestinal metaplasia.

Histologic pattern	Diagnosis (organ)	No. of cases (n=96)
Glandular, pure (n=15)	Adenocarcinoma (colon and appendix)	**7**
	Adenocarcinoma (pancreas / bile ducts)	5
	Adenocarcinoma (breast, adnexa, lung)	3
Glandular with papillary/micropapillary component (n=9)	Serous carcinoma (adnexa =8, endometrium = 1)	9
Solid / diffuse, small cell type (n= 20)	Melanoma (skin)	2
	Invasive lobular carcinoma (breast)	14
	Small cell carcinoma (lung)	1
	Merkel cell carcinoma (skin)	1
	Well differentiated neuroendocrine tumor (pancreas)	1
	Myeloid sarcoma	1
Solid/ diffuse, medium to large cell type (n=28)	Melanoma (skin and ocular)	14
	Squamous cell carcinoma (lung, skin)	2
	Poorly differentiated carcinoma (lung, breast, salivary gland)	8
	Seminoma (testis)	1
	Epithelioid trophoblastic tumor (uterus)	1
	Hepatocellular carcinoma (Liver)	2
Solid / diffuse, pleomorphic cell type (n= 6)	Choriocarcinoma (testis)	1
	Pleomorphic lobular carcinoma (breast)	2
	Poorly differentiated ductal carcinoma (breast)	1
	Undifferentiated sarcoma (bladder)	1
	Osteosarcoma (bone)	1
Solid, clear cell type (n=15)	Clear cell carcinoma (kidney)	14
	Osteosarcoma (bone)	1
Solid, spindle cell type (n=3)	Leiomyosarcoma (mediastinum)	1
	Synovial sarcoma (soft tissue)	1
	Undifferentiated sarcoma (uterus)	1

Figure 1 - 805

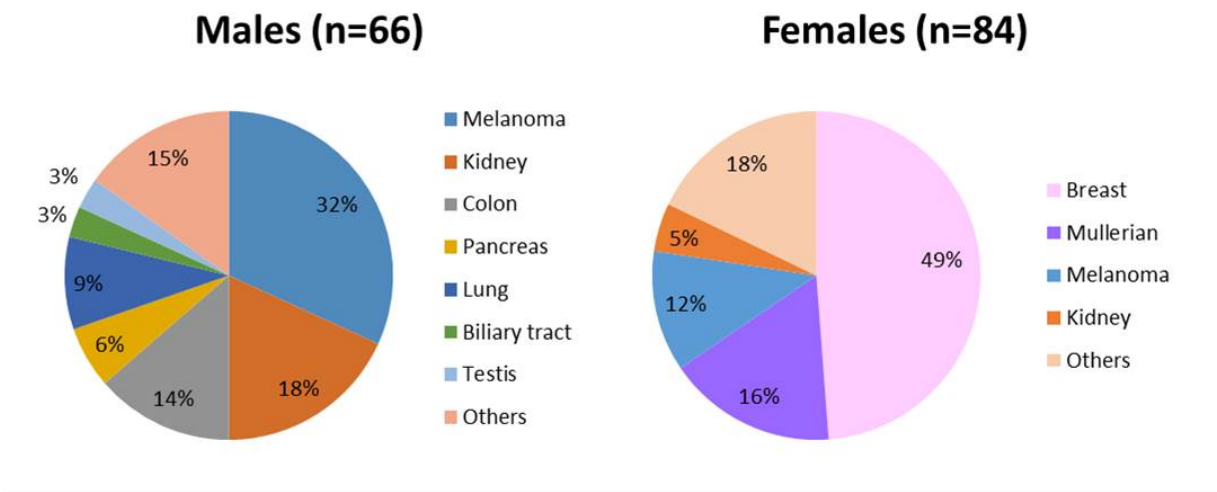

Figure 2 - 805

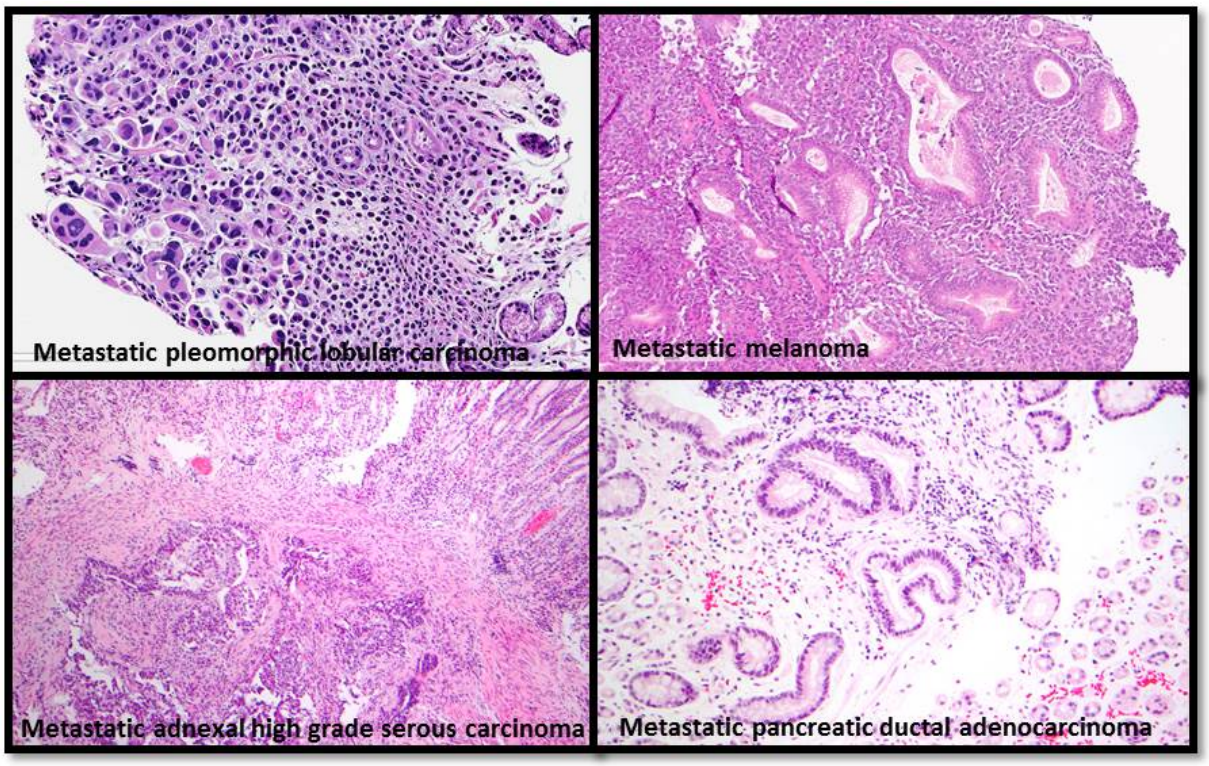

Conclusions: Our large series of metastatic tumors to the stomach shows that women are more commonly affected due to the high frequency of metastatic mammary tumors. Metastasis can be the first manifestation of disease (15% in our series) and should always be considered in tumors with a predominantly solid/diffuse (non-glandular) growth pattern and in all patients with a known primary.

806 Pathological Assessment of Adenoviral Gastroenteritis in Post Hematopoietic Stem Cell Transplant (HSCT) Patients

Ritika Walia[1], Teresa Hyun[1], David Myerson[1], Cecilia Yeung[1]
[1]Fred Hutchinson Cancer Research Center, Seattle, WA

Disclosures: Ritika Walia: None; Teresa Hyun: None; David Myerson: None

Background: Background: Adenovirus (ADV) gastroenteritis is a serious infection in post-HSCT recipients associated with concurrent GVHD warranting critical treatment decisions. Pathological diagnosis is required to guide treatment without which it is frequently fatal. Except for a few case reports, gastrointestinal (GI) ADV infection has not been well described in transplant patients. The objective of this study was to identify the morphological features associated with ADV infection in GI biopsies and compare assay performance of ADV immunohistochemistry (IHC) to PCR and culture.

Design: Design: Pathology archives from Jan 2006 to May 2019 were searched for cases where ADV IHC was performed. 25 patients identified to have ADV gastroenteritis confirmed by ADV IHC and PCR/shell vial culture were compared to 25 sequential patients who had negative IHC. Morphological features were assessed by four pathologists. IHC was scored (1-3) depending upon the number of positive cells in the surface epithelium.

Results: Results: Diagnostic intranuclear viral inclusions were identified in the surface epithelium in 13/25 cases. Two types of inclusions were noted: Amphophilic geographic inclusions were seen in 7, round eosinophilic in 3 and both types in 3 cases. Piling up of nuclei on the surface epithelium was seen in all 13 cases. 85% cases with inclusions had a higher IHC score while 83% cases without inclusions had only rare positive cells. All IHC positive cases also displayed focal loss of polarity, nuclear enlargement, smudgy hyperchromasia, and irregular nuclear contours in areas corresponding to IHC positivity. No viral inclusions were noted in any of the cases negative by both IHC and PCR. However, other features described in the positive cases were seen in variable combinations in the negative controls. Using PCR and viral culture as the gold standard, ADV IHC had a sensitivity and specificity of 81% and 90% respectively. A higher IHC score (2+,3+) also correlated with heavy ADV viremia. Concurrent GVHD of varying severity was found in 23/25 cases.

Figure 1 - 806

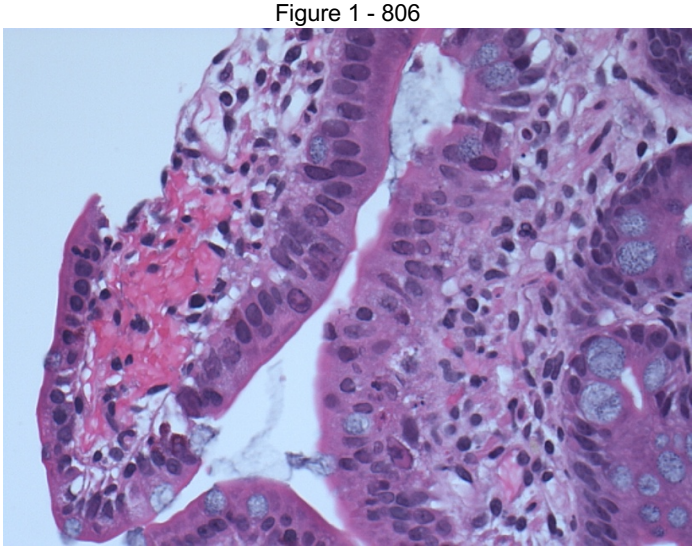

Figure 2 - 806

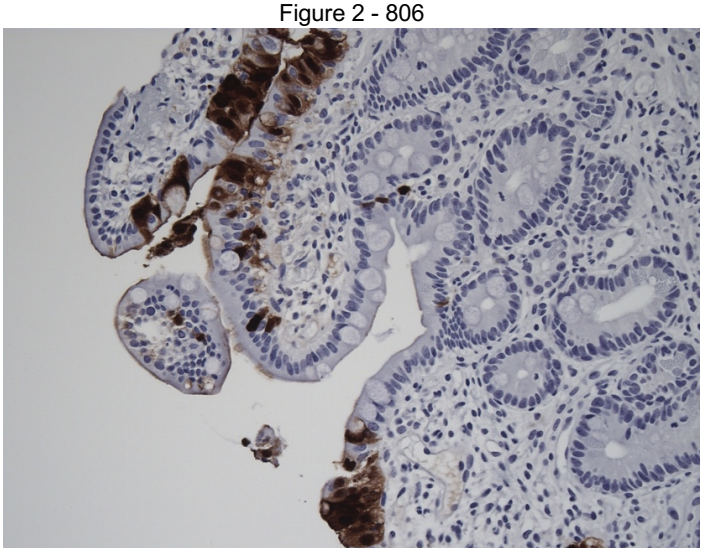

Conclusions: Conclusion: ADV can be diagnosed on H&E in 50% cases where intranuclear inclusions are identified in the surface epithelial cells. Other supportive features described above should prompt us to perform IHC which is highly specific. A low threshold should be adopted to suspect ADV infection as the morphological features can be subtle and frequently overlooked. Morphology and IHC should be correlated with PCR and viral culture studies.

807 Sarcina ventriculi: A Case Series of Ten Patients

Douglas Walton[1], Vincent Quoc-Huy Trinh[1], Chanjuan Shi[1], Safia Salaria[1]
[1]Vanderbilt University Medical Center, Nashville, TN

Disclosures: Douglas Walton: None; Vincent Quoc-Huy Trinh: None; Chanjuan Shi: None; Safia Salaria: None

Background: *Sarcina ventriculi* (SV) (also referred to as *Clostridium ventriculi*) is a gram positive anaerobic coccus with a characteristic refractile tetrad pattern that can be identified by light microscopy (figure 1). In the last decade, SV has been increasingly documented in biopsy (bx) and resection material. It is associated with gastric outlet obstruction, emphysematous gastritis, and perforation. We present the largest case series to date of 10 patients with SV including adult and pediatric examples as well as one pregnant woman.

Design: We queried the electronic medical record system of our institution and found ten patients affected by SV from the years 2013 to 2019. We compiled the following: age, gender, race, specimen location, histologic features, relevant clinical history, endoscopic or surgical findings, treatment, and follow-up.

Results: The results are summarized in Table 1. This series had a male predilection (7/10), which is counter to prior reports. 3 cases involved prior GI surgery. Nausea, vomiting, and abdominal pain were the most common presenting symptoms. There was no co-occurring *H pylori,* but coinfection with *Candida* was seen in 3 cases. Significant mucosal injury was seen in 7 patients, with mucosal (figure 2) to transmural necrosis in 1 patient. Treatment regimens varied but were primarily directed at either treating the underlying disease or no treatment at all. Only patient #9 died soon after medical intervention. Despite medication, patient #8 continued to have symptoms regarding his chronic gastroparesis up to 4 months after bx. The pregnant woman received a proton pump inhibitor prior to bx and had complete resolution of GI symptoms. Patient #6 had a persistent ulcer 1 month after bx despite receiving high dose acid suppression. The patient was later diagnosed with Crohn's disease. After receiving antibiotics patient #2 had additional biopsies that did not show SV but revealed gastric adenocarcinoma.

#	Age	Sex	Race	Clinical History	Macroscopic	Location	Microscopic
1	4	M	W NH	Noonan's syndrome s/p nissen fundiplication with a gastrocutaneous fistula	large gastrocutaneous fistula with possible prolapsed mucosa	Gastrocutaneous Fistula	Ulcerated gastric mucosa
2	17	M	H	H/o gastric ulcer with N/V, epigastric pain	Erosive esophagitis and narrowing in the duodenal bulb	Distal esophagus	Neutrophilic infiltrate and surface erosion
3	11	M	W NH	Nausea and vomiting	Partially digested food material in stomach	Stomach	Normal besides organisms
4	54	F	W NH	Acute onset abdominal and back pain with N/V, emphysematous gastric by CT, s/p nissen fundiplication	Severe gastric distention with gastric volvulus, 3 areas of full-thickness gangrene on posterior stomach	Stomach	Transmural ischemic changes, necrosis, ulceration, serositis and abcess formation
5	64	F	W NH	Dysphagia h/o GERD	Patchy candidiasis was found in the entire esophagus	Esophagus	Squamous mucosa with mild reactive changes and *Candida*
6	22	M	W NH	Epigastric discomfort with a sense of pressure and vomiting	deep gastric ulcer with stigmata of bleeding	Stomach & GEJ	Acute and chronic gastritis with erosions
7	23	F	AA	Pregnant patient with generalized abdominal pain and dyspepsia	small amount of food in the stomach	Stomach	Mild reactive changes
8	59	M	W NH	DM1 with persistent abdominal pain in the setting of long standing gastroparesis and recent gastric pneumatosis	A large amount of food in stomach; One nonbleeding gastric ulcer	Stomach	Chronic active gastritis with ulceration and budding yeast
9	66	M	W NH	Substance abuser found down at home 2 weeks after abdominal hernia repair in septic shock	Thick exudate throughout the abdominal cavity, necrotic debris, patchy necrosis of the proximal small bowel with possible perforation	Small Bowel	Focal transmural necrosis and extensive mucosal necrosis
10	75	M	W NH	Known esophageal ulcer and stricture	Esophageal diverticulum and minimal erosion; salmon colored mucosa	Esophagus	Intestinal metaplasia, erosion, yeast, hyphae, and no dysplasia

Figure 1 - 807

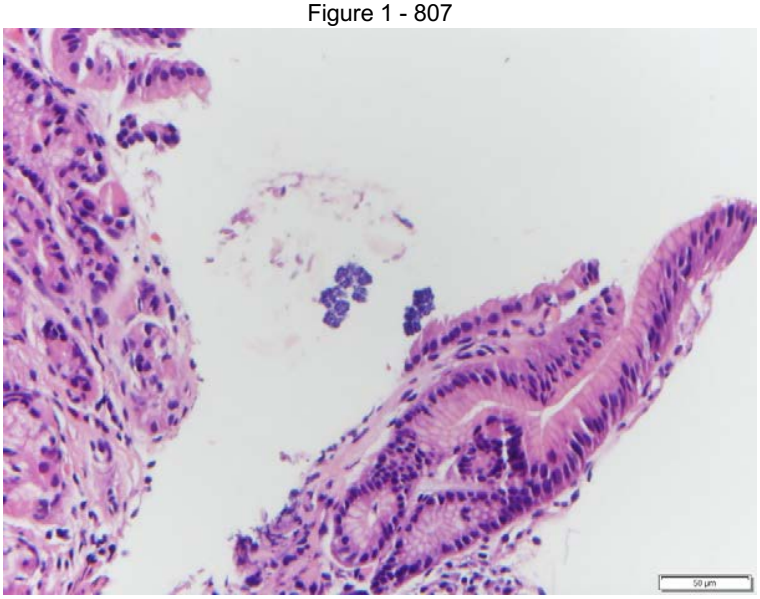

Figure 2 - 807

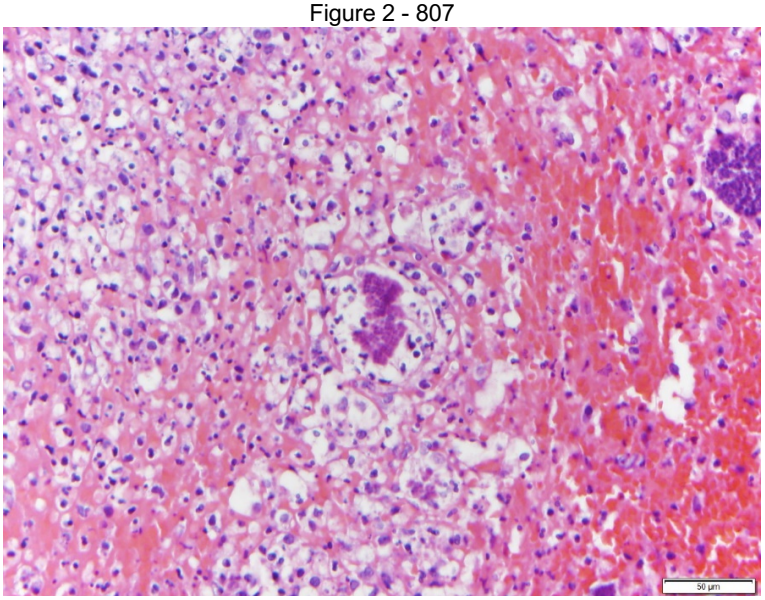

Conclusions: It is still unclear if SV is merely a colonizing organism or a causative agent. Yet, 9 out of 10 of our cases had another valid cause for the symptomatology outside of SV. Regardless, pathologist should be able to recognize SV and be vigilant of its potential presence in circumstances of gastroparesis and mucosal injury.

808 Distinct Morphologic Features Associated with Epithelial Atypia in Primary-Sclerosing-Cholangitis-Associated Inflammatory Bowel Disease

Chiyun Wang[1], James Conner[2], Richard Kirsch[2]
[1]Toronto, ON, [2]Mount Sinai Hospital, Toronto, ON

Disclosures: Chiyun Wang: None; James Conner: None; Richard Kirsch: None

Background: Primary sclerosing cholangitis (PSC) affects up to 5% of patients with inflammatory bowel disease (IBD), who are at further increased risk of colorectal neoplasia. We have noted distinctive features associated with epithelial atypia in colonic biopsies from PSC-IBD patients. This study aimed to (1) document these morphologic features, (2) evaluate their correlation to, sensitivity and specificity for PSC status, and (3) determine the interobserver agreement for their identification.

Design: A discovery cohort of photomicrographs from areas of atypia in biopsies from patients with PSC-IBD and IBD controls were reviewed, independently then collaboratively, by two gastrointestinal (GI) pathologists (JC, RK) to reach consensus on morphologic features seen more frequently in PSC-IBD. Subsequently, 61 additional surveillance biopsies from 26 patients with IBD-PSC and 64 biopsies from 40 IBD patients without PSC were identified. Dysplasia status in the cohort were: PSC-IBD: 11 negative with reactive atypia (NEG), 38 indefinite for dysplasia (IND), 12 low-grade dysplasia (LGD); PSC-negative IBD: 9 NEG, 45 IND, 10 LGD. H&E slides were randomized, blindly reviewed independently by JC and RK, and classified as positive or negative for the predetermined PSC features. One observer required multiple morphologic characteristics for positivity but also marked select cases as borderline for PSC features.

Results: PSC-associated features identified in the discovery cohort included small, angulated basal crypts lined by cuboidal to low columnar cells, with enlarged angulated/teardrop-shaped nuclei, intense hyperchromasia, variation in nuclear orientation, and an alternating light-dark appearance to individual crypts (pseudostratification, dark nuclei, pale cytoplasm). Using this morphologic profile, a significant association was found between PSC features and PSC-IBD for both observers (see Table). Individual sensitivities were 75% and 31%, while specificities were 75% and 88%. Interobserver agreement was fair and moderate (Cohen's κ = 0.32, 0.53) when excluding and including borderline cases, respectively.

Table: Association Between Identification of Morphologic Features and Clinical PSC Status

Legend: *: additionally includes borderline cases from observer 2; Either/Both: cases positive for PSC features as scored by either/both observer(s); +/- / +/-: patient PSC-positive/-negative / PSC features present/absent; PPV: positive predictive value; NPV: negative predictive value.

Rater	+/+ (n)	-/+ (n)	+/- (n)	-/- (n)	*p*-value	Sensitivity	Specificity	PPV	NPV	Accuracy
Observer 1	45	16	15	48	<0.001	0.750	0.750	0.738	0.762	0.750
Observer 2	19	8	42	56	0.020	0.311	0.875	0.704	0.571	0.600
Observer 2*	31	11	30	53	<0.001	0.508	0.828	0.738	0.639	0.672
Either	47	18	13	46	<0.001	0.783	0.719	0.723	0.780	0.750
Either*	47	19	13	45	<0.001	0.783	0.703	0.712	0.776	0.742
Both	17	6	43	58	0.013	0.283	0.906	0.739	0.574	0.605
Both*	29	8	31	56	<0.001	0.483	0.875	0.784	0.644	0.685

Conclusions: Two GI pathologists recognized distinctive histologic patterns of atypia associated with PSC-IBD with statistically significant accuracy. Sensitivity and specificity varied based on the stringency with which criteria were applied. These findings suggest that a proportion of PSC-IBD cases with epithelial atypia have distinct morphologic features that can be discerned on H&E.

809 African Americans Have Increased Tumor Budding in Colorectal Carcinoma - A Predictor of Poor Prognosis

Donghai Wang[1], Mouyed Alawad[1], Anthony Nicastri[1], Raag Agrawal[2], M. Haseeb[1], Raavi Gupta[1]
[1]SUNY Downstate Medical Center, Brooklyn, NY, [2]SUNY Downstate, Brooklyn, NY

Disclosures: Donghai Wang: None; Mouyed Alawad: None; Anthony Nicastri: None; Raag Agrawal: None; M. Haseeb: None; Raavi Gupta: None

Background: African Americans (AA) with colorectal carcinoma (CRC) suffer from worst clinical outcomes among all ethnic groups. Although contributing socioeconomic factors have been extensively studied, its biological basis is largely unknown. Tumor budding, a cognate of epithelial-mesenchymal transition, has been suggested as a measurement of aggressiveness in several tumor types. With the standardization of the tumor budding by the International Tumor Budding Consensus Conference in 2016, it has become possible to investigate the tumor budding activity in CRC accurately. In this study we correlated tumor budding in CRC patients with various clinicopathological factors in different races to predict its prognostic significance.

Design: Colorectal resection specimens from 70 AA and 35 non-AA (age-and sex-matched) patients with CRC were identified. Single cells or clusters (up to 4 tumor cells) along the invasive front of the tumor were counted at the 'hot spots' at x20 magnification. Final counts were normalized to counts/0.785 mm^2. Areas of dense neutrophilic infiltration, glandular fragmentation or tumor cells floating in the mucin were not counted. The 3-tier category was used to classify tumor budding groups. Correlation with clinicopathologic variables with different tumor budding groups was performed with Chi-Squared test (SPSS, v.22.0).

Results: Higher tumor budding was significantly associated with AA ethnicity (p=0.036), high tumor stage (p=0.001), right-sided tumors (p=0.037) and high CEA levels (p=0.006) in 3-tier classification. Tumor budding was not associated with grade, lymphovascular or perineural invasion (Figure 1).

Figure 1 - 809

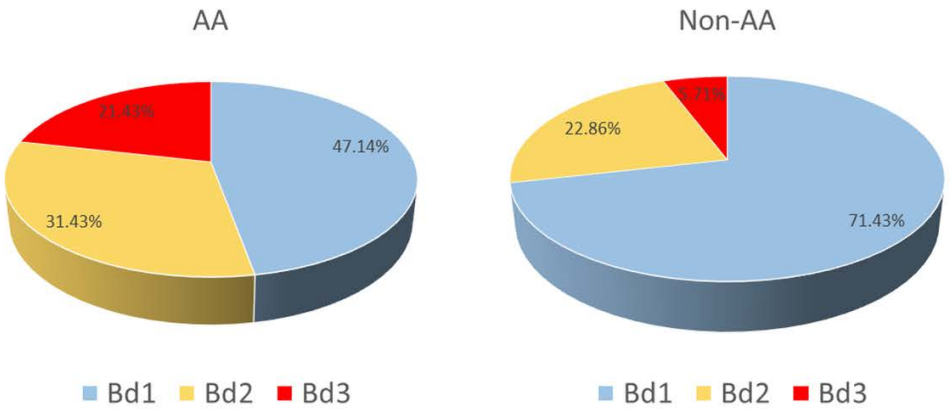

Figure 1. Frequency of 3 categories of tumor budding in AA and non-AA patient population with CRC

Conclusions: We present the first evidence of increased tumor budding in CRC in AA patients as compared to those in other racial groups. These findings provide insight into biological mechanisms of tumor progression and adverse prognosis in this population.

810 Intestinal Nodular Lymphoid Hyperplasia, and Possible Underlying Immunodeficiency in Patients with Cowden Syndrome

Guoliang Wang[1], Yujun Gan[2], Deepthi Rao[3], Katsiaryna Laziuk[4]
[1]University of Missouri, Columbia, MO, [2]Department of Pathology and Anatomical Sciences, School of Medicine, University of Missouri, Columbia, MO, [3]University of Missouri School of Medicine, Columbia, MO, [4]Columbia, MO

Disclosures: Guoliang Wang: None; Yujun Gan: None; Deepthi Rao: None; Katsiaryna Laziuk: None

Background: Cowden syndrome is an autosomal dominant inherited disorder caused by mutation in *PTEN* gene. With a prevalence of about 1 in 200,000 people, it is characterized by multiple hamartomas and increased risk of developing cancers. Nodular lymphoid hyperplasia, a histologic finding usually associated with immunodeficiency state was assessed in Cowden patients.

Design: In this study, we performed an electronic search of the pathology records at the University of Missouri, Columbia for a 20 years period between January 2000 and September 2019 for all patients with Cowden syndrome. The histological slides of gastrointestinal biopsies were reviewed independently by two board certified pathologists specialized in gastrointestinal pathology and hematopathology, respectively.

Results: Our study revealed nine patients with Cowden syndrome. Of them, eight had gastrointestinal endoscopy examination and biopsies(8/9). Gastrointestinal lymphoid aggregates were consistently noted in all patients(8/8). Interestingly, nodular lymphoid hyperplasia, characterized by the presence of histologically markedly hyperplastic, mitotically active germinal centers, and well-defined lymphocytes mantles, in lamina propria and/or superficial submucosa was identified among six of eight patients (6/8). Other findings include colonic tubular adenoma(5/8), ganglioneuroma(3/8), and gastric fundic gland polyp(1/8).

Conclusions: In this study, we identified an impressively high occurrence rate(6/8) of nodular lymphoid hyperplasia in patients with Cowden syndrome. Nodular lymphoid hyperplasia, a known histologic finding in immunodeficiency state, is also a risk factor for lymphomas. Thus, active GI endoscopic surveillance with histopathologic evaluation is recommended in patients with Cowden syndrome to assess for the underlying immunodeficiency and lymphoma, in addition to surveillance of dysplastic polyps and carcinoma.

811 Intestinal-Type Epithelium Minimally Extends Beyond the Gastroduodenal Junction into the Gastric Pylorus

Kai Wang[1], David Hernandez Gonzalo[2], Michael Feely[1]
[1]University of Florida, Gainesville, FL, [2]University of Florida-Shands, Gainesville, FL

Disclosures: Kai Wang: None; David Hernandez Gonzalo: None; Michael Feely: None

Background: Gastric intestinal metaplasia is associated with an increased risk of neoplasia such that this diagnosis may subject patients to further surveillance. While a diagnosis of intestinal metaplasia within the gastric body or proximal antrum is relatively straightforward, interpretation of such findings on biopsies from the gastric pylorus can be problematic as the normal mucosa in this region has not been well-characterized. The purpose of this study was to evaluate whether intestinal-type epithelium (ITE) may innately extend into this pyloric region.

Design: We identified resection specimens from our archives in which sampling of the gastroduodenal junction or pyloric ring was performed. Cases were excluded if the primary pathology was gastric in nature, a secondary review demonstrated more than minimal chronic gastritis, or they had insufficient histologic features for assessment. Individual slides were examined for the presence of ITE in relation to histologic landmarks of the gastroduodenal junction including the proximal extent of submucosal Brunner glands and the apex of the muscular pyloric ring.

Results: A total of 158 cases met the selection criteria which were comprised of a nearly equal distribution of women (n=80) and men (n=78) with a mean age of 64 (range 23-87). Indications for the original resection included pancreatic (n=95), duodenal/ampullary (n=36), or biliary neoplasia (n=11) as well as pancreatic inflammatory disorders (n=14) and metastatic disease (n=2). ITE was noted to extend proximally from the Brunner glands in 72 (46%) cases for a mean length of 2.8 mm in these instances. Fewer cases had ITE extend beyond the apex of the pyloric ring (n=52; 33%), a more proximal landmark of the gastroduodenal junction. This extension ranged from 0.1 to 14.5 mm with a mean length of 2.5 mm. Most cases demonstrated a continuous extension of ITE into the pylorus with a minor subset exhibiting a patchy distribution (n=15).

Conclusions: A notable proportion of individuals exhibit extension of ITE into the gastric pylorus, albeit to a minimal degree. A prior complementary study looking into this landmark demonstrated encroachment of foveolar epithelium distally into the duodenal bulb. This heterogeneous mucosa within this transition point should dissuade gastroenterologists from routinely obtaining gastric biopsies immediately prior to intubation of the pyloric ring. Pathologists should also be aware of this phenomenon so as not to overinterpret ITE as pathologic intestinal metaplasia.

812 Straightening Signet Rings via Convoluted Networks --- The Utility of Convolutional Neural Networks for Screening and Staging Signet Ring Cell Carcinoma on Digital Slides in Gastrointestinal Pathology

Yaohong Wang[1], Yongchao Li[1], Shuyu E[1], Jie Zhang[1], Lauren King[2], Farhan Khan[2], Nour Yadak[3], Richa Jain[4], Ian Clark[5], Alan Boom[2], Joel Gradowski[6], David Robins[7], Rodolfo Laucirica[1], Jing Huang[8], Steve Jin[8], Richard Kinsey[9], Mahul Amin[10]
[1]University of Tennessee Health Science Center, Memphis, TN, [2]The University of Tennessee Health Science Center, Memphis, TN, [3]UTHSC, Bartlett, TN, [4]Banner-University Medical Center, Tucson, AZ, [5]University of Tennessee, Memphis, TN, [6]University of Tennessee Health Sciences Center, Germantown, TN, [7]West Cancer Clinic, Memphis, TN, [8]Hipposcan Intelligence Inc., Collierville, TN, [9]Poplar Healthcare, Memphis, TN, [10]Methodist University Hospital, Memphis, TN

Disclosures: Yaohong Wang: None; Yongchao Li: None; Shuyu E: None; Lauren King: *Employee*, Pfizer Pharmaceuticals; Farhan Khan: None; Nour Yadak: None; Ian Clark: None; Joel Gradowski: None; Rodolfo Laucirica: None; Jing Huang: None; Steve Jin: None; Richard Kinsey: None; Mahul Amin: *Consultant*, UroGen; *Consultant*, Advanced Clinical; *Advisory Board Member*, Cell Max; *Advisory Board Member*, Precipio Diagnostics

Background: Despite the overall decline in the incidence and mortality of gastric carcinoma, the incidence of gastrointestinal signet-ring cell carcinoma (SRCC) is increasing. In Asia, the United States and Europe, it currently accounts for 35% to 45% of all gastric adenocarcinoma. The histologic findings in SRCC are often subtle. Pathologists spend extra time on gastric biopsies searching for these subtle signet ring cells (SRC) with some advocating the use of routine immunohistochemical stains to help identify small clusters or rare isolated SRC on all gastric biopsies while others examining all gastric biopsies on high power. Manual detection is both time consuming, labor intensive and prone to error. Convolutional neural networks (CNNs) have been used in recent years for deep learning and histology image recognition. CNNs have achieved clinical grade performance on complex visual tasks. This study will apply CNNs to assist pathologists in detecting SRC for diagnosis as well as pathological staging.

Design: The dataset consists of 600 de-identified whole slide images (WSIs) of gastric mucosa and intestine specimens from 120 patients. The tissue was stained with hematoxylin and eosin and scanned on Leica Biosystems AT2 digital slide scanners. Supervised frameworks are deployed for computer training. Deep learning models are deployed for the detection. We use Keras to access tensorflow engine to build our deep learning models.

Results: Total of 10,000 tiles with SRC and 18,000 tiles with no SRC are annotated by experienced pathologists. They are used as input training dataset to train our CNNs models. Additional 30 patients' 150 images and annotations of 5,000 cells are utilized as testing dataset for evaluation. Overall our model reached 95% accuracy with training dataset and more than 99% with testing dataset in SRC detection on both resection and biopsy slides. And in the meanwhile, the invasive front of single or small cluster of tumor cell(s) can be labeled on the digital slide and the depth of invasion is measured, that will facilitate the pathologic staging.

Figure 1 - 812

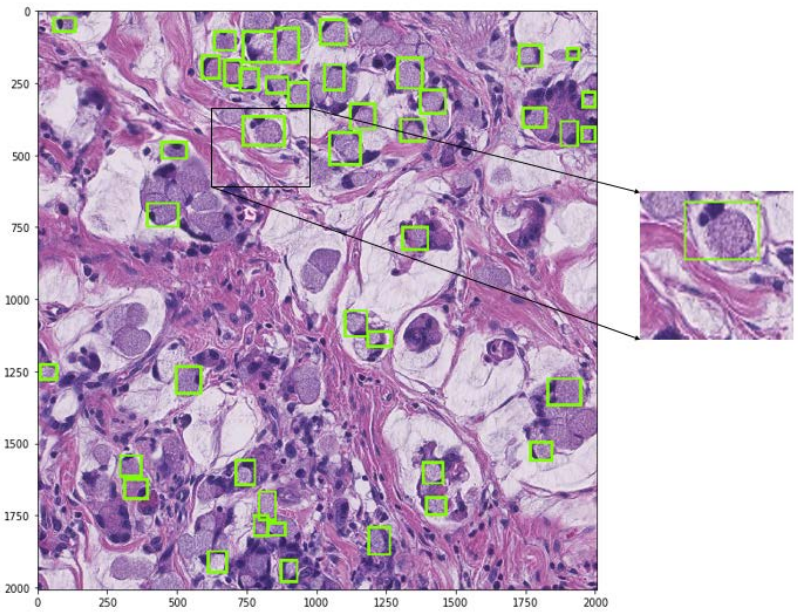

Fig. 1, WSI annotation. Each signet ring cell is labeled with a green box. Each signet ring cell is sliced into a tile with 256x256 pixel size as input training data. The location of signet ring cell in relation to tile border is randomly assigned.

Figure 2 - 812

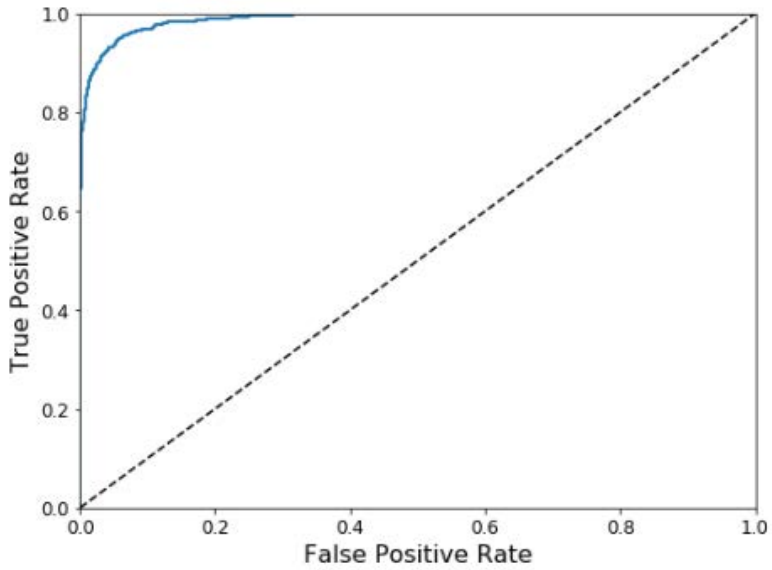

Conclusions: CNNs method can assist pathologists to screen for unexpected or challenging SRC detection and label the invasive front of carcinoma cell(s), which can be readily applied in the clinical trials. The CNNs method shows promise as an assistant screening and staging tool; improving the sensitivity and efficiency for SRC detection; however, for its use in confirmatory diagnosis, further training with a more diverse dataset will be required.

813 Assessment of Surface Cell Polarity (the "Four Lines") Distinguishes Gastric Dysplasia from Reactive Gastropathy: A Comprehensive 2 Institution 5-Year (2008-2012) Histologic and Clinical Review

Kevin Waters[1], Danielle Hutchings[2], Kevan Salimian[3], Lysandra Voltaggio[4], Elizabeth Montgomery[5]
[1]Cedars-Sinai Medical Center, Los Angeles, CA, [2]Johns Hopkins Medicine, Baltimore, MD, [3]Johns Hopkins, Baltimore, MD, [4]Baltimore, MD, [5]Johns Hopkins Medical Institutions, Baltimore, MD

Disclosures: Kevin Waters: None; Danielle Hutchings: None; Kevan Salimian: None; Lysandra Voltaggio: None; Elizabeth Montgomery: None

Background: Gastric dysplasia is a risk factor for both synchronous and subsequent gastric carcinoma. Assessing dysplasia is challenging as striking nuclear atypia can accompany reactive gastritis. We previously showed that assessment of surface cytologic architecture/cell polarity (4 lines: 1) apical mucin cap, 2) base of mucin cap, 3) cytoplasm, and 4) nucleus) improved the evaluation of dysplasia in Barrett esophagus. We studied the utility of this feature in distinguishing gastric dysplasia from reactive changes and correlated with findings on follow-up (f/u) biopsies.

Design: We identified all biopsied cases of incident gastric dysplasia (n=95) at two tertiary care centers over a 5-year period (2008-2012) and compared them to reactive gastropathy cases (n=60) from 2008. Demographic variables and the results of clinical and pathologic f/u were collected. Each biopsy was evaluated by 2 gastrointestinal pathologists for either maintenance or loss of the "4 lines."

Results: Patients with dysplasia versus reactive gastropathy were similar in mean age (67 vs 63) and gender (44% vs. 38% male) but patients with dysplasia were more likely to be Hispanic (6% vs. 0%) or Asian (19% vs. 3%). Intestinal metaplasia (67% vs. 5%), autoimmune metaplastic atrophic gastritis (14% vs. 3%), and prevalent or prior *H. pylori* infection (16% vs. 0%) were more common in the dysplasia group. The "four lines" were lost in all 92 dysplasia cases with evaluable surface; 3 cases lacked surface dysplasia to evaluate. Surface cytologic architecture was maintained in all 57 cases of reactive gastropathy with evaluable surface, but 17 (28%) showed focal loss of the "4 lines" adjacent to erosion in fibrinous exudate. In the dysplasia group, 48% had low-grade dysplasia (LGD), 35% high-grade (HGD), and 16% at least intramucosal carcinoma (≥IMC). On f/u, 14% (4/28) of the LGD cases progressed to HGD and 21% (5/24) of the HGD cases progressed to ≥IMC. Progression was more common in flat lesions (56% 5/9) than polypoid ones (9%; 4/43; $p<0.001$). Dysplasia arising in fundic gland polyps did not progress (0/15). No cases of reactive gastritis with f/u biopsy progressed to dysplasia over 100 person-years.

Conclusions: Surface cell polarity is a useful tool to differentiate gastric dysplasia from reactive gastritis and the loss of the "four lines" was associated with dysplasia and progression. This feature cannot be relied on in dysplastic cases without evaluable surface and adjacent to erosions in reactive gastropathy.

814 RNA in situ Hybridization (ISH) Staining is a Sensitive and Specific Test for Chlamydia Proctitis

Kevin Waters[1], Brian Cox[1], Maha Guindi[2], Stacey Kim[1], Brent Larson[1], Lysandra Voltaggio[3], Bonnie Balzer[1]
[1]Cedars-Sinai Medical Center, Los Angeles, CA, [2]Cedars-Sinai Medical Center, Beverly Hills, CA, [3]Baltimore, MD

Disclosures: Kevin Waters: None; Brian Cox: None; Maha Guindi: None; Stacey Kim: None; Brent Larson: None; Lysandra Voltaggio: None; Bonnie Balzer: None

Background: Chlamydia proctitis cannot be reliably diagnosed by histology as its features overlap with other infections and inflammatory bowel disease. There is no commonly available stain for chlamydia infection and the diagnosis is made by nucleic acid amplification (NAA), culture, or direct immunofluorescence of a rectal swab. We evaluated an RNA in situ hybridization stain in cases of Chlamydia proctitis.

Design: Anorectal samples from 12 cases were identified in our surgical pathology archives in patients with a rectal swab positive for Chlamydia NAA within 3 months. 10 comparison proctitis cases from other causes (5 rectal; 5 anal) were selected. Each case was tested for Chlamydia with an RNAscope® ISH probe targeting Chlamydia 23S rRNA using red chromogenic detection on the Leica Bond RX platform. A negative control (dapB) was negative in each case. Clinical characteristics were recorded and sensitivity and specificity were calculated.

Results: The mean age of the Chlamydia group was 42 and all were male. 9/12 were HIV+ and 1 each had concurrent syphilitic and CMV proctitis. 8 biopsies were from the rectum and 4 were from the anus or anorectal junction. Reason for biopsy included: rectal bleeding (n=5), condyloma (n=3), mass (n=1), ulceration (n=1), diverticulitis (n=1), hemorrhoid (n=1), and soft stools (n=1). Acute inflammation was mild except for cases with ulceration and/or concomitant CMV infection. 8 showed prominent plasma cells. 9 had lymphoid aggregates including one that was worked up for lymphoma. Other than basal plasmacytosis, features of chronic proctitis (crypt distortion, Paneth cell metaplasia) were absent in rectal biopsies. The sensitivity was 75% as 9/12 Chlamydia cases had definitive positive staining. 1 additional case had 2 focal dots of equivocal staining that may reflect treatment effect as the biopsy was done 17 days after the positive NAA test. 2 anal condyloma biopsies with only focal inflammation were negative. The positive staining was characterized by red chromogenic dots

present both singly and in clusters in both columnar and squamous epithelium as well as inflammatory cells. The specificity was 100% as none of the control proctitis cases were definitively positive. 1 case did have a single dot of equivocal staining in rectal stroma.

Conclusions: RNA ISH staining is a sensitive and specific method for detection of Chlamydia infection in rectal and anal biopsies. Additional studies are necessary to examine this method in other tissue types and in treated cases.

815 Lymphocytic and Collagenous Colitis in Pediatric Patients Revisited: Clinicopathologic Analysis and Patient Outcomes in 25 Patients

Annika Windon[1], Danielle Hutchings[2], Kevan Salimian[3], Naziheh Assarzadegan[4], Lysandra Voltaggio[5]
[1]Johns Hopkins Hospital, Baltimore, MD, [2]Johns Hopkins Medicine, Baltimore, MD, [3]Johns Hopkins, Baltimore, MD, [4]Department of Pathology, The Johns Hopkins Medical Institutions, Baltimore, MD, [5]Baltimore, MD

Disclosures: Annika Windon: None; Danielle Hutchings: None; Kevan Salimian: None; Naziheh Assarzadegan: None; Lysandra Voltaggio: None

Background: Microscopic colitis (MC) is a condition characterized by clinical symptoms of chronic watery diarrhea, endoscopically normal findings, and abnormal histology. While this condition is mostly seen in adults, pediatric cases are rare with few case series published to date.

Design: Our Pathology Data System was searched from 1984-2019 for cases of lymphocytic colitis (LC) or collagenous colitis (CC) in patients 20 years of age and younger. Twenty-five cases were retrieved and slides were reviewed together with pertinent clinical findings.

Results: Twenty-five cases of microscopic colitis (21 LC, 4 CC) were identified in 25 individual patients. Mean age was 10 years (range, 4-18) and there was a female predominance (N=16, 64%). The majority were Caucasian (N=21, 84%) with three cases of LC (12%) occurring in African Americans. Most patients (N=24, 96%) presented with prolonged non-bloody diarrhea/loose stools with or without additional symptoms including abdominal pain (N=17, 68%), flatulence (N=6, 24%), and nausea/vomiting (N=5, 20%). Abnormal endoscopic findings including aphthous ulcers, edema, friability, erythema, and lymphoid hyperplasia were found in a subset of patients (N=9, 36%). In addition to the classical features of each MC subtype, cryptitis and apoptosis were identified in 28% (N=7) and 24% (N=6) of cases, respectively. Immune dysregulation was documented in 44% of the patients (immunodeficiency syndromes [N=6, 24%], celiac disease [N=3, 12%], juvenile idiopathic arthritis [N=2, 8%]). Clinical and/or pathologic follow up data was available for twenty-one patients (84%) with a mean of 4.2 years (range, 4 months to 12 years). Ten of these twenty-one patients had subsequent biopsies available for review; seven displayed persistent histologic features of MC (70%), despite clinical improvement. Though none of the patients developed histologic features of inflammatory bowel disease (IBD), 11 patients experienced varying degrees of symptomatic relief after management with IBD medications (infliximab, 6-mercaptopurine, mesalamine, adalimumab).

Conclusions: In keeping with previous studies, LC was more common in this age group than CC, associations with autoimmune conditions were frequent, and atypical histologic findings such as apoptosis and neutrophilia were not infrequent. Unlike prior series, our cohort demonstrated abnormal colonoscopic findings in over 1/3 of the patients. Patients may improve clinically despite histologic persistence of the inflammatory process.

816 Expression of Claudin-18 in Precursor Lesions of the Stomach

Mary Wong[1], Carissa Huynh[2], Stacey Kim[3], Maha Guindi[4], Brent Larson[3], Mariza De Peralta-Venturina[5], Bonnie Balzer[3], Kevin Waters[3]
[1]Arcadia, CA, [2]Cedars-Sinai Medical Center, Palmdale, CA, [3]Cedars-Sinai Medical Center, Los Angeles, CA, [4]Cedars-Sinai Medical Center, Beverly Hills, CA, [5]Cedars-Sinai Medical Center, West Hollywood, CA

Disclosures: Mary Wong: None; Carissa Huynh: None; Stacey Kim: None; Maha Guindi: None; Brent Larson: None; Mariza De Peralta-Venturina: None; Bonnie Balzer: None; Kevin Waters: *Advisory Board Member*, Astella Pharma

Background: Claudin-18 plays a key role in constructing tight junctions and altered claudin-18 expression has been documented in various malignancies. Antibody-based cancer therapies have been emerging as promising therapeutics in oncology, including one that targets claudin-18 in gastric carcinoma that is currently being evaluated in clinical trial. Intestinal metaplasia (IM), autoimmune metaplastic atrophic gastritis (AMAG) and gastric dysplasia have been shown to be risk factors for gastric carcinoma. In this retrospective study, we evaluated the expression of claudin-18 in gastric IM, IM in AMAG, and gastric dysplasia to investigate the clinical-pathologic profile of these processes.

Design: Biopsy cases with gastric IM not due to AMAG (15), IM in AMAG (10) and gastric dysplasia (20) were identified from departmental surgical archives. Each case was stained for claudin-18 (CLDN18 (43-14A), Ventana Medical Systems). Staining of claudin-18 in IM and gastric dysplasia was evaluated base on intensity and extent of staining.

Results: 64% (9/14) with IM not due to AMAG were positive, ranging from weak to strong in intensity and patchy to diffuse in extent, and 89% (8/9) of the positive cases showed complete IM. All 6 negative cases had complete metaplasia. The IM on the fifteenth case was lost on subsequent slides. All ten cases with IM in AMAG were negative. 18 of the dysplasia cases had low-grade dysplasia and 2 cases had high-grade dysplasia. Of these 25% (5/20) showed positive staining for claudin-18, ranging from weak to strong and patchy to diffuse in extent. Of the 13 cases with both IM and dysplasia, 38.4% (5/13) of cases showed positive staining in the IM, with 80% (4/5) of these cases also showing positive staining in dysplasia. The two cases with high-grade dysplasia were negative for claudin-18 in both the IM and gastric dysplasia.

Conclusions: Our findings show similar rate of positivity of claudin-18 in IM (not due to AMAG) and dysplasia compared to the reported rate in gastric adenocarcinomas (~40%). In contrast, IM in the background of AMAG showed 100% negative staining for claudin-18 indicating that IM in this setting differs from other forms of IM. Additional cases with paired carcinoma will be necessary to determine if claudin-18 expression in precursor lesions is predictive of expression in paired carcinoma.

817 Claudin-18 is a Sensitive and a Specific Marker for Gastric Neuroendocrine Tumors

Mary Wong[1], Carissa Huynh[2], Stacey Kim[3], Deepti Dhall[4], Maha Guindi[5], Brent Larson[3], Mariza De Peralta-Venturina[6], Bonnie Balzer[3], Kevin Waters[3]
[1]Arcadia, CA, [2]Cedars-Sinai Medical Center, Palmdale, CA, [3]Cedars-Sinai Medical Center, Los Angeles, CA, [4]The University of Alabama at Birmingham, Birmingham, AL, [5]Cedars-Sinai Medical Center, Beverly Hills, CA, [6]Cedars-Sinai Medical Center, West Hollywood, CA

Disclosures: Mary Wong: None; Carissa Huynh: None; Stacey Kim: None; Deepti Dhall: None; Maha Guindi: None; Brent Larson: None; Mariza De Peralta-Venturina: None; Bonnie Balzer: None; Kevin Waters: *Advisory Board Member*, Astella Pharma

Background: Antibody-based cancer therapies have been emerging as promising therapeutics in oncology, including one currently in clinical trials that targets claudin-18, a protein that is expressed in normal gastric epithelium and in some gastric adenocarcinoma. Currently, we have no markers for gastric well-differentiated neuroendocrine tumors (NETs). In this retrospective study, we evaluated the expression of claudin-18 protein in gastric neuroendocrine hyperplasia in the setting of autoimmune metaplastic atrophic gastritis (AMAG), gastric NETs and NETs from other organs to investigate the expression profile of claudin-18 in gastric NETs.

Design: Seven biopsy cases of gastric ECL-cell neuroendocrine hyperplasia with AMAG and eleven gastric NETs biopsies and resections were identified from departmental surgical archives. Additionally, two tissue microarrays (TMA) of NETs were also used that include NETs of gastric (4), pancreatic (26), small bowel (24), colorectal (7), appendiceal (6), and lung (25) origin. All gastric NETs and TMAs of NETs were stained with claudin-18 (CLDN18 (43-14A), Ventana Medical Systems). Staining quality of claudin-18 was evaluated base on intensity and extent of staining.

Results: Thirteen of fourteen cases (92.9%) with neuroendocrine hyperplasia were positive for claudin-18 expression, ranging from moderate to strong in intensity and all with diffuse positivity. Thirteen of fifteen (86.7%) cases of gastric NETs (including 2 cases from TMAs) were positive for membranous claudin-18 staining, ranging from moderate to strong in intensity and patchy to diffuse in extent. Of these cases, 80.0% (8/10) of type I, 100.0% (4/4) of type III, and 100.0% (1/1) of unknown type of gastric NETs were positive for claudin-18. All 88 WDNETs in the TMAs from pancreas, small bowel, colorectum, appendix, and lung were negative (P<0.001). The sensitivity and specificity of claudin-18 for gastric NETs was 86.7% (95% CI 62.1-97.7%) and 100.0% (95% CI 0-4.2%), respectively.

Conclusions: Expression of claudin-18 appears to be maintained in the vast majority of gastric NETs. Diagnostically claudin-18 appears to be very sensitive and specific for gastric NETs compared to NETs from other primary sites and may be a useful marker for gastric origin in a metastatic setting. The membranous expression of claudin-18 in gastric NETs, including in the more aggressive type III cases, indicates that they may be susceptible to anti-claudin 18 therapy.

818 Intraepithelial Gamma-Delta T Cells are Comparatively Increased in the Duodenum but not Colon of Patients with Celiac Disease and Lymphocytic Colitis

Elizabeth Wu[1], Ashlee Sturtevant[2], Sonja Chen[3], Murray Resnick[4]
[1]Rhode Island Hospital/Brown University, Providence, RI, [2]Brown University, Providence, RI, [3]Rhode Island Hospital, Providence, RI, [4]Sharon, MA

Disclosures: Elizabeth Wu: None; Ashlee Sturtevant: None; Sonja Chen: None; Murray Resnick: *Consultant*, PathAI

Background: Celiac disease (CeD) is strongly associated with lymphocytic colitis (LyC; defined as >20 intraepithelial lymphocytes per 100 enterocytes with epithelial injury). Intraepithelial gamma-delta T cells are increased in the duodenum of patients with CeD; however, their distribution at other luminal sites have not been well characterized. The aim of this study is to compare the degree of intraepithelial gamma-delta lymphocytosis in LyC diagnosed in CeD patients compared to patients negative for CeD.

Design: We included all biopsies from LyC patients with known celiac serologies on chart review who had both duodenal and colorectal biopsies. Demographic, serologic, endoscopic findings, and medication history were reviewed. Immunohistochemistry for gamma-delta, CD3, CD4, and CD8 were performed and lymphocytes counted.

Results: Twenty-eight adult and pediatric patients with 56 biopsies were evaluated (Table 1). Thirteen patients had LyC and confirmed CeD; one patient had compatible histology and symptoms with response to a gluten free diet. Fourteen patients had LyC and negative TTG, with duodenal biopsies showing either few or no intraepithelial lymphocytes. Eleven patients (78.6%) with CeD were diagnosed concurrently with LyC, while 3 (21.4%) were diagnosed with CeD prior to LyC. Moreover, patients with CeD were more likely to have an endoscopically abnormal duodenum (p = 0.029). Most patients with CeD had evidence of histologic villous blunting (12/14, 85.7%), while the rest had intact villous architecture. In addition, the number of duodenal intraepithelial gamma-delta, CD3-positive, and CD8-positive intraepithelial T cells was significantly higher in CeD patients compared to controls (p = 0.021, 0.003, and 0.005). In contrast, colonoscopic findings were similar in both groups, and there was no significant difference between colonic gamma-delta, CD3-positive, and CD8-positive intraepithelial T cells between patients with and without CeD. There was no difference in use of SSRIs, NSAIDs, PPIs, and statins between patients with and without CeD.

Table 1. Demographic characteristics, endoscopic findings, and intraepithelial lymphocyte subsets in celiac and non-celiac patients				
		Celiac	**Non-celiac**	**p-value**
Age (median, range)		46 (17-66)	42 (6-71)	0.05
M/F		14 F	1M, 13 F	NS
TTG (median, range)		83.8 (16.1 to >200)	4.4 (1.4 to 7.9	<0.00001
Presenting symptoms (number, %)	Diarrhea	11 (78.6%)	14 (100%)	NS
	Positive FOBT	1 (7.1%)	0 (0%)	
	No data available	2 (14.3%)	0 (0%)	
Upper endoscopic findings (number, %)	Normal	6 (42.9%)	11 (78.6%)	0.029
	Scalloping	6 (42.9%)	1 (7.1%)	
	Other (ulceration, erythema)	2 (14.3%)	0 (0%)	
	No data available	0 (0%)	2 (14.3%)	
Colonoscopic findings (number, %)	Normal	12 (85.7%)	13 (92.9%)	NS
	Mild erythema or inflammation	1 (7.1%)	1 (7.1%)	
	No data available	1 (7.1%)	0 (0%)	
Duodenum gamma-delta T cell count (median, range)		11.5 (1-26)	4 (0-9)	0.021
Duodenum CD3 count (median, range)		66 (32-131)	33 (24-52)	0.0033
Duodenum CD8 count (median, range)		55 (30-83)	26 (15-50)	0.005
Colon gamma-delta T cell count (median, range)		8.5 (0-37)	6 (0-22)	NS
Colon CD3 count (median, range)		55.5 (21-125)	43.5 (22-85)	NS
Colon CD8 count (median, range)		43.5 (21-107)	39 (16-70)	NS

Conclusions: The findings suggest that gamma-delta immunohistochemistry may have utility in distinguishing CeD and non-celiac related duodenal lymphocytosis, including in adult patients. Intraepithelial gamma-delta T cells do not appear to differ between CeD and non-CeD patients with LyC. Larger series of patients with clinicopathologic follow-up data are needed to confirm this finding and further evaluate this association.

819 Molecular and Clinicopathological Features of Colorectal Adenocarcinoma with Enteroblastic Differentiation

Yuya Yamashiro[1], Tsuyoshi Saito[2], Takuo Hayashi[3], Takashi Murakami[2], Yuka Yanai[4], Sho Tsuyama[5], Yoshiyuki Suehara[2], Kazuya Takamochi[2], Takashi Yao[6]
[1]Juntendo University Hospital, Tokyo, Japan, [2]Juntendo University, School of Medicine, Tokyo, Japan, [3]Juntendo University Graduate School of Medicine, Tokyo, Japan, [4]Juntendo University, Bunkyo-ku, Tokyo, Japan, [5]Juntendo University Graduate School of Medicine, Bunkyo-ku, Tokyo, Japan, [6]Juntendo University, Tokyo, Japan

Disclosures: Yuya Yamashiro: None; Tsuyoshi Saito: None; Takuo Hayashi: None; Takashi Murakami: None; Yuka Yanai: None; Sho Tsuyama: None; Yoshiyuki Suehara: None; Kazuya Takamochi: None; Takashi Yao: None

Background: Gastric adenocarcinoma with enteroblastic differentiation (GAED) is a rare variant of gastric adenocarcinoma characterized as having a primitive intestine-like structure with clear cytoplasm and positive for at least one of the following antibodies, AFP, Glypican-3 and SALL4 (enteroblastive markers) by immunohistochemistory (IHC). In contrast, several cases of its colorectal counterpart, namely adenocarcinoma with enteroblastic differentiation (CAED), have been reported so far (Murakami et al. Histopathology 2019). The aims of this study are to elucidate the frequency of CAED and to establish its molecular and clinicopathological characteristics.

Design: In addition to 3 cases recently diagnosed as CAED, colorectal carcinoma (CRC) with expression of enteroblastic markers were selected by using IHC on tissue microarray of 988 advanced CRC. We employed the next-generation sequencing (NGS) and Sanger sequencing. IHC for p53 and HER2, HER2 FISH and MSI status were also investigated. Survival analyses for clinicopathologic parameters were performed using Kaplan-Meier methods.

Results: Among 988 cases, 971 cases were adequate for IHC evaluation. Thirty-nine cases (4.0%) were positive for at least one enteroblastic markers. Histological evaluation of total 42 cases revealed that 10 cases contained tumor cells with clear cytoplasm. Enteroblastic markers positive cases tended to show higher pT and TNM stages, frequent venous invasion and lymph nodes metastasis. Lymphatic invasion was more frequently observed (P< .001). Overall survival and recurrence-free survival analysis revealed that enteroblastic markers positive cases showed poorer prognosis than negative cases (P<.01 and P<.05 respectively). NGS revealed *TP53* as the most frequently mutated gene. Combined with the subsequent Sanger sequences, the rate of *TP53* mutation was 52.4% (22/42). The rate of HER2 positive cases and MSI-H cases were 9.5% (4/42) and 12.2% (5/41), respectively. Among these 42 cases, there was no molecular and clinicopathological differences according to the presence of tumor cells with clear cytoplasm.

Conclusions: Enteroblastive marker-positive CRC could be grouped together as CAED regardless of clear cell cytoplasm. By this definition, the frequency of CAED was rarer than GAED. Enteroblastic markers may be an indicator of aggressive behavior and poor prognosis in CRC. The frequencies of *TP53* mutation, HER-2 positive, MSI-H are similar to those reported in conventional CRC.

820 NTRK Fusion in Japanese Colorectal Adenocarcinomas

Yuya Yamashiro[1], Taisei Kurihara[2], Takuo Hayashi[3], Yoshiyuki Suehara[2], Takashi Yao[4], Shunsuke Kato[2], Tsuyoshi Saito[2]
[1]Juntendo University Hospital, Tokyo, Japan, [2]Juntendo University, School of Medicine, Tokyo, Japan, [3]Juntendo University Graduate School of Medicine, Tokyo, Japan, [4]Juntendo University, Tokyo, Japan

Disclosures: Yuya Yamashiro: None; Taisei Kurihara: None; Takuo Hayashi: None; Yoshiyuki Suehara: None; Takashi Yao: None; Shunsuke Kato: None; Tsuyoshi Saito: None

Background: *NTRK* fusions have been reported to be less frequent in cancers across organs except for specific cancer types such as infantile fibrosarcoma and mammary analog of secretary carcinoma. *NTRK* fusion positive tumors are reported to show high sensitivity to the TRK inhibitor such as Larorectinib and Entrectinib, therefore identification of patients with potential benefit by these inhibitors is very important. In colorectal carcinoma (CRC), the frequency of *NTRK* fusion is reported to up to 0.3%, however, its frequency in Japanese patients with CRC is unknown.

Design: We performed pan-trk immunohistochemistry (IHC) using tissue microarray (TMA) in a large cohort of consecutive Japanese CRC samples. Positive cases were further analyzed by Nanostring containing 90 tyrosine kinase genes and subsequent target RNA sequences. Furthermore, microsatellite instability (MSI) analysis and IHC for p53, β-Catenin and Ki-67 were performed.

Results: We found three CRC cases showing positive staining for pan-trk IHC from among 971 consecutive Japanese CRC cases. Two out of three cases showed strong and diffuse membranous and cytoplasmic staining, whereas the remaining case showed weak but diffuse cytoplasmic staining. Clinicopathologically, histological types of these three cases were tub2>por1, tub2 and muc>tub2, respectively. Pathological stages were Stage I, Stage IIA, and Stage IIIB, respectively. All three cases with *NTRK* fusions did not show overexpression for p53, and all cases showed β-catenin membranous staining without nuclear staining. MIB-1 LI was evaluated and were approximately 80%, 50% and 50%, respectively. MSI analysis revealed that two of three cases were classified as MSI-H, whereas the remaining case was judged as MSS. All these three CRC showed imbalanced expressions (5'-side vs 3'-side) of *NTRK1*, suggesting the formation of *NTRK1* fusions. RNA target sequences are in progress to determine the fusion partners. Regarding prognosis, one patient had been

followed -up for short period, and another patient has been no evidence of recurrence/metastasis for 100 months. The remaining patient with Stage IIIB died 1 year after surgery.

Conclusions: This is a first report regarding the frequency of *NTRK* fusion in Japanese CRC. *NTRK* fusion positive CRC seemed to have distinct pathogenesis compared to conventional CRC. It is necessary to await the accumulation of positive cases to clarify the biological behavior of CRC with *NTRK* fusion.

821 Clinicopathological and Comprehensive Mutational Analysis in Esophageal Basaloid Squamous Cell Carcinoma

Yuka Yanai[1], Tsuyoshi Saito[2], Takuo Hayashi[3], Sho Tsuyama[4], Yoshiyuki Suehara[2], Takashi Yao[5]
[1]Juntendo University, Bunkyo-ku, Tokyo, Japan, [2]Juntendo University, School of Medicine, Tokyo, Japan, [3]Juntendo University Graduate School of Medicine, Tokyo, Japan, [4]Juntendo University Graduate School of Medicine, Bunkyo-ku, Tokyo, Japan, [5]Juntendo University, Tokyo, Japan

Disclosures: Yuka Yanai: None; Tsuyoshi Saito: None; Takuo Hayashi: None; Sho Tsuyama: None; Yoshiyuki Suehara: None; Takashi Yao: None

Background: Esophageal basaloid squamous cell carcinoma (EBSCC) is a poorly differentiated variant of squamous cell carcinoma and is a rare tumor accounting for 0.77-5% of esophageal cancer. The aim of this study is to examine the clinicopathological/molecular biological characteristics of EBSCCs.

Design: We examined 58 cases of surgically or endoscopically resected EBSCCs. Clinicopathological factors such as age, gender, tumor size, tumor site, tumor type (elevated, depressed and unclassifiable type), lymphovascular invasion, INF, intramural invasion, TNM stage and dominant histological-typewere examined.EBSCC are classified histologically into 4 types (solid, cribri, micronestic and ductal type) according to the dominant histology. We performed Kaplan-Meier survival analysis to elucidate the prognostic impact of each factor. Cancer hotspot panel by next-generation sequencing (NGS) were performed for 19 cases. Target sequences were performed for the remaining 39 cases using the same primer pairs as NGS for *TP53,* and loss of heterozygosity (LOH) analysis for*TP53*, *ATM* and *RB1* in all case. We also performed immunohistochemical staining of p53, ATM and RB1 for all cases.

Results: The average observation period was 55.8 months (from 3 to 135). Overall survival (OS) rate was 68%, and relapse free survival (RFS) rate was 53.2%. Solid-type was the most frequently observed histological feature in EBSCC (79.3%). As for *TP53,* mutation and LOH, overexpression by IHC rate were high (66.6%, 67.5% and 56.4%, respectively), however the frequency was not different from those reported in conventional esophageal squamous cell carcinoma. NGS revealed TP53as the most frequent mutated gene, and ATMand RB1 aslost genes by the copy number variation (CNV). LOH of RB1and ATMrate were also high (67.2% and 55.3%, respectively). LOH status for TP53, ATM, and RB1 was not consistent with protein expression by IHC. Macroscopic tumor type (unclassifiable type), lymphatic invasion, venous invasion, intramural metastasis, depth of wall penetration and TNM stage affected on the relapse-free survival. Besides, intramural metastasis and dominant-histological type (microcystic type) affected on overall survival.

Conclusions: Only the conventional clinicopathological factors had the prognostic impacts in EBSCC. Genetic alterations such as *TP53*, *ATM, and RB1* statusdid not affect patients' prognosis. Genetic alteration other than these genes were rare in EBSCC on this hotspot panel.

822 Clinical Significance of Basaloid Features in Squamous Cell Carcinoma of the Esophagus

Jing Yang[1], Deepa Patil[2], Jon Wee[3], Agoston (Tony) Agoston[2], Vikram Deshpande[4], Lei Zhao[3]
[1]Brigham and Women's Hospital, Harvard Medical School, Belmont, MA, [2]Brigham and Women's Hospital, Boston, MA, [3]Brigham and Women's Hospital, Harvard Medical School, Boston, MA, [4]Massachusetts General Hospital, Boston, MA

Disclosures: Jing Yang: None; Deepa Patil: None; Jon Wee: None; Agoston (Tony) Agoston: None; Vikram Deshpande: *Grant or Research Support*, Advanced Cell Diagnostics; *Advisory Board Member*, Viela; *Grant or Research Support*, Agios Pharmaceuticals; Lei Zhao: None

Background: Although some believe that basaloid features in esophageal squamous cell carcinoma (SCC) suggest worst prognosis, there are conflicting results in the literature regarding its biological behavior. In this study, we compared clinicopathological features of esophageal SCC with basaloid features with conventional SCC using surgical resections of treatment naïve esophageal carcinomas.

Design: Esophageal SCC resected between 1990 to 2016 were retrieved from our pathology archive. Clinical information was collected by reviewing electronic medical records. Pathologic features were evaluated by examination of all slides. HPV infection status was tested by p16 immunohistochemistry and HPV (high risk strains) mRNA ISH. Survival analysis was calculated using the Kaplan-Meier estimate.

Results: Twenty-two cases of esophageal SCC with basaloid features were identified. Thirty-eight cases of conventional SCC matched by tumor stage were used as control [Table 1]. Among 22 cases of esophageal SCC with basaloid features, 10 cases showed pure basaloid morphology and 12 cases showed additional morphologic features including well-differentiated keratinizing SCC, poorly differentiated SCC and sarcomatoid SCC. Survival analysis was carried out between SCC with basaloid features versus conventional SCC, and pure basaloid SCC versus conventional SCC (matched for tumor stage). No statistical difference was seen in any of the analyses.

SCC with basaloid features were more frequently associated with diffuse or multifocal squamous dysplasia. Two of the 13 patients with stage T1 SCC with basaloid features had lymph node metastasis, but both cases also showed areas of poor differentiation. P16 IHC was positive in 2 of 13 cases tested, but HPV mRNA ISH was negative in 17 out of 17 cases tested (including both cases with positive P16 IHC).

	T1 Tumors			T2 and above Tumors		
	SCC with basaloid features n=13	Conventional SCC n=19	*p*	SCC with basaloid features n= 9	Conventional SCC n= 19	*p*
Age	68.5 (56-79)	65.7 (47-85)	0.43	66.6 (53-82)	71 (51-83)	0.21
Gender	Male: 7 Female: 6	Male: 11 Female: 8	0.05	Male: 7 Female: 2	Male: 8 Female: 11	0.11
Tumor location	Upper/mid: 8 Lower: 5	Upper/mid: 8 Lower: 11	0.295	Upper/mid: 3 Lower: 6	Upper/mid:11 Lower: 8	0.42
Tumor Size (cm)	2.1 (0.3-3.8)	2.65 (0.5-9.5)	0.45	3.08 (1.7-5.3)	4.3 (1.9-11)	0.15
Lymph node status	Positive: 2 Negative: 11	Positive: 0 Negative:19	0.038*	Positive: 4 Negative: 5	Positive: 6 Negative: 13	0.67
Associated with diffuse or multifocal dysplasia	Positive: 6 Negative: 7	Positive: 1 Negative: 18	0.01*	Positive: 6 Negative: 3	Positive: 0 Negative: 19	<0.001*

Conclusions: Our study shows that esophageal SCC with basaloid features are more frequently associated with diffuse or multifocal dysplasia. However, it is not associated with HPV infection and the survival is similar to conventional SCC.

823 Validation of a Rapid PCR Assay for Microsatellite Instability Testing in Colorectal Cancer

Hadi Yaziji[1], Richard Chiu[2], Iryna Mazur[3], Altaf Taher[4]
[1]Vitro Molecular Laboratories, LLC, Miami, FL, [2]Larkin Community Hospital, Hialeah, FL, [3]Boca Raton, FL, [4]St Johns, NL

Disclosures: Hadi Yaziji: None; Richard Chiu: None; Iryna Mazur: None

Background: Detection of microsatellite instability (MSI) continues to gain clinical importance, particularly in light of targeted therapy approval of checkpoint inhibitors in patients whose solid tumors are MSI high. Several methods of testing already exist, including PCR-based capillary-gap electrophoresis and next generation sequencing. Most of these methods suffer a prolonged turnaround time, which may impact/delay treatment decisions.

Design: We wished to evaluate and validate a relatively novel rapid PCR assay (Idylla; Biocartis) for MSI testing on a cohort of 72 colorectal cancers (CRC). The assay was validated against a clinically validated immunohistochemistry-based mismatch-repair protein assay that was previously clinically validated using outcome data from a large cohort of stage II colon cancer patients samples (QUASAR trial). The MMR assay included four antibodies against MLH1, MSH2, MSH6 and PMS2. We also wished to evaluate the east of use of the rapid molecular assay, failure rate and turnaround time. Following automated DNA extraction from a single, 5-micron section, the polymerase chain reaction was accompanying by simultaneous generation of melting curves via fluorescence detection. The multiplex assay detects tumor-specific mutations in 7 MSI loci which are ACVR2A (2p22.3-q23.1), BTBD7 (14q32.12), DIDO1 (20q13.33), MRE11 (11q21), RYR3 (15q13.3-q14), SEC31A (4q21.22), and SULF2 (20q13.12). Amplification of < 5 markers renders the test results invalid. Otherwise, the tumor is either classified as MSI-H (MSI-high) or MSS (MS - stable).

Results: All but one of the 72 tumors yielded a valid result (failure rate 1.3%). The valid results only required a single tissue section, and the entire procedure from extraction to PCR and detection lasted only 2.5 hours. 12 tumors (16%) were classified as MSI High (MSI-H), all of which also show deficiency in either MLH1/PMS2 or MSH2/MSH6 protein complexes. All 60 MSI-stable (MSI-S) tumors also show MMR proficiency by immunohistochemistry.

Conclusions: This study validate the clinical use of a relatively novel MSI PCR-based assay on a cohort of 72 CRC samples, by showing 100% correlation with MMR protein status in a clinically validated MMR assay. The extremely fast turnaround time, ease of use and very low failure rate are advantageous for adopting this platform for molecular MSI testing.

824 Double Negative for Expression of YAP1 and CDX2 Defines a Subgroup of Colitis-Associated Colorectal Cancer with Early Onset and Aggressive Features

Feng Yin[1], Hao Xie[2], Jinping Lai[3], Jixin Dong[4], Xiuli Liu[5]
[1]University of Missouri, Columbia, MO, [2]Mayo Clinic, Rochester, MN, [3]Kaiser Permanente Sacramento Medical Center, Sacramento, CA, [4]Eppley Institute for Research in Cancer and Allied Diseases, Fred and Pamela Buffett Cancer Center, University of Nebraska Medical Center, Omaha, NE, [5]University of Florida, Gainesville, FL

Disclosures: Feng Yin: None; Hao Xie: None; Jinping Lai: None; Jixin Dong: None; Xiuli Liu: None

Background: Hippo signaling is an evolutionarily conserved tumor suppressor pathway. The correlation of YAP1 with CDX2 in colorectal cancer has not been investigated. In addition, the expression of YAP1 in colitis-associated colorectal cancer (CAC) has not been explored.

Design: A cohort of 57 CAC from year 1992 to 2010 were included in this study. Chronic colitis was confirmed by clinical history and histology in all cases. Three tissue microarrays were constructed from the representative area of these CACs and subjected to immunohistochemistry for YAP1, CK7, CDX2, p53, AMACR, and beta-catenin. Expression of YAP1 expression is correlated with clinicodemographics, tumor histologic features, and other examined markers.

Results: Analysis of TCGA database revealed a positive correlation between gene expression of YAP1 and CDX2 in invasive colorectal adenocarcinoma (P=0.00072) (Figure 1). Twenty-nine out of 57 (55.5%) CACs showed expression of YAP1. Table 1 summarizes YAP1 expression in relation to clinicodemographics and other features. Briefly, YAP1 expression in tumor was associated with old age (P=0.029) and CDX2 positivity (P=0.001). On the other hand, tumors with no expression of YAP1 showed a trend of having signet ring feature (P=0.144) and medullary feature (P=0.112). Forty out of 57 (70.2%) CACs showed expression of CDX2. Majority of CACs with YAP1 expression showed CDX2 expression (89.7%). In contrast, only half of the CACs with no YAP1 expression showed CDX2 expression (50.0%). Double negative YAP1(-)/CDX2(-) subgroup of CACs was often found in younger patients (mean age 45.3 years) (P=0.036). Morphologically this subgroup more likely has a feature of dirty necrosis (P=0.049). Most importantly, double negative YAP1(-)/CDX2(-) subgroup of CACs was more frequently presented with higher pathologic tumor stage (92.9% with pT3/pT4), as compared with the rest of cohort (62.8%; P=0.036). Double negative YAP1(-)/CDX2(-) subgroup of CACs was also more likely to have nodal metastasis (64.3% vs. 30.2% for the rest of cohort, P=0.031). Expression of YAP1 was not associated with other markers such as CK7, p53, AMACR, or beta-catenin nuclear immunoreactivity.

	YAP1 (-)	YAP1 (+)	*P* value
Mean age (SD)	46.5 (13.3)	55.5 (16.8)	**0.029 ***
pT3/pT4	20 (71.4%)	20 (69.0%)	1
Nodal metastasis	13 (46.4%)	9 (31.0%)	0.283
Right side	10 (35.7%)	12 (41.4%)	0.787
No dirty necrosis	17 (60.7%)	19 (65.5%)	0.787
Mucinous feature	17 (60.7%)	14 (48.3%)	0.429
Signet ring feature	6 (21.4%)	2 (6.9%)	**0.144**
Medullary feature	3 (10.7%)	0 (0%)	**0.112**
Crohn like feature	13 (46.4%)	18 (62.1%)	0.292
Heterogeneity	12 (42.9%)	9 (31.0%)	0.417
Well differentiation	12 (42.9%)	11 (37.9%)	0.790
CK7 +	16 (57.1%)	17 (58.6%)	1
CDX2 +	14 (50.0%)	26 (89.7%)	**0.001 ***
p53 +	16 (57.1%)	18 (62.1%)	0.790
AMACR +	4 (14.3%)	8 (27.6%)	0.331
Beta-catenin +	3 (10.7%)	3 (10.3%)	1
Total	28	29	
	YAP1 (-)/CDX2 (-)	YAP1 (-)/CDX2 (+) YAP1 (+)/CDX2 (-) YAP1 (+)/CDX2 (+)	*P* value
Mean age (SD)	45.3 (11.5)	53.0 (16.6)	**0.036 ***
pT3/pT4	13 (92.9%)	27 (62.8%)	**0.044** *
Nodal metastasis	9 (64.3%)	13 (30.2%)	**0.031 ***
Right side	7 (50%)	15 (34.9%)	0.356
No dirty necrosis	6 (42.9%)	32 (74.4%)	**0.049 ***
Mucinous feature	7 (50%)	25 (58.1%)	0.758
Signet ring feature	3 (21.4%)	5 (11.6%)	0.391
Medullary feature	2 (14.3%)	1 (2.3%)	**0.146**
Crohn like feature	6 (42.9%)	25 (58.1%)	0.367
Heterogeneity	7 (50%)	14 (32.6%)	0.340
Well differentiation	5 (35.7%)	20 (46.5%)	0.548
CK7 +	7 (50%)	28 (65.1%)	0.356
p53 +	9 (64.3%)	25 (58.1%)	0.762
AMACR +	2 (14.3%)	10 (23.2%)	0.710
Beta-catenin +	1 (7.1%)	5 (11.6%)	1
Total	14	43	

Figure 1 - 824

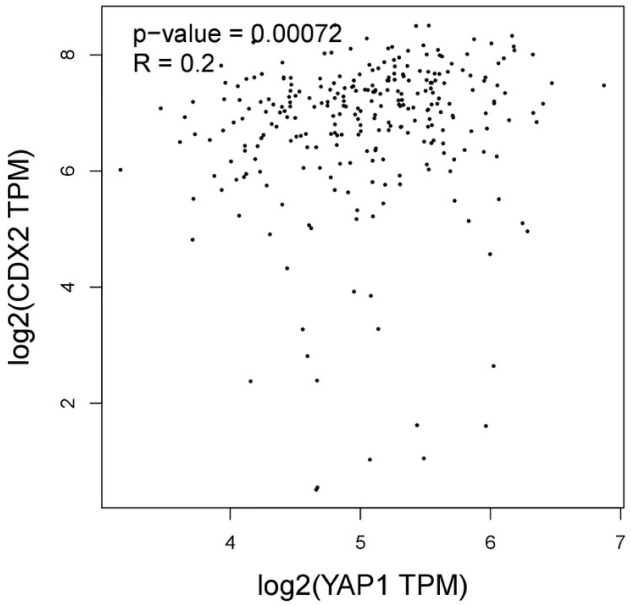

Conclusions: Gene expression levels of YAP1 and CDX2 are positively correlated in colorectal adenocarcinoma including CACs. Double negative for expression of YAP1 and CDX2 defines a subgroup of CACs, which is more often presented in younger patients with aggressive features, as indicated as higher tumor stage and frequent lymph node metastasis.

825 Deleterious Mutations in Esophageal Carcinoma Cuniculatum Detected by Next Generation Sequencing

Feng Yin[1], Kai Wang[2], Petr Starostik[2], Kimberly Newsom[2], Michael Feely[2], Xiuli Liu[2]
[1]University of Missouri, Columbia, MO, [2]University of Florida, Gainesville, FL

Disclosures: Feng Yin: None; Kai Wang: None; Petr Starostik: None; Kimberly Newsom: None; Michael Feely: None; Xiuli Liu: None

Background: Esophageal carcinoma cuniculatum (ECC) is a rare form of extremely well differentiated squamous cell carcinoma that is often misdiagnosed preoperatively. The etiology and molecular changes underlying ECC remain unknown. This study aimed to examine the molecular changes underlying invasive ECC as well as adjacent non-invasive components using next generation sequencing (NGS).

Design: Four cases of ECC were collected from our pathology database from 2014 to 2019. They were diagnosed based on criteria previously published [Laudau M et al., 2012; Chen D et al, 2013]. Areas of normal squamous mucosa, non-invasive components (n=2) and invasive components (n=4) of ECC were selected for analysis. Genomic DNA extracted from the microdissected tissue was sequenced using the GatorSeq NGS Panel and on the Illumina NextSeq500 to high uniform depth. Sequence data was processed using a customized analysis pipeline (GatorSeq) designed to accurately detect base substitutions and insertions/deletions using human genome version hg19 as the reference. Deleterious mutations, as predicted by SIFT, were identified using tumor/normal pairs and annotated by amino acid change.

Results: Four [three females and one male, mean age 57 years (range 37-67)] patients were included in this study. One patient received chemoradiation and the remaining three patients were treatment naïve. NGS identified *Notch 1* mutations in 3 (75%) cases, *TP53* mutations in 2 (50%) patients, mismatch repair gene (*MSH6* and *MLH1*) in 2 (50%) patients, and *KRAS* mutation in 1 (25%) case. Other deleterious gene mutations included *PIK3CA* (phosphoinositide-3-kinase catalytic alpha polypeptide), *SETD2* (SET domain-containing protein 2) and *TLR2* (toll-like receptor 2). Two cases had both non-invasive and invasive components evaluated. The mutation profiles in the non-invasive and invasive components were identical with one case showing deleterious mutation in *MSH6*, *PIK3CA*, and *TP53*, and the other case in *Notch 1*, *SETD2*, *KRAS*, *MLH1*, and *TP53*. Table 1 summaries the deleterious gene mutations detected in these four ECCs.

Table 1. Deleterious mutations observed in 4 invasive esophageal carcinoma cuniculatum.

Case	Age	Gender	Specimen type	Pathology stage	Deleterious mutations based SIFT predicted amino acid change
1	58	Female	Esophagectomy	ypT3N0	MSH6 c.2474T>A; p.Ile825Asn (US) PIK3CA c.1624G>A; p.Glu542Lys (GOF) TP53 c.733G>A; p.Gly245Ser (LOF)
2	67	Female	Endoscopic resection	N/A	Notch 1 c.1363G>A; p.Glu455Lys (LOF) SETD2 c.6365G>T; p.Arg2122Leu (LOF) SETD2 c.6364C>T; p.Arg2122Trp (LOF) KRAS c.35G>A; p.Gly12Asp (GOF) MLH1 c.1930G>A; p.Asp644Asn (US) TP53 c.817C>T; p.Arg273Cys (LOF)
3	37	Female	Esophagectomy	pT3N0	Notch 1 c.1393 G>A, pAla465Thr (LOF)
4	67	Male	Biopsy	N/A	Notch 1 c.1253T>C; p.Leu418Pro (US) TLR2 c.1624C>A; p.Leu542Ile (US)

GOF: gain of function; LOF: loss of function; US: uncertain significance.

Conclusions: ECCs demonstrate deleterious mutations in several genes including *Notch 1*, *TP53*, *MLH1*, *MSH6*, *KRAS*, *SETD2*, *TLR2*, and *PIK3CA*. The mutations were also identified in the corresponding non-invasive components. These results suggest that molecular testing may aid in the pre-operative diagnosis and the mutated proteins may provide potential therapeutic targets in patients with advanced or unresectable ECC.

826 Correlation of Histologic Features with Etiologies of Lymphocytic Gastritis

Raymond Yip[1], Lawrence Lee[2], Lik Hang Lee[3], David Schaeffer[4], Hui-Min Yang[1]
[1]Vancouver General Hospital/University of British Columbia, Vancouver, BC, [2]Vancouver, BC, [3]University of British Columbia and St. Paul's Hospital, Vancouver, BC, [4]Vancouver General Hospital, Vancouver, BC

Disclosures: Raymond Yip: None; Lawrence Lee: None; Lik Hang Lee: None; David Schaeffer: None; Hui-Min Yang: None

Background: Lymphocytic gastritis (LG) is an injury reaction pattern of the stomach characterized by intraepithelial lymphocytosis and lamina propria chronic inflammation. In our prior study of LG, we assessed topography and morphologic features such as glandular microabscesses, intestinal metaplasia, and lymphoid aggregates in cases of LG associated with gluten-sensitive enteropathy (GSE), NSAID injury, and *H. pylori* infection. In this new iteration of our LG study, we examined additional histologic features such as the number of intraepithelial lymphocytes (IELs) per 100 gastric epithelial cells, the distribution of IELs at the surface vs in the pit, the degree of acute and chronic inflammation in the lamina propria, and the presence or absence of lymphoid follicles and their association with the common etiologies of LG.

Design: Cases of LG were collected from our institution between August 2011 and September 2017, confirmed via histologic assessment by two study pathologists. We examined histologic features including the number and distribution of IELs, the degree of acute and chronic inflammation in the lamina propria, and the presence and absence of lymphoid follicles.

Results: Of the 32 total cases of LG, all 5 cases associated with NSAID injury had over 45 IELs per 100 epithelial cells, compared to only 2 of 8 (25%) cases associated with GSE and 1 of 6 (17%) cases associated with *H. pylori* infection. The distribution of IELs was mostly in either the surface epithelium only or both the surface and pit epithelium, and was not associated with specific etiologies. All LG cases associated with *H. pylori* infection (6/6) and 3 of 5 cases associated with NSAID injury showed severe chronic inflammation in the lamina propria. Lymphoid follicles were identified only in LG cases associated with *H. pylori* infection (2 of 6 cases) and not with other etiologies.

Conclusions: In cases of severe LG where there are greater than 45 IELs per 100 epithelial cells, LG is more likely to be associated with NSAID injury. The distribution of IELs does not appear to be associated with specific etiologies. Severe lamina propria chronic

inflammation is most likely associated with *H. pylori* infection or NSAID injury. The presence of lymphoid follicles is highly specific for *H. pylori* infection. In the absence of other features such as *H. pylori* or duodenal biopsies to suggest GSE, the severity of intraepithelial lymphocytosis can be evaluated to suggest NSAID use as the cause of injury and to allow for proper treatment.

827 TTF-1, SATB2, and SSTR2A Can Help Differentiate Between Gastroenteropancreatic and Pulmonary Neuroendocrine Carcinomas

Sanhong Yu[1], Jason Hornick[2], Raul Gonzalez[3]
[1]Tufts Medical Center, Boston, MA, [2]Brigham and Women's Hospital, Harvard Medical School, Boston, MA, [3]Beth Israel Deaconess Medical Center, Boston, MA

Disclosures: Sanhong Yu: None; Jason Hornick: *Consultant*, Eli Lilly; *Consultant*, Epizyme; Raul Gonzalez: None

Background: Primary gastroenteropancreatic neuroendocrine carcinoma (GEP-NEC) is a rare, aggressive malignancy that cannot be distinguished morphologically from pulmonary neuroendocrine carcinoma (P-NEC). This can present a significant diagnostic challenge in cases where the site of origin cannot be readily determined (typically when a patient presents with metastatic disease, given the high rate of dissemination in NEC). Although immunohistochemical (IHC) staining may help determine primary site for metastatic well-differentiated neuroendocrine tumors, to date no markers have been identified that can reliably distinguish among visceral NEC.

Design: We constructed two 3mm tissue microarrays, one containing 15 GEP-NECs and the other containing 20 P-NECs, all of which were retrieved from our departmental archives and reviewed to confirm the diagnosis. IHC for the following 18 cancer-related proteins was performed on both microarrays: AE1/AE3, CK7, CK20, synaptophysin, chromogranin, CD56, SSTR2A, TTF1, Napsin A, CDX2, SATB2, p53, Rb, progesterone receptor, GATA3, SMAD4, PAX8, and AFP. Each marker was assessed for percentage of cells at each level of staining intensity (0-3+), and an H-score was calculated. Each stain's H-score was compared between GEP-NEC and P-NEC using the *t* test, with significance set at $P<0.05$.

Results: The GEP-NECs included 6 small cell and 9 large cell NECs, from the esophagus (n=2), stomach (n=1), small bowel (n=4), colorectum (n=7), and pancreas (n=1). The P-NECs included 7 small cell and 13 large cell NECs. H-score data are summarized in the **Table**. For GEP-NEC, the most strongly expressed marker was synaptophysin (mean H-score 235), while AE1/AE3 was the most strongly expressed in P-NEC (mean H-score 230), which was stronger than in GEP-NECs ($P=0.0061$). Other markers that were stronger overall in P-NEC than in GEP-NEC included CK7 ($P<0.0001$) and TTF1 ($P=0.0002$), although 6 P-NEC were negative for TTF1. Markers that were stronger overall in GEP-NEC than in P-NEC included SSTR2A ($P=0.0061$) and SATB2 ($P=0.024$), but not CDX2 ($P=0.15$), which was only expressed in 3 GEP-NEC. SMAD4, Rb, and P53 showed similar rates of abnormal protein expression.

Table: Detailed Expression Data for NEC

IHC stain	GEP-NEC mean H-score	P-NEC mean H-score	*P*-value
AE1/AE3	148	230	**0.0061**
CK7	42	209	**<0.0001**
CK20	32	4	0.11
Synaptophysin	235	188	0.22
Chromogranin	170	165	0.91
CD56	145	157	0.78
SSTR2A	107	14	**0.0061**
TTF1	20	177	**0.0002**
Napsin A	0	10	0.32
CDX2	11	0	0.15
SATB2	99	35	**0.024**
PR	0	0.1	0.22
GATA3	4	6	0.79
PAX8	29	24	0.78
AFP	0	0	n/a

Conclusions: Organ-specific IHC markers that can help distinguish GEP-NEC from P-NEC include TTF1 and SATB2; CDX2 is not useful in this regard. Additionally, AE1/AE3, CK7, and SSTR2A may assist in this differential diagnosis.

828 PD-L1 Expression Patterns in Mismatch Repair Deficient Colorectal Cancer

Dongwei Zhang[1], Xiaoyan Liao[1], Huijie Liu[2], Karina Hiroshige[3], Meenal Sharma[4], Rebecca Amorese[5], Elena Gupta[6], Laura Frado[7], Caitlin Foor-Pessin[8], Qi Yang[9], Danielle Marino[3], Raul Gonzalez[10], Jennifer Findeis-Hosey[1]
[1]University of Rochester Medical Center, Rochester, NY, [2]University of Rochester Medical Center, West Henrietta, NY, [3]University of Rochester, Rochester, NY, [4]Unity Hospital, Rochester Regional, Rochester, NY, [5]University of Rochester, Mohegan Lake, NY, [6]Cornell University, Ithaca, NY, [7]University of Rochester, New York, NY, [8]University of Rochester Medical Center, Ithaca, NY, [9]Pittsford, NY, [10]Beth Israel Deaconess Medical Center, Boston, MA

Disclosures: Dongwei Zhang: None; Xiaoyan Liao: None; Huijie Liu: None; Karina Hiroshige: None; Meenal Sharma: None; Rebecca Amorese: None; Elena Gupta: None; Laura Frado: None; Caitlin Foor-Pessin: None; Qi Yang: None; Danielle Marino: None; Raul Gonzalez: None; Jennifer Findeis-Hosey: None

Background: The checkpoint proteins programmed cell death-1 (PD-1) and PD-1 ligand (PD-L1) receptors allow tumor cells to keep the host immune response in check. Checkpoint blockade therapy, currently approved by the U.S. Food and Drug Administration, shows dramatic response rates and durability of response in mismatch repair deficient (dMMR) colorectal cancer (CRC). The aim of this study is to characterize the expression profile of PD-L1 in dMMR CRC and correlate with histomorphologic features and outcome.

Design: Sixty-four surgically resected dMMR CRCs between the years of 2012 and 2016 were retrieved from our institution. Histological examination and PD-L1 immunohistochemical study were performed using tissue microarray slides, and a *Combined Positive Score* [*CPS*] (number of PD-L1 staining cells [tumor cells, lymphocytes, and macrophages], divided by total number of viable tumor cells, then multiplied by 100) was calculated for each case.

Results: The 64 CRC came from 27 males and 37 females, with an average age of 74 years (range: 27-99). Among them, 57 (89.0%) showed MLH1/PMS2 loss, 3 (4.3%) PMS2 loss, and 4 (6.7%) MSH2/MSH6 loss. Some degree of positive PD-L1 staining was observed in 47 (73.4%) cases, among which 34 (53.1%) showed positivity in tumor-infiltrating immune cells, 5 (7.8%) showed positivity in tumor cells, and 8 (12.5%) showed positivity in both. The 47 positive cases were further divided into three categories: CPS≤1 and >10 (n=22, 46.8%), CPS≥10 and <50 (n=21, 44.7%), and CPS≥50 (n=4, 8.5%). All 4 cases with CPS≥50 showed PD-L1 expression on tumor cells only. PD-L1 expression was more frequent in medullary (7/8, 87.5%) and conventional adenocarcinoma (33/40, 82.5%) than in adenocarcinoma with mucinous features (7/13, 53.8%). PD-L1 expression did not correlate with tumor differentiation. After a median follow-up of 37 months (range: 2-72, 61 cases), the PD-L1 positive and negative cases did not show statistically significant differences in patient survival.

Conclusions: More than 70% of dMMR CRC in our study were positive for PD-L1, and PD-L1 expression was more frequently observed in tumor-infiltrating immune cells. Cases with high PD-L1 expression (CPS≥50) demonstrated positivity in tumor cells only. PD-L1 expression was associated with CRC histologic subtype but not tumor differentiation or patient survival.

829 Can Multi-Target Stool DNA Test (Cologuard) Replace Colonoscopy to Detect Colorectal Cancer? A Single Institutional Experience

Kuixing Zhang[1], Hanlin Wang[2]
[1]University of California Los Angeles, San Diego, CA, [2]David Geffen School of Medicine at UCLA, Los Angeles, CA

Disclosures: Kuixing Zhang: None; Hanlin Wang: None

Background: The current guidelines for colorectal cancer (CRC) screening recommended by the American Cancer Society include colonoscopy every 10 years or fecal immunochemical test (FIT) for occult blood every year for average-risk adults starting at age 45. In 2014, the FDA approved the first stool DNA-based multitarget CRC screening test, the Cologuard test. In addition to hemoglobin immunoassay, Cologuard test also includes molecular assays for *KRAS* mutations and aberrant *NDRG4* and *BMP3* methylation using beta-actin as a reference gene. For detecting CRC or advanced precancerous lesions, Cologuard has shown a higher sensitivity but lower specificity than FIT. There have been no data available for the positive predictive value of this test.

Design: A total of 55 patients were tested positive for Cologuard and followed by colonoscopy at UCLA from 2016 to 2019. There were 27 males and 28 females. The patients' age ranged from 38 to 86 years, with an average age of 62 and a median age of 71.

Results: On colonoscopy, 1 patient (1.8%) was found to have invasive adenocarcinoma, 24 (43.6%) had ≤2 adenomas (tubular adenoma and/or sessile serrated adenoma), 16 (29.1%) had ≥3 adenomas or an adenoma(s) with villous architecture or high-grade dysplasia, and 14 (25.5%) had negative findings. The positive predictive value is 1.8% (1/55) for adenocarcinoma, 30.9% (17/55) for adenocarcinoma and high-risk adenoma, and 74.5% (41/55) for adenocarcinoma and any adenomatous lesion.

Conclusions: Cologuard test offers a convenient, non-invasive option for CRC screening for those who are reluctant or not readily available to do a colonoscopy. It has a higher sensitivity than the conventional FIT test since it incorporates stool hemoglobin immunoassay into the CRC-related DNA assay. However, Cologuard test suffers from a lower specificity, which leads to unnecessary colonoscopy in some patients.

In this study, up to 25% of patients with a positive Cologuard test are free of any cancerous or precancerous lesion in the colorectum. Only 1 patient (<2%) in our cohort is found to have CRC. Thus, Cologuard test has a low positive predictive value for malignancy and a positive result should always be followed by colonoscopy. Colonoscopy remains to be the gold standard for early CRC detection in the era of molecular medicine.

830 Histologic Patterns of Immune-Related Adverse Events in the Colon

Mingjuan Zhang[1], Azfar Neyaz[2], Angela Shih[1], Deepa Patil[3], Vikram Deshpande[1]
[1]Massachusetts General Hospital, Boston, MA, [2]Massachusetts General Hospital, Malden, MA, [3]Brigham and Women's Hospital, Boston, MA

Disclosures: Mingjuan Zhang: None; Azfar Neyaz: None; Angela Shih: None; Deepa Patil: None; Vikram Deshpande: *Grant or Research Support*, Advanced Cell Diagnostics; *Advisory Board Member*, Viela; *Grant or Research Support*, Agios Pharmaceuticals

Background: Immune checkpoint inhibitors (ICIs) are increasingly used to treat a variety of malignancies and are also associated with gastrointestinal (GI) immune-related adverse events (GI-irAEs). The aim of this study was to describe the spectrum of histological alterations seen in colonic biopsies following ICI therapy.

Design: 40 patients treated with ICIs and had a subsequent colon biopsy were identified. We recorded clinical data and endoscopic findings and reviewed their colonic biopsies. The diagnosis of GI-irAE was based on the improvement of GI symptoms following immunosuppressive therapy. Active colitis was defined as neutrophils involving >5 crypts, and apoptosis was defined as >5 apoptotic cells/10 HPFs.

Results: The mean age was 60.2 years; 23 (58%) were female. 25 (63%) patients were treated with an anti-programmed cell death protein 1 (PD1)/anti-programmed cell death ligand 1 (PD-L1) antibody alone, and 14 (35%) were treated with a combination of anti-cytotoxic T-lymphocyte-associated protein-4 and anti-PD1 antibodies. 36 (90%) patients presented with diarrhea. 31 (78%) and 9 (23%) patients were diagnosed clinically as positive and negative for GI-irAEs, respectively (Table). Increased numbers of colonic lamina propria mononuclear cells and neutrophilic activity were significantly associated with a clinical diagnosis of GI-irAE (p=0.015 and p=0.005, respectively). We identified four patterns of colitis: 1) acute self-limiting colitis (n=11), 2) lymphocytic colitis (n=9), 3) collagenous colitis (n=2), and 4) apoptosis only (n=3); the colonic mucosa was histologically unremarkable in the remaining 15 cases. None of the cases showed histologic evidence of chronic colitis. There was no difference in the histologic spectrum of patients treated with anti-PD1/PD-L1 alone vs. anti-PD1/anti-CTLA4 combination therapy.

Table. Comparison of Patients Diagnosed as Positive and Negative for Gastrointestinal Immune-Related Adverse Events

Histological features	All patients, *n* (%)	Negative for GI-irAEs, *n* (%)	Positive for GI-irAEs, *n* (%)	*P*-value
	N = 40	N = 9	N = 31	
ICI-associated colonic injury	25 (63)	1 (11)	24 (77)	**<0.001**
Increased numbers of lamina propria lymphocytes and plasma cells*	15 (38)	0 (0)	15 (48)	**0.015**
Increased number of intraepithelial lymphocytes	11 (28)	1 (11)	10 (33)	0.399
Neutrophilic activity*	17 (43)	0 (0)	17 (55)	**0.005**
Increased apoptotic activity*	9 (23)	0 (0)	9 (29)	0.090

*Criteria used to define immune checkpoint inhibitor-associated colonic injury.

ICI, immune checkpoint inhibitor; GI-irAE, gastrointestinal immune-related adverse events.

Conclusions: The morphological spectrum of ICI-related GI disease is broad and overlaps with other inflammatory diseases, highlighting the need for careful correlation with clinical findings and exclusion of other diseases associated with the acute self-limiting colitis and lymphocytic/collagenous colitis patterns of injury.

831 Risk Prediction Model Based on Prognostic Factors Beyond Lymph Node Status in Colorectal Cancer Stages II/III: An Integration of Mixed Clinicopathologic Data Using Bayesian Ensemble Trees

Melissa Zhao[1], Mai Chan Lau[1], Koichiro Haruki[1], Juha Väyrynen[2], Sara Väyrynen[2], Andressa Dias Costa[2], Jennifer Borowsky[3], Simeng Gu[1], Carino Gurjao[4], Kenji Fujiyoshi[1], Kota Arima[1], Tsuyoshi Hamada[5], Jochen Lennerz[6], Charles Fuchs[7], Andrew Chan[8], Kimmie Ng[4], Kana Wu[1], Xuehong Zhang[9], Jeffrey Meyerhardt[2], Mingyang Song[8], Jonathan Nowak[1], Marios Giannakis[2], Nishihara Reiko[1], Shuji Ogino[1]

[1]Brigham and Women's Hospital, Boston, MA, [2]Dana-Farber Cancer Institute, Boston, MA, [3]The Royal Brisbane & Women's Hospital, Brisbane, QLD, Australia, [4]Dana Farber Cancer Institute, Boston, MA, [5]The University of Tokyo, Boston, MA, [6]Massachusetts General Hospital, Harvard Medical School, Boston, MA, [7]Yale Cancer Center, New Haven, CT, [8]Massachusetts General Hospital, Boston, MA, [9]Brigham and Women's Hospital

Disclosures: Melissa Zhao: None; Mai Chan Lau: None; Koichiro Haruki: None; Juha Väyrynen: None; Sara Väyrynen: None; Andressa Dias Costa: None; Jennifer Borowsky: None; Simeng Gu: None; Carino Gurjao: None; Kenji Fujiyoshi: None; Jochen Lennerz: None; Charles Fuchs: *Consultant*, CytomX Therapeutics; *Consultant*, Eli Lilly; *Consultant*, Agios; *Consultant*, Merck; *Consultant*, Bayer; Jeffrey Meyerhardt: *Consultant*, Ignyta; *Consultant*, Taiho Pharmaceutical; *Consultant*, COTA Healthcare; Jonathan Nowak: None; Marios Giannakis: *Grant or Research Support*, Bristol Myers-Squibb; *Grant or Research Support*, Merck; Shuji Ogino: None

Background: Colorectal cancer TNM staging reflects local invasion and metastasis of tumor cells. However, difficulties in pathological assessment of tumor spread and pathogenic heterogeneity of colorectal cancer may contribute to imprecision in patient-specific survival prediction. Thus, we aimed to first determine important variables that influence colorectal cancer TNM stage, and then refine a survival prediction model by integrating TNM stage with tumor and immune characteristics.

Design: Utilizing databases of 1449 colorectal cancer cases with clinicopathologic, tumor molecular, immune, and microbial variables, we constructed Bayesian Additive Regression Trees (BART) models for classification of TNM stage II vs stage III and prediction of patient survival. We examined model stability in performance and variable selection through five-fold cross-validation and random runs, and compared BART model performance to other machine learning models such as LASSO linear regression, Stochastic Gradient Boosting, Random Forest, Support Vector Machine, and Artificial Neural Network using a multiple random validation strategy.

Results: Tumor depth of invasion (pT stage), number of negative lymph nodes, tumor-area memory cytotoxic T cell density, microsatellite instability status, and tumor differentiation were consistently important factors in the classification of stage II vs stage III. Additional predictors that were not important in stage classification, including extent of extraglandular necrosis and age, were stable important factors in colorectal cancer-specific survival prediction model. For patients with stage II/III cancer, hierarchical clustering of important variables demonstrated significant intra-stage survival differences of two major clusters in a multivariable-adjusted Cox proportional hazards regression model (Hazard Ratio = 0.272, P-value = 0.0004).

Conclusions: Our results indicate that the integrated bioinformatic analyses of pertinent factors can more robustly stratify patients into prognostic groups compared to TNM stage alone.

832 Utility of Metabolic Profiling of Formalin-Fixed Paraffin-Embedded Tissue Materials in Colorectal Cancer

Melissa Zhao[1], Kota Arima[1], Mai Chan Lau[1], Juha Väyrynen[2], Keisuke Kosumi[3], Koichiro Haruki[1], Hideo Baba[3], Massimo Loda[4], Andrew Chan[5], Nishihara Reiko[1], Jeffrey Meyerhardt[2], Marios Giannakis[2], Charles Fuchs[6], Jonathan Nowak[1], Shuji Ogino[1]

[1]Brigham and Women's Hospital, Boston, MA, [2]Dana-Farber Cancer Institute, Boston, MA, [3]Kumamoto University, Kumamoto, Kumamoto, Japan, [4]Weill Cornell Medicine, New York, NY, [5]Massachusetts General Hospital, Boston, MA, [6]Yale Cancer Center, New Haven, CT

Disclosures: Melissa Zhao: None; Mai Chan Lau: None; Juha Väyrynen: None; Koichiro Haruki: None; Jeffrey Meyerhardt: *Consultant*, Ignyta; *Consultant*, Taiho Pharmaceutical; *Consultant*, COTA Healthcare; Marios Giannakis: *Grant or Research Support*, Bristol Myers-Squibb; *Grant or Research Support*, Merck; Charles Fuchs: *Consultant*, CytomX Therapeutics; *Consultant*, Eli Lilly; *Consultant*, Agios; *Consultant*, Merck; *Consultant*, Bayer; Jonathan Nowak: None; Shuji Ogino: None

Background: Accumulating evidence suggests that metabolic reprogramming has a critical role in carcinogenesis and tumor progression. The usefulness of formalin-fixed paraffin-embedded (FFPE) tissue material for metabolomics analysis as compared with fresh frozen tissue material remains unclear.

Design: Liquid chromatography tandem mass spectrometry-based metabolomics analysis was performed on 11 pairs of matched tumor and normal tissues in both FFPE and fresh frozen tissue materials from colorectal carcinoma patients. Permutation t-test was applied to identify metabolites with differential abundance between tumor and normal tissues.

Results: A total of 200 metabolites were detected in the FFPE samples and 536 in the fresh frozen samples. The preservation of metabolites in FFPE samples was diverse according to classes and chemical characteristics, ranging from 78% (energy) to 0%

(peptides). Compared with the normal tissues, 34 (17%) and 174 (32%) metabolites were either accumulated or depleted from the tumor tissues in FFPE and fresh frozen samples, respectively. Among them, 15 metabolites were common in both FFPE and fresh frozen samples. Notably, branched chain amino acids were highly accumulated in tumor tissues. Using KEGG pathway analyses, glyoxylate and dicarboxylate metabolism, arginine and proline, glycerophospholipid, and glycine, serine and threonine metabolism pathways distinguishing tumor from normal tissues were found in both FFPE and fresh frozen samples.

Conclusions: This study demonstrates that informative data of metabolic profiles can be retrieved from FFPE tissue materials. Our data suggest potential value of metabolic profiling using FFPE tumor tissues.